TORRES STRAIT EXTREME WATER LEVEL STUDY

Final Report
July 2011

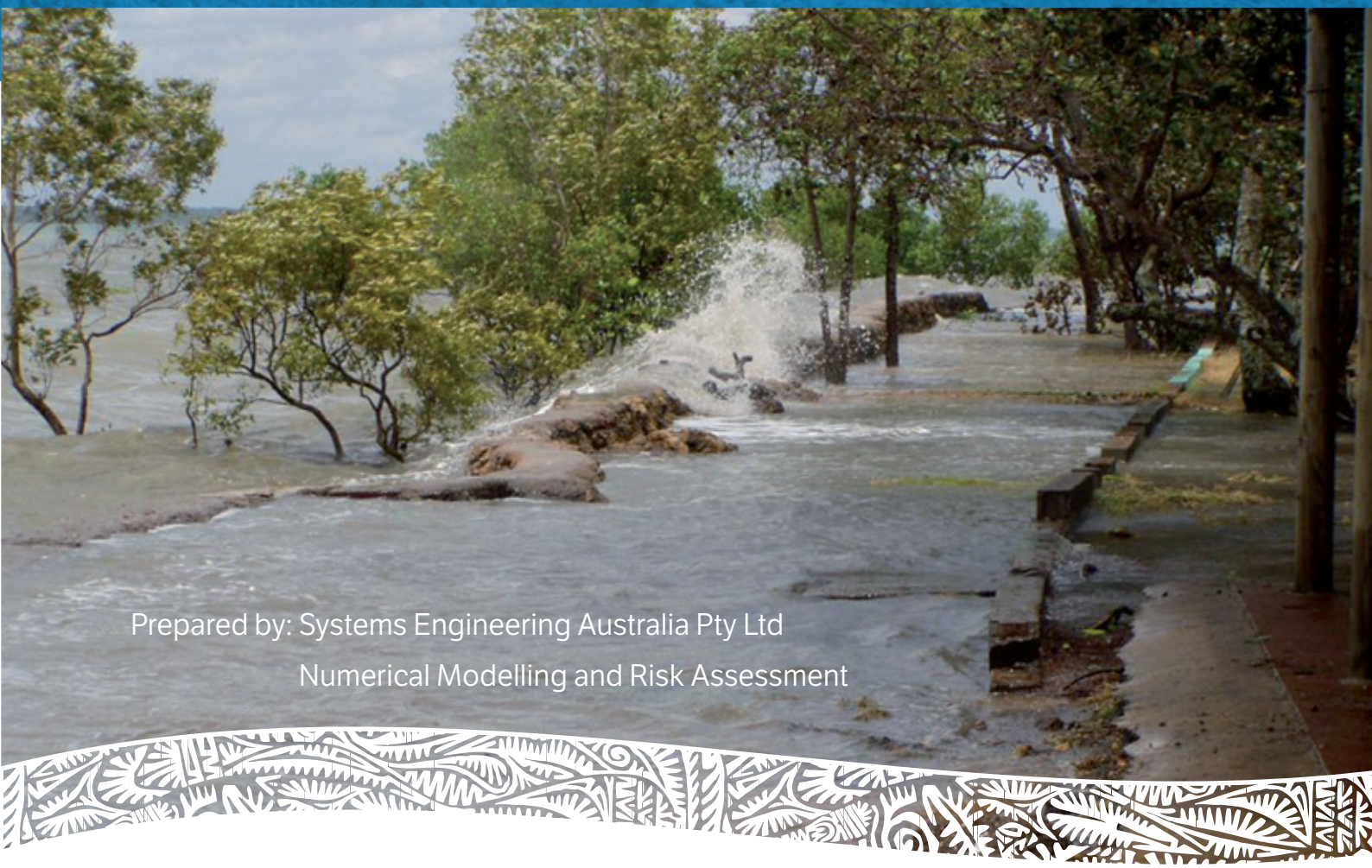

Prepared by: Systems Engineering Australia Pty Ltd
Numerical Modelling and Risk Assessment

Australian Government
TORRES STRAIT REGIONAL AUTHORITY
SEA

Cover Details:

Top: TSRA-supplied photographs of flooding by the sea at Saibai, January 2009 (D. Hanslow).

Bottom: Example modelled Category 4 tropical cyclone storm surge pattern (left) and simulated broadscale 100 year Return Period water level pattern (right).

Torres Strait Regional Authority

Torres Strait Extreme Water Level Study

Final Report

July 2011

Systems Engineering Australia Pty Ltd
ABN 65 073 544 439
http://www.systemsengineeringaustralia.com.au
PO Box 3125
Newstead Qld 4006

J0907-PR002C

ACKNOWLEDGEMENTS

The support provided by the Torres Strait (TSRA) Land and Sea Management Unit (Mr David Hanslow and Mr John Rainbird) is gratefully acknowledged.

This project was facilitated by the cooperation of many organisations, e.g.

- Australian Marine Safety Organisation (AMSA)
- Australian Hydrographic Service (AHS)
- Bureau of Meteorology (BoM) and the National Tidal Centre (NTC)
- Department of Environment and Resource Management Queensland (DERM)
- Geoscience Australia (GA)
- James Cook University (JCU)
- Maritime Safety Queensland (MSQ)

SEA Project team members were:

- Systems Engineering Australia Pty Ltd (SEA); Dr Bruce Harper;
- University of Tasmania, Australian Maritime College, Marine Modelling Unit (UTAS/AMC/MMU); Mr Luciano Mason;
- GHD Pty Ltd (GHD); Dr Ivan Botev, Mr Mitchell Smith;
- Jeff Callaghan Consulting (JCC), Mr Jeff Callaghan;
- Gassman Development Perspectives Pty Ltd (GDP); Mr Peter Todd.

LIMITATIONS OF THE REPORT

The information contained in this publication is based on the application of conceptual computer models of atmospheric and ocean hazards and provides an estimate only of the likely impacts of such events. The analyses have been undertaken in accordance with generally accepted consulting practice and no other warranty, expressed or implied, is made as to the accuracy of the data and professional advice provided herein. The results should be interpreted by qualified professionals familiar with the relevant meteorological, oceanographic and statistical concepts.

Systems Engineering Australia Pty Ltd (SEA) has taken all reasonable steps and due care to ensure that the information contained herein is correct at the time of publication. SEA expressly excludes all liability for errors or omissions, whether made negligently or otherwise, for loss, damage or other consequences that may result from the application of advice given in this publication.

TABLE OF REVISIONS

Version	Description	Date	Prepared By	Approved By
A	Issued as draft.	30-Jan-2011	B. A. Harper BE PhD CPEng RPEQ L.B. Mason BE	B.A. Harper
B	Final	24-Jul-2011	B.A. Harper	B.A. Harper
C	Revised Saibai HAT	25-Apr-2013	B.A. Harper	B.A. Harper

RELEASE STATUS

Client Confidential

TABLE OF CONTENTS

Page

LIST OF APPENDICES

LIST OF TABLES

LIST OF FIGURES

EXECUTIVE SUMMARY

This report describes the probabilistic assessment of extreme ocean water levels and inundation hazard in Torres Strait under present and projected future climate conditions (2010, 2050 and 2100). The study was commissioned by the Torres Strait Regional Authority though its Land and Sea Management Unit.

The Torres Strait is a remote region having significant complexity and diversity of geophysical parameters, low levels of reliable insitu information and with a widespread community vulnerable to the impacts of the sea. Although there have been many individual studies over time into various aspects of the geomorphology, oceanography, tides and meteorology of the region, this report has for the first time addressed the quantification of the extreme ocean water levels that can possibly occur. This information can now be used to perform detailed community vulnerability mapping and risk assessments as well as forming a rational basis for adaptation planning and assisting in the design of emergency services. The study has also significantly improved knowledge of the land-sea elevation datums across the various island communities and provides estimates of the risks from extreme winds.

The analysis confirms existing community experiences of periodic encroachment from the sea at many communities. On a 5 y average return period, equivalent to a 20% chance in any year, five communities are affected to some extent. The most vulnerable is Saibai, where the modelling suggests an annual likelihood of encroachment into some habitation areas of up to 0.5 m in depth and up to 1 m in an extreme 1000 y return period situation (a 0.1% chance in any single year or a 5% chance over any 50 y period). The next most vulnerable is Boigu, where the annual event is about 0.1 m depth, reaching up to 0.8 m by 1000 y return period. This is followed by Masig, Warraber and Iama. Other communities start to become vulnerable at the most extreme 10,000 y condition (0.01% chance in any year). This includes Erub, Hammond, Mabauig, Moa_St_Pauls, Ngurupai, Poruma, Seisia and Waiben. The remaining communities appear relatively free of encroachment to current habitation ground levels in present climate conditions. In terms of the geographic island clusters, it is the Top Western group (Saibai and Boigu) and some Central group islands (Masig, Warraber, Iama) that are the more affected at the shorter return periods but the Inner and Western groups are increasingly vulnerable at high return periods. In comparison the Eastern group is the least impacted.

Future climate change considerations have included increases in mean sea level and changes in the intensity and frequency of tropical cyclones. For the projected future climate of 2050, the existing five communities that are already principally affected will be further impacted

by the possible 0.3 m sea level rise. Erub is also affected then at the 5 y return period, Hammond is increasingly vulnerable by the 25 y level and Poruma becomes at risk around 100 y. It is likely that by 2050, five communities (Saibai, Boigu, Warraber, Iama and Masig) would be experiencing significantly adverse impacts. Notwithstanding these chronic incursions by the sea there would be increased stress placed on emergency services in the event of a higher magnitude event (longer return period) occurring.

By 2100, with a possible 0.8 m sea level rise and with increased tropical cyclone intensities, a total of 13 sites are affected beyond the 5 y level and 11 of these sites are affected across the full return period range. It is likely that 8 communities (Saibai, Boigu, Warraber, Masig, Iama, Erub, Poruma and Hammond) would be experiencing significantly adverse impacts. Where retreat is likely not to be possible, such as at the low lying islands of Saibai, Boigu, Masig, Warraber and Poruma, communities may have to consider the viability of maintaining permanent habitation on these islands. Again, emergency services will come under increasing stress across the remaining communities.

The extensive analyses required for these estimates have been based on robust numerical and statistical techniques that have been designed to capture the principal atmospheric, astronomic and other broadscale forcing that modulates ocean water levels in the region. In addition, the localised impacts of tropical cyclones have been considered. Wherever possible, the analyses have been checked and validated against reliable measured data for winds, tides, storm surge and community impacts.

The analysis concludes that ocean water levels in the region are dominated by the highly variable astronomical tide but that extreme water levels are caused by often subtle combinations of relatively small inter-annual changes in the regional ocean level, strong seasonal variability due to the prevailing winds and occasional high energy weather events (monsoon surges and tropical cyclones). The interplay of these components on a range of time and space scales likely leads to periods of both enhanced and reduced impacts of the ocean water levels on the various communities. This would appear consistent with community experiences during recorded history.

The results of the analyses are presented in a very comprehensive manner, both tabular and graphical, that should permit wide ranging application for studies into geomorphological processes, environmental and sustainability issues, community infrastructure and emergency services. Important advice on the interpretation of Return Period and ARI estimates has also been provided to assist in the correct perception of the estimated hazard probabilities. It is recommended that various long-term geophysical data collection studies in the region be continued and expanded to ensure reliable data is available for future studies.

1. Introduction

This report documents analyses undertaken to provide a probabilistic assessment of extreme ocean water levels and inundation hazard in Torres Strait. Appendix A contains the Scope of Work.

1.1 Aims and Objectives

The purpose of the study is to quantitatively assess the risks of extreme ocean water levels and inundation hazards in Torres Strait generally and in particular at each of the established communities, many of which are low-lying. With potential rises in sea level under predicted climate change and the possibility of more intense tropical cyclones, existing inundation risks are likely to increase and require either mitigation or adaptation. It is also acknowledged that lower than expected water levels can also be an issue for shipping and port activities, but these are not specifically addressed in this study.

1.2 The Challenge

The Torres Strait is a complex ocean interface between the Coral Sea and the Arafura Sea, with influences also emanating from the Gulf of Carpentaria. The eastern boundary is fringed by the northern Great Barrier Reef and the western perimeter is defined by a string of islands, reefs, sand cays and banks stretching from Cape York to Papua New Guinea (Figure 1-1). The area is generally shallow (<15 m) and considered largely protected from ocean swell but there is a pronounced seasonal current through-flow – westerly during the dominance of the trade winds, and easterly during the monsoon. The principal ocean driver in the region is known to be the astronomical tide, with tidal ranges rapidly varying from 5 m to 4 m across the strait and high currents (>2 m/s) in some passages, which can cause difficulties for shipping. Although tidal data is reasonably comprehensive in some specific areas, it is known that there is much variability in mean sea level as a result of the seasonal influences and the tidal dynamics. Additionally, although relatively rare, severe tropical cyclones can affect the area.

1.3 The Communities

The Torres Strait is home to 18 island and two Northern Peninsula Area (NPA) communities. The islands are scattered over a geographic area of 48,000 km^2, from the tip of Cape York, north towards the borders of Papua New Guinea and Indonesia (TSRA 2009).

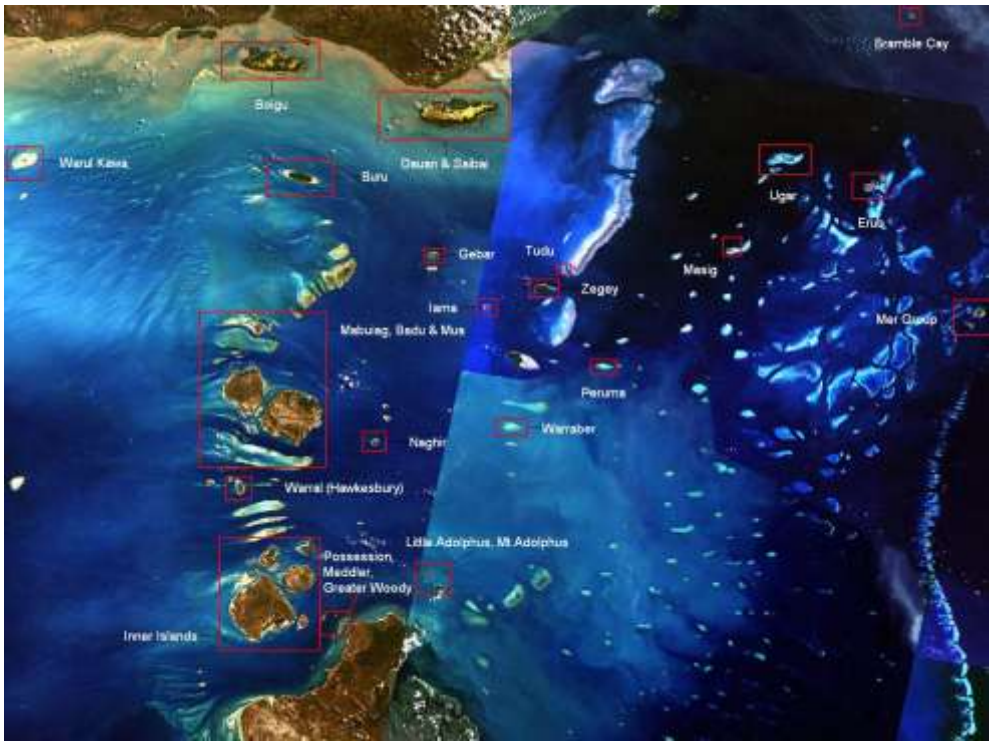

Figure 1-1 The Torres Strait communities (image supplied by TSRA).

There are five traditional island clusters, reflecting various ethnic and historical links. However, to facilitate discussion in the present study, the communities to be addressed are treated alphabetically:

- Badu Island
- Boigu Island
- Dauan Island
- Erub (Darnley Island)
- Gealug (Friday Island)
- Hammond Island (also known as Kiriri)
- Iama (Yam Island)
- Mabuiag Island
- Masig (Yorke Island)
- Mer (Murray Island)
- Moa Island (Communities of Kubin and St Pauls)
- Muralag (Prince of Wales Island)
- Ngurupai (Horn Island)

- Poruma (Coconut Island)
- Saibai Island
- Seisia/Bamaga (mainland)
- Ugar (Stephen Island)
- Waiben (Thursday Island)
- Warraber (Sue Island)

Of the above, the northernmost communities of Boigu and Saibai are especially low-lying, although several other islands are also adversely impacted by elevated ocean levels. Appendix B provides further information regarding each of the island communities[1].

1.4 Definitions

All severe weather systems are capable of producing a *storm surge*, which can increase coastal and ocean water levels for periods of several hours to days and significantly affect over 1000 km of coastline (Harper 2001). Tropical cyclones (TCs) are the most damaging storm surge events in northern Australia but their greatest impacts are typically limited to within 100 km of the centre, last for less than 12 hours and are relatively rare in the Torres Strait. Meanwhile, the more common and regular tropical monsoon can also be energetic, affect much wider areas and persist for several days at much lower levels of impact. The combination of these events with the astronomical tide in areas that are low lying and susceptible to inundation can be very significant.

The storm surge (or meteorological tide), is an atmospherically forced ocean response caused by the high surface winds and low surface pressures associated with severe and/or persistent offshore weather systems. An individual storm surge is measured relative to the tide level at the time. It is generated by the combined action of the severe surface winds (TC winds circulate clockwise around a storm centre while strong monsoon winds tend to be more frontal in nature), generating ocean currents, and the decreased atmospheric pressure, causing a local rise in sea level (the so-called inverted barometer effect). When a severe TC crosses the coast, the strong winds perpendicular to the land are responsible for the greater proportion of the surge (also called wind setup).

[1] Site names used throughout the report may sometimes alternate between the indigenous community name (e.g. Poruma) and the historical geographic name (e.g. Coconut Island) depending on the particular discussion context. No disrespect to community members is intended in this regard.

The total water level experienced at a site during the passage, say, of a severe TC will be made up of relative contributions from a number of different effects, as depicted in Figure 1-2. The combined or total water level is then termed the *storm tide*, which is an absolute vertical level, referenced in this report to *Mean Sea Level* (MSL)[2]. Local inundation depths must be referenced to the land elevation and are best indicated via mapping in situations where overland flooding is described.

It is important to appreciate the many water level components that can comprise the total storm tide. The relative contribution of these effects can vary throughout any given region depending on the local conditions. With reference to Figure 1-2:

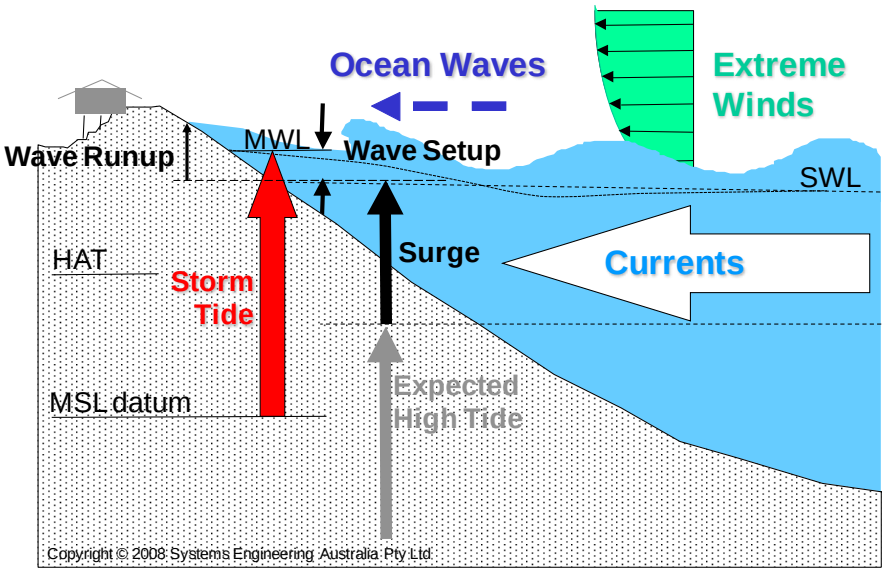

Figure 1-2 Water level components of an extreme storm tide.

(a) The Astronomical Tide

This is the regular periodic variation in water levels due to the gravitational effects of the moon and sun, which can often be predicted with generally very high accuracy at any point in time (past and present) where sufficiently long and precise measurements are available[3].

[2] MSL is normally similar to *Australian Height Datum* (AHD) but, as discussed in Section 9, the Torres Strait region AHD datums are still being evaluated.

[3] The minimum desirable period is not less than about 40 days, while many years of data are normally required to determine so-called seasonal corrections.

In practice, the analysis of tides often also includes non-astronomical components that are persistent and have a fixed periodicity. This includes components such as the radiation tide which is driven by the daily solar cycle and the annual tide created by seasonal variations in wind and atmospheric pressure.

The highest expected tide level at any location is termed the *Highest Astronomical Tide* (HAT) and occurs theoretically once each 18.6 y period, although at some sites tide levels similar to HAT may occur several times per year. The variability in tidal range across the region is significant and the tidal datums at many of the islands, which are critical for relating sea and land elevations, have been subject to review and assessment as part of this study (refer Section 9).

(b) Storm Surge

By some definitions, the “storm surge” is simply the difference between the expected (predicted) astronomical tide and the actual (measured) average sea level at some point in time and space. This difference is typically termed the “residual” water level variation. However, because of non-linear interactions in some situations, the residual often does not fully represent the incident non-astronomical wave-form.

As previously introduced, the storm surge is perhaps best referred to as the *meteorological tide* because it is the combined result of atmospheric pressure gradients and wind shear stress acting on the underlying ocean. While these influences are universally active everywhere, and are present at many time and space scales (e.g. refer (f) later), the effects are significantly greater during the enhanced forcing provided by what we might colloquially call *storms*.

The storm surge manifests as a long period “wave” capable of sustaining above-normal or below-normal water levels over a number of hours. The wave travels with and ahead of the storm system and may be amplified as it progresses into shallow waters or is confined by coastal features. The magnitude of the surge can be affected by many factors such as storm intensity, size, speed and angle of approach to the coast and the coastal bathymetry (undersea depths). The storm surge will add to the normally expected tide over a large area, combining to produce the so-called “still water level” or SWL. This is the highest water level at a point on the shoreline if wave action is smoothed out.

(c) Breaking Wave Setup

Severe wind fields also create abnormally high sea conditions and extreme waves may propagate large distances from the centre of a storm as ocean swell. As the waves enter shallower waters they refract and steepen under the action of shoaling until their stored energy is dissipated by wave breaking either offshore in shallow regions or at a beach or reef. Through the continuous action of many breaking waves,

shoreward water levels can rise above the still-water level (SWL), creating a locally higher “mean water level” (MWL) at the shore.

This increase in water level after wave breaking is known as *breaking wave setup* and applies to most natural beaches and reefs. Seawards of the breaker zone there is also a region of *wave setdown*. Importantly, wave setup needs some type of a vertical barrier that will act to sustain the water level gradient that balances the incoming wave momentum. Accordingly, wave setup generally is not expected to be significant in river mouths or protected swampy lands. The presence of irregular (i.e. 2-D) natural banks and channels can also act to dissipate the products of wave setup.

(d) Breaking Wave Runup

Notwithstanding wave setup, there remains some residual energy in the form of individual waves that will generate intermittent vertical *runup* and may cause localised impacts and erosion at elevations above that of the nominated storm tide (MWL) level. These effects can only be estimated with specific information about the land-sea interface, which may even be changing in time as the storm tide increases in height. This would include the slope of the shoreline, the porosity, vegetation and the incident wave height and period.

(e) Overland inundation and wave penetration

When normally dry land becomes inundated during a severe storm tide episode, the sea begins to quickly flood inland as an intermittent “wave front”, driven by the initial momentum of the surge, products of wave setup and the local surface wind stress. This flow then reacts to the local ground contours and the hydraulic roughness due to either natural vegetation or housing and other infrastructure. It will continue inland until a dynamic balance is reached between the applied hydraulic gradients and the land surface resistance or until it becomes constrained by elevation. As the new “stillwater” surface gradually reforms behind the propagating front, the exact extent to which individual unbroken or partially reformed ocean waves might further penetrate into a coastal region will be very site specific. As the storm surge abates or the tide reduces, an ebb flow is created which is often responsible for much of the damage and scouring after such events.

(f) Other Effects on Sea Level

There remain other related phenomena that also have an effect on the local ocean water level. These include annual and inter-annual variations in the sea level caused by large scale wind-forced ocean currents and their associated temperature changes. These meteorological tides are relatively large contributors to sea level variability in the Torres Strait on an annual basis. In addition, there exist low amplitude long period shelf waves that can propagate large

distances and affect the predicted tidal elevation over periods of several days. Many of these effects are implicitly included in the present study to the extent that they are represented by the 2-D barotropic modelling.

Finally, where there is a high exposure to large swell waves, the wave setup effect can be further modulated by unsteady “surf beat”. While this effect is unlikely for the majority of Torres Strait communities, some may be affected by localised stormwater and/or river runoff in specific situations. The present study does not consider these specific effects and nor does it consider tsunami events.

2. Methodology Overview

The following provides an outline of the study methodology and Figure 2-1 is a schematic of the activities that are addressed in more detail in each section below.

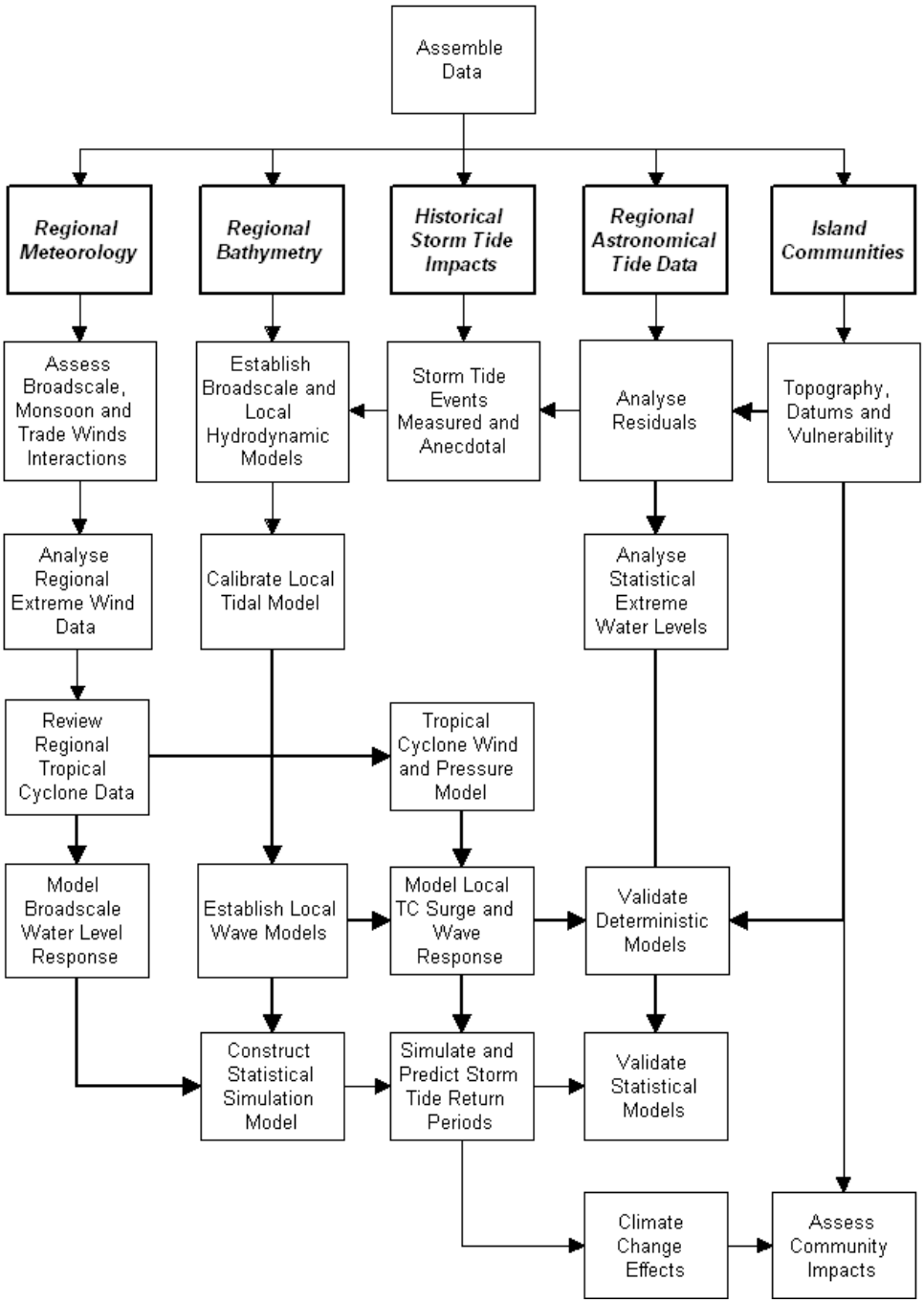

Figure 2-1 Methodology flowchart

2.1 Working Hypothesis

Based on the collective experience of the Study Team, it was qualitatively hypothesised that extreme water levels impacting Torres Strait communities would likely be determined by, in order:

a) Frequent broadscale wind and pressure forcing (monsoon or trade wind driven) coinciding with periods of high tides (especially the so-called King Tides);

b) Annual remote TC influences, principally from the Gulf of Carpentaria, that interact with monsoon surges;

c) Rare close approach TCs;

d) Inter-decadal sea level variability and increasing climate change influences on the above (predominantly sea level rise);

e) Local bathymetry and topography affecting breaking wave setup and runup on beaches or reefs.

These assumptions necessarily underpinned the subsequent approaches to modelling and parameterisation of the many expected influences on extreme water levels in the region. However, illustrations of the appropriateness of these assumptions compared with available data and other independent modelling are presented in support of the adopted methodology.

The outcome from the study is a quantitative assessment of the ocean inundation risks. The specific issues relating to each of the above study components are described in detail in the relevant sections.

2.2 Data Assembly

This section summarises the various data sets that were assembled for the project and notes any specific issues associated with that process.

2.2.1 Previous Regional Studies

The Torres Strait remains an essentially remote region about which there is incomplete information on a wide range of bio-physical parameters. Over time though, the gradually increasing number of studies that have been conducted in or adjacent to the region have assisted in building a degree of understanding of the meteorology and the hydrodynamics. For example, some of the earlier work is due to the Australian Institute of Marine Science (e.g. Wolanski et al. 1988) and James Cook University (e.g. Bode and Mason 1995). Noting that the Torres Strait is an important sea trade route, the latter authors also addressed marine navigation, maritime rescue matters and sediment issues in other studies.

More recently CSIRO / Geoscience Australia (Saint-Cast 2008) provides a valuable history of some previous studies and a contemporary overview of the hydrodynamics of the region at a range of scales, focusing on the estimation of sediment movement of importance to assessing seagrass dieback. In particular, the updated bathymetry collated by Geoscience Australia for use by that study (Daniell 2008) also underpins the present investigation.

In the risk management context Arup (2006) provides an overview of regionally relevant natural hazards and provides qualitative analysis of risk treatments and the like. This study importantly highlighted the significant issue of the accuracy of land and sea elevation datums across the region, which are mostly known to have been inaccurate or remained unstated. In particular, this made the task of providing meaningful storm tide threat mapping especially difficult.

In terms of social and community aspects Green (2006) and Green et al. (2009) considers the potential impacts of climate change related social upheaval and concerns over recent sea level incursions into some communities during periods of adverse weather coupled with King Tides. It is also noted that instances of persistent inundation have occurred in the past in association with strong monsoon or TC events. For example, events in 1948 led to the subsequent relocation of islanders from Boigu and Saibai that led to the formation of new communities on the mainland at Bamaga and Seisia. Duce et al. (2010) summarises a number of studies addressing the detailed geomorphology of the region and island-specific issues of inundation and erosion.

2.2.2 Meteorological Data

A wide variety of data and other qualitative information on the meteorology of the area was assembled for the project. These include:

- US National Center for Environmental Prediction (NCEP/NCAR) reanalysed gridded surface winds and pressures, 6 hourly from 1948 onwards (e.g. Kistler et al. 2001);
- Bureau of Meteorology (BoM) National Climate Centre (NCC) regional site-specific long term wind and pressure datasets and associated metadata;
- BoM/NCC TC track dataset (as revised) and unpublished Regional Office reports;
- BoM LAPS (Limited Area Prediction System) modelled surface wind and pressure fields (9 years supplied by AMC)
- Published and unpublished meteorological discussions;
- Systems Engineering Australia Pty Ltd proprietary TC dataset;

- Meteorological analyses by Mr Jeff Callaghan (BoM retired).

2.2.3 Bathymetric and Topographic Data

- The publicly available Geoscience Australia bathymetric grid for the Gulf of Papua and Northern Australia (Daniell 2006);
- AMC/MMU composite electronic datasets comprising digitised charts and AHS survey information;
- TSRA-provided topographic datasets of selected communities (comprising orthophoto, LiDAR) plus advice on beach slopes, dune heights, breakwater crests and the like;
- Geomorphological study data (e.g. DERM/JCU)
- DERM-provided land and sea datum information;
- Maritime Safety Queensland (MSQ) local harbour information.

2.2.4 Tidal Information

- Long term raw tidal records of sea level height in electronic format obtained from AMSA, MSQ and BoM/NTC;
- Tidal analyses as above, including tidal plane estimates and predictions (ANTT and MSQ);
- Various reports and technical papers (published and unpublished as available).

2.2.5 Historical Storm Tide Data

- Measured tides from AMSA and MSQ regional tide gauges;
- BoM (Queensland) storm tide impacts database (ex J. Callaghan);
- Published and unpublished technical sources;
- Eye witness accounts, cultural records, photographs etc.

2.2.6 Projected Climate Change

- CSIRO and BoM-derived statements on projected rises in sea level and potential changes in mean and extreme winds;
- DERM recommendations;
- World Meteorological Organization (WMO) sponsored expert advice on projected TC frequency and intensity;
- WMO Intergovernmental Panel on Climate Change (IPCC) statements as applicable.

2.3 An Overview of the Steps in the Analyses

Following the data assembly task, which was a very significant aspect of the present study, the analyses were undertaken in a series of steps as illustrated further in Figure 2-1. The principal processes as reported in the remaining report chapters are outlined here:

Chapter 3 Regional Meteorology

This considers the broadscale wind and pressure forcing that influences water levels in Torres Strait by examining the long-term wind speed records at specific locations and the available numerically hindcast wind and pressure fields. TC aspects are treated in detail in Chapter 6.

The long-term site-specific wind data is analysed to determine the regional variability of extreme conditions so that the later veracity of the developed statistical wind models (both broadscale and TC related) can be assessed. The suitability of the hindcast modelled surface wind and pressure datasets are then assessed relative to the site specific data. Such data are also used for deterministic checks of historical events.

Chapter 4 Astronomical Tides

The astronomical tide in the region is extremely complex and is the dominant modulator of ocean water levels. Additionally, an important element of the methodology is the ability to treat the tide as being independent of the other ocean (weather related) processes. This is due to the separate forcing (gravity versus atmospheric) and the very large spatial scale of the tide, such that it is largely insensitive to local water level variations caused by atmospheric effects.

This chapter analyses the available tide data to extract the harmonic components of the tide and to obtain the non-astronomical water level residuals for later statistical analysis. The bathymetric data for the region is then utilised to construct a numerical hydrodynamic model that is calibrated to reproduce the measured tidal data to a high level of accuracy. Importantly, the so-called *seasonal* tidal constituents are excluded in this analysis, as they are more correctly a part of the broadscale meteorological forcing. The resulting numerical tidal model then provides a spatially consistent representation of the tide behaviour across the entire Torres Strait region.

Chapter 5 Modelling the Broadscale Sea Level Variability

This addresses the non-tidal ocean response on a scale that is much larger than the local Torres Strait region and later combines that with the tidal response. This additional hydrodynamic model utilises bathymetric data extending into the Arafura and Coral Sea as well as the Gulf of Carpentaria. The model is then forced with the available hindcast meteorological data for the past 60 y to identify seasonal variability in the ocean water levels and also to capture the broadscale TC

influences. In addition, the inter-annual variability of the ocean levels external to the model are represented.

This provides a baseline 60 y of broadscale water level variability across the Torres Strait that is then used to additionally force the tidal model to obtain a combined water level response. This modelled response is then validated against the available tide gauge data deterministically.

To form the basis of the statistical analysis of broadscale extreme ocean conditions, this 60 y reconstruction is then extended out to an effective data period of over 1000 y by a random resampling of the tidal phase. This is validated statistically by similarly resampling the measured tide residual record (typically about a 20 y record) by the modelled tidal phase. This shows good agreement of the modelled and measured ocean water levels that are associated with the broadscale forcing.

Projected future climate change influences on the broadscale processes are also considered.

Chapter 6 Tropical Cyclone Climatology

While TCs are the most energetic of the atmospheric forcings in the tropics, they are known to be relatively rare in the immediate Torres Strait. While their broadscale effects are deemed to have been captured separately, it remains necessary to consider the possible effects of close approach storms through the region.

Because of the remoteness of the region generally, and the scarcity of observations over time, the quality of the historical TC record must be questioned before utilising the data in a statistical analysis. Accordingly a review of the TC record is undertaken to identify the most likely sources of significant error. This has resulted in a number of adjustments being made to the TC intensity estimates in the official Bureau of Meteorology record.

The adjusted TC data record is then statistically analysed to provide the basis for a simulation model that is later used to enable the modelling of wind, storm surge and wave effects. Projected future climate change influences on TCs are also considered.

Chapter 7 Numerical Tropical Cyclone Storm Surge Modelling

The modelling of close approach TCs is considered in this Chapter. Numerical hydrodynamic models are constructed in an analogous manner to the broadscale forcing models but the influences of the broadscale ocean and atmospheric forcing are ignored, as well as the astronomical tide.

A series of scenarios are used to illustrate the potential impacts of close approach TC events in the region and the relative effects at the various communities due to their specific locations and exposures.

The numerical TC storm surge model is then later used as part of a combined broadscale and local ocean forcing simulation.

Chapter 8 Numerical Wave Modelling

In addition to the long-period ocean sea level response from tide and weather, surface wave effects can have localised impact on water levels through the processes of breaking wave setup and runup. Accordingly, separate models are developed to provide estimates of surface wave impacts due to both broadscale and local TC forcing.

Due to the considerable computational burden associated with high resolution spectral wave modelling in a statistical context, this Chapter describes the approach needed to enable a practical description of the wave effects. In the TC context this involves comparisons between a full spectral wave model and simplified fetch-limited models to justify use of a simplified model. In the broadscale context a simplified model is shown to perform well after adjustment of the available hindcast wind data. Both approaches rely on the assumption that the Torres Strait region is protected from remotely generated ocean swell.

Chapter 9 Land Elevation Datums

The lack of reliable land elevation datums in the region was a considerable handicap to this study that significantly delayed completion of the work and complicated the assessment of tidal data. However, the broadscale modelling undertaken here has significantly improved this situation by providing guidance on the tidal variability both spatially and seasonally. This Chapter summarises the adopted land datum shifts needed to correctly interpret the vulnerability of each of the island communities.

Chapter 10 Deterministic Hindcast Modelling

This Chapter provides further validation of the various modelling components by illustrating the reasonable reproduction of a number of known historical events. Necessarily this is compromised to some extent by the lack of measured data in many cases, but it confirms the robustness of the methodology that underpins the statistical projections.

Chapter 11 Statistical Storm Tide Simulation Modelling

This Chapter describes the process by which the various statistical and deterministic elements of the analyses are combined to provide a numerical simulation of ocean water levels at all the Torres Strait community sites over a 50,000 y period. This synthetic data record then forms the basis of the statistical analysis that provides estimates of the likelihood of ocean inundation on a Return Period or Average Recurrence Interval (ARI) basis. This allows the relative ranking of community vulnerability and a comparison with present experiences. Projected future climate change influences on global sea level and weather processes are also considered for the years 2050 and 2100.

3. Regional Meteorology

The large scale meteorology of the Torres Strait region is dominated predominantly by the influences of, *inter alia*:

- The summer NW Monsoon, and
- The winter SE Trade Winds.

The seasonality, strength and persistence of these two major influences dictate the mean oceanic response. TCs are then capable of intermittently influencing and interacting with these larger scale influences during summer. The dominant regional winds play a significant part in the cultural and economic lifestyle of the indigenous communities and are locally named[4] as *Kuki* (NW) and *Sager* (SE), with the lesser winds known as *Zey* (S) and *Nay Gay* (N).

On the larger scale, inter-annual coupled atmospheric-oceanic influences due to the El Niño/Southern Oscillation (ENSO) (e.g. Nicholls 1984, 1985ab, 1992) and potential inter-decadal influences such as the Interdecadal Pacific Oscillation (IPO) (e.g. Power et al. 1999, Allan 1991) act to adjust the background conditions.

3.1 Synoptic Patterns and Winds

The Torres Strait region meteorology is dominated by the summer NW monsoon and the winter SE Trade circulations, as summarised in Figure 3-1 and Figure 3-2. The monsoon trough typically develops in late October and moves southwards during the summer, being located over the Arnhem Land region in January, and then ascends once again by April. During the monsoon trough descent and ascent periods, TCs have an enhanced opportunity to form in the Arafura and Coral Sea.

For the remainder of the year the region is under the influence of high pressure systems far to the south. The resulting generally persistent SE Trade winds are illustrated in Figure 3-3 by the wind roses from Thursday Island. These are strongest in autumn and winter.

Figure 3-4 summarises the regional seasonal wind statistics for Thursday Island, Horn Island, Coconut Island and Willis Island (refer Figure 3-5 for mapped locations). The latter site is far outside of the Torres Strait region but provides a useful reference because of its exposed open ocean location and length of record. These data are from the BoM online data summary statistics.

[4] http://www.gabtitui.com.au

Of interest again is the dominance of the SE Trades during the winter half-year. Also of interest is the significant diurnal variation at Thursday Island and Horn Island, which probably reflects their closer position to the mainland and also the relatively large surrounding islands. Meanwhile at Coconut and Willis, there is very little diurnal variability evident, as might be expected.

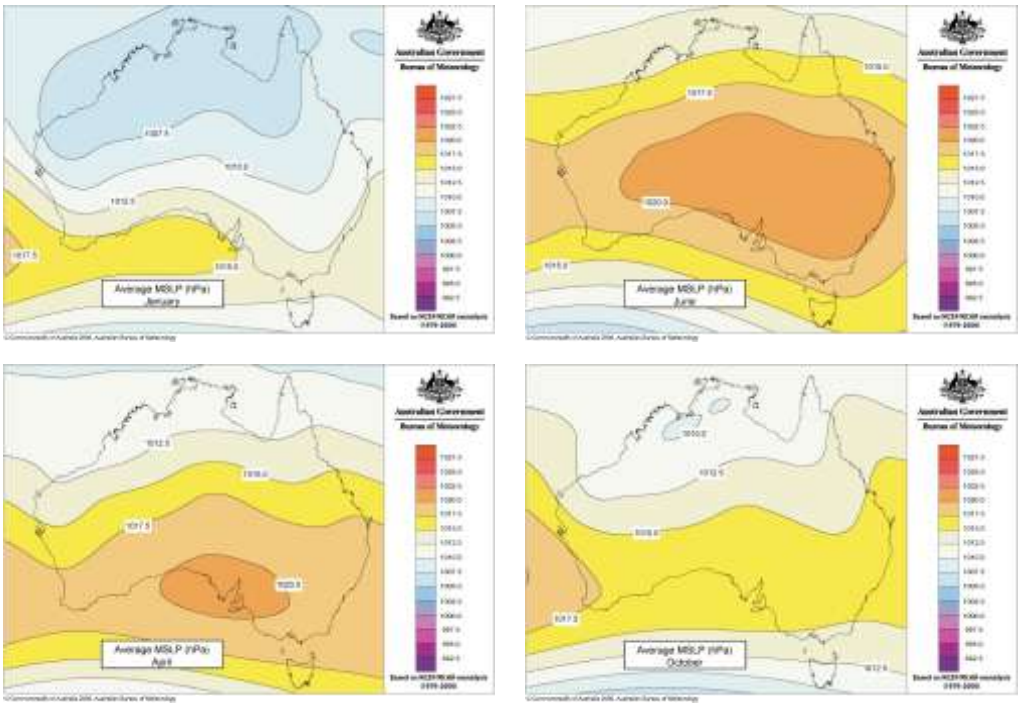

Figure 3-1 Seasonal mean synoptic pressure patterns (BoM analysis NCEP/NCAR 1979-2000).

The data record length in these site summaries varies considerably but it is clear that the long term regional Thursday Island observation site (Waiben), closed in February 1993, experienced the higher wind speeds relative to nearby Horn Island (Ngurupai) and also the more north-eastern Coconut Island (Poruma). Wind data in the immediate region is limited to these three sites.

Notwithstanding that it is possible there is some regional enhancement of winds near Cape York, it is argued here that the Thursday Island site experiences topographic enhancement that almost certainly increases the apparent wind speeds from certain directions. It may also experience local modifications from some of the surrounding islands. Section 8.3.1 further considers these matters in association with the use of broadscale NCEP/NCAR winds for regional wave modelling.

Many of the regional anemometer sites experience some degradation of exposure and in the next section attempts are made to correct for some of the likely significant effects

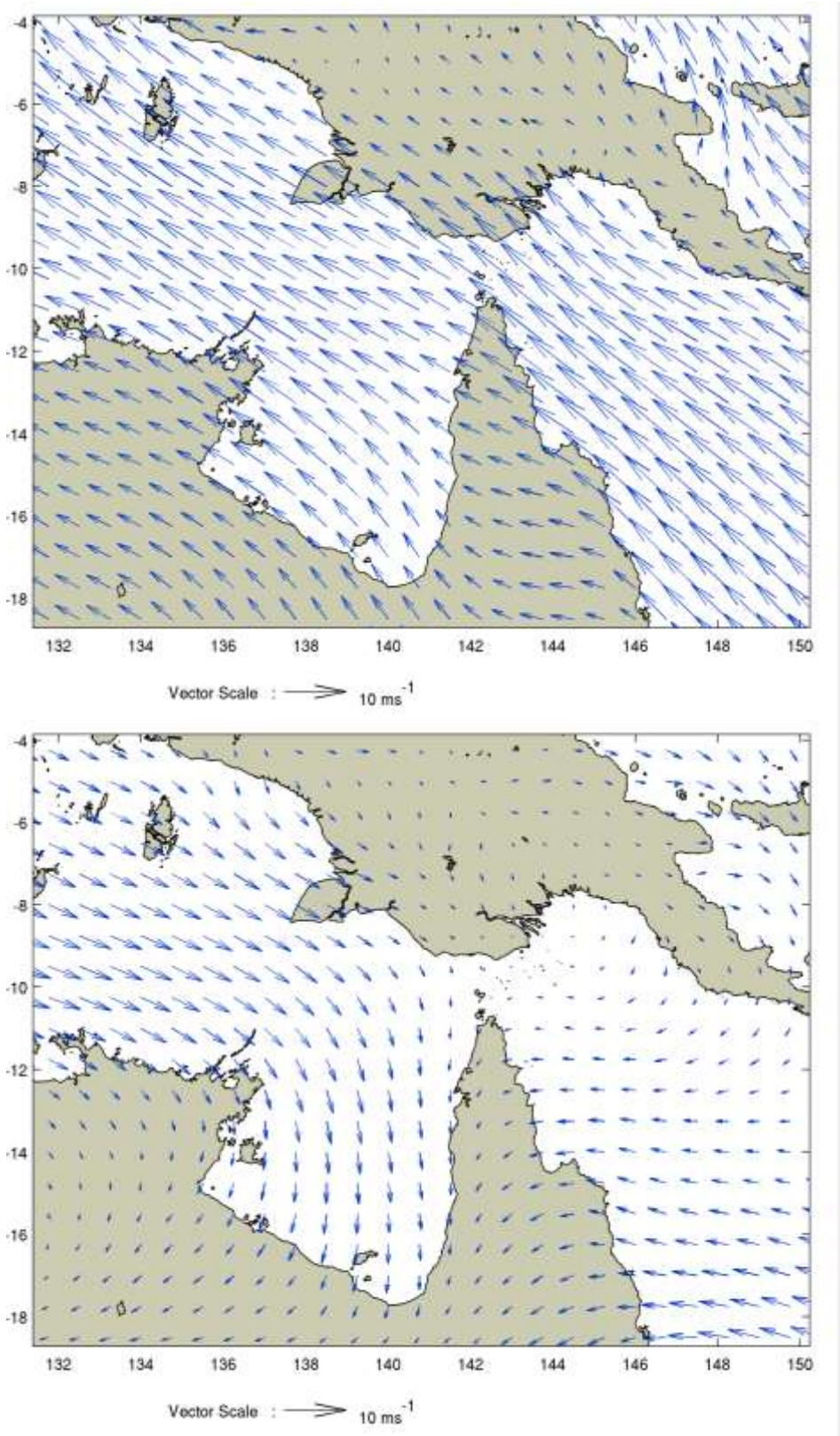

Figure 3-2 Seasonal mean synoptic wind patterns for January (top) and July (bottom) from BoM LAPS model 1996-2008.

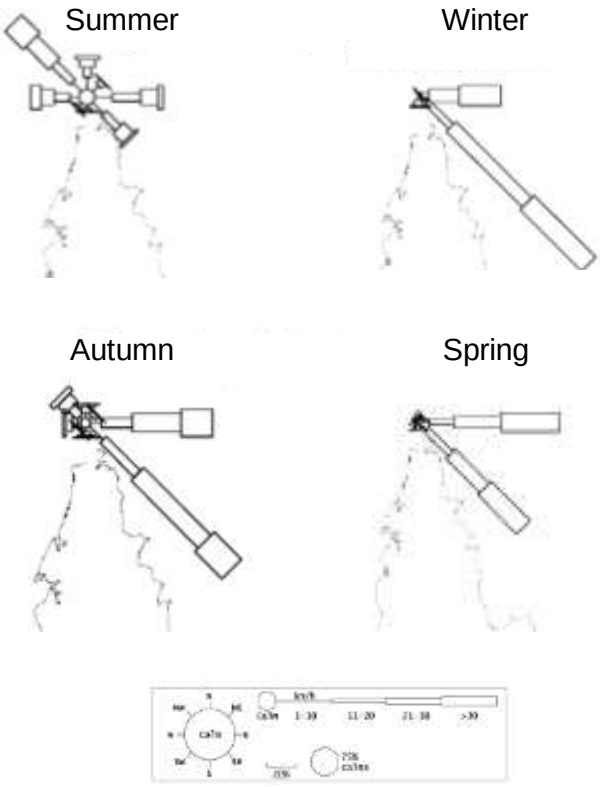

Figure 3-3 Thursday Island mean wind speed roses (BoM analysis 1961-1990).

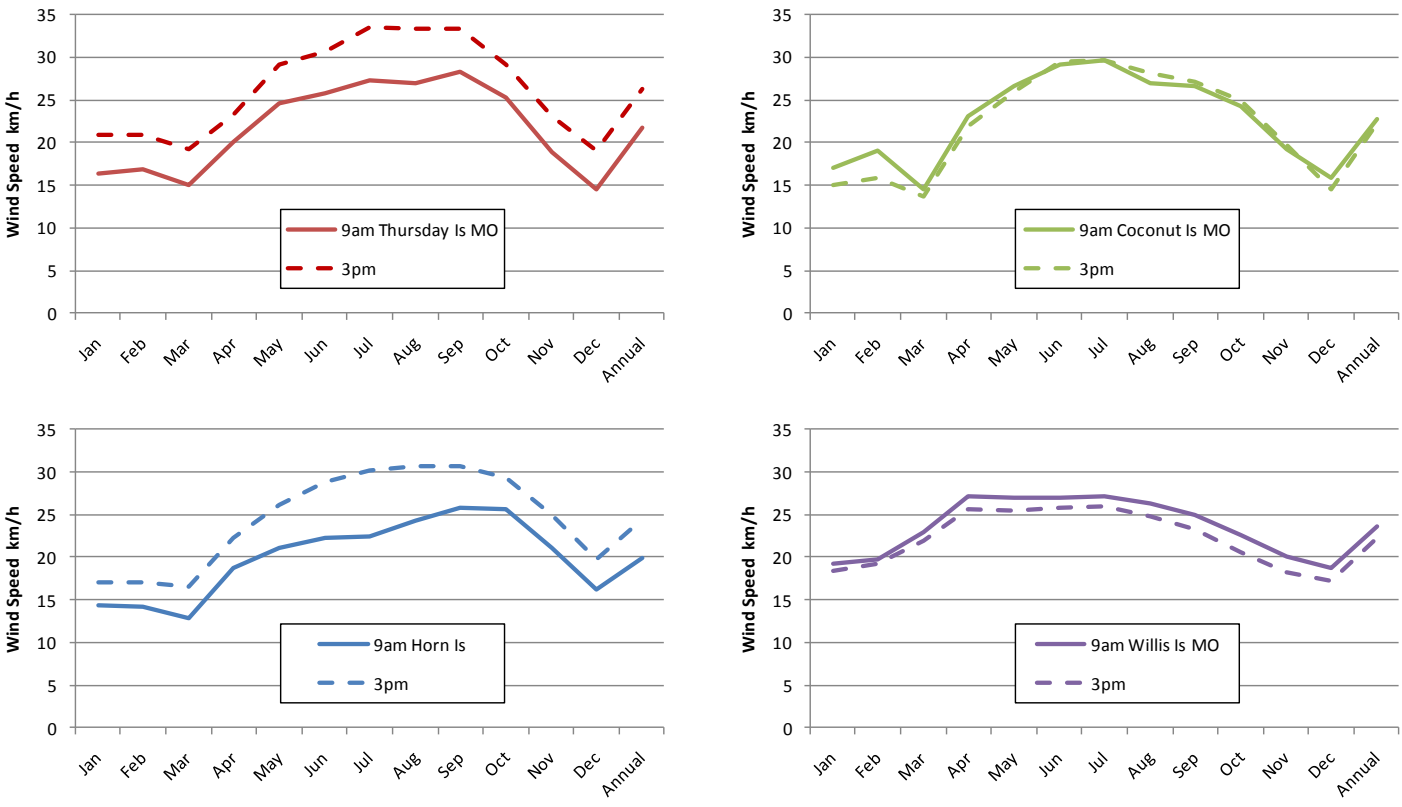

Figure 3-4 Seasonal synoptic mean wind summary (BoM online data).

3.2 Regional Extreme Wind Analyses

Although there is an insufficient record of coastal wind speeds in the immediate region upon which to infer extreme wind statistics, the available regional record is very valuable in assessing the broadscale variability and providing some order of magnitude verification for the later statistical modelling of winds that leads to estimates of extreme water levels (refer Section 11.2).

In this section, wind data from 10 regional sites is considered. After adjustments for station exposure, the peak 10-min mean (V_{600}) and 3-s peak daily gusts (V_3) are then analysed to estimate long term Return Periods (or Average Recurrence Intervals ARI).

3.2.1 Regional Wind Data

The BoM stations used for the extreme wind analysis are indicated on Figure 3-5 with site details provided in Table 3-1.

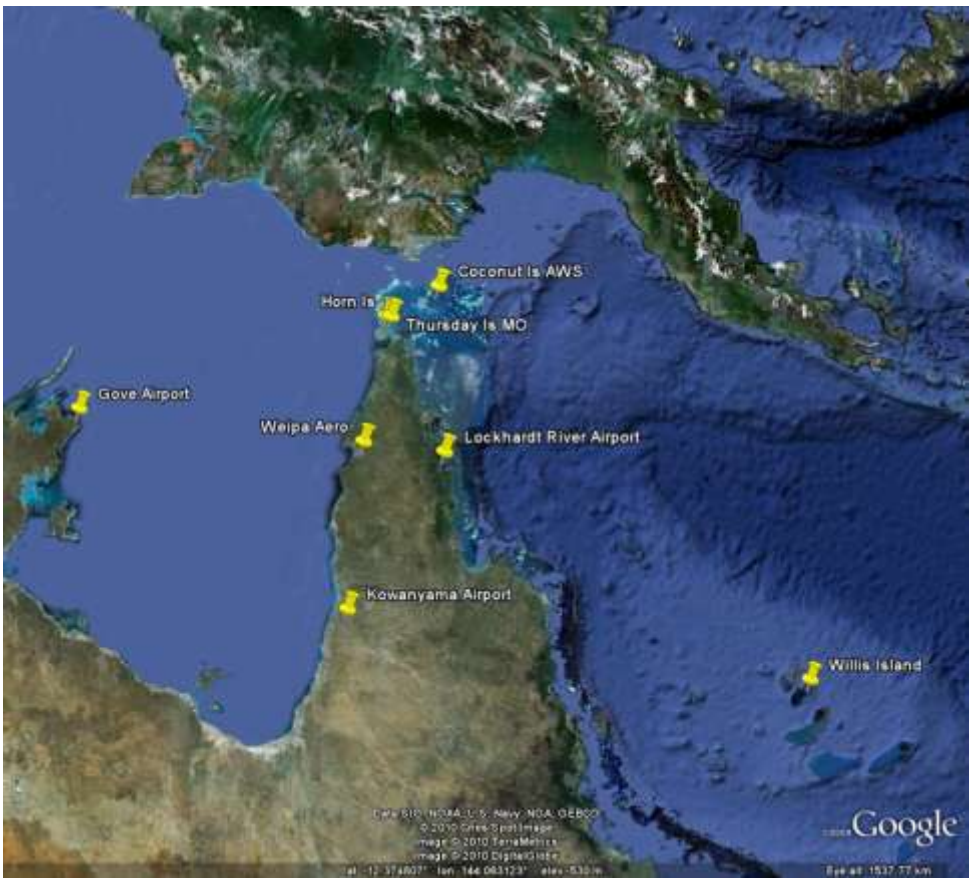

Figure 3-5 Location of BoM regional wind stations.

Table 3-1 Summary of regional wind station metadata and raw peak winds.

3-sec Peak Daily Gust Winds V3

Station	Name	Lat	Lon	Station Ht	Start	End	Span	Avail	Record	Raw Peak Wind V3	Date
		deg	deg	m MSL			y	%	y	m/s	
27022	THURSDAY ISLAND MO	-10.5853	142.2100	57.6	04/09/1950	28/02/1993	42.5	81	34.3	30	24/02/1991
27058	HORN ISLAND	-10.5844	142.2900	4.0	11/10/1995	30/07/2009	13.8	63	15.0	24	06/02/2007
27054	COCONUT ISLAND	-10.0511	143.0686	3.5	21/07/1988	30/07/2009	21.0	28	6.0	22	21/01/2005
27045	WEIPA AERO	-12.6778	141.9208	18.0	30/10/1980	30/07/2009	28.8	87	29.0	28	09/03/1996
27042	WEIPA EASTERN AVE	-12.6267	141.7475	20.0	02/01/1959	28/02/1994	35.2	84	31.0	32	10/01/1992
27045	WEIPA (combined)	-12.6267	141.8836	18.0	02/01/1959	30/07/2009	50.6	86	45.0	28	09/03/1996
29038	KOWANYAMA AIRPORT	-15.4839	141.7475	9.6	29/11/1965	30/07/2009	43.7	21	9.4	54[5]	01/02/2001
28008	LOCKHART RIVER AIRPORT	-12.7850	143.3047	18.5	01/01/1965	30/07/2009	44.6	60	30.0	29	09/05/1989
200283	WILLIS ISLAND	-16.2878	149.9652	8.1	07/11/1921	30/07/2009	87.8	76	71.0	56	08/02/1957
14508	GOVE (combined)	-12.2741	136.8203	51.6	02/03/1972	19/12/2006	34.8	77	27.3	32	12/03/2005

10-min Mean Winds (3hourly or Hourly) V600

Station	Name	Lat	Lon	Station Ht	Start	End	Span	Avail	Record	Raw Peak Wind V600	Date
		deg	deg	m MSL			y	%	y	m/s	
27022	THURSDAY ISLAND MO	-10.5853	142.2100	57.6	03/09/1950	28/02/1993	42.5	73	42.0	26	19/01/1952
27058	HORN ISLAND	-10.5844	142.2900	4.0	11/10/1995	30/07/2009	13.8	63	15.0	16	11/01/2009
27054	COCONUT ISLAND	-10.0511	143.0686	3.5	20/07/1988	22/08/2004	16.1	65	17.0	17	08/03/1991
27045	WEIPA AERO	-12.6778	141.9208	18.0	11/10/1995	30/07/2009	13.8	99	14.0	27	05/01/1999
27042	WEIPA EASTERN AVE	-12.6267	141.7475	20.0	01/01/1959	28/02/1994	35.2	25	31.0	19	02/03/1961
27045	WEIPA (combined)	-12.6267	141.8836	18.0	01/01/1959	22/08/2004	45.7	42	42.0	19	02/03/1961
29038	KOWANYAMA AIRPORT	-15.4839	141.7475	9.6	28/11/1965	22/08/2004	38.8	10	38.0	40[5]	18/10/2003
28008	LOCKHART RIVER AIRPORT	-12.7850	143.3047	18.5	31/12/1964	22/08/2004	39.7	12	39.0	21	08/03/1977
200283	WILLIS ISLAND	-16.2878	149.9652	8.1	06/11/1921	14/07/2004	82.7	12	79.0	40	08/02/1957
14508	GOVE (combined)	-12.2741	136.8203	51.6	31/08/1966	20/12/2006	40.3	60	35.0	23	11/03/2005

[5] Deemed unreliable or possible thunderstorm.

In addition to these sites, data from Cape Wessel, north of Gove, was also considered due to its exposure to the monsoon. However many errors were uncovered[6] that required dismissing of this dataset. Winds at Port Moresby were also considered but deemed to be too affected by Papua New Guinea mainland effects. The Thursday Island Township site was deemed unsuitable for analysis due to its location, short record and manual observations

After considering the many gaps in the data, it can be seen in Table 3-1 that the longest wind record available in the region is for peak daily wind gust at Weipa. This assumes that the Aero and Eastern Avenue datasets can be merged to form a single recoverable 45 y record (refer next section). This is closely followed by the 10-min mean wind record at the same merged Weipa site. The Thursday Island record is the next longest with 34.3 y for peak gusts and also 42 y for mean winds. Lockhart River Airport then follows with 30 to 40 y of data, followed by Gove[7] with 27 to 35 y. However, Willis Island, which is the furthest removed from the area, has the longest and best exposed record of 70 to 80 y.

The mean wind dataset is often a mixture of synoptic (3-hourly) and hourly mean winds as a result of various changes in instrumentation and the shift from manual to automatic operation at many sites, especially airports. These changes unavoidably act to reduce the homogeneity of the record in ways that cannot be readily identified or corrected.

Table 3-1 also indicates the peak raw wind speeds from each of the datasets for reference. Willis Island, with its very long record in an area of significant TC activity, has a peak gust of 56 ms^{-1} and a peak mean wind of 40 ms^{-1}. The values from the short record at Kowanyama, which seem almost equivalent to the Willis Island values, are however deemed unreliable (J. Callaghan, *personal communication*). The majority of sites have experienced peak gusts to about 25 to 30 ms^{-1} and peak mean winds of about 20 to 25 ms^{-1}.

3.2.2 Adjustment of the Raw Wind Data

Before the raw station wind data is subjected to analysis for statistical extremes, adjustments are applied in an attempt to correct each site for unfavourable exposures so that data from the various sites can be more usefully compared and conclusions drawn in regard to possible climatological differences.

[6] These issues were referred to the BoM NT Regional Office for resolution and most of the larger wind speed values were subsequently confirmed as erroneous. Time did not permit incorporating the remainder of the dataset into this analysis.

[7] The Gove Airport record has been merged here with that from the Wallaby Beach site.

The WMO standard (WMO 2008) and conforming BoM guidelines seek to ensure that all wind observing stations will measure winds in “open terrain” at a height above local ground level of 10 m. On land, a basic requirement for the siting of instrumentation is to avoid upstream aerodynamic effects and “open terrain” is defined by WMO as an area where the distance between the anemometer and any obstruction is at least 10 times the height of the obstruction. However, there are many practical matters that often work to compromise these standards and much work remains to be done to develop appropriate wind station calibration records (Harper 2009). Importantly though, all of the wind stations considered here conform to the 10 m height standard.

However, for quantitative purposes (e.g. Standards Australia 2002; Powell et al. 1996) it is also necessary to account for the directional effects of terrain roughness changes and possible topographic effects due to nearby hills. These latter effects should be assessed so that all wind measurements can consistently be expressed in terms of an “open terrain” defined to be nearly-flat and with a surface roughness height of approximately 0.03 m (Harper et al. 2010).

The most compromised station in the Torres Strait is unfortunately at Thursday Island, where the Dines anemometer was located at about 60 m elevation on the ridgeline of a steep hill as shown in Figure 3-6. While this position ensured that the site would be “well exposed” to the prevailing winds, the steepness and variability of the approach slopes makes this a very difficult site to assess and correct for “open terrain” conditions. This station was closed in 1993 and the new regional reference station was later established adjacent to the airport on Horn Island on flat terrain and with notably different exposure. Coconut Island, albeit located on a small island of low elevation and in an open ocean context, may also be influenced by the close presence of a palm fringed sand dune ridge and azimuthally varying roughness effects. All of the wind station sites in the immediate region have been manually assessed for these types of exposure effects (refer Appendix C).

While it is desirable that insitu calibrations, wind tunnel modelling or numerical modelling be undertaken to assess the wind response at a measuring site, such sophisticated studies were outside the present scope. Accordingly, the process of adjustment undertaken for this study is to apply the analytical rules in Standards Australia (2002) that are used for the design of wind-resisting structures, namely the estimation of:

- The terrain multiplier M_t, with a typical range of 1.1 to 0.75, which represents the effects of surface roughness changes, and
- The topographic multiplier M_h, with a typical range of 1.0 to 1.7, which represents the influence of changes in surface slope and location of an instrument relative to the crest of a hill.

Figure 3-6 Steep site of the former Thursday Island MO wind station. (Google Earth™ images)

The factoring of M_t and M_h values with the reference wind speed in "open terrain" yields the site-specific estimate of the wind at the measurement site. Accordingly, the inverse factoring will convert the measured site wind into an estimate of the "open terrain" reference speed that is sought for comparison purposes, e.g.

$$V_{ref} = \frac{V_{site}}{M_t M_h} \quad (1)$$

While Standards Australia (2002) formulae for M_t and M_h strictly apply to the nominal V_3 wind gust speed, they have for convenience here also been applied to the mean V_{600} wind speeds[8]. The adjustments undertaken for each site are summarised in Appendix C, which shows the regional setting of each station, an azimuthal 1 km radius wind rose of 30° resolution and the resulting azimuthally varying M_t and M_h values that have been determined using the aforementioned methodology.

3.2.3 Analysis of Station Adjusted Wind Extremes

Following the site-specific directional wind adjustments, each station record was further analysed as follows:

- The time series were "windowed" using a 5 day period to approximate the independence of event peak winds;
- The data were separated into "combined", "non-cyclonic" and "cyclonic" classifications;
- The "cyclonic" classification was based on whether a TC centre (as estimated by the "best track file", refer later) was within 300 km of the station at the time of the reading;
- The resulting peak data were fitted to an EV Type 1 (Gumbel) statistical distribution (Benjamin and Cornell 1970) using the Method of Maximum Likelihood.

The results of the individual curve fits to the measured data peaks are presented in Appendix D, while Figure 3-7 summarises the fitted distributions for peak wind gusts and Figure 3-8 for mean winds across the region, stratified into all-data, cyclonic-only and non-cyclonic categories. In regard to the peak gusts, the applicable Region C regional design wind speed from Standards Australia (2002) is also illustrated for reference and can be seen to lie comfortably above the various objective analyses. While these results are presented to provide a regional overview, the interested reader should also consult the Appendix to judge the quality of the various fits, which do vary between sites and categories and as a function of the length of record. In particular, the Kowanyama, Horn Island and Coconut Island results are not presented here due to their generally very short records.

[8] This may tend to under-adjust the V_{600} speeds to some extent.

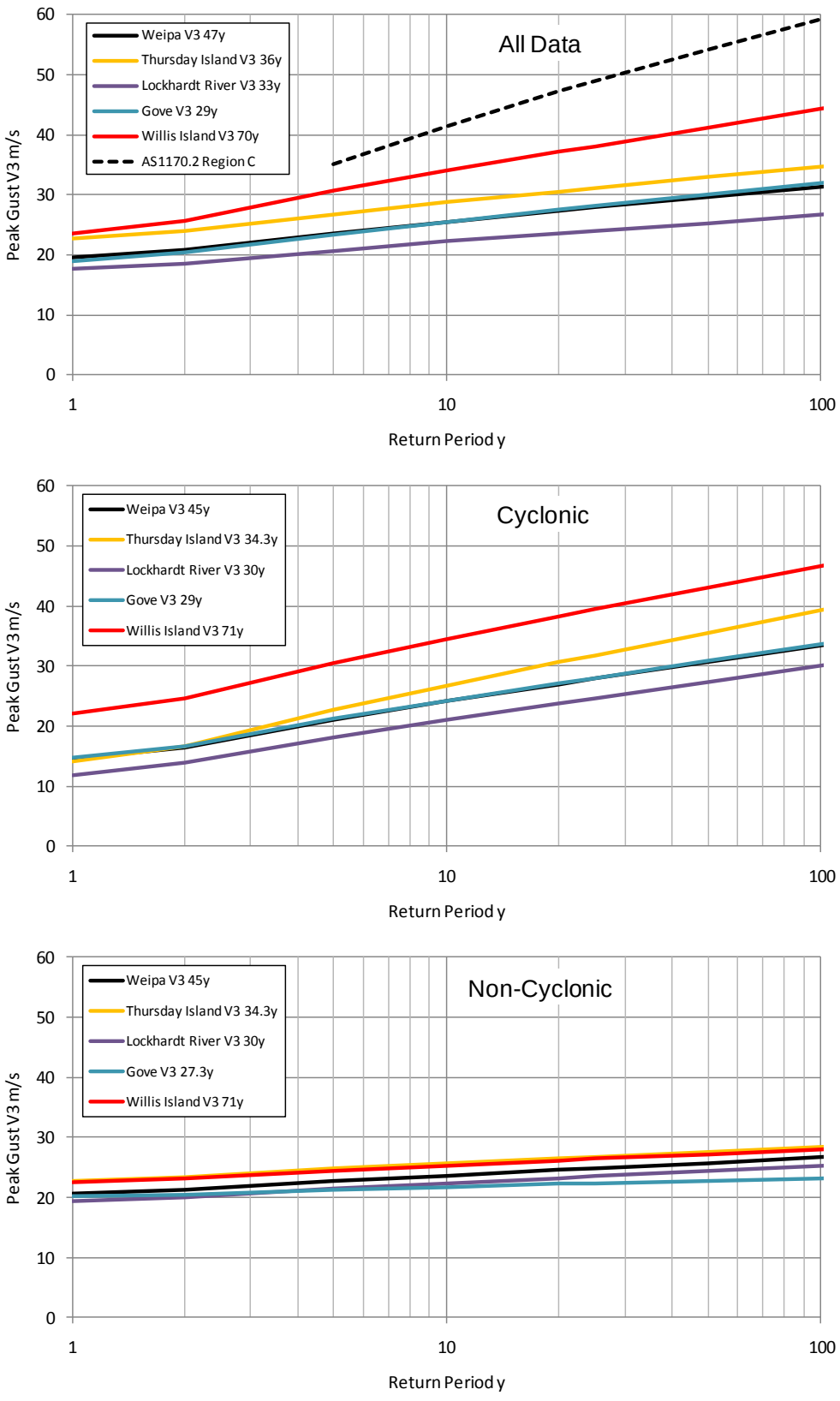

Figure 3-7 Statistical analysis of regional peak gust wind speeds.

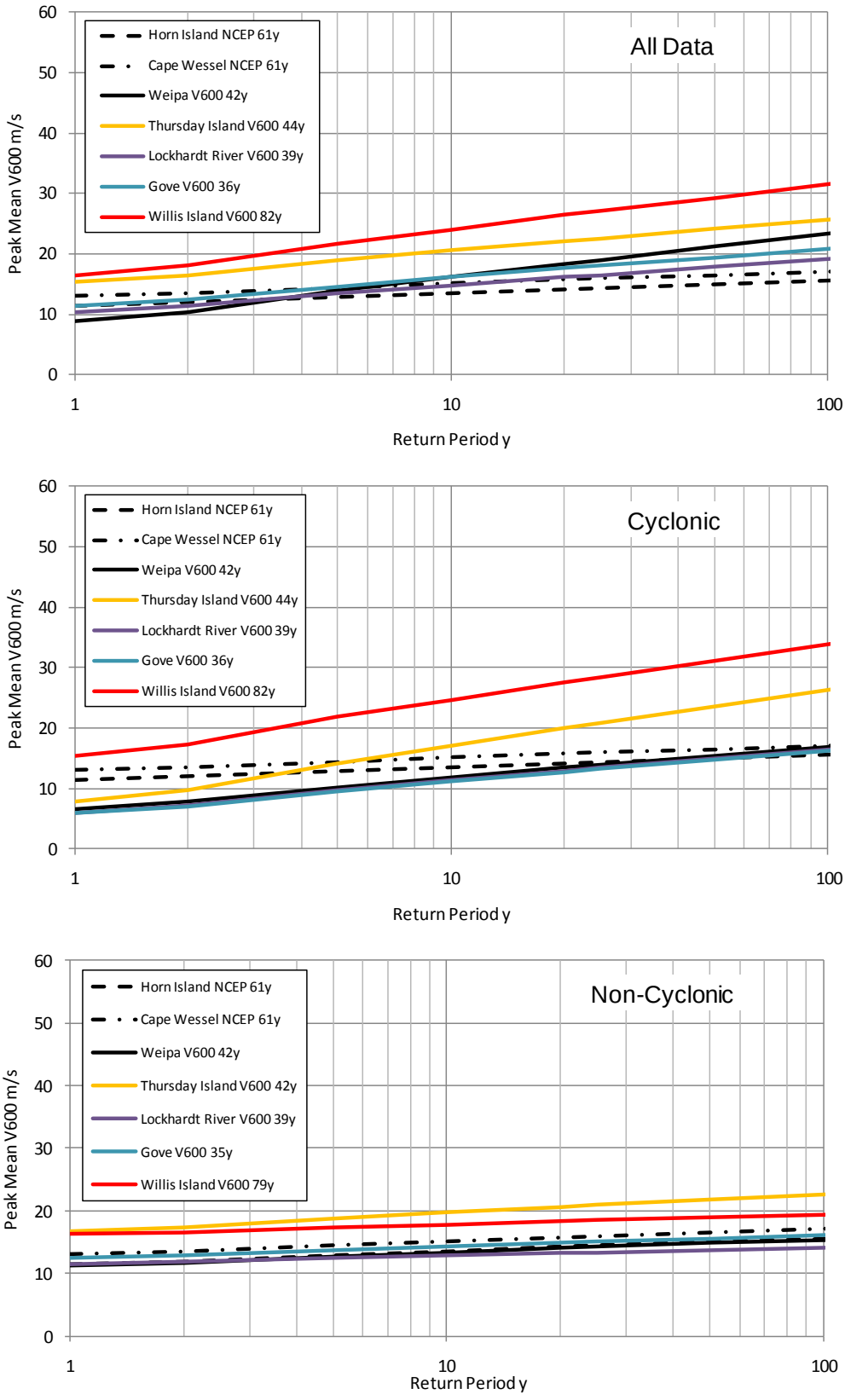

Figure 3-8 Statistical analysis of regional peak mean wind speeds.

Considering the peak gust analyses, there is a very clear differentiation between the cyclonic and non-cyclonic results for all sites. Willis Island, with its very long record and exposed location, experiences a significantly higher combined wind risk than the other sites. However Thursday Island is the next highest, followed by Gove and Weipa with essentially identical results. Although the Weipa record is longer, this similarity with Gove may well be related to their like latitude on either side of the Gulf of Carpentaria. The lowest combined wind risk appears to be at Lockhart River Airport. However, when considering the non-cyclonic analyses, there is much less variability between the sites, and Willis Island and Thursday Island are almost identical. This could be indicative of both being strongly influenced by the SE Trades.

Considering the mean wind analyses, the relative wind risks are similar to the gusts but with less differentiation between the sites. Included in these graphs are the equivalent analyses of the hindcast NCEP/NCAR data for locations averaged at Cape Wessel, north of Gove, and centred at Horn Island in the Torres Strait. Due to the low resolution (6 hourly and 2°) of these data they are most appropriately compared with the non-cyclonic subset, where they can be seen to be very similar to Gove and Weipa. This is to be expected since the reanalysis would take much of its regional input from these sites. However, Thursday Island still lies significantly above these curves and is higher than Willis Island.

3.2.4 Discussion

The foregoing analyses were undertaken to generally inform and quantitatively assign wind risk throughout the region so as to better understand the scale interactions between cyclonic and non-cyclonic influences that influence extreme water levels.

It would appear that the Thursday Island winds are higher than others in the immediate region. Given that these winds have already been attenuated here to help account for topographic effects, this could be evidence of a real broadscale atmospheric amplification related to convergence between Cape York and Papua New Guinea. Alternatively, the simplified Thursday Island site adjustments here may simply not be sufficient to reliably normalise the data. Of interest, Figure 3-9 compares adjusted daily peak 10-min winds for Thursday Island and Poruma for the 10 years 1994 to 2004, suggesting a mean 15% increase at Thursday Island, albeit with large scatter.

3.3 Representativeness of the Local NCEP Winds

Finally, with the preceding conclusion in mind, attention is turned to the suitability of the broadscale NCEP/NCAR wind dataset for the regional modelling of wave effects. For example, Figure 3-10 compares the raw NCEP winds averaged to a point in the vicinity of Horn Island, with the measured winds at the more exposed Poruma site for a 10 year period.

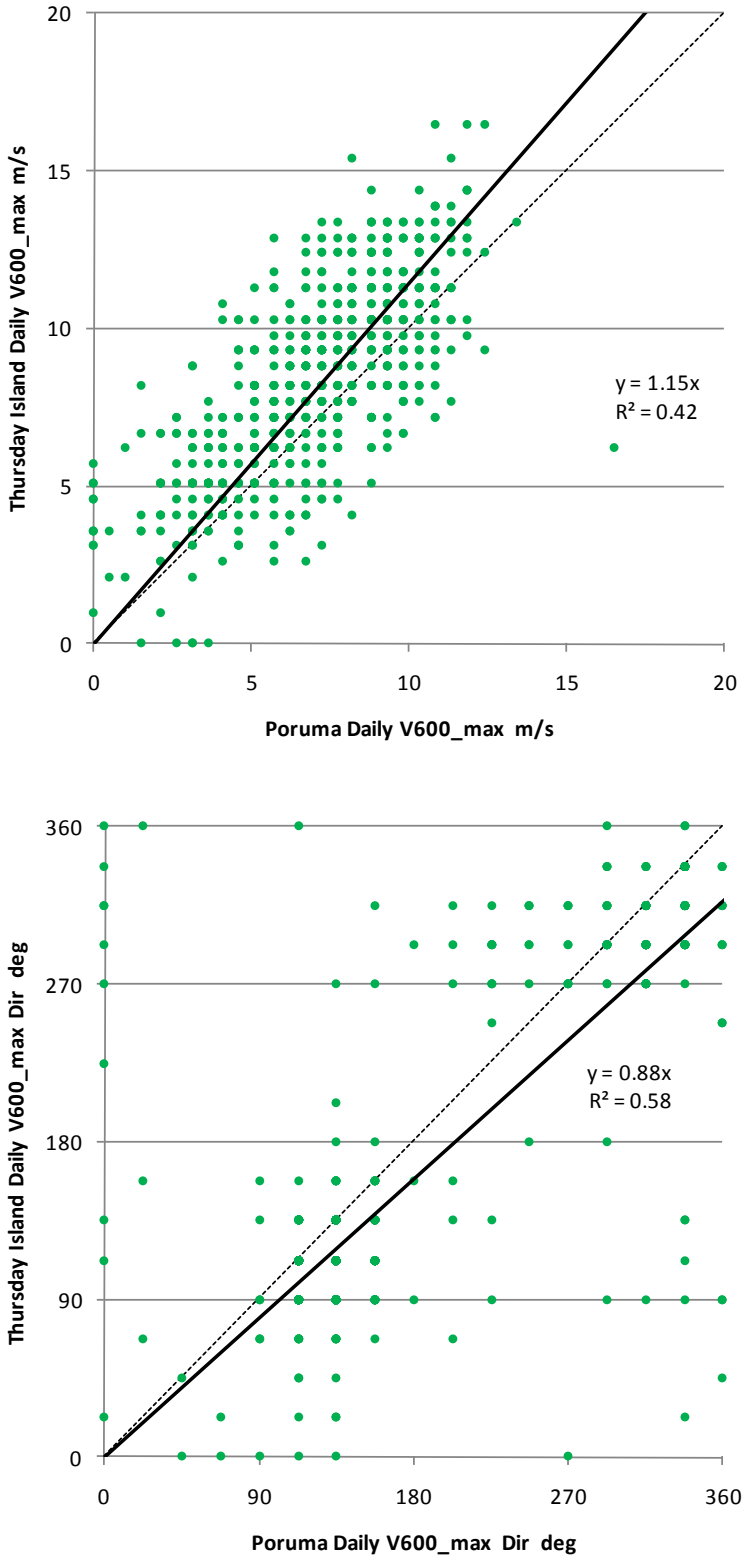

Figure 3-9 Comparison of adjusted Thursday Island and Poruma winds 1994 – 2004.

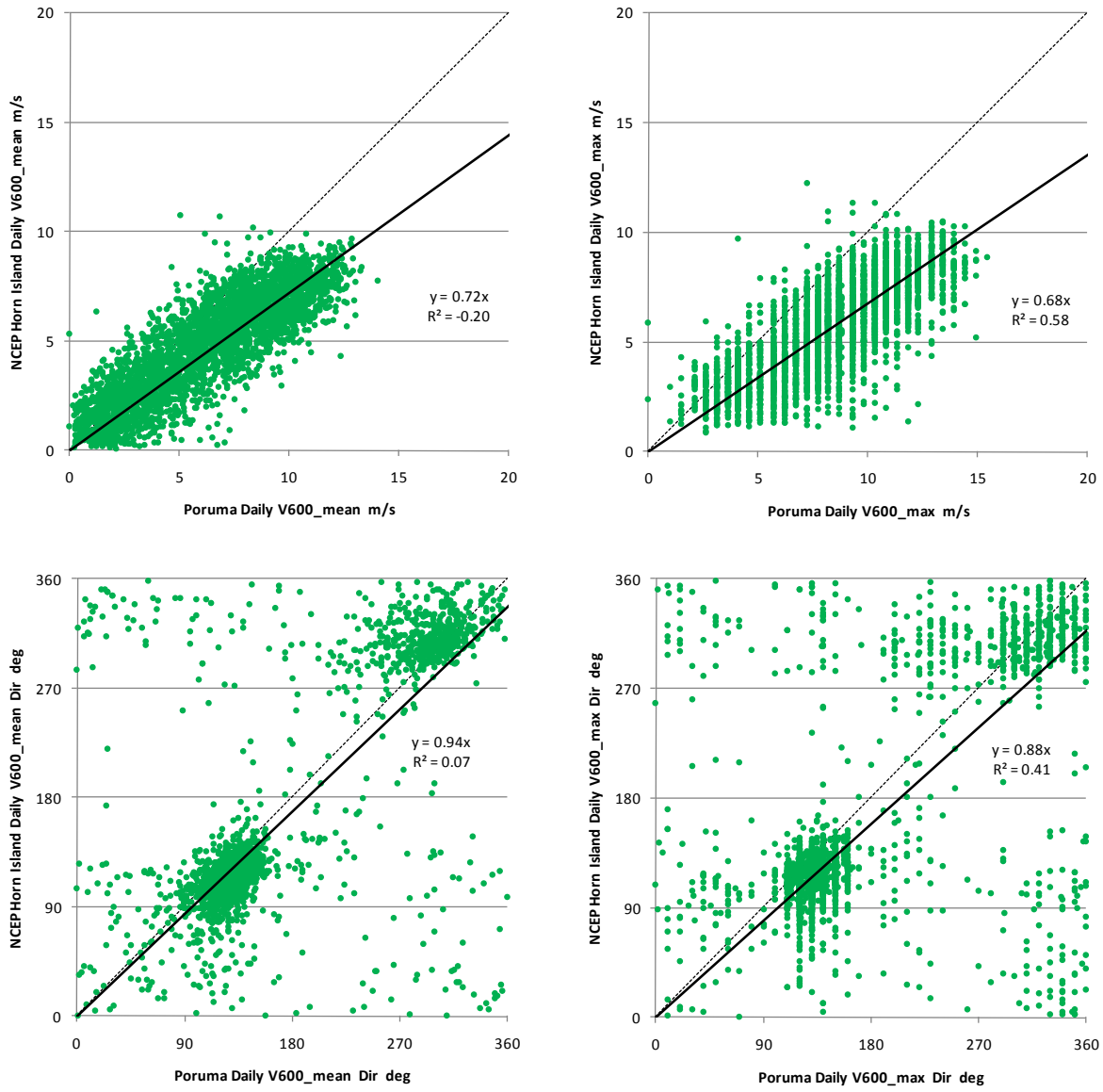

Figure 3-10 Comparison of raw NCEP wind estimates vicinity Horn Island and adjusted Poruma measured winds 1994-2004.

Both the daily mean V_{600} winds and the daily maximum V_{600} winds are compared. These graphs show that there is a slightly higher correlation between the daily mean V_{600} than the daily maximum, reflecting perhaps the difference in the 6-hourly NCEP and the 3-hourly Poruma data, but that the NCEP estimate significantly underpredicts the Poruma wind speeds, although the wind directions are generally reasonable. Likewise in Figure 3-11, where two years at random are compared in a time history context, there is a significant offset evident in the wind speed.

In order to ensure that locally-generated waves are not under-stated in the subsequent simulation modelling, a simple linear adjustment of the

locally-averaged NCEP winds is used to correct for the bias evident at the Poruma site. This nominal[9] bias adjustment was based on the linear best fit line of 1.0/0.72 = 1.38 for the daily mean V_{600}. Section 8.3.1 further justifies the need for this adjustment by comparing estimates of wave heights based on the raw NCEP data with those available from independent satellite altimeter pass data.

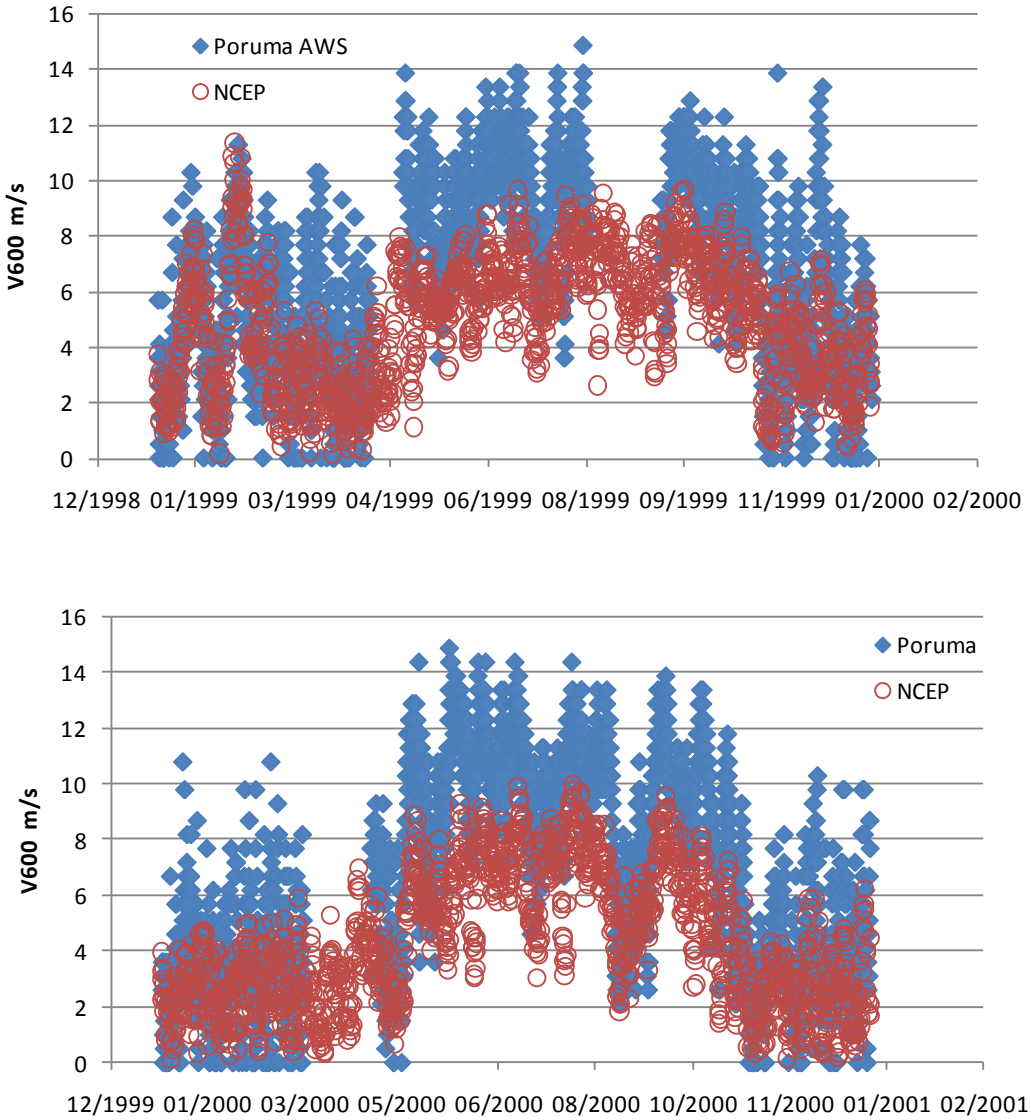

Figure 3-11 Comparison of time history of all raw NCEP wind and adjusted Poruma winds for 1999 and 2000.

[9] Strictly the comparison should be done with the NCEP as the independent data but the adopted adjustment is of the same order.

4. Astronomical Tides

The Torres Strait is situated essentially at the junction of two oceans – the Coral Sea to the east and the Arafura Sea to the west - each with significantly different tidal regimes as a result of the continental separation formed by Australia, Papua New Guinea and the so-called Maritime Continent of SE Asia. This commonly leads to situations where the astronomical tide is approaching high water on one side of the Strait while the other side is near low water, resulting in the generation of steep water level gradients and strong tidal currents. Because the Torres Strait is also shallow and partially blocked by a number of reefs and islands, the high water level gradient generated by the tide is focused along the chain of islands and reefs directly north of Cape York.

4.1 Analysis of Regional Tide Gauge Data

The measured tidal data in the region is the primary source of information regarding storm tide events from both broadscale and TC origins. It is therefore necessary to separate, as much as possible, the periodic astronomical signal from the raw signal to obtain the estimates of both the tidal constituents and the residual non-tidal water levels. This was done by harmonic analysis of the water level records using software developed by the AMC/MMU.

Long term tidal data was available for the sites listed in Table 4-1 with their locations shown on Figure 4-1. Five of these gauges service the navigational needs in the area, providing real time information to ship's masters via the Australian Maritime Safety Authority (AMSA) to enable their safely-timed passage through the shallow and narrow shipping channels. The Thursday Island gauge services the main island community port of Waiben and is the Standard Port gauge for the region (MSQ 2010).

Table 4-1 Long-term tide gauges available for analysis.

Authority	Name	Latitude ° GDA94	Longitude ° GDA94	Data Record y
AMSA	Booby_Is_TG	-10.60111	141.91120	>39
AMSA	Goods_Is_TG	-10.56019	142.15281	>35
AMSA	Ince_Pt_TG	-10.51249	142.30591	>38
AMSA	Nardana_Patches_TG	-10.50331	142.24490	>4
AMSA	Turtle_Head_TG	-10.52019	142.21281	>20
MSQ	Thursday_Is_TG	-10.58181	142.21780	>19

Figure 4-1 Location of long-term tide gauges in the region.
(yellow markers)

The results of the tidal analyses for the major diurnal and semi-diurnal tidal constituents (O_1, K_1, N_2, M_2 and S_2) are given in Table 4.2 and extraction of residuals is summarised graphically in Figure 4-2 for each of the long term tidal stations. The upper blue panels show the full time history of the raw water level signal while the lower red panels show the residual water level signal after accounting for the astronomical tide variability obtained from harmonic analysis of the identifiable tidal constituents (up to 150 at some locations). At this compressed scale the considerable annual variability in the residual water levels is quite evident. Note that for this work the astronomical tide analysis does not include annual variations (e.g. S_a), which are treated as part of atmospheric forcing in the broadscale synoptic modelling.

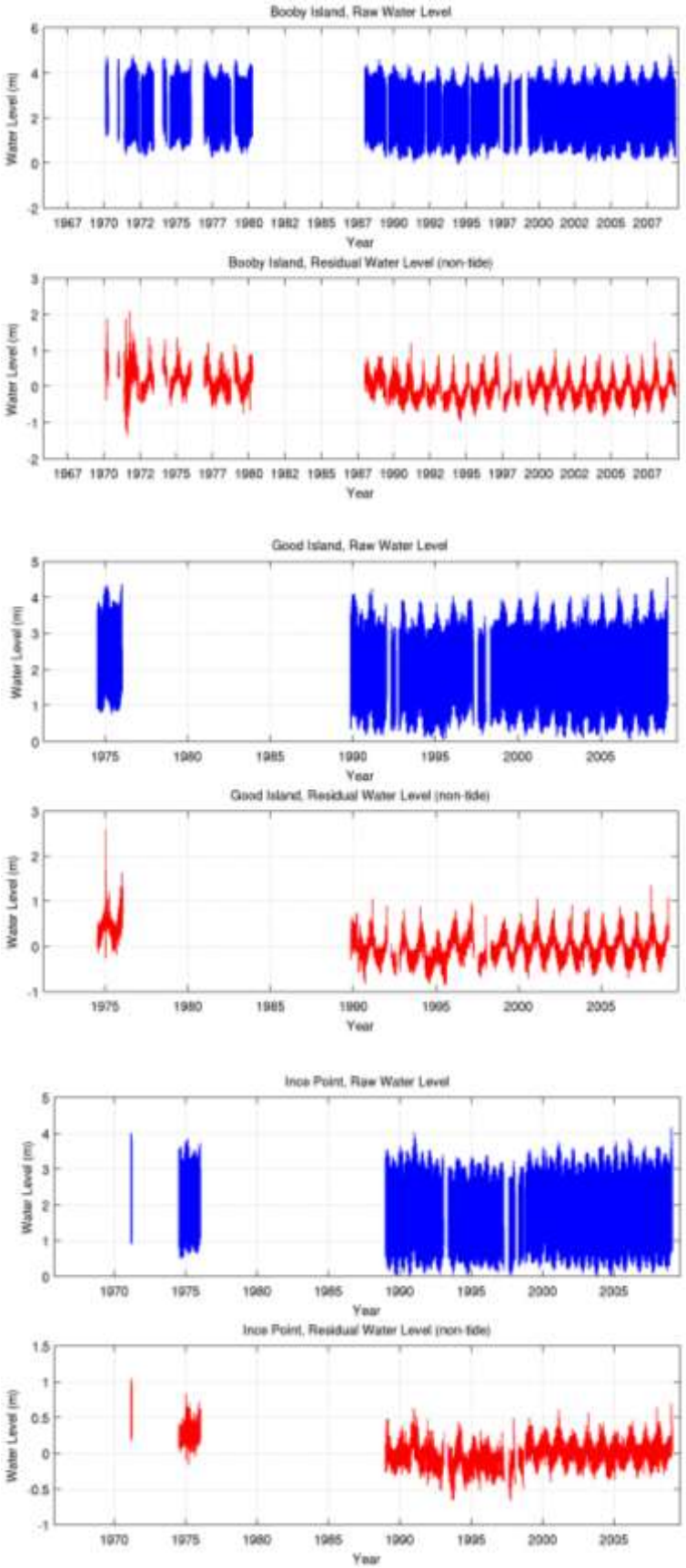

Figure 4-2 Example of the tidal residual extraction process.

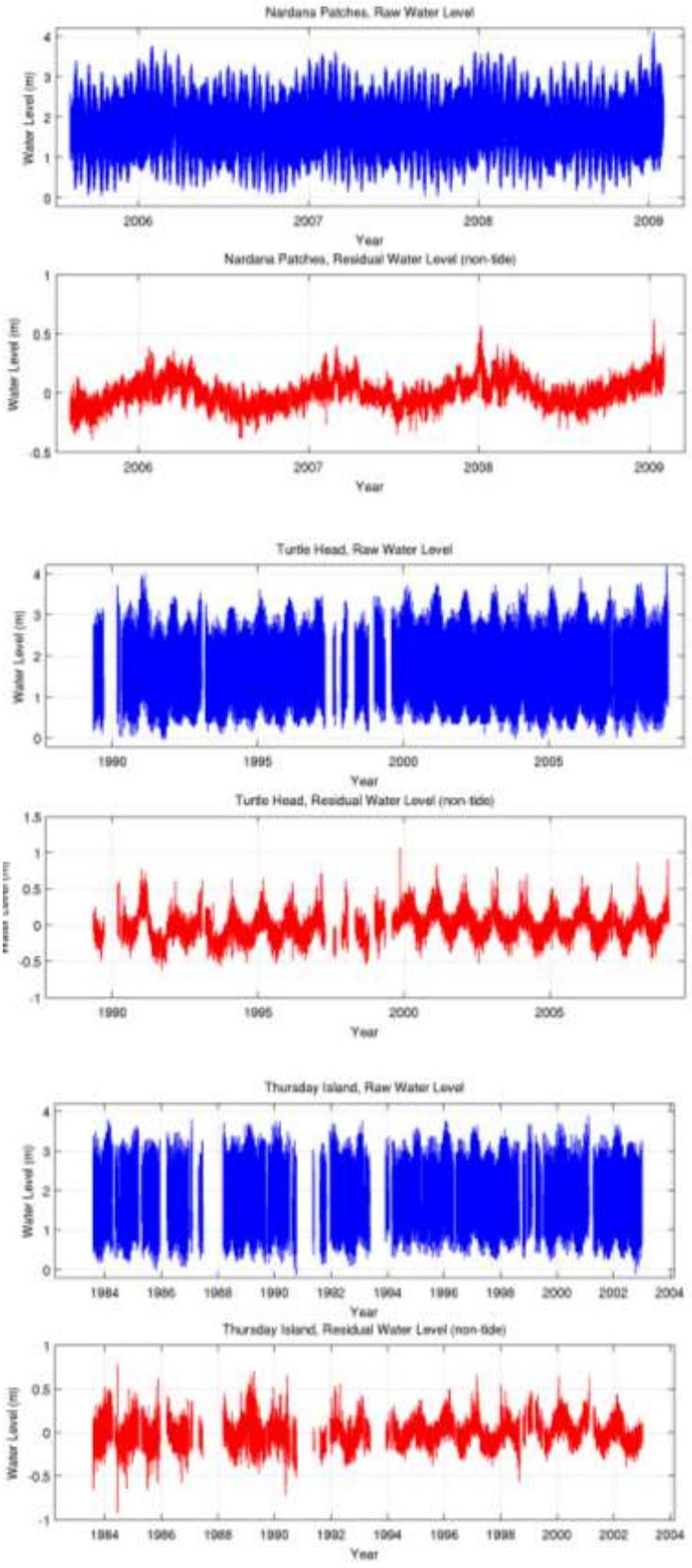

Figure 4-2 Example of the tidal residual extraction process (contd.)

Missing data (indicated by gaps) does not interfere with the harmonic extraction process but does act to limit the value of the analysis. It can be seen that Booby Island recorded a very significant non-tidal event in 1971 that is deemed due to bad data. The early data collected is often plagued with timing errors that then appear as large residuals. It also appears that the earlier segments of the data have some slight datum shifts relative to the more recent data. Accordingly, in the following work only the residuals after 1988 are used in the statistical analysis for extreme water levels.

Other recent shorter-term tide data was also made available to assist in the model calibration and the determination of land elevation datums (refer Section 9). Figure 4-4 indicates where tidal data was available during these periods (also includes the long-term sites), consisting of measurements for DERM by Griffith University (GU; Zier et al. 2009, Lemckert et al. 2009) and for the AHS by Fugro (2010). The results of the tidal analyses for the major semi-diurnal and diurnal tidal constituents are given in Table 4.2.

4.2 Bathymetry of the Torres Strait

The bathymetry of the region is generally shallow and particularly complex with likely morphological changes at a local level on a seasonal basis as a result of tidal, non-tidal and incoming wave influences (Saint-Cast 2008).

The available sounding data has only recently been composited into a high quality digital elevation dataset (Daniell 2008) providing a resolution of about 100 m horizontally. Further data collection is understood to be either underway or planned by a number of authorities (D. Hanslow, *personal communication*).

An extract from this dataset is displayed in Figure 4-4, showing the major features as:

- The eastern Coral Sea deepwater boundary and northern Great Barrier Reef region consisting of numerous reefs, shoals and some isolated islands in intermediate depth of 20 to 50 m;
- A middle shallowing region typically below 20 m depth, comprising numerous coral cays and shoals;
- The central island chain extending north beyond Cape York comprising mainland islands interspersed with large banks and shoals, often with depths below 15 m. Further to the north, the island chain reduces to extensive areas of banks and shallows below 10 m, culminating in the muddy coast of Papua New Guinea;
- The western extent comprising generally open water gradually deepening westward to the Arafura Sea, with a horizontal extent similar to that of the middle region on the eastern side.

Table 4-2 Measured amplitude and local phase of major tidal constituents

Station Name	Latitude	Longitude	Constituents									
			O_1		K_1		N_2		M_2		S_2	
			Amp	Phase	Amp	Phase	Amp	Phase	Amp	Phase	Amp	Phase
Booby Island (AMSA)	-10.6000	141.9167	0.426	133	0.692	193	0.169	84	0.718	131	0.139	262
Daru	-9.0667	143.2000	0.191	165	0.400	212	0.253	316	0.762	326	0.507	317
Frederick Point	-10.7167	142.5833	0.190	157	0.446	207	0.212	334	0.603	352	0.514	328
Goods Island (AMSA)	-10.5667	142.1667	0.400	139	0.677	199	0.137	76	0.525	132	0.200	302
Hammond Rock	-10.5167	142.2167	0.326	146	0.598	204	0.132	42	0.340	98	0.301	327
Harrington Reef	-10.8167	142.7200	0.190	159	0.427	204	0.280	312	0.774	335	0.569	313
Ince Point (AMSA)	-10.5000	142.3167	0.266	150	0.538	208	0.174	13	0.365	42	0.413	341
Nardana Patches (AMSA)	-10.5000	142.2500	0.277	148	0.548	207	0.177	23	0.343	59	0.374	342
Thursday Island (MSQ)	-10.5833	142.2167	0.285	144	0.552	207	0.163	23	0.352	65	0.351	338
Turtle Head (AMSA)	-10.5167	142.2167	0.343	146	0.617	207	0.133	42	0.323	100	0.294	331
Twin Island (AMSA)	-10.4500	142.4333	0.226	155	0.494	209	0.194	352	0.502	12	0.504	337
Badu Island (GU)	-10.1701	142.1681	0.362	141	0.622	204	0.191	66	0.442	125	0.266	331
Boigu Island (GU)	-9.7507	143.4060	0.277	161	0.600	227	0.246	108	0.454	156	0.434	43
Coconut Island (GU)	-10.0493	143.0640	0.171	163	0.407	206	0.256	317	0.715	334	0.475	320
Darnley Island (GU)	-9.5975	143.7601	0.161	160	0.352	200	0.256	288	0.718	310	0.395	288
Hammond Island (GU)	-10.5614	142.2194	0.250	147	0.507	206	0.195	24	0.343	57	0.381	338
Mabuiag Island (GU)	-9.9512	142.2013	0.216	153	0.515	215	0.217	37	0.385	59	0.499	359
Murray Island (GU)	-9.9150	144.0397	0.139	154	0.300	194	0.213	269	0.572	292	0.325	264
Saibai Island (GU)	-9.3800	142.6136	0.201	178	0.514	233	0.188	49	0.388	43	0.542	37
Stephen Island (GU)	-9.5048	143.5469	0.161	154	0.351	200	0.253	293	0.746	314	0.399	295
Thursday Island (GU)	-10.5861	142.2216	0.251	147	0.509	205	0.195	26	0.345	61	0.339	341
Warraber Island (GU)	-10.2046	142.8225	0.175	163	0.417	212	0.229	338	0.613	349	0.495	340

Station Name	Latitude	Longitude	Constituents									
			O_1		K_1		N_2		M_2		S_2	
			Amp	Phase	Amp	Phase	Amp	Phase	Amp	Phase	Amp	Phase
Yam Island (GU)	-9.8997	142.7663	0.178	168	0.439	217	0.219	354	0.577	1	0.529	356
Yorke Island (GU)	-9.7489	143.4016	0.164	163	0.373	204	0.255	300	0.727	320	0.433	305
Badu-Moa_Channel (Fugro)	-10.1537	142.1853	0.380	139	0.672	208	0.171	67	0.460	123	0.256	331
East_Strait_Islet (Fugro)	-10.4576	142.4357	0.226	159	0.485	212	0.215	5	0.530	14	0.493	339
Hawkesbury Island (Fugro)	-10.3006	142.0987	0.404	135	0.702	202	0.176	76	0.585	133	0.195	301
Mid 437 (Fugro)	-10.1531	142.5031	0.229	166	0.490	219	0.211	9	0.563	12	0.536	346
Muknab Rock (Fugro)	-10.3648	142.3581	0.242	156	0.516	214	0.195	9	0.487	24	0.471	341
NE Badu Island Mooring (Fugro)	-10.0337	142.2176	0.231	157	0.647	210	0.222	22	0.411	52	0.389	350
NE Moa Island (Fugro)	-10.1500	142.3400	0.229	162	0.505	216	0.221	18	0.563	23	0.560	349
NW_Boundary (Fugro)	-9.9711	141.8192	0.451	128	0.777	196	0.220	86	0.919	137	0.118	256
Orman Reefs (Fugro)	-9.8787	142.3612	0.240	166	0.517	220	0.221	26	0.539	27	0.577	355
South Badu (Fugro)	-10.2058	142.1611	0.376	138	0.692	206	0.158	71	0.521	130	0.224	315
South Sassie Reef (Fugro)	-10.1465	142.9217	0.200	164	0.432	214	0.187	342	0.653	341	0.513	326
Sue (Warraba) Island (Fugro)	-10.2050	142.8200	0.208	166	0.445	216	0.173	354	0.601	350	0.511	333
SW Badu Island Mooring (Fugro)	-10.1903	141.9178	0.404	135	0.855	193	0.190	86	0.766	138	0.109	278
SW_Boundary (Fugro)	-10.4484	141.8192	0.425	128	0.712	195	0.182	81	0.752	129	0.131	255
Travers_Island_Mooring (Fugro)	-10.3651	142.3185	0.223	157	0.609	207	0.223	2	0.445	27	0.387	337
Travers_Island_TP (Fugro)	-10.3647	142.3604	0.228	153	0.623	205	0.211	4	0.405	32	0.361	333
West Badu (Fugro)	-10.1224	142.0808	0.429	132	0.746	200	0.197	86	0.739	140	0.171	294
West Island (Fugro)	-10.4032	142.0984	0.399	134	0.697	200	0.164	73	0.575	132	0.195	292
West Island TP (Fugro)	-10.3556	142.0448	0.391	136	0.838	194	0.177	79	0.645	136	0.137	288
Yam Island (Fugro)	-9.8993	142.7661	0.227	175	0.478	225	0.184	16	0.541	8	0.536	355

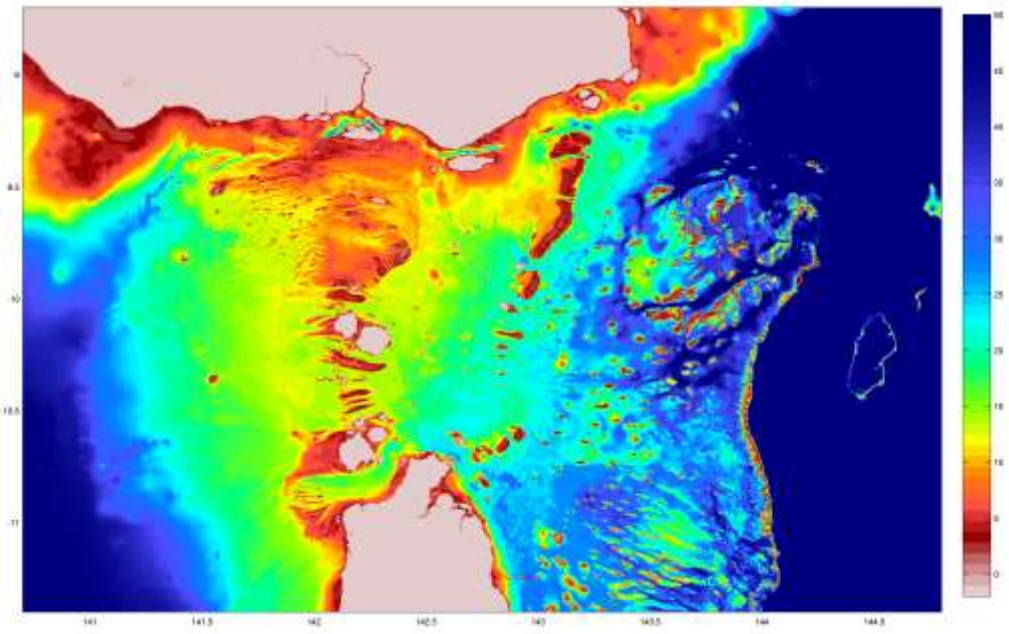

Figure 4-3 Bathymetry of the Torres Strait region.

4.3 Numerical Hydrodynamic Modelling of the Regional Astronomical Tide

In order to obtain estimates of the statistical distribution of extreme water levels at each of the community locations it is necessary to construct a numerical model that encompasses the entire Torres Strait and at a resolution sufficient to represent the tidal scale processes and the coastal features. The adopted model domain, which makes use of the aforementioned bathymetry data, is termed here the Torres Strait (TS) model and is illustrated in Figure 4-4. The spatial resolution is 1' (one minute of arc or 1.85 km) and the model is driven by tidal signals along its eastern and western boundaries guided by previous AMC regional modelling and further manually calibrated here.

The numerical tidal model used is based on Bode and Mason (1994, 1995) and Bode et al. (1997) and is a rectilinear-nested three-dimensional barotropic model with an implicit finite difference numerical scheme. The two-dimensional (depth-integrated) model mode was used for the tidal modelling. The nested rectilinear domains provide for highly efficient numerical performance and the model's ability to incorporate internal sub-grid scale boundary conditions provides for enhanced resolution of reefs, banks and shoals (Bode and Mason 2005).

The TS tidal model was then calibrated using all suitable tide stations to ensure that the principal tidal components would each be well

represented. A total of 36 major and minor tidal constituents are included. The model's ability to reproduce the tide is initially evaluated at the individual constituent level by comparing the measured and modelled amplitudes and local phases. Data for the 5 major tidal constituents O_1, K_1, N_2, M_2 and S_2 (Table 4-2) can be compared with those produced by the model (Table 4-3).

The full predictive value of the output from the TS model is best illustrated by considering the modelled propagation of the principal tidal components in terms of their amplitude and relative phase. This is illustrated in Figure 4-5 which shows the modelled amplitude of the major semi-diurnal constituent (M_2) across the study region as a series of height contours and the propagation phase angle as a colour-coded background. The islands and reefs are also shown and can be seen to playing a principal part in the propagation pattern of this, the major semi-diurnal tide harmonic in the region, which contributes to twice-daily high and low tides.

In particular, the colour-coding shows the significant phase separation between east and west and the contours show the concentration of amplitude variation along that separation line, which follows the central line of islands, shoals and reefs. The highest tidal amplitude can be seen concentrated in the upper left hand side against the Papua New Guinea coastline. Similar results are obtained for the other harmonics and Appendix E presents the modelled patterns for the semi-diurnal S_2 and N_2 and the O_1 and K_1 principal diurnal harmonics, which further modulate the semi-diurnal tides to create diurnal inequalities. These combinations of harmonics, plus shallow water sub-harmonics, which are generated by the tidal flow interaction with the bathymetry, are responsible for giving the tide its special and complex character across the region.

Table 4-3 Modelled amplitude and local phase of major tidal constituents

Station Name	Latitude	Longitude	I	J	Constituents									
					O1		K1		N2		M2		S2	
					Amp	Phase	Amp	Phase	Amp	Phase	Amp	Phase	Amp	Phase
Booby Island (AMSA)	-10.6000	141.9167	50	31	0.406	132	0.696	193	0.173	88	0.714	131	0.134	266
Daru	-9.0667	143.2000	127	123	0.182	167	0.393	212	0.248	305	0.786	320	0.498	323
Frederick Point	-10.7167	142.5833	90	24	0.205	161	0.471	211	0.225	338	0.584	354	0.505	337
Goods Island (AMSA)	-10.5667	142.1667	65	33	0.382	138	0.687	200	0.132	81	0.508	135	0.213	310
Hammond Rock	-10.5167	142.2167	68	36	0.324	147	0.625	206	0.115	44	0.287	106	0.305	333
Harrington Reef	-10.8167	142.7200	98	18	0.187	161	0.428	206	0.277	315	0.775	335	0.538	316
Ince Point (AMSA)	-10.5000	142.3167	74	37	0.235	155	0.522	211	0.194	5	0.426	30	0.466	349
Nardana Patches (AMSA)	-10.5000	142.2500	70	37	0.252	150	0.545	208	0.169	18	0.356	53	0.399	348
Thursday Island (MSQ)	-10.5833	142.2167	68	32	0.310	143	0.608	205	0.126	43	0.306	100	0.304	336
Turtle Head (AMSA)	-10.5167	142.2167	68	36	0.324	147	0.625	206	0.115	44	0.287	106	0.305	333
Twin Island	-10.4500	142.4333	81	40	0.215	160	0.496	212	0.216	353	0.511	13	0.518	347
Badu Island (GU)	-10.1701	142.1681	66	56	0.309	142	0.622	206	0.131	65	0.379	122	0.286	346
Boigu Island (GU)	-9.2300	142.2190	68	113	0.353	159	0.724	225	0.179	125	0.578	178	0.369	41
Coconut Island (GU)	-10.0493	143.0640	119	64	0.193	165	0.431	212	0.228	320	0.652	334	0.511	331
Darnley Island (GU)	-9.5975	143.7601	161	91	0.156	158	0.339	198	0.233	281	0.703	300	0.416	290
Hammond Island (GU)	-10.5614	142.2194	68	33	0.273	149	0.566	208	0.159	24	0.336	64	0.375	347
Mabuiag Island (GU)	-9.9512	142.2013	67	70	0.245	160	0.571	218	0.161	38	0.301	69	0.491	12
Murray Island (GU)	-9.9150	144.0397	177	72	0.141	158	0.302	197	0.182	270	0.530	289	0.304	274
Saibai Island (GU)	-9.3800	142.6136	92	105	0.265	171	0.584	228	0.122	29	0.176	12	0.579	22
Stephen Island (GU)	-9.5048	143.5469	148	97	0.162	159	0.356	201	0.248	287	0.755	306	0.456	299
Thursday Island (GU)	-10.5861	142.2216	68	32	0.310	143	0.608	205	0.126	43	0.306	100	0.304	336

Station Name	Latitude	Longitude	I	J	Constituents									
					O1		K1		N2		M2		S2	
					Amp	Phase	Amp	Phase	Amp	Phase	Amp	Phase	Amp	Phase
Warraber Island (GU)	-10.2046	142.8225	104	55	0.207	166	0.470	215	0.216	336	0.574	348	0.532	343
Yam Island (GU)	-9.8997	142.7663	101	73	0.221	169	0.504	220	0.196	350	0.493	357	0.573	358
Yorke Island (GU)	-9.7489	143.4016	139	82	0.175	162	0.389	206	0.244	301	0.731	318	0.481	314
Badu-Moa_Channel (Fugro)	-10.1537	142.1853	66	58	0.247	150	0.563	213	0.156	42	0.322	81	0.412	6
East_Strait_Islet (Fugro)	-10.4576	142.4357	81	40	0.215	160	0.496	212	0.216	353	0.511	13	0.518	347
Hawkesbury Island (Fugro)	-10.3006	142.0987	61	49	0.404	138	0.721	200	0.149	92	0.609	142	0.199	306
Mid 437 (Fugro)	-10.1531	142.5031	85	58	0.220	164	0.509	216	0.211	356	0.496	10	0.569	355
Muknab Rock (Fugro)	-10.3648	142.3581	76	45	0.225	157	0.515	211	0.201	2	0.446	25	0.497	350
NE Badu Island Mooring (Fugro)	-10.0337	142.2176	68	65	0.227	161	0.542	216	0.196	24	0.410	50	0.535	8
NE Moa Island (Fugro)	-10.1500	142.3400	76	58	0.221	162	0.518	215	0.214	3	0.483	21	0.573	357
NW_Boundary (Fugro)	-9.9711	141.8192	44	69	0.428	133	0.762	197	0.219	104	0.891	142	0.102	273
Orman Reefs (Fugro)	-9.8787	142.3612	77	74	0.229	165	0.540	219	0.198	14	0.410	30	0.594	6
South Badu (Fugro)	-10.2058	142.1611	65	55	0.329	139	0.644	204	0.136	76	0.451	131	0.245	340
South Sassie Reef (Fugro)	-10.1465	142.9217	110	58	0.199	165	0.452	213	0.229	328	0.629	341	0.536	337
Sue (Warraba) Island (Fugro)	-10.2050	142.8200	104	55	0.207	166	0.470	215	0.216	336	0.574	348	0.532	343
SW Badu Island Mooring (Fugro)	-10.1903	141.9178	50	56	0.418	134	0.740	197	0.193	99	0.796	141	0.133	282
SW_Boundary (Fugro)	-10.4484	141.8192	44	40	0.412	130	0.707	192	0.183	90	0.762	132	0.130	257
Travers_Island_Mooring (Fugro)	-10.3651	142.3185	74	45	0.229	156	0.519	211	0.197	6	0.431	31	0.481	351
Travers_Island_TP (Fugro)	-10.3647	142.3604	77	45	0.223	159	0.509	212	0.209	0	0.475	21	0.511	351
West Badu (Fugro)	-10.1224	142.0808	60	60	0.416	137	0.747	200	0.183	103	0.751	146	0.154	303
West Island (Fugro)	-10.4032	142.0984	61	43	0.389	137	0.698	199	0.142	87	0.570	137	0.197	305
West Island TP (Fugro)	-10.3556	142.0448	58	46	0.402	136	0.715	199	0.158	93	0.650	140	0.175	297
Yam Island (Fugro)	-9.8993	142.7661	101	73	0.221	169	0.504	220	0.196	350	0.493	357	0.573	358

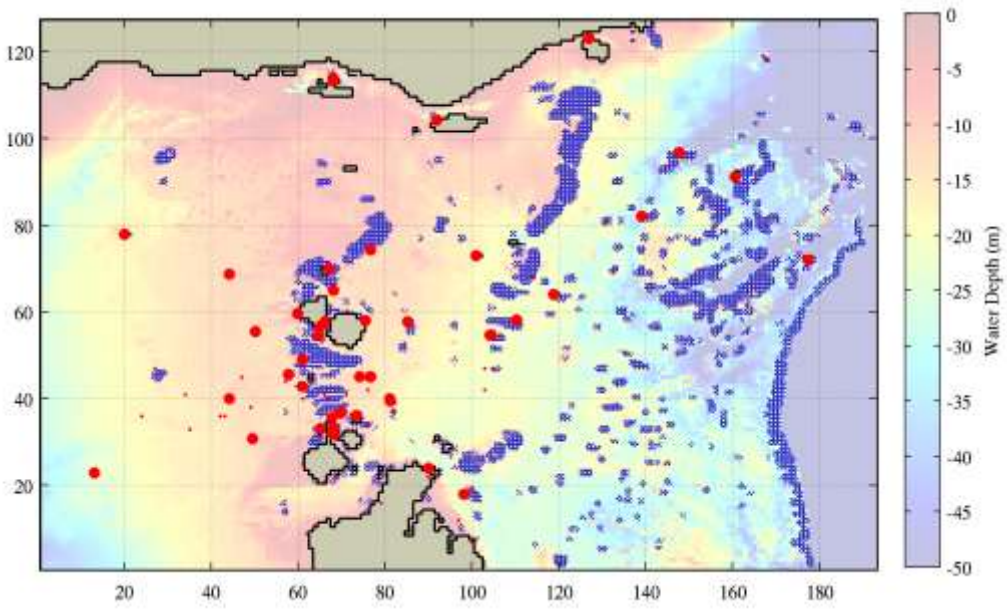

Figure 4-4 Torres Strait model with red markers indicating locations where some measured tide data was available.

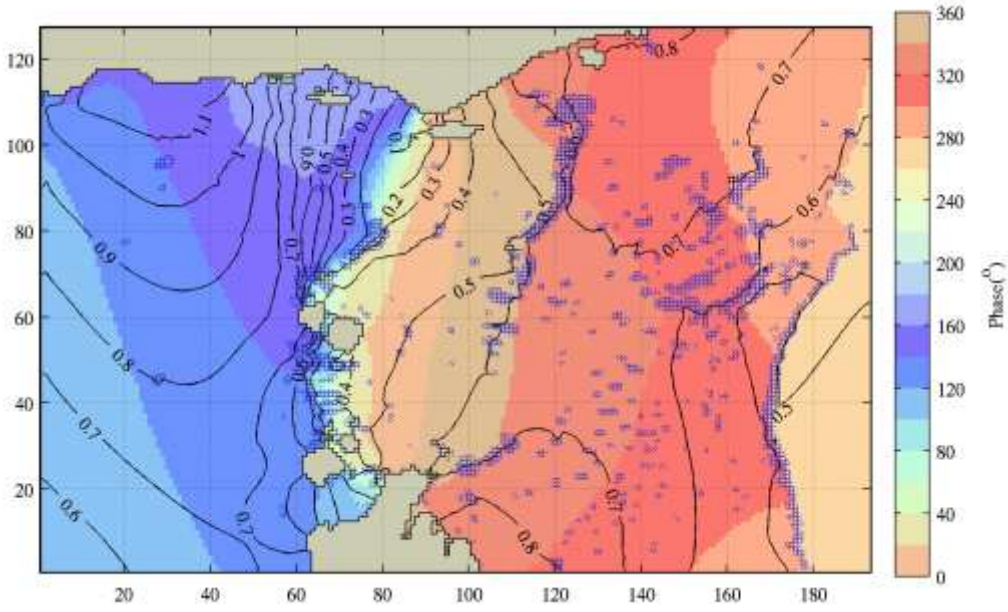

Figure 4-5 The TS-modelled M_2 component tidal propagation pattern.

5. Modelling the Broadscale Sea Level Variability

To obtain a reliable estimate of the extremes of the sea level across the region it is also necessary to model the non-tidal water level gradients and associated currents passing through the Torres Strait. The mean oceanic levels (i.e. ignoring the tide) on either side of the strait are influenced by seasonal changes in oceanic water level in the Coral and Arafura seas. Meanwhile, the sea level in the nearby Gulf of Carpentaria, because of its relatively shallow waters, is strongly influenced by both seasonal changes in synoptic wind patterns and other intense synoptic scale weather systems such as the monsoon and TCs. The basic approach to modelling these various elements is to separately address the principal scales of forcing.

5.1 The Broadscale Numerical Hydrodynamic Model

To model these effects within the Torres Strait, a relatively coarser outer model domain (10 km resolution) is added to the inner TS tidal model. This outer domain is termed the Gulf of Carpentaria and Coral Sea model (GCCS) and covers both the Gulf of Carpentaria and the western Coral Sea on a synoptic scale, as shown in Figure 5-1.

The GCCS model is designed to capture the broadscale water level response to regional synoptic weather systems, as represented by the hindcast NCEP surface wind and pressure data, the annual water variations that were excluded in the tidal analyses and also inter-annual effects. The NCEP resolution of about 210 km is relatively coarse, and so is not capable of adequately representing the presence of TCs, unless they are very large in scale (refer section later regarding the unusual TC *Charlotte*). This suits our purposes because the effect of intense TC forcing is separately treated later as a “local” or small scale forcing within the Torres Strait region (Section 7).

The GCCS model open boundaries are designed to be used to represent the slowly varying oceanic water levels that are separated from the immediate synoptic scale. We consider two broadscale boundary components in this regard:

- The annual average water level signal; and the
- Inter-annual mean water level variation that represents effects that may last for a year or more (e.g. ENSO)

The annual average signal has been based on tide stations across the region comprising very long datasets. The inter-annual variation has been estimated by examining the ENSO climate sequence, and determining the likely nature of that signal.

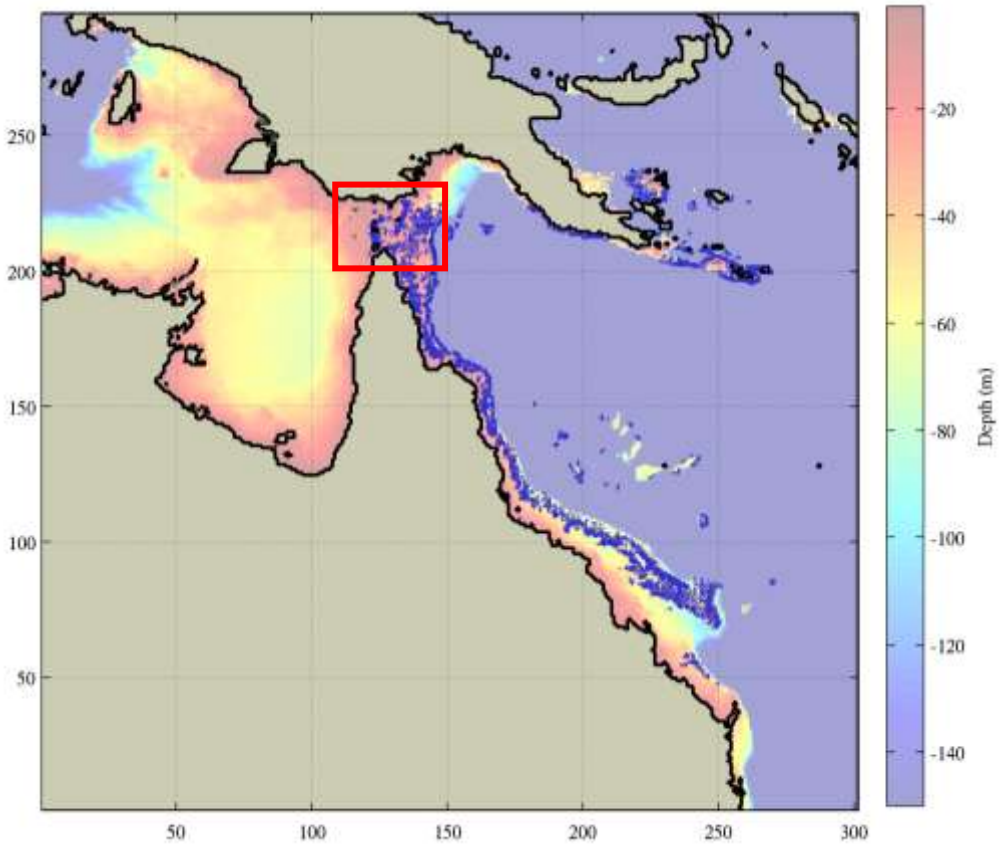

Figure 5-1 The numerical hydrodynamic model domains; inner fine-scale Torres Strait (TS) and outer broad-scale Gulf of Carpentaria and Coral Sea Model (GCCS).

5.2 The Annual Average Water Level Boundary Signal

Changes in water level associated with the seasonal weather cycle are reasonably small for most locations on the east Queensland coast and have amplitudes that are generally less than 0.1 m. However in the Gulf of Carpentaria this seasonal response is much larger and reaches an amplitude of about 0.4 m at Karumba in the southernmost part. On the western side of Torres Strait it is of the order of 0.3 m and forms a significant part of the total water level variation in the region. Although a large proportion of this seasonal water level response is generated locally within the Gulf by wind and pressure variations a significant signal still exists at the north-western boundaries of the GCCS model (~0.12 m).

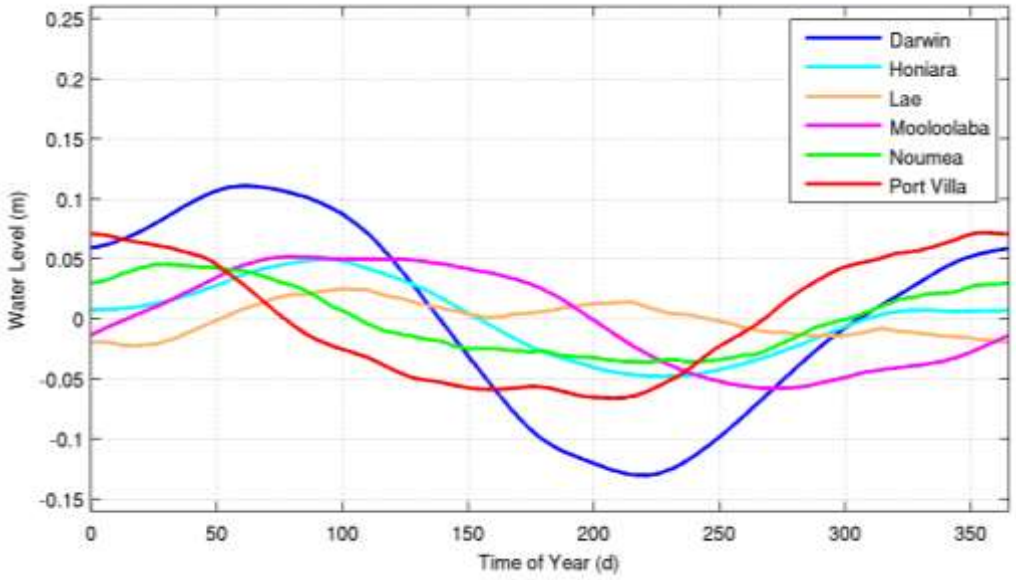

Figure 5-2 Annual water level signals used on the boundaries of the GCCS model.

To represent this seasonal effect, analysed tidal gauge records from Darwin in the Arafura Sea to the west and Honiara, Lae, Mooloolaba, Noumea and Port Villa in the Coral Sea to the east were used (refer Figure 5-2). The Darwin tide gauge annual water level signal is applied uniformly along the western boundary of the GCCS model and a composited annual signal from the other stations is used on the eastern boundary. These are chosen to produce water levels that are consistent with the annual variation of the East Australian Current (EAC) and act to change the water level slope across the inflow/outflow regions of the EAC (Bode and Mason 1995).

5.3 The Inter-Annual Water Level Boundary Signal

In order to account for the expected inter-annual variability of water levels in the region, which are likely linked to the broadscale Pacific Ocean EL Niño Southern Oscillation (ENSO), the simplified Southern Oscillation Index (SOI) was examined.

The SOI signal has the advantage of being of much longer duration than the available NCEP wind record and is expected to correlate well with water level changes in the Gulf of Carpentaria because it is based on atmospheric pressure differences between Darwin and Tahiti.

To investigate if the measured SOI could be used to create a proxy for the inter-annual water level variation, a correlation analysis was undertaken between the low-pass filtered SOI (Figure 5-3) and water

level signals for tide stations in the region. On that basis Darwin and Mooloolaba have r^2 values of 0.7662 and 0.4788 respectively. This means that an SOI-based model will act as a reasonable proxy for water level variation (77%) at the boundaries of the Gulf of Carpentaria but in the Coral Sea the SOI will explain less than 50% of the inter-annual water level variations. Figure 5-4 shows the resulting SOI-driven inter-annual water level model compared with the actual filtered tidal records at Darwin, Port Moresby, Townsville and Mooloolaba. Although far from perfect, it can be seen that this simple SOI-proxy provides some significant portion of the inter-annual signal and suits the present purposes. To improve on this simple approximation would likely be a difficult and time consuming modelling task.

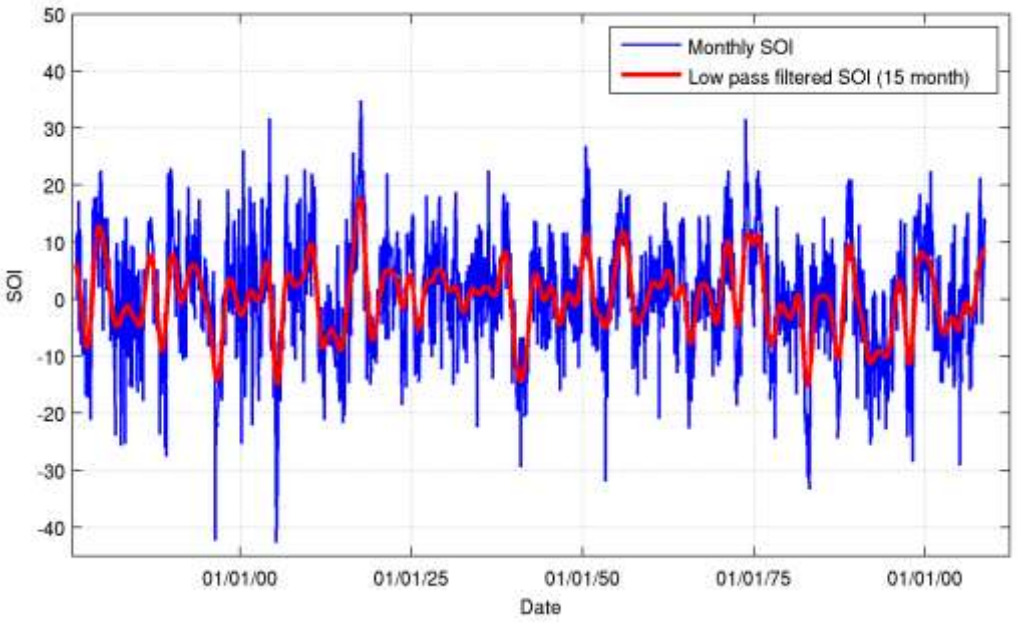

Figure 5-3 The raw and filtered SOI record.

5.4 Statistical Broadscale Modelling of Water Level

The GCCS model has been used to simulate the 60 year period of available NCEP/NCAR surface wind and pressure data (since 1948), with the open boundaries forced by the annual (tide gauge derived) and inter-annual (SOI) signals discussed previously. No astronomical tides are included in this simulation, such that the resulting modelled water elevations can be considered as “residuals” relative to the background tide.

The inner fine scale TS model was then run for the same 60 year period, but with its open boundaries forced by the combination of the GCCS broadscale signal and the astronomical tide. These results are then examined to determine the matching with the actual residual water levels at the available tidal stations.

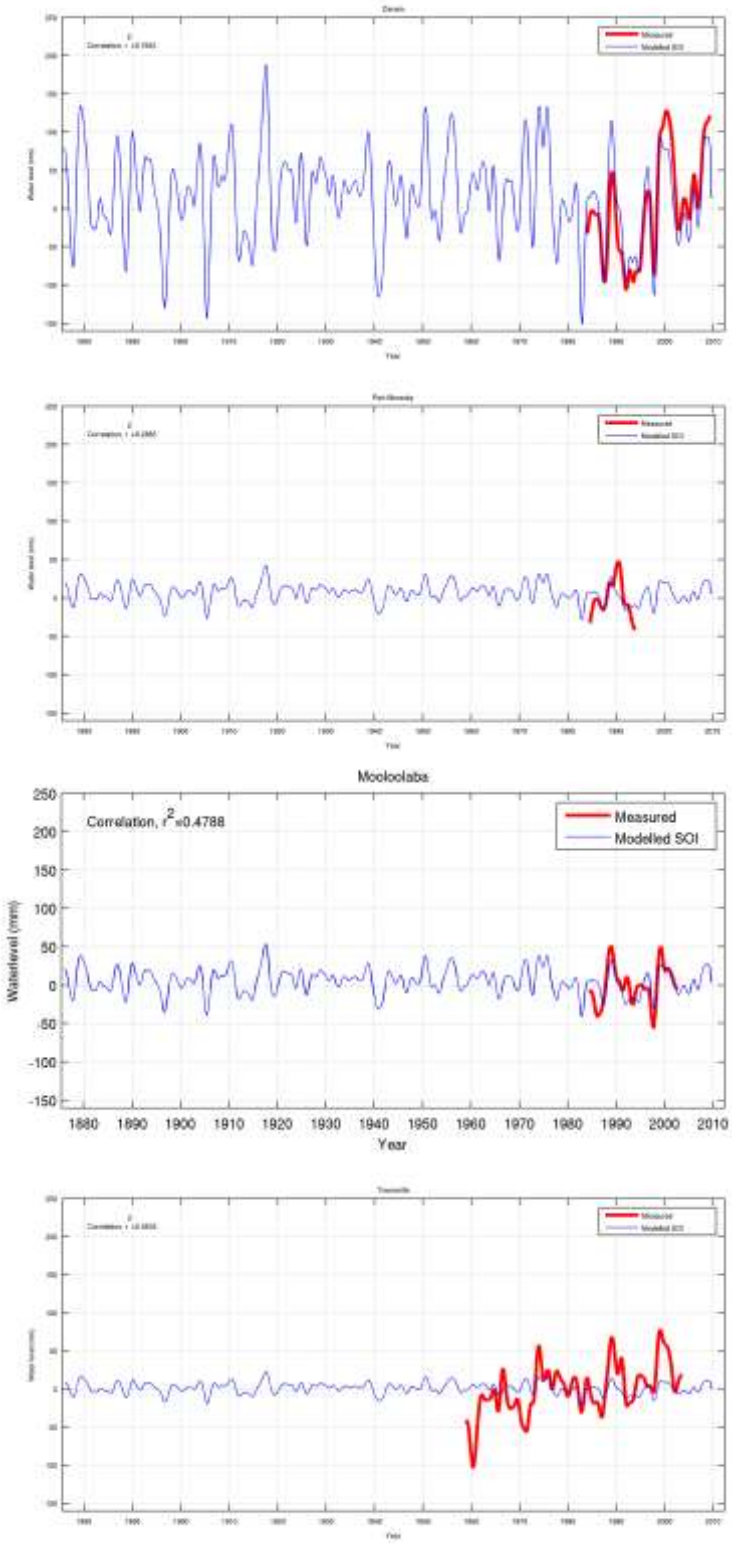

Figure 5-4 The GCCS modelled SOI-driven water level.

Table 5-1 summarises the model site-specific performance in terms of an r^2 statistic and also a linear correlation slope *s*. Figure 5-5 shows these results graphically, indicating a generally high level of correspondence, especially to the longer term AMSA gauges located in open water. The *s* value is typically slightly less than unity, which shows a tendency for the model to slightly overpredict the measured water levels. Due to the significant tidal gradients, gaps in the bathymetric accuracy and the influence of the seasonal features on the shorter period measurements, agreement is not ideal at all locations. Appendix F provides more detailed graphical comparisons of model and measured data at each of the gauge sites for the interested reader.

Table 5-1 Comparisons between raw measured and modelled water levels at tide gauge locations.

Station Name	Source	Longitude Station	Latitude Station	r^2	s	comment
				Raw Water Levels		
Badu Island (GU)	GU	142.1681	-10.1701	0.935	1.019	35d
Boigu Island (GU)	GU	143.4060	-9.7507	0.903	0.854	35d
Booby Island (AMSA)	MSQ	141.9167	-10.6000	0.939 0.959	0.960 0.984	39 y (with gaps) last 9y
Coconut Island (GU)	GU	143.0640	-10.0493	0.954	0.984	35d
Darnley Island (GU)	GU	143.7601	-9.5975	0.972	0.996	35d
Goods Island (AMSA)	MSQ	142.1667	-10.5667	0.926 0.943	0.981 1.002	35y (with gaps) last 9y
Hammond Island (GU)	GU	142.2194	-10.5614	0.940	0.930	35d
Ince Point (AMSA)	MSQ	142.3167	-10.5000	0.919 0.933	0.982 1.004	38y (with gaps) last 9y
Mabuiag Island (GU)	GU	142.2013	-9.9512	0.905	0.959	35d
Murray Island (GU)	GU	144.0397	-9.9150	0.964	1.025	35d
Nardana Patches (AMSA)	MSQ	142.2500	-10.5000	0.954	0.977	4y
Saibai Island (GU)	GU	142.6136	-9.3800	0.901	0.962	35d
Stephen Island (GU)	GU	143.5469	-9.5048	0.965	0.949	35d
Thursday Island (GU)	GU	142.2216	-10.5861	0.932	0.923	35d
Thursday Island (MSQ)	MSQ	142.2167	-10.5833	0.920	0.895	1 Aug 1983 to 1 Jan 2003
Turtle Head (AMSA)	MSQ	142.2167	-10.5167	0.930 0.932	0.994 0.997	20y (with gaps) last 9y
Warraber Island (GU)	GU	142.8225	-10.2046	0.959	0.935	35d
Yam Island (GU)	GU	142.7663	-9.8997	0.952	0.941	35d
Yorke Island (GU)	GU	143.4016	-9.7489	0.973	0.940	35d

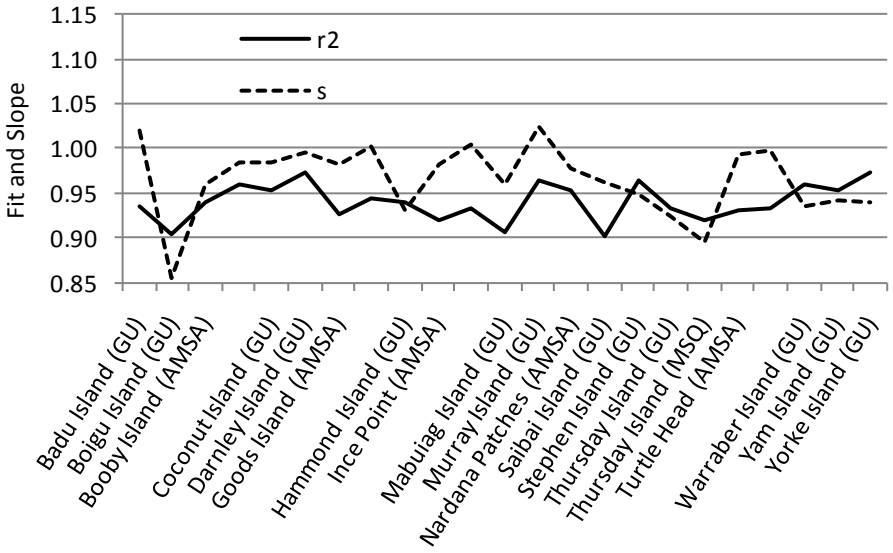

Figure 5-5 Torres Strait model summary error statistics.

The final aim of the project is to produce water level statistics (e.g. the 100 y Return Period ocean water level) for the various island communities and, to ensure the model is performing correctly, tests are done to verify that the broadscale water level statistics are well represented. To achieve this, the statistics of the total 60 y of simulated broadscale water levels are compared with the statistics of the long term well-exposed tide gauges such as Booby Island, Goods Island, Round Island, Turtle Head and Ince Point. These are presented in Figure 5-6 and Figure 5-7, where the blue lines are the frequency-ranked *measured* extreme annual water levels for each gauge, with data periods of between 20 and (almost) 40 years as per Table 4-1. The green line is then the 60 y ranked *modelled* extreme water levels.

At Booby Island and Goods Island, the more westward sites, the blue and green curves are reasonably sympathetic, but with the green 60 y sample showing increased amplitude over the shorter gauge record. This is not unreasonable given the different record lengths and the results are quite encouraging that the broadscale effects have been well represented. At the more easterly sites of Turtle Head and Ince Point, the differences between blue and green appear more exaggerated. One possible reason for this is that the tide variability in the vicinity of these eastern sites is particularly high, with even small errors in location accuracy (of the order of 1 km) capable of modifying these results.

We note at this point that the astronomical tide and weather driven water level variations are largely independent: one is driven by gravity and the other by input from solar energy. Additionally the tide is largely predictable into the past and future given an accurate analysis of the tidal constituents.

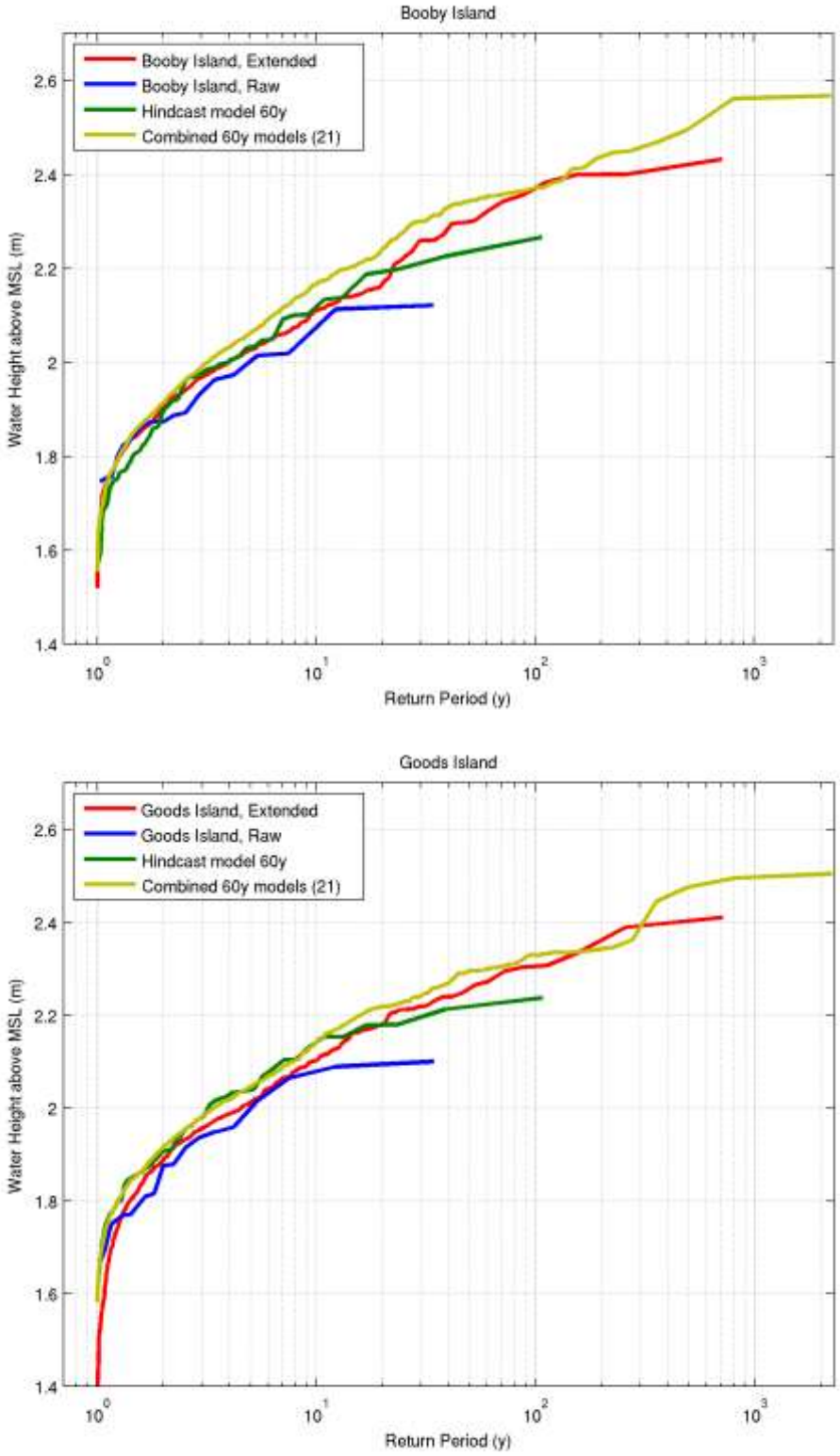

Figure 5-6 Simulated broadscale water levels based on tide gauge residuals – Booby Island and Goods Island .

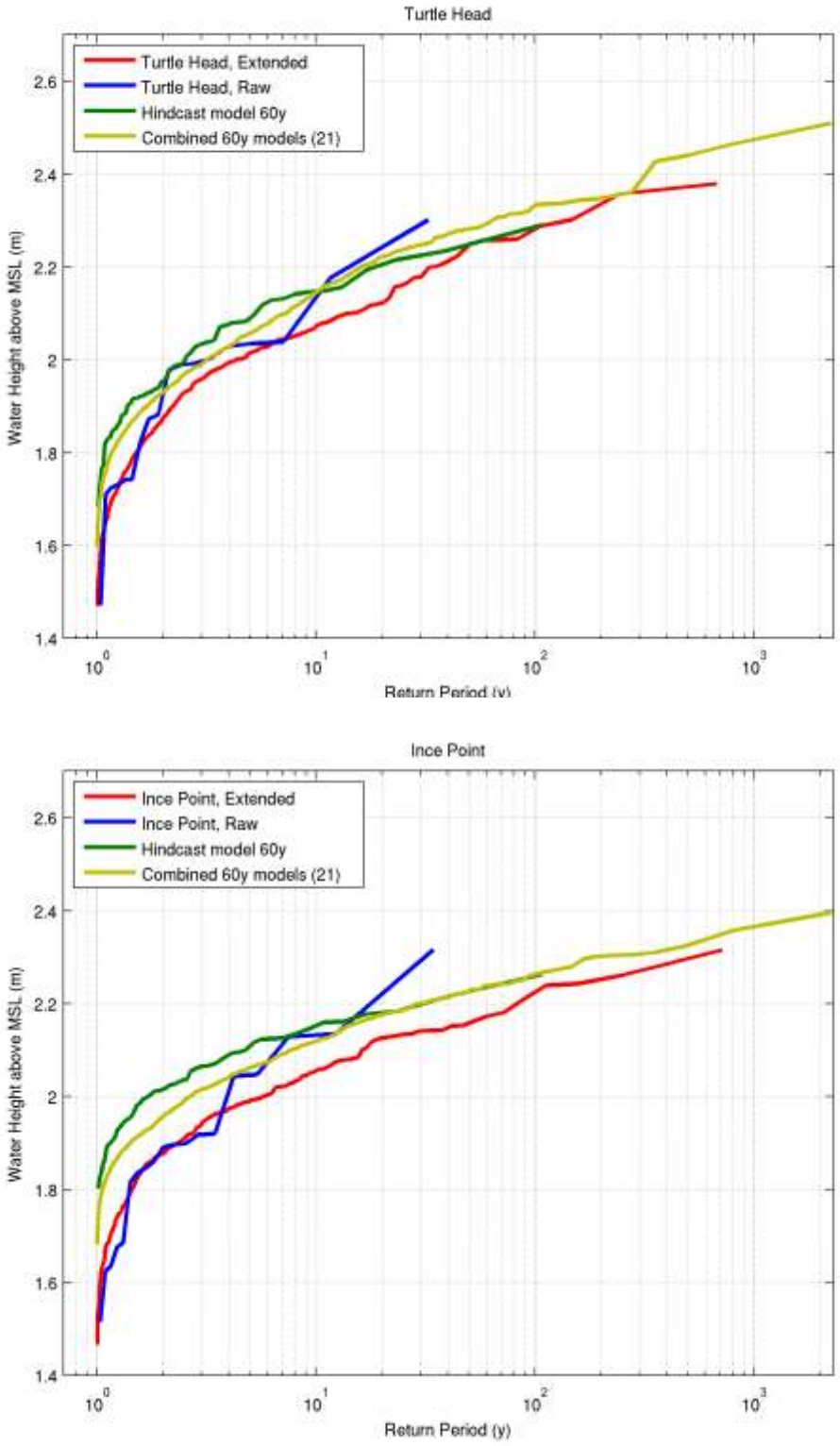

Figure 5-7 Simulated broadscale water levels based on tide gauge residuals – Turtle Head and Ince Point.

This intrinsic independence of water level components and the predictability of the tide can be used to extend the water level statistics by recombining the residual water level (e.g. Figure 4-2) with “new” tides. Although independent, the water level components do have some correlations that must be treated correctly in the recombination process. The residual water levels have a strong seasonal signal which must be aligned with the tidal maxima whose envelope also show an annual variation. This correlation can be accounted for by combining the two components in yearly lots where the seasonal phasing is retained.

Additionally, where a strong semi-diurnal spring-neap cycle is present the highest tides occur near the same time of day due to the solar locked S_2 constituent. To ensure that any peak in the residual water level component is matched with a variety of tides a small random perturbation in the time of the residual signal is introduced. Here we use a random offset of ±1 week, which does not affect the seasonality of the signal.

Therefore, in order to account for the tidal variability influencing these comparisons, the raw data residuals (e.g. Figure 4-2) have been combined with 20 alternate tide sequences (annually locked) to create a re-sampled record approximately equivalent to a 700 y sample (red lines).

A similar process is applied to extend the modelled statistics given that there is only 60y of NCEP wind and pressure available. Here the GCCS and TS models are re-run a further 20 times. For each instance of the GCCS model the SOI-derived inter-annual boundary water levels are offset by 3 years from each other, beginning at the start of the SOI signal. The TS models are then run with differing tides, giving a total synthetic water level record of $21 \times 60 = 1260$ y (yellow line).

The re-sampling procedure used to extend both the model and measured statistics reduces the statistical uncertainty, at the lower return periods, associated with short records. The comparison between the yellow and red line return period slope and bias is then quite compelling at all sites, with maximum differences of the order of 0.05 m. The fit at Goods Island is particularly close.

Based on this verification of concept, modelled return period curves for broadscale water levels can be produced for each point in the TS model domain, This then allows mapping of the estimated broadscale water level return periods across the Torres Strait, as shown in Figure 5-8 for the 10 y and 100 y return period. These patterns can be seen to generally follow the base tidal amplitude pattern (e.g. Figure 4-5) but are further modulated by the applied broadscale forcing patterns. Note that the above statistics are produced relative to the modelled mean water level (MWL) and therefore can be added to the local MWL to produce water levels relative to a local datum.

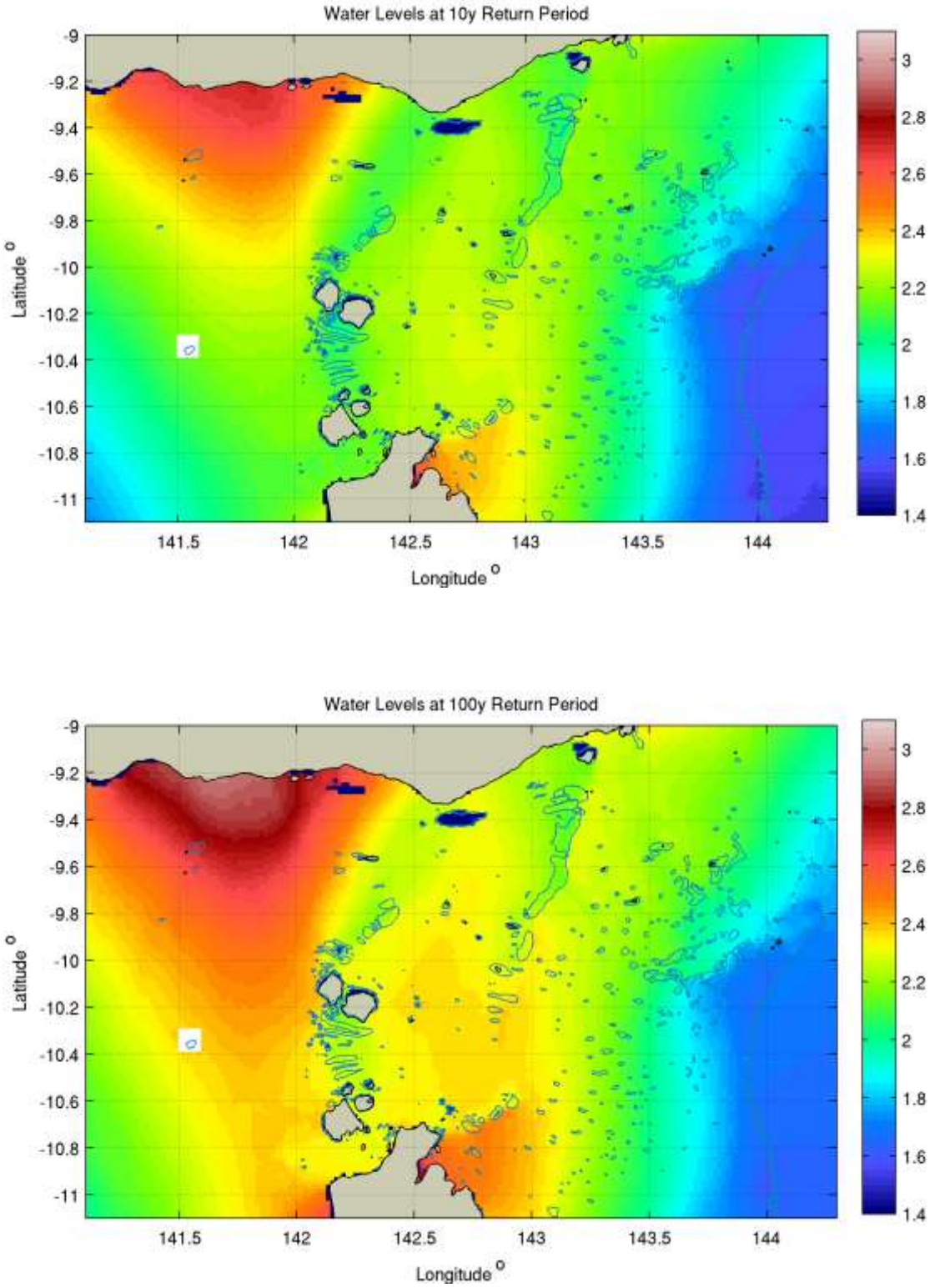

Figure 5-8 Simulated broadscale return period water levels.

Also of significant interest is the mean water level across the region. Unfortunately the model derived MWL, which is shown in Figure 5-9, still does not represent the “true” MWL. This is because the western and eastern boundaries are independent (not connected) and not part of a global model. To assess the veracity of this result, public domain analyses from the OCCAM[10] global ocean model were obtained for comparison with the TS model (refer Figure 5-10). The OCCAM model, due to its coarse resolution, cannot be expected to adequately model the steep tidal gradients within the Strait but, in this more expansive view, shows how it depicts ocean dynamical effects on the mean sea level in the Coral Sea. Because the two models have different intrinsic mean level datums we can only usefully compare the water level gradients with the present study and the colour scales have been chosen to assist in this.

Although the models have significantly different resolution and detailed physics, the results show good matching in the western region. However there are differences in the northern and eastern domains where a lack of data precludes better closure here. Both show the relative super-elevation of the MWL in the vicinity of the centre of the Strait of ~0.1 m. The output from this broadscale modelling is then used as input to the combined broadscale and local TC forcing in Section 11.

5.5 Potential Future Climate Change

This has been limited to consideration of future changes in MSL only, whereby it is implicitly assumed that the tidal characteristics will not alter significantly (relative to the current uncertainties) by the year 2100.

5.5.1 Potential Changes in Mean Sea Level (MSL)

The principal reference in this regard is IPCC (2007), also known as “Assessment Report 4” or “AR4”. CSIRO (2007) provides some specific model details of projected sea level rise around Australia, showing a tendency for slightly above-global-average values across northern Australia. However, it is stated that the reliability of regional projections of sea level rise is poor and no specific recommendations are available from CSIRO. Accordingly, nominal values of maximum expected sea level rise have been adopted here of +0.30m by 2050 and +0.80m by 2100. These are similar to values adopted by the Queensland Government (e.g. DERM 2009) and earlier recommendations from Engineers Australia (NCCOE 2004).

[10] http://gcmd.nasa.gov/records/GCMD_OCCAM.html

5.5.2 Potential Changes in Regional Wind Forcing

The available advice (CSIRO 2007, IPCC 2007) in regard to potential changes in regional mean wind speed and direction, ENSO and other broadscale forcing was considered either of minor significance compared with the modelling assumptions here or too qualitative to usefully incorporate into the analysis.

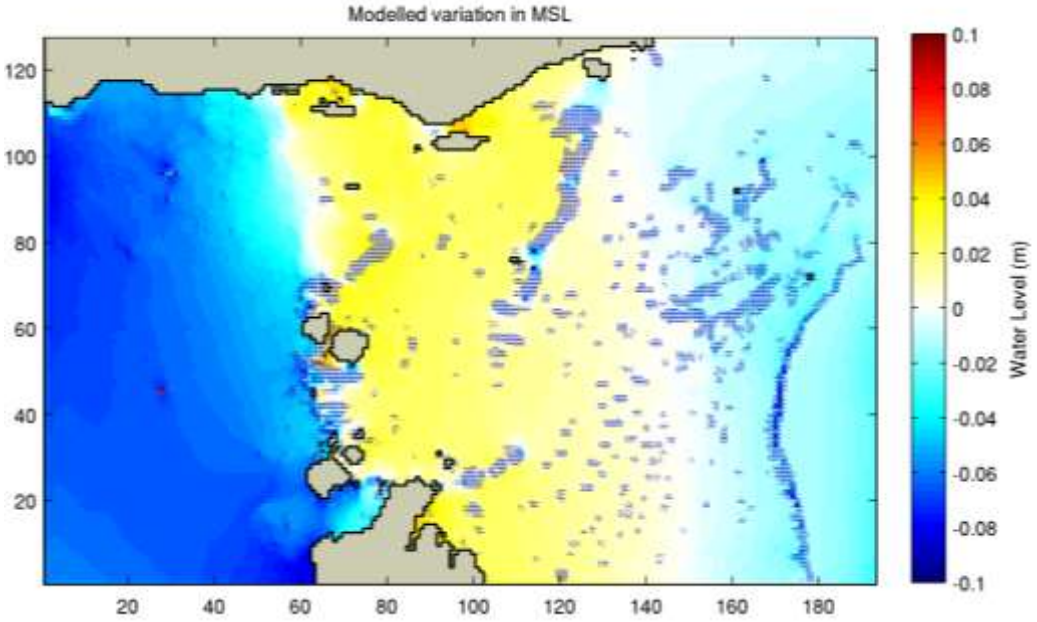

Figure 5-9 The TS model variation in the mean water level over 60 yr.

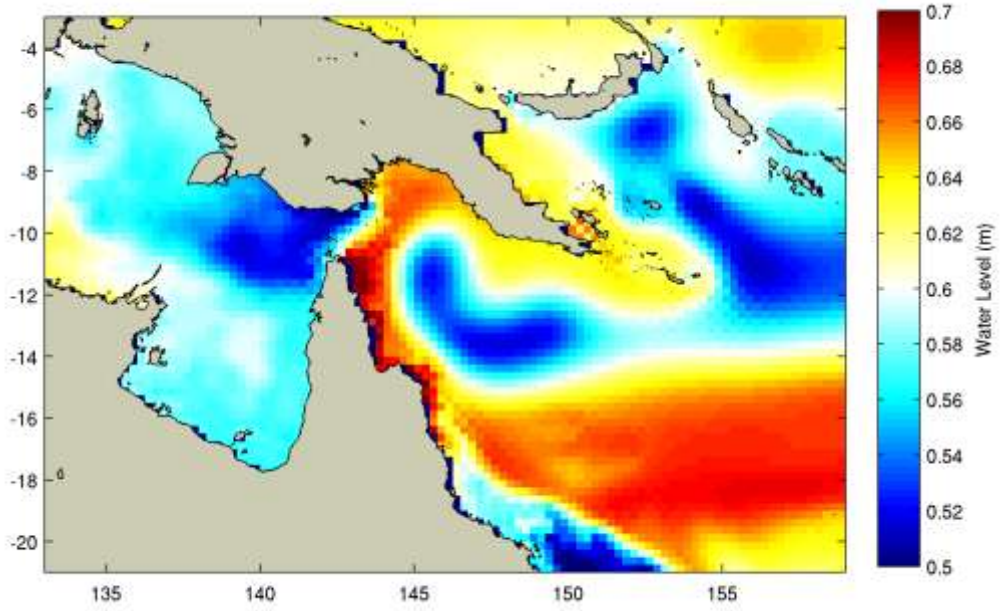

Figure 5-10 The OCCAM global model regional mean water level.

5.6 Deterministic Validation of the Broadscale Hydrodynamic Model

This has been undertaken with regard to reproducing the well documented broadscale influence of TC *Charlotte*, which although it was named as a TC, was a very large scale low pressure circulation of modest intensity located in the southern Gulf of Carpentaria as shown in Figure 5-11. Appendix H has more details of this event, which lasted for several days while the centre moved to the south-east. The circulation was so broad that much of the east coast of North Queensland was affected and even Townsville experienced elevated ocean levels that rivalled the storm tide produced by TC *Althea* in 1971 (e.g. Harper et al. 2001).

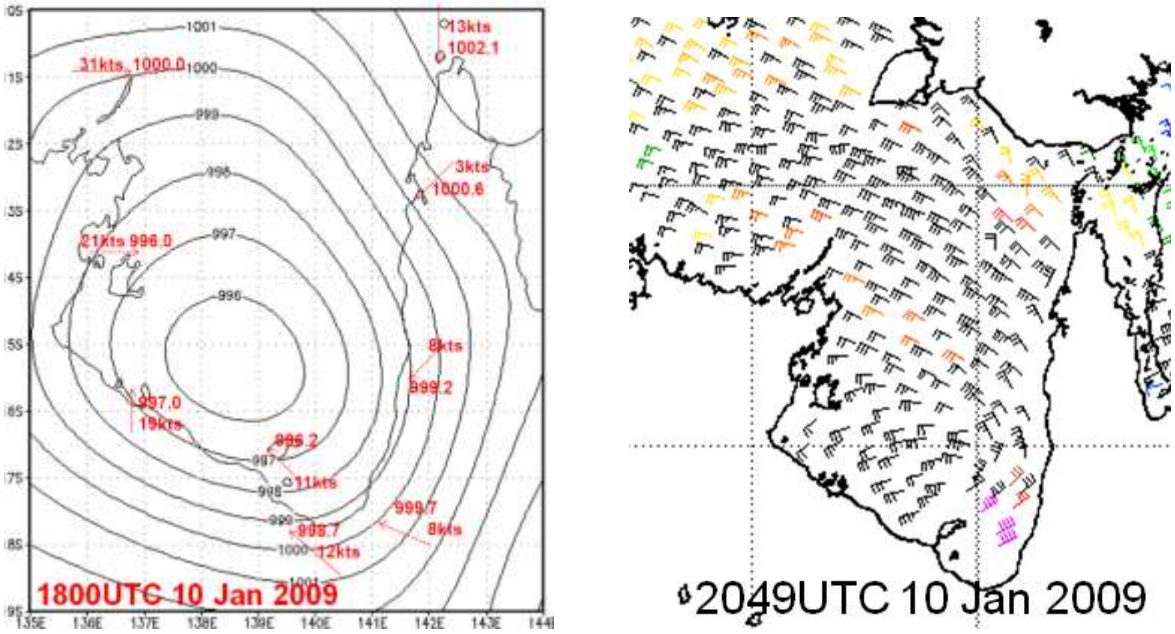

Figure 5-11 US-NOAA high-resolution modelled MSL pressure (left) and QuikSCAT satellite surface measured winds during TC *Charlotte*.

The results of hydrodynamic modelling of this event are shown in Figure 5-12, being an extract for this period from the 60 y long-term regional broadscale modelling that uses the coarser resolution NCEP winds. The modelled values are compared with the measured water levels from the AMSA tide gauges and show that the peak levels near the 11th Jan are well-matched, although there are some slight under predictions over the several days prior to and after the TC *Charlotte* event. This comparison confirms that the NCEP-resolution winds, in partnership with the model extent, bathymetry, wind stress and other physics assumptions, are well capable of representing these regional broadscale events.

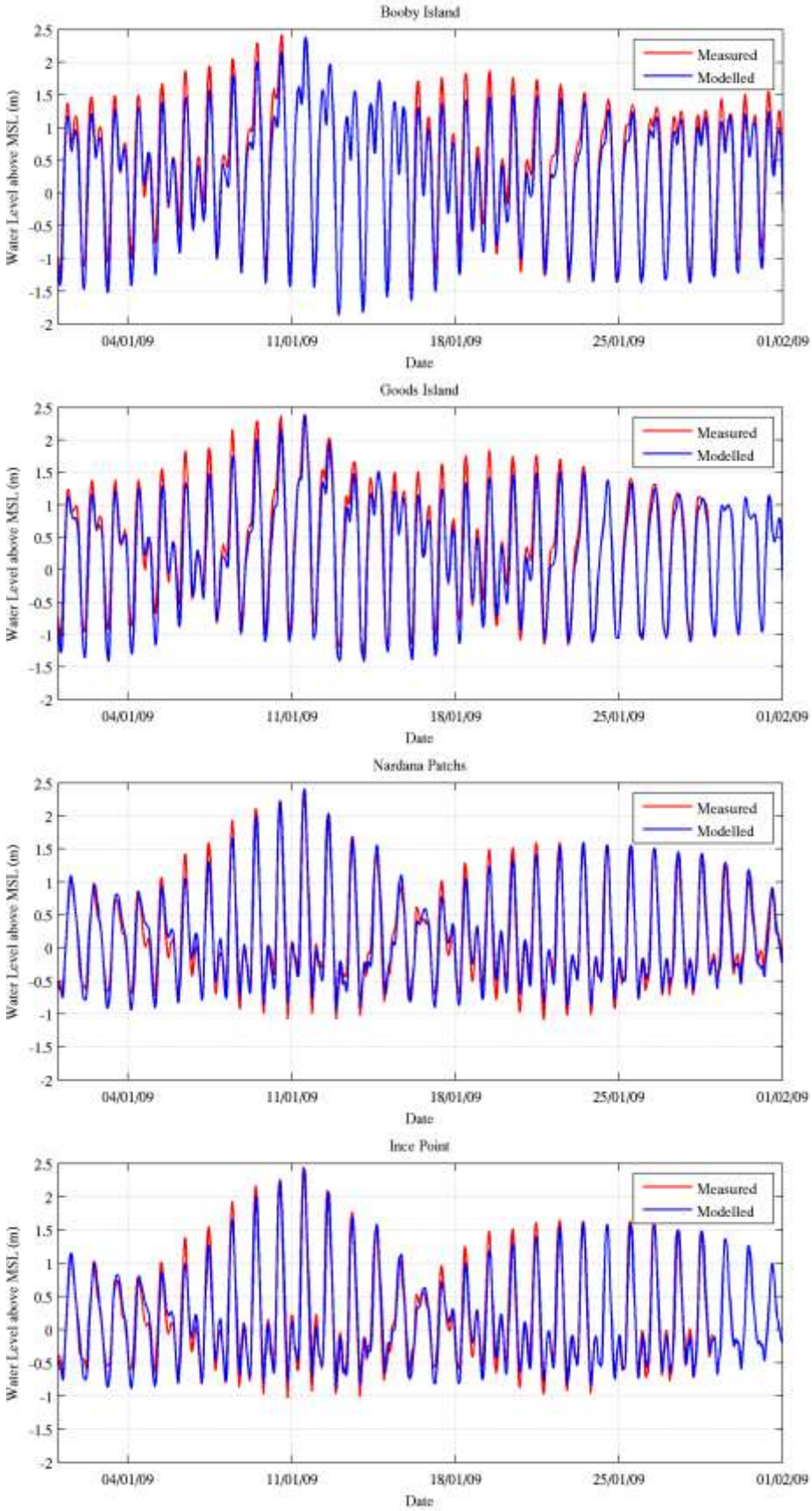

Figure 5-12 Modelled versus measured hydrodynamic response to TC *Charlotte* in Torres Strait.

6. Tropical Cyclone Climatology

TCs are the most energetic of the regional weather systems and represent the more significant source of life-threatening inundation episodes if they make a close approach. However, existing historical records suggest that the regional threat is relatively low and has even markedly decreased during the past 50 years. Notwithstanding this, it is known that the historical record of TC intensity is subject to a variety of limitations (e.g. Harper et al. 2008) and a selective review of the intensity and scale of TCs likely to have affected the Torres Strait area, directly or indirectly, has been undertaken. Appendix G provides details of this work while Appendix H provides a compendium of historical TC events in North-Eastern Australia assembled by Mr Jeff Callaghan.

6.1 Definitions

The TC is a large scale and potentially very intense tropical low pressure weather system that can affect the Torres Strait region typically between November and April (SEA 2005). In Australia, such systems are upgraded to *severe* tropical cyclone status (referred to as *hurricanes* or *typhoons* in some countries) when average, or so-called sustained, surface wind speeds exceed 120 km h^{-1}.

The accompanying shorter-period destructive wind gusts are higher still, up to 20% in the open ocean and often 50% or higher over land (Harper et al. 2010). In the southern hemisphere, TC winds circulate clockwise around the centre, as seen in the spiral cloud patterns of the satellite image of severe TC *Ingrid* in Figure 6-1.

There are three components of a TC that combine to make up the total storm hazard - strong winds, intense rainfall and induced ocean effects, including extreme waves, currents, storm surge and resulting storm tide. The destructive force of TCs is usually expressed in terms of the strongest wind gusts likely to be experienced. Maximum wind gust is related to the central pressure and structure of the system, whilst extreme waves and storm surge, are linked more closely to the combination of the *mean* surface winds, central pressure and regional bathymetry.

The Commonwealth Bureau of Meteorology (BoM) uses the five-category system shown in Table 6-1 for classifying TC intensity in Australia. Severe TCs are those of Category 3 and above.

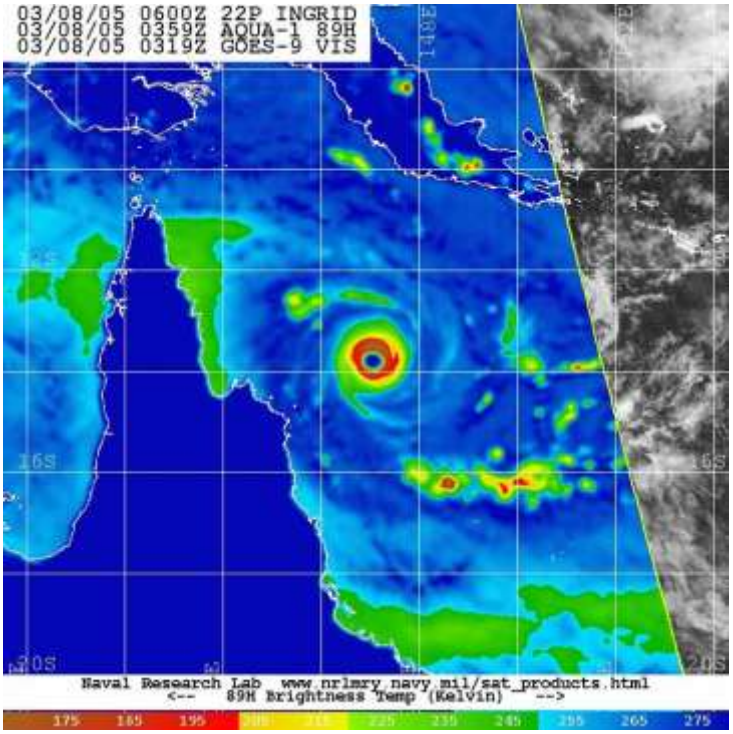

Figure 6-1 Severe tropical cyclone *Ingrid* approaching Cape York when at estimated Category 5 intensity in March 2005. (US Navy processed image)

Table 6-1 Australian tropical cyclone category scale.

Category	Maximum Wind Gust ($km\ h^{-1}$)	Potential Damage
1	<125	minor
2	125-164	moderate
3	165-224	major
4	225-279	devastating
5	>280	extreme

The main structural features of a severe TC at the earth's surface are the eye, the eye wall and the spiral rainbands. The eye is the area at the centre of the storm at which the surface atmospheric pressure is lowest. It is typically 20 to 50 km in diameter, skies are often clear and winds are light. The eye wall is an area of cumulonimbus clouds, which swirls around the eye. Tornado-like vortices of even more extreme winds may also occur associated with the eye wall and outer rain bands. The rain bands spiral inwards towards the eye and can extend over 1000 km or

more in diameter. The heaviest rainfall and the strongest winds, however, are usually associated with the eye wall.

For any given central pressure, the spatial size of individual TCs can vary enormously. Generally, smaller storms occur at lower latitudes and larger storms at higher latitudes, but there are many exceptions. Large TCs can have impacts far from their track, especially on waves and storm tide.

Cyclonic winds circulate clockwise in the Southern Hemisphere and the wind field within a moving TC is generally asymmetric so that winds are typically stronger to the left of the direction of motion of the system (the "track"). This is because on the left-hand side the direction of storm movement and circulation tends to act together; on the right-hand side, they are opposed. During a coast crossing in the Southern Hemisphere, the wind direction is onshore to the left of the eye (seen from the storm) and offshore to the right.

Given specifically favourable conditions, TCs can continue to intensify until they are efficiently utilising all of the available energy from the immediate atmospheric and oceanic sources. This maximum potential intensity (MPI) is a function of the climatology of regional sea surface temperature (SST) and atmospheric temperature and humidity profiles. Thankfully, it is rare for any storm to reach its MPI because environmental conditions often act to limit intensity development in a region.

6.2 TC Climatology Analyses

A number of aspects of the TC climatology were examined in order to develop a sound basis for understanding of the regional threats and how to best represent their impacts on extreme water levels.

6.2.1 Base Tropical Cyclone Dataset

The SEA proprietary TC dataset for Australia forms the basis of the climatology assessment. This dataset was originally compiled from a variety of BoM sources in the mid-1980s and has been continuously updated and corrected since that time as a result of many separate TC risk studies (e.g. Harper 2001), with corrections made in consultation with BoM Regional Office staff in Brisbane, Darwin and Perth. The errors and omissions discovered were provided to BoM over time and this assisted the ongoing improvement of the official best track database. The types of errors and omissions typically discovered over time included:

- Missed storms;
- Duplicate storms;
- Incorrectly named storms;

- Incomplete tracks;
- Miss-classified systems (east coast lows etc);
- Typographical errors.

The dataset was firstly updated to include all official BoM storm tracks up until 2008/2009 and an illustration of the pattern of TC tracks in the region is given in Figure 6-2.

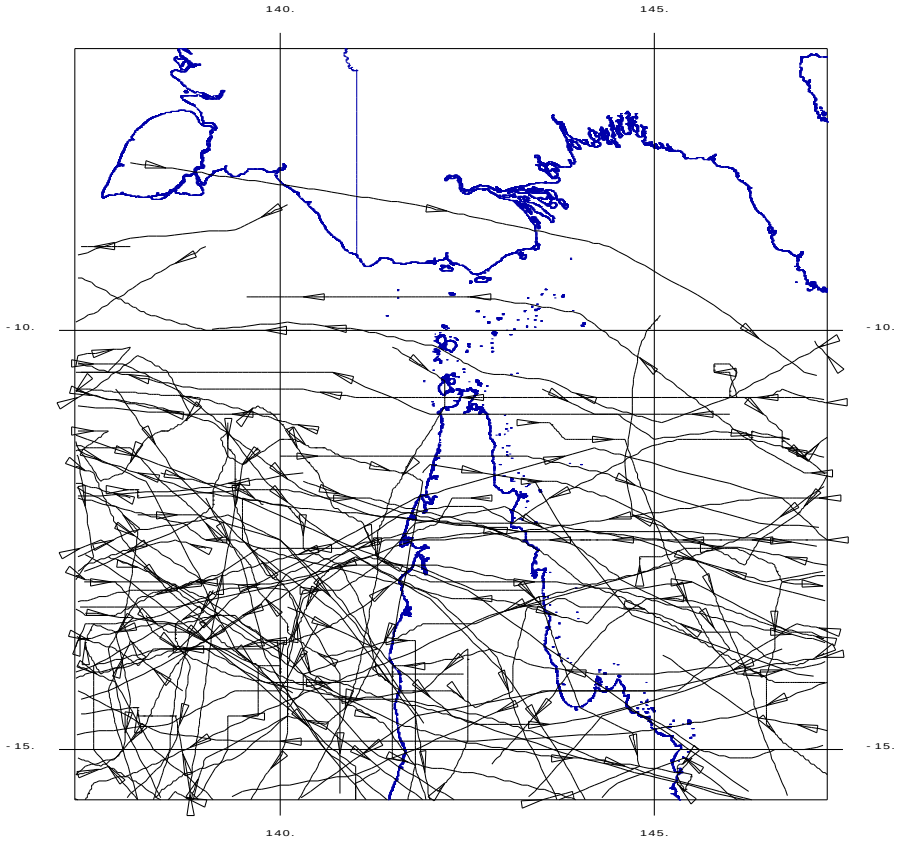

Figure 6-2 Tropical cyclone tracks within 500 km of Thursday Island for the 50 year period 1959/60 to 2008/09.

6.2.2 Review of Historical Tropical Cyclones in the Region

A review of the more significant historical TCs in the region was then undertaken by sub-consultant Mr Jeff Callaghan[11] to provide increased confidence in the statistical foundation for the climatology analysis.

Justification

A major justification for the review is the knowledge that, over time, there have been changes in the operational procedures applied in BoM

[11] Former Senior Forecaster and Manager of the Severe Weather Section in Brisbane.

to the estimation of TC intensity (e.g. as documented by Harper 2002, 2004b, Harper and Callaghan 2006, Harper et al. 2008). These changes have resulted mainly through increasing knowledge and skill in the use of the Dvorak TC intensity analysis system (Dvorak 1984, Velden et al. 2006) that relied solely on satellite cloud patterns prior to 1984, but later included more objective satellite-derived infra-red cloud-top temperatures. Without the benefits of aerial reconnaisaance, such as available in the USA, this method is still the principal means of estimating TC intensity in Australia and throughout the world.

In the Dvorak analysis method the so-called tropical T number is taken directly from the satellite cloud features and has a dynamic range of 1.0 through 8.0 (the most intense rating). The T number is adjusted according to a series of ancilliary rules and eventually is converted into a measure of the peak surface wind speed in the storm. The Dvorak analysis system was developed with a constraint on the rate of intensification of a storm to better match the original observations that were available for its development (circa 1972). For example, for a storm with an initial T number greater than 4.0 the method limits the change in T number to 1.0 in 6 h, 2.0 over 18 h and 2.5 in 24 h. Where the T number is initially less than 4.0 the rate of change is limited to 0.5 over a 6 h period. Increasingly however, greater rates of change in T numbers have been observed over time with the benefit of better satellite coverage and higher temporal and spatial resolution. Accordingly the basis for this constraint has been widely questioned and, based on recent objective studies, is recommended to be abandoned in the future (Knaff et al. 2010). This factor is especially relevent to northeastern Australia because many population centres are located adjacent to the monsoon trough, where rapid tropical cyclogenesis can occur and this feature may not have been detected sufficiently frequently in the historical context.

Well-documented Rapid Intensification Examples

Examples of rapid cyclogenesis near a large population centre in Australia include TC *Celeste*, which formed just off the north Queensland coast near Townsville, and TC *Rona*, which formed near Cairns. Both reached severe TC intensity (maximum average winds over a 10 min period reaching at least 65 knots) 12 and 15 h after formation, respectively resulting in T number increases of 2.5 in 12 h whereas for such systems the T number increase is technically limited to 0.5 increments every 6 h.

A study of reconnaissance data by Holliday and Thompson (1979) indicated that 75% of all western North Pacific TCs deeper than 920 hPa have experienced a period of rapid intensification of 42 hPa per day or more. Extreme deepening rates of nearly 100 hPa per day have been observed which would be equivalent to four T numbers per day. More recently, the central pressure of Hurricane *Rita* (September 2005) deepened 70 hPa in 24 h. The largest 6, 12 and 24 h drops in best track

central pressure for Hurricane *Wilma* (October 2005) were 54, 83 and 97 hPa, respectively. The central pressure of Hurricane *Charley* (2004), as measured by US reconnaissance aircraft, reduced from 969 hPa to 947 hPa (22 hPa change) in a 6 h period (about 1.5 T numbers)[12]. Near landfall, a reconnaissance aircraft observation within Hurricane *Gabrielle* (Molinari et al 2006), experienced a 20 hPa pressure fall over the preceding 3 h. Likewise, in a recent paper Reasor et al. (2009) show, using recconnaisanse data, that the rapid intensification of a hurricane was associated with a burst of eyewall convection to which the hurricane quickly responded.

In Fiji during April 2004 forecasters were unprepared when a severe TC developed within a 5 h period. The sequence of enhanced infrared satellite imagery shown in Figure 6-3 (the black circle marking the location of Nadi) shows the left-most (earliest) image showed no evidence of a developing TC beneath the cloud. Five hours later (centre image) there was the familiar image of a dense central overcast associated with a developing TC. This system moved across Fiji (northern part of the island of Viti Levu) on 8th April and caused severe flooding in the country and destructive winds, severe damage, and with around 20 lives lost. This was a very small storm system that proved quite difficult to track until it moved within the range of the Nadi radar. The minimum central pressure recorded there was 990hPa and one of the automatic weather stations in Fiji reported sustained winds of 43 knots before loss of data. Meanwhile, numerical weather models failed to forecast the development of this system.

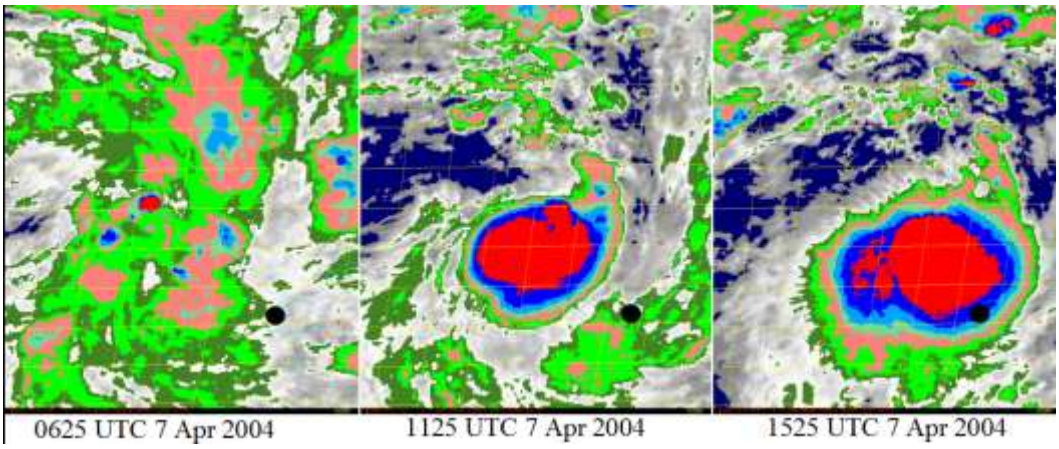

Figure 6-3 Enhanced infrared satellite imagery during the rapid intensification of an unnamed tropical cyclone near Fiji in April 2004. The green encloses areas with temperatures colder than -30 ^{0}C grading to -80 ^{0}C in the red areas (indicator of a cloud structure of an intense storm system).

[12] NOAA National Hurricane Center reports; http://www.nhc.noaa.gov/pastall.shtml

Review Methodology and Outcomes

Due to the scarcity of objective wind, pressure and storm tide measurements – even today – it can be difficult to accurately assign a TC intensity. However, as demonstrated by the extensive incidence of impacts (Appendix H) it is highly likely that many storm strengths were underestimated. On this basis, the historical dataset within the Gulf of Carpentaria / Cape York / Torres Strait region was scanned to identify potential rapid intensification situations that had probably not been identified at the time of the forecasts and subsequent "best track" post-analyses.

A total of 10 storms have been considered in the review, nine of which resulted in modifications to the official intensity estimates (increases), and the other is a new track estimated for a known impact storm event in December 1952 that does not exist in the official database. The tracks of these storms are provided in Figure 6-4, while Appendix G contains the individual storm reassessments and Table 6-2 provides a summary of the changes.

Table 6-2 Summary outcome of the historical TC review.

Storm	Radius from Thursday Island	Revised Maximum Intensity		Resulting Intensity Change	
	km	UTC	hPa	hPa	%
Torres_Strait_1952	51	01-Dec-1952 12:00	982		
Dora_1964	447	02-Feb-1964 23:00	955	-19	59
Flora_1964	659	05-Dec-1964 11:00	955	-37	264
Fiona_1971	466	19-Feb-1971 05:00	925	-38	88
Ted_1976	170	18-Dec-1976 11:00	930	-30	65
Dominic_1982	132	07-Apr-1982 09:00	920	-30	54
Felicity_1989	648	15-Dec-1989 12:00	965	-20	95
Ivor_1990	347	19-Mar-1990 12:00	930	-50	192
Nina_1992	264	25-Dec-1992 12:00	975	-5	19
Agnes_1995	223	18-Apr-1995 12:00	945	-20	49

Based on the above, it can be seen that most of the storms that have been adjusted through this review process made landfall on Cape York several hundred kilometres away from Torres Strait. The one exception is the added 1954 event which is estimated to have passed much closer. The tabulated changes in the central pressures are quite significant, especially for Flora_1964 and Ivor_1990, and collectively the adjustments do influence the regional statistics, as shown in the central

pressure return period plot of Figure 6-5 that compares the official BoM central pressures with the modified dataset developed here.

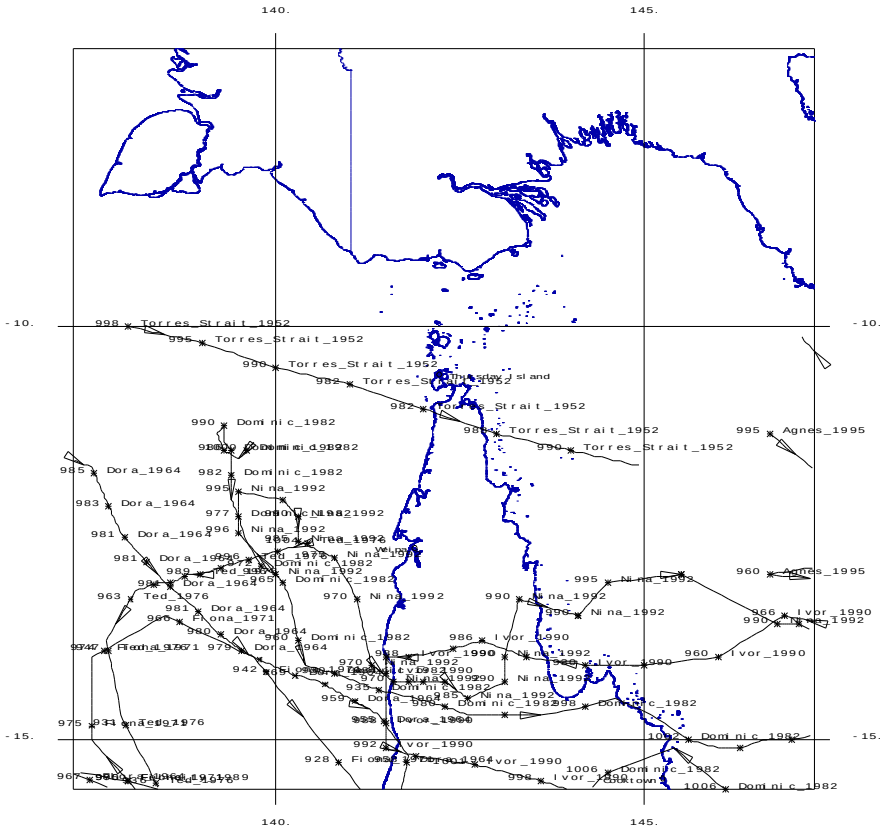

Figure 6-4 Tracks of the 10 historical storms that were considered in the review.

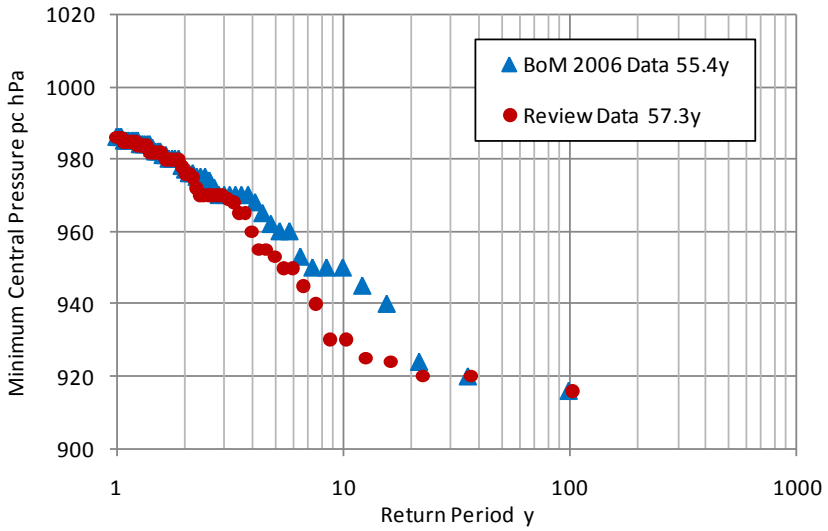

Figure 6-5 Statistical comparison of the alternate intensity estimates using data since 1951/52 and within an 800 km radius of Thursday Island.

6.2.3 Consideration of Regional Synoptic Patterns Influencing Tropical Cyclone Formation, Movement and Intensity

The tracks of TCs in the Torres Strait region are known to be strongly influenced by the persistent background zonal steering patterns (east-west or west-east) and by the relative location of the monsoon trough and the coastline. As a result, the most intense storms tend to move south of Torres Strait.

The more common TC-related scenario affecting water levels is identified as being due to storms located west of Torres Strait or in the Gulf of Carpentaria that are capable of interacting with and enhancing the monsoon influence to the north. Examples of these interactions were used to investigate the possibility of developing a statistical climatology of TC and monsoon interactions and were based on examining selected NOAA/NCEP reanalysed datasets of wind and pressure at various levels in the atmosphere.

Unfortunately it became evident that, although there are significant patterns of interaction that can be identified, it would not be possible to undertake the necessary analyses and develop a robust model of these features within the timeframe available for the study. Accordingly, further investigation of these interactions remains as a recommendation for future work, which might provide a physically-based framework to further fine-tune regional TC risks.

6.2.4 Data Quality Issues and Radius of Influence Analysis

The accuracy and homogeneity of the TC dataset is always of concern when being used as the basis for a statistical analysis. Based on previous studies that have considered the evolution of measurement techniques, the advent of satellite imagery, radars and many other factors, the earliest dependable start date for frequency of occurrence and track data in the Australian region is the 1959/60 season (e.g. Harper 2001, Harper et al. 2008). In regard to intensity estimates, it can be argued that the advent of the Dvorak method circa 1975 was the start of improved consistency in intensity values, although in practice many studies have been compelled to utilise data from 1959/60 onwards in order to obtain sufficiently large datasets for analysis.

It is useful to explore the spatial variability of TC frequency and intensity as a precursor to developing a rational model for simulation purposes and a radius of influence analysis is presented in Figure 6-6. This provides insight into the differences between the full historical dataset comprising all storms since 1906 (but of known inhomogeneity) and only the subset since 1959/60 that is deemed suitably reliable. The analysis shows the minimum central pressure for each historical storm within a given radius of Thursday Island compared with the estimated pressure at closest radius, together with the total storm count.

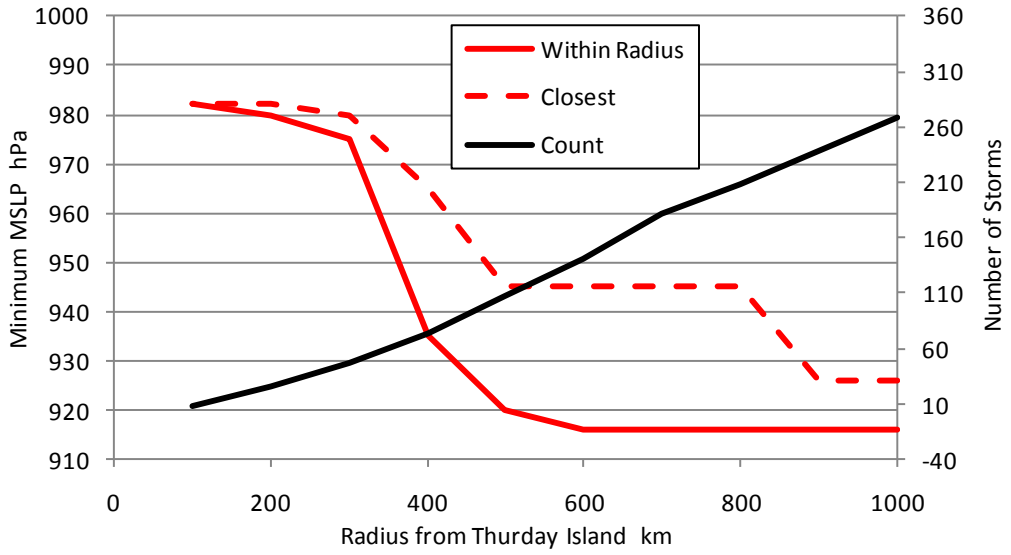

(a) All data since 1906

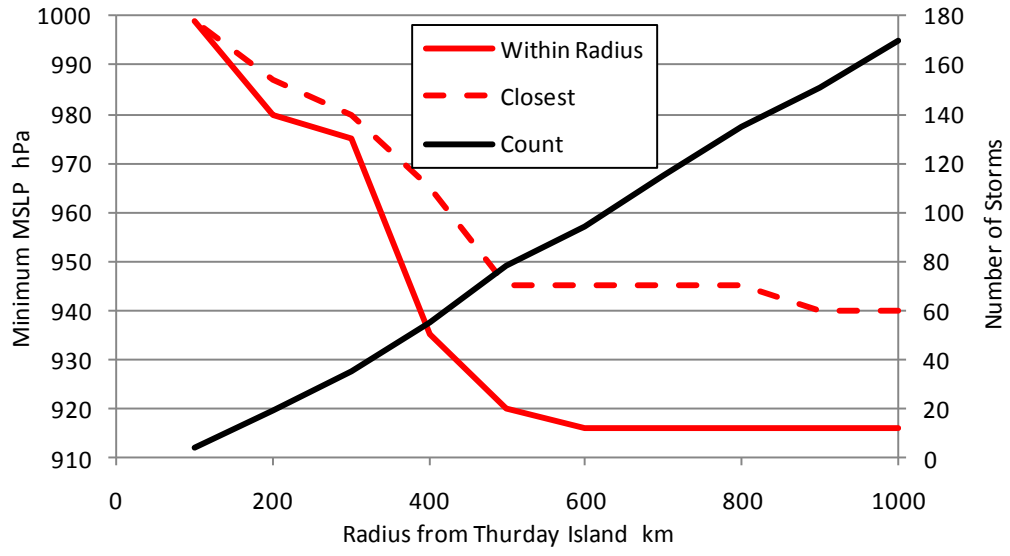

(b) Data for period 1959/60 to 2008/09

Figure 6-6 Summary of radial analysis of TC occurrence and intensity.

The analysis has been done in steps of 100 km radius and the frequency counts show that there are only approximately 50% more storms in the 105 year record as the 51 year record, confirming the anticipated undersampling prior to 1959[13]. However, the graph shows that within a radius of 500 km of Thursday Island, the maximum intensity from both datasets is about 920 hPa. The full dataset also indicates that it contains more intense storms (lower pressures) within 100 km and that the storms beyond 800 km were also more intense in the earlier period.

While it is not appropriate to make too much of these differences, given the uncertainties in the earlier data, it nevertheless seems that the spatial distribution of storm events is relatively homogeneous in a radial extent, and that the maximum intensity will be sampled by taking a radius of about 500 km. Beyond 800 km of course, the influence of the southern extent of the Gulf of Carpentaria becomes limiting.

Taking the post-1959 dataset and analysing the intensity statistics as a function of radius produces the result in Figure 6-7, which shows objectively fitted Extreme Value Type 1 distributions (Benjamin and Cornell 1970) to the datasets.

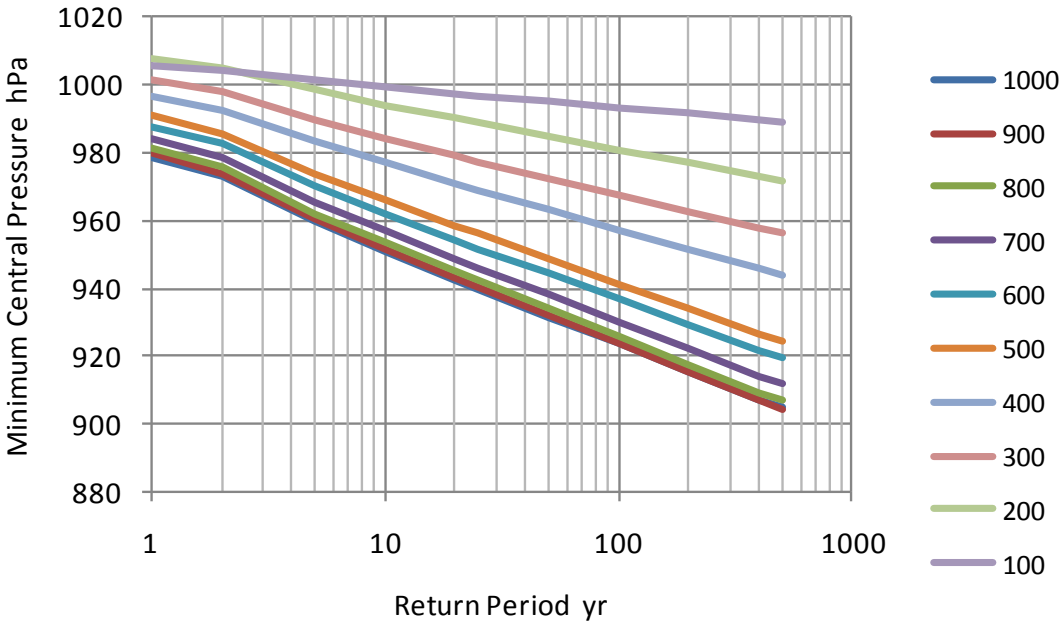

Figure 6-7 Radial-sampling sensitivity of EV analysis of TC intensity.

This graph shows that as the sample size increases with increasing radius, the objectively fitted intensity distributions adjust rapidly, but become much more stable at and beyond the 500 km radius. This result is not intended to be used for simulation purposes (refer later) but is supported by analogous assessment of goodness of fit statistics

[13] This reflects a global issue that had erroneously been attributed by some as a "climate change" signal but is now accepted as a sampling problem (e.g. WMO 2006).

suggesting that the intensity dataset is reasonably well conditioned as EV Type 1 within the 500 km radius.

On these bases, it was decided to adopt a nominal 500 km radius of influence for the statistical analysis of TC risks, albeit noting that the site of interest is located near the northernmost point of the physical TC basin for this region.

6.2.5 Identification of the Principal Tropical Cyclone Parameters

A total of 78 TCs have been registered as occurring within the 50 season record from 1959/60 to 2008/09 and within the 500 km radius study region, averaging 1.56 cyclones per season. The time history of the annual frequency of occurrence is shown in Figure 6-8(a), showing a fluctuation about a 5 year averaged value of between 1 and 2 storms per year. Several years indicate zero storms within the 500 km radius while the maximum number during this time has been up to 5 storms in one season.

The variability in cyclone occurrences over a 3 to 5 year span on the east coast of Queensland (Coral Sea) is known to be strongly associated with the so-called El Niño - Southern Oscillation (ENSO) phenomenon (e.g. Nicholls 1992, Basher and Zheng 2000). ENSO refers to a quasi-biennial oscillation of the sea surface temperatures (SST) in the eastern tropical Pacific Ocean. During a so-called El Niño period, the SST is warmer than normal in the east and rainfall and TC activity in northern Australia tends to decrease. In the reverse situation, called La Niña, the SST in the eastern Pacific is cooler than normal and rainfall and TC activity increases along the east coast of Australia. The Southern Oscillation Index (SOI) is a measure of the strength of the ENSO episodes, derived from surface pressure data at Darwin and Tahiti. The SOI is also plotted on Figure 6-8(a), but there is no strong relationship evident with the storm frequencies. In fact, during the 1970s and 1980s, the storm frequency is highest during the below-average SOI period, which is counter to the normal Coral Sea behaviour.

The corresponding time history of minimum storm central pressures is shown in Figure 6-8(b), illustrating the great variety possible in intensities. The 5 year average line in this case never falls below 980 hPa but it is the extreme intensity values that control the storm tide risk.

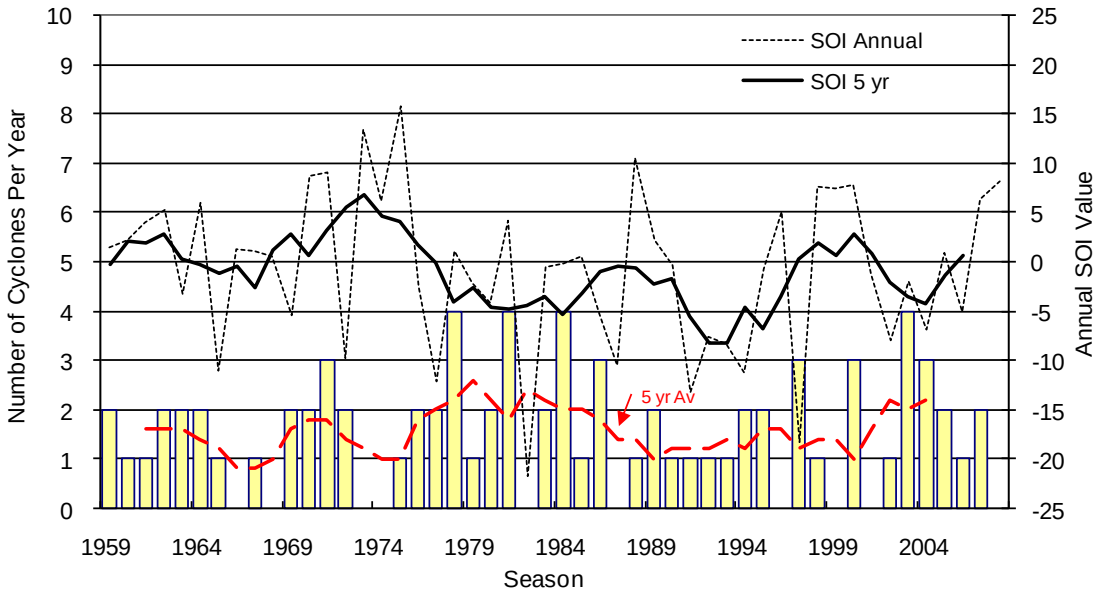

(a) Frequency of occurrence and SOI variation.

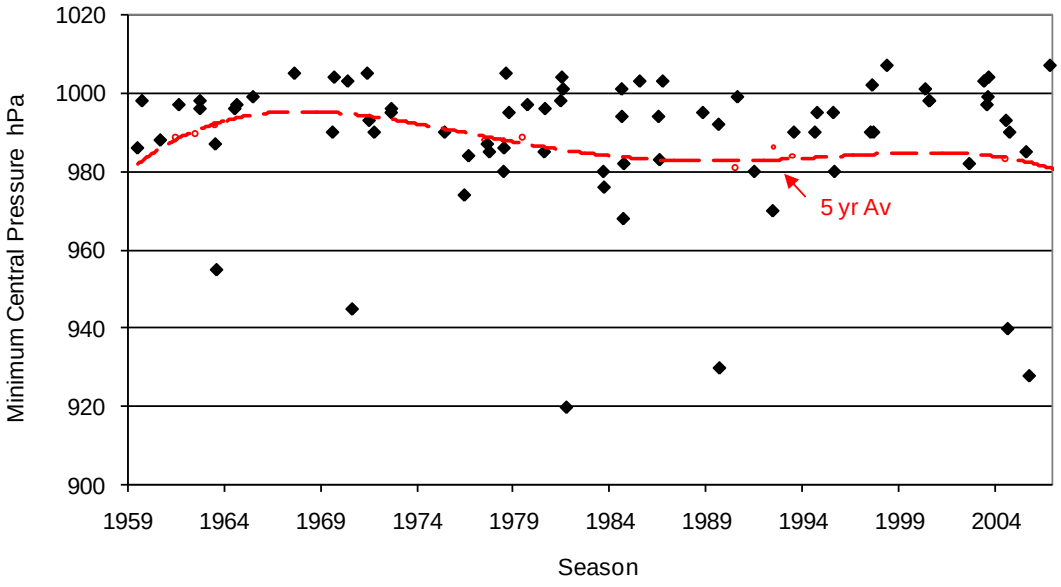

(b) Intensity variation.

Figure 6-8 Time history of TC frequency and intensity from 1959/60 to 2008/09 and within 500 km radius of Thursday Island.

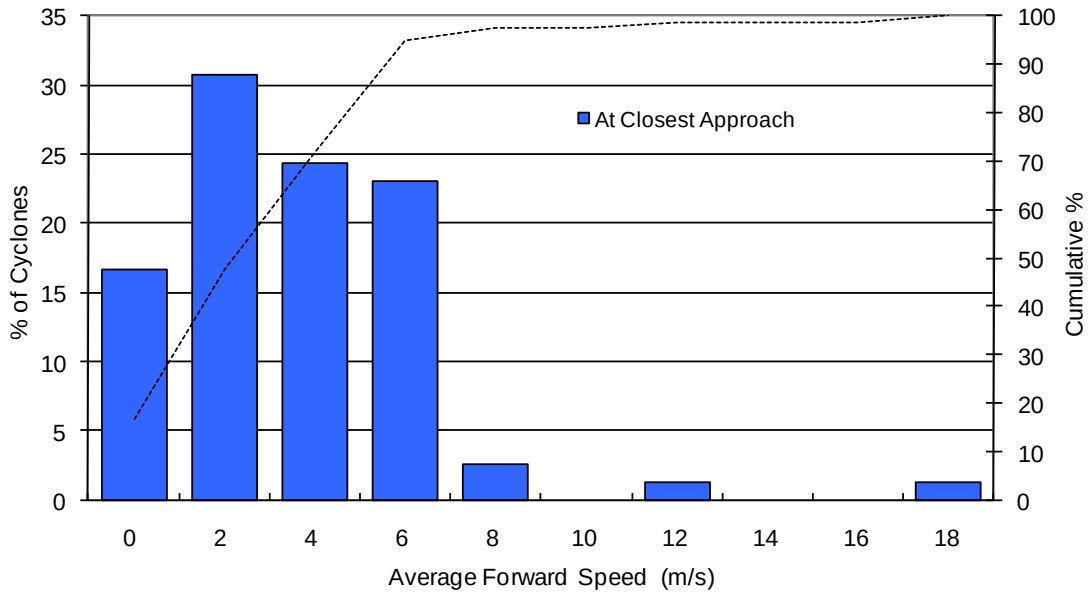

(a) Forward speed distribution.

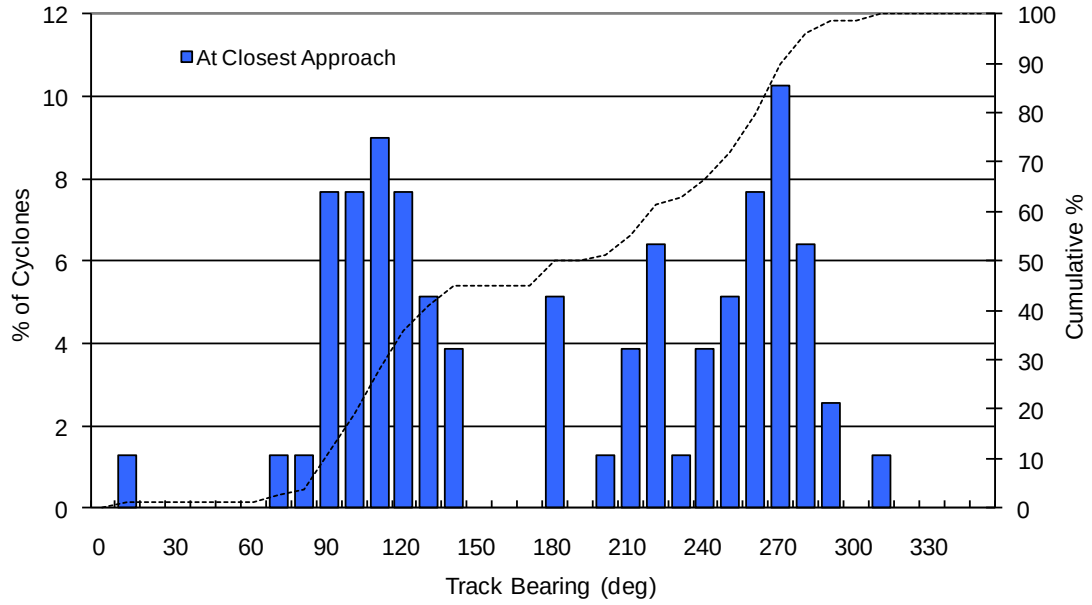

(b) Track distribution.

Figure 6-9 Statistical distributions of TC forward speed and track from 1959/60 to 2008/09 at time of closest approach and within 500 km radius of Thursday Island.

The tracks of TCs often appear random and chaotic but a more cohesive structure can be seen when the storms are grouped into what are evident to be common statistical populations that relate to areas of genesis and broadscale movement. In Figure 6-9(a) the distribution of forward speeds indicates a very wide range is possible, ranging from a high proportion of slow movers (<4 ms^{-1}) and, except for a few exceptions, a cut-off at 6 ms^{-1}. Meanwhile the track distribution in Figure 6-9(b) shows the very strongly zonal behaviour, with a very low incidence of north-moving storms.

After investigation and testing of various options, it has been assumed that the population of TCs in the region can be reasonably represented by three basic track classes - easterly moving (18%), westerly moving (32%) and southerly moving (50%). The 78 storm sample of Figure 6-2 is shown split into these classes in Figure 6-10, where it can be seen that there is a clear reduction in TC effects towards the Torres Strait region.

The most significant parameter affecting regional storm tide is the intensity of the TC winds. This is typically indirectly represented by the central pressure of the storm but also depends in part on other scale parameters. The estimated minimum central pressure for all of the 78 storms was statistically analysed using Extreme Value Theory (Benjamin and Cornell 1970) to obtain the likelihood of particularly intense storms occurring anywhere within the 500 km radius region. The statistical analyses were undertaken firstly for each separate track class and then combined into a single regional prediction shown graphically in Figure 6-11 in terms of return period and the approximate intensity category based on Table 6-1. The initially objective analyses were augmented by visually-assessed adjustments to overcome what were relatively poor distribution fits, which are likely a reflection of the accuracy and homogeneity of the estimates, notwithstanding the review that was undertaken. Nevertheless, it is considered that the finally adopted relationship is likely conservative in respect of the TC risk to the Torres Strait.

It can be shown that the most intense storms are contributed mainly by the southerly class, which typically represent storms that have developed either within the Gulf of Carpentaria basin or the Coral Sea and their southerly steering currents allow them to avoid land contact sufficiently long to allow development. The westerly class are the next dominant, developing in the Coral Sea but typically disrupted by their passage across Cape York, The easterly moving class tends to be the weakest, perhaps because of the limited area of development available in the Gulf before moving across Cape York. On this combined track basis, the 100 y return period TC intensity within a 500 km radius of Thursday Island is predicted to be approximately 910 hPa.

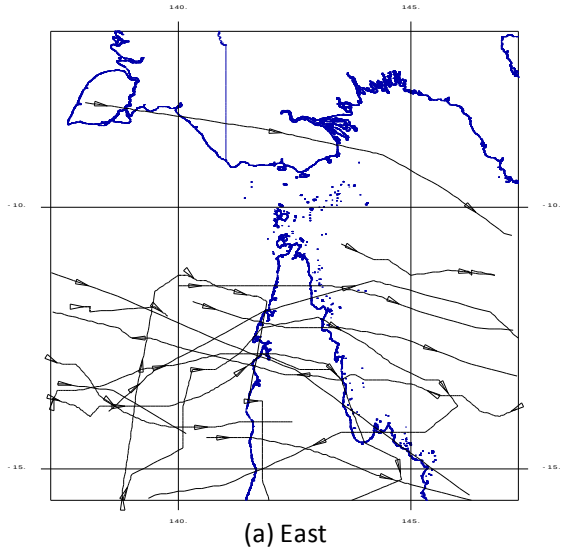

(a) East

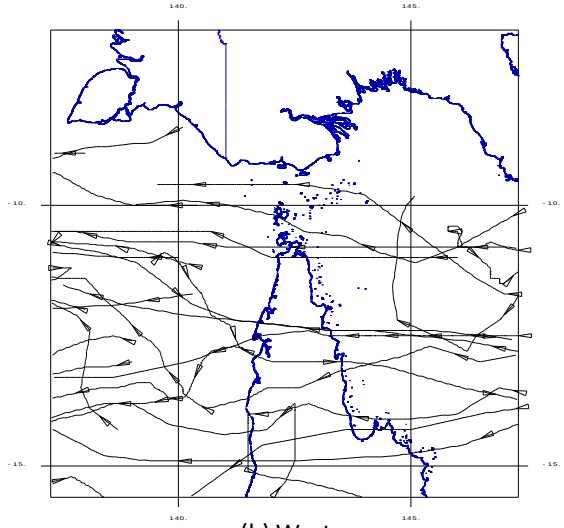

(b) West

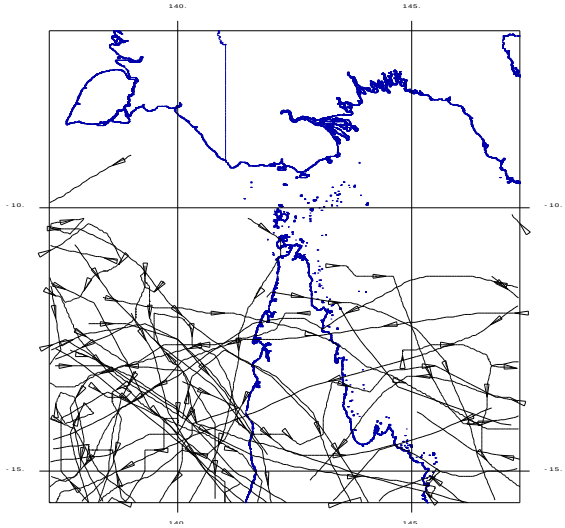

(c) South

Figure 6-10 Separation of the TC tracks into directional classes.

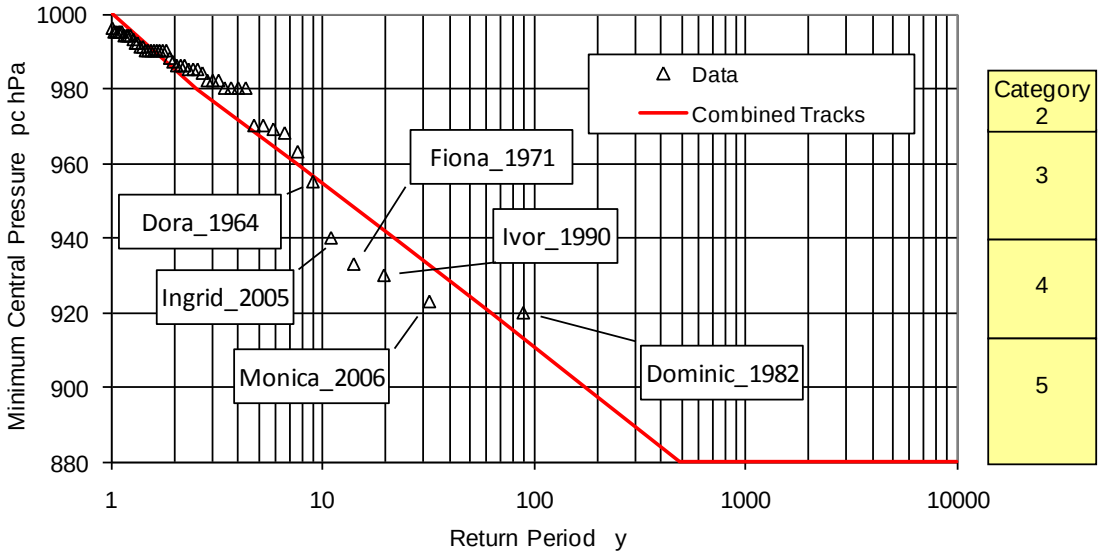

Figure 6-11 Extreme value analysis of TC intensity within 500 km of Thursday Island.

Coupled with this theoretical (normally unbounded) analysis there needs to be a consideration of the maximum potential intensity (MPI) that might be achievable in any region. This is a function of a number of physical parameters but principally the sea surface temperature and the upper atmosphere profile (Holland 1997b). For the Torres Strait region the MPI is assessed as 880 hPa (Holland 1997) and, based on the present analysis, this MPI value has a return period of approximately 500 y anywhere within the study region.

Many other storm parameters are also extracted during the analysis phase. For example, the spatial distribution of storm tracks is accounted for, together with the tendency for a proportion of storms to weaken (fill) as they move closer to the site of interest. The ambient or environmental pressure is also required for modelling and is based on the long term summer mean sea level pressures for Thursday Island of 1007 hPa.

The historical track datasets typically do not provide information on the spatial scale of the storms (radius to maximum winds *R*), although this parameter directly affects the storm tide risk. A number of model sensitivity tests were undertaken to gauge the effect of this parameter on the generated extreme wind speeds at Thursday Island and the empirical formulation after Vickery et al. (2000) was adopted, which is derived from US aerial reconnaissance-based hurricane data:

$$\ln R = 2.636 - 5.086\times10^{-5}\Delta p^2 + 0.0394899\phi \qquad (2)$$

where *R* is in km, *Δp* is the central pressure deficit in hPa and *Φ* is latitude. This relationship is graphed in Figure 6-14.

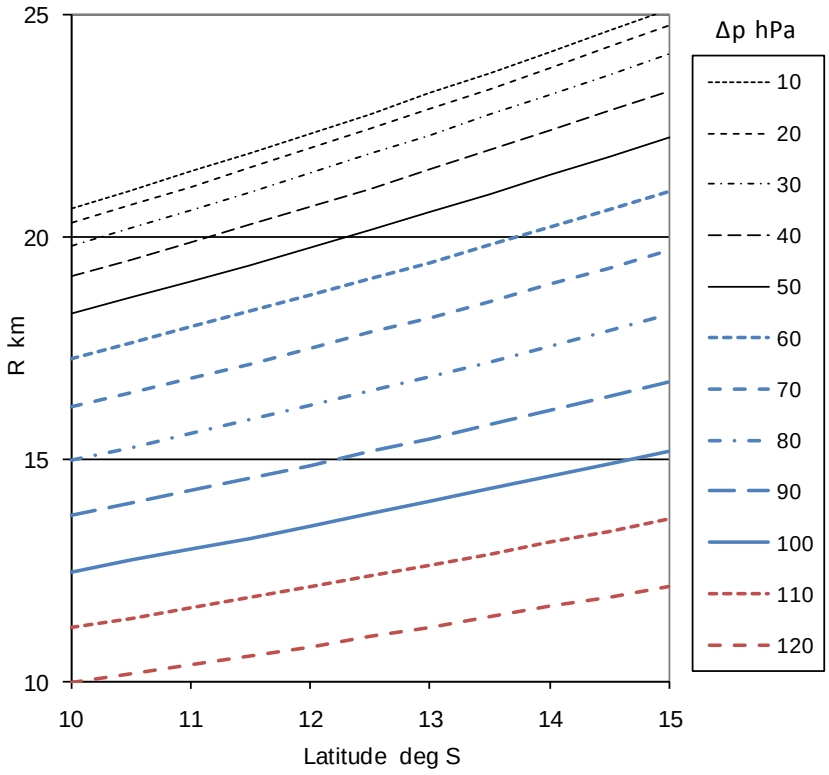

Figure 6-12 Assumed radius to maximum wind variability (after Vickery at al. 2000)

Likewise, the Holland peakedness parameter *B* (Holland 1980) is also required to complete the wind field model representation. Again, based on sensitivity testing, a relationship based on the tendency of the Atkinson and Holiday (1977) wind-pressure relationship was adopted:

$$B = 1.47 + \Delta p / 160 \qquad (3)$$

This relationship is graphed in Figure 6-13 and follows the Holland (1980) recommendation assuming a surface to gradient wind reduction factor of 0.75.

The *R* and *B* assumptions support the generally accepted concept that intense northern Australian cyclones tend to be relatively small in size and have highly peaked wind fields (e.g. *Kathy*, *Ingrid* and *Monica*).

All of the above statistical estimates of TC behaviour and strength are then assembled for use by the statistical storm tide model and used as a "template" to allow the generation of many thousands of synthetic TC storm events.

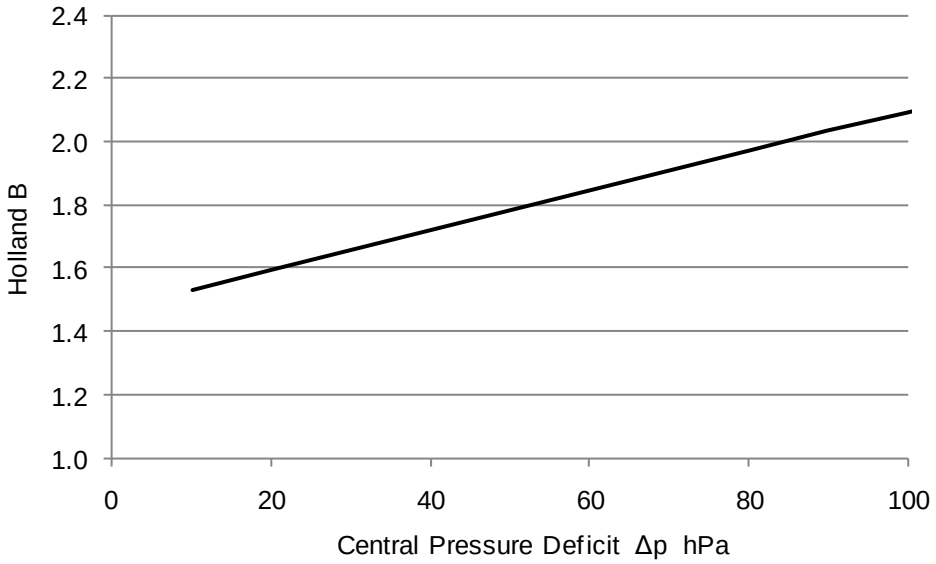

Figure 6-13 Assumed Holland B variability.

6.3 Potential Future Climate Change

The sensitivity of the regional risk of TC storm tide under potential future climate (Enhanced-Greenhouse) conditions is assessed through the adoption of scenarios that may modify the mean sea level (MSL), the maximum intensity of TCs (MPI) and their frequency of occurrence by the year 2050 and 2100. The components of each scenario have been agreed with TSRA and are based on a variety of sources as described below.

6.3.1 Potential changes in Tropical Cyclone Intensity

Although IPCC (2007) does address aspects of future TC climatology, there has been significant controversy over some of the initial statements on trends in intensity to date (e.g. Landsea et al. 2006). This area of research is advancing rapidly and the preferred reference is Knutson et al. (2010), which arose from initiatives at WMO (2006). This latest review and consensus expert statement summarises the status of current research in this area and concludes that there is a likely increase in the MPI of TCs as the mean global temperature rises, of between +3 to +21% by the year 2100 (between +2 and +11% if expressed as maximum wind speed rather than central pressure deficit). This has been nominally assumed to be represented by a 10% increase in MPI by 2050 and a 20% increase by 2100.

The future climate intensity is assumed to be able to be appropriately represented by maintaining the estimated probability of TCs achieving the regional MPI state but increasing the intensity magnitudes (decreasing the MPI pressures) for 2050 and 2100 climates. This allows

realistic blending of the future climate intensity distribution with the present climate description, as summarised graphically in Figure 6-14.

6.3.2 Potential changes in Tropical Cyclone Frequency and Track

Likewise, Knutson et al. (2010) report that the consensus from many advanced modelling studies is that the global frequency of TCs will either decrease or remain essentially unchanged.

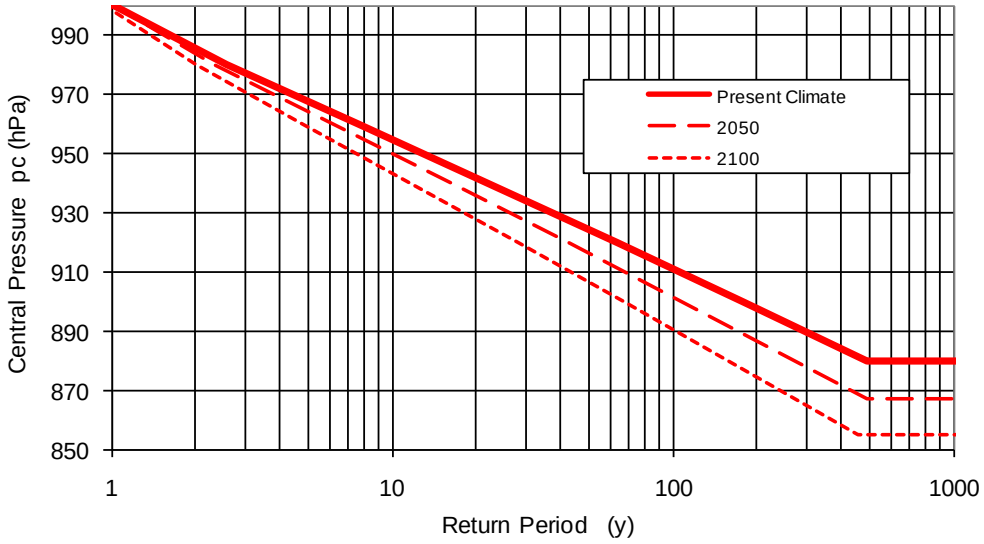

Figure 6-14 Estimated present and future climate TC intensity distributions within 500 km of Thursday Island.

In particular, there is an expressed low confidence in some global modelling studies that project changes ranging from -6 to -34% globally, and up to ±50% or more in individual basins by 2100. Regarding tracks, there is low confidence in estimates of changed areas of genesis or tracks. Accordingly no changes are adopted here for the year 2050, but a nominal precautionary allowance for a +10% change in frequency has been assumed by the year 2100.

The adopted future climate change scenarios are summarised below in Table 6-3, and Table 6-4 indicates where these scenarios modify the simulation model storm climatology.

Table 6-3 Adopted climate change scenarios.

Planning Year	2050	2100
MSL Increase[14] (m)	0.30	0.80
TC MPI Increase	10%	20%
TC Frequency Change	0%	10%

Table 6-4 Key statistical TC climatology parameters adopted for the Torres Strait region for present and future climates.

Track Population	Statistical Model Parameters					
	Name	Variable	Units	2010	2050	2100
	Ambient Pressure	p_n	hPa	1007	1007	1007
East Moving	% This Track			18	18	18
	Av. No. Per Year			0.28	0.28	0.30
	Gumbel Intensity pc	U	hPa	995.0	994.5	993.9
	Parameters	α		0.0900	0.0814	0.0743
	Max Potential Intensity pc	MPI	hPa	880	867	855
West Moving	% This Track			32	32	32
	Av. No. Per Year			0.50	0.50	0.54
	Gumbel Intensity pc	U	hPa	1004.0	1004.4	1004.8
	Parameters	α		0.070	0.0633	0.0578
	Max Potential Intensity pc	MPI	hPa	880	867	855
South Moving	% This Track			50	50	50
	Av. No. Per Year			0.78	0.78	0.84
	Gumbel Intensity pc	U	hPa	1000.0	1000.0	1000.0
	Parameters	α		0.0500	0.0452	0.0413
	Max Potential Intensity pc	MPI	hPa	880	867	855

[14] MSL changes are relative to the nominal 1990 sea level.

7. Numerical Tropical Cyclone Storm Surge Modelling

There are two aspects to storm surge considered in this study; the first is the broadscale effect attributed to remote forcing on a wide range of time and space scales, while the second is the localised effect of TCs (nominally passing within a radius of 300 km of Thursday Island). The former has been addressed by the analysis of tidal residuals combined with considerations of ENSO and annual variability in the sea level, as described in Section 5. The latter TC surge is the more energetic and life threatening event, and while such events have been known to occur in the past (refer Section 6.2) they are deemed relatively rare. This Section describes the numerical modelling of TC storm surge that has been undertaken for the Torres Strait.

7.1 Philosophy

While severe TCs are known to be rare events in the region, they nevertheless remain possible, and the complexity of the Torres Strait environment means that the resulting storm surge response will likewise be complex. Accordingly, unlike many previous studies (e.g. GHD/SEA 2003, 2007, 2009) where parametric storm surge models were developed to inform the final statistical analysis, a decision was undertaken to undertake discrete numerical modelling of all statistically-generated storms.

This decision placed considerable stress on the efficiency of the deterministic numerical modelling because a total of 11,625 individual storms were required to represent the 50,000 year model time-span desirable for describing the present climate. This compares with modelling approximately 500 storms when developing a parametric storm surge model. In addition, 11,787 storms were needed for the 2050 future climate and 12,690 for the 2100 climate. Due to some commonality as a result of discrete storm parameter values being used, 33,816 individual model simulations were required to satisfy the 2010, 2050 and 2100 climates.

7.2 The Numerical Storm Surge Model

The adopted model is MMUSURGE[15] (Mason and McConochie 2001), developed as part of the Queensland Climate Change Study (e.g. Harper 2001) where it was verified against several historical storms. The model has since been used extensively for storm surge studies across

[15] MMU refers to the Marine Modelling Unit, originally at James Cook University and currently at the University of Tasmania, Australian Maritime College in Launceston.

Queensland and the Northern Territory (e.g. GHD/SEA 2003, 2007, 2009; SEA 2004, 2005, 2006, 2007).

The model is 2-D depth integrated on a rectilinear spherical coordinate mesh with an implicit numerical scheme that is identical to the TS tidal model described in Section 4.3. Likewise, MMUSURGE is able to represent sub-grid scale effects of complex reefs, shoals and banks through the use of special internal boundary conditions (Bode et al. 1997) or alternatively through nesting of model domains at increasing resolution. The surface wind forcing of TCs is provided by an implementation of the Holland (1980) analytical wind and pressure model following Harper (2001). The model can accommodate wetting and drying

While the 1 nmile resolution TS tidal model accepts either tidal boundaries or input from the GCCS model, the TC version similarly requires open boundary forcing from a larger domain that ensures the storm wind and pressure fields can be correctly represented. This “A” domain, with a resolution of 7.5 nmile, is shown in Figure 7-1, with the inner “B” grid being identical in coverage and detail to the TS tide model.

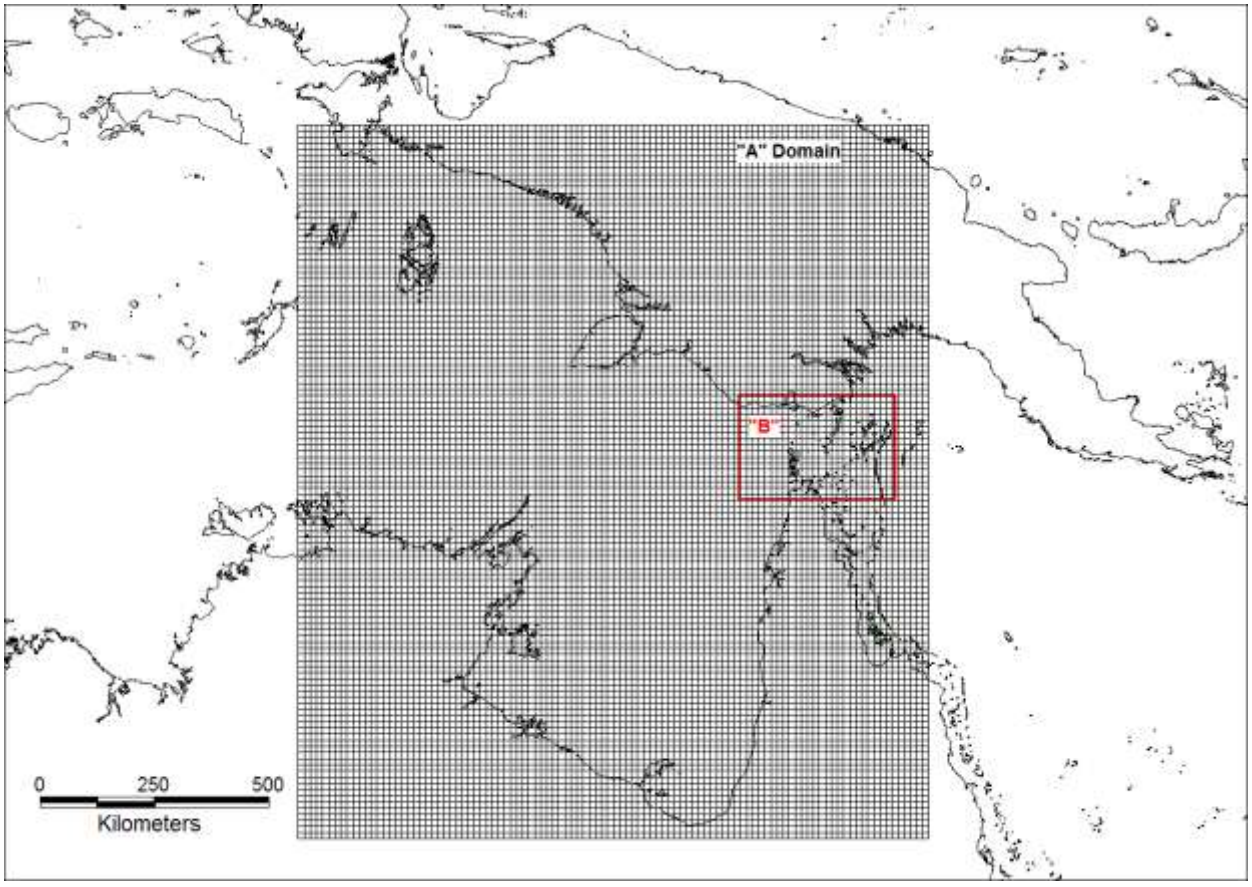

Figure 7-1 The 7.5 nmile “A” and 1nmile “B” storm surge domains.

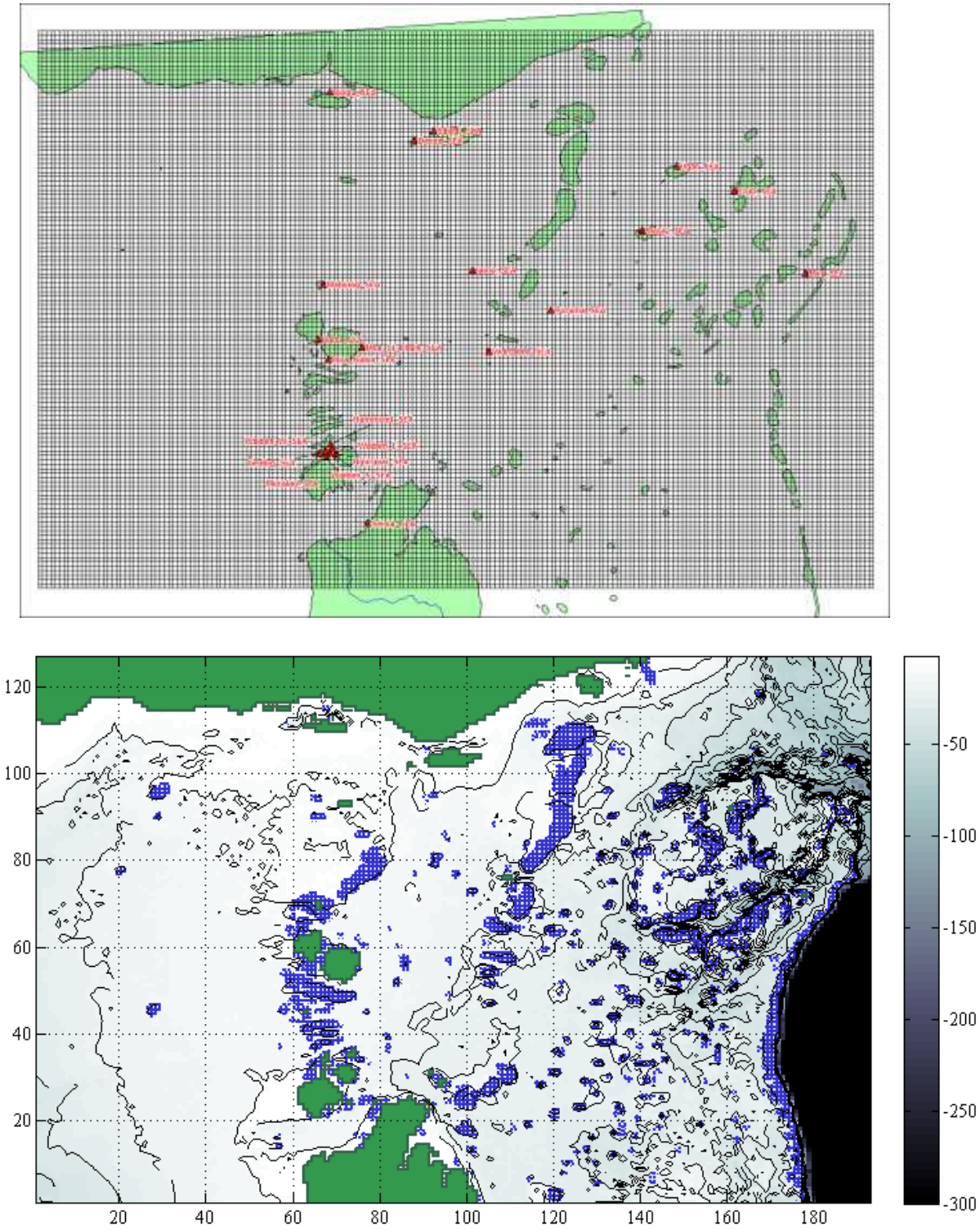

Figure 7-2 The 1 nmile TS storm surge model; Top: Resolution and sites; Bottom: Bathymetry, land, model reef and barrier structures.

The “A” domain is less extensive than the GCCS model and is designed to extend only over the shallow waters to the east (limited) and west of the Torres Strait (more extensively) so that the close-approach TC winds and pressures are well represented prior to any storm entering the inner “B” domain. The resolution of the “B” domain is illustrated in the upper panel of Figure 7-2 together with the community locations, while the lower panel highlights the bathymetry and the special model reef and boundary elements (in blue). In addition to the “A” and “B” storm surge domains a higher 0.2 nmile (371m) “C” domain was also available. This was used to prepare localised “C” domains in the vicinity of the central islands and also Boigu and Saibai (as detailed in Appendix J and discussed below).

7.3 Storm Surge Model Testing and Calibration

7.3.1 Domain Resolution

Because of the decision to undertake discrete TC storm surge modelling, the computational burden of a “C” grid was deemed to be too great within the timeframe available. In addition, much of the region was deemed reasonably well represented at the 1 nmile resolution, but with some suspect areas near Thursday Island and also near the northernmost islands of Boigu, Saibai and Dauan. Accordingly, a series of tests were undertaken to determine the suitability of the 1 nmile “B” domain resolution during TC forcing.

For example, Figure 7-3 shows the representation of “B” domain depths near the centre island chain and the detail near the confluence of Prince of Wales, Horn and Hammond Islands (green in lower panel represents land that is > 10 m elevation and is assumed to remain always dry). Notably, the Thursday Island landmass is not able to be fully resolved at this scale and so the model uses a series of short barriers (black) to produce the equivalent resistance to flow as represented by the actual island. Numerous other barriers and reefs (blue) can be seen throughout the area in response to the various shoals. The difference between “barriers” and “reefs” is simply that a reef, in addition to providing a blockage, allows flow over its crest, whereas a barrier is simply a blockage. The length of each barrier or reef represents the proportion of the blockage relative to the size of a full model cell.

This final arrangement of barriers and reefs was decided after a series of tests using a NW-SW Category 4 TC such that the “B” domain closely reproduced the result from a “C” domain at the same modelled grid position. Comparisons were also done between the “B” and true “C” grid position and these are summarised in Appendix J. Likewise, tests were also undertaken for the northernmost islands but using a SW-NW TC track for maximum impact. Differences in all cases were limited to about 5% and justified the use of the “B” domain for modelling.

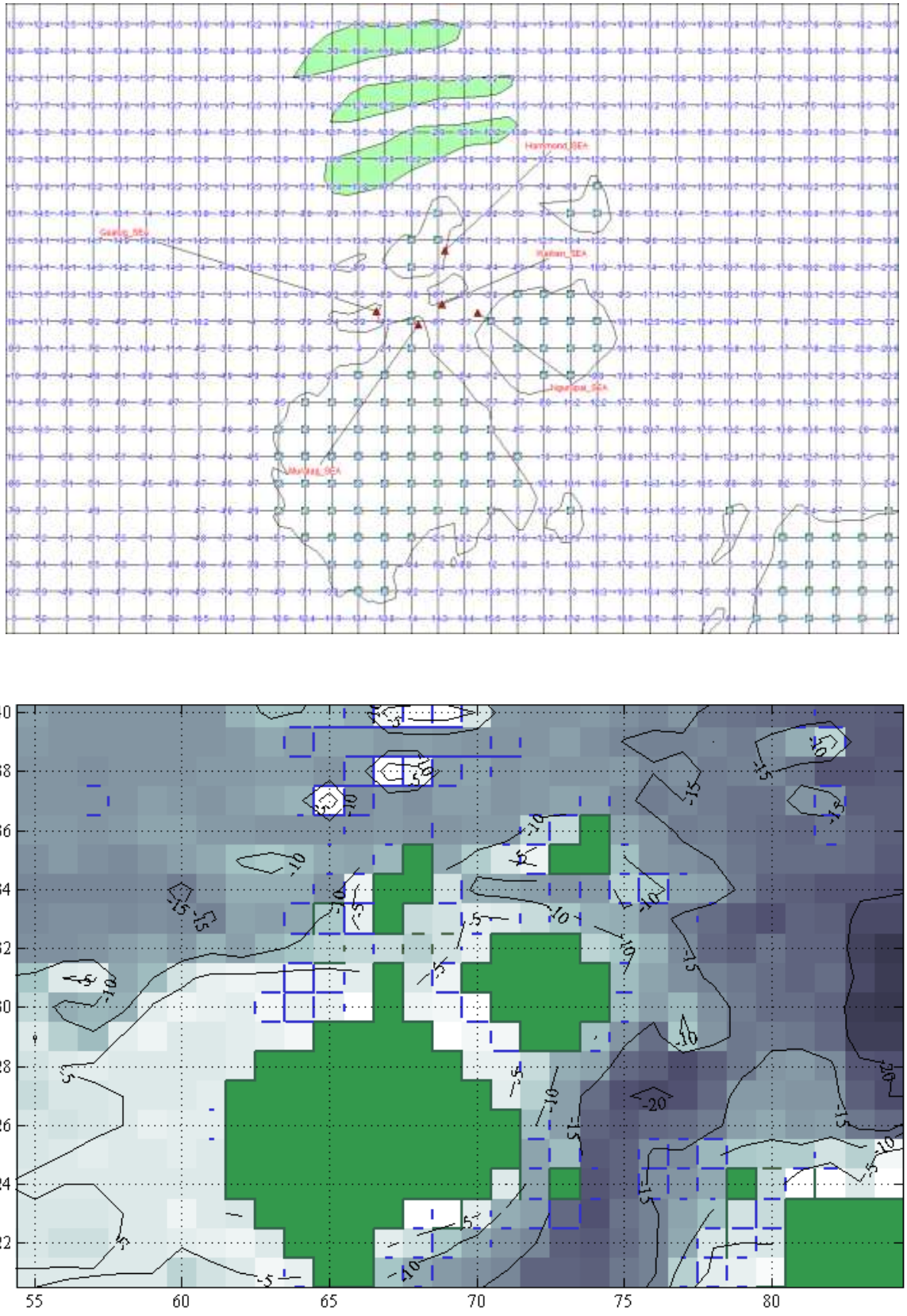

Figure 7-3 TS storm surge model “B” domain detailed views.

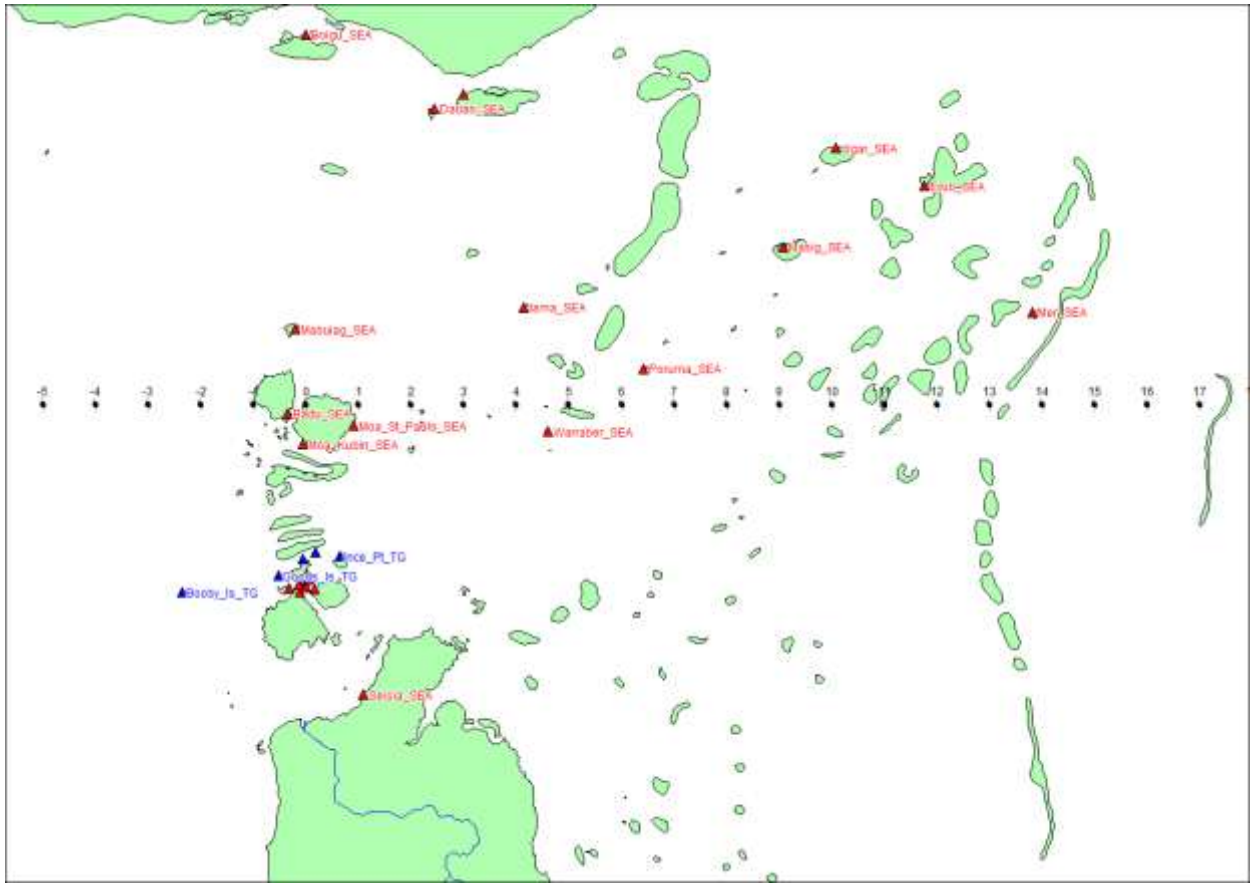

Figure 7-4 Example Cat 4 W-E Centre extreme TC scenario.

7.3.2 Deterministic Extreme TC Scenario Testing

A series of extreme TC scenarios were devised to test the stability of the storm surge modelling system and also provide some insight into the possible impacts of a very severe close-approach storm. A nominal Category 4 storm (without tide effects) was devised having the following Holland model parameters:

p_c = 940 hPa

R = 20 km

B = 1.8

V_{fm} = 4 ms^{-1}

A number of different storm tracks were then tested, each with a duration of 36 hours, and the full set of results are summarised in Appendix I. In addition, aspects of the "W-E" scenario are illustrated here. The track is shown in Figure 7-4 with hourly positions relative to Badu, while Figure 7-5 shows the modelled wind speed pattern 3 hours before crossing over Badu.

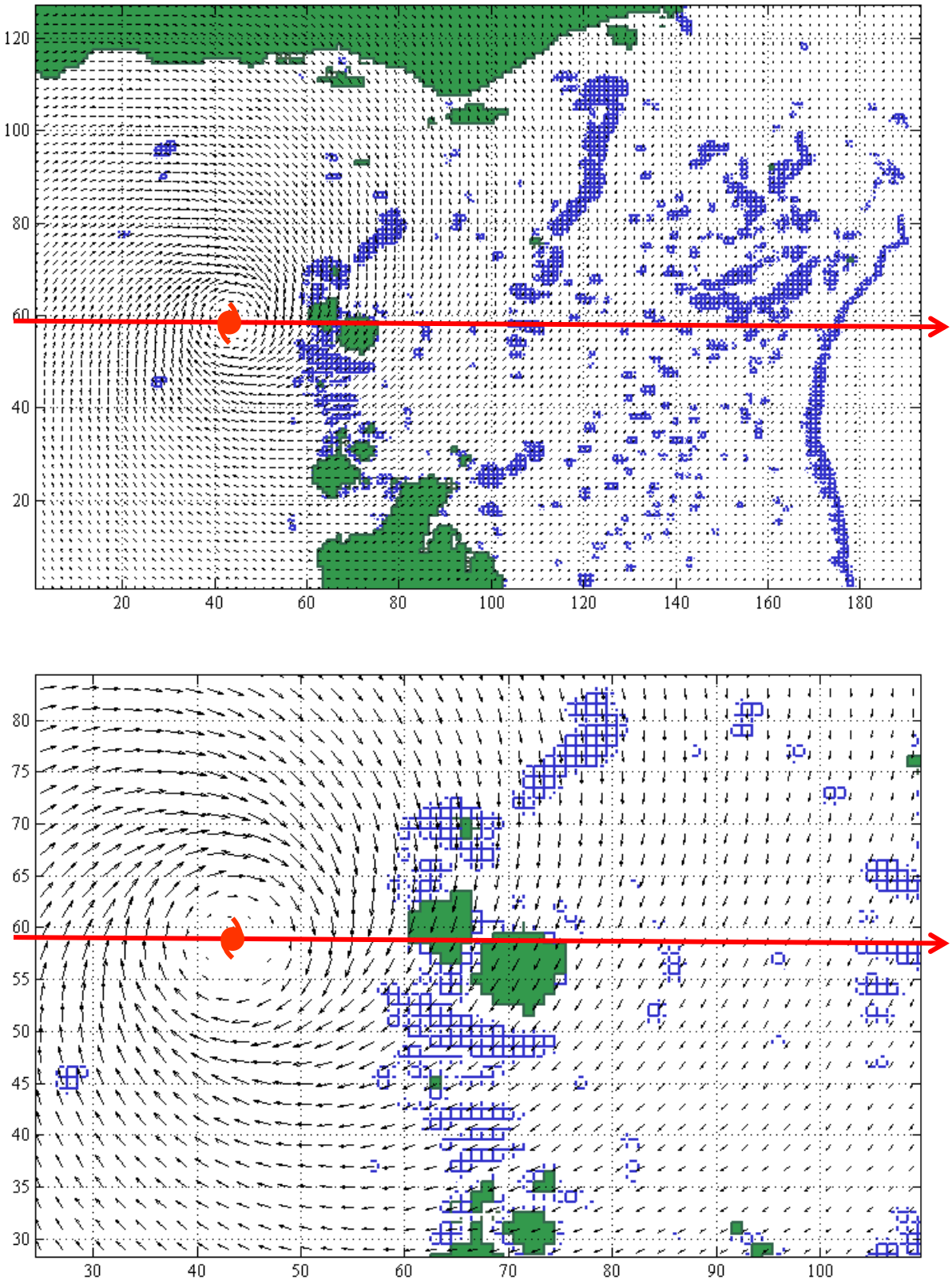

Figure 7-5 Example Cat 4 W-E Centre extreme wind pattern.

The characteristic clockwise vortex of winds is shown, which increase exponentially towards the radius of maximum winds. This band of winds, which are expected to produce 3-sec gusts up to 64 m s^{-1} (230 km h^{-1}) in this example, is still located to the west of Badu in this figure. Between the radius of maximum winds and the centre of the storm the winds decrease to eventually form the quiescent “eye” of the storm.

Figure 7-6 then shows the equivalent views of the modelled storm surge pattern, where the labelled contours show the surge height in metres above the mean sea level. The surge build-up can be seen to be concentrated on the left-hand side and forward of the position of the storm centre, which is where the wind speeds are highest. The innermost height contour at this time is 1.2 m and it can be seen that the various island and reef clusters are acting to modify the overall surge height pattern.

Appendix I provides some further views of this storm scenario at different times, but Figure 7-7 here provides the so-called envelope of the highest surge levels throughout the full 36 hour simulation. This shows that the highest surge of about 1.4 m was predicted to occur near Badu, immediately below the centre of the storm. This is caused by the concentration of the extreme winds pushing the surge between Badu and Moa Island. This open-water result is different from a typical coast-crossing TC scenario where the maximum surge will normally occur about one radius of maximum winds distance to the left of the track (refer Appendix I for a suitable example).

Table 7-1 summarises the peak surge magnitudes at all of the community sites for this specific scenario, showing that the St Pauls and Kubin communities on Moa Island are experiencing the next highest magnitudes of about 1.2 m. The full modelled time histories of the surge response are then shown graphed in Figure 7-8. This indicates the differences in the time of arrival of the surge and the steepness of the rise, as well as the fact that some sites would experience a “negative surge” prior to the arrival of the “positive surge”. Boigu, for example, shows one of the highest negative surges (also termed *drawdown*) as the initial winds tend to draw water away from the shallow Papua New Guinea coastline, but later experiences the positive surge from the winds in the rear of the storm after it passes further to the east.

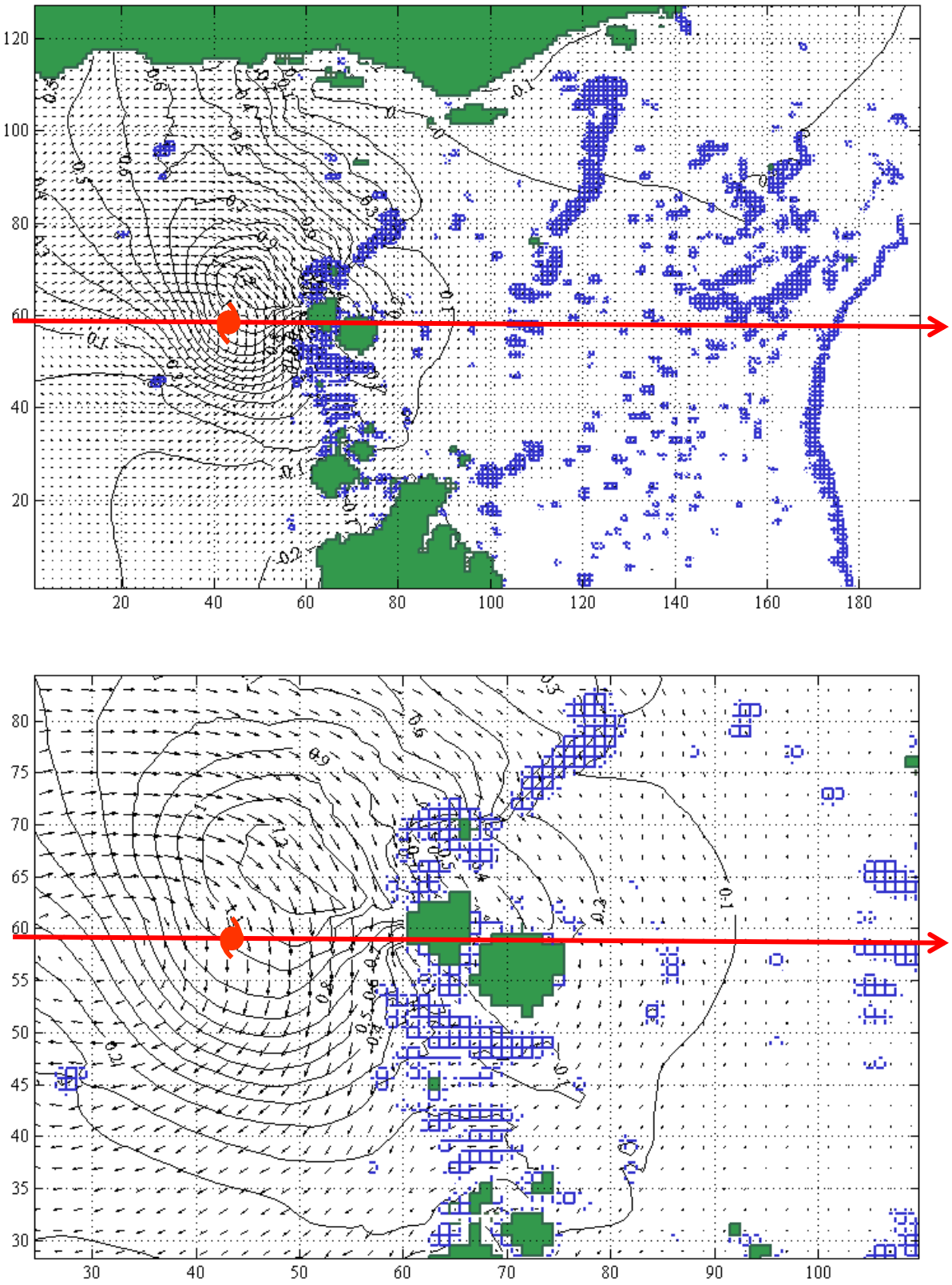

Figure 7-6 Example Cat 4 W-E Centre extreme surge pattern.

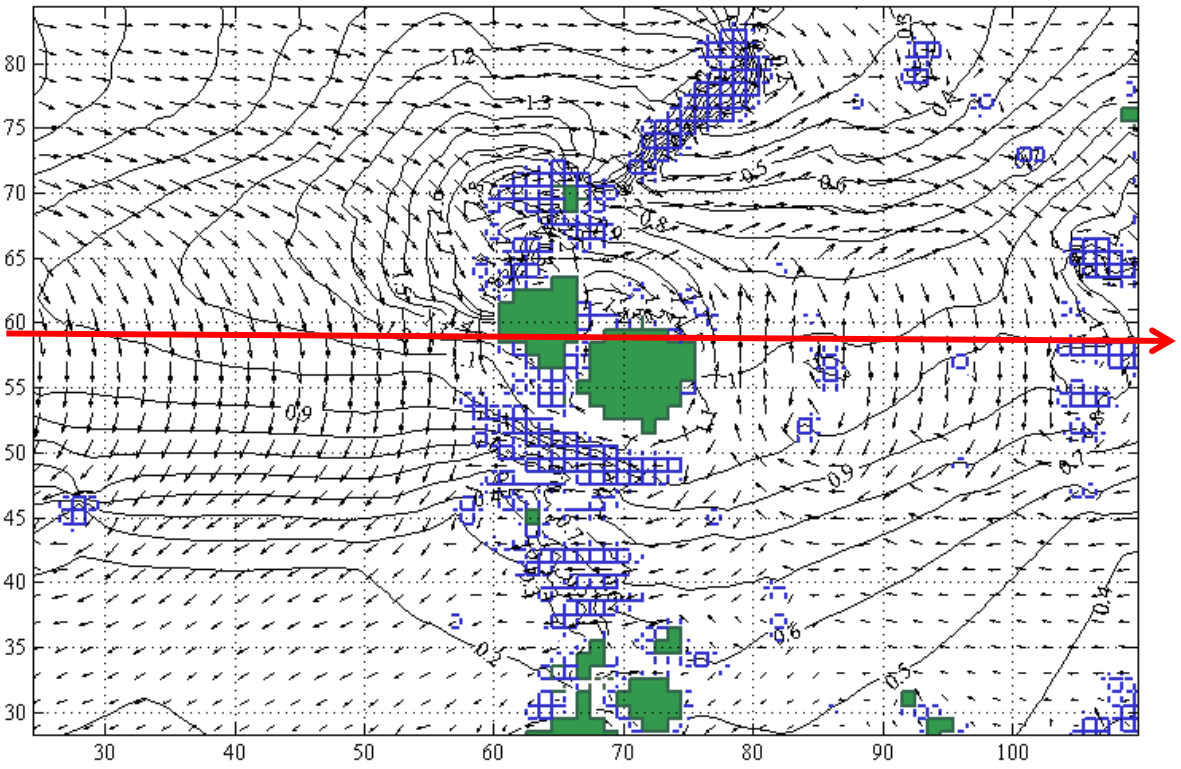

Figure 7-7 Example Cat 4 W-E Centre envelope of maximum surge magnitude and current velocities.

Table 7-1 Summary of peak storm surge magnitudes for Cat4 W-E Centre extreme TC scenario.

Community	Surge	Community	Surge
	m		m
Badu_SEA	1.36	Moa_Kubin_SEA	1.18
Boigu_SEA	0.65	Moa_St_Pauls_SEA	1.18
Dauan_SEA	0.37	Muralag_SEA	0.56
Erub_SEA	0.17	Ngurupai_SEA	0.53
Gealug_SEA	0.14	Poruma_SEA	0.70
Hammond_SEA	0.48	Saibai_SEA	0.3
Iama_SEA	0.66	Seisia_SEA	0.13
Mabuiag_SEA	0.97	Ugar_SEA	0.17
Masig_SEA	0.33	Waiben_S_SEA	0.34
Mer_SEA	0.38	Warraber_SEA	0.87

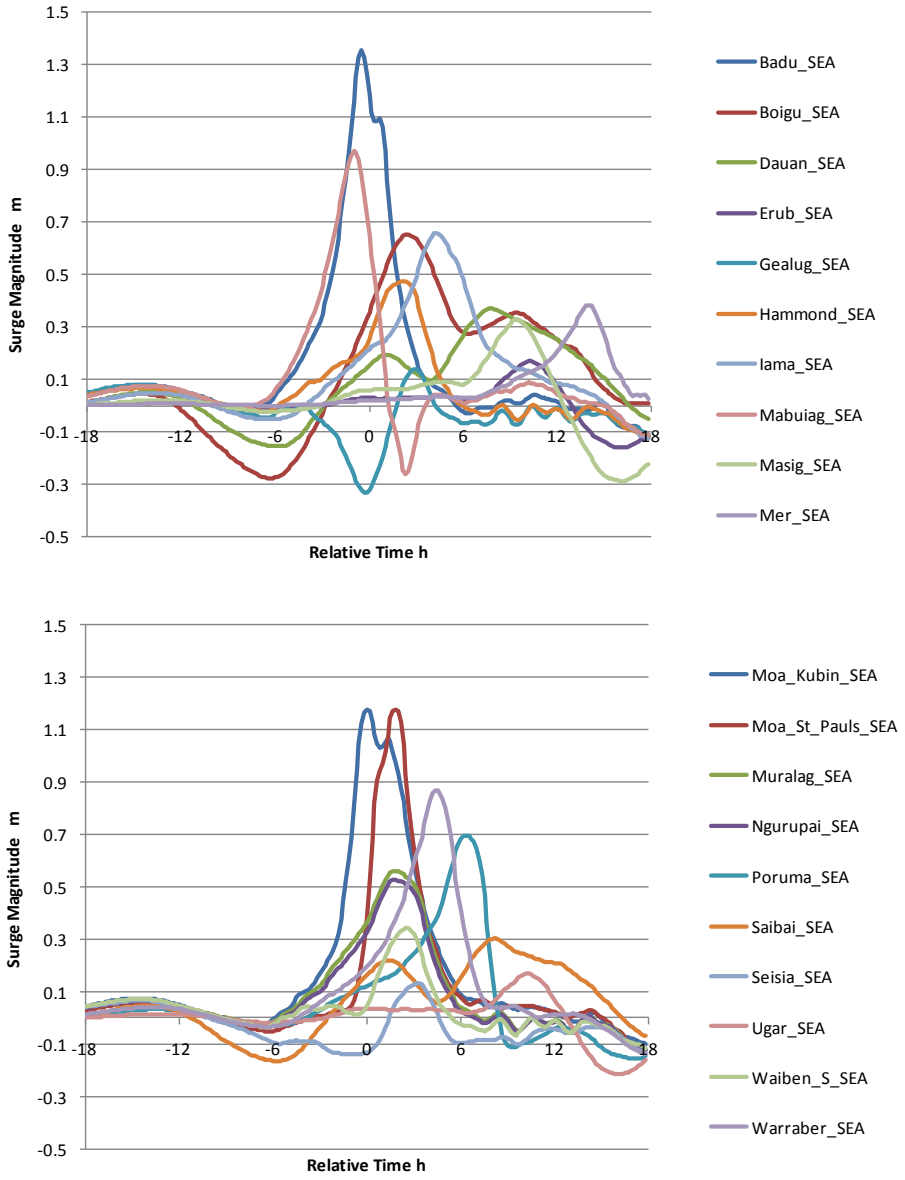

Figure 7-8 Example Cat 4 W-E Centre time histories of surge magnitude at each community site.

8. Numerical Wave Modelling

There are no known insitu measurements of wave conditions in the Torres Strait region that could be used in an analogous manner to the analysis of long term tide gauges as used to estimate the broadscale water level variability in Section 5. Numerical spectral modelling is the only option available to estimate the potential site-specific influence of waves on extreme storm tide levels. However, some comparisons with satellite altimeter data are able to be made that provide some confidence in the modelled broadscale wave climate.

8.1 Philosophy

As discussed in Section 1.2 the Torres Strait communities are protected from the long period ocean swell that normally emanates from higher latitudes by the Great Barrier Reef to the east, the broad shallow regions to the west and the numerous central banks and shoals. On this basis it is assumed that wave effects at the communities will be dominated by those generated locally by the prevailing winds, subject to the significant seasonality described in Section 3.1, with rare but significant incursions from TCs. No remote wave forcing is therefore considered, thus allowing a simplification of approach that assumes waves will be fetch-limited by the bathymetric constraints.

Spectral wave modelling is adopted in order to efficiently cover the necessary area of interest, although it must be acknowledged that this approach can only offer representative wave conditions at each community. The very small scale influences of small banks, shoals, reefs and channels cannot be represented as many features are below the resolution of the bathymetric data. Accordingly, the analyses here are meant to be sufficiently informative to show the relative differences between wave effects at the various communities, which might justify more detailed studies and insitu measurements if warranted.

8.2 Spectral Wave Modelling

While a variety of spectral modelling approaches are possible, the very long periods required to be modelled (thousands of years) has necessitated a pragmatic approach that focuses on computational efficiency.

To suit the final statistical modelling a parametric wave modelling approach was considered (e.g. Harper 2004c). However, as argued in Section 7 with respect to TC surge effects, the region was considered potentially too complex to enable a consistent approach without multiple models having to be developed. Given more time, parametric approaches would undoubtedly be of use in specific circumstances or to assist in real-time forecasting of waves and storm surge.

8.2.1 The Unsteady Directional Fetch Model TS_Wave

The adopted spectral wave model has been based on the fetch-limited method described by Walker (1989), whereby the Radiative Transfer Equation is solved for a set of discrete frequencies using finite-differences in a directional fetch arrangement rather than a full 2-D orthogonal grid. The model is computationally efficient, allowing the practical generation of very long-term time series of wave heights.

The model (termed *TS_Wave*) includes standard source terms (following and opposing winds), a modified saturated P-M spectrum and can include bed friction. Variation in depth along a series of radiating fetches centred at each site influences the wave energy propagation and the directional spectrum at the centre of each set of fetches is summed to provide a time-varying estimate of the wave energy. The energy frequency spectrum is then integrated to provide significant wave height Hs, peak spectral wave period Tp and mean wave direction.

The principal assumptions of the simplified model are that:

- Waves are mainly locally generated;
- Refraction effects are small due to reasonably constant depth;
- Diffraction effects are negligible;
- Bed friction effects are negligible;
- Wave breaking effects can be neglected;
- Wave-current interactions are minor.

Although the shallow waters of the Torres Strait do not necessarily fit with all these assumptions, a similarly simplified model has been shown to produce reliable wave estimates in Great Barrier Reef environments (e.g. EPA 2005) where wave data was available for comparison.

After considerable sensitivity testing, a total of 32 equally-spaced wave directions and 10 wave frequencies were considered at each site. The 32 directions were necessary to accommodate some of the more narrow channels between the Centre and Inner groups of islands in particular[16] and compensates slightly for the lack of refraction effects. Figure 8-1 indicates the resulting pattern of fetches that were developed and the specific case of Mabuiag. The directional depths where obtained by interpolating the fine-scale 0.2 nmile (370 m) bathymetric grid at a constant spatial step of 1 km. Special considerations were necessary for isolated small island sites (e.g. Erub, Iama, Poruma etc) whereby the fetch generation ignored the presence of the island itself, treating it as a point in the ocean. Non-land points were set to a minimum depth of 2 m.

[16] Any future work could consider the use of non-equally-spaced directions to preserve the necessary directional resolution but reduce the computational burden even further.

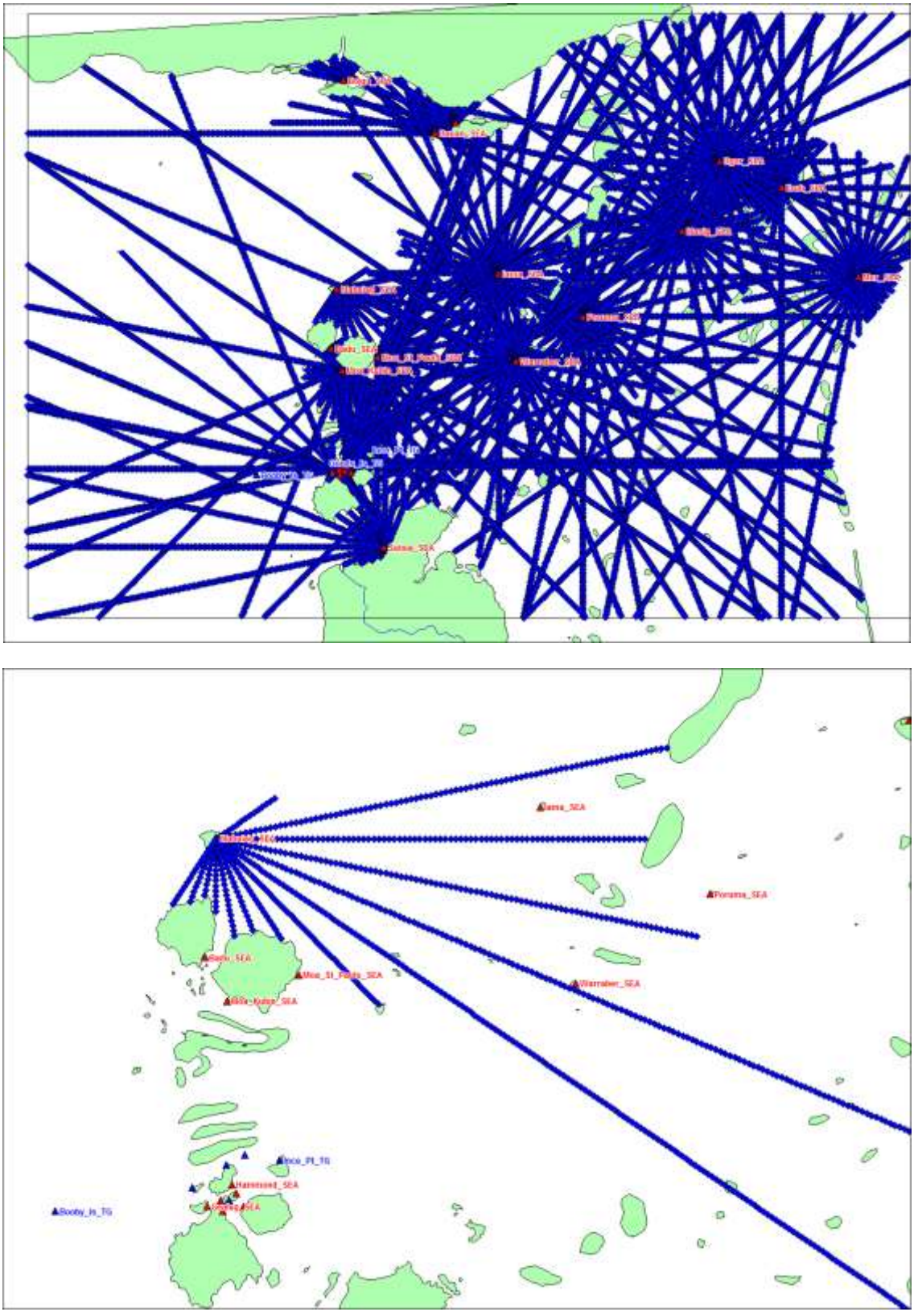

Figure 8-1 Example modelled wave fetches within Torres Strait.

8.2.2 Comparisons with a Steady-State Non-Directional Model

During the model development, an even simpler and much more economic steady-state model version was also built and tested. This made use of the same directional fetch information for each site but utilised the one-dimensional wave growth formula after Young and Verhagen (1996). A comparison of the steady-state and unsteady wave models is given in Appendix K for four years of selected regionally-modified NCEP wind forcing from 1949 to 1952.

It can be seen that the steady-state model compares reasonably favourably with the unsteady *TS_Wave* model at a number of communities, mostly those that are well exposed such as Masig, Mer, Moa St Pauls and Ugar. However, at the more sheltered sites it tends to perform less well, such as at Waiben and Ngurupai. This is likely to be due to the poorer effective directional resolution of the unsteady model whereby the winds are always only applied to the 1-D fetch that is most closely aligned with the wind direction, rather than being the integrated result from a number of directional fetches. Generally the steady-state model slightly overestimates Hs and underpredicts Tp relative to the unsteady directional model.

8.3 Wave Model Testing and Calibration

8.3.1 Broadscale Winds and Altimeter Data

Satellite altimetry wave height and associated scatterometer non-directional surface wind speed data for the northern Australian region for the period May 1985 to November 2008 was provided by Prof Ian Young from Swinburne University of Technology. The altimeter tracks and summary time series of significant wave heights is shown in Figure 8-2, which indicates a significant data gap from September 1986 to April 1992. It can be seen that the availability of data within the Torres Strait area of interest is significantly reduced, no doubt because of the quality checking algorithms rejecting values that have been deemed to be land-affected.

The data was first filtered to only include values within the immediate Torres Strait (142.46°E to 143.35°E and 9.9°S to 10.6°S) and then any multiple estimates on the same day were averaged. This resulted in a total of 271 d of wind or wave estimates being available within the data span of 23.5 y. The data is summarised in Figure 8-3 as a time history of the wind and wave values (upper left panel), wave versus wind correlation (lower left panel) and distributions of the wind and wave data sets (right hand panels). The maximum wind speed in the record is 13.6 ms^{-1}, occurring on 28/05/2000, and the maximum significant wave is 1.7 m, occurring on 10/11/1995. As expected, there is a strong correlation evident between the wind and wave estimates. The average wind speed for the sample is 6.9 ms^{-1} and the average wave is 0.8 m.

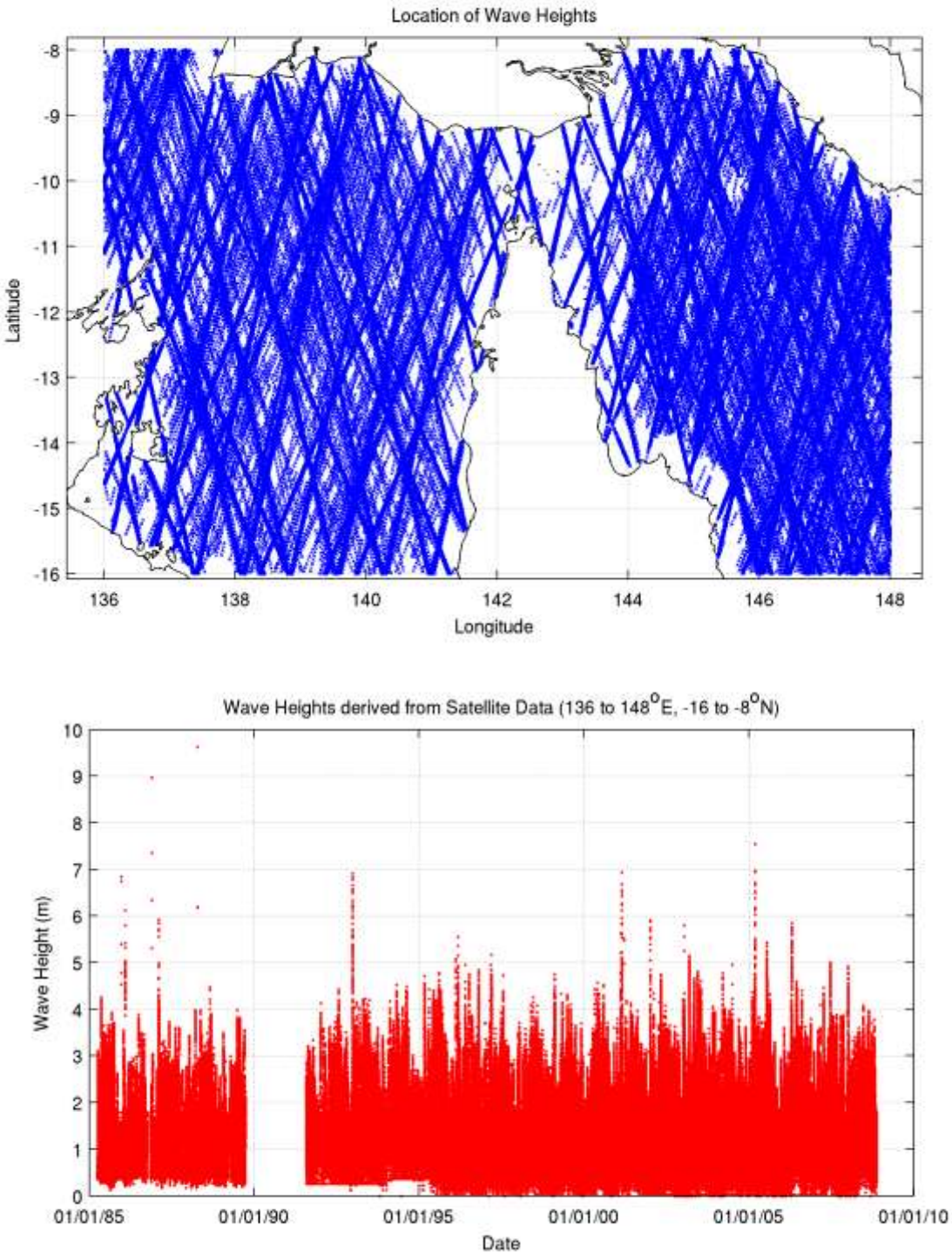

Figure 8-2 Altimeter data available for the northern region.

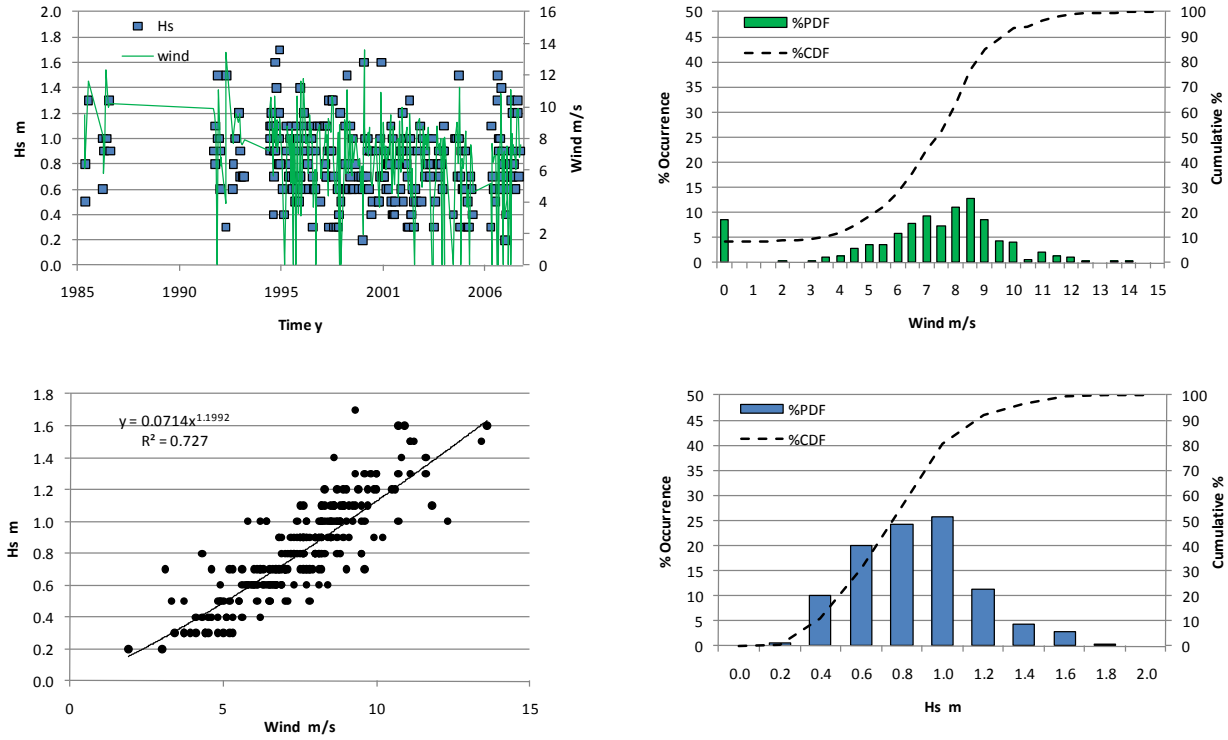

Figure 8-3 Summary of altimeter data within the Torres Strait.

This dataset was then further culled to the 10 y period from 01/01/1995 to 31/12/2004 to avoid altimeter data gaps and also to match the period of quality controlled winds available at Poruma Island (refer Section 3.3). Because Poruma is reasonably centrally-located in the area it provides a basis for intercomparison of the NCEP-derived regional winds, the locally measured winds and the altimeter wave and wind dataset. This is then used to assess the performance of the steady-state wave model and especially the fetch-limited wave growth assumptions.

Although the altimeter dataset is limited, the comparison of the daily non-directional mean wind in Figure 8-4 shows a very high correlation with the coincident site-adjusted wind speeds at Poruma. The scatterometer winds are also higher than the NCEP winds as derived for the location of Horn Island, consistent with the analysis of Section 3.3 that leads to adoption of a regional adjustment. On this basis, a comparison between modelled waves and altimeter waves during these periods is warranted, recognising that there is a reliance on the assumption that winds are reasonably steady on a daily basis.

This is done in Figure 8-5, where the steady-state unidirectional fetch-limited wave model has been applied to the Poruma location, driven by the regionally-adjusted NCEP winds. The resulting comparison shows that the model result is highly correlated with the data, although there is much scatter. The distribution of modelled heights is likewise similar. As altimeter wave data is the only objective source of wave data, this is some justification for the wave model fetch-limiting assumptions.

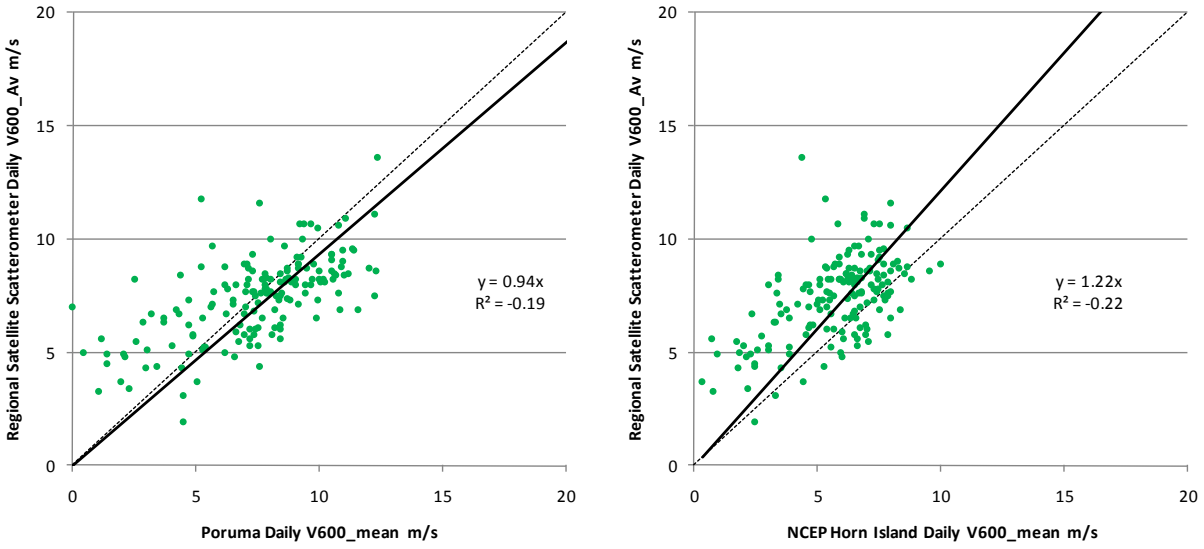

Figure 8-4 Inter-comparison of coincident scatterometer winds, and mean daily winds at Poruma and mean daily NCEP winds at Horn Island 1995 to 2004.

8.3.2 Tropical Cyclone Waves

There is no quantitative wave data in the region associated with TCs that can be used for direct comparison with wave modelling options. Accordingly the approach taken has been to compare the performance of the preferred unsteady directional fetch-limited wave model *TS_Wave* with that of a fully dynamic 2-D spectral model for a number of selected TC scenarios.

The chosen dynamic 2-D spectral model was *ADFA1* (Young 1988), which has been proven very reliable in a number of verification studies (e.g. GHD/SEA 2009 for TC *Larry* and GHD/SEA 2007 for TC *Aivu*) in complex reef environments. The model operates at a fixed water level (MSL in this case), using 16 equally-spaced directions and 10 frequency bands, a computational resolution of 1 nmile (same as the TS model) but with wave ray paths based on the fine scale 0.2 nmile (371 m) bathymetry grid.

Considering the extreme Category 4 storm scenario ‘W-E Centre’, as shown earlier in Figure 7-4 for the storm surge example, Figure 8-6 shows that the ADFA1 modelled wave conditions are predicted to be complex. The upper panel shows a view when the storm is at the centre of image, heading east. The wave heights are labelled showing peak heights of about 6 to 7 m and peak spectral period directional vectors are at 4 nmile spacing. The lower panel shows the maximum wave height envelope throughout the entire passage of the storm where highest wave heights are typically 5 to 6 m, with isolated maxima up to10 m in the eastern region.

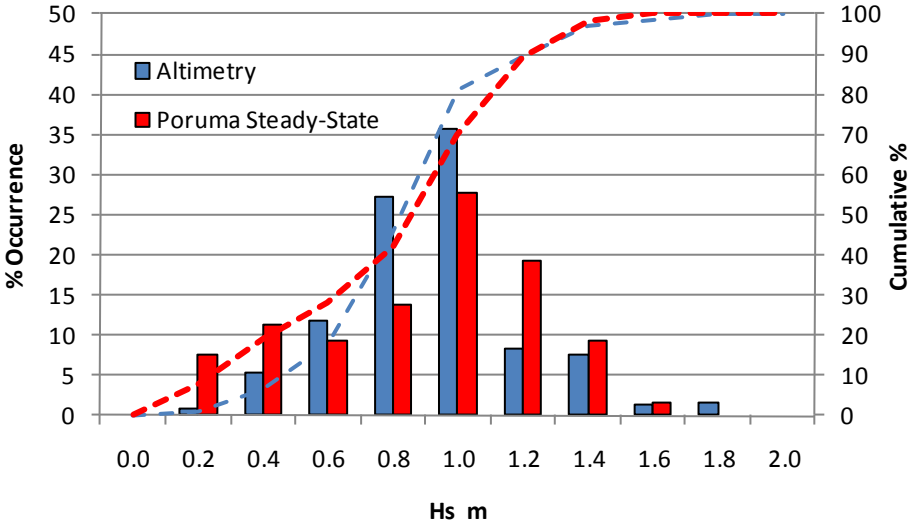

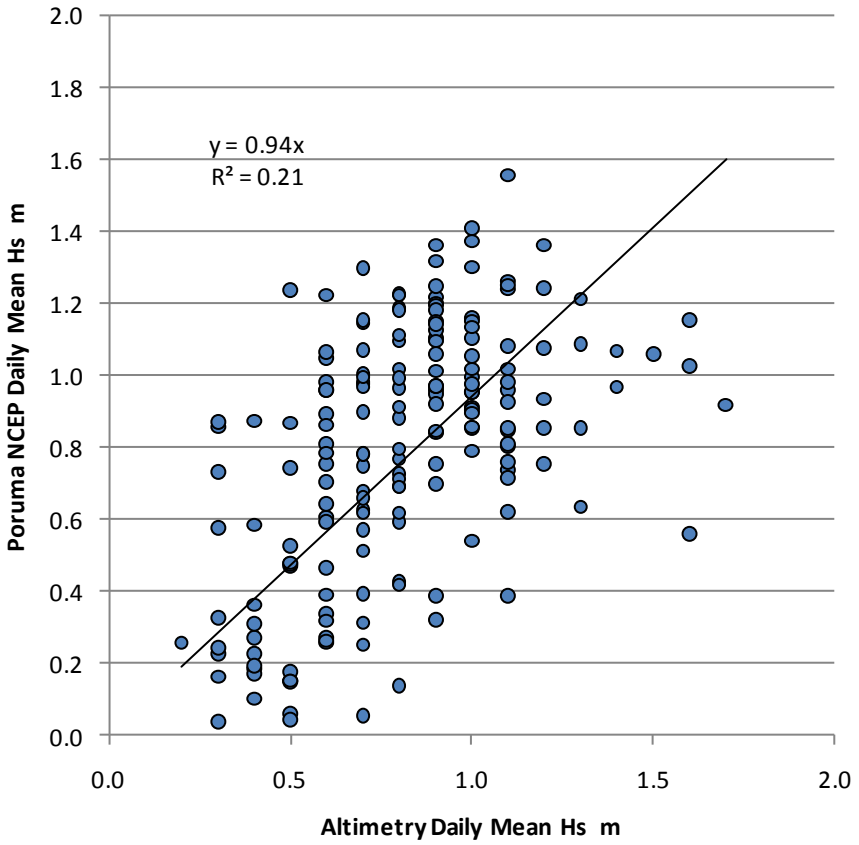

Figure 8-5 Comparison of altimeter waves 1995-2008 and NCEP-adjusted winds driving the steady-state unidirectional wave model centred at Poruma Island.

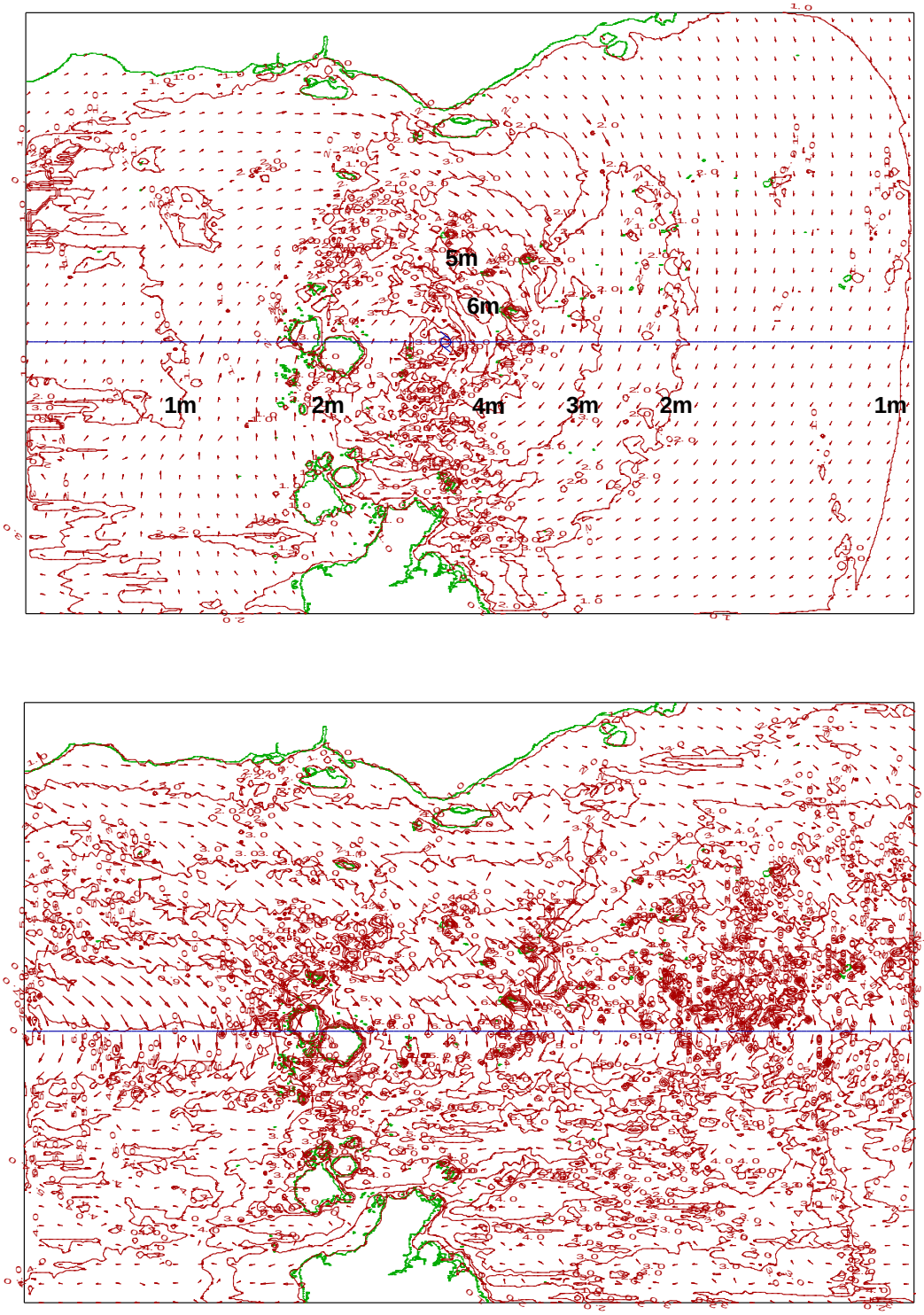

Figure 8-6 Example W-E Centre Category 4 TC wave height, period and direction on 1 nmile grid. Top: Snapshot at time storm is centre of image; Bottom: Envelope over entire passage.

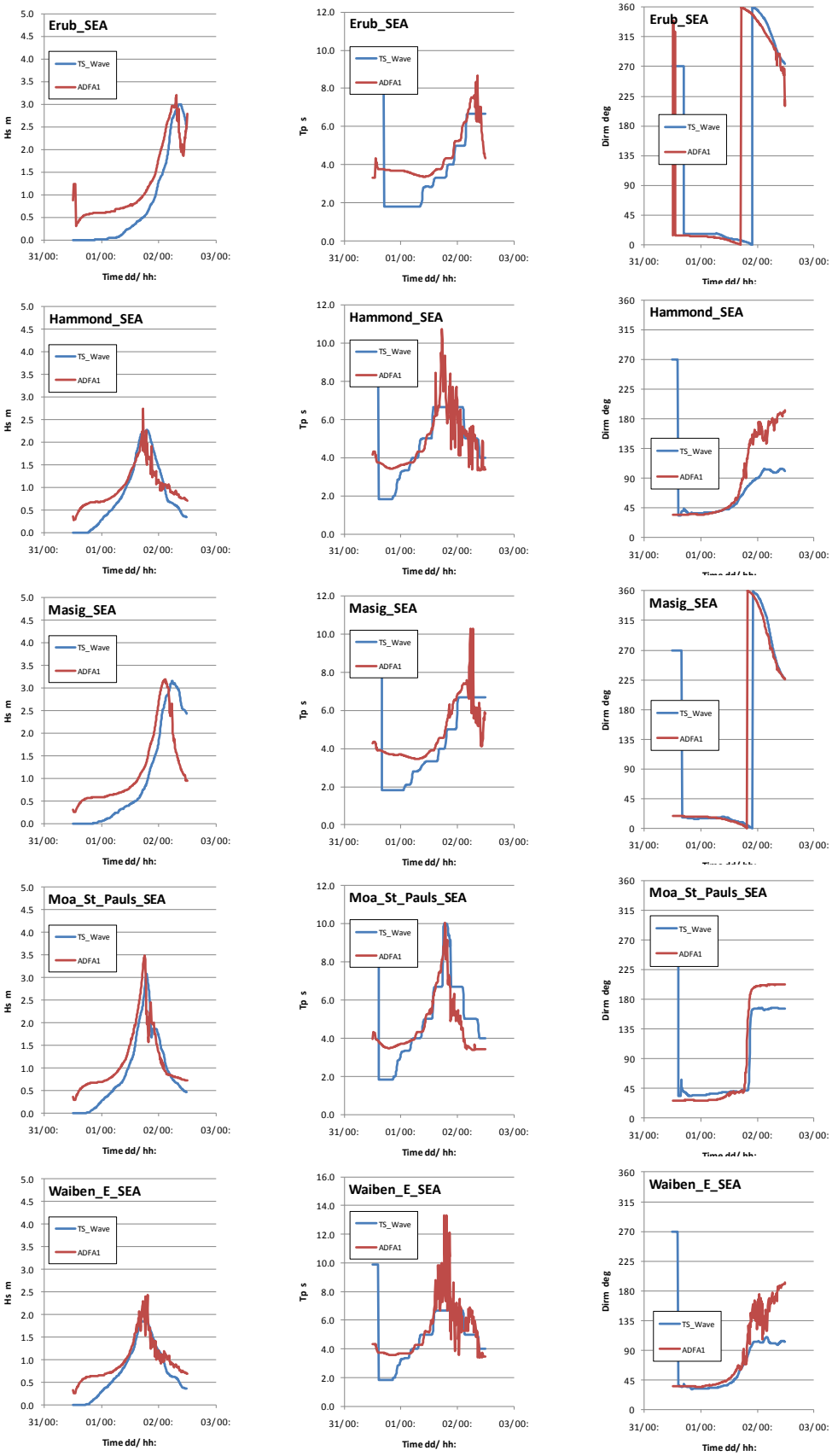

Figure 8-7 Example W-E Centre scenario time history comparisons.

With interest in the performance of the *TS_Wave* model in this context, the same wind field is applied to each of the site-specific fetch-limited definitions applicable to each community location. The intercomparison of *TS_Wave* and *ADFA1* is summarised in Figure for some of the better performing locations, showing a reasonably good matching of the shape, timing and peak conditions for Hs, Tp and mean direction. Considering the approximations made in *TS_Wave* this is a good result, however many other sites do not compare as favourably as these and Figure 8-8 summarises the model comparison of peak Hs and associated Tp and direction for each site. The most scatter is evident in Tp, where *TS_Wave* tends to underestimate the *ADFA1* value, although Tp is typically a somewhat unstable parameter. Comparison of the wave ray paths in *ADFA1* with the fixed rays in *TS_Wave* shows that refraction enables a greater penetration into some sites with a longer generation path and this is likely the principal reason for the relative underprediction in *TS_Wave*. This also has an impact on Hs, such that typically *TS_Wave* tends to underestimate the *ADFA1* values. Notwithstanding this, the 16 directions used for *ADFA1* are also relatively coarse and this tends to overemphasise the influence of some specific wave rays that manage to get through the complex bathymetry, whereas it can be expected that in reality there would be significant shielding and diffraction acting to limit the wave energy propagation through the reef margins.

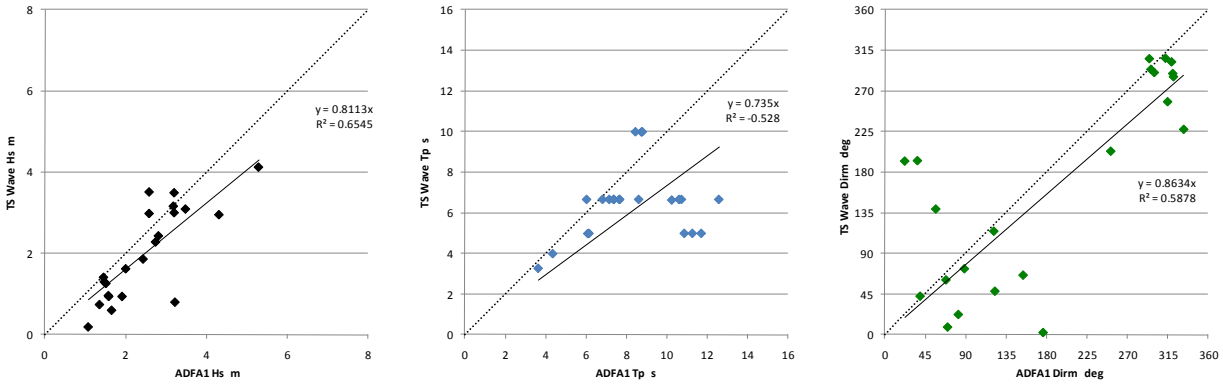

Figure 8-8 Summary of W-E Centre scenario model comparisons.

However, with a view to “calibrating” *TS_Wave* against the more sophisticated *ADFA1*, Appendix L provides the full set of site comparisons for this test and three further extreme scenarios that were examined. These consist of the reverse ‘E-W Centre’ case and two complementary tracks that pass further to the south, near the tip of Cape York. One of the poorest performing sites in the model inter-comparisons was Mabuiag where the Hs value was consistently underestimated by *TS_Wave* by as much as 80% of the ADFA1 result. Although it does not seem to have the most complex exposure (refer Figure 8-1), it would appear to be more affected by refractive processes.

Some other sites also performed badly in some scenarios and so a simple linear "calibration" has been applied to all sites. This was achieved by averaging the peak error in Hs and Tp across each of the four scenarios at each site and inverting the resulting linear coefficient to normalise the results. The adopted coefficients[17] are listed in Appendix N as site-specific input to the SATSIM statistical model.

The results of this calibration process are summarised in Figure 8-9, whereby the results for each of the four scenarios are colour-coded and scenario-specific linear fits are indicated for the Hs and Tp results. The grouped scenario trend is also shown, which reflects the calibration process forcing an unbiased result, albeit with some significant scatter. This is a relatively crude attempt to construct a wave model for the region that has some reasonable level of skill for the very complex situation of a TC yet still provide a practical means of modelling over extended periods. Importantly, the reason for modelling waves is to obtain an estimate of breaking wave setup that will potentially add to the storm tide elevation at many sites (see below).

8.4 Breaking Wave Setup and Wave Runup

The statistical SATSIM model (Section 11) is used to estimate the total quasi-steady water level at a coastal site as a function of tide + surge and breaking wave setup components. Due to the variety of coastal morphologies in the region, this is separated into exposed beaches and fringing reef classes.

8.4.1 Exposed Beaches

Breaking wave setup at exposed sandy beaches is estimated using the empirical method of Hanslow and Nielsen (1993), whereby the shoreline superelevation η relative to the MSL is assumed to be:

$$\eta = 0.048\sqrt{H_{orms} L_o} \quad (4)$$

where H_{orms} is the incident equivalent deepwater root-mean-square wave height and L_o is the deepwater wave period. This relationship is based on extensive field monitoring of wave setup on a range of sandy beaches under varying incident wave conditions. The additional effect of vertical wave runup has also been considered but in a generalised way only, noting that wave runup is typically influenced by many localised factors, including beach slope. Wave runup must also be considered in a statistical manner, and a nominal 1% exceedance wave run-up estimate has been based on Nielsen and Hanslow (1991), as described in Harper (2001).

[17] The Mabuiag Hs calibration factor was subjectively reduced after unreasonably high wave conditions were generated using the directly derived calibration coefficient.

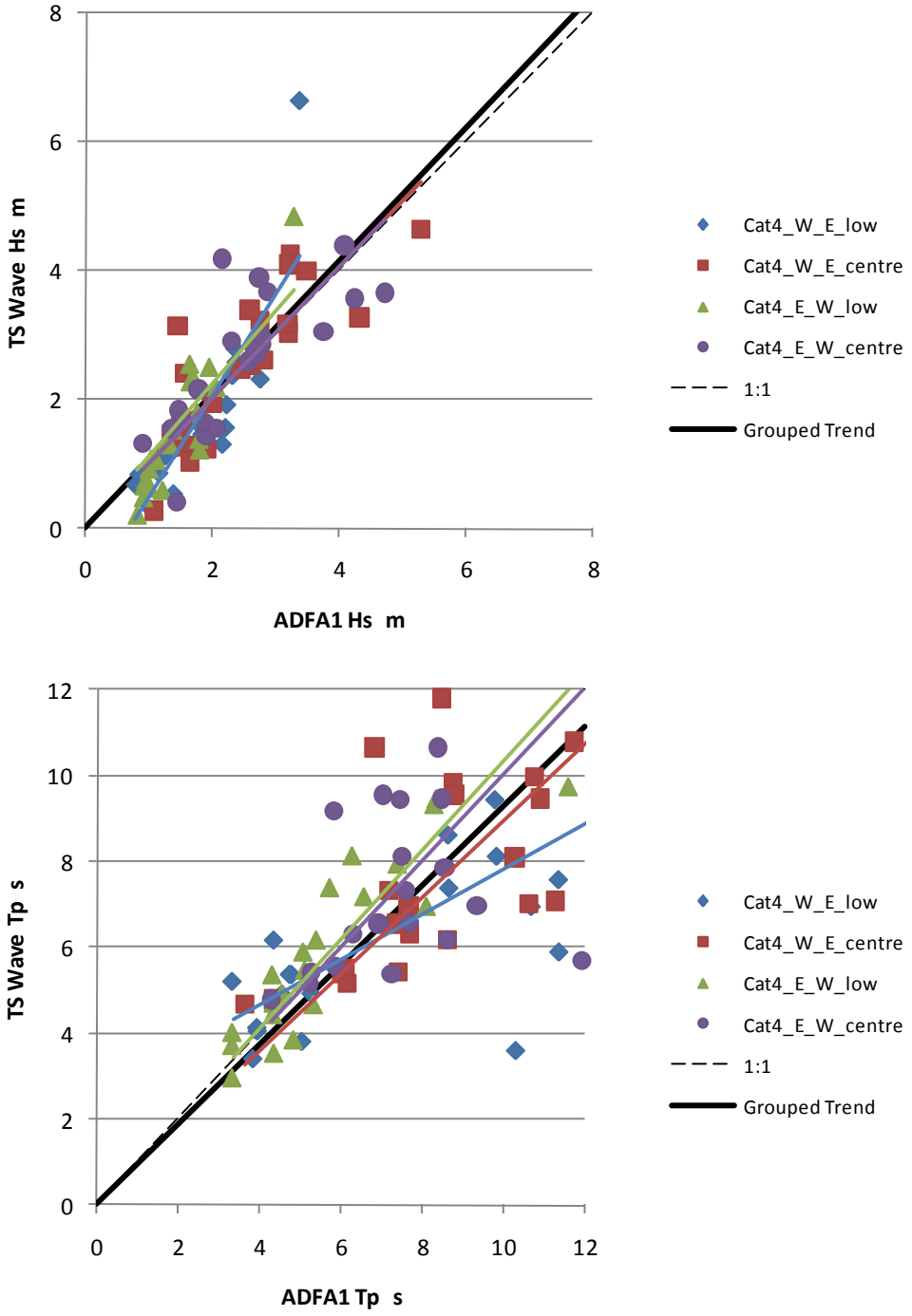

Figure 8-9 The calibrated *TS_Wave* vs *ADFA1* performance for the selected tropical cyclone scenarios.

8.4.2 Fringing Reefs

Many of the community shorelines are more appropriately described as fringing reefs, with a narrow upper beach. These present a specific set of physical characteristics that can create very significant wave setup, raising the water levels on the reef-top, and driving reef-top current systems that may control lagoon flushing and sediment transport processes.

In extreme situations, reef-top wave setup can be responsible for overtopping and flooding of low lying islands, and is likely to be the largest component of storm tide at deepwater islands with a fringing reef. In particular, the combination of astronomical tide variation, storm surge and incident wave height and period present a very dynamic and sensitive wave setup environment, as schematised in Figure 8-10. Wave runup can also occur on the upper beach caused by the remaining transmitted wave energy.

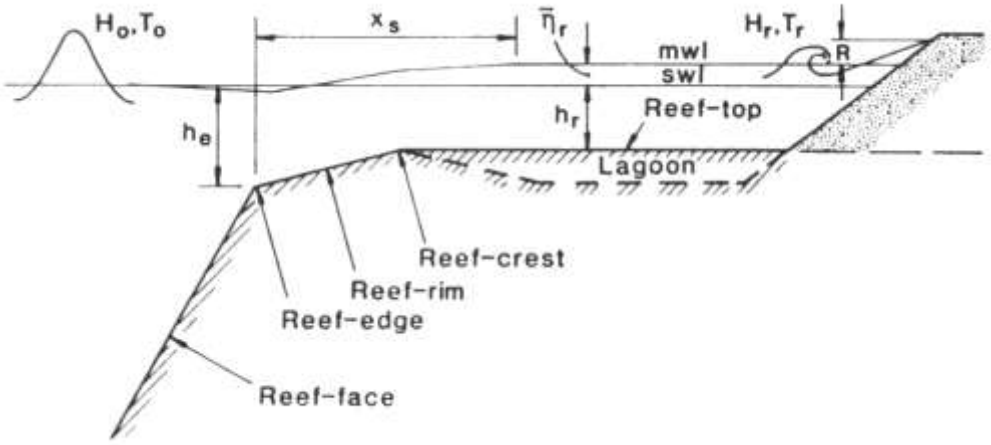

Figure 8-10 Fringing reef wave setup definitions (after Gourlay 1997).

A number of geometric parameters are required to describe this complex situation, and these have been estimated based only on very limited information such as that available from aerial photography or satellite images, together with advice from TSRA (D. Hanslow). The adopted site-specific parameters are listed in Appendix N.

8.5 Production Wave Modelling

While the economical steady-state wave model performed reasonably well compared with the unsteady *TS_Wave* model at many communities, it was decided to apply the unsteady model to the broadscale wind climate for the baseline 60 y period of NCEP winds. The regionally-adjusted NCEP winds were then used as the representative winds within the Torres Strait for local fetch-limited wave growth.

9. Land Elevation Datums

One of the principal sources of uncertainty in the present study has been the estimation of land elevation heights relative to the modelled Mean Sea Level (MSL). Accurate land elevation is a critical parameter needed to assess the relative impacts of storm tide events on the various communities and to enable detailed inundation mapping that can assist in future planning decisions, especially in regard to projected sea level rise.

9.1 Background

Historically there has been difficulty in establishing accurate land elevation datums due to the complex tidal regime and the paucity of long term sea level measurements in the region. This has led to a variety of methods being used for the different Torres Strait communities over time, many on an ad-hoc basis, that have resulted in anomalous estimates of MSL and the various tidal planes being used for infrastructure projects. This has contributed to the poor performance of some facilities and infrastructure.

Prior to the long-term tidal measurements established for shipping in the 1970s (AMSA), the Thursday Island (MSQ) tide gauge has been the sole source of regionally specific sea level information. However, as is evident from the discussion in Section 4, the regional tidal variability is such that these data have only limited areal significance and traditional simplified methods of inter-island datum transfer are not reliable.

In preparation for the present study, TSRA and DERM acted to help resolve the lack of tidal data in the region by commissioning a field study during May-June of 2008, whereby tide data was successfully collected at 13 sites across the Torres Strait by Griffith University (GU) researchers (Zier et al. 2009). While of significant benefit to the present study, the limited observation periods of 35 days, the need for non-overlapping deployments and various practical difficulties meant that this dataset was also below the level of accuracy normally desirable for the accurate determination of land datums.

While it was not within the scope of the present study to specifically address these issues, it became apparent during the course of the work that the detailed sea level numerical modelling being undertaken would likely be a principal contributor to improving the accuracy of regional land datum estimates by informing assumptions regarding seasonality during the period of the GU measurements. As a result, TSRA requested MSQ to incorporate the regional MSL modelling results into a revised estimate of the tidal datums across the region (MSQ 2009).

An additional complication and delay during the course of the work was the revision by Geoscience Australia of the Australian Geoid

(AUSGeoid09), which was not originally intending to include the Torres Strait region in its scope. With significant additional encouragement from DERM[18], the Torres Strait was ultimately included and promised a significant improvement in datum accuracy across the region.

9.2 Adopted Land Elevation Datums

Notwithstanding the interim MSQ (2009) recommendations on tidal planes and datums, an alternative interpretation of the seasonal MSL corrections was adopted based on the analysis in Appendix M. This was deemed to be necessary to retain the full value of the broadscale modelling in better describing the high tidal gradients across the region.

The seasonal adjustments were then incorporated into the AUSGeoid09 framework by DERM, who advised specific datum shifts to be applied to the available community topographic mapping. This enabled the estimation of suitable "dune crest heights" and the typical "lowest habitation level" (LHL) of each Torres Strait community to complete the statistical model description and to allow estimation of impacts. Both of these values are somewhat nominal, given that a single parameter is adopted to represent what are spatially varying situations, but this is consistent with the overall high-level statistical modelling approach. Subsequent detailed re-mapping of the regional topography is planned that will extend the modelling beyond the point-specific nature of this assumption and enable a comprehensive impacts assessment.

The outcome of this process is summarised in Table 9-1 and Figure 9-1, whereby the DERM-supplied datum shifts have been applied to the interpretation of the available topographic mapping for each community. This yields the local MSL-relative heights for the dune crest (used by the modelling to modulate the effects of wave setup and runup) and the LHL (used for assessing impacts). Also shown are a selection of HAT estimates available from MSQ and ANTT, as well as the modelled HAT and LAT levels from this study[19]. Likewise, as a reference, the harmonically-based estimate of the MHHW level is indicated, which is based on a combination of the O_1, K_1 and M_2 constituent magnitudes (average of modelled and measured values has been used).

The very significant datum shifts at some locations reflects the previous use of estimated low water and other types of temporary datums. Also, it is immediately evident that the communities likely to be at greatest risk from inundation are those where the HAT level is close to (e.g. Masig) or even exceeds the estimated LHL (e.g. Boigu and Saibai).

[18] Due to the efforts of project team member Peter Todd from Gassman Development Projects, who had at this time returned to employment with DERM.

[19] This is based on utilising measured constituents where available but adopting the modelled Sa and Ssa values (except at Waiben) plus measured Mm and Msf. Epoch used is 1992-2012 with 10 min sampling.

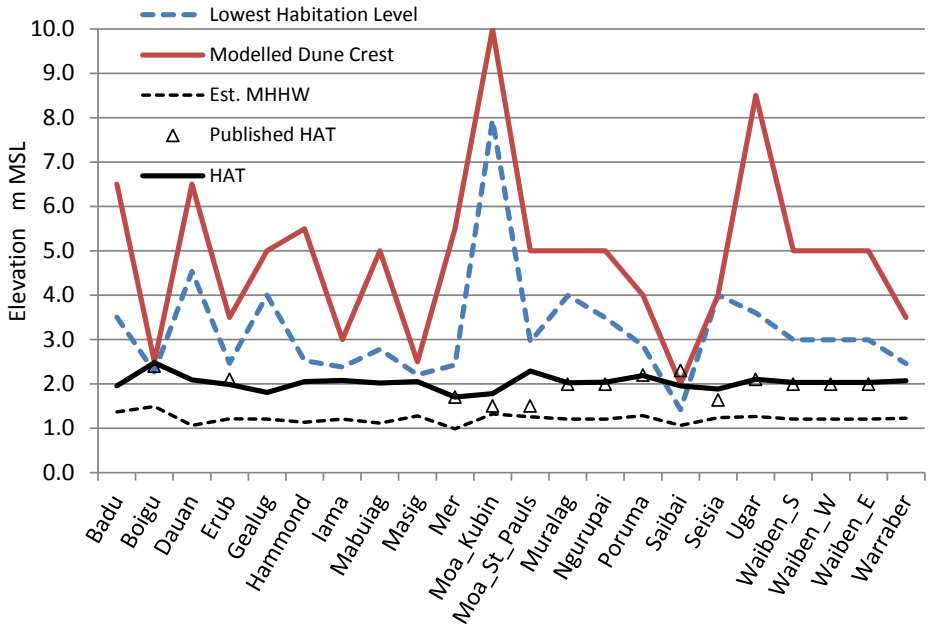

Figure 9-1 Adopted local MSL-relative datums.

Table 9-1 Adopted local MSL-relative datums.

Community	DERM ICC Datum Shift m	Modelled HAT m MSL	Modelled LAT m MSL	Lowest Habitation Level m MSL	Assumed Dune Crest m MSL
Badu	0.006	2.0	-1.9	3.5	6.5
Boigu	-1.929	2.5	-2.0	2.3	2.5
Dauan	1.033	2.1	-1.7	4.5	6.5
Erub	-1.534	2.0	-1.8	2.5	3.5
Gealug	0.000	1.8	-2.3	4.0	5.0
Hammond	0.023	2.1	-1.7	2.5	5.5
Iama	-0.615	2.1	-1.7	2.4	3.0
Mabuiag	-0.216	2.0	-2.0	2.8	5.0
Masig	1.705	2.1	-1.9	2.2	2.5
Mer	0.424	1.7	-1.5	2.4	5.5
Moa_Kubin	-0.050	1.8	-1.8	8.0	10.0
Moa_St_Pauls	-0.050	2.3	-1.7	3.0	5.0
Muralag	-0.006	2.0	-1.7	4.0	5.0
Ngurupai	-0.006	2.0	-1.7	3.5	5.0
Poruma	-3.385	2.2	-1.9	2.9	4.0
Saibai	-2.078	2.0	-1.7	1.4	2.0
Seisia	0.000	1.9	-1.8	4.0	4.0
Ugar	-1.898	2.1	-1.6	3.6	8.5
Waiben_S	-0.006	2.0	-1.7	3.0	5.0
Waiben_W	-0.006	2.0	-1.7	3.0	5.0
Waiben_E	-0.006	2.0	-1.7	3.0	5.0
Warraber	-2.041	2.1	-1.7	2.5	3.5

10. Deterministic Hindcast Modelling

While the principal goal of the simulation model is to provide a statistical basis for estimating extreme winds, waves and water levels it is also important to demonstrate that it has deterministic skill compared with some known historical events. One example of that was provided in Section 5.6 in regard to the broadscale hydrodynamic model's simulated water level response to TC *Charlotte* in the Gulf of Carpentaria in January 2009. In this section TC *Charlotte* is again considered, but this time in the combined simulation modelling context. Another recorded example of broadscale-driven water level impacts in January 2006 is also considered. As a final demonstration, the *Douglas Mawson* TC event of 1923 is modelled to compare with the limited available anecdotal information.

10.1 Modelled Impacts of Remote TC *Charlotte* in Jan 2009

The background to TC *Charlotte* was discussed earlier and comparisons with the AMSA tide gauges in the region were reasonably good. Here we provide output from the simulation model at various sites.

Figure 10-1 Impacts from TC *Charlotte* at Saibai on 12-Jan-2009 (D. Hanslow photos)

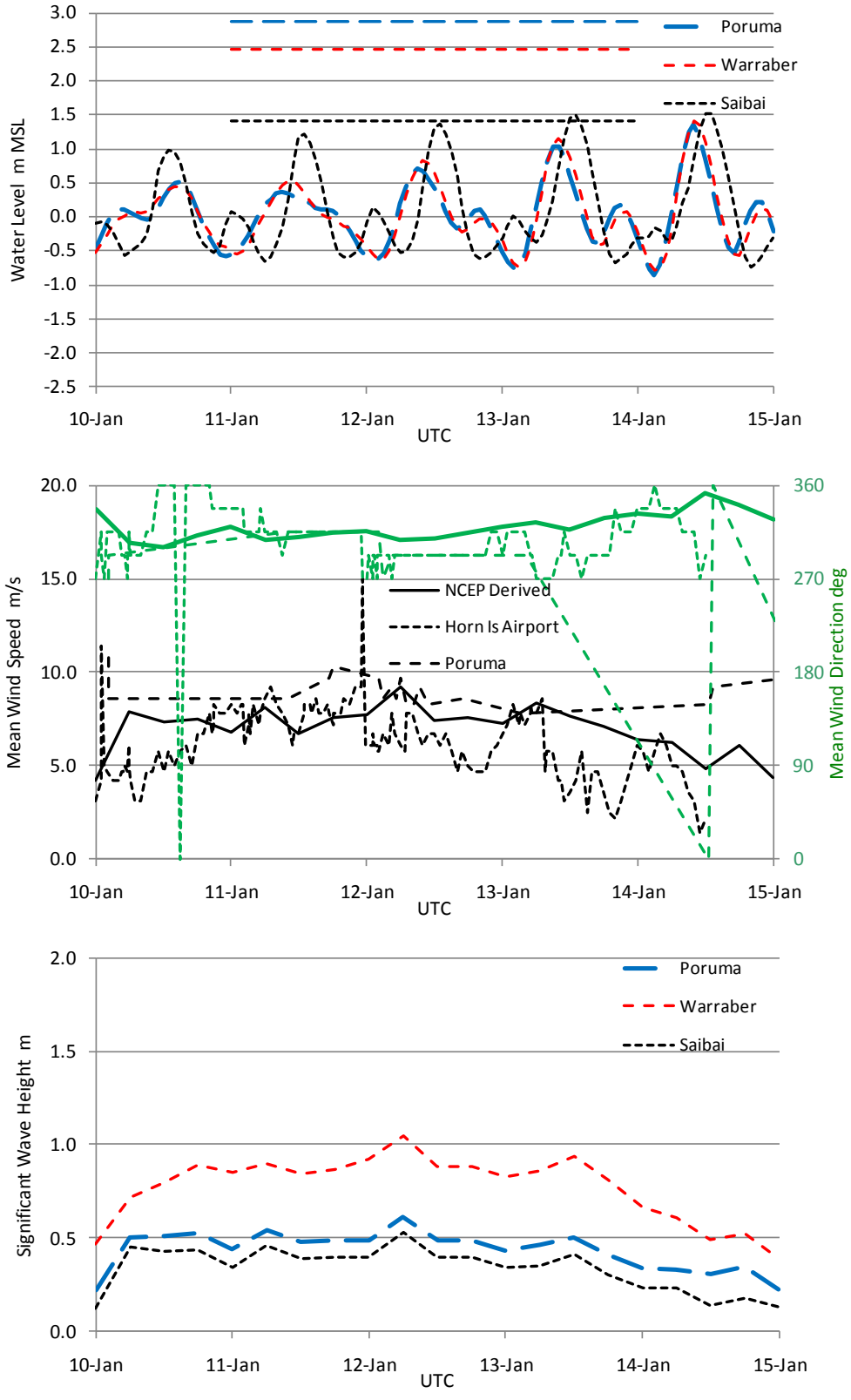

Figure 10-2 Simulation model outputs during TC *Charlotte*.

Figure 10-1illustrates the typical impacts of these types of events at the low lying community of Saibai. Figure 10-2 presents the modelled time history of the combined tide+surge water level (top panel), the modelled and measured winds during the same period (middle panel) and the modelled wave heights (bottom panel) for the selected community sites of Poruma, Warraber and Saibai.

The top panel of Figure 10-2 also shows the estimated LHL at each community, whereby it can be seen that Saibai was modelled to experience impacts at around this time. The other communities experienced much lower water levels but (refer bottom panel) all were expected to have significant wave action.

The middle panel shows the actual recorded winds from Horn Island Airport and Poruma, compared with the model-assumed winds, which are based on the adjusted NCEP time series as previously discussed. It can be seen that these model-assumed winds compare quite favourably with the local measurements (which are raw/uncorrected in this case) both in speed and direction.

10.2 Modelled Impacts of “King Tides” in Jan 2006

A similar water level impact event was chronicled by the EPA in 2006, with the photographs in Figure 10-3 taken from the EPA publication of the time. This shows inundation at Saibai and water levels at Poruma and Warraber reaching jetty deck levels, together with significant wave activity.

The corresponding modelled conditions are shown in Figure 10-4 and suggest more severe impacts than during TC *Charlotte* at each of these locations. The modelled inundation at Saibai is of the order of 0.5 m in some habitation areas and, although not directly inundated, both Poruma and Warrraber are predicted to have had significant wave impacts, with additional contribution from wave setup also being likely. The wind comparison shows that the adjusted NCEP winds are typically well in excess of the raw Horn Island record (as desired, based on the foregoing arguments) but may tend to overpredict the event in this instance. There are no winds available for Poruma during this event.

10.3 Modelled Impacts of the TC *“Douglas Mawson”* in March 1923

This event pre-dates any quantifiable data but a reconstruction is attempted here to illustrate the possible impacts indicated by the models developed for this investigation. After some trial reconstructions, the official BoM track (refer Figure 10-5) and central pressure estimates were adopted together with nominal values for radius to maximum winds (30 km) and Holland B (1.2) when in the vicinity of the Torres Strait. The later reported severe impacts at Groote Eylandt were not examined.

Figure 4 – Sabai Island late January 2006 (courtesy Qbuild).

Figure 5 – Poruma (Coconut Island) on 30 Jan 2006 (courtesy Poruma Island Council).

Figure 6 – Warraber Island late January 2006 (courtesy Warraber Island Council.

Figure 7 – Poruma (Coconut Island) on 28 February 2006 (courtesy Poruma Island Council).

Figure 10-3 Impacts from "King Tides" in 2006

(From EPA Qld FACT SHEET 2006 King Tides in Torres Strait http://www.derm.qld.gov.au/services_resources/item_details.php?item_id=200392&topic_id=54)

As noted in Appendix H, the anecdotal impacts are of significant damage to Darnley (Erub), Coconut (Poruma), Mabuiag and Murray (Mer) communities, comprising houses being unroofed, trees down, gardens damaged and pearl luggers dismasted. The Erub community was reported to have been virtually destroyed with banks of living coral 4 to 5 feet high dashed up by the waves.

The reconstructed wind field (Figure 10-6) using the assumed parameters produces peak winds in the area around 26th March, with gusts of up to 32 ms^{-1} at Erub (116 km h^{-1} or 63 kt) and only slightly lower values at Mabauig, Mer and Poruma. Gale force mean winds are also estimated to have affected Thursday Island further to the west.

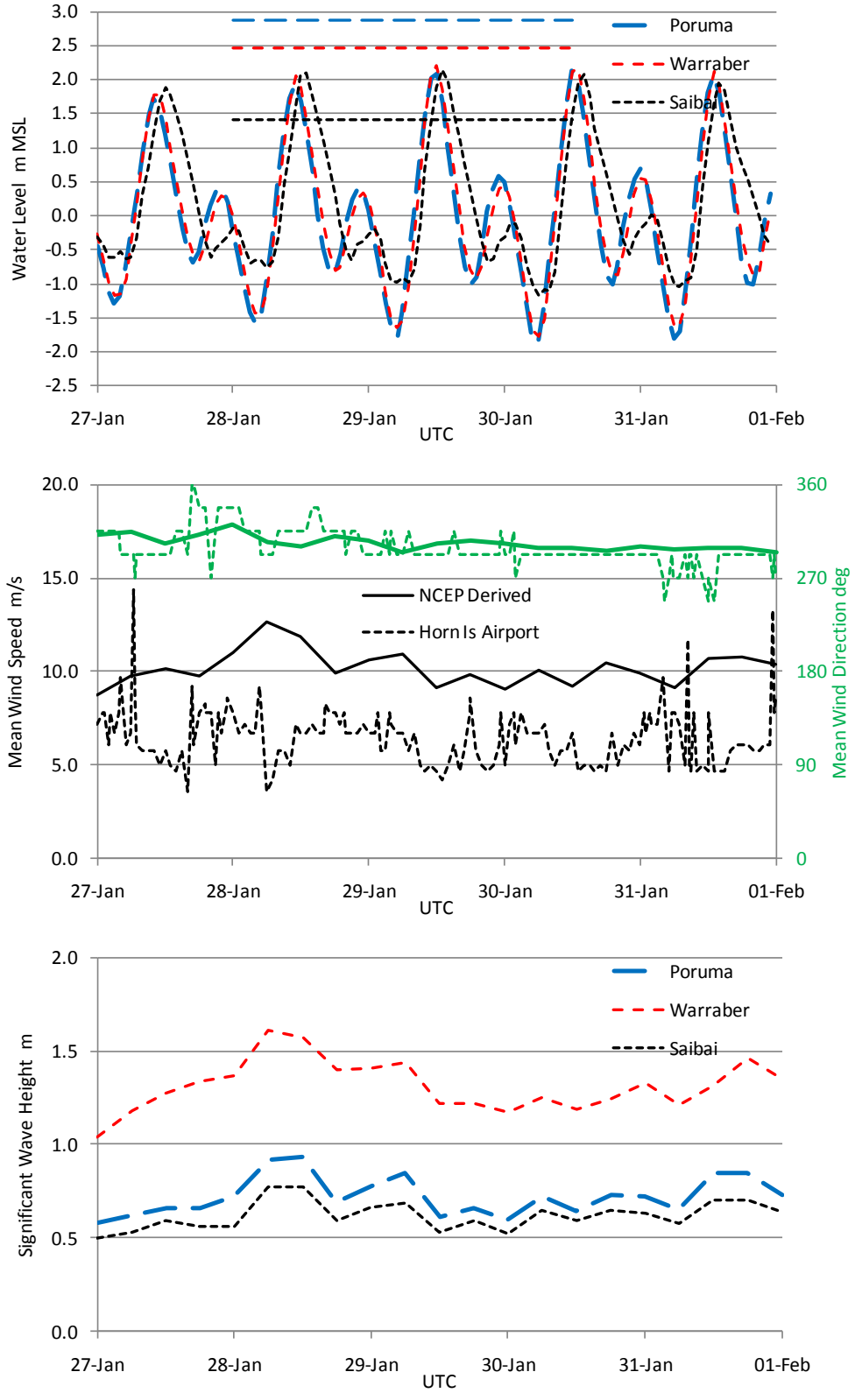

Figure 10-4 Simulation model outputs during “King Tide” event in 2006.

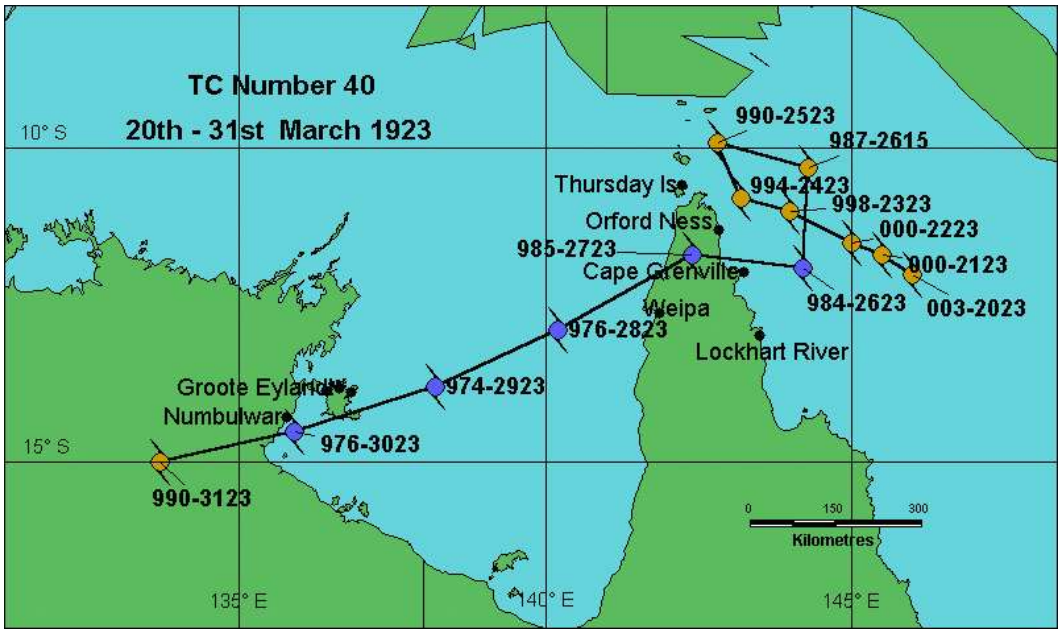

Figure 10-5 The historical track for the TC *Douglas Mawson* in 1923.

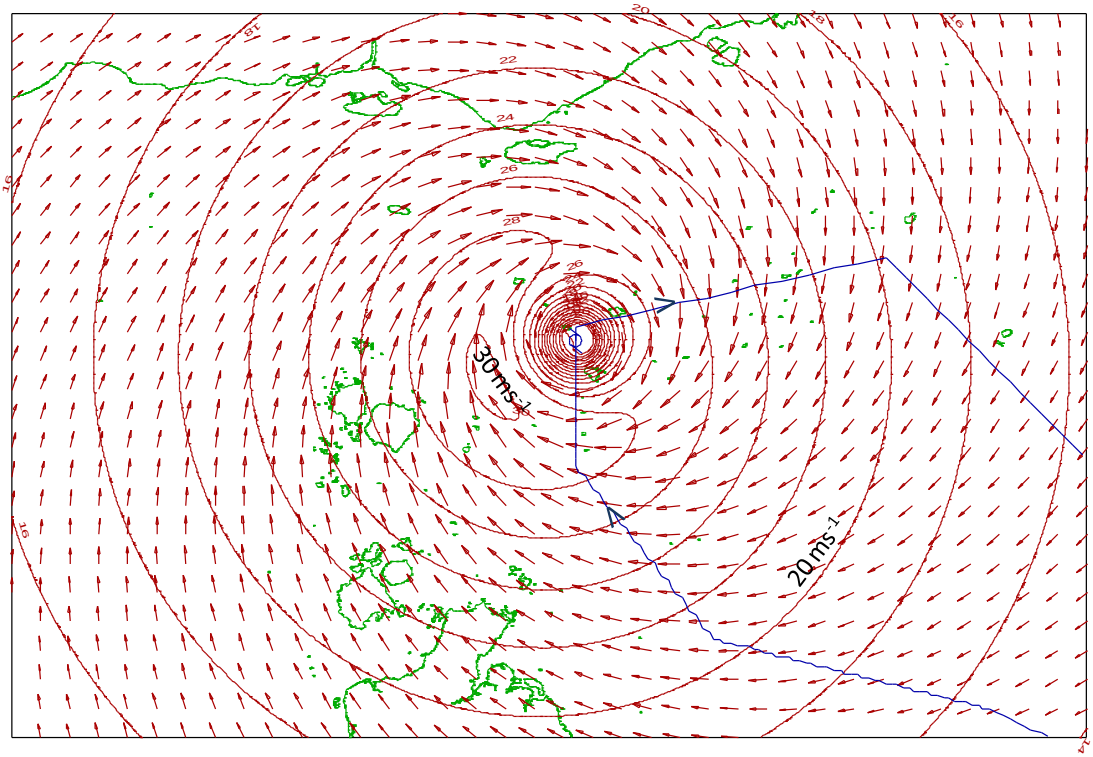

Figure 10-6 Modelled wind gust field of the TC *Douglas Mawson* 25/03/1923 22:00 UTC.

Figure 10-7 presents the results of the numerical modelling of tide plus surge, winds and waves for a selection of sites in Torres Strait, including those that were noted as having significant impacts.

Firstly, the tide plus surge at various sites shows very little evidence of any significant storm surge and the levels are well below the approximate LHL in each case. The highest modelled storm surge in the region during this event was 0.5 m at Boigu (not shown), associated with the later passage of the storm across Cape York and into the Gulf of Carpentaria. Surge magnitudes at the various islands that had reported impacts were typically of the order of 0.2 m. Of some significance though is the fact that the easterly islands such as Mer, Erub, Poruma and Warraber were likely experiencing a neap tide period, whereby it can be seen that the predicted tides were close to MSL and varied only slightly during the period of the maximum winds and waves. This may have exacerbated the effects of waves on the fringing reefs, whereby the near constant water level may have increased the amount of reef damage.

The modelled wind speeds show that all islands in the region likely experienced some significant impacts, which because of the near-circular track over several days, increased the period of exposure as well as varying the wind direction. Here Erub and Mer have the higher winds but Warraber also experiences an eye passage.

The predicted waves tend to follow the trend in winds, with Erub and Mer indicated to have experienced significant wave heights up to 2.5 m and peak spectral periods of about 7 s, which would have been capable of causing extensive damage and breaking wave setup (not modelled in this case).

It is again stressed that the *Douglas Mawson* simulation here is more of a demonstration than a validation of the modelling techniques because of the lack of verifying quantitative information and the nominal values adopted for some of the necessary storm parameters. The official track and intensity must also be regarded as very approximate also. Nevertheless, the models indicate that a significant impact on the islands is indicated, which is reasonably consistent with the anecdotal information.

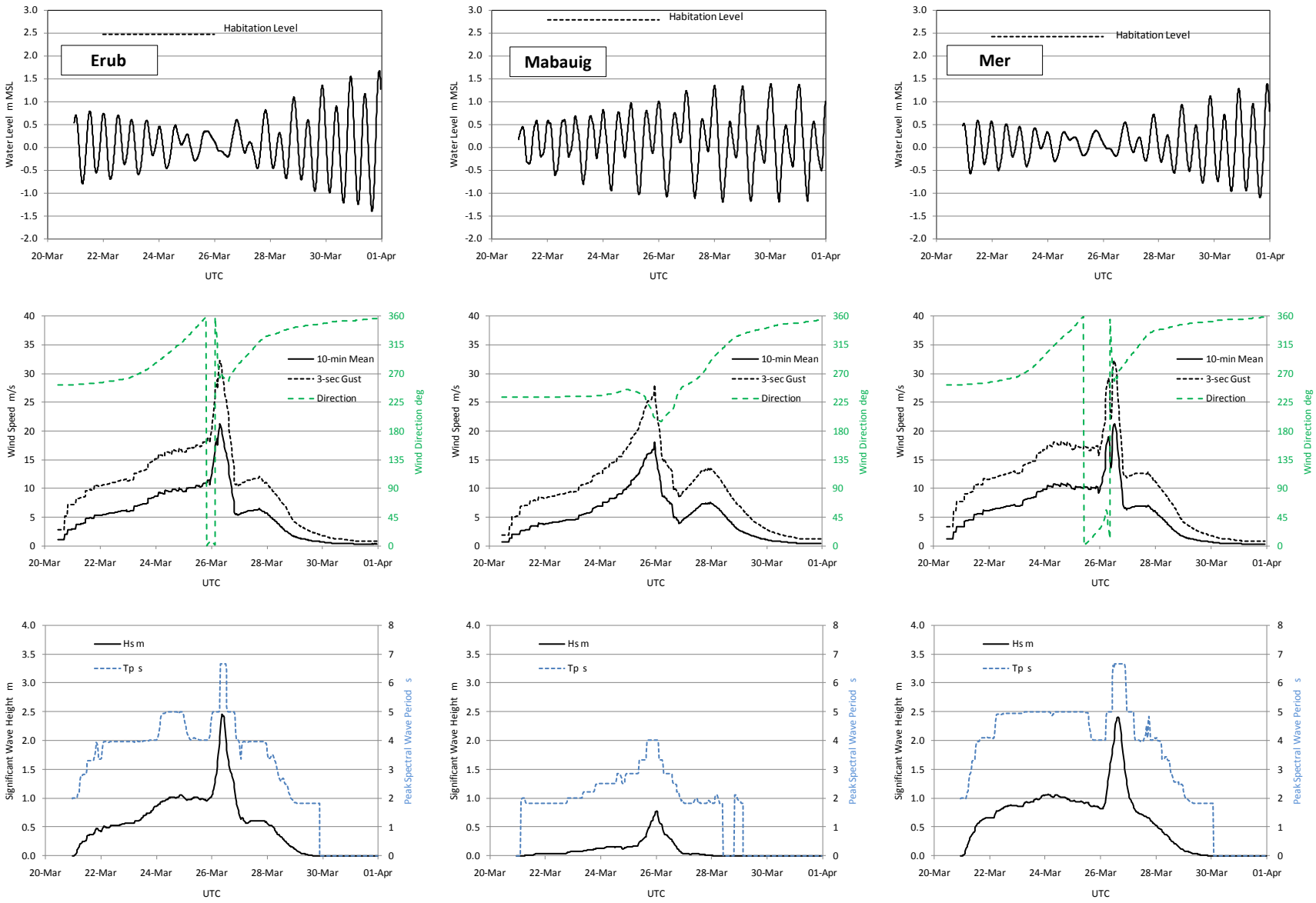

Figure 10-7 Modelled water level (top), winds (middle) and waves (bottom) of the TC *Douglas Mawson*

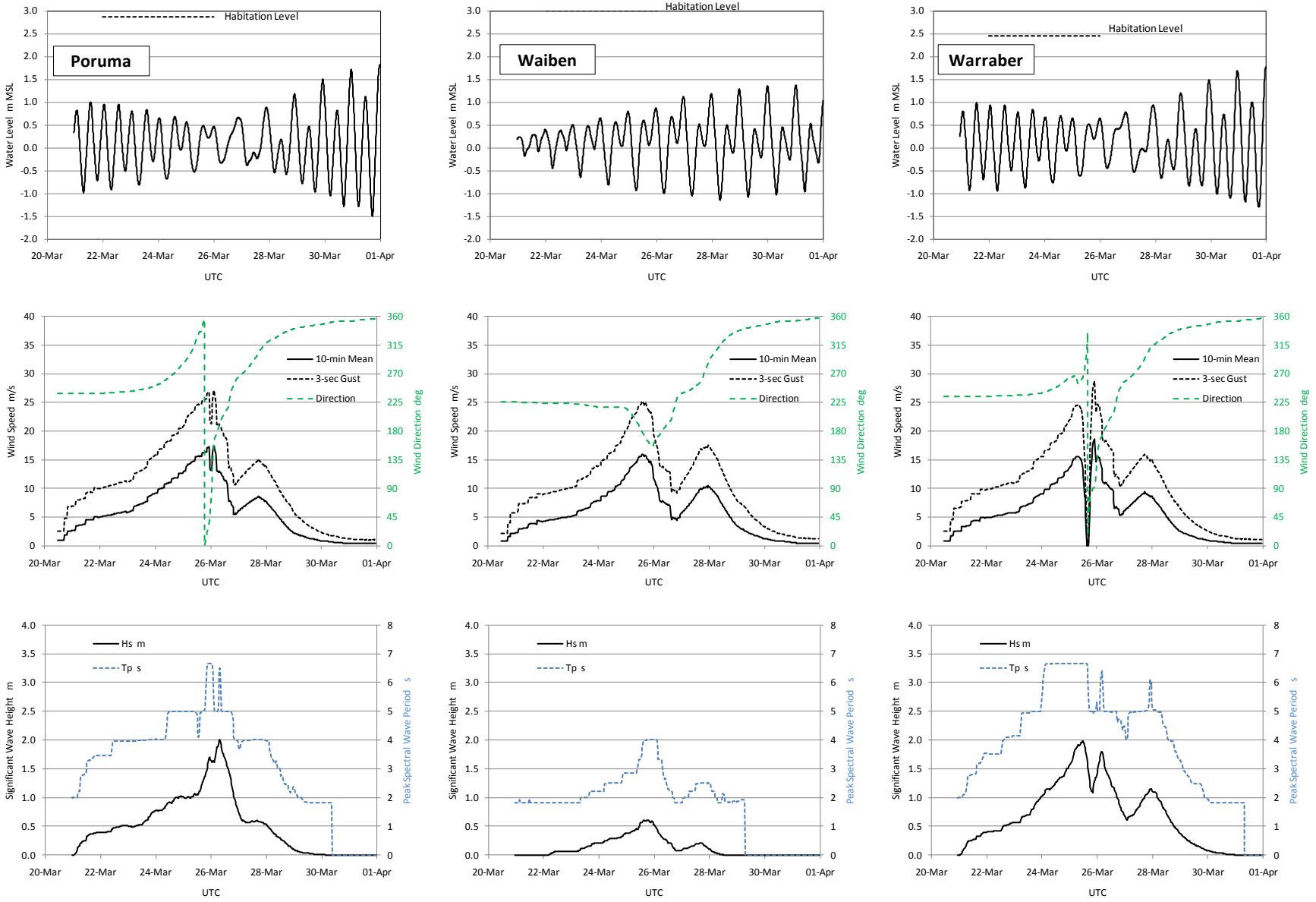

Figure 10-7 Modelled water level (top), winds (middle) and waves (bottom) of the TC *Douglas Mawson (contd.)*

11. Statistical Storm Tide Simulation Modelling

The regional water levels are statistically modelled using a specially-developed variant of the SEA numerical model SATSIM (Surge And Tide SIMulation). This is a discrete Monte-Carlo event sampling model that operates at a 30 min timestep and accumulates exceedance statistics of winds, tide+surge, wave height, breaking wave setup and runup at all of the Torres Strait community sites. The typical length of a simulation is 50,000 y, which for example provides 50 values to form the basis of the average 1000 y return period water level estimate. Importantly, the modelling methodology retains all seasonally-locked information, such as the astronomical tide, the annual broadscale forcing and the summer-only TC influences.

11.1 Overview of the Climate Simulation Process

Figure 11-1 provides a schematic of the operation of the model, which is initialised in time at the start of the NCEP hindcast winds sequence in 1949. The model then steps forward by one week at a time and treats each week as an independent climate event window. Only the highest exceedance of any parameter of interest within each week and at each site is counted and included in the statistics.

Broadscale Forcing

The broadscale modelled parameters from Section 5 for the week of interest are first considered. This consists of the surface mean wind speed and direction for the nominal Horn Island site, which is adjusted according to the calibration process described in Section 3.3 to be more representative of the “local” Torres Strait wind. This broadscale wind condition is assumed to apply at all community sites.

The broadscale modelled water level (tide + surge) is also retrieved for the week of interest and this varies across the modelled sites as a function of the combined tidal, NCEP wind and external inter-annual and inter-decadal forcing, as discussed in Section 5.

Tropical Cyclone Forcing

For each week of interest, the model checks to see if a TC is scheduled to be active in the region. This condition is controlled by the climatology description of Section 6.2.5, whereby each defined track class has an associated average inter-arrival interval (the Poisson statistic). Each of the three TC track classes is considered and it remains possible that more than one storm might exist in the same week within the chosen 500 km radius. Only the summer half-year is considered capable of generating a TC event.

The mean and gust wind speeds are then modelled for each TC that is present, using the parametric wind and pressure model detailed in

Harper (2001), based on the Holland (1980) approach. If a specific storm generates winds at the Horn Island location that are greater than the corresponding broadscale winds, then that TC is considered a contender for inclusion, else it is rejected and its effects are ignored. This is consistent with the assumption of separation of scale between local and broadscale. The TC contender with the highest winds that exceed the broadscale condition is then retained, if any. The TC generated wind, surge and wave time series is then retrieved for all sites and blended into the equivalent broadscale parameters for the week of interest. Surge-tide interaction factors are included at this time so that the modelled TC storm surge time history is sensitive to the underlying broadscale tide+surge level.

Breaking Wave Setup and Runup

With each complete week's time series of tide+surge, directional wave height and period being available, the breaking wave setup and runup is calculated according to the methods of Section 8.4. These parameters are then sensitive to site-specific water depth, beach slope, reef configuration and dune crest elevation as applicable. The total storm tide level is then calculated as the tide+surge+setup combination.

Exceedance Statistics

The time history of each parameter of interest during the modelled week is then analysed to determine the equalled or exceeded count of a set of discrete event levels of 0.05 m vertical resolution. Each level exceedance is only counted once for each week. Hence, if total storm tide variation at the 30 min resolution exceeds 2 m on three separate occasions, say 2.0, 2.1, and 2.2, only one count of equalling or exceeding each level is recorded. In addition, the time-persistence statistics of each parameter is retained, which provides insight into the distribution of individual event exceedances.

Time Stepping

The model is then advanced by one week in time to repeat the process. After each year of 52 weeks, the year is advanced. When the simulation year exceeds the broadscale re-sampled time period at the year 3208, the model resets the simulated year back to the start of 1949 so that the broadscale variability is sampled again and in the same sequence. Subsequent TCs however are allowed to continue to vary randomly, thus allowing for further variability in the combined broadscale and TC forcing. After 50,000 y of simulation the model ends and the final statistical results are available for each parameter of interest and at each site.

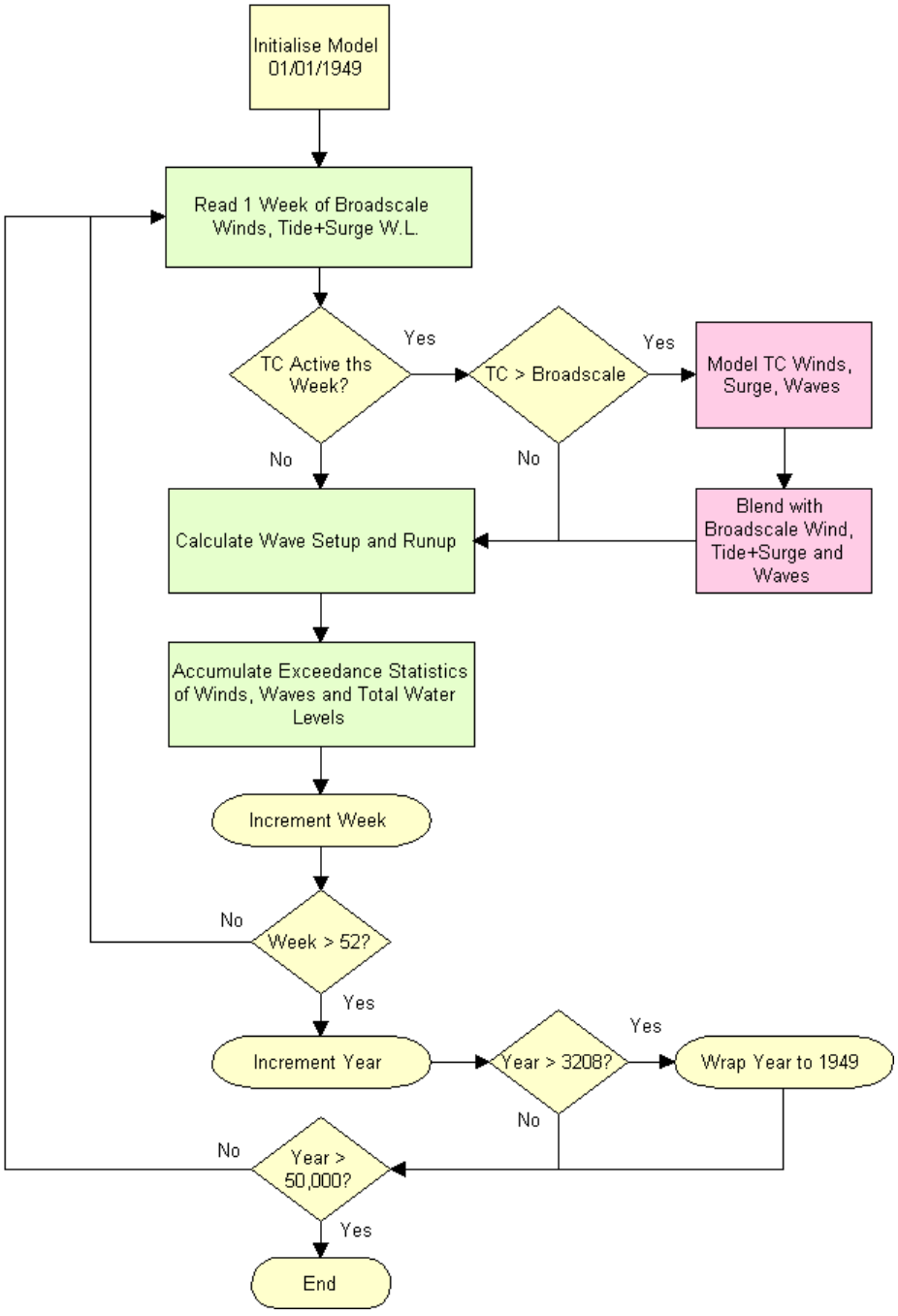

Figure 11-1 Schematic of the operation of the Torres Strait SATSIM model.

11.2 Statistical Verification of the Simulation Model

11.2.1 Simulated Broadscale Wind Climate

This is achieved by comparing a short 1000 y SATSIM simulation without TC influences being active, to the regionally-recorded stratified non-cyclonic wind speeds from Section 3.2.3 and the raw NCEP winds averaged to a point near Horn Island.

The NCEP comparison is shown in Figure 11-2, where the EV1 (Gumbel) line is fitted to the blue raw NCEP data and the dashed black line is the blue line simply adjusted upwards here by 1.38 according to the calibration process in Section 3.3. The red triangles are the SATSIM simulation result, which falls between these two lines. This is a satisfactory result, showing that the model statistics are incorporating the adjusted NCEP winds, even though it does not match the dashed line at short return periods. This is because the linear adjustment of the dashed line does not correctly represent the effect of the 1.38 factor in an exceedance context and it is used here as a reference only.

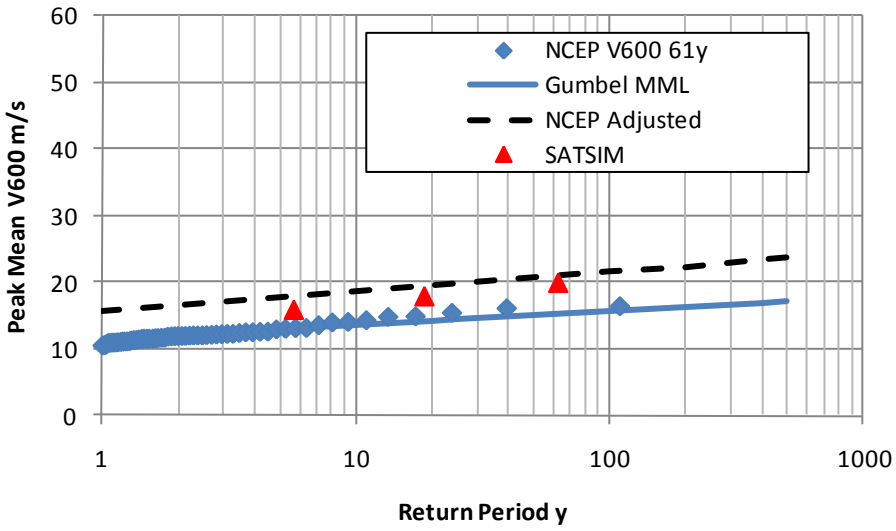

Figure 11-2 Comparison of the broadscale modelled NCEP winds (raw and adjusted) and the simulated SATSIM mean wind climate for the nominal Thursday Island site.

Next, the SATSIM simulated winds are compared with site-adjusted winds from the regionally-representative Thursday Island and Coconut Island sites. This is done in Figure 11-3, where the mean winds are shown in the top panels and the peak daily gusts in the lower panels. By these comparisons, the Thursday Island site still appears to be underpredicted by the simulation model, especially in the gust context. However the Coconut Island comparisons, albeit of lesser duration, are

reasonably well represented. It should be noted that the SATSIM model assumes a $G_{3,600}$ gust factor of 1.41, which can be regarded as slightly overconservative (high biased) relative to the more likely gust factor of 1.38 or less for nearshore conditions (Harper et al. 2010) that are likely representative of the shallow Torres Strait environment. However, as discussed in Section 3.2.4, the gust record at Thursday Island remains problematical, likely due to the complex topography and the surrounding island influences.

Importantly, the SATSIM-sampled NCEP-adjusted winds are seen to be performing well at Coconut Island, where the 1.38 factor was derived.

Given the issues with data quality this is deemed a satisfactory simulation outcome for the broadscale wind component, which is used by SATSIM to generate the local non-cyclonic wave climate.

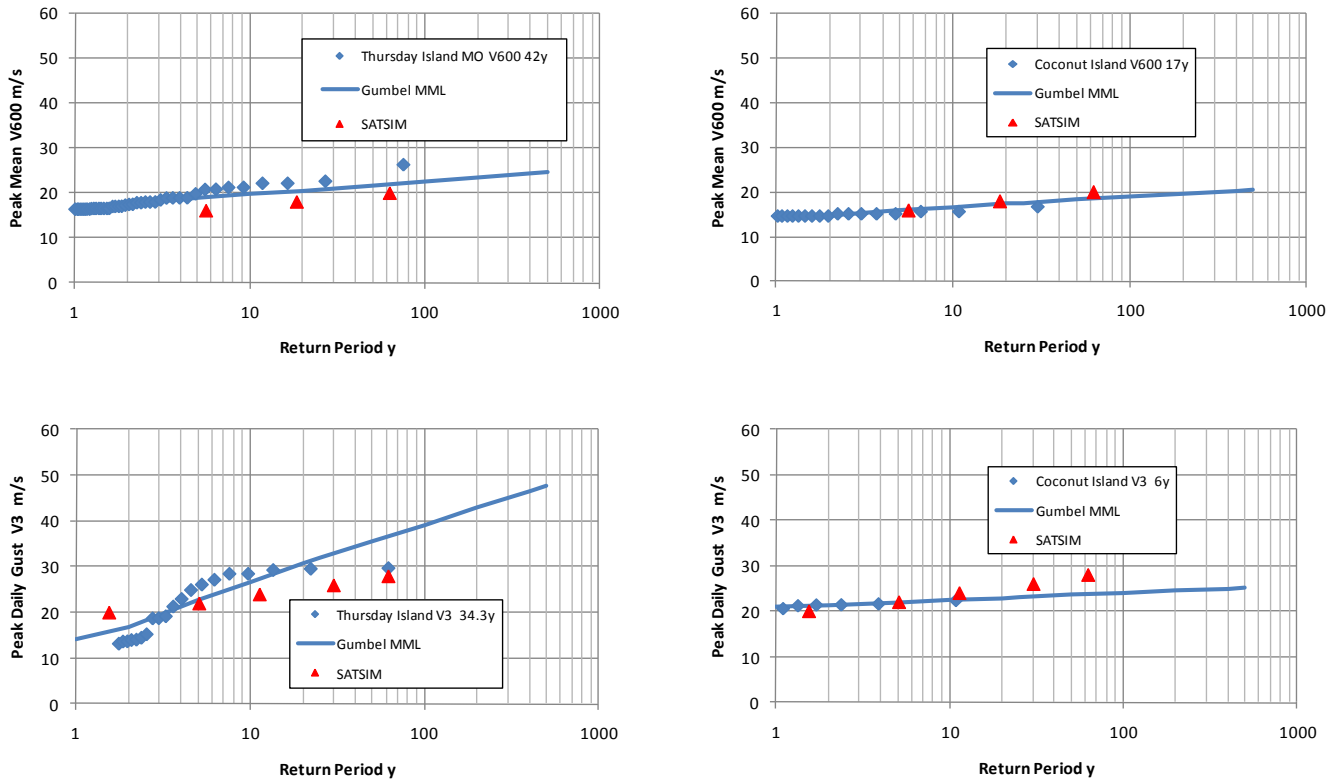

Figure 11-3 Comparisons of the adjusted measured mean and gust wind climate for Thursday Island (left) and Coconut Island (right) with the broadscale SATSIM simulation assigned to the whole of the Torres Strait.

11.2.2 Simulated Combined Broadscale and Tropical Cyclone Wind Climate

The verification of the TC-related simulated winds is the more difficult to demonstrate due to the noted rarity of intense TCs that have made a close approach within the period of measured wind data. Hence the veracity of the SATSIM result hinges on the various assumptions made in Section 6.2 and the range of sensitivity analyses that were done. Inevitably these are relatively subjective, but with similarly conceived assumptions, the model has been found to be quite reliable in many previous studies (e.g. Harper 1999, SEA 2001, 2005, 2007; GHD/SEA 2003, 2004, 2005, 2007, 2009).

Firstly, it is instructive to consider the range and distribution of the TC tracks that are generated by the model. These are controlled by the parameterisations of Section 6.2.5 that identified the three principal track populations within the 500 km radius from Thursday Island. The result of 100 y of simulation is provided in Figure, showing that there is a noticeable reduction in storm tracks north of Cape York, but a finite number of tracks that do pass through the Torres Strait.

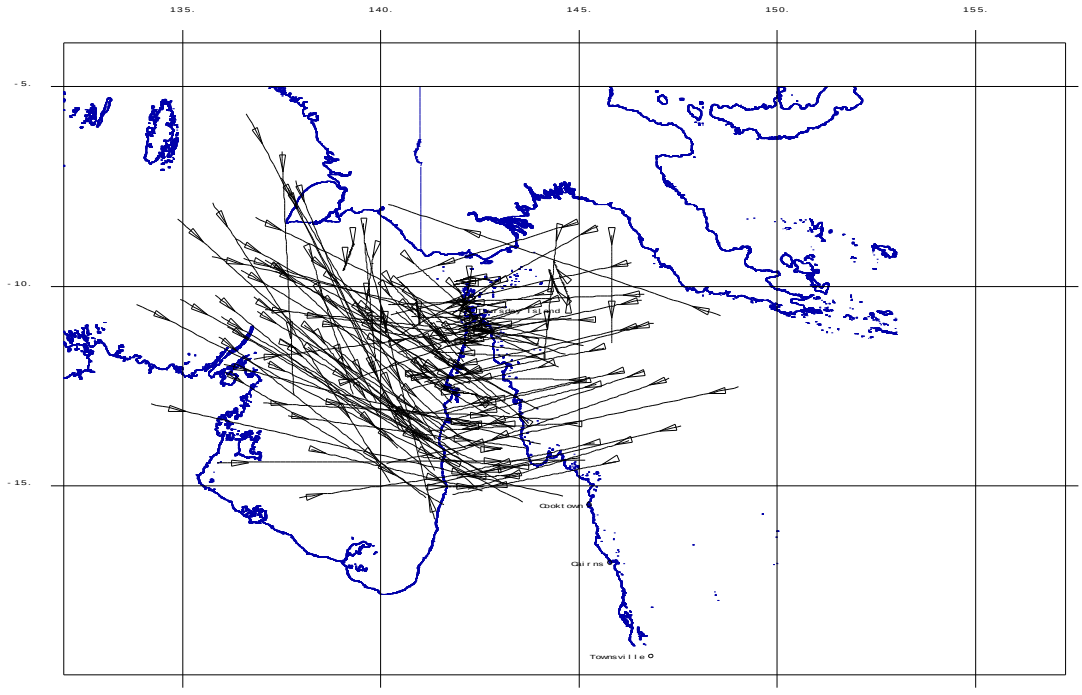

Figure 11-4 Example of 100 years of SATSIM-simulated tropical cyclone tracks within 500 km of Thursday Island.

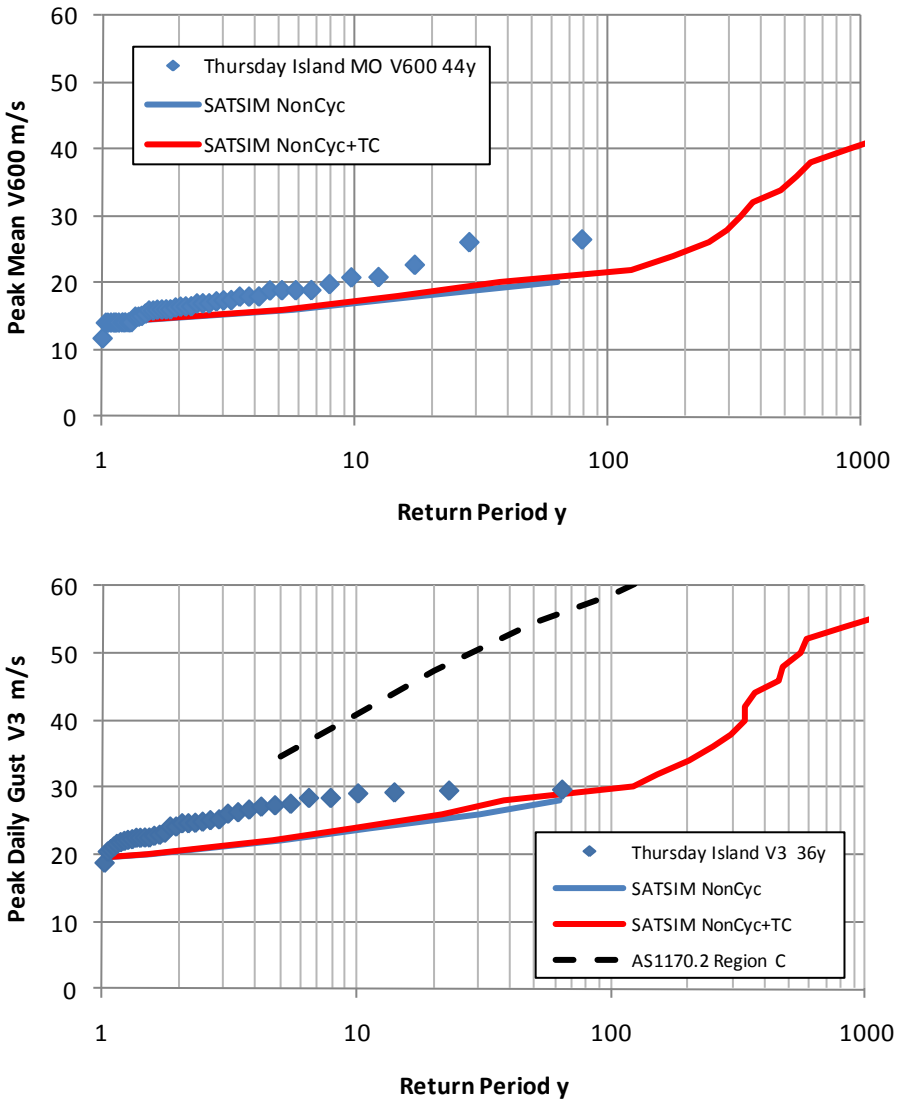

Figure 11-5 SATSIM-simulated wind speeds at Thursday Island for a 50,000 y period compared with the available (adjusted) wind speed record.

By way of comparison with what is regarded as a more stable wind reference location, Figure 11-6 shows the same comparison with the wind data from Weipa, which is of slightly longer record. In this case the regionally simulated Torres Strait winds and the measured Weipa winds seem more consistent. The basis of accepting a good match in this case would be that Weipa and Thursday Island experience a similar wind climate. This may not be the case, and one can argue that Weipa is a more protected site, but given that the model places Weipa in a much more TC-threatened environment (refer Figure) it further supports the thesis that the measured winds at Thursday Island are probably overstated and that the simulated TC winds are likely reasonable or even potentially conservative.

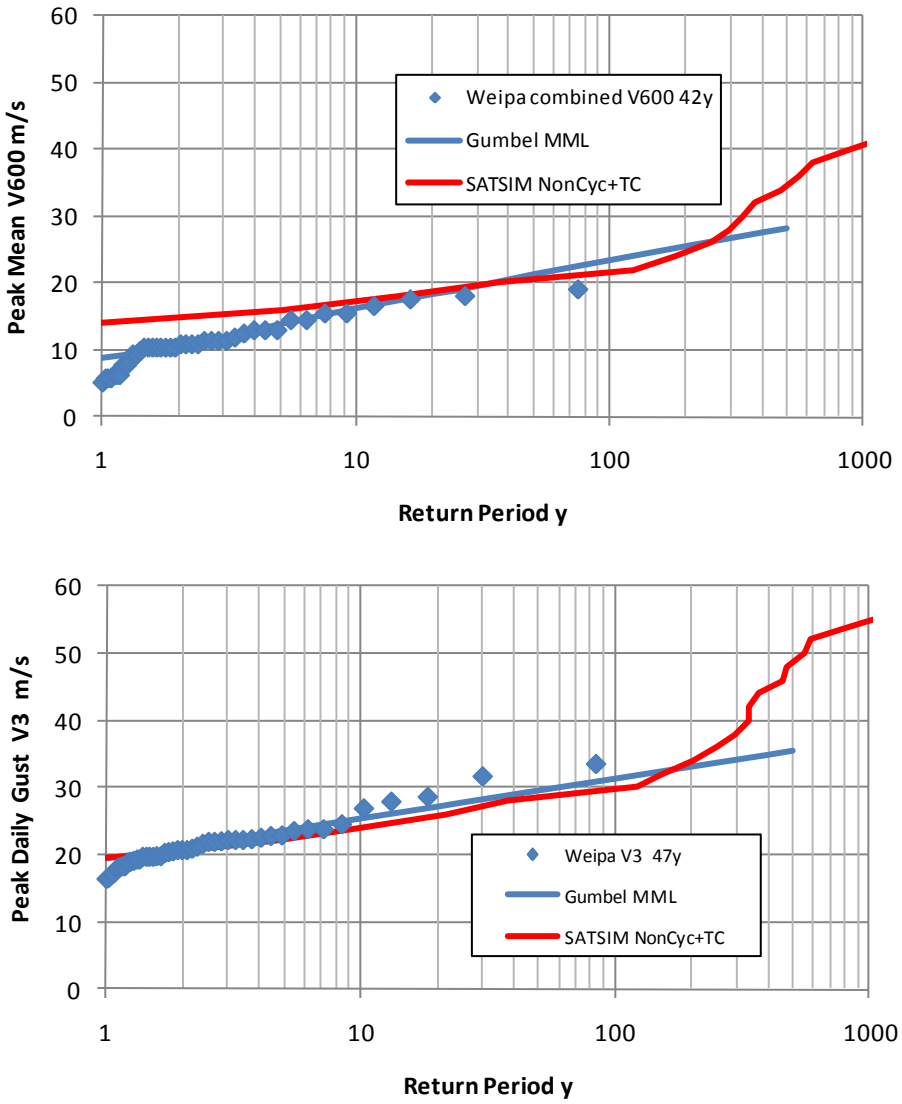

Figure 11-6 SATSIM-simulated wind speeds at Thursday Island for a 50,000 y period compared with the available (adjusted) wind speed record at Weipa.

11.2.3 Simulated Extreme Broadscale-Forced Water Levels

The methodology of simulating the broadscale water level response outlined in Section 5.4 does not require validation *per se*, as it is simply a random phase-shifted re-sampling of the modelled residual water levels in concert with the 60 y NCEP wind sequences and the annual and inter-annual background signals. However, for completeness, Figure 11-7, presents the simulated broadscale "total storm tide" level comprising tide plus surge plus setup water level return periods for each of the modelled communities. These are relative to the modelled MSL at each of the islands.

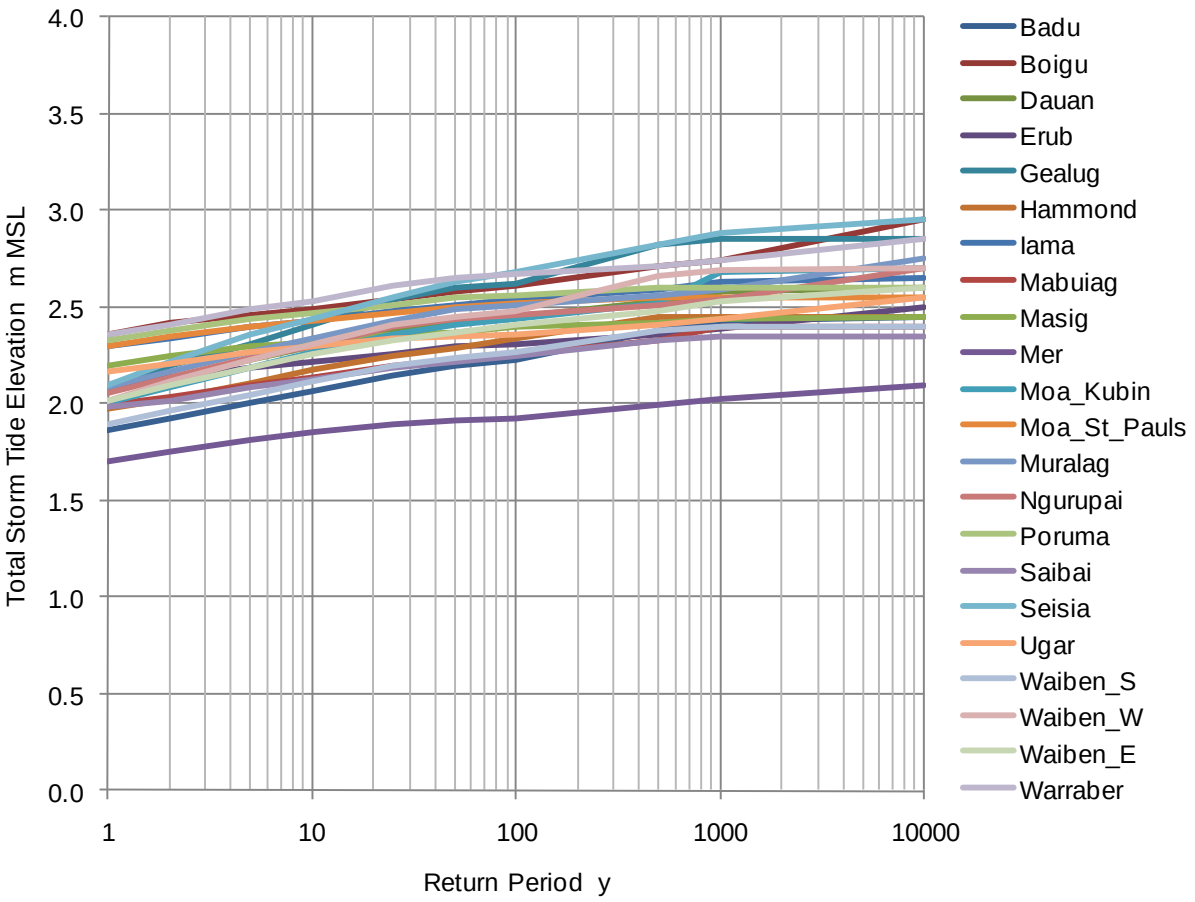

Figure 11-7 SATSIM-simulated broadscale-forced tide plus surge plus setup levels.

It can be seen that the bulk of the communities could expect a 100 y return period broadscale tide plus surge plus setup level between 2.2 and 2.4 m, which is bounded by about the 1000 y return period. However Mer has a much lower level of risk due to its easterly location nearer deep water and Boigu has a much higher risk due to its close proximity to the area shown in Figure 5-8 adjacent to the Papua New Guinea coast, where the tidal and wind forcing effects tend to be concentrated.

11.3 Simulated Combined Storm Tide Levels for Present Climate (2010)

The results of the simulation of combined broadscale and local TC forcing for a 50,000 y period are summarised for all communities in Figure 11-8 and Table 11-1. These are the “total storm tide” level referenced to local MSL, which comprises the effects of the astronomical tide, storm surge and breaking wave setup components.

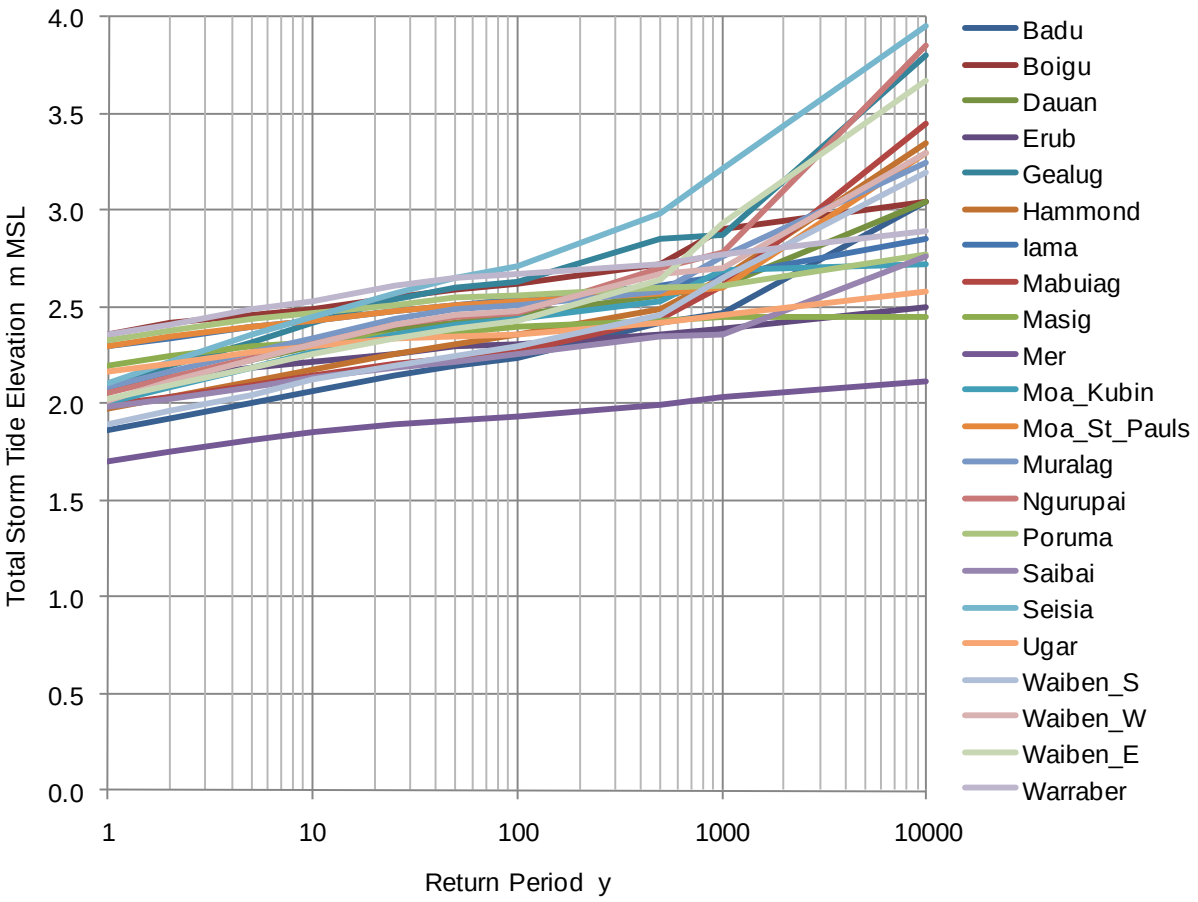

Figure 11-8 Simulated tide plus surge plus setup return period water levels for present climate (2010) relative to MSL.

As previously described, the magnitude of the breaking wave setup component is limited by the defined “dune crest” elevation in all cases.

From the graph it is evident that, compared with Figure 11-7, the local TC forcing begins to influence some communities at around the 100 y return period and dominates their response at the very low risk levels (high return periods). These communities are ones located closest to the mainland or in close proximity to other islands. The water level at the more remote isolated islands are largely unaffected by TC events. Appendix O also graphs these results in small community groups for more clarity.

Table 11-1 Estimated return period of total storm tide level for 2010 climate relative to MSL datum.

Site	1 y m MSL	2 y m MSL	5 y m MSL	10 y m MSL	25 y m MSL	50 y m MSL	100 y m MSL	500 y m MSL	1000 y m MSL	10000 y m MSL	HAT m MSL	LHL m MSL
Badu	1.86	1.92	2.01	2.07	2.15	2.20	2.24	2.42	2.47	3.05	1.96	3.51
Boigu	2.36	2.42	2.46	2.49	2.55	2.59	2.62	2.72	2.90	3.05	2.48	2.27
Dauan	2.07	2.14	2.23	2.30	2.39	2.42	2.46	2.56	2.61	3.05	2.09	4.53
Erub	2.09	2.14	2.19	2.22	2.26	2.30	2.31	2.36	2.39	2.50	1.99	2.47
Gealug	2.09	2.20	2.32	2.42	2.54	2.60	2.63	2.85	2.87	3.80	1.81	4.00
Hammond	1.97	2.04	2.12	2.18	2.26	2.31	2.36	2.49	2.65	3.35	2.06	2.52
Iama	2.30	2.34	2.40	2.43	2.48	2.51	2.54	2.61	2.66	2.85	2.08	2.39
Mabuiag	1.99	2.04	2.10	2.15	2.21	2.24	2.27	2.44	2.61	3.45	2.02	2.78
Masig	2.20	2.25	2.30	2.32	2.36	2.37	2.40	2.43	2.45	2.45	2.06	2.21
Mer	1.70	1.75	1.81	1.85	1.89	1.91	1.93	1.99	2.04	2.12	1.70	2.42
Moa_Kubin	2.00	2.09	2.19	2.27	2.36	2.41	2.44	2.53	2.69	2.72	1.78	7.95
Moa_St_Pauls	2.30	2.35	2.40	2.43	2.48	2.51	2.53	2.57	2.60	3.30	2.29	2.95
Muralag	2.09	2.17	2.27	2.34	2.44	2.49	2.51	2.58	2.76	3.25	2.03	3.99
Ngurupai	2.06	2.14	2.24	2.31	2.41	2.45	2.47	2.70	2.78	3.85	2.04	3.49
Poruma	2.33	2.38	2.44	2.47	2.51	2.55	2.56	2.60	2.61	2.77	2.19	2.87
Saibai	1.98	2.03	2.09	2.14	2.19	2.22	2.26	2.35	2.36	2.76	1.96	1.42
Seisia	2.11	2.22	2.36	2.45	2.57	2.65	2.71	2.98	3.22	3.95	1.89	4.00
Ugar	2.17	2.21	2.27	2.30	2.34	2.35	2.36	2.42	2.46	2.58	2.11	3.60
Waiben_S	1.89	1.96	2.05	2.13	2.20	2.25	2.30	2.46	2.65	3.20	2.03	2.99
Waiben_W	2.02	2.12	2.23	2.31	2.41	2.46	2.48	2.67	2.70	3.30	2.03	2.99
Waiben_E	2.03	2.10	2.19	2.26	2.34	2.39	2.43	2.64	2.93	3.67	2.03	2.99
Warraber	2.36	2.41	2.49	2.53	2.61	2.65	2.67	2.72	2.77	2.89	2.07	2.46

Table 11-1 lists the estimated total storm tide levels relative to the 2010 MSL datum for a range of return periods and also shows the height of the modelled HAT (Highest Astronomical Tide) and the LHL (Lowest Habitation Level). In this case the LHL levels should be regarded as approximate only pending detailed mapping of the community elevations.

In terms of assessing the vulnerability of the communities, it is then appropriate to consider the estimated water level elevations relative to the LHL. The results of performing this simple elevation shift is graphed in Figure 11-9 and similarly tabulated in Table 11-2 (alphabetical by site) and Table 11-3 (by island cluster). This presentation immediately highlights the most vulnerable communities, where the community curve moves above the 0.0 level, indicating that water level will likely enter onto present day inhabited land and the vulnerable community levels are highlighted in red. A negative value in this context means that the community is not subject to inundation at that return period.

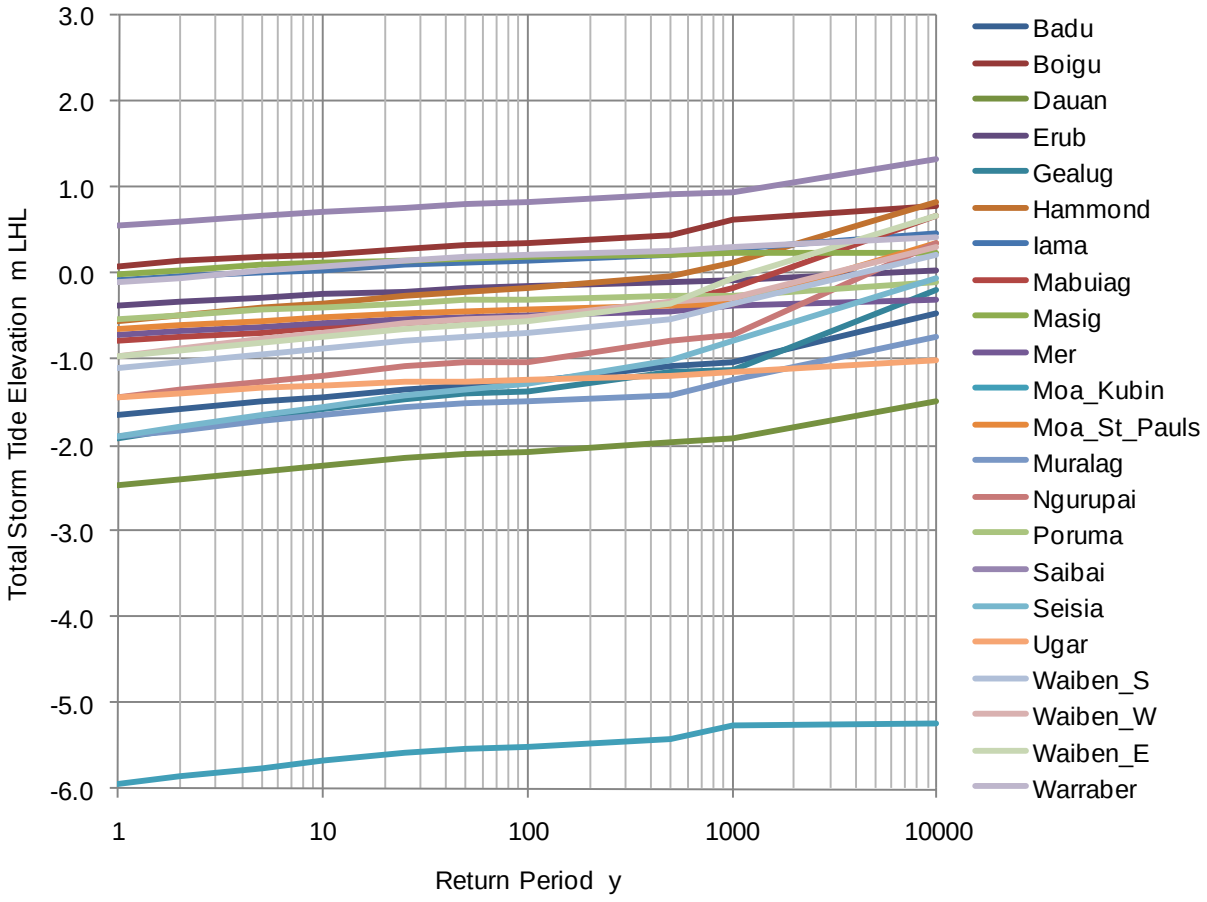

Figure 11-9 Simulated tide plus surge return period water levels for present climate (2010) relative to LHL datum.

Table 11-2 Estimated return period of total storm tide level for 2010 climate relative to LHL datum.

Site	1 y m LHL	2 y m LHL	5 y m LHL	10 y m LHL	25 y m LHL	50 y m LHL	100 y m LHL	500 y m LHL	1000 y m LHL	10000 y m LHL	HAT m LHL	LHL m LHL
Badu	-1.65	-1.59	-1.50	-1.44	-1.36	-1.31	-1.27	-1.09	-1.04	-0.46	-1.55	0.00
Boigu	0.09	0.15	0.19	0.22	0.28	0.32	0.35	0.45	0.63	0.78	0.21	0.00
Dauan	-2.46	-2.39	-2.30	-2.23	-2.14	-2.11	-2.07	-1.97	-1.92	-1.48	-2.44	0.00
Erub	-0.38	-0.33	-0.28	-0.25	-0.21	-0.17	-0.16	-0.11	-0.08	0.03	-0.48	0.00
Gealug	-1.91	-1.80	-1.68	-1.58	-1.46	-1.40	-1.37	-1.15	-1.13	-0.20	-2.19	0.00
Hammond	-0.55	-0.48	-0.40	-0.34	-0.26	-0.21	-0.16	-0.03	0.13	0.83	-0.47	0.00
Iama	-0.09	-0.04	0.02	0.05	0.10	0.13	0.16	0.23	0.28	0.47	-0.31	0.00
Mabuiag	-0.79	-0.74	-0.68	-0.63	-0.57	-0.54	-0.51	-0.34	-0.17	0.67	-0.76	0.00
Masig	0.00	0.05	0.10	0.12	0.16	0.17	0.20	0.23	0.25	0.25	-0.15	0.00
Mer	-0.72	-0.67	-0.61	-0.57	-0.53	-0.51	-0.49	-0.43	-0.38	-0.30	-0.72	0.00
Moa_Kubin	-5.95	-5.86	-5.76	-5.68	-5.59	-5.54	-5.51	-5.42	-5.26	-5.23	-6.17	0.00
Moa_St_Pauls	-0.65	-0.60	-0.55	-0.52	-0.47	-0.44	-0.42	-0.38	-0.35	0.35	-0.66	0.00
Muralag	-1.90	-1.82	-1.72	-1.65	-1.55	-1.50	-1.48	-1.41	-1.23	-0.74	-1.96	0.00
Ngurupai	-1.43	-1.35	-1.25	-1.18	-1.08	-1.04	-1.02	-0.79	-0.71	0.36	-1.46	0.00
Poruma	-0.54	-0.49	-0.43	-0.40	-0.36	-0.32	-0.31	-0.27	-0.26	-0.10	-0.68	0.00
Saibai	0.56	0.61	0.67	0.72	0.77	0.80	0.84	0.93	0.94	1.34	0.54	0.00
Seisia	-1.89	-1.78	-1.64	-1.55	-1.43	-1.35	-1.29	-1.02	-0.78	-0.05	-2.11	0.00
Ugar	-1.43	-1.39	-1.33	-1.30	-1.26	-1.25	-1.24	-1.18	-1.14	-1.02	-1.50	0.00
Waiben_S	-1.10	-1.03	-0.94	-0.86	-0.79	-0.74	-0.69	-0.53	-0.34	0.21	-0.96	0.00
Waiben_W	-0.97	-0.87	-0.76	-0.68	-0.58	-0.53	-0.51	-0.32	-0.29	0.31	-0.96	0.00
Waiben_E	-0.96	-0.89	-0.80	-0.73	-0.65	-0.60	-0.56	-0.35	-0.06	0.68	-0.96	0.00
Warraber	-0.10	-0.05	0.03	0.07	0.15	0.19	0.21	0.26	0.31	0.43	-0.39	0.00

Table 11-3 Estimated return period of total storm tide level for 2010 climate relative to LHL datum by island cluster.

Cluster	Site	1 y m LHL	2 y m LHL	5 y m LHL	10 y m LHL	25 y m LHL	50 y m LHL	100 y m LHL	500 y m LHL	1000 y m LHL	10000 y m LHL	HAT m LHL	LHL m LHL
Top Western	Boigu	0.09	0.15	0.19	0.22	0.28	0.32	0.35	0.45	0.63	0.78	0.21	0.00
	Dauan	-2.46	-2.39	-2.30	-2.23	-2.14	-2.11	-2.07	-1.97	-1.92	-1.48	-2.44	0.00
	Saibai	0.56	0.61	0.67	0.72	0.77	0.80	0.84	0.93	0.94	1.34	0.54	0.00
Western	Badu	-1.65	-1.59	-1.50	-1.44	-1.36	-1.31	-1.27	-1.09	-1.04	-0.46	-1.55	0.00
	Mabuiag	-0.79	-0.74	-0.68	-0.63	-0.57	-0.54	-0.51	-0.34	-0.17	0.67	-0.76	0.00
	Moa_Kubin	-5.95	-5.86	-5.76	-5.68	-5.59	-5.54	-5.51	-5.42	-5.26	-5.23	-6.17	0.00
	Moa_St_Pauls	-0.65	-0.60	-0.55	-0.52	-0.47	-0.44	-0.42	-0.38	-0.35	0.35	-0.66	0.00
Central	Iama	-0.09	-0.04	0.02	0.05	0.10	0.13	0.16	0.23	0.28	0.47	-0.31	0.00
	Masig	0.00	0.05	0.10	0.12	0.16	0.17	0.20	0.23	0.25	0.25	-0.15	0.00
	Poruma	-0.54	-0.49	-0.43	-0.40	-0.36	-0.32	-0.31	-0.27	-0.26	-0.10	-0.68	0.00
	Warraber	-0.10	-0.05	0.03	0.07	0.15	0.19	0.21	0.26	0.31	0.43	-0.39	0.00
Inner	Gealug	-1.91	-1.80	-1.68	-1.58	-1.46	-1.40	-1.37	-1.15	-1.13	-0.20	-2.19	0.00
	Hammond	-0.55	-0.48	-0.40	-0.34	-0.26	-0.21	-0.16	-0.03	0.13	0.83	-0.47	0.00
	Muralag	-1.90	-1.82	-1.72	-1.65	-1.55	-1.50	-1.48	-1.41	-1.23	-0.74	-1.96	0.00
	Ngurupai	-1.43	-1.35	-1.25	-1.18	-1.08	-1.04	-1.02	-0.79	-0.71	0.36	-1.46	0.00
	Seisia	-1.89	-1.78	-1.64	-1.55	-1.43	-1.35	-1.29	-1.02	-0.78	-0.05	-2.11	0.00
	Waiben_S	-1.10	-1.03	-0.94	-0.86	-0.79	-0.74	-0.69	-0.53	-0.34	0.21	-0.96	0.00
	Waiben_W	-0.97	-0.87	-0.76	-0.68	-0.58	-0.53	-0.51	-0.32	-0.29	0.31	-0.96	0.00
	Waiben_E	-0.96	-0.89	-0.80	-0.73	-0.65	-0.60	-0.56	-0.35	-0.06	0.68	-0.96	0.00
Eastern	Erub	-0.38	-0.33	-0.28	-0.25	-0.21	-0.17	-0.16	-0.11	-0.08	0.03	-0.48	0.00
	Mer	-0.72	-0.67	-0.61	-0.57	-0.53	-0.51	-0.49	-0.43	-0.38	-0.30	-0.72	0.00
	Ugar	-1.43	-1.39	-1.33	-1.30	-1.26	-1.25	-1.24	-1.18	-1.14	-1.02	-1.50	0.00

These results suggest that five communities are already vulnerable to encroachment from the sea by at least the 5 y return period, equivalent to a 20% chance in any year. The most vulnerable is Saibai, where the modelling suggests an annual likelihood of encroachment up to 0.56 m in depth and up to 1 m in an extreme 1000 y return period situation. The next most vulnerable is Boigu, where the annual event is about 0.1 m depth, reaching up to 0.8 m by 1000 y. This is followed by Masig, Warraber and Iama. However, some other communities start to become vulnerable at the extreme 10,000 y condition. This includes Erub, Hammond, Mabauig, Moa_St_Pauls, Ngurupai, Poruma, Seisia and Waiben. The remaining communities appear relatively free of encroachment but (refer the detailed model results in Appendix P) some are possibly affected by wave runup. The relative vulnerabilities are shown ranked in Figure 11-10 below according to the community 50 y return period level.

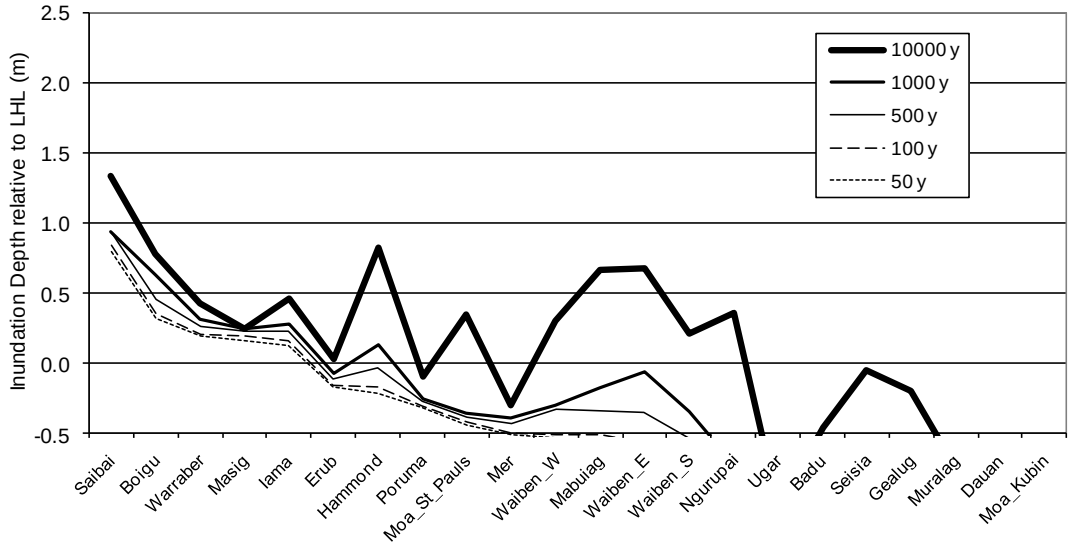

Figure 11-10 Inundation for present 2010 climate ranked by the community 50 y return period value.

It should be noted that these conclusions are based on the assumed LHL levels that have been manually interpreted from presently available topographic mapping and imagery and in some cases are very approximate. After the results of recent LiDAR capture, the ratification of the various datums and detailed topographic mapping is complete, these LHL levels could change – perhaps by as much as 0.5 m or more. Accordingly the return periods discussed above will also shift. For example, the conclusion above that Saibai has an annual encroachment of up to 0.6 m could readily change to a less frequent value, perhaps more consistent with the community experience. Nevertheless, the model estimates appear reasonably consistent with anecdotal

information. Planned vulnerability mapping will then allow the better quantification of these impacts spatially across each of the communities, thus informing adaptation and response strategies.

Before considering the potential impacts of climate change, an example of the detailed modelling results available in Appendix P is presented in Figure 11-11 for the community of Waiben_S. This shows the relative contributions of the various storm tide components at this location, which is on the south-facing shore of Thursday Island, where the business district and port infrastructure is located.

The left-hand vertical axis is water level (to the datums indicated in the curve legends) and the right-hand axis is significant wave height, which is the short-dashed black curve mostly laying above all the other curves. The coloured horizontal lines refer to the left-hand axis and are the estimated **HAT** level (m MSL), the **LHL** level (m MSL) and the model's **Dune Crest** level (m MSL). The remaining black lines in the various dash styles are either storm tide magnitudes (m), which are relative to an instantaneous tide level during an event, or storm tide levels (m MSL) relative to the MSL datum.

The values plotted in Figure 11-8 and tabulated in Table 11-1 are the "Total Storm Tide Level m MSL" shown as the heavy solid black line. Above that lies the "Total Wave Runup Level m MSL" as a heavy dot-dash, and below it is the "Tide + Surge m MSL" heavy dashed, which does not include wave setup. The light solid line is the "Surge m" magnitude, indicating that the highest single storm surge event at this location is expected to be about 2.5 m high above whatever the tide might be and the light dashed line is the equivalent "Setup m" magnitude, showing a peak of about 1.2 m.

At this site, the model estimates that HAT will be exceeded on average about every 2 y and that the LHL level will first be reached by wave runup around 100 y. Wave runup is predicted to increase at longer return periods while the dune crest is still exposed. The LHL will be reached by the Total Storm Tide at about the 2000 y return period (0.05% per annum risk). Previous comments in regard to the selection of the nominal and approximate LHL level apply to these comments. In respect of wave conditions, the annual expected significant wave height is about 0.5 m (right-hand axis) but increases significantly beyond the 10 y return period. For specific infrastructure assessments, these estimates should be subject to further site-specific analyses.

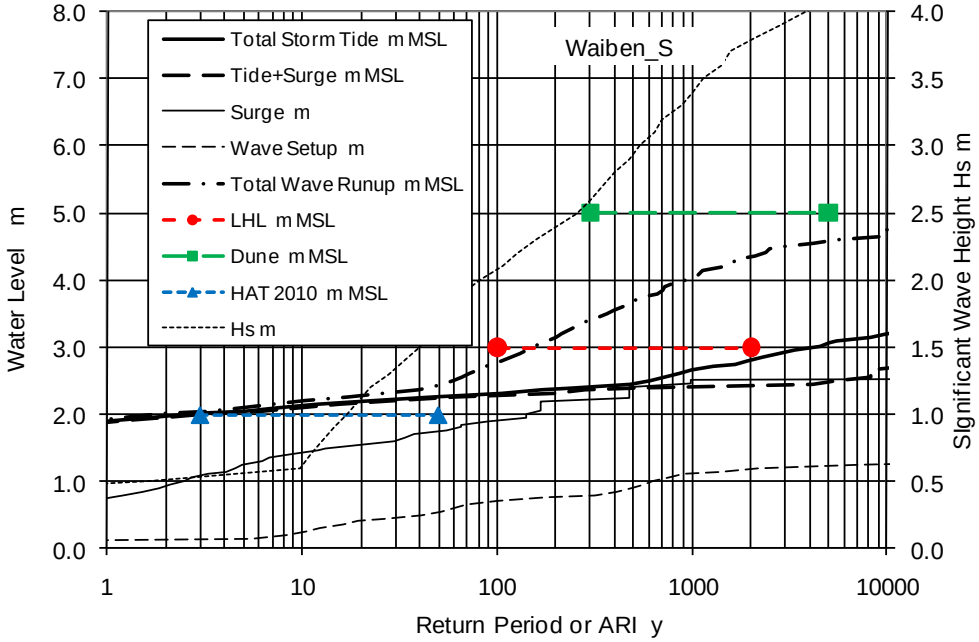

Figure 11-11 Detailed simulation results for the site of Waiben_S for present (2010) climate.

11.4 Simulated Combined Storm Tide Levels for Projected Future Climates (2050 and 2100)

These results are presented in a variety of ways. Firstly, Appendix Q presents a series of comparison graphs for each community showing the changed total storm tide lines relative to the present 2010 MSL datum and the LHL levels. Appendix R then provides a tabulation of the changes in levels for a range of return periods relative to the 2010 levels. This highlights the fact that for the majority of communities the principal change is due to the assumed sea level rise component, being 0.3 m by 2050 and 0.8 m by 2100. Considering that no changes in wind conditions of future climates have been considered in the broadscale context, this is consistent with the predicted small impact of local TC effects on Torres Strait water levels generally. Nevertheless the simulation does consider other depth-dependent feedbacks.

For consistency with the 2010 climate summary Figure 11-9, and to focus on the vulnerability relative to the LHL level, Figure 11-12 presents the equivalent 2050 condition and Figure 11-13 presents the 2100 condition. It can be seen that the number of communities expected to be impacted above the LHL level (above 0.0 on the vertical axis) increases

significantly. The actual values are then tabulated in Table 11-4 and Table 11-5 respectively.

By 2050, the existing five communities that are already principally affected are further impacted by the 0.3 m sea level rise. Erub is also affected now at the 5 y return period, Hammond is increasingly vulnerable by the 25 y level and Poruma becomes at risk around 100 y. It is likely that 5 sites (Saibai, Boigu, Warraber, Iama and Masig) would be experiencing significantly adverse impacts by this time. Notwithstanding these chronic incursions by the sea there would be increased stress placed on emergency services in the event of a higher magnitude event (longer return period) occurring.

By 2100, with a possible sea level rise of 0.8 m and increased TC intensities, a total of 13 sites are affected beyond the 5 y level and 11 of these sites are affected across the full return period range. It is likely that 8 sites (Saibai, Boigu, Warraber, Masig, Iama, Erub, Poruma and Hammond) would then be experiencing significantly adverse impacts. Where retreat is likely to not be possible, such as at the low lying islands of Saibai, Boigu, Warraber, Masig and Poruma, communities may have to consider the viability of maintaining permanent habitation on these islands. Some islands that have higher ground, such as Iama, may still prove impractical for retreat because of their rugged terrain. Again, emergency services will come under increasing stress across the remaining communities.

Finally, for consistency with Figure 11-10, the ranked community inundation estimates for 2050 are presented in Figure 11-14 and for 2100 in Figure 11-15. It can be seen that beyond the 50 y return period there are significant changes indicated in the relative impacts across the various communities.

It is recommended that Appendix S be consulted for advice on the interpretation of the statistical return periods discussed in this report. For example, the 1000 y Return Period (or ARI) is equivalent to an annual probability of exceedance of 0.1% and, over an exposure period of 50 y, has a probability of exceedance of 5%. It can be thought of as being equivalent to an annual lottery containing only 1000 tickets. Similarly other Return Periods should be interpreted in this way to avoid the common misconception that the likelihood of some of these impacts is very unlikely.

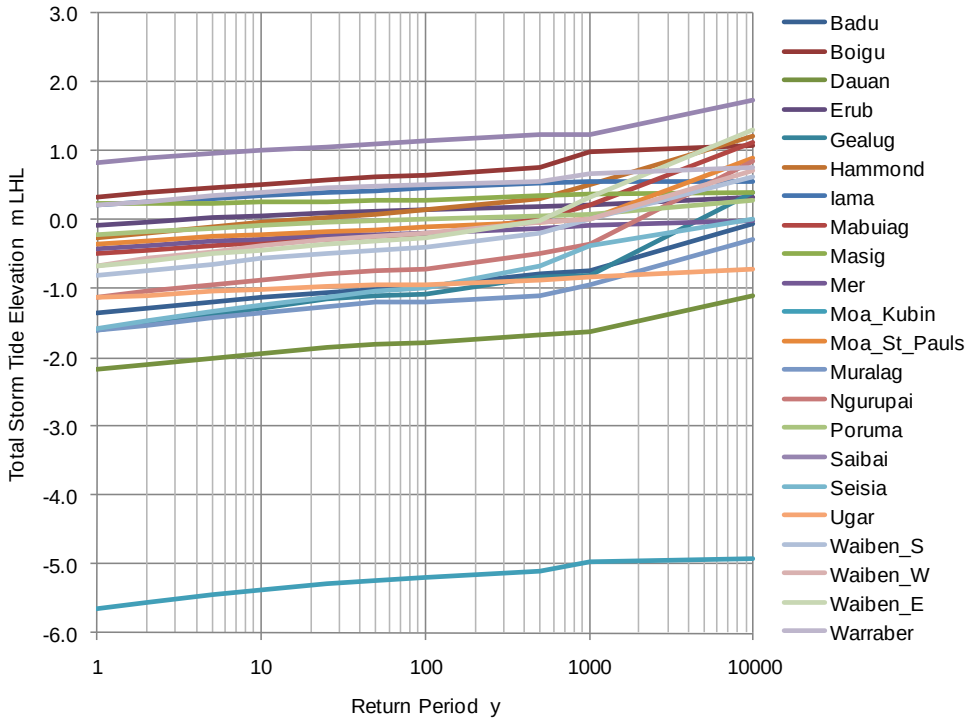

Figure 11-12 Simulated tide plus surge plus setup return period water levels for projected climate (2050) relative to LHL datum.

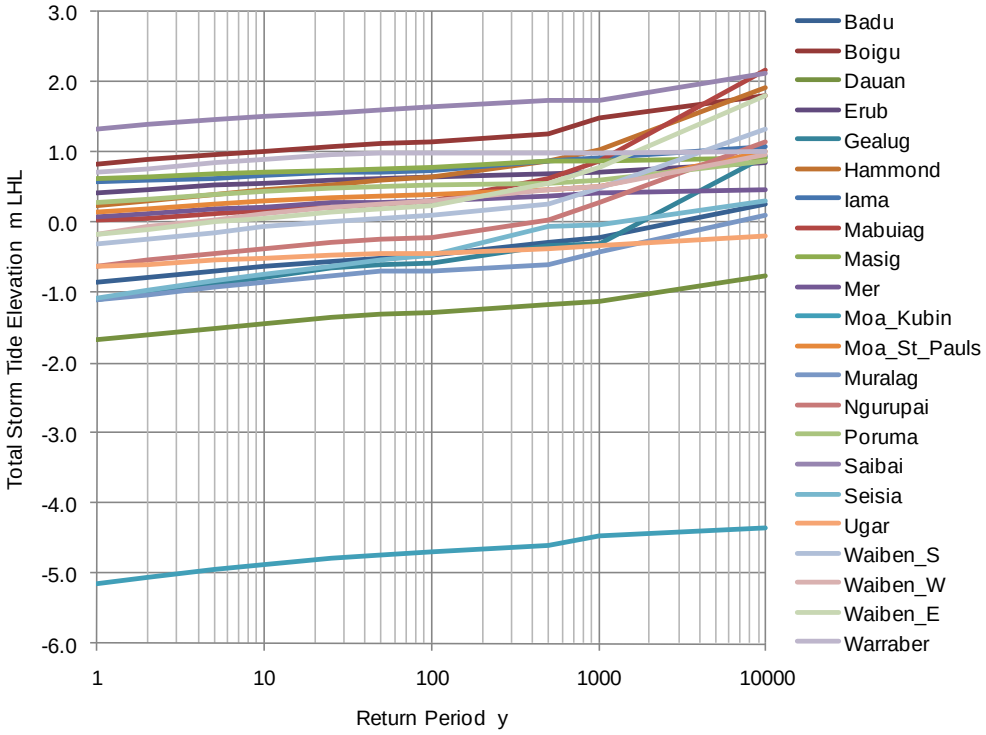

Figure 11-13 Simulated tide plus surge plus setup return period water levels for projected climate (2100) relative to LHL datum.

Table 11-4 Estimated return period of total storm tide level for 2050 climate relative to LHL datum.

Site	1 y m LHL	2 y m LHL	5 y m LHL	10 y m LHL	25 y m LHL	50 y m LHL	100 y m LHL	500 y m LHL	1000 y m LHL	10000 y m LHL
Badu	-1.35	-1.29	-1.20	-1.14	-1.06	-1.01	-0.97	-0.79	-0.74	-0.06
Boigu	0.34	0.39	0.46	0.51	0.58	0.62	0.65	0.75	0.98	1.08
Dauan	-2.16	-2.09	-2.00	-1.93	-1.84	-1.81	-1.77	-1.67	-1.62	-1.11
Erub	-0.08	-0.03	0.02	0.05	0.09	0.13	0.14	0.19	0.22	0.33
Gealug	-1.61	-1.50	-1.38	-1.28	-1.15	-1.10	-1.07	-0.84	-0.81	0.40
Hammond	-0.25	-0.18	-0.10	-0.03	0.04	0.09	0.15	0.32	0.52	1.21
Iama	0.22	0.27	0.32	0.35	0.40	0.43	0.46	0.53	0.57	0.57
Mabuiag	-0.48	-0.43	-0.38	-0.33	-0.27	-0.24	-0.21	0.02	0.21	1.12
Masig	0.25	0.25	0.25	0.26	0.26	0.28	0.30	0.36	0.39	0.41
Mer	-0.42	-0.37	-0.31	-0.27	-0.22	-0.21	-0.19	-0.13	-0.08	0.00
Moa_Kubin	-5.65	-5.56	-5.45	-5.38	-5.29	-5.24	-5.20	-5.10	-4.96	-4.92
Moa_St_Pauls	-0.35	-0.30	-0.24	-0.21	-0.16	-0.14	-0.10	-0.04	0.00	0.90
Muralag	-1.60	-1.52	-1.42	-1.35	-1.25	-1.20	-1.18	-1.10	-0.93	-0.29
Ngurupai	-1.13	-1.04	-0.95	-0.88	-0.78	-0.74	-0.72	-0.48	-0.34	0.86
Poruma	-0.22	-0.18	-0.12	-0.08	-0.04	-0.01	0.01	0.06	0.08	0.28
Saibai	0.84	0.91	0.97	1.02	1.07	1.10	1.14	1.23	1.24	1.74
Seisia	-1.59	-1.47	-1.33	-1.25	-1.13	-1.04	-0.98	-0.68	-0.37	0.00
Ugar	-1.13	-1.09	-1.03	-1.00	-0.96	-0.95	-0.94	-0.88	-0.82	-0.71
Waiben_S	-0.80	-0.73	-0.64	-0.56	-0.48	-0.44	-0.39	-0.19	0.02	0.63
Waiben_W	-0.67	-0.56	-0.46	-0.38	-0.28	-0.23	-0.20	-0.02	0.02	0.71
Waiben_E	-0.66	-0.59	-0.49	-0.43	-0.35	-0.30	-0.26	0.00	0.34	1.31
Warraber	0.21	0.26	0.34	0.39	0.46	0.49	0.51	0.56	0.66	0.76

Table 11-5 Estimated return period of total storm tide level for 2100 climate relative to LHL datum.

Site	1 y m LHL	2 y m LHL	5 y m LHL	10 y m LHL	25 y m LHL	50 y m LHL	100 y m LHL	500 y m LHL	1000 y m LHL	10000 y m LHL
Badu	-0.85	-0.79	-0.70	-0.64	-0.56	-0.51	-0.47	-0.28	-0.23	0.25
Boigu	0.84	0.89	0.96	1.01	1.08	1.12	1.15	1.25	1.48	1.80
Dauan	-1.66	-1.59	-1.50	-1.43	-1.34	-1.31	-1.27	-1.17	-1.12	-0.76
Erub	0.42	0.47	0.52	0.55	0.59	0.63	0.64	0.69	0.72	0.84
Gealug	-1.11	-1.00	-0.88	-0.78	-0.65	-0.60	-0.57	-0.34	-0.31	0.95
Hammond	0.25	0.32	0.40	0.47	0.54	0.60	0.66	0.88	1.04	1.93
Iama	0.58	0.60	0.64	0.67	0.71	0.73	0.74	0.87	0.92	1.09
Mabuiag	0.03	0.07	0.13	0.17	0.23	0.27	0.30	0.63	0.87	2.17
Masig	0.62	0.66	0.70	0.71	0.75	0.77	0.80	0.87	0.89	0.92
Mer	0.08	0.13	0.19	0.23	0.28	0.29	0.31	0.37	0.42	0.48
Moa_Kubin	-5.15	-5.06	-4.95	-4.88	-4.79	-4.74	-4.70	-4.61	-4.46	-4.35
Moa_St_Pauls	0.15	0.20	0.26	0.30	0.35	0.37	0.40	0.46	0.51	1.01
Muralag	-1.10	-1.02	-0.92	-0.85	-0.75	-0.70	-0.68	-0.60	-0.42	0.11
Ngurupai	-0.63	-0.54	-0.45	-0.38	-0.28	-0.24	-0.22	0.04	0.28	1.16
Poruma	0.28	0.34	0.39	0.43	0.48	0.50	0.53	0.57	0.59	0.88
Saibai	1.34	1.41	1.47	1.52	1.57	1.60	1.64	1.73	1.74	2.13
Seisia	-1.09	-0.97	-0.83	-0.75	-0.63	-0.54	-0.47	-0.05	-0.04	0.30
Ugar	-0.63	-0.59	-0.53	-0.50	-0.46	-0.45	-0.44	-0.38	-0.32	-0.20
Waiben_S	-0.30	-0.23	-0.14	-0.06	0.01	0.06	0.11	0.27	0.49	1.33
Waiben_W	-0.17	-0.06	0.04	0.12	0.22	0.27	0.30	0.48	0.51	0.96
Waiben_E	-0.16	-0.09	0.01	0.07	0.16	0.20	0.25	0.56	0.78	1.81
Warraber	0.71	0.77	0.84	0.89	0.96	0.99	0.99	0.99	0.99	1.01

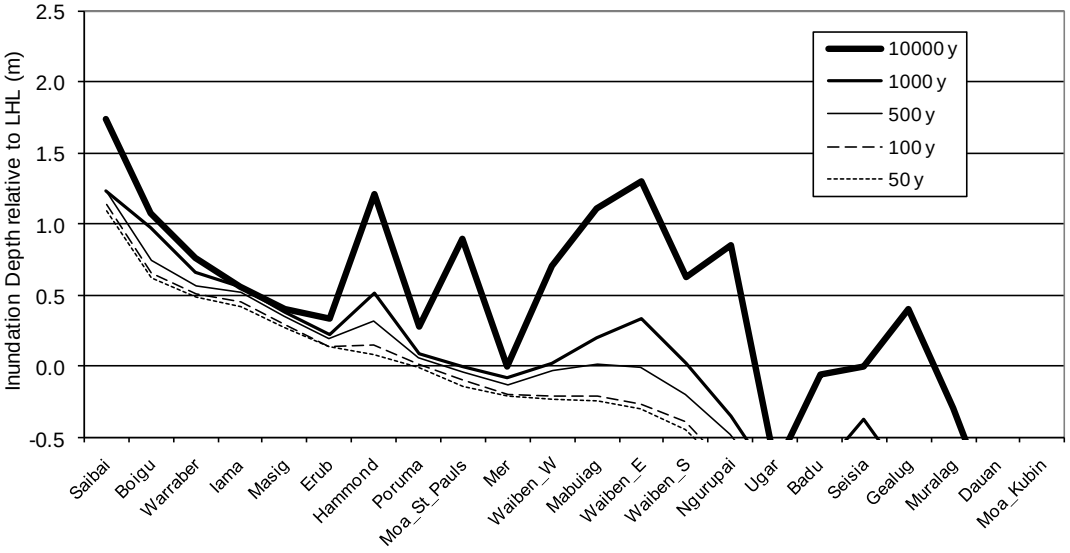

Figure 11-14 Inundation for future 2050 climate ranked by the community 50 y return period value.

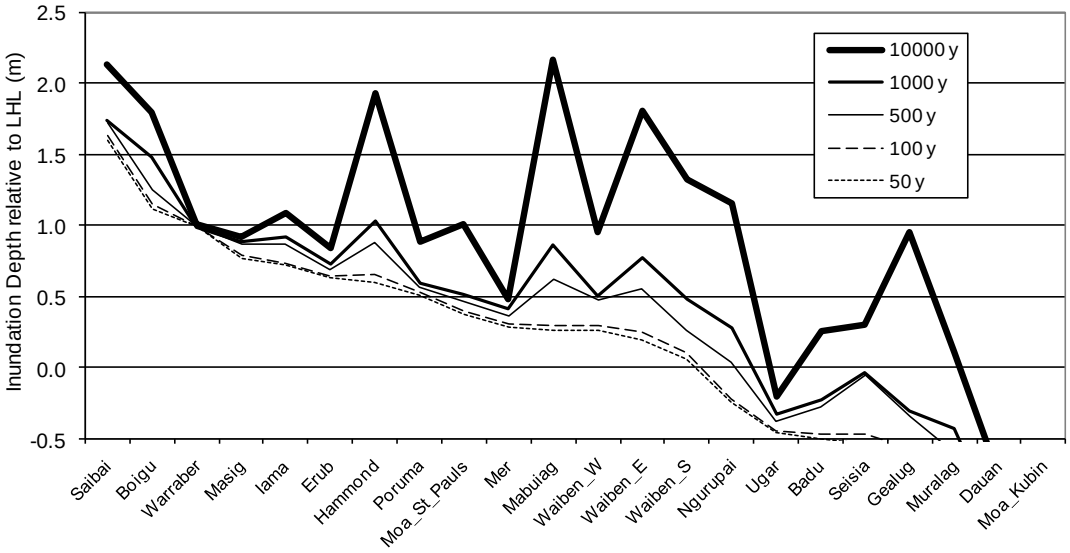

Figure 11-15 Inundation for future 2100 climate ranked by the community 50 y return period value.

12. Conclusion

This report has for the first time addressed the quantification of extreme ocean water levels in the Torres Strait – a remote region having significant complexity and diversity of geophysical parameters, low levels of reliable insitu information and with a widespread community vulnerable to the impacts of the sea. Both present (2010) and projected future (2050 and 2100) climate and sea level rise scenarios have been considered.

The extensive analyses have been based on robust numerical and statistical techniques that have been designed to capture the principal atmospheric, astronomic and other broadscale forcing that modulates ocean water levels in the region. In addition, the localised impacts of TCs have been considered. Wherever possible, the analyses have been checked and validated against reliable measured data for winds, tides, storm surge and community impacts.

A principal aspect of the analyses has been the calibration of a regional astronomical tide model that shows good accuracy compared with the available tide data and highlights the very complex dynamics of the tide across and within the Strait.

Broadscale ocean modelling has then been undertaken that captures the principal seasonal and inter-annual sea level variability as well as the effects of remote TCs. These results have been synthetically extended by recombination with the astronomical tide to provide a robust statistical basis for determination of water level return periods beyond the 1000 y return period. This has also provided estimates of the variability of the mean water level throughout the region essential for establishing accurate land elevation datums.

Although close approach TCs are deemed rare in the Torres Strait, their potential wind, storm surge and wave impacts have also been considered. Due to doubts surrounding the accuracy of the historical TC records in this remote area, an expert review was undertaken that led to adopting increased intensities for a number of Gulf of Carpentaria events. This data was then used to construct a synthetic TC record and to overlay a simulated TC storm surge climate onto the broadscale ocean and tide modelling. More than 33,000 TC events were numerically modelled.

Numerical wave modelling was also undertaken for both the broadscale and close-approach TC climate conditions and estimates of breaking wave setup and wave runup were made based on nominal beach and reef morphology for each community.

The deterministic model results for the broadscale and locally-forced conditions were then combined into a sophisticated numerical simulation

model capable of estimating the statistics of ocean water levels for an extended period of 50,000 y for each of the Torres Strait communities. These statistics are then used to provide estimates of the Return Period or Average Recurrence Interval of the Total Storm Tide level (defined as tide + surge+ wave setup), Tide plus Surge and Tide plus Surge plus Runup level. Likewise the probability of the specific storm surge magnitude, wave height, wave setup and runup magnitudes are also provided.

The analysis concludes that ocean water levels in the region are dominated by the highly variable astronomical tide but that extreme water levels are caused by subtle combinations of relatively small inter-annual changes in the regional ocean level, strong seasonal variability due to the prevailing winds and occasional high energy weather events (monsoon surges and TCs). The interplay of these components on a range of time and space scales likely leads to periods of both enhanced and reduced impacts of the ocean water levels on the various communities. It is concluded that ocean water levels are controlled by generally broadscale processes up until around the 100 y return period, after which close-approach TCs may increasingly begin to impact wind, wave and water levels at some communities.

The results of the analyses are presented in a very comprehensive manner, both tabular and graphical, that should permit wide ranging application for studies into geomorphological processes, environmental and sustainability issues, community infrastructure and emergency services. Important advice on the interpretation of Return Period and ARI estimates has also been provided to assist in the correct perception of the estimated hazard probabilities.

The analysis estimates that five communities are already vulnerable to encroachment from the sea by at least the 5 y return period, equivalent to a 20% chance in any year. The most vulnerable is Saibai, where the modelling suggests an annual likelihood of encroachment up to 0.56 m in depth and up to 1 m in an extreme 1000 y return period situation. The next most vulnerable is Boigu, where the annual event is about 0.1 m depth, reaching up to 0.8 m by 1000 y. This is followed by Masig, Warraber and Iama. These statistics appear broadly consistent with anecdotal information regarding recent community impacts and provide confidence in the ability of the analyses to estimate longer return period events that will assist in planning and adaptation strategies.

For example, other communities start to become vulnerable at the extreme 10,000 y condition. This includes Erub, Hammond, Mabauig, Moa_St_Pauls, Ngurupai, Poruma, Seisia and Waiben. The remaining communities appear free of encroachment in present climate conditions. In terms of the geographic island clusters, it is therefore the Top Western group (Saibai and Boigu) and some of the Central group islands (Masig, Warraber, Iama) that are the more affected at the shorter

return periods but the Inner and Western groups are increasingly vulnerable at high return periods. In comparison the Eastern group is the least impacted.

For the projected climate of 2050, the existing five communities that are already principally affected are further impacted by the 0.3 m sea level rise. Erub is also affected now at the 5 y return period, Hammond is increasingly vulnerable by the 25 y level and Poruma becomes at risk around 100 y. It is likely that 5 sites (Saibai, Boigu, Warraber, Iama and Masig) would be experiencing significantly adverse impacts by this time. Notwithstanding these chronic incursions by the sea there would be increased stress placed on emergency services in the event of a higher magnitude event (longer return period) occurring.

By 2100, with a possible 0.8 m sea level rise and increased TC intensities, a total of 13 sites are affected beyond the 5 y level and 11 of these sites are affected across the full return period range. It is likely that 8 sites (Saibai, Boigu, Warraber, Masig, Iama, Erub, Poruma and Hammond) would be experiencing significantly adverse impacts. Where retreat is likely not to be possible such as at the low lying islands of Saibai, Boigu, Warraber, Masig and Poruma, communities may have to consider the viability of maintaining permanent habitation on these islands. Some islands that have higher ground, such as Iama, may still prove impractical for retreat because of their rugged terrain. Again, emergency services will come under increasing stress across the remaining communities.

It is recommended that data collection studies in the region be continued and expanded to ensure reliable geophysical data is available for future studies. In particular, permanent tide gauges are highly desirable at each of the principal island communities to provide long term data of use in better mapping the tidal variability, establishing accurate land elevation datums and to assist in emergency services. These should be matched by an expansion of and site calibration of standard meteorological observation sites and strategically placed wave monitoring buoys and current measuring devices, or other composite instrumentation. Bathymetric data is also still scarce in some areas and this should continue to be addressed. It is noted that land elevations are already subject to an extensive LiDAR survey.

13. References

Allan R.J. (1991) In: Teleconnections linking worldwide climate anomalies. Glantz M. et al. (Eds), Cambridge Uni. Press, Cambridge, UK, 73-120 pp.

ANTT (2006) Australian national tide tables. Australian Hydrographic Service, *Royal Australian Navy*.

ARUP (2006) Torres Strait Natural Disaster Risk Management Study. *ARUP Consultants*, Brisbane.

Atkinson, G.D. and Holliday, C.R., (1975) Tropical cyclone minimum sea level pressure – maximum sustained wind relationship for western North Pacific. FLEWEACEN Tech. Note: JTWC 75-1, *US Fleet Weather Centra*l, Guam, 20pp.

Benjamin and Cornell (1970) Probability, statistics and decision for civil engineers*, McGraw-Hill*.

Bode, L. and Mason, L.B. (1994) Application of an implicit hydrodynamic model over a range of spatial scales, *Computational Techniques and Applications: CTAC93*, D. Stewart, H. Gardner and D. Singleton, Eds., World Scientific Press, 112--121

Bode L. and Mason L.B. (1995) Tidal modelling in Torres Strait and the Gulf of Papua. *Proc Pacific Congress on Marine Science and Technology*: PACON 94, Townsville, O. Bellwood, H. Choat and N. Saxena, Eds., 55--65.

Bode, L. and Mason, L.B. (2005) Evaluation of a nonlinear reef parameterisation for steady flows, *12th Biennial Computational Techniques and Applications: CTAC2004*, R. May and A. J. Roberts, Eds., ANZIAM J., VOL. 46 (E), pp 1017--1034.

Bode L., Mason L.B. and Middleton J.H. (1997) Reef parameterisation schemes for long wave models. *Progress in Oceanography*, Special issue on tidal science in honour of David E. Cartwright, Vol. 40, No. 1-4, pp. 285–324.

Church J.A., White N.J., Hunter J.R. and Lambeck K. (2008) Briefing: a post-IPCC AR4 update on sea-level rise. Antarctic Climate and Ecosystems Cooperative Research Centre, MB01_080911, 12pp.

CSIRO (2007) Climate change in Australia – technical report. CSIRO in association with the Bureau of Meteorology and the *Australian Greenhouse Office*. 148pp.

Daniell J., (2008) The development of a bathymetric grid for the Gulf of Papua and adjacent areas—a note describing its development. *Journal of Geophysical Research* 113, F01S15, doi:10.1029/2006JF000673.

DERM (2009) Draft Queensland Coastal Plan, Draft State Planning Policy Coastal Protection. *Department of Environment and Resource Management*, Aug, 56pp.

Duce S.J., Parnell K.E., Smithers S.G. and McNamara K.E. (2010) A Synthesis of Climate Change and Coastal Science to Support Adaptation in the Communities of the Torres Strait. Synthesis Report prepared for the Marine and Tropical Sciences Research Facility (MTSRF). *Reef & Rainforest Research Centre Limited*, Cairns, 64pp.

Dvorak, V.F. 1984: Tropical Cyclone Intensity Analysis Using Satellite Data. *NOAA* Technical Report NESDIS 11. 45pp

EPA (2005) Mackay coast study. Environmental Protection Agency, Queensland Government. RE 488, Jan, 119pp.

EPA (2006) Mitigating the adverse impacts of storm tide inundation. State Coastal Management Plan Guideline, Ecoaccess Environmental Licences and Permits, 061218, *Environmental Protection Agency, Queensland*, 47pp.

EPA (2006) Fact Sheet: King Tides in Torres Strait. www.epa.qld.gov.au/publications/p01864aa.pdf/2006_King_Tides_in_Torres_Strait.pdf

Fugro (2010) Tide data in the Torres Strait. Provided by TSRA.

GHD/SEA (2003) Whitsunday Storm Surge Study. Prepared for Whitsunday Shire Council. Nov, 150pp.

GHD/SEA (2005) Rarotonga Coastal Protection Study. Prepared for SOPAC.

GHD/SEA (2007) Townsville-Thuringowa Storm Tide Study. Prepared for Townsville and Thuringowa City Councils, April, 210pp.

GHD/SEA (2009) Cassowary Coast Storm Tide Study. Prepared for Cassowary Coast Regional Council, June, 240pp.

Gourlay M.R. (1997) Wave setup on coral reefs: some practical applications. Proc. 13th Aust Conf Coastal and Ocean Engin., *Centre for Advanced Engineering*, Christchurch, Sept, 959-964.

Green D. (2006) How might climate change affect island culture in the Torres Strait? *CSIRO Marine and Atmospheric Research* Paper 011, Nov, 14pp.

Green D., Alexander L., McInnes K., Church J., Nicholls N. and White N. (2009) An assessment of climate change impacts and adaptation for the Torres Strait Islands, Australia. *Climatic Change*, DOI 10.1007/s10584-009-9756-2.

Hanslow D.J. and Nielsen P. (1993) Shoreline setup on natural beaches. *J Coastal Res*, Special Issue 15, 1-10.

Hardy T.A., McConochie J.D. and Mason L.B. (2001) A wave model for the Great Barrier Reef. *Ocean Engineering*, 28 (1), 45-70.

Hardy T.A., Mason L.B. and Astorquia A. (2004) Queensland climate change and community vulnerability to tropical cyclones - ocean hazards assessment - stage 3: the frequency of surge plus tide during tropical cyclones for selected open coast locations along the Queensland east coast. Report prepared by James Cook University

Harper B.A (1999) Numerical modelling of extreme tropical cyclone winds APSWE Special Edition, *Journal of Wind Engineering and Industrial Aerodynamics*, 83, 35 - 47.

Harper B.A. (ed) (2001) Queensland climate change and community vulnerability to tropical cyclones - ocean hazards assessment - Stage 1, Report prep by Systems Engineering Australia Pty Ltd in association with James Cook University Marine Modelling Unit, *Queensland Government*, March, 375pp.

Harper B.A. (2002) Tropical cyclone parameter estimation in the Australian region: Wind-Pressure Relationships and Related Issues for Engineering Planning and Design, *Systems Engineering Australia Pty Ltd* for Woodside Energy Ltd, Perth, May, 83pp. [available from http://www.uq.net.au/seng/download/Wind-Pressure%20Discussion%20Paper%20Rev%20E.pdf]

Harper B.A. (2004a) Queensland climate change and community vulnerability to tropical cyclones – ocean hazards assessment – Synthesis Report. Prepared by Systems Engineering Australia Pty Ltd, *Queensland Government*, August, 38pp.

Harper B.A. (2004b) Globalisation, calibration and opportunities for enhancement of the Dvorak technique, 30 yr of the Dvorak Technique Special Session, *American Meteorological Society*, 26th Conference on Hurricanes and Tropical Meteorology, Miami, May, 8A.1, 218-219.

Harper B.A. (2004c) Queensland climate change and community vulnerability to tropical cyclones – ocean hazards assessment: Stage 1a – Operational Manual, *Queensland Government*, Mar, 75pp.

Harper B.A. and Callaghan J. (1998) Modelling of severe thunderstorms in South East Queensland. Proc. Sixth Australian Severe Storms Conference, *Bureau of Meteorology*, Brisbane, Aug.

Harper B.A. and Callaghan J. (2006) On the importance of reviewing historical tropical cyclone intensities. *American Meteorological Society*, 27th Conference on Hurricanes and Tropical Meteorology, 2C.1, Monterey, Apr.

Harper B.A., Gourlay M.R. and Jones C.M. (2001) Storm tide risk assessment for the Cocos (Keeling) Islands, Proc 15th Australasian

Conference on Coastal and Ocean Engin, Coasts & Ports 2001, *Engineers Australia*, Gold Coast, Sept, 75-80.

Harper B.A., Hardy T.A. and Mason L.B. (2007) Developments in Storm Tide Modelling and Risk Assessment in The Australian Region. *Proc. WMO/IOC JCOMM 1st Scientific and Technical Symposium on Storm Surges*, Seoul, Korea, 2-6 Oct.

Harper B.A., Hardy T.A., Mason L.B. and McConochie J.D. (2001) Cyclone *Althea* revisited, Proc 15th Australasian Conference on Coastal and Ocean Engin, Coasts & Ports 2001, *Engineers Australia*, Gold Coast, Sept, 140-145.

Harper, B.A. and Holland, G.J. (1999) An updated parametric model of the tropical cyclone. Proc. 23rd Conf. Hurricanes and Tropical Meteorology, *American Meteorological Society*, Dallas, Texas, 10-15 Jan, 1999.

Harper B.A., Stroud S.A., McCormack M. and West S. (2008) A review of historical tropical cyclone intensity in north-western Australia and implications for climate change trend analysis. *Australian Meteorological Magazine*, Vol. 57, No. 2, June, 121-141.

Harper B.A., Kepert J. and Ginger J. (2010) Guidelines for converting between various wind averaging periods in tropical cyclone conditions. *World Meteorological Organization*, TCP Sub-Project, WMO/TD-No. 1555, August, 60pp.

Harper B.A. (2009) Forecasting surface wind, wave and storm surge impacts. WMO 2nd International Workshop on Tropical Cyclone Landfall Processes, *CAS Tropical Meteorology Research Programme (TMRP)*, Shanghai, China, 19-23 October.

Holland G.J. (1980) An analytic model of the wind and pressure profiles in hurricanes, *Monthly Weather Review*, Vol 108, No.8, Aug, pp 1212-1218.

Holland G.J. (1997). The maximum potential intensity of tropical cyclones. *J. Atmos. Sci*., 54, Nov, 2519-2541.

Holliday, C.R. and Thompson, A. H. 1979. Climatological characteristics of rapidly intensifying typhoons. *Monthly Weather Review: Vol. 107, pp. 1022-1034.*

IPCC (2007) Climate Change 2007: The Physical Science Basis. Contribution of Working Group I to the Fourth Assessment Report of the Intergovernmental Panel on Climate Change [Solomon, S., D. Qin, M. Manning, Z. Chen, M. Marquis, K.B. Averyt, M. Tignor and H.L. Miller (eds.)]. *Cambridge University Press*, Cambridge, United Kingdom and New York, NY, USA, 996 pp.

James M.K. and Mason L.B. (2005) A Synthetic Tropical Cyclone Database. *Journal of Waterway, Port, Coastal and Ocean Engineering*, Am. Soc. Civil Eng. ., 131, No. 4, pp. 181-192.

Kistler R., Kalnay E., Collins W., Saha S., White G., Woollen J., Chelliah M., Ebisuzaki W., Kanamitsu M., Kousky V., van den Dool H., Jenne R. and Fiorino M. (2001) The NCEP–NCAR 50–Year Reanalysis: Monthly Means CD–ROM and Documentation. *Bulletin of the American Meteorological Society*, 82, 2, Feb, 247–267.

Knaff J.A, Brown D.P, Courtney J., Gallina G.M. and Beven J.L. (2010) An evaluation of Dvorak technique-based tropical cyclone intensity estimates. *Weather and Forecasting*, early online release.

Knutson T.R., McBride J.L., Chan J., Emanuel K., Holland G., Landsea C., Held I., Kossin J.P., Srivastava A.K. and Sugi M., 2010: Tropical cyclones and climate change. *Nature Geoscience*, 3, 15 –163.

Landsea C.W., Harper B.A., Hoarau K., and Knaff J. (2006) Can we detect trends in extreme tropical cyclones? *Science*, 313, 28 July, (10.1126/science.1128448).

Lemckert C.J., Zier J. and Gustafson J. (2009). Tides in Torres Strait. *Journal of Coastal Research,* SI 56: 524-528.

Mason L.B. and McConochie J.D. (2001) MMUSURGE user's guide. School of Engineering, Marine Modelling Unit, *James Cook University*, Townsville.

Molinari, J., D. Vollaro, P. Dodge, and F. Marks Jr., 2006: Mesoscale aspects of the downshear reformation of a tropical cyclone. *J.Atmos. Sci.,* **63,** 341–354.

MSQ (2009) Torres Strait tidal survey – datum analysis. Maritime Safety Queensland, Prep. For Torres Strait Regional Authority, *Department of Transport and Main Roads*, Queensland Government.

MSQ (2010) Queensland Tide Tables 2010. Maritime Safety Queensland, *Department of Transport and Main Roads*, Queensland Government.

NCCOE (2004) Guidelines for responding to the effects of climate change in coastal and ocean engineering. National Committee on Coastal and Ocean Engineering, *Engineers Australia*, *EA Books*, Barton, ACT, 76 pp.

Nicholls N. (1984) The Southern Oscillation, sea surface temperature, and interannual fluctuations in Australian tropical cyclone activity. *J. Climatology*, 4, 661 670.

Nicholls N. (1985a) Towards the prediction of major Australian Droughts. *J. Climatology*, 5, 553-560.

Nicholls N. (1985b) Predictability of interannual variations of Australian seasonal tropical cyclone activity. *Mon. Weath. Rev*., 113, 1144 1149.

Nicholls N. (1992) Historical El Niño/Southern Oscillation variability in the Australian region. In: Nicholls, N., 1992: Recent performance of a method for forecasting Australian seasonal tropical cyclone activity. *Aust. Meteor. Mag*., 40, 105 110.

Nielsen P. and Hanslow D.J. (1991) Wave runup distributions on natural beaches. *J Coastal Res*, Vol 7, No 4, pp 1139-1152.

Power S., Casey T., Folland C., Colman A. and Mehta V. (1999) Inter-decadal modulation of the impact of ENSO on Australia. *Climate Dynamics*, 15, 319-324.

Powell M. D., Houston S.H., and Reinhold T.A., (1996) Hurricane Andrew's landfall in South Florida. Part I: Standardizing measurements for documentation of surface wind fields. *Weather and Forecasting*, 11, 304–328.

Reasor, Paul D., Matthew D. Eastin, and John F. Gamache. (2009), Rapidly Intensifying Hurricane Guillermo (1997). Part I: Low-wavenumber Structure and Evolution, February 2009 *Monthly Weather Review*.

Saint-Cast F. (2008) Multiple time-scale modelling of the circulation in Torres Strait – Australia. *Continental Shelf Research*, 28, 2214-2240.

SEA (2001) Cocos (Keeling) Island Storm Surge Study. Prep for Commonwealth Department of Transport and Regional Services, Aug.

SEA (2004) Queensland climate change and community vulnerability to tropical cyclones – ocean hazards assessment – Stage 1a: Operational manual. Prepared by Systems Engineering Australia Pty Ltd, *Queensland Government*, Mar, 85pp.

SEA (2005) Darwin TCWC Northern Region Storm Tide Prediction System - System Development Technical Report. Prep by *Systems Engineering Australia Pty Ltd* for the Bureau of Meteorology, Darwin. SEA Report J0308-PR001C. December.

SEA (2006) Darwin Storm Tide Mapping Study 2006. Prep by *Systems Engineering Australia Pty Ltd* for NT Emergency Services, SEA Report J0606-PR001C, 119pp, Nov.

SEA (2007) Gove Storm Tide Study 2007. Prepared for Alcan Gove Pty Ltd by *Systems Engineering Australia Pty Ltd* in association with James Cook University Cyclone Testing Station. Aug, 124pp. Updated July 2008 to include climate change estimates and impacts.

Sobey R.J. and Young I.R. (1986) Hurricane wind waves -- A discrete spectral model. *J. Waterways Port Costal Ocean Eng*., ASCE, 112, 370-389.

Standards Australia (2002) AS/NZS 1170.2 – 2002. Structural design actions - Part 2: wind actions. 88pp, as amended.

Tonkin H., Holland G.J., Holbrook N., Henderson-Sellers A., (2000) An evaluation of thermodynamic estimates of climatological maximum potential tropical cyclone intensity. *Monthly Weather Review*, 128, 3, 746–762.

TSRA (2009) Personal communications, *Torres Strait Regional Authority*.

Velden C., B. Harper, F. Wells, J. L. Beven, R. Zehr, T. Olander, M. Mayfield, C. Guard, M. Lander, R. Edson, L. Avila, A. Burton, M. Turk, A. Kikuchi, A. Christian, P. Caroff, P. McCrone (2006) The Dvorak tropical cyclone intensity estimation technique: a satellite-based method that has endured for over 30 years. *Bulletin American Meteorological Society*, Vol 87, Sept, 1195-1210.

Vickery P.J., Skerlj P.F. and Twisdale L.A., (2000) Simulation of hurricane risk in the U.S. using empirical track model. *J. Structural Engineering*, ASCE, 126,10, Oct, 1222-1237.

Walker D.J. (1989) An efficient wave hindcasting model. Proc 9th Australasian Conf Coastal and Ocean Engin., *IEAust*, Adelaide, 4-8 Dec, 117-121.

WMO (2006) Statement on tropical cyclones and climate change. Outcome of the Sixth International Workshop on Tropical Cyclones (IWTC-VI), Costa Rica, *World Meteorological Organization,* WMO-TCP, Geneva, Nov, 13pp.

WMO (2008) Guide to meteorological instruments and methods of observation. *World Meteorological Organization,* WMO-No. 8, 7th Ed, 681pp.

Wolanski E., Ridd P., Inoue M., (1988) Currents through Torres Strait. *Journal of Physical Oceanography* 18, 1535–1545.

Young I.R. (1988) A shallow water spectral wave model. *J. Geophys. Res.*, 93, 5113-5129.

Young I.R. and Verhagen L.A. (1996) The growth of fetch limited waves in water of finite depth. Part 1. Total energy and peak frequency. *Coastal Engineering*, 29, 47-78.

Zier J.B, Gustafson J. and Lemckert C. (2009) Torres Strait tidal survey. Prep. For Dept Natural Resources and Water by *Griffith University Centre for Infrastructure Engineering and Management (GCIEM),* Reference No: 03/12/1237_1.

Appendix A

Scope of Work

TORRES STRAIT REGIONAL AUTHORITY

REQUEST FOR QUOTATION

FOR

CONSULTANCY FOR PROJECT:

Probabilistic Assessment of Extreme Ocean Water Levels and Inundation Hazard in Torres Strait

1. INTRODUCTION

The Torres Strait Regional Authority (TSRA) is a Commonwealth statutory authority responsible for coordinating the delivery of policies and programs that benefit Torres Strait Islander and Aboriginal people living in the Torres Strait region.

As part of TSRA's coastal management program TSRA's Land & Sea Management Unit (LSMU) is seeking to undertaken an assessment of Extreme Ocean Water Levels and Inundation Hazard in Torres Strait.

Ocean inundation is a significant issue in Torres Strait impacting many Island communities. Early records suggest inundation has a been a problem for many years with an event on Saibai in 1948 leading to the relocation of a portion of the population to the Northern Cape York Peninsula. More recently an event in 2006 and 2009 impacted several island communities.

Conversely lower than predicted water levels can also be an issue for shipping activity and port activities.

With potential sea level rise inundation risk is likely to increase over time with events expected to become more frequent and severe over time. Potential changes to the frequency and intensity of cyclones and possibly other drivers of tidal anomalies may also result in increased inundation risk.

2. TERMS OF REFERENCE

2.1 Main Task

The main task is to undertake a probabilistic assessment of ocean water levels and mapping of inundation hazard to Torres Strait Island and Northern Cape York Peninsula communities.

2.2 Study Area

The study area is the Torres Strait and focuses on all inhabited island communities as well as Seisia on Cape York Peninsula.

2.3 Project Scope

Specific tasks to be undertaken within this engagement include:

- Identification of contributors to ocean water levels in Torres Strait and their relative importance. This is to include assessment of potential variability in contributors between Island communities.
- Probabilistic assessment of tidal anomalies (deviation from predicted tides) for each Torres Strait island community. This should be undertaken

assuming current conditions and greenhouse enhanced conditions for 2100 (high, med, low scenarios).

- Probabilistic assessment of water level extremes (combined probability of tides and other contributors to ocean water levels) for each Torres Strait Island community. This should be undertaken assuming current conditions and greenhouse enhanced conditions for 2100 (high, med, low scenarios).

- Probabilistic mapping of inundation within each community for 1, 100, 1000, 10000 ARI events under current conditions and greenhouse enhanced conditions for 2100.

2.4 Suggested methodology

It is envisaged that the project will involve:

- Review of existing studies and literature relevant to ocean water levels in eastern and northern Australia.

- Analysis of existing ocean water level data from gauges within Torres Strait and the processes contributing to these.

- Modelling of storm surge and other contributors to extreme ocean water levels. Ideally any modelling undertaken will also be designed to assist event based forecasting and warning in association with cyclone occurrence.

- Noting potential issues with the accuracy of existing datum's the scope of the project includes assessment of tidal anomalies (deviations from predicted tide) enabling easy update of map layers should better datum and tidal plain information become available.

- Simple methods of including wave effects including wave setup and runup where these are likely to be significant (e.g. Iama).

2.5 Expected Output/reporting

The consultant shall attend meetings with TSRA representatives to discuss the progress of the project. Meetings will be held at the consultant's preferred office or TI. The consultant shall allow for the costs of up to 3 meetings in the project fee. In addition the consultant will be expected to present the draft findings of the study to the Torres Strait Coastal Management Committee.

Preliminary report on data analysis and modelling: a preliminary report should be prepared outlining initial data analysis and modelling results by 15 June 2009.

Draft Report: The results of the study should be should be presented in a draft report to be provided by October 2009 in digital format together with at least 3 printed copies.

Final Report: The final report should be provided in digital format together with at least 20 printed copies by November 2009.

The report is expected to as a minimum include:

- A description of the processes contributing to extreme water level events within Torres Strait.
- A description of the methods used in the study
- Return interval plots for tidal anomalies and ocean water level within Torres Strait island communities. (including confidence limits)
- Tabulated return period tidal anomalies and ocean water level within Torres Strait island communities. (including confidence limits)
- Maps of inundation within each community for 1, 100, 1000, 10000 ARI events under current conditions and greenhouse enhanced conditions for 2100 (high, med, low scenarios).
- Maps showing depth of inundation within each community for 1, 100, 1000, 10000 ARI events under current conditions and greenhouse enhanced conditions for 2100 (high, med, low scenarios).

All mapping output should also be provided in ARCGIS compatible format.

2.6 Program

The project is to be completed by November 2009

The following milestones are to be met for the project.

Date	Milestone / Data Output
April	1. Acceptance of contract
15 June	2. Preliminary report on data analysis and modelling
1 Nov	3. Final report.

The consultant shall attend meetings with TSRA representatives to discuss the progress of the project. Meetings will be held at the consultant's preferred office or TI. The consultant shall allow for the costs of up to 3 meetings in the project fee. In addition the consultant will be expected to present the draft findings of the study to the Torres Strait coastal Management committee.

The Consultant will be required to sign a Consultancy Agreement with the LSMU

2.7 Payments

As sole supplier, TSRA will simply initiate purchase orders based on meeting the milestones outlined in the Terms of Reference. 50% will be paid on milestone 1 and 50% on meeting milestone 2.

The Consultant will be required to sign a Standard Short Form Contract with LSMU (See Attachment A).

2.8 Lodging a response to this request for Quotation

A response is to be lodged by 17th of April 2009 and should be addressed to the Project Manager identified below.

The Consultant's submission for the project shall include the following information:

- an outline of the proposed methodology addressing the terms of reference
- a detailed costing, project plan and timeline.
- the structure of the proposed project team, together with roles and responsibilities of team members;
- brief curriculum vitae of team members concentrating on experience in similar projects and experience with the proposed procedure/model;
- suggestions and costing of any additional work considered necessary.

A fee schedule is to be presented, based on the identified activities in each stage of the project, together with estimated time inputs for each team member on each major task. Support staff and sub-consultant costs should be distinguished, together with reimbursables estimates for report preparation and printing; travel and accommodation; and other services.

All costs, particularly the unit costs for team members, are to be those which currently apply. Cost items not identified in the proposal will not be allowed in the final contract. The specified charge-out rates shall also apply for any additional work.

2.9 Project Manager

All enquires and correspondence for this Request for Quotation are to be directed to:

David Hanslow

Land & Sea Management Unit

PO Box 261, Thursday Island, QLD 4875

Ph: 07 4069 2957

Fax: 07 4069 2967

Email: david.hanslow@tsra.gov.au

Appendix B

Torres Strait Community Profiles and Modelled Locations

The following community information has been assembled mainly from TSRA-supplied material and the images are from Google Earth™. The mapped locations shown are those used in the numerical and statistical modelling to nominally represent each of the study communities.

Badu Island

Badu Island (10° 10'S, 142° 10'E) is located approximately 65 km north-east of Thursday Island, approximately half-way between the mainland of Australia and PNG. The island is approximately 10 km wide by 10 km long with two thirds consisting of granite hills, the highest point being Mulgrave peak (198 m ASL).

Badu Island is covered with scattered forest and scrub, with low-lying regions tending towards swamps and mangrove. Seagrass beds are widespread amongst the shallow waters around the island. The waters to the west and north are dotted with numerous small, rocky islands and outcrops, each surrounded by narrow fringing reefs.

The village is located on the south-east coast of the island within an area of 100 ha between the beach and the foothills to the north-west. Badu Community comprises residential areas with supporting facilities, e.g., Church, Government (FNQEB and Telstra, Council office, IBIS Store, workshop), hospital, sporting facilities and local private enterprises.

Boigu Island

Boigu Island is the most northerly of the inhabited islands and lies just 6 km off the mainland of Papua New Guinea (PNG) at approximately latitude 9^{o} 17' S and longitude 142^{o} 12' E in the Top Western group of islands within the Torres Strait.

Boigu Island is a large low flat island approximately 20 km long by 6 km wide formed from alluvial mud deposited on decayed coral platforms by the adjacent large river systems in PNG. Typical of the 'mud' islands, Boigu is very flat with large interior swamps filled with brackish water. Mangroves line the entire perimeter shores except in front of the Community. The remaining vegetation on the island consists of coconut, almond, fig and mango trees within the village. Established gardens produce cassava and sweet potato.

The low-lying and swampy nature of Boigu Island confines the Community to an area of approximately 500 m x 200 m on the northern shore of the Island.

Dauan Island

Dauan Island (9^{o}25'S, 142^{o} 32'E) is located in the Top Western group of Torres Straits, approximately 120 km north of Thursday Island. The island is roughly triangular in shape and is approximately 2 km wide by 2.5 km long. Topography is very steep composed of granite and acid volcanic rocks with the highest peak, Mt Cornwallis, at 242 m ASL. The Community is located on a narrow 0.5 km mostly elevated strip following the shore and consists of residential areas with supporting facilities provided by Churches, Government (Power Generation, Health Centre, School) and Council (Office, Workshop). There is no airstrip on Dauan. Air access is by helicopter or by fixed-wing aircraft to Saibai airstrip and then by dinghy to Dauan.

The Island has reticulated water and electricity. There is no airport on Dauan, with the nearest on Saibai, 6km to the northeast. The community is built along narrow coastal lowland, backed by steep granite peaks. Like other islands of the Torres Straits, municipal services are provided by the local Community Council of Dauan Island.

Erub Island

Erub or Darnley Island (9^{o} 35'S, 143^{o} 45'E) is located 185 km north east of Thursday Island and is one of the Eastern Group of islands within Torres Strait and is approximately 3 km long by 2 km wide. Terrain consists of steep basaltic slopes rising to a central peak 181 m ASL. The area of island is approximately 375 hectares. As with the other islands in this group (the other being Mer and Ugar) Darnley is steep and of volcanic origin.

Four major and numerous minor creeks drain to the coastline. The Island is at the western end of a reef, which extends approximately 0.5 km in the south to 5 km in the west. Grass burnoffs during summer have destroyed much of the previous dense vegetation on the island and contribute to sheet and gully erosion during the wet season.

The coast line is indented with small sandy beaches and pockets of lush vegetation in the valleys. Surrounding the island is a well developed fringing reef which supports well established coral communities, reef fish and invertebrates. The fringing reef today still has well preserved stone fish traps which dominate the aerial view of the reefs.

Gealug Island

Gealug (Friday Island; 10° 35'S, 142° 10'E) is located immediately west of Thursday Island within the Inner Island Cluster of Torres Strait and is approximately 1.5 km wide by 3 km long. The terrain is typical of the surrounding island, being composed of granite hills.

The main community is located on the eastward-facing sandy shore and consists of only a few scattered houses.

Hammond Island

Hammond Island (10° 33'S, 142° 12'E) is located immediately north of Thursday Island within the Inner Island Cluster of Torres Strait and is approximately 3 km wide by 6 km long. The coastline varies markedly from mangroves and mudflats, to granite hills and sandy beaches at the back of dead coral reefs. The terrain is generally quite hilly except for a narrow coastal strip on the eastern side where part of the Community lies. It is noted for its natural, permanent, freshwater springs.

Settlement is along a long narrow ribbon of shore land or elevated above the shore on a plateau between hills further inland. This plateau slopes gently westward and is drained by a creek that becomes tidal 200 m west of the Community.

The township of Hammond is split into two distinct areas. The main township area is located on an elevated plateau and the other part of the township is located along a narrow coastal strip with clusters of house extending along the coastal strip. Future township expansion is constrained by topography although there are opportunities for consolidation and expansion within existing housing areas.

Iama Island

Iama or Yam Island (9° 54'S, 142°41'E) is located is approximately 97 km north east of Thursday Island in the Central Group of Islands in the Torres Strait. It consists of a large steep mass of granite fringed with coral sand flats, the largest being at the north-western end of the island on which the village is located. Vegetation includes thick scrub and mangroves. Iama has an area of 145 ha.

The area of settlement is a triangular area 300 x 300 m on reasonably flat land. The majority of the community consists of residential areas (54 occupied dwellings) with supporting facilities including; Council offices, hall, medical aid post, church, IBIS food store, state primary school, Council 'motel', and AQIS office. There are telecommunications facilities and an Ergon power station. Transport facilities include an airstrip, and a barge landing area.

Industry includes a fish factory and there are two privately owned freezer processing plants established on the island. CDEP has a participant level of 124.

Mabuiag Island

Mabuiag Island (9^{o} 58'S, 142^{o} 10'E) is located in the Near Western of islands in Torres Strait. Mabuiag is loosely described as a 'granitic' island; essentially a submerged remnant of the Australian mountain chain. The Island is roughly triangular in shape, having an area of 626 ha, being approximately 4 km long by 3.5 km across its widest point. Terrain consists of steep mountains rising to a maximum height of 263 m.

The main Community is located in a small valley or 'cove' approximately 700 m x 200 m following the shoreline. The majority of Mabuiag Community consists of residential areas with supporting facilities provided by Churches, Government (Power Generation, Health Centre, School) and Council (Office, Workshop).

The village is substantially located within an area of approximately 15 ha along the shoreline. The layout is essentially an elongated pattern with major streets parallel to the shore. The majority of the village consists of residential areas supported by Council offices, churches, Ergon, health centre, IBIS Store and Council workshops.

Masig Island

Masig or Yorke Island (9°45'S, 143°24'E) is located in the Central Group of islands in Torres Strait, and is approximately 160 km from Thursday Island.

Masig is a coral cay, approximately 2700 m long and 800 m wide at its widest point, located on the west end of a narrow east-west orientated reef system. Topography is flat with ground level generally 3 m above local mean sea level. Vegetation consists of dense trees. Soils are medium to coarse grain sand overlying a cemented 'horizon of beach rock'.

Mer Island

Mer Island (9°55'S, 144°03'E) is located 200 km from Thursday Island in the Eastern Island Group of islands in the Torres Strait and is the most easterly of the communities.

Mer is of volcanic origin, roughly oval in shape and approximately 7.8 km^2. The island rises steeply from the shoreline to a central plateau about 80 m ASL. Gelam Paser, a crater rim on the western end of the island is the highest point reaching 230 m. Dense timber and scrub vegetation exists within the central plateau formed by the major lava flow, with clearings for banana, cassava, taro and sweet potato gardens.

The village is in a ribbon pattern 3 houses wide by 3 km long on the north-eastern side of the island, along the narrow sand strip at the base of the ash rim.

Moa Island

Moa Island (10^{o}14'S, 142^{o}13'E) in the Near Western group of islands is located approximately 60 km north-east from Thursday Island. It is a circular granite island of approximately 160km^2; just over 17 km in diameter at its widest point. A large sandy alluvial plain rimmed by hills covered in open forest drains a significant portion of the island westward and to the north. A granite ridge, Mt Augustus (399m ASL) is the highest point in the Torres Strait. There are numerous creeks with seasonal freshwater wetlands found in the alluvial areas adjacent to creeks. Some tidal wetlands are located on the island. The island is fringed by an extensive but patchy mangrove forest which are most developed on the south, west and north coasts.

There are two communities on Moa Island - Kubin and St Pauls.

Kubin Community Profile

Kubin is situated on the south eastern corner of Moa Island. The Community is located on a small hilly headland near the south-west corner of the island. Most of the housing is located 18 to 10 m above mean sea level in an area 400 x 300 m. A natural drainage path bisects the Community. The village is predominantly located on a small hilly headland near the south-west corner of the island. Most of the housing is located on a sloping plateau within this headland which varies from 10 to 18 metres above mean sea level.

The majority of the community consists of residential areas, supported by Council offices, church, primary school, store, health centre, Council workshop and Ergon. The community has access to a small sheltered harbor and boat ramp and is serviced by regular airline flights from Horn Island and weekly barges.

St Pauls Community Profile

St Pauls community is located on the eastern side of Moa Island with older settlement within an area of 40 ha along a beach front sand dune and the swampy areas to the west. Recent residential development has occurred on higher ground to the west of the main village.

The majority of the community consists of residential areas, supported by Council offices, church, primary school, store, health centre, Council workshop and Ergon. St Pauls' Council has initiated a number of small industries, and these have made a significant contribution to the general economy of the community.


Moa_Kubin_SEA
Google


Moa_St_Pauls_SEA
Google

Muralag

Muralag (Prince of Wales Island) is a small coastal community on the lower coastal flats towards the northern end of what is a large hilly island with limited development. It is within easy reach of Waiben by boat.

Ngurupai

Ngurupai is located on Horn Island, immediately opposite Waiben, and is host to the regional Airport.

Poruma

Poruma or Coconut Island (10°3'S 143° 4'E) is located approximately 100 km north-east from Thursday Island in the Central Island Group in Torres Strait.

Poruma is a narrow, elongated coral cay approximately 2 km long by 0.3 km wide with an area of 44.6 ha. The terrain is reasonably flat except along the southern side of the Island where higher sand dunes are found. Vegetation predominantly comprises coconut palms, with some low scrub on the eastern side. The natural vegetation cover was largely depleted many years ago for firewood. There are serious concerns as to erosion and other impacts from development.

The narrowness of the Island has resulted in a ribbon like development, predominantly centred on the main street, located on the western end of the Island. The majority of the community consists of residential areas. Supporting facilities include: council offices, medical aid post; churches, kindergarten and store.

Saibai

Saibai Island (9°24'S, 142°41'E) lies in the Top Western Group of is located approximately 5km south of Papua New Guinea. It is one of the largest Torres Strait Islands, being approximately 26 km long by 8 km wide. It is composed of alluvial sediments apparently originating from the Fly River of Papua New Guinea. Similar to Boigu Island, it is locally referred to as a 'mud' island.

Saibai is very flat with large interior swamps filled with brackish water. Mangroves line the entire perimeter shores except in front of the Community.

The Community is located on a narrow 1.7 km long embankment along the north shore; sufficient only in width for a roadway and one row of houses at some locations.

Seisia

Seisia community is situated on the coast of the Northern Peninsula Area. Its population is largely made up of Saibai Islander descendents, who moved to the mainland following flooding in the late 1940s and 1950's. It has a significant passing trade from tourists travelling to the tip of Cape York, offering a large camping ground and holiday park for travellers.

Ugar

Ugar or Stephen Island (9°30'S, 143°33'E) is approximately 185 km north east of Thursday Island and located within the Eastern Group of islands within the Torres Strait. Its closest neighbour is Darnley Island.

Ugar is the smallest of the inhabited volcanic islands at approximately 700 m long by 500 m wide covering approximately 35 hectares. The Island consists mainly of a central plateau elevated 20 to 30 m ASL, with escarpments on all sides falling away steeply to narrow beaches on the north and south. The village is situated on a small plateau 46m above sea level. The rich red soil supports dense vegetation where it has not been cleared. There are no defined rivers or stream channels evident on the island. The island is fringed by extensive coral reefs.

Waiben

Waiben or Thursday Island (10°34'E, 142°13'S) is located 35 km north-west of Cape York and is one of the Prince of Wales Island Group.

Thursday Island (or "TI") is approximately 7km x 3km in size. Similar to the other Western islands, the island is a remnant of the Great Dividing Range which runs the length of the east coast of Australia. Thursday Island is hilly, rocky and generally has poor soil. There are tiny pockets of rainforest but most of the island is covered with open scrubland.

There are approximately 4000 people living permanently on TI. More than 90% are Torres Strait Islanders with the rest made up of Europeans, with a mixture of Asians from Japan, Indonesia and Malaysia. It is a cultural melting pot, which gives TI its own unique lifestyle.

Warraber

Warraber Island (10°13'S, 142°49'E), previously Sue Island, is located 72 km north-east of Thursday Island in the Central Islands Groups of the Torres Strait. The island is an elliptical coral cay island, approximately 1400 m long and 750 m wide at its widest point with an area of 93.2 hectares, located on the north-west corner of a large reef flat on an east-west alignment. There is a large shallow lagoon in the northern reef area with a narrow outlet in front of the village. The island is fringed with sandy beaches with coral rock outcrops along the northern beach.

The Warraber Island Community has developed a conventional grid layout contained within an area of approximately 500 m by 300 m, located on the eastern half of the island. The majority of the community consists of residential areas which are extensively planted with coconut trees. Dense tree cover exists over the areas not yet developed for houses.

Appendix C

Regional Wind Station Corrections


Google


Google

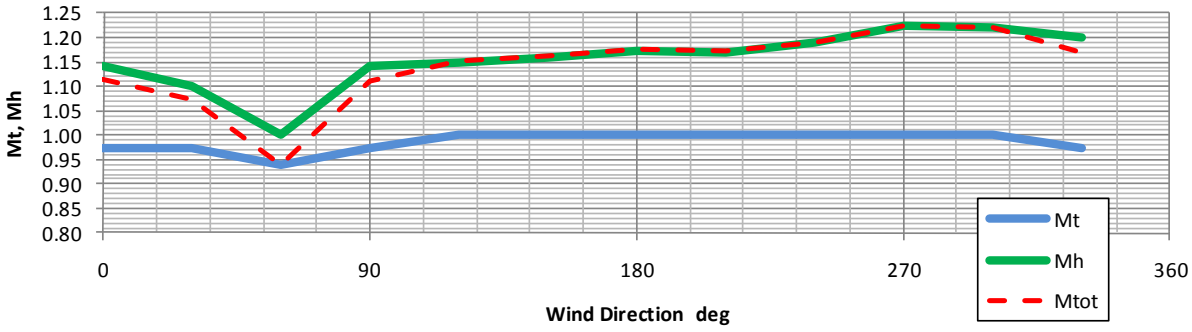
1.25
1.20
1.15
1.10
1.05
1.00
0.95
0.90
0.85
0.80
Mt, Mh
0
90
180
270
360
Wind Direction deg
Mt
Mh
Mtot

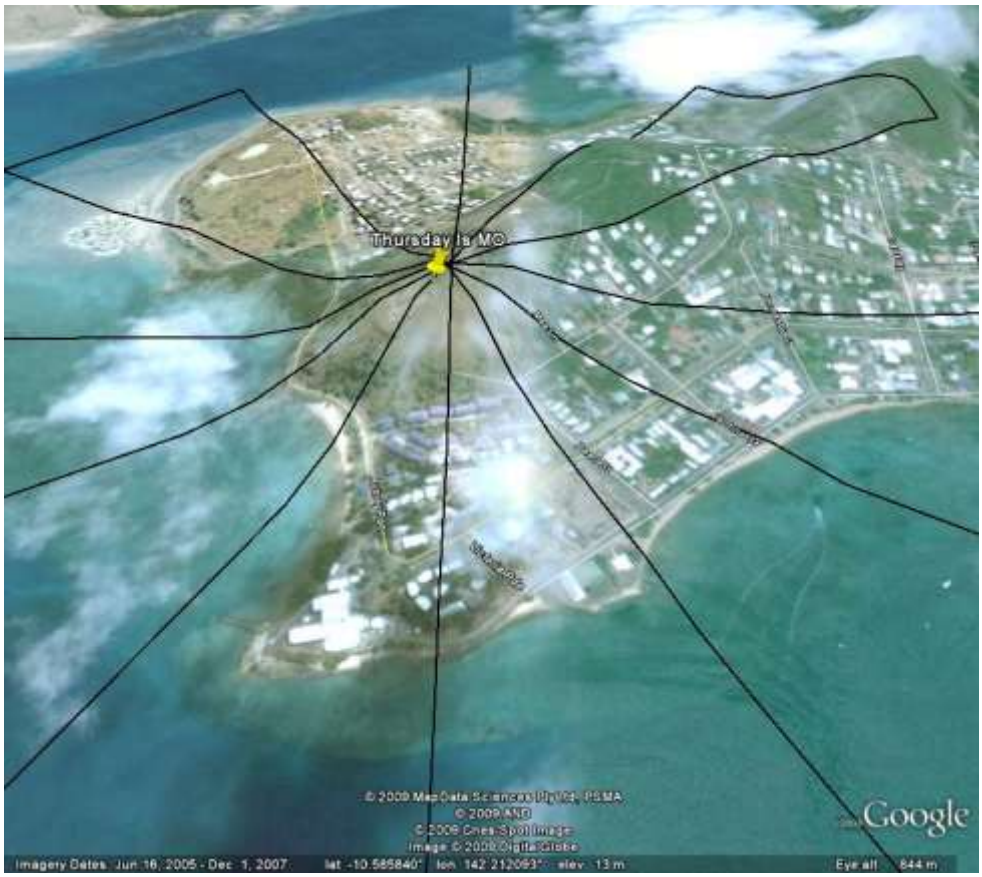
Thursday Is MO
Google

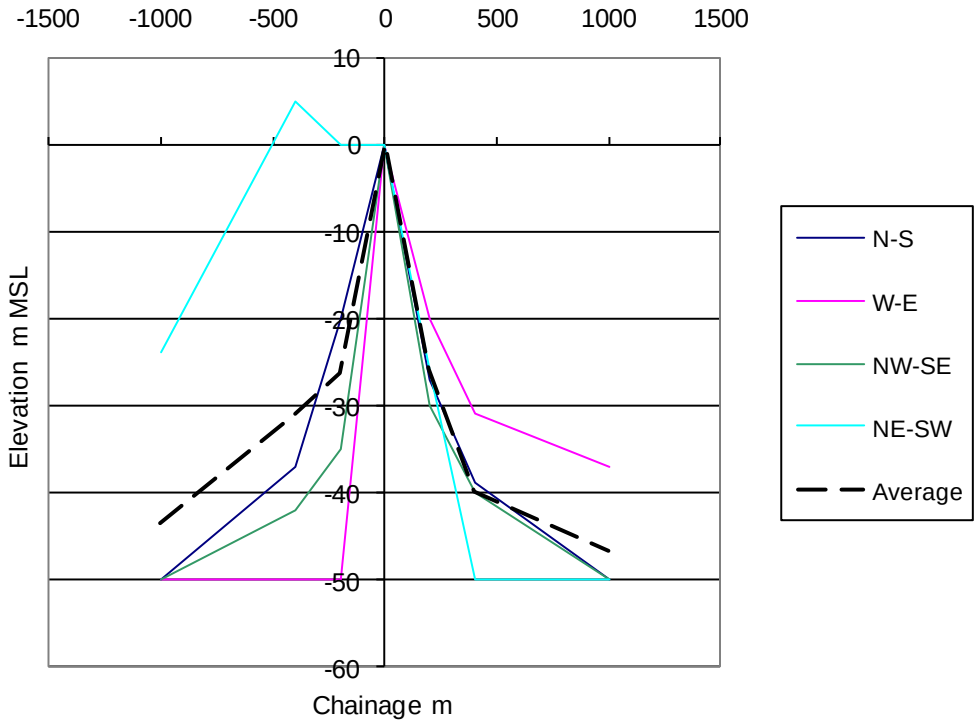
-1500
-1000
-500
0
500
1000
1500
10
0
-10
-20
-30
-40
-50
-60
Elevation m MSL
Chainage m
N-S
W-E
NW-SE
NE-SW
Average

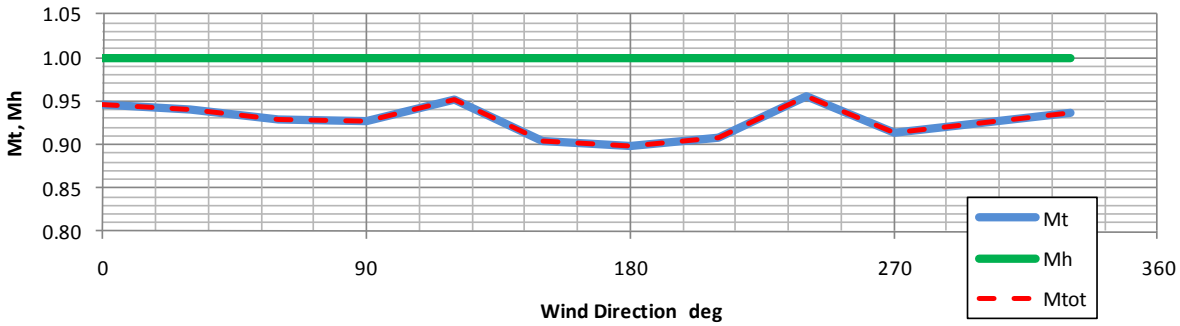
1.05
1.00
0.95
0.90
0.85
0.80
Mt, Mh
0
90
180
270
360
Wind Direction deg
Mt
Mh
Mtot

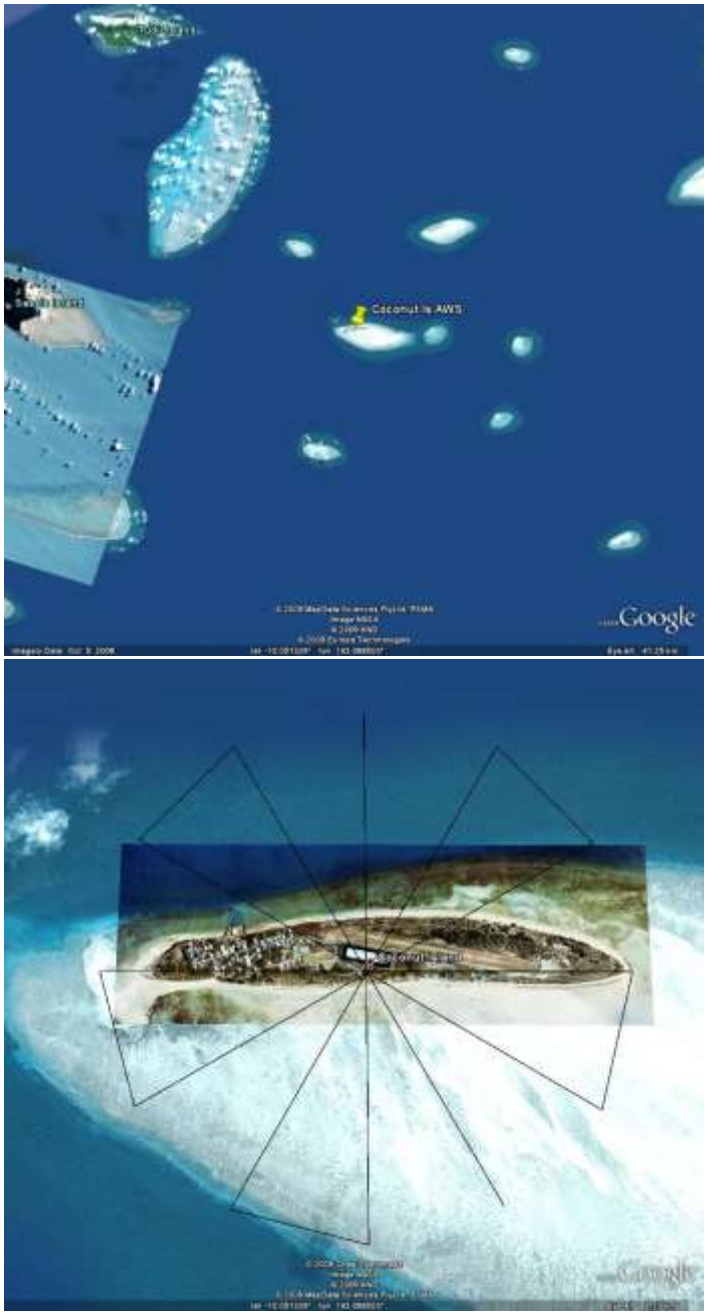
Coconut Is AWS
Google

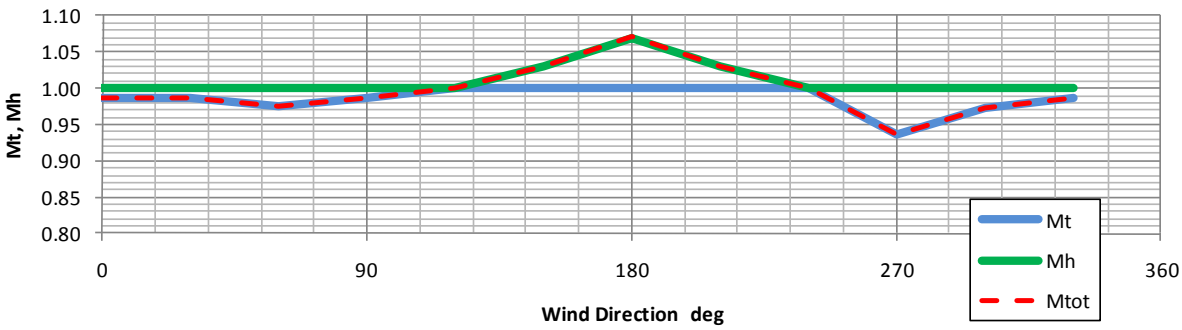
1.10
1.05
1.00
0.95
0.90
0.85
0.80
Mt, Mh
0
90
180
270
360
Wind Direction deg
Mt
Mh
Mtot

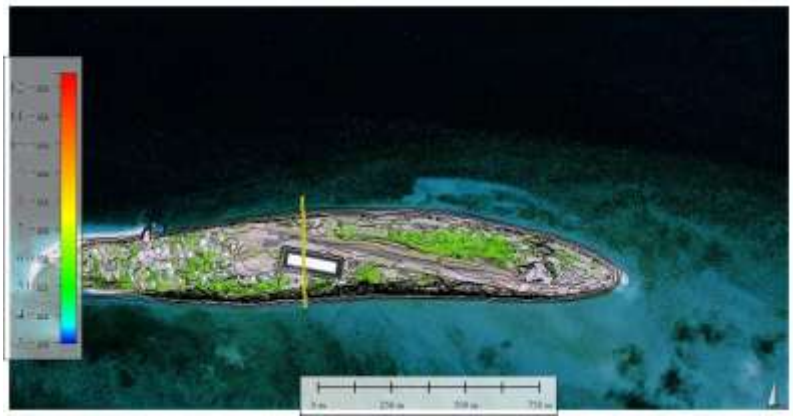

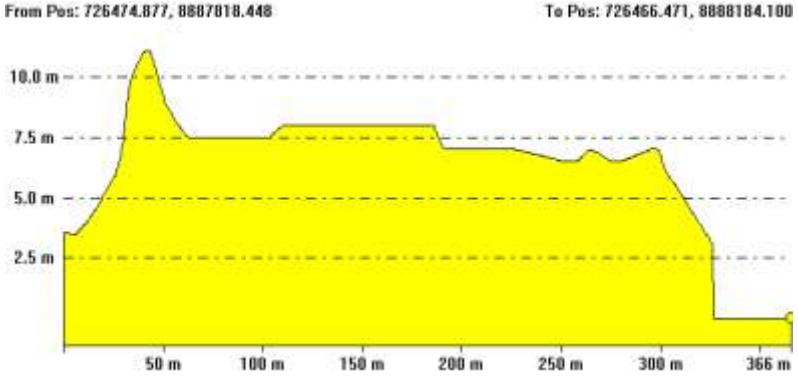
From Pos: 726474.877, 8887818.448
To Pos: 726466.471, 8888184.100
10.0 m
7.5 m
5.0 m
2.5 m
50 m
100 m
150 m
200 m
250 m
300 m
366 m

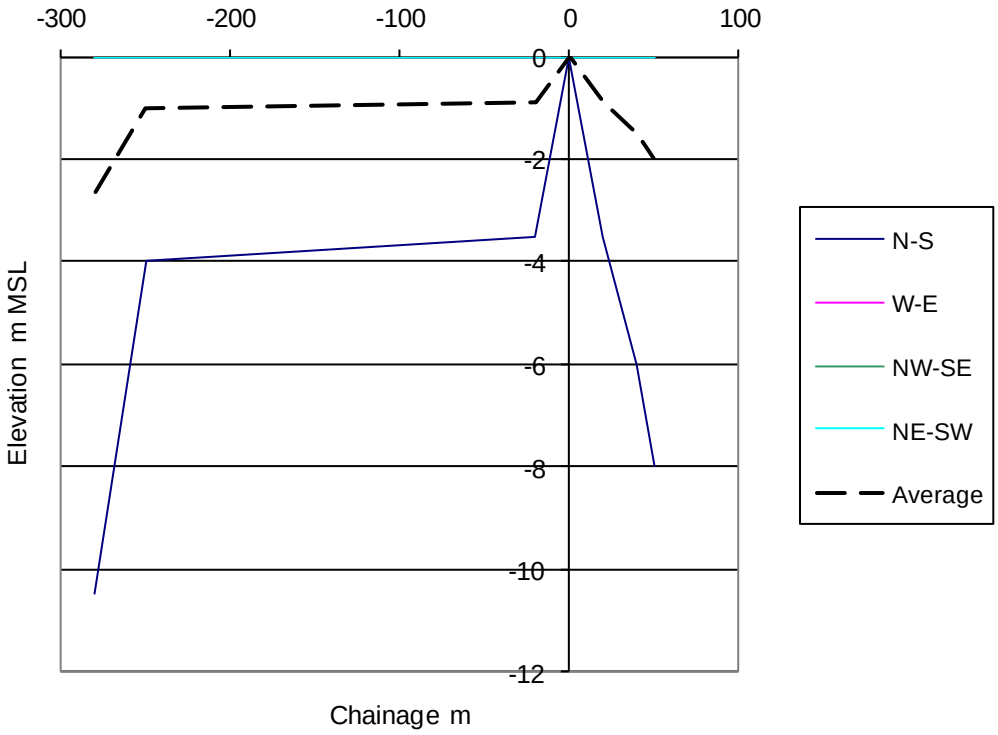
-300
-200
-100
0
100
0
-2
-4
-6
-8
-10
-12
Elevation m MSL
Chainage m
N-S
W-E
NW-SE
NE-SW
Average


Google


Google

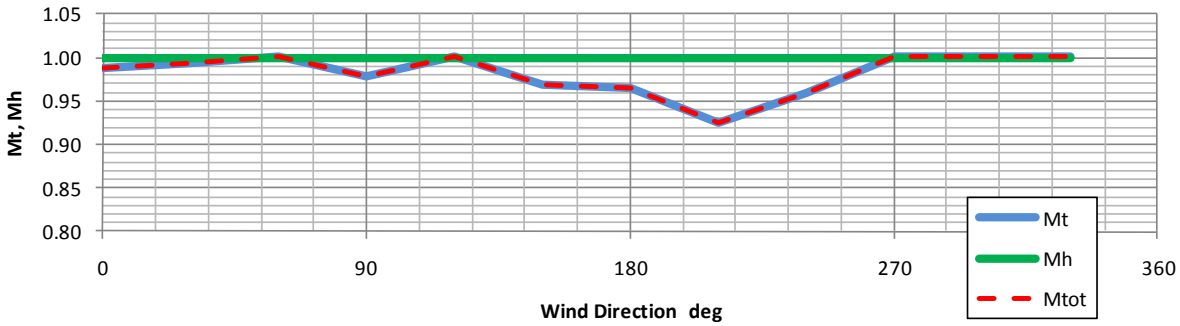
1.05
1.00
0.95
0.90
0.85
0.80
Mt, Mh
0
90
180
270
360
Wind Direction deg
Mt
Mh
Mtot


Google


Google

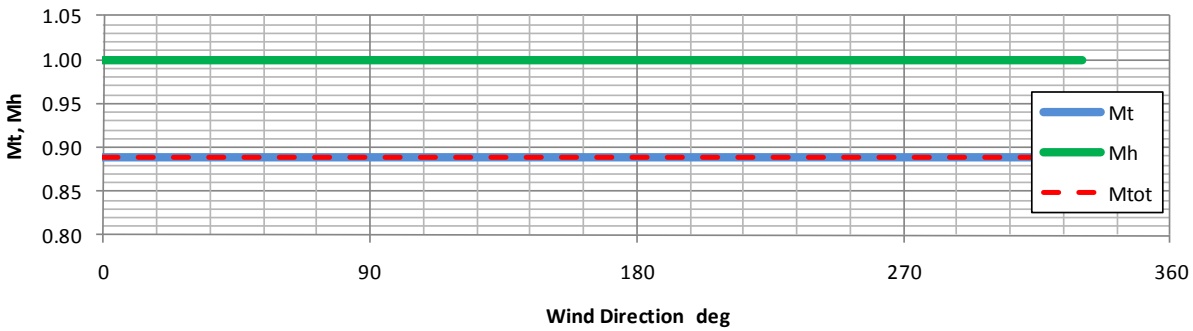
1.05
1.00
0.95
0.90
0.85
0.80
Mt, Mh
0
90
180
270
360
Wind Direction deg
Mt
Mh
Mtot


Lockhardt River Airport
Google
Lockhardt River Airport
Google

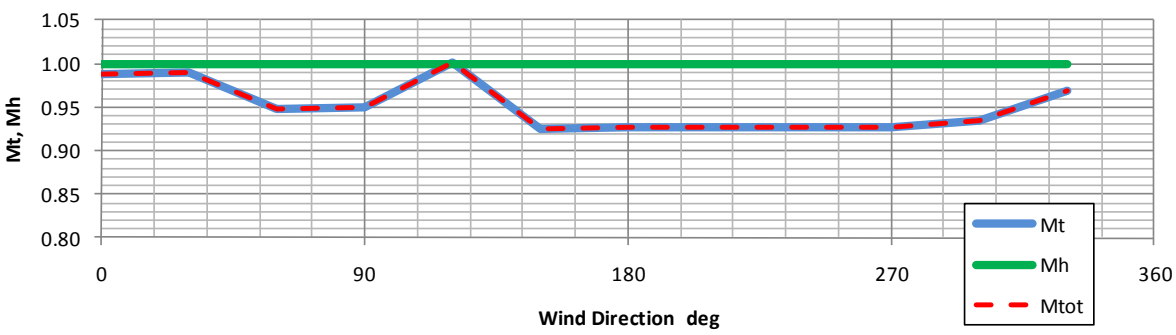
1.05
1.00
0.95
0.90
0.85
0.80
Mt, Mh
0
90
180
270
360
Wind Direction deg
Mt
Mh
Mtot

Appendix D

Extreme Value Analysis of Measured Winds

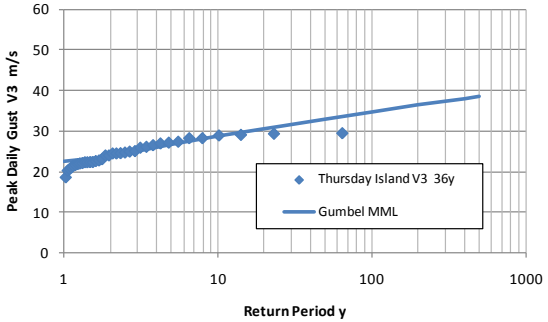

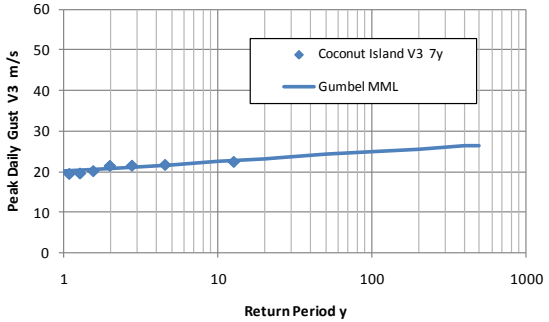

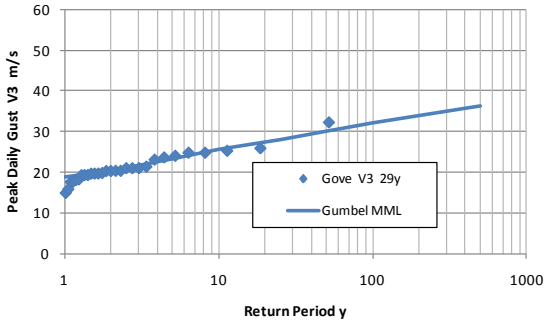

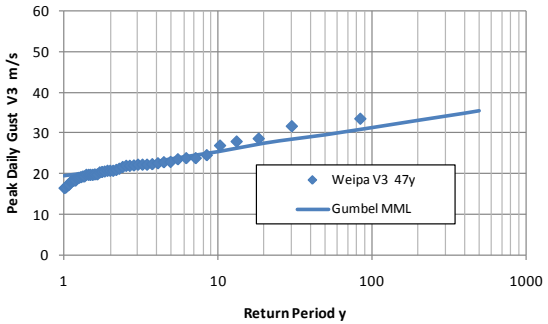

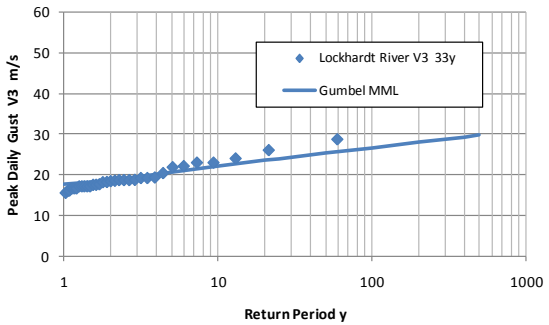

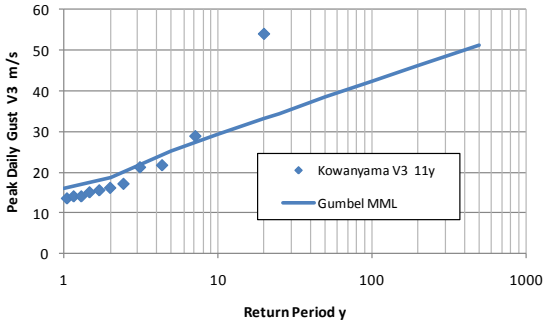

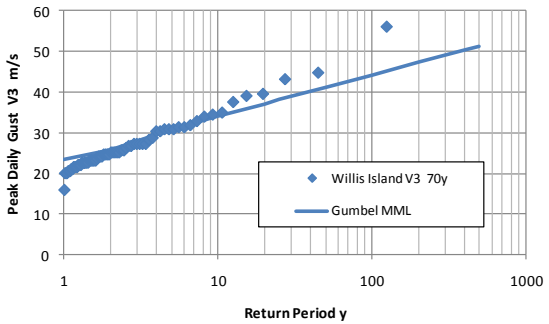

ALL WIND DATA - PEAK DAILY GUST V3

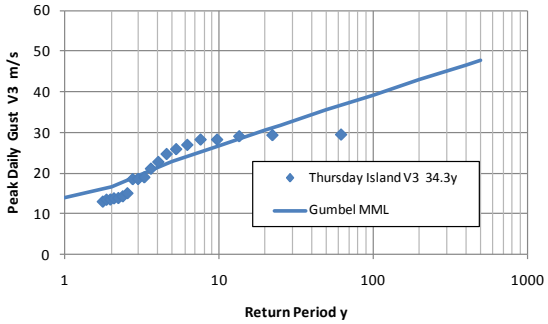

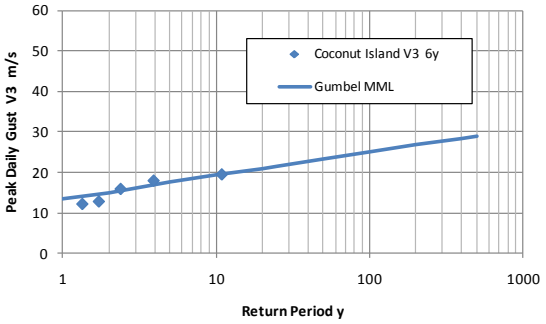

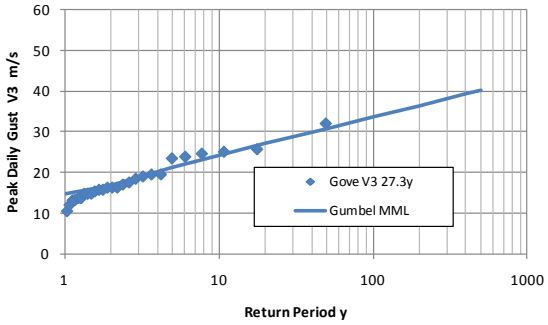

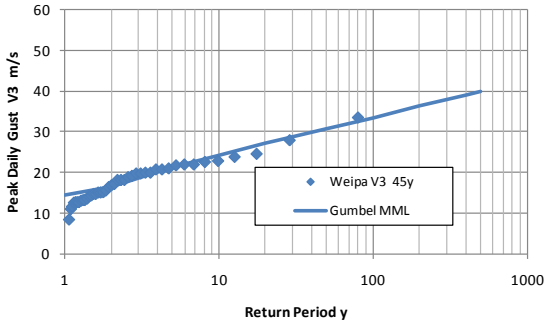

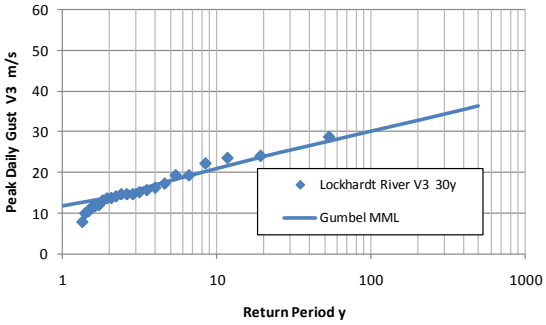

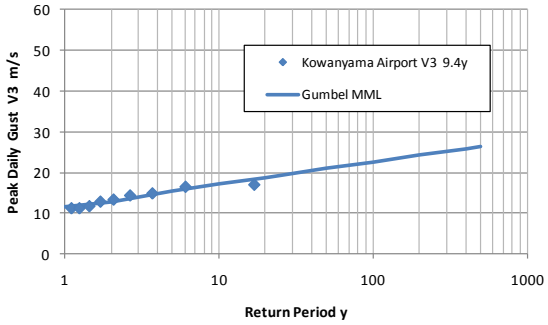

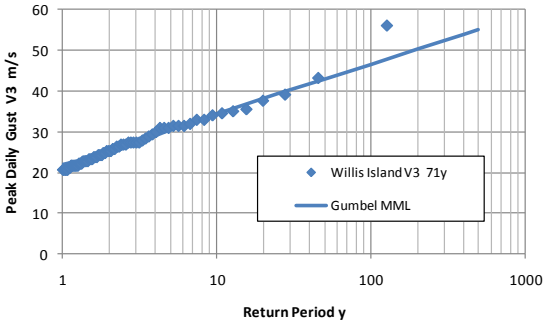

CYCLONIC WIND DATA - PEAK DAILY GUST V3

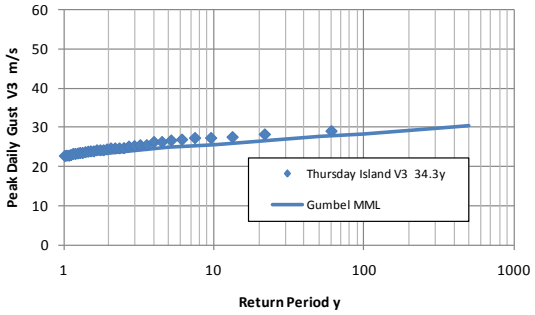

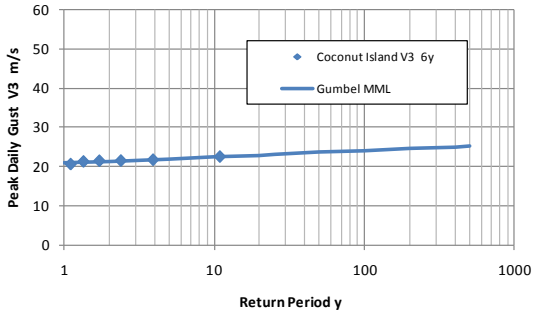

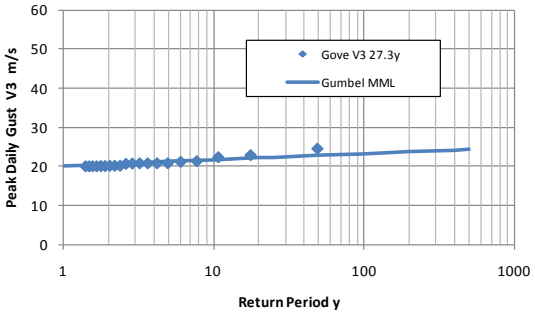

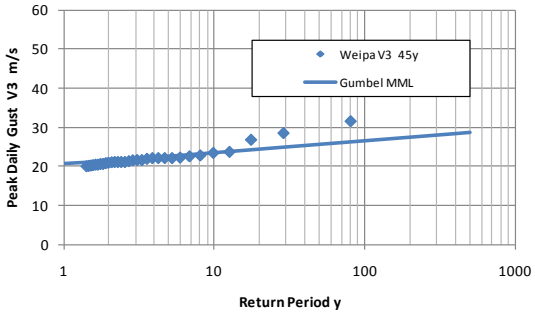

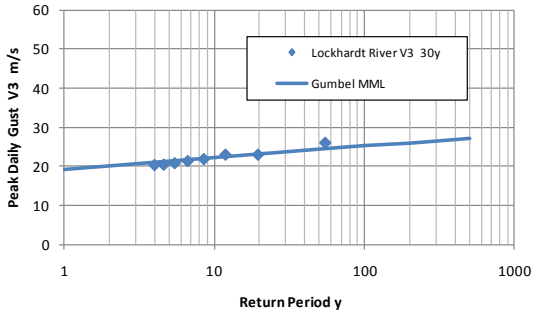

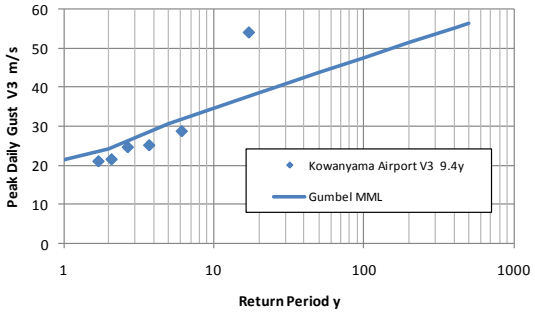

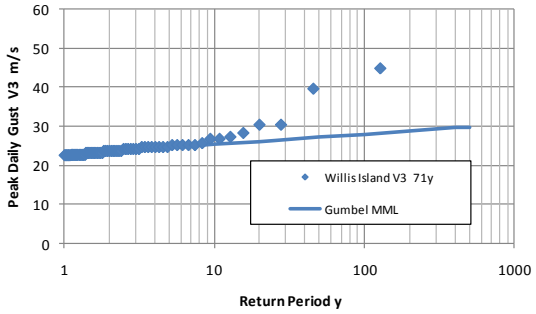

NON-CYCLONIC WIND DATA - PEAK DAILY GUST V3

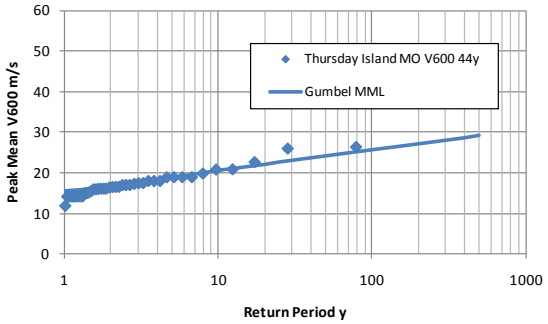

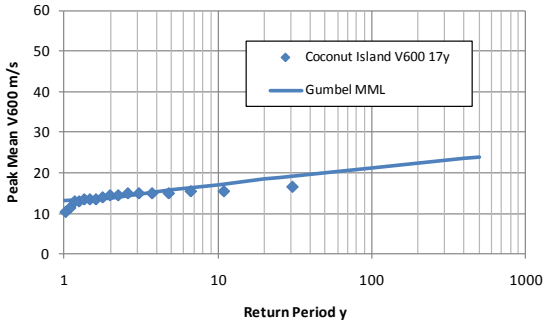

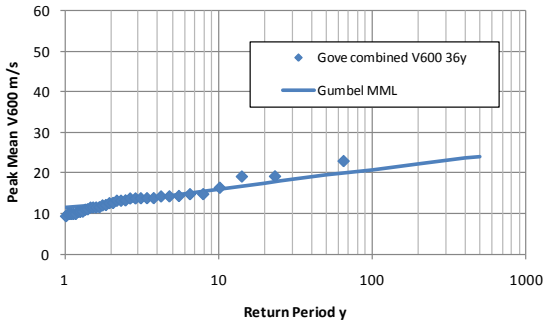

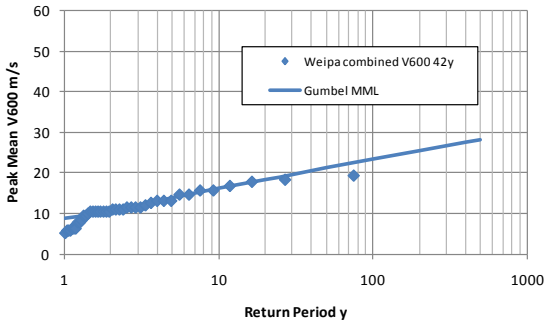

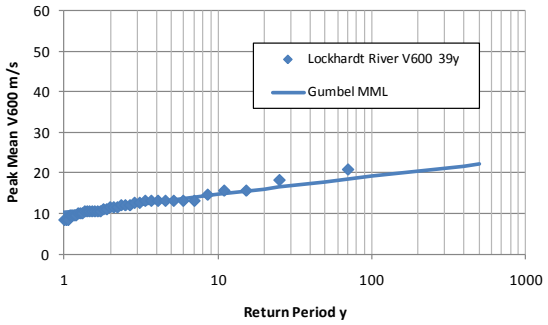

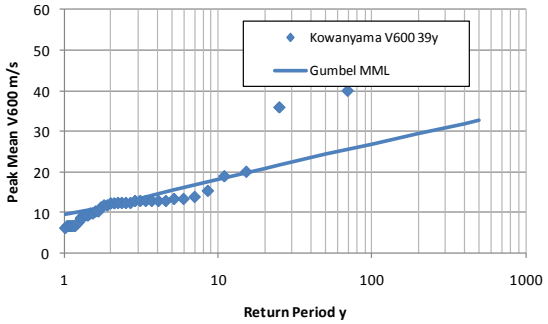

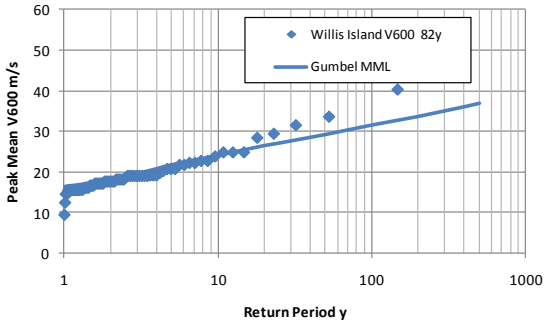

ALL WIND DATA - MAXIMUM MEAN WINDS V600

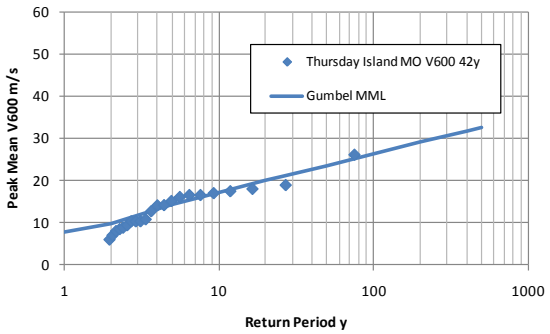

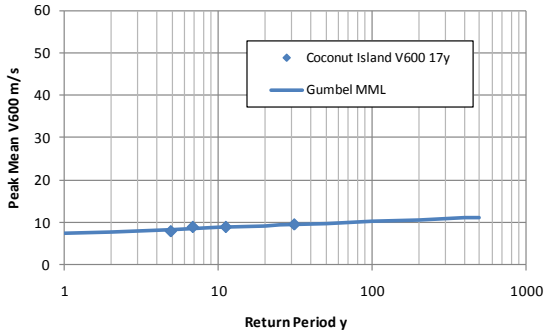

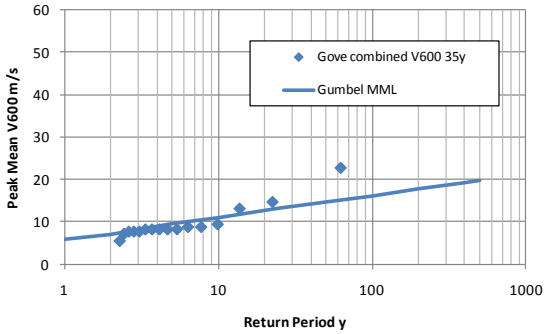

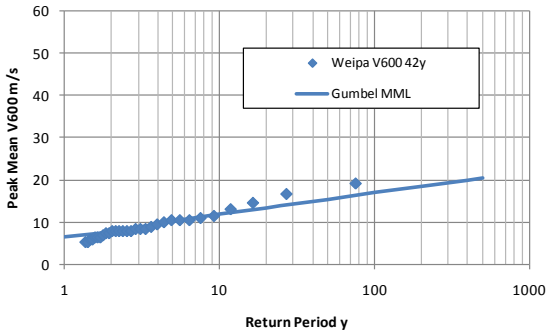

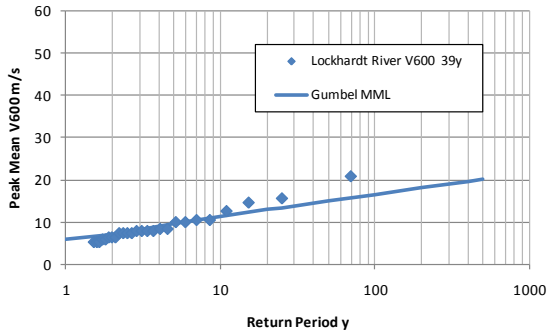

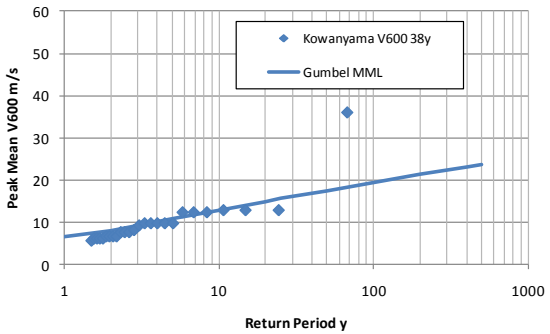

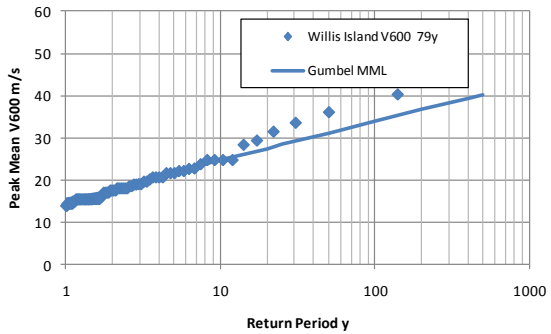

CYCLONIC WIND DATA - MAXIMUM MEAN WINDS V600

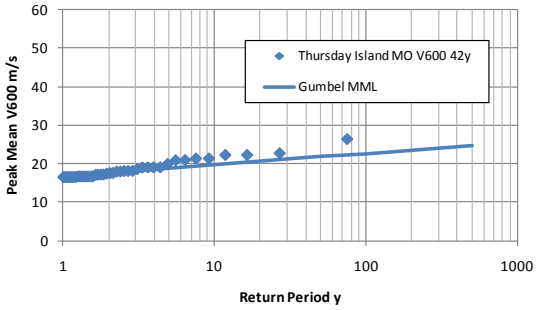

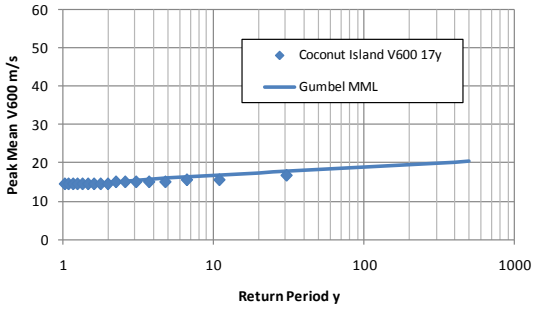

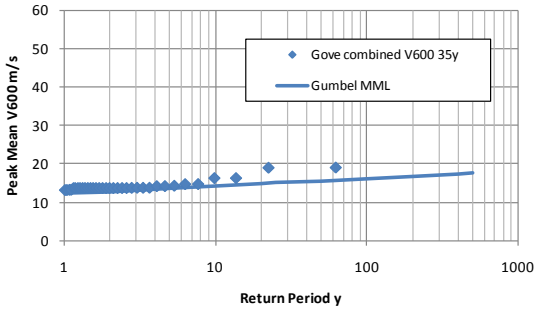

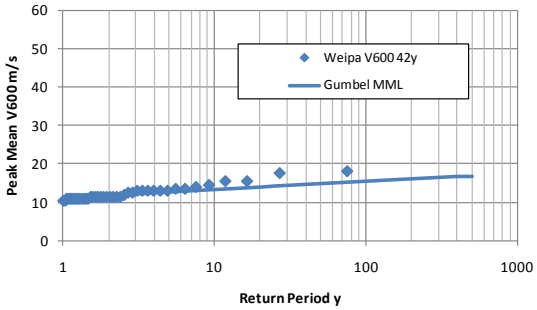

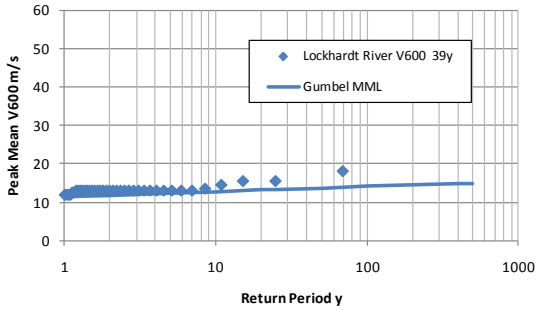

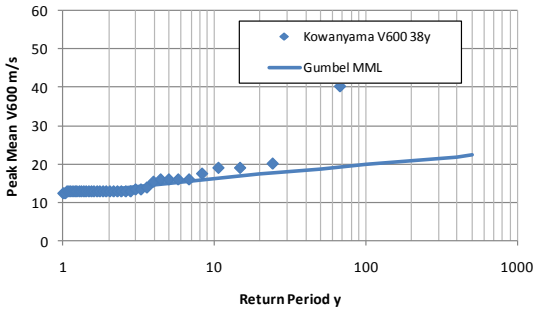

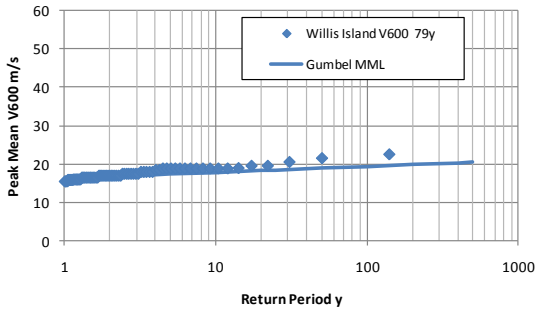

NON-CYCLONIC WIND DATA - MAXIMUM MEAN WINDS V600

Appendix E

Regional Tidal Modelling – Major Harmonics

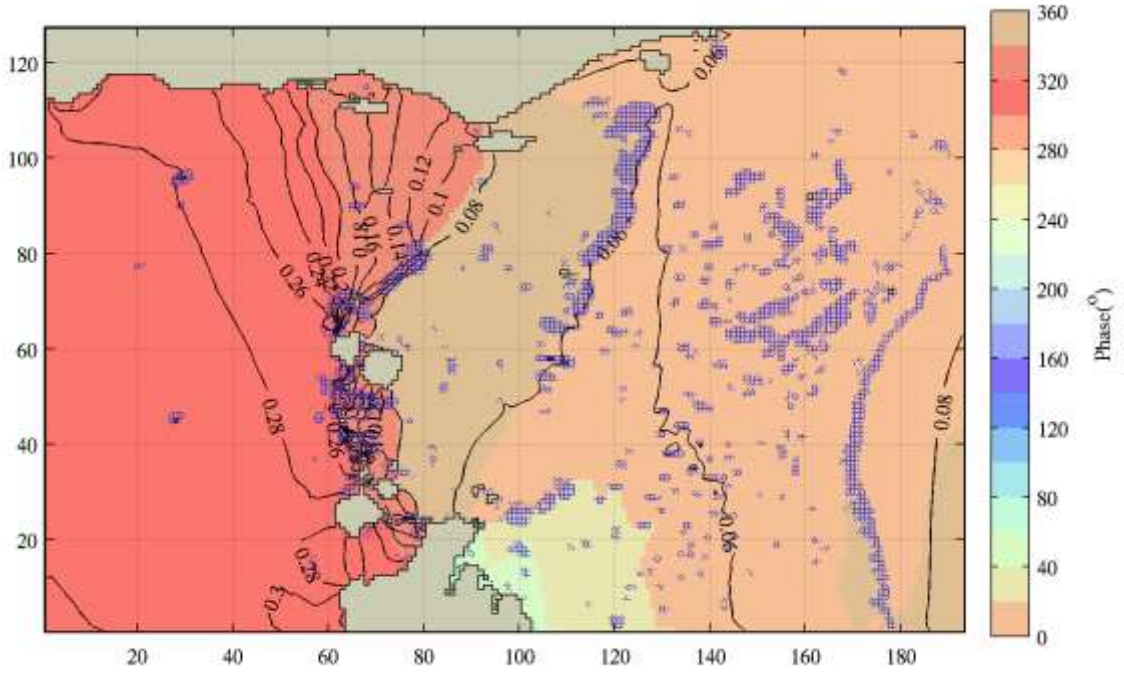

Figure E-1 Amplitude and Phase of S_a

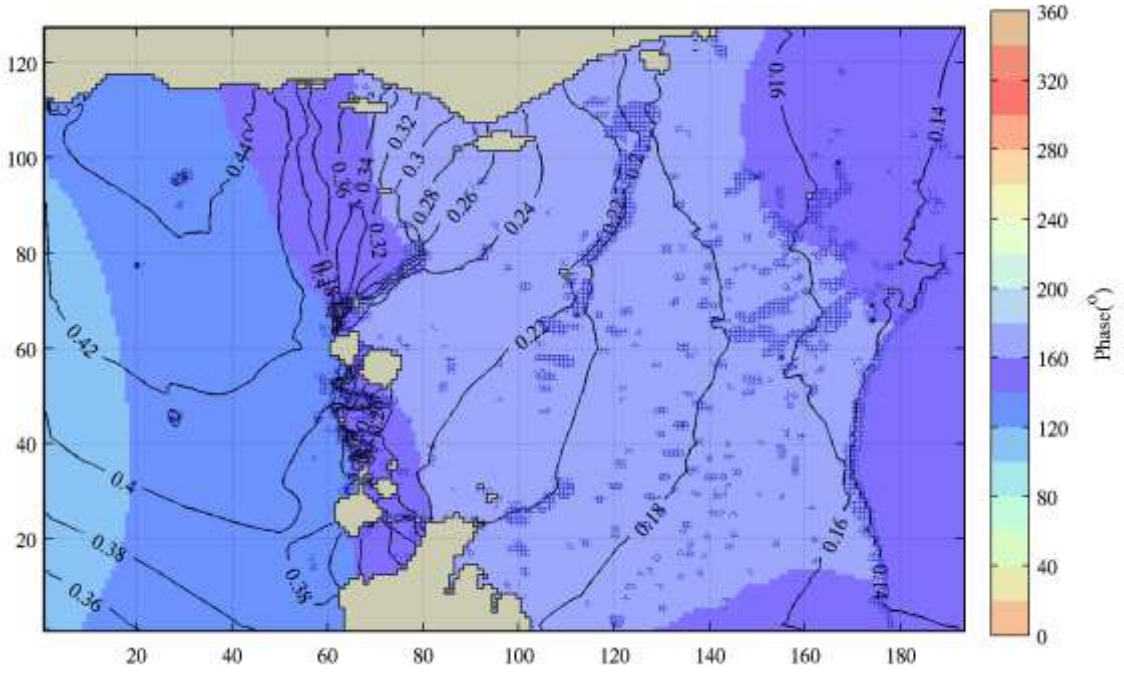

Figure E-2 Amplitude and Phase of O_1

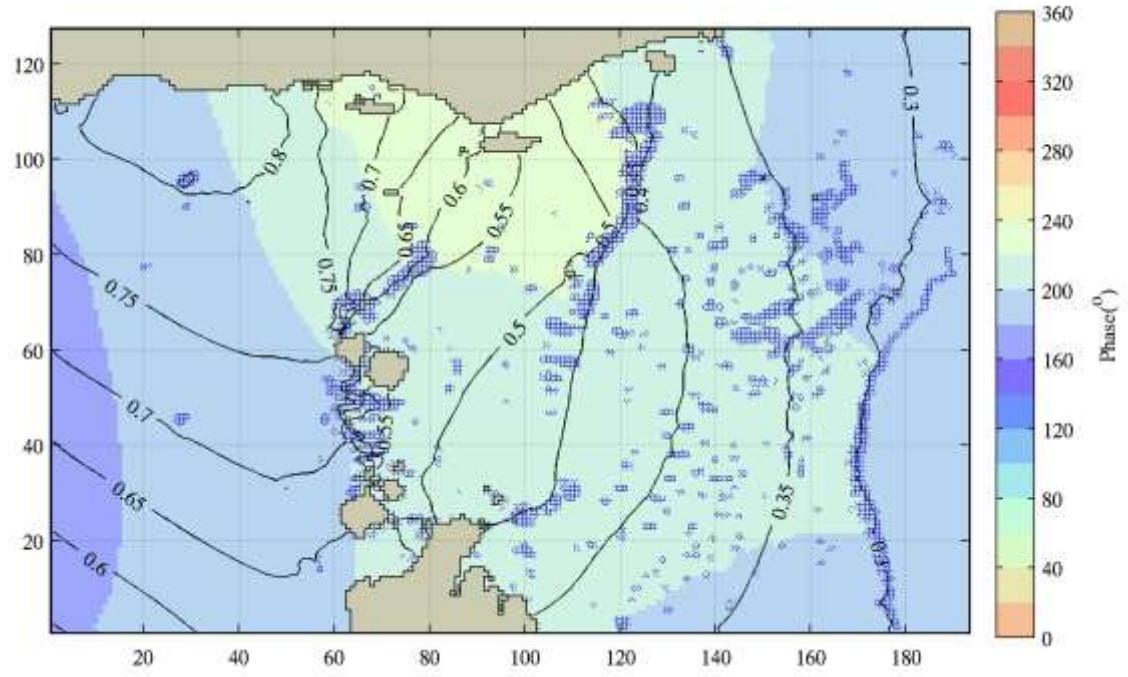

Figure E-3 Amplitude and Phase of K_1

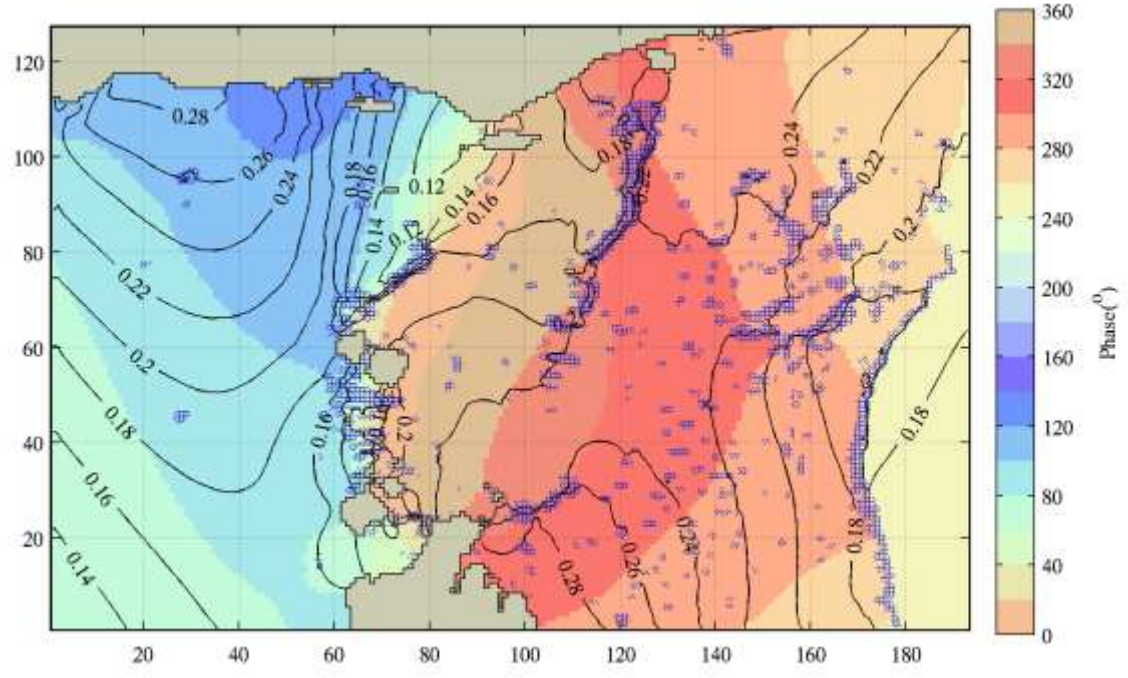

Figure E-4 Amplitude and Phase of N_2

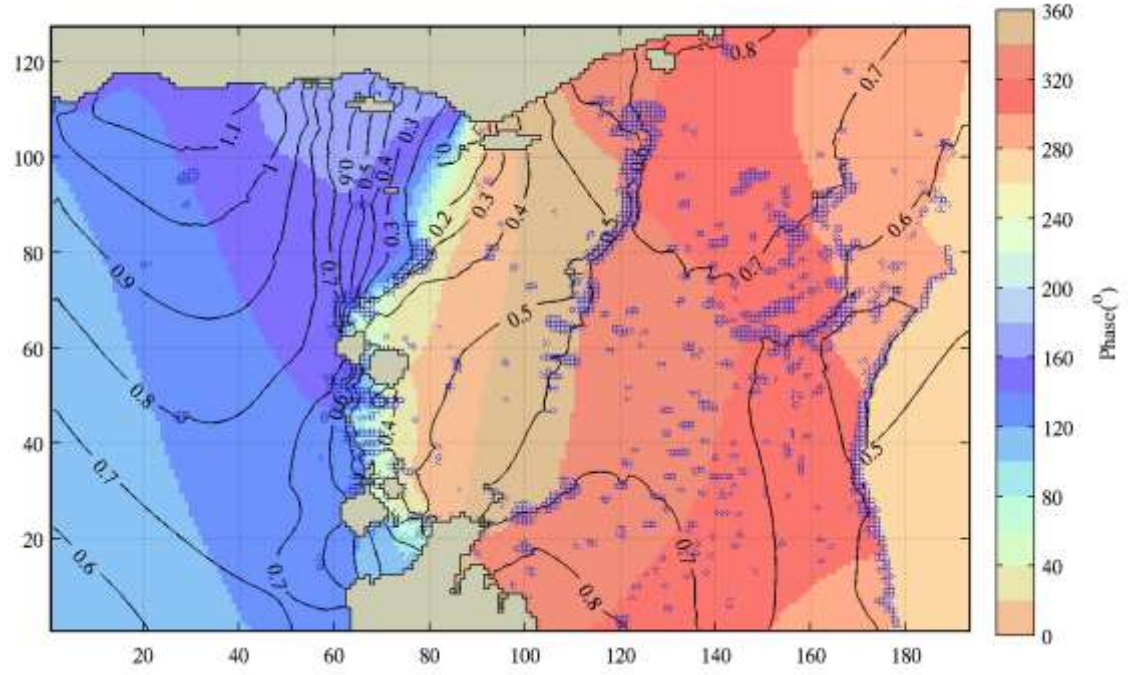

Figure E-5 Amplitude and Phase of M_2

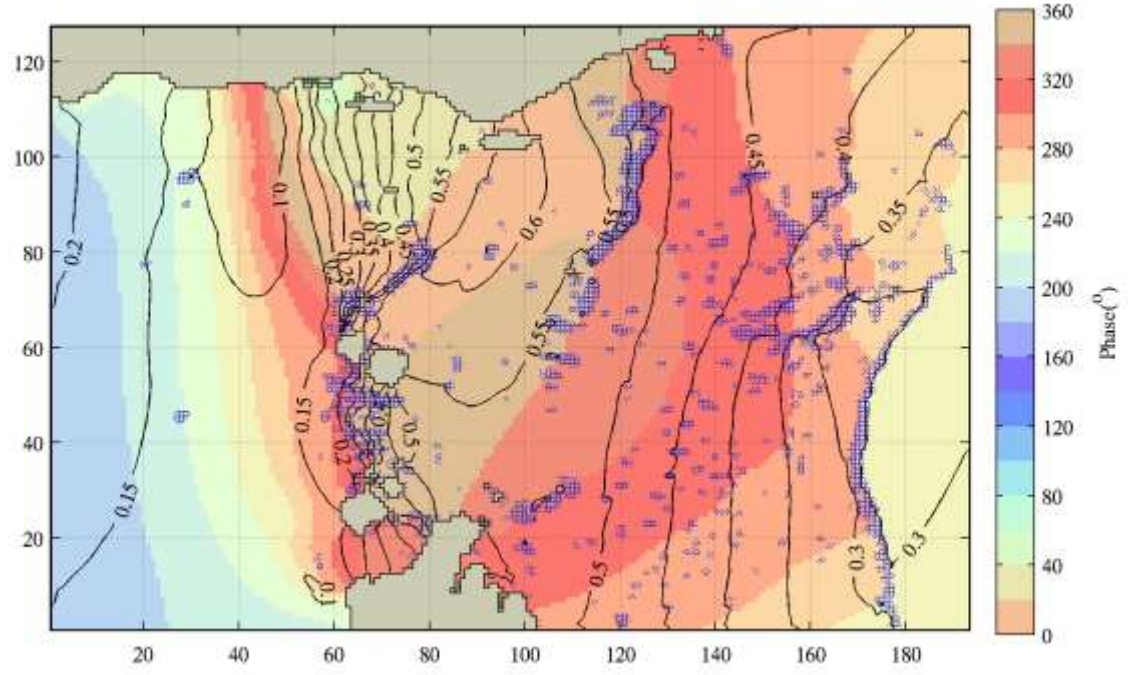

Figure E-6 Amplitude and Phase of S_2

Appendix F

Broadscale Ocean Water Level Modelling – Site Comparisons

Red is measured

Blue is modelled

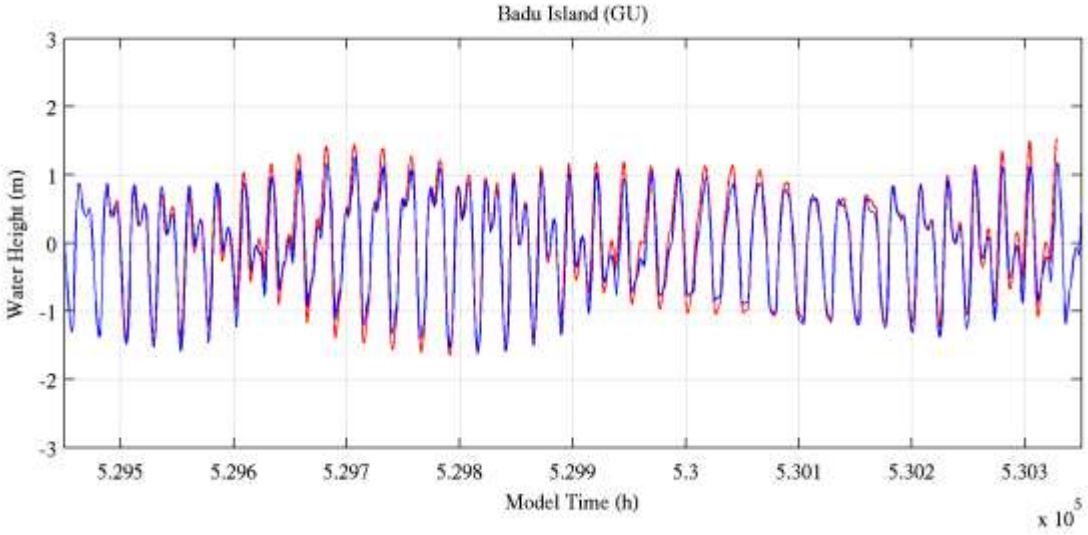
Badu Island (GU)
Water Height (m)
Model Time (h)
x 10^5
3
2
1
0
-1
-2
-3
5.295
5.296
5.297
5.298
5.299
5.3
5.301
5.302
5.303

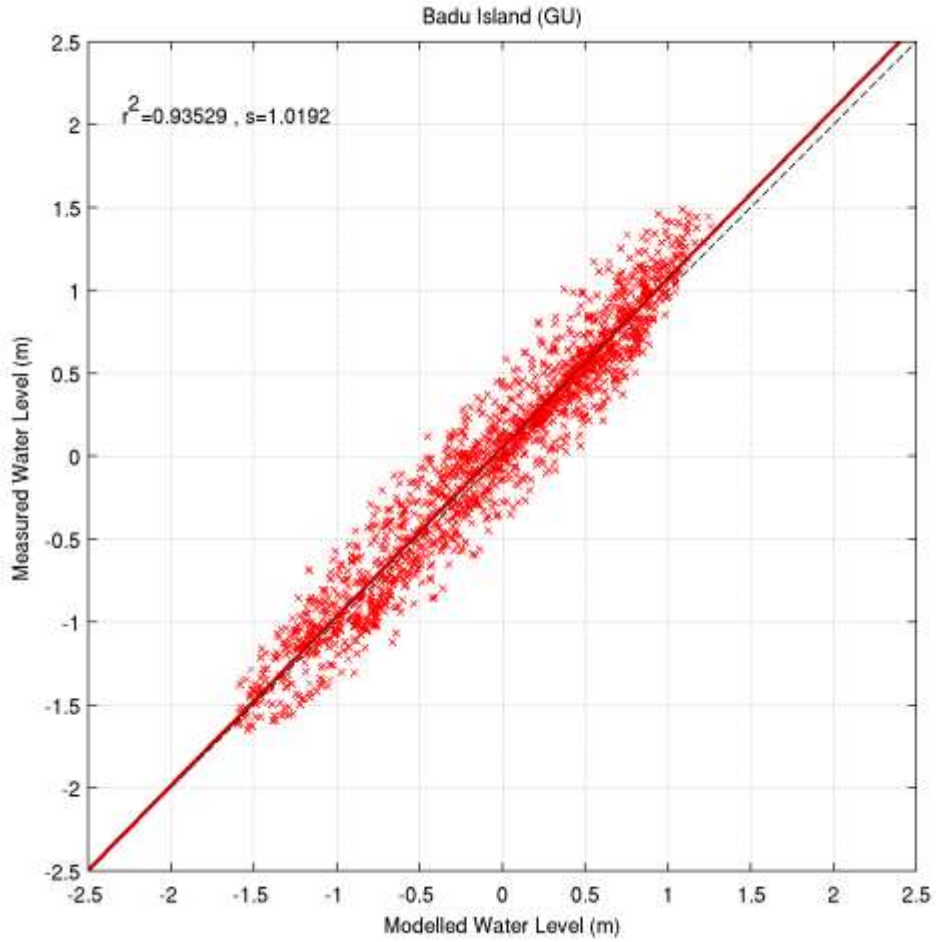
Badu Island (GU)
r^2=0.93529 , s=1.0192
Measured Water Level (m)
Modelled Water Level (m)
2.5
2
1.5
1
0.5
0
-0.5
-1
-1.5
-2
-2.5

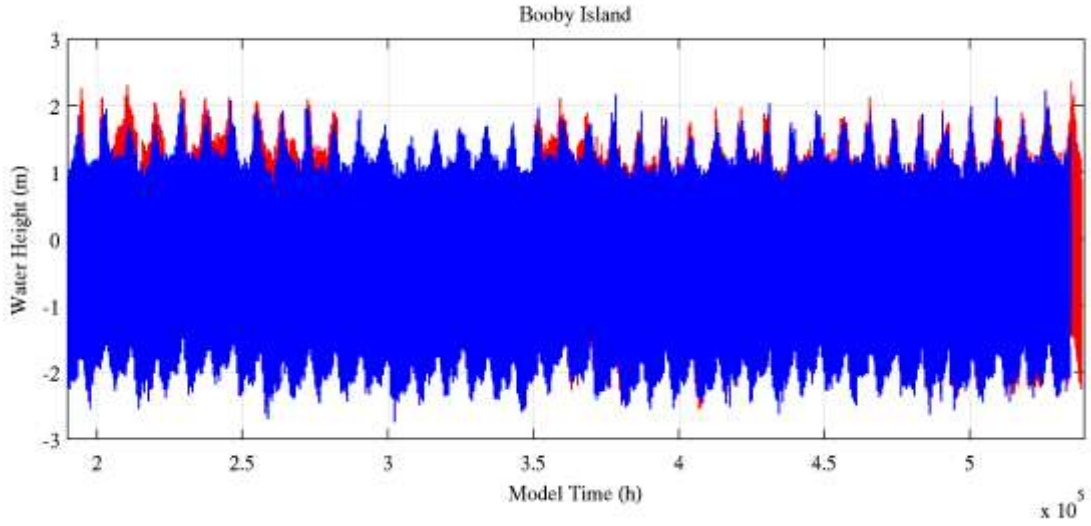
Booby Island
Water Height (m)
Model Time (h)
x 10^5

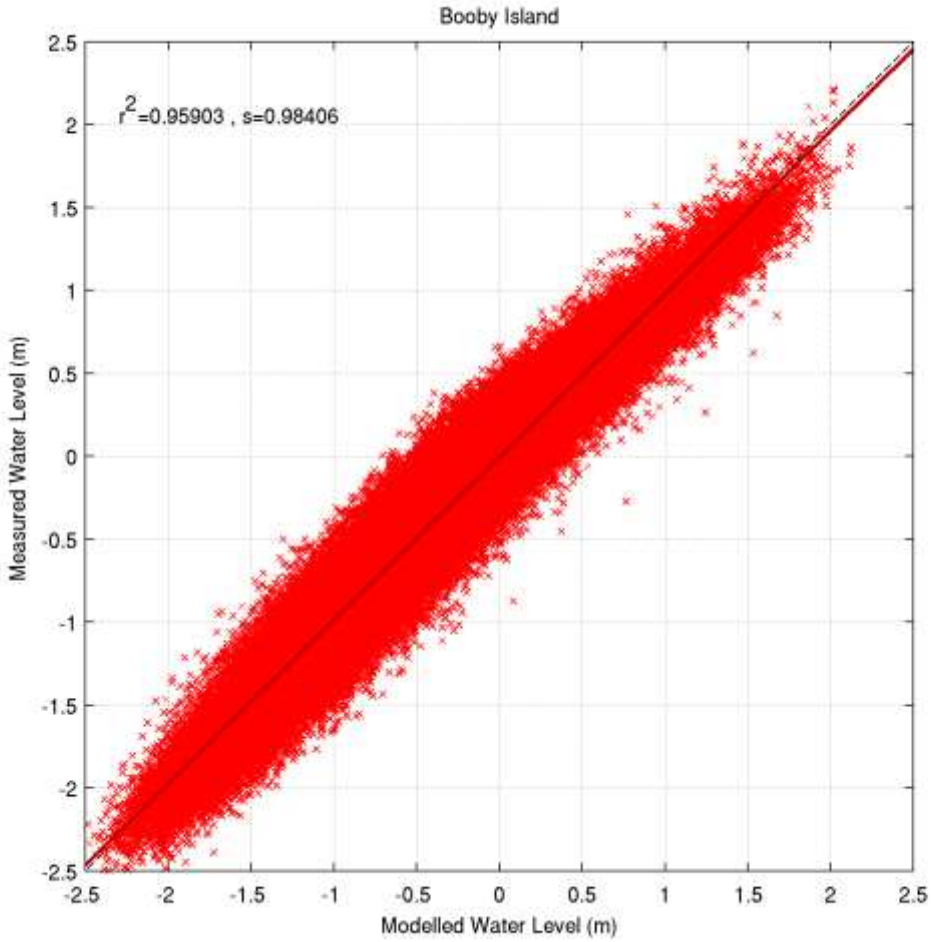
Booby Island
r^2=0.95903 , s=0.98406
Measured Water Level (m)
Modelled Water Level (m)

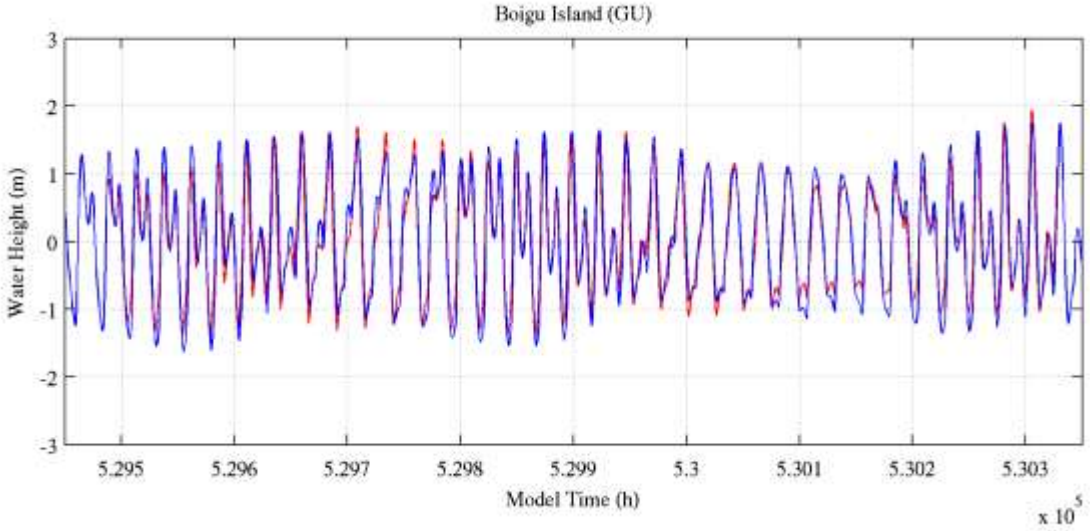
Boigu Island (GU)
Water Height (m)
Model Time (h)
x 10^5

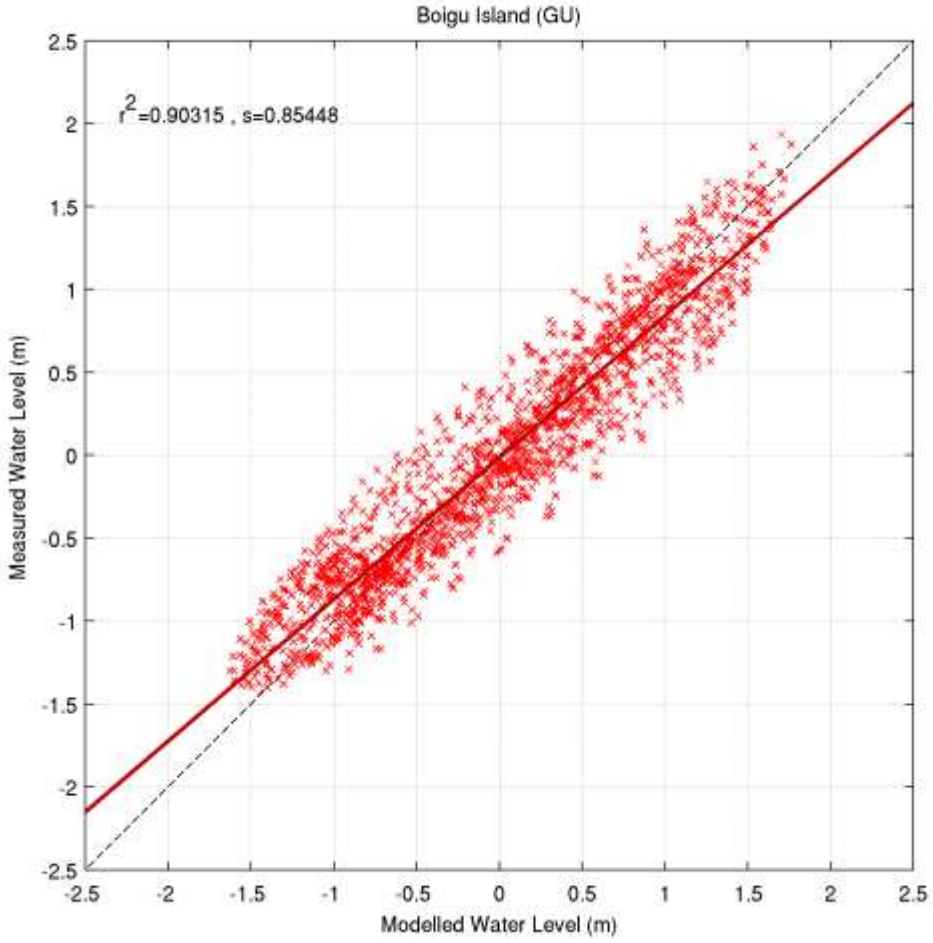
Boigu Island (GU)
r^2=0.90315 , s=0.85448
Measured Water Level (m)
Modelled Water Level (m)

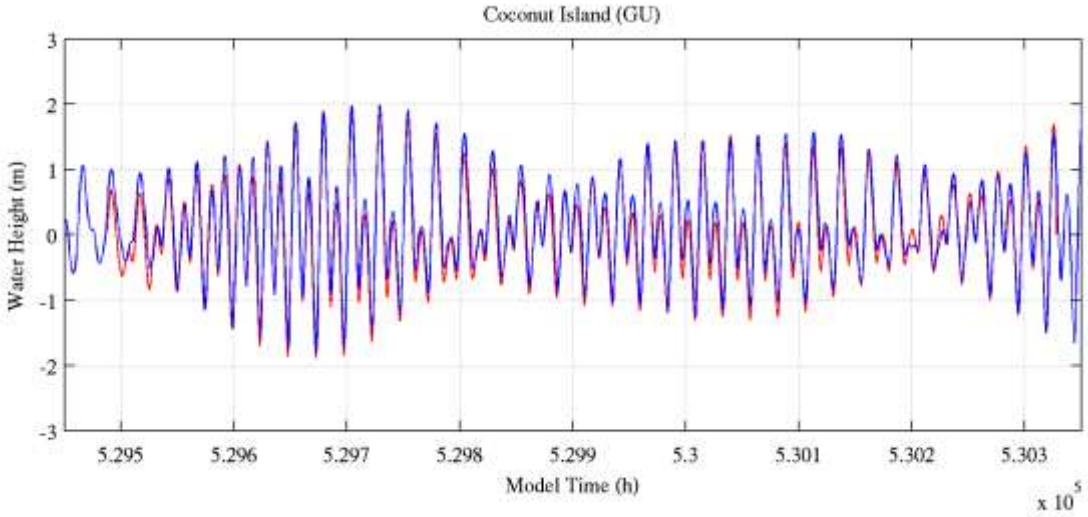
Coconut Island (GU)
Water Height (m)
Model Time (h)
x 10^5

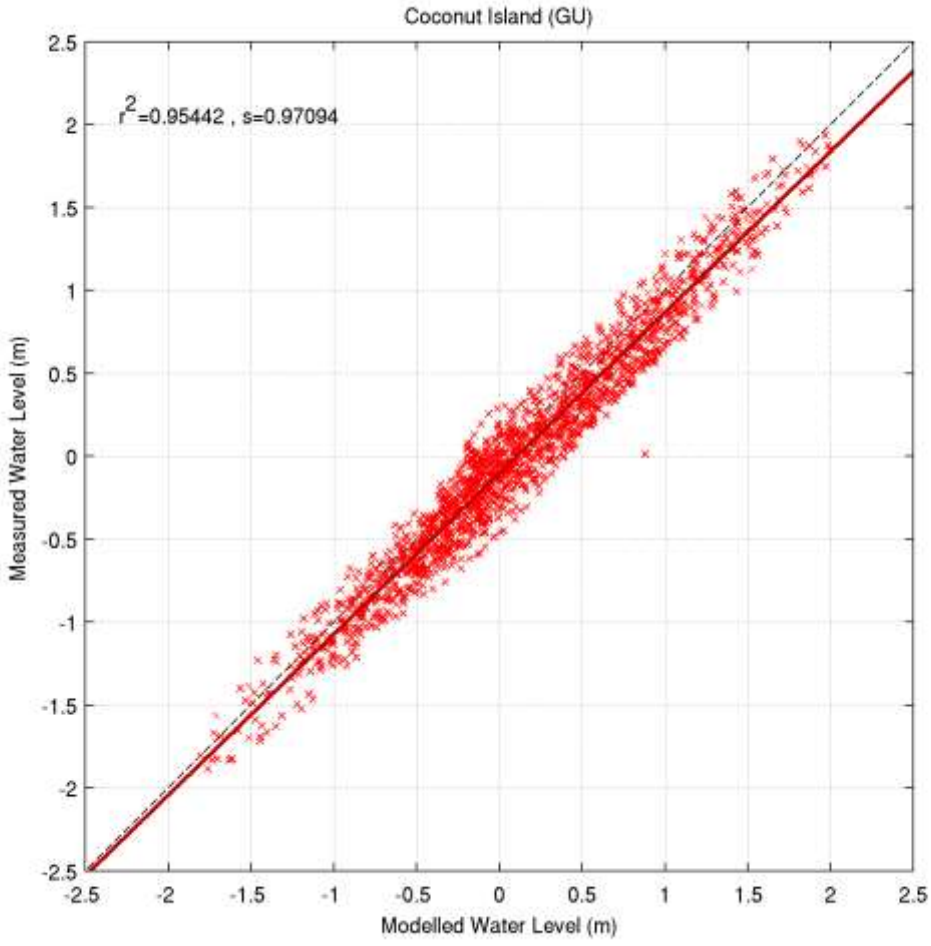
Coconut Island (GU)
r^2=0.95442 , s=0.97094
Measured Water Level (m)
Modelled Water Level (m)

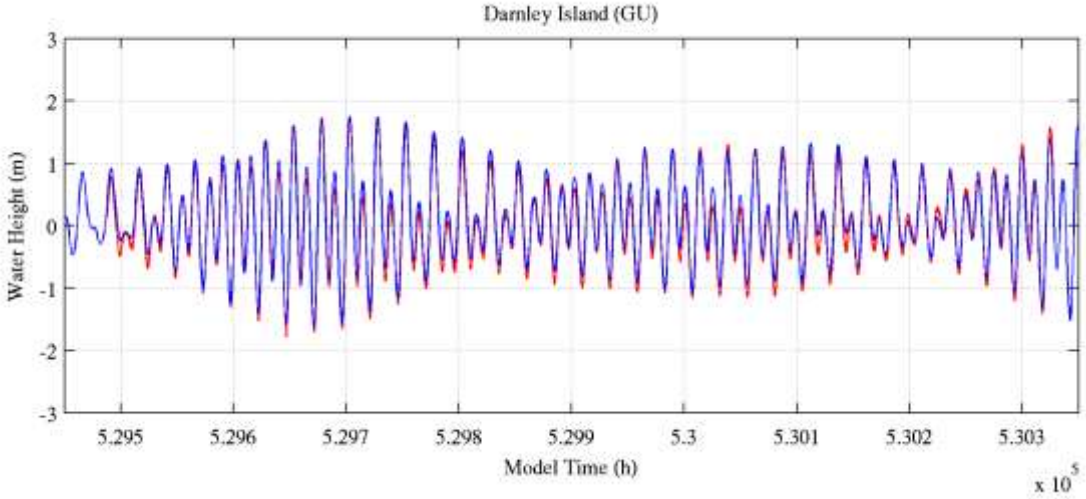
Darnley Island (GU)
Water Height (m)
3
2
1
0
-1
-2
-3
5.295
5.296
5.297
5.298
5.299
5.3
5.301
5.302
5.303
Model Time (h)
x 10^5

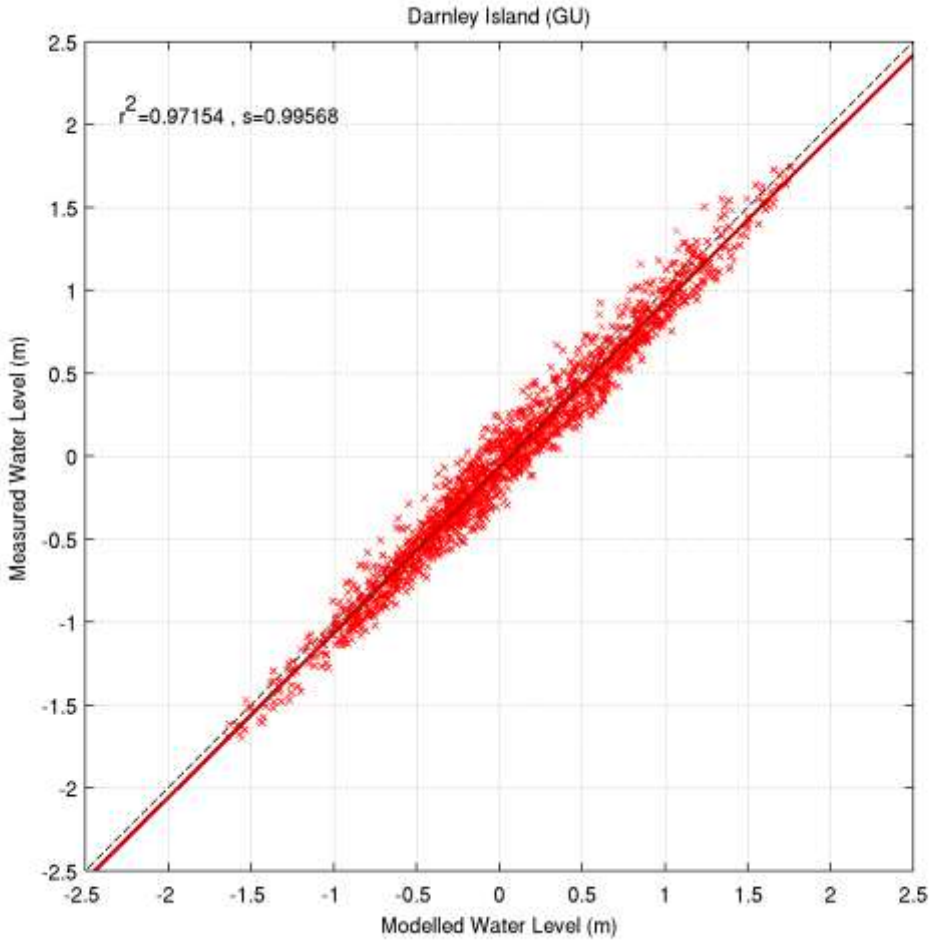
Darnley Island (GU)
r^2=0.97154 , s=0.99568
Measured Water Level (m)
Modelled Water Level (m)
2.5
2
1.5
1
0.5
0
-0.5
-1
-1.5
-2
-2.5

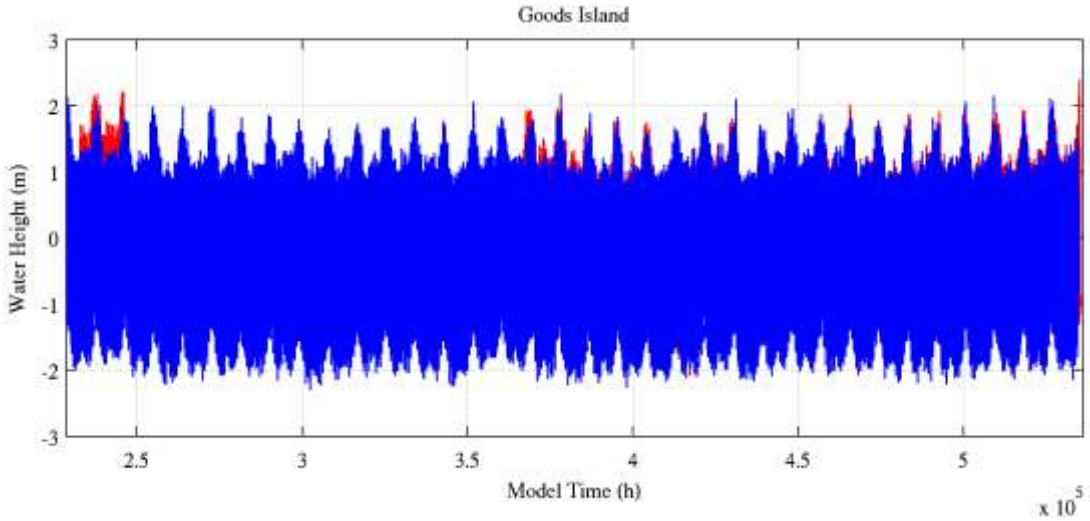
Goods Island
Water Height (m)
Model Time (h)
x 10^5

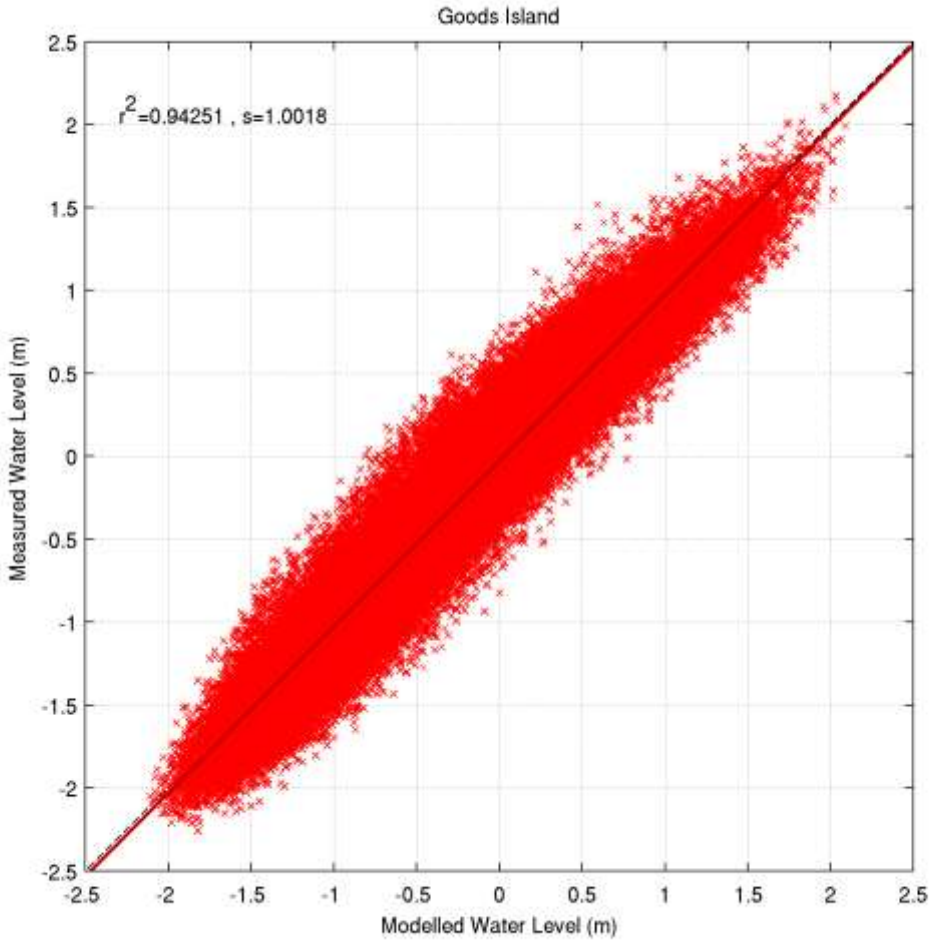
Goods Island
r^2=0.94251 , s=1.0018
Measured Water Level (m)
Modelled Water Level (m)

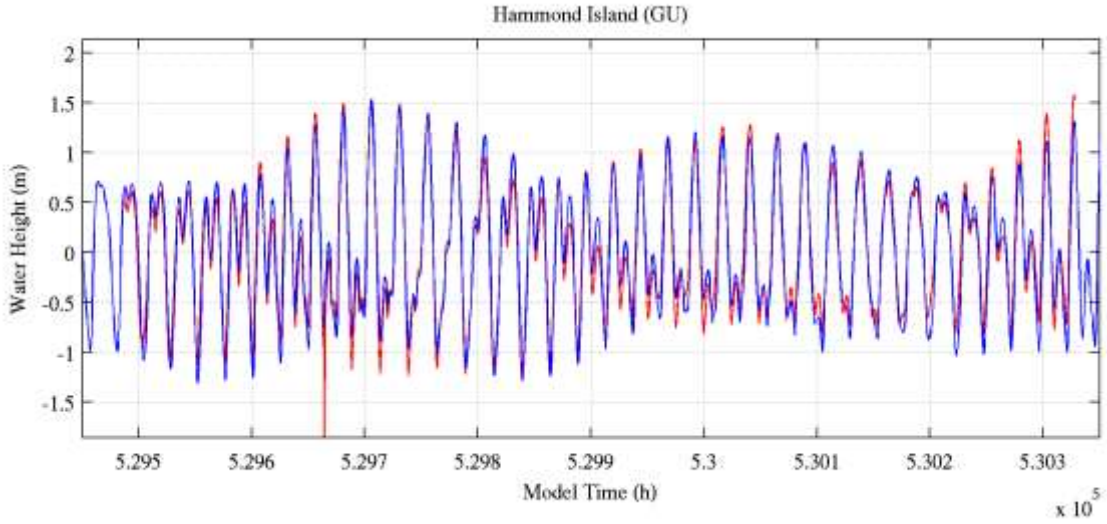
Hammond Island (GU)
Water Height (m)
2
1.5
1
0.5
0
-0.5
-1
-1.5
5.295
5.296
5.297
5.298
5.299
5.3
5.301
5.302
5.303
Model Time (h)
x 10^5

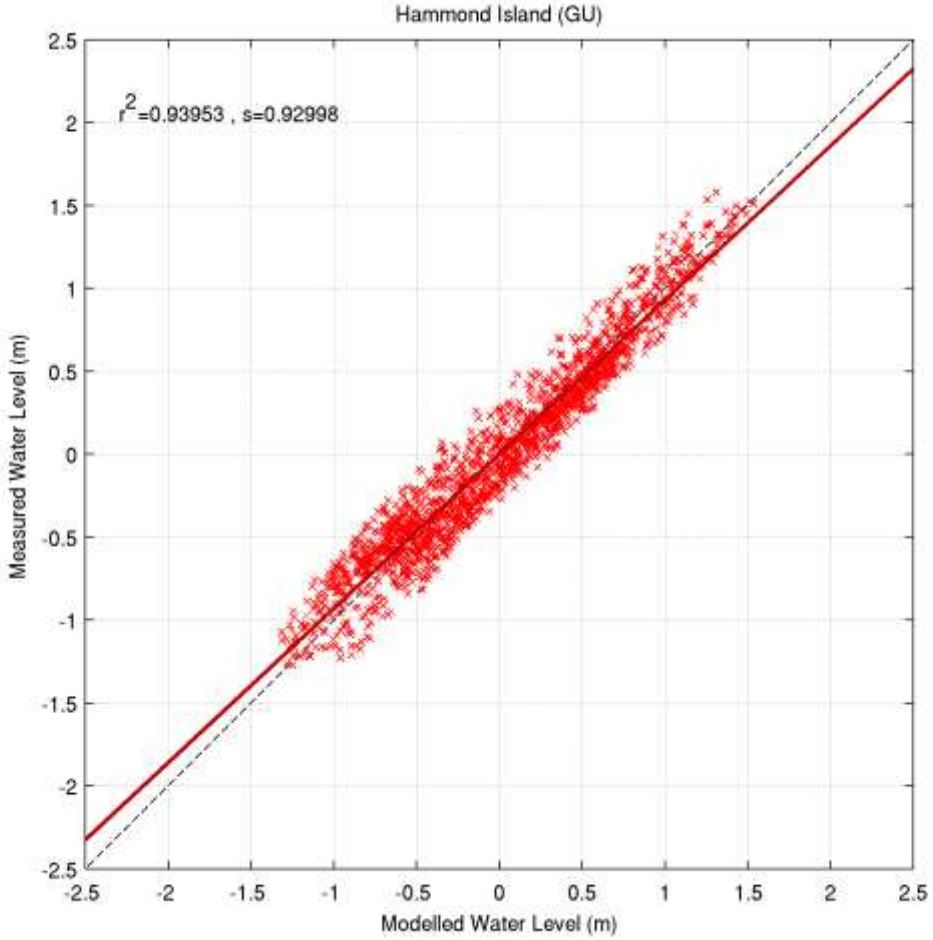
Hammond Island (GU)
r^2=0.93953 , s=0.92998
Measured Water Level (m)
Modelled Water Level (m)
2.5
2
1.5
1
0.5
0
-0.5
-1
-1.5
-2
-2.5

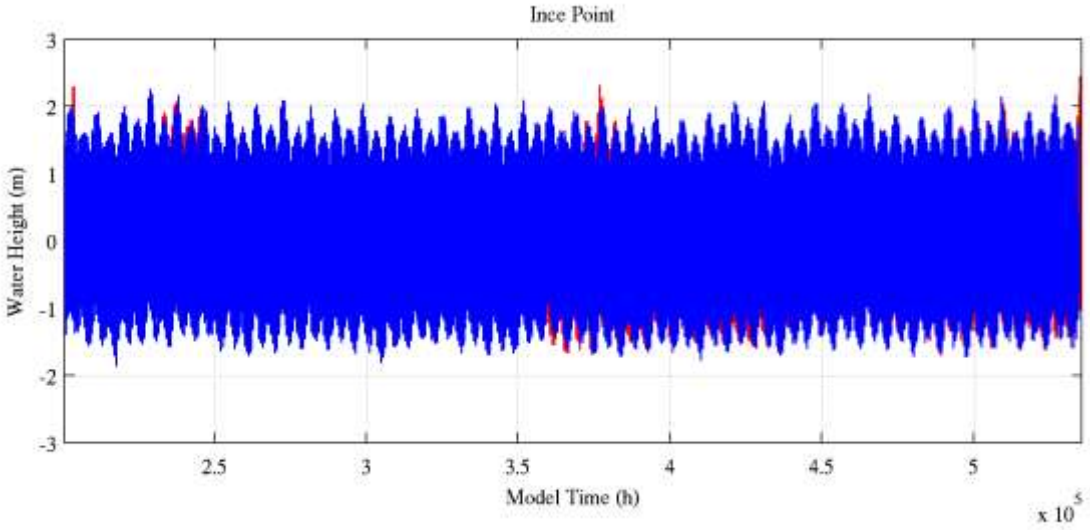
Ince Point
Water Height (m)
Model Time (h)
x 10^5

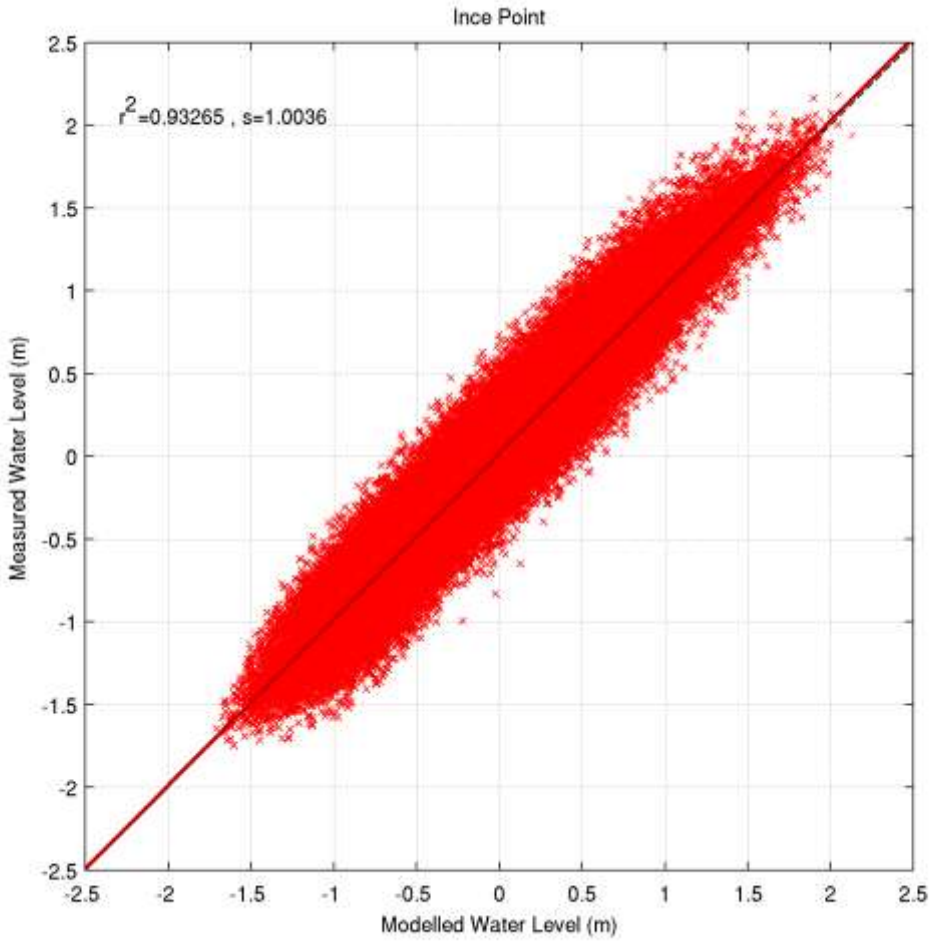
Ince Point
r^2=0.93265 , s=1.0036
Measured Water Level (m)
Modelled Water Level (m)

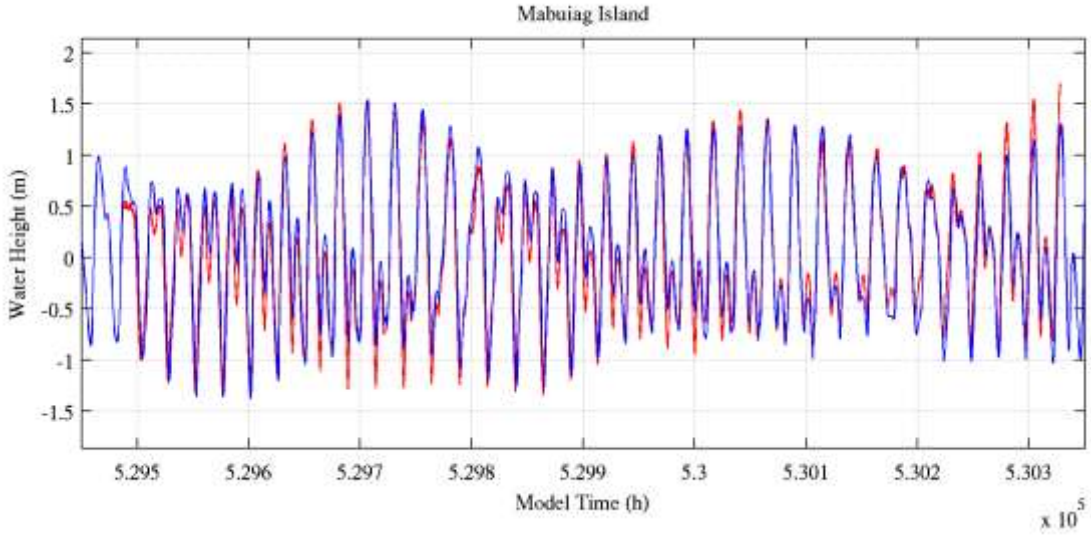
Mabuiag Island
Water Height (m)
2
1.5
1
0.5
0
-0.5
-1
-1.5
5.295
5.296
5.297
5.298
5.299
5.3
5.301
5.302
5.303
Model Time (h)
x 10^5

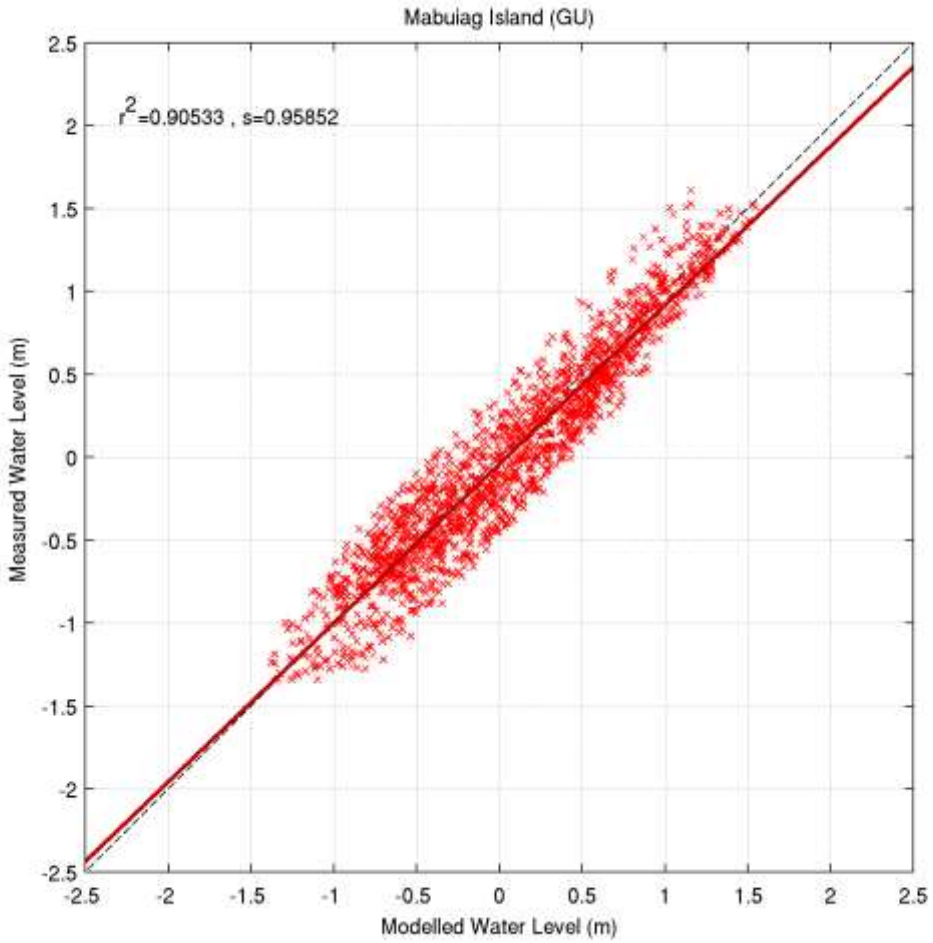
Mabuiag Island (GU)
r^2=0.90533 , s=0.95852
Measured Water Level (m)
Modelled Water Level (m)
2.5
2
1.5
1
0.5
0
-0.5
-1
-1.5
-2
-2.5

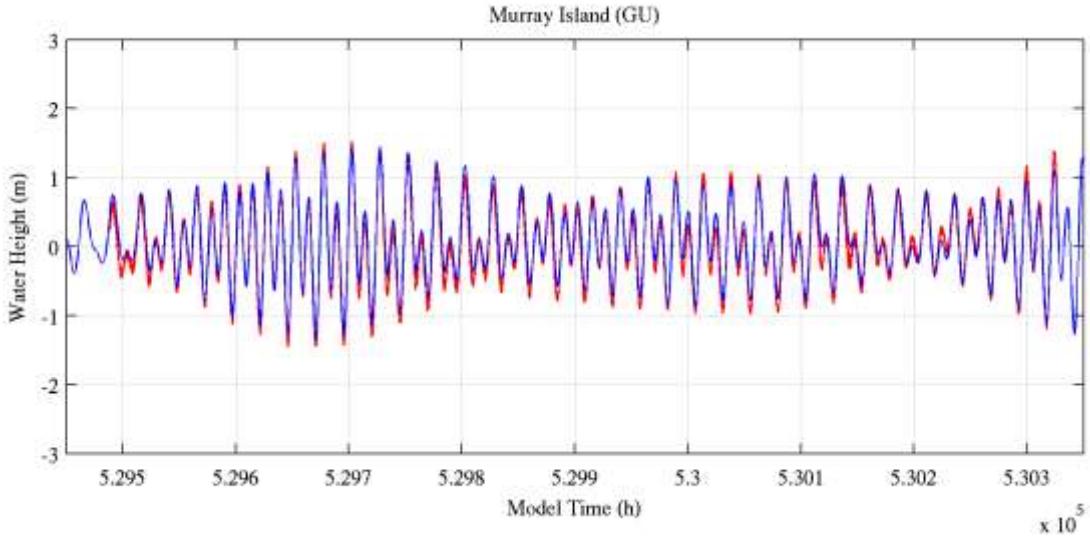
Murray Island (GU)
Water Height (m)
Model Time (h)
x 10^5

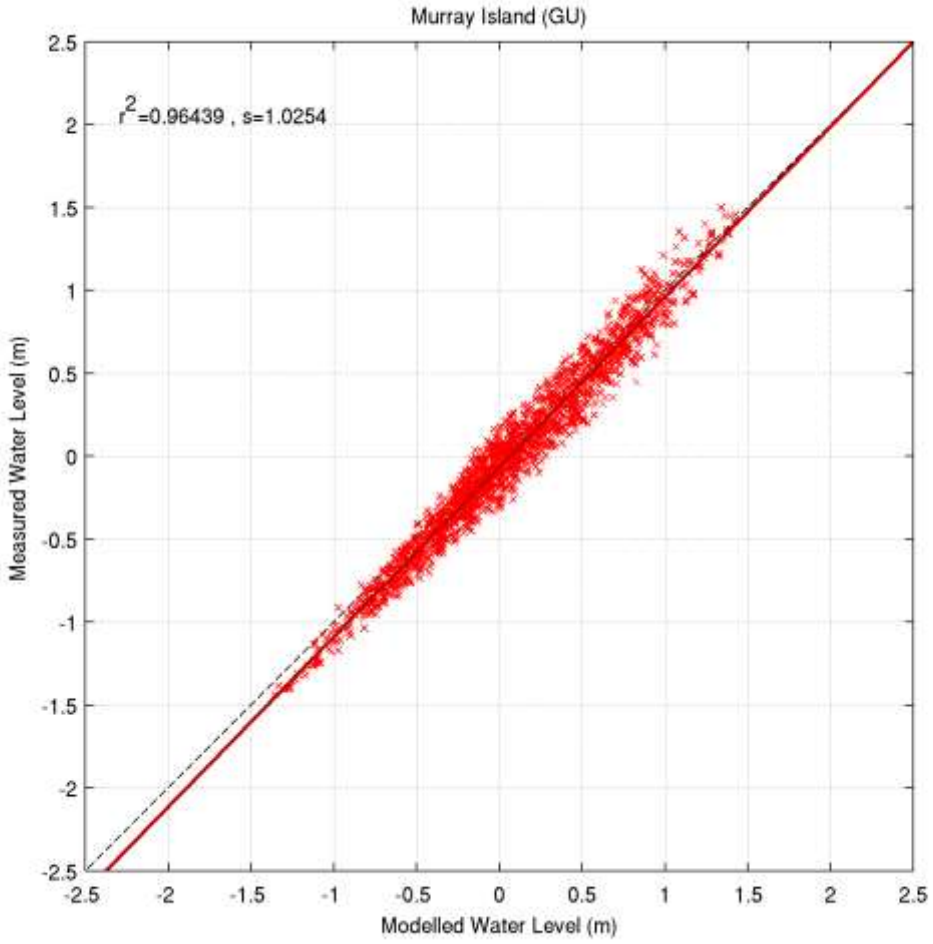
Murray Island (GU)
r^2=0.96439 , s=1.0254
Measured Water Level (m)
Modelled Water Level (m)

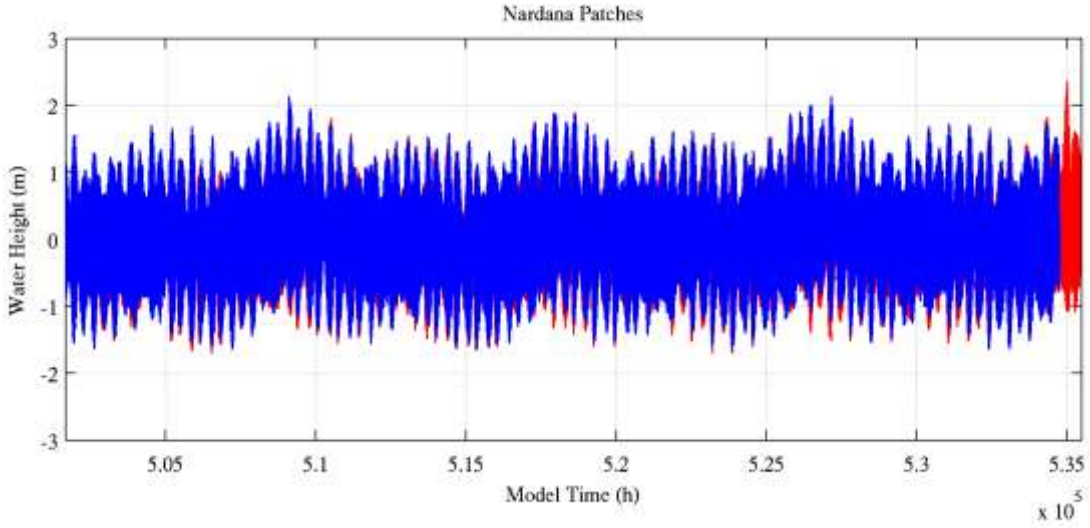
Nardana Patches
Water Height (m)
Model Time (h)
x 10^5
3
2
1
0
-1
-2
-3
5.05
5.1
5.15
5.2
5.25
5.3
5.35

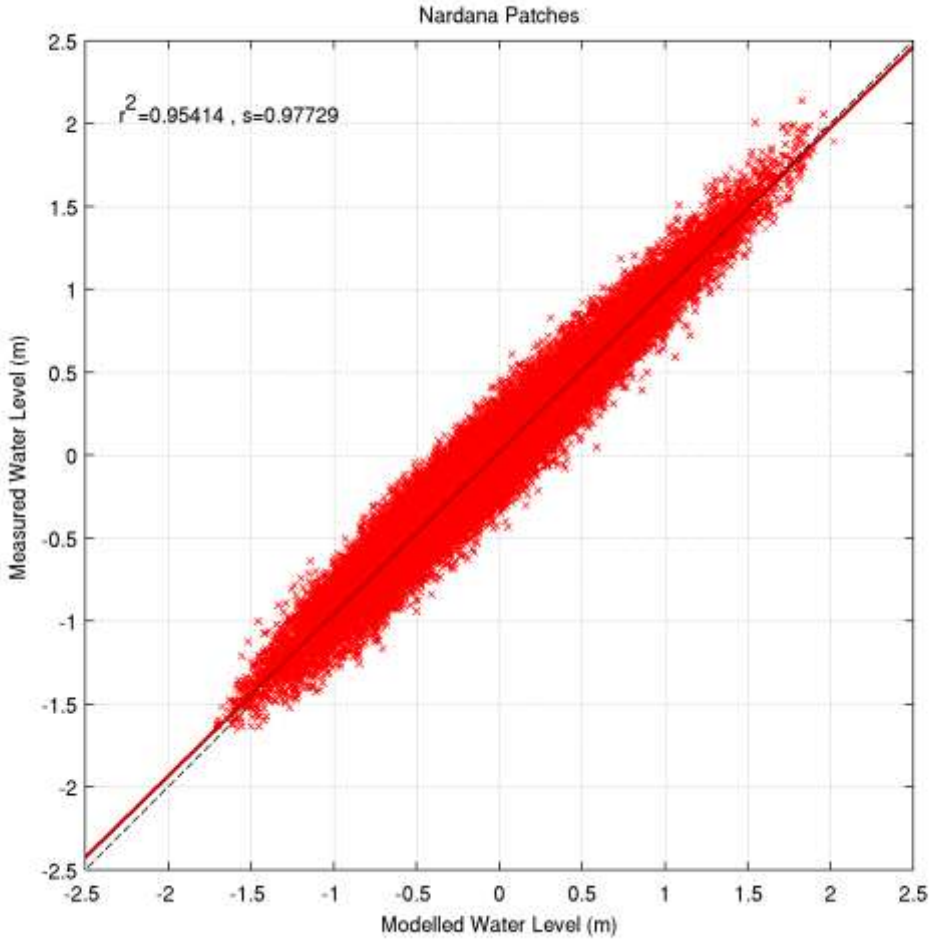
Nardana Patches
r^2=0.95414 , s=0.97729
Measured Water Level (m)
Modelled Water Level (m)
2.5
2
1.5
1
0.5
0
-0.5
-1
-1.5
-2
-2.5

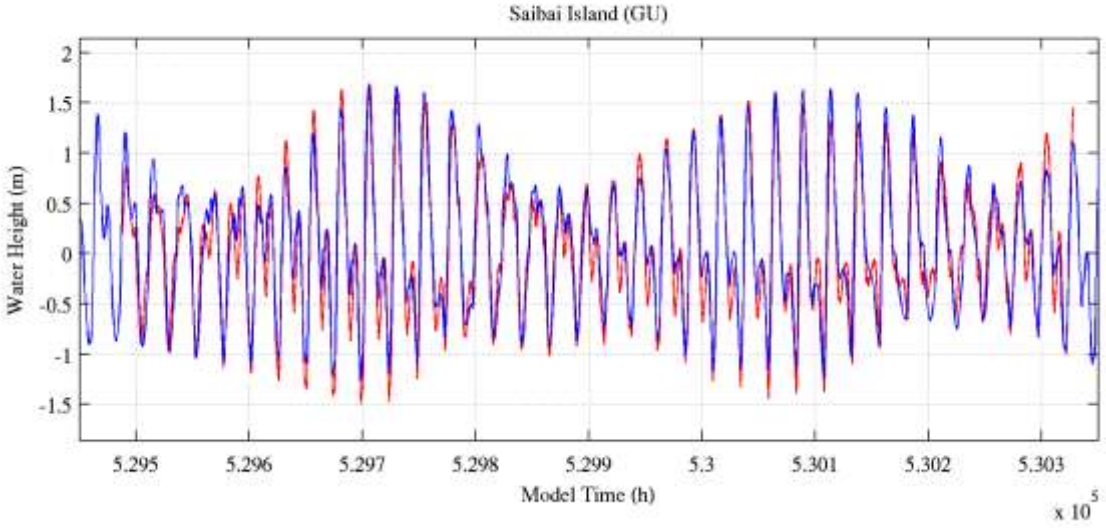
Saibai Island (GU)
Water Height (m)
Model Time (h)
x 10^5

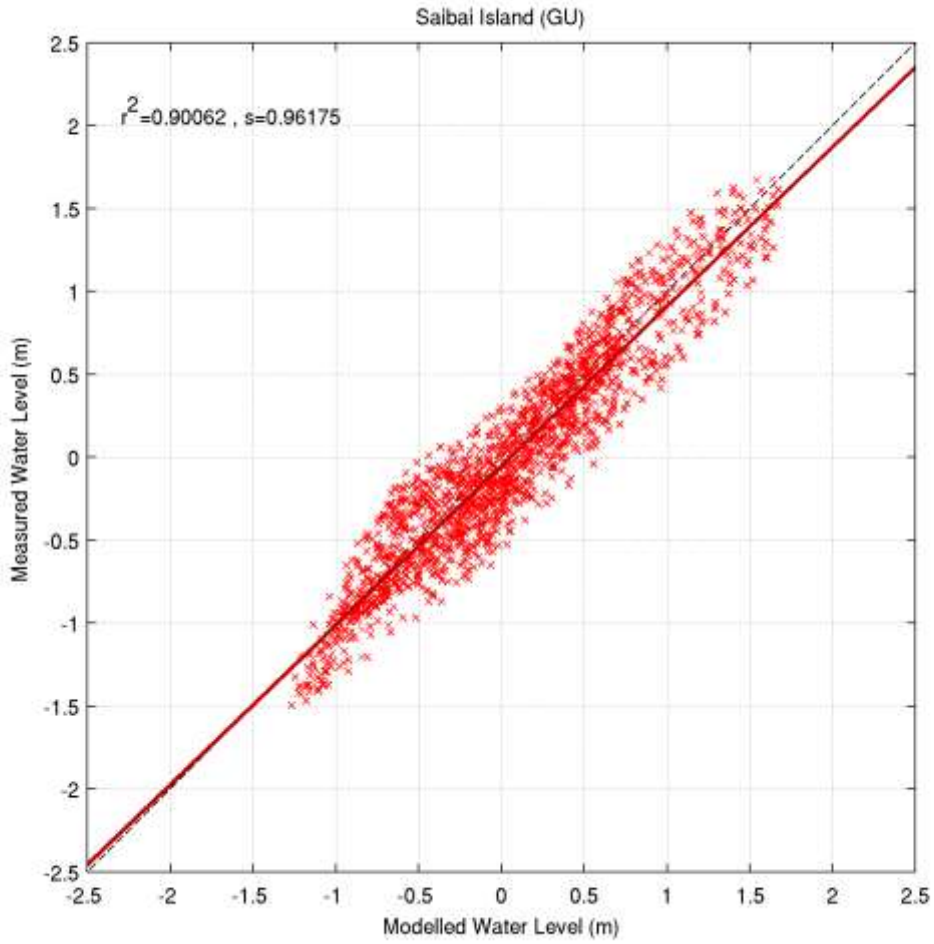
Saibai Island (GU)
r^2=0.90062 , s=0.96175
Measured Water Level (m)
Modelled Water Level (m)

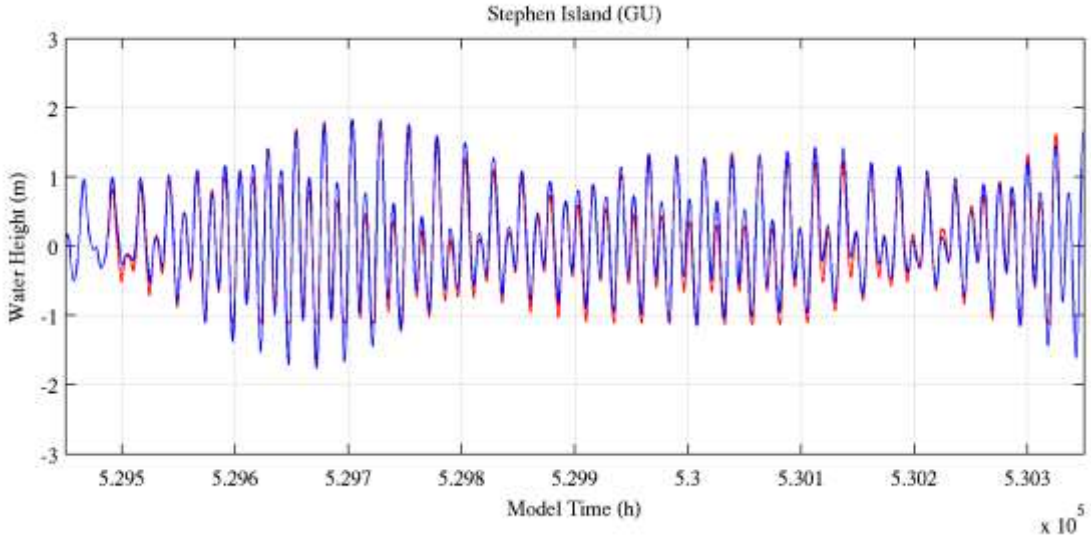
Stephen Island (GU)
Water Height (m)
Model Time (h)
x 10^5
3
2
1
0
-1
-2
-3
5.295
5.296
5.297
5.298
5.299
5.3
5.301
5.302
5.303

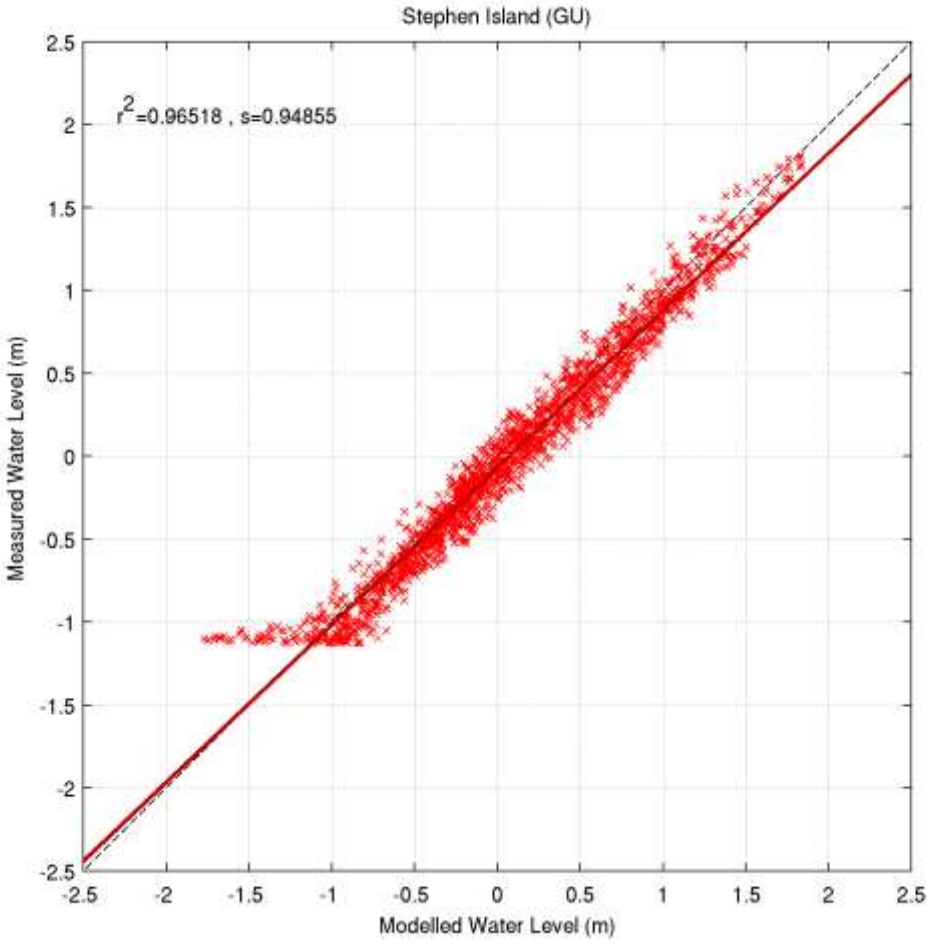
Stephen Island (GU)
r^2=0.96518 , s=0.94855
Measured Water Level (m)
Modelled Water Level (m)
2.5
2
1.5
1
0.5
0
-0.5
-1
-1.5
-2
-2.5

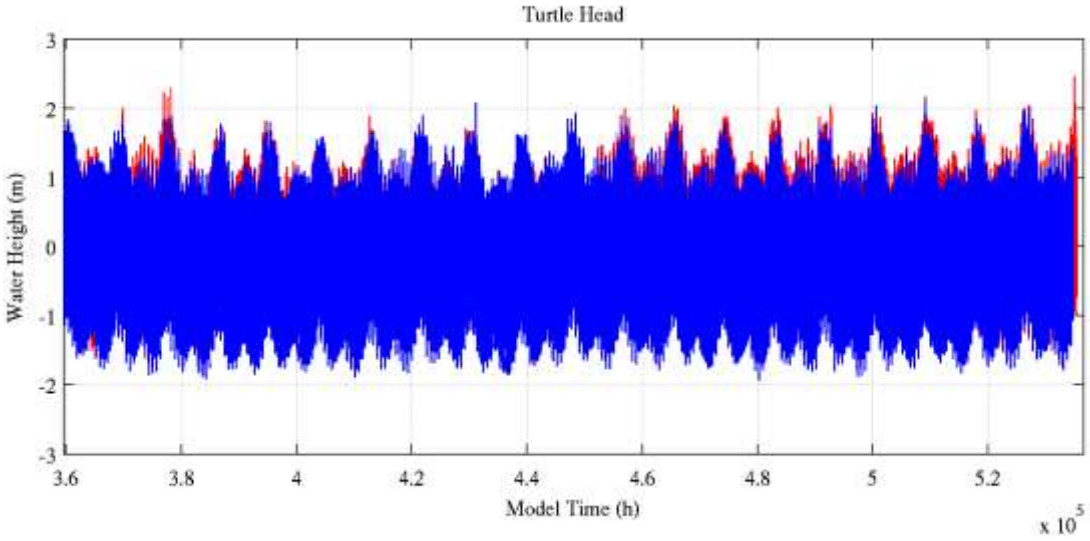
Turtle Head
Water Height (m)
Model Time (h)
x 10^5

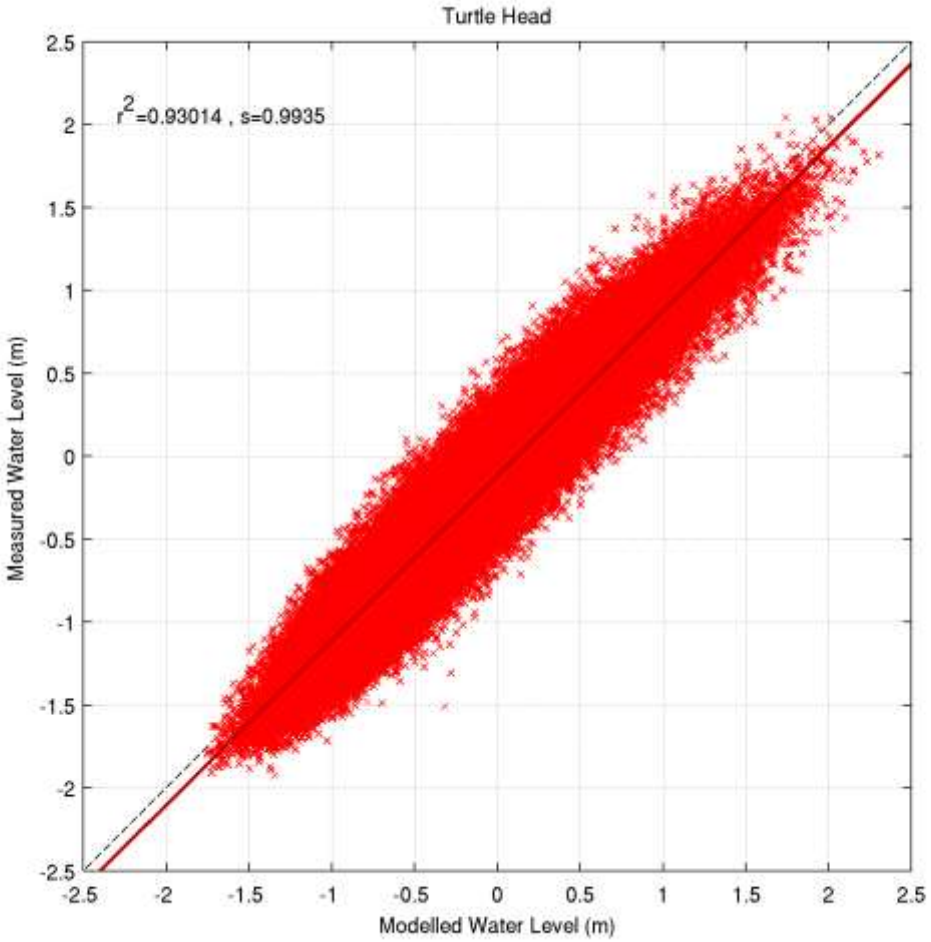
Turtle Head
r^2=0.93014 , s=0.9935
Measured Water Level (m)
Modelled Water Level (m)

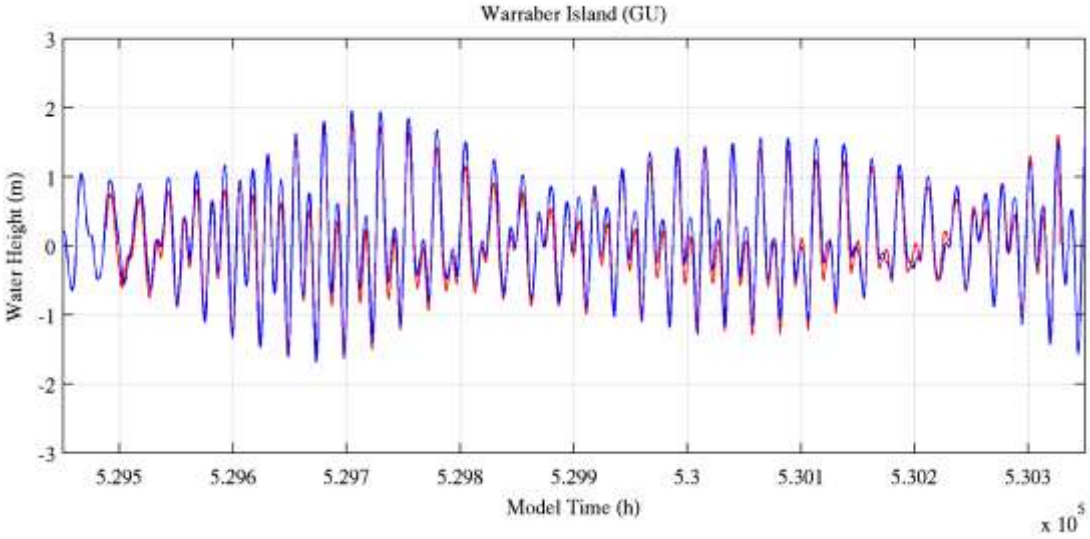
Warraber Island (GU)
Water Height (m)
Model Time (h)
x 10^5
3
2
1
0
-1
-2
-3
5.295
5.296
5.297
5.298
5.299
5.3
5.301
5.302
5.303

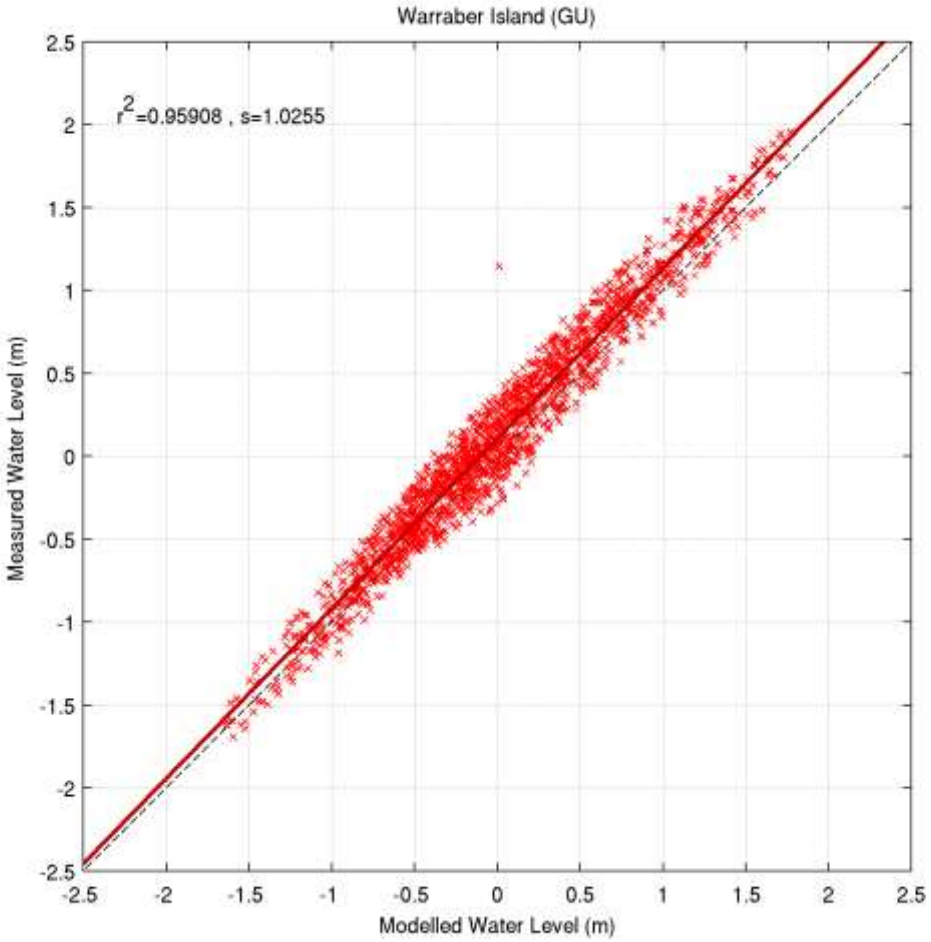
Warraber Island (GU)
r^2=0.95908 , s=1.0255
Measured Water Level (m)
Modelled Water Level (m)
2.5
2
1.5
1
0.5
0
-0.5
-1
-1.5
-2
-2.5

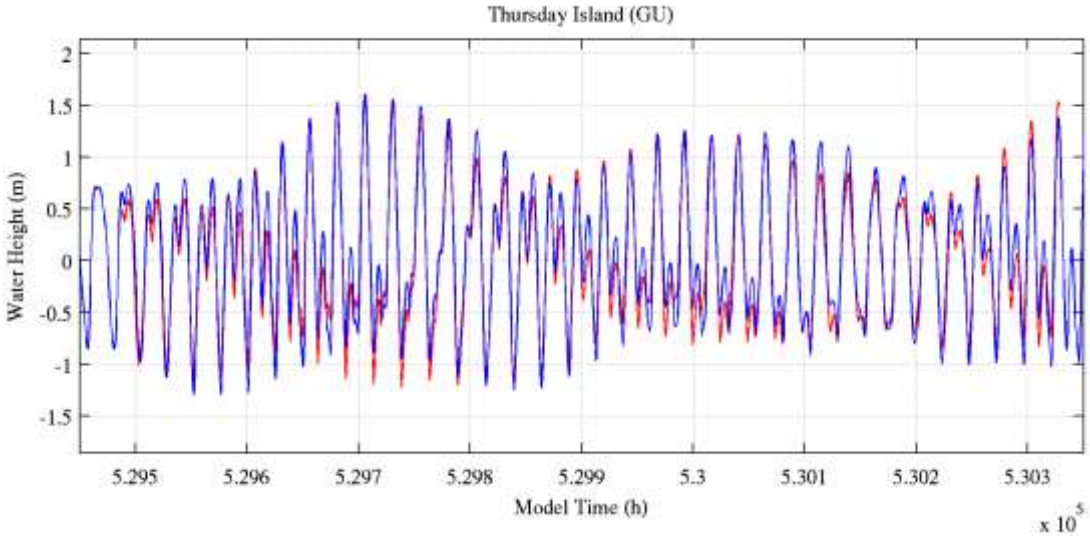
Thursday Island (GU)
Water Height (m)
Model Time (h)
x 10^5

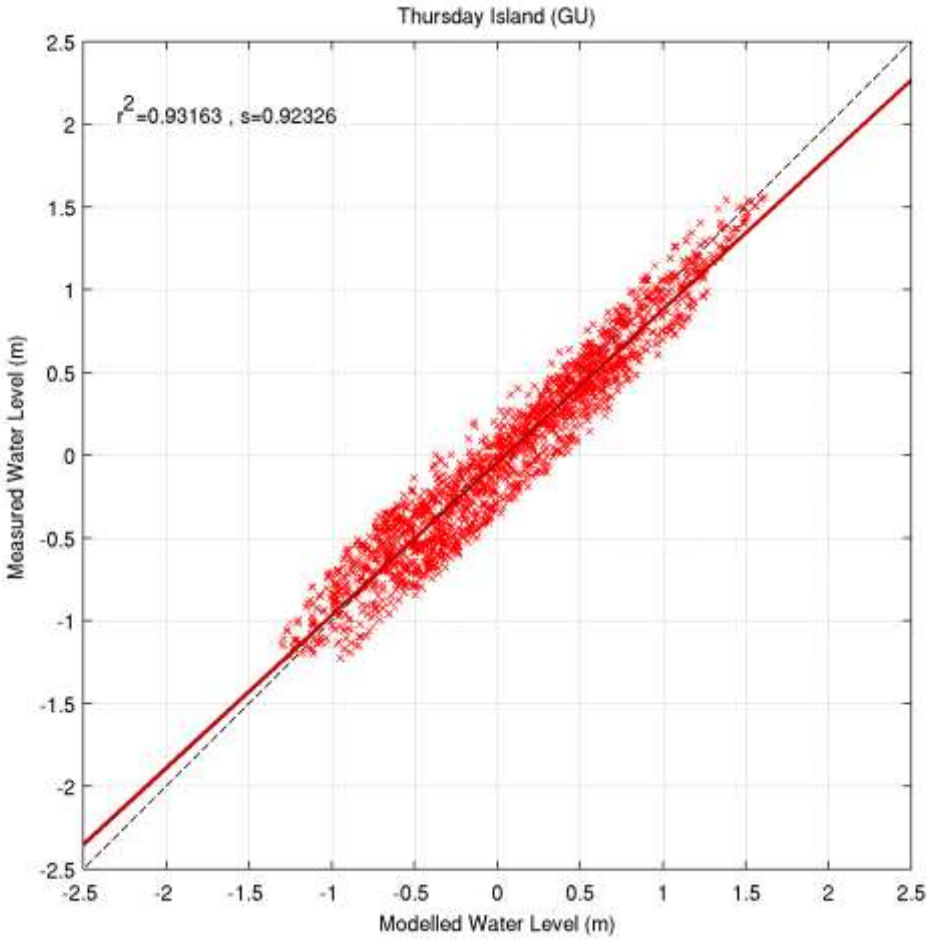
Thursday Island (GU)
r^2=0.93163 , s=0.92326
Measured Water Level (m)
Modelled Water Level (m)

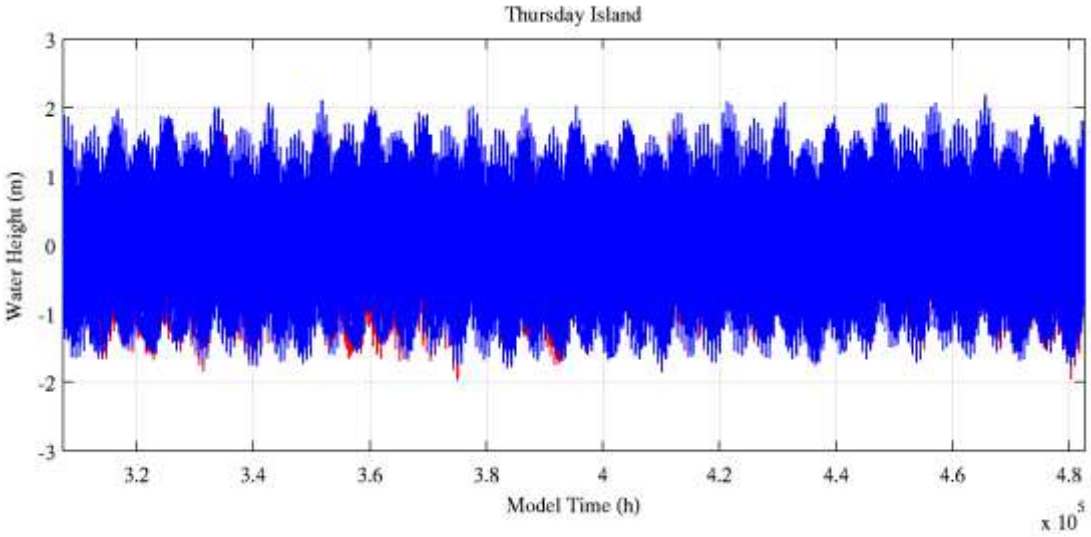
Thursday Island
Water Height (m)
Model Time (h)
x 10^5

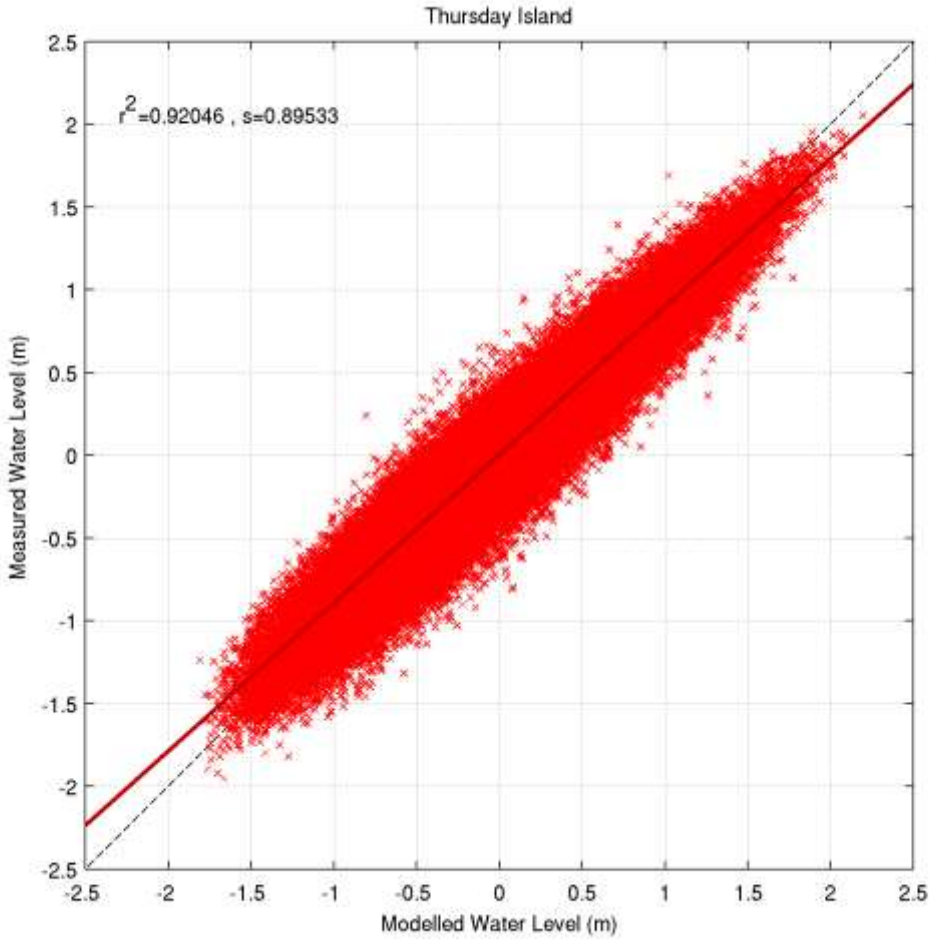
Thursday Island
r^2=0.92046 , s=0.89533
Measured Water Level (m)
Modelled Water Level (m)

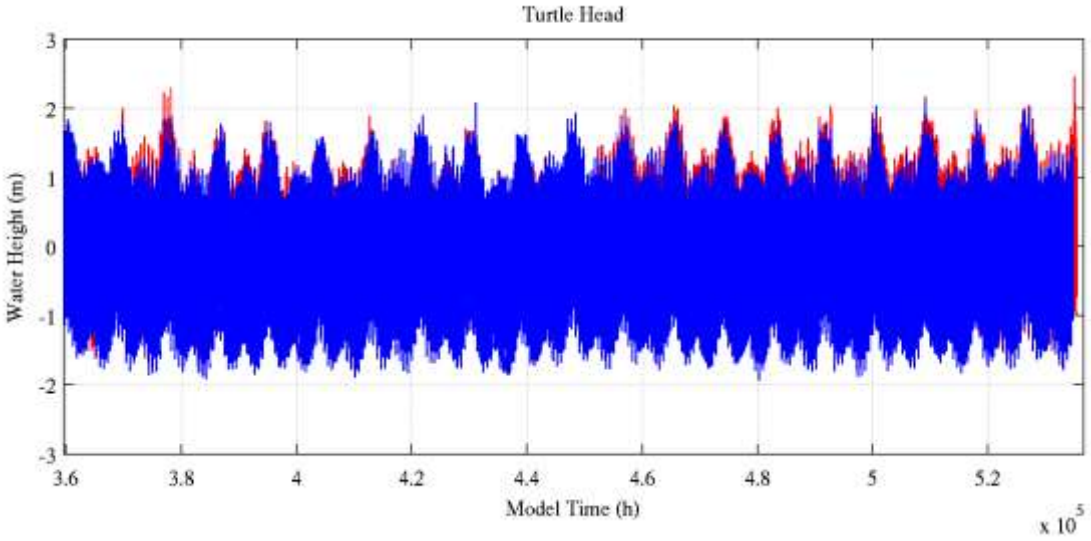
Turtle Head
Water Height (m)
Model Time (h)
x 10^5

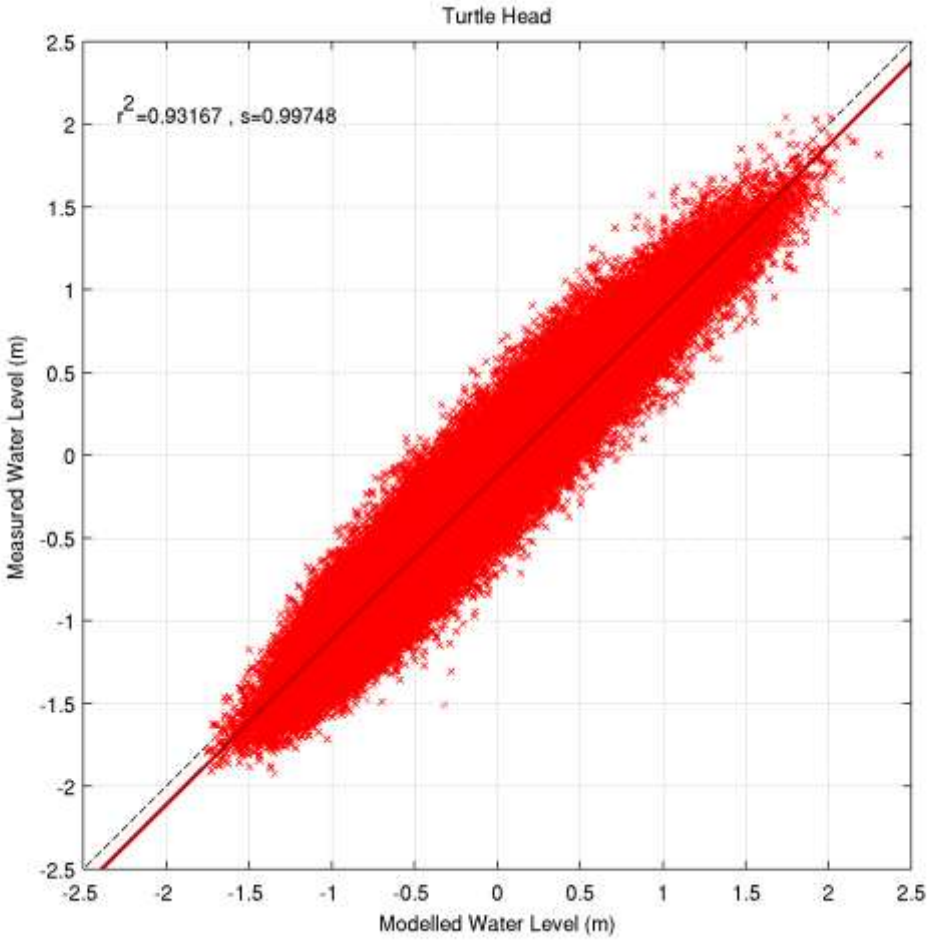
Turtle Head
r^2=0.93167 , s=0.99748
Measured Water Level (m)
Modelled Water Level (m)

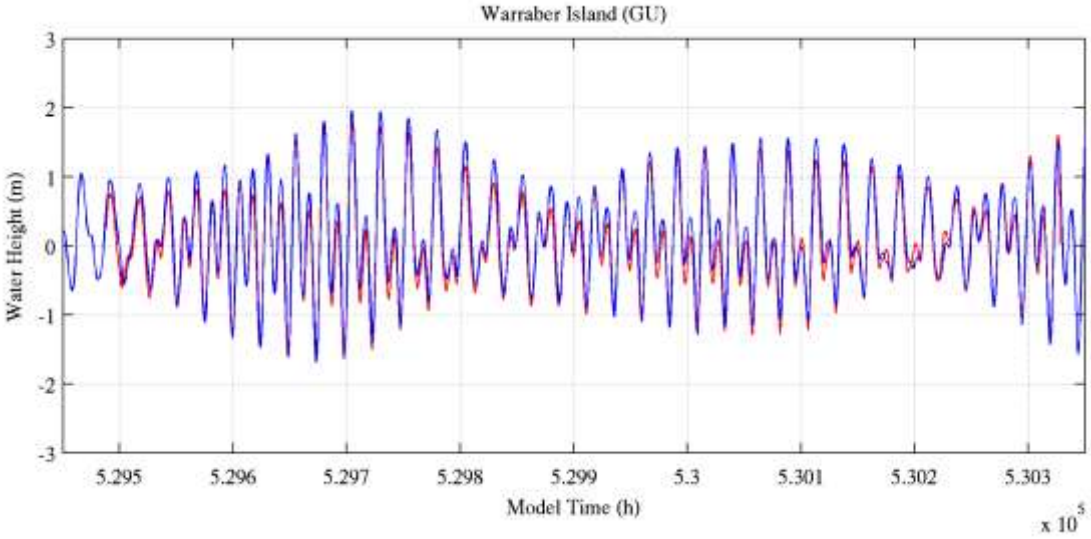
Warraber Island (GU)
Water Height (m)
Model Time (h)
x 10^5
3
2
1
0
-1
-2
-3
5.295
5.296
5.297
5.298
5.299
5.3
5.301
5.302
5.303

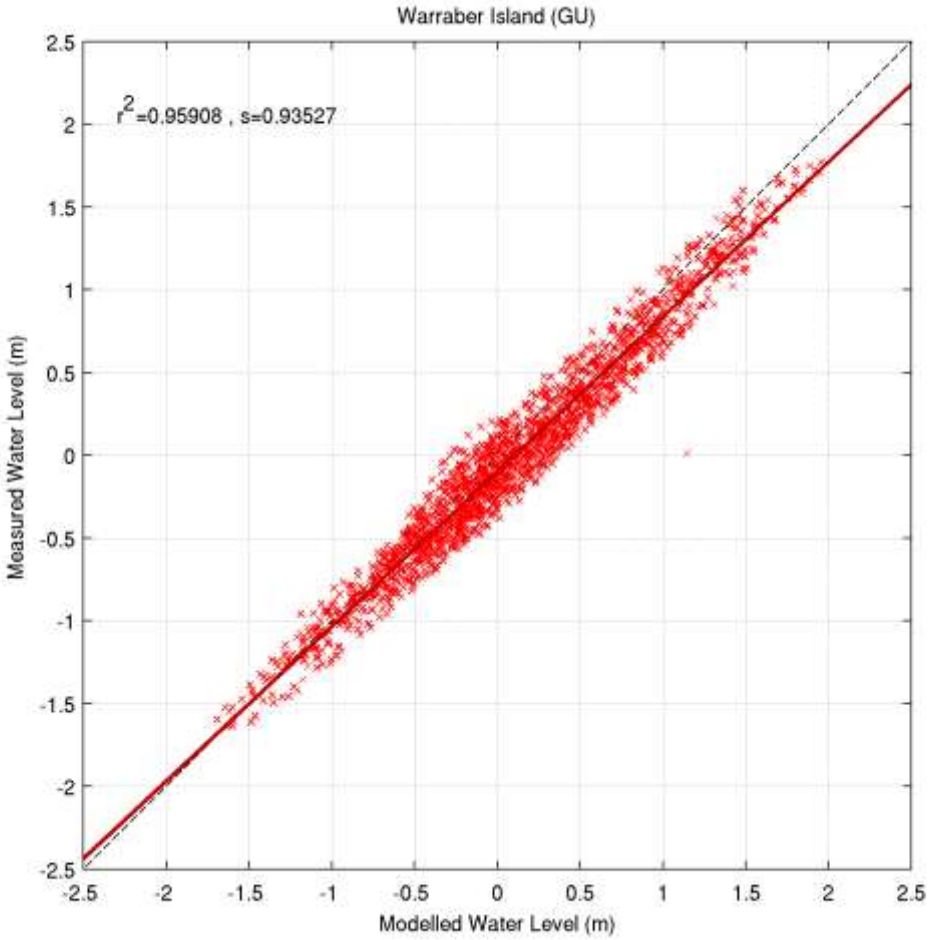
Warraber Island (GU)
r^2=0.95908 , s=0.93527
Measured Water Level (m)
Modelled Water Level (m)
2.5
2
1.5
1
0.5
0
-0.5
-1
-1.5
-2
-2.5

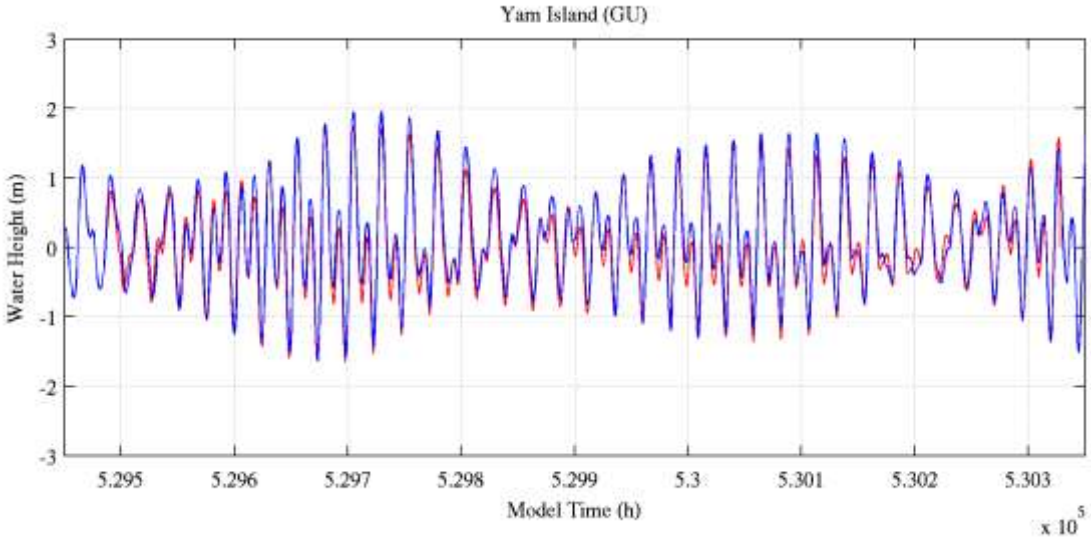
Yam Island (GU)
Water Height (m)
3
2
1
0
-1
-2
-3
5.295
5.296
5.297
5.298
5.299
5.3
5.301
5.302
5.303
Model Time (h)
x 10^5

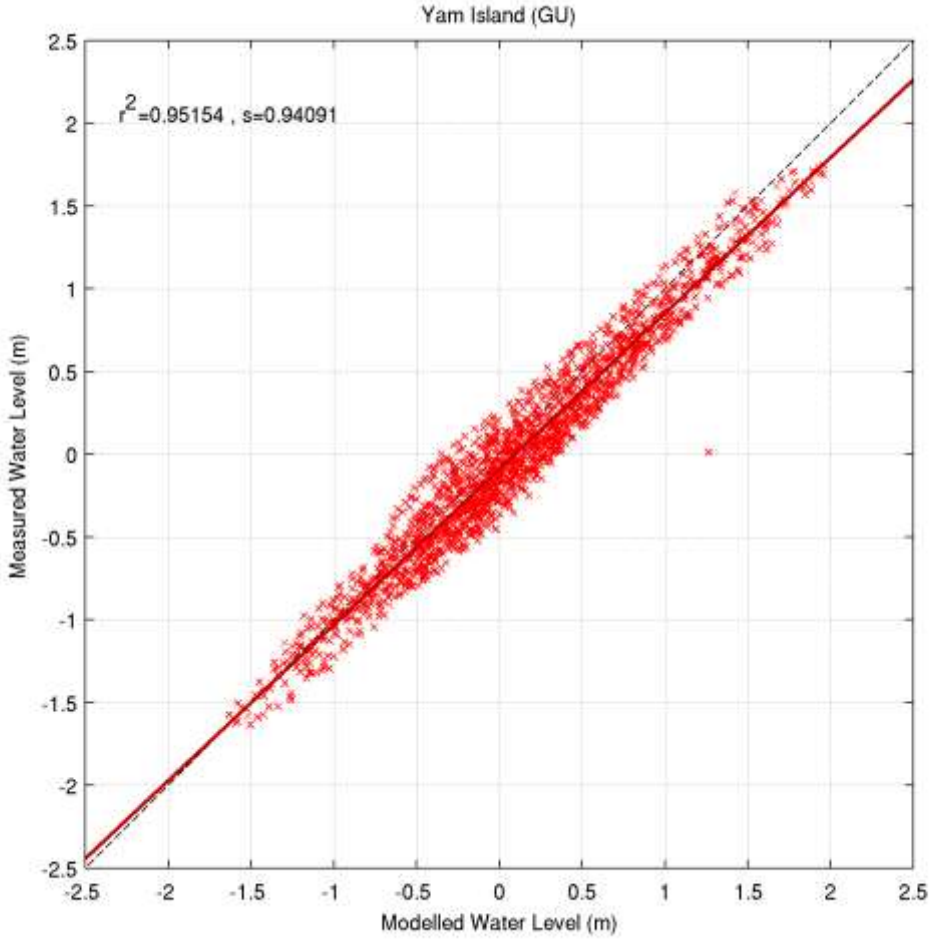
Yam Island (GU)
r^2=0.95154 , s=0.94091
Measured Water Level (m)
Modelled Water Level (m)
2.5
2
1.5
1
0.5
0
-0.5
-1
-1.5
-2
-2.5

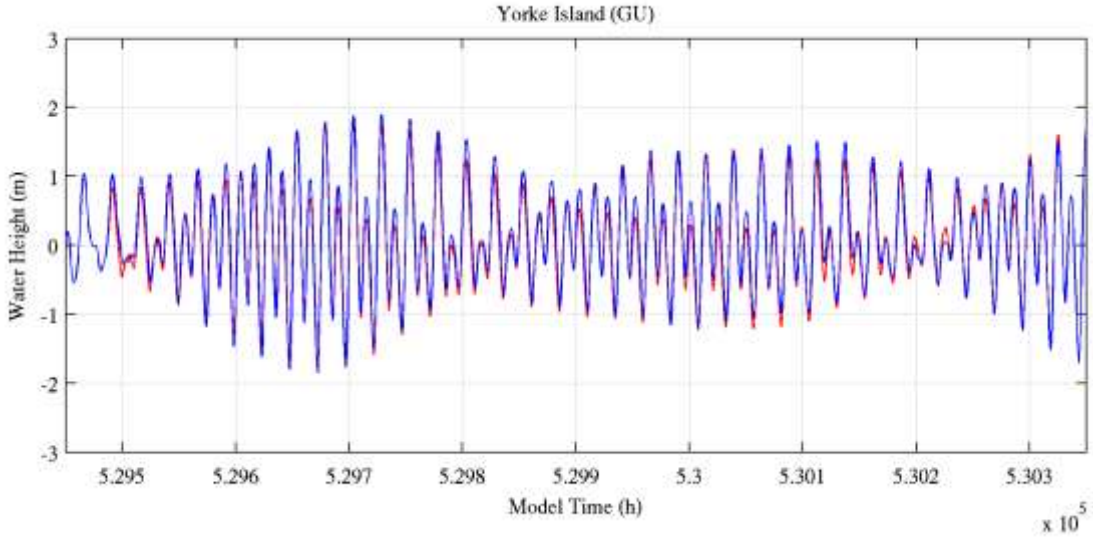
Yorke Island (GU)
Water Height (m)
Model Time (h)
x 10^5
3
2
1
0
-1
-2
-3
5.295
5.296
5.297
5.298
5.299
5.3
5.301
5.302
5.303

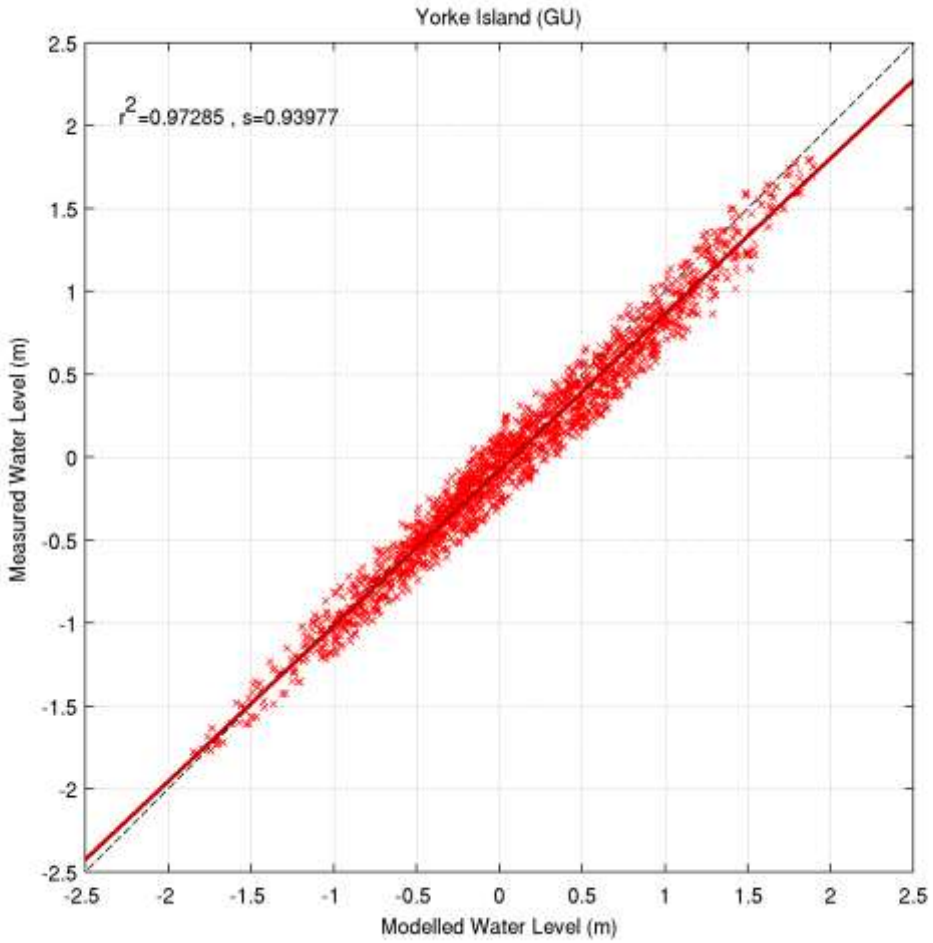
Yorke Island (GU)
r^2=0.97285 , s=0.93977
Measured Water Level (m)
Modelled Water Level (m)
2.5
2
1.5
1
0.5
0
-0.5
-1
-1.5
-2
-2.5

Appendix G

Review of Regional Tropical Cyclone Intensity in North-Eastern Australia

by J.J. Callaghan

1. Tropical cyclone *Dominic* 1982

The enhanced infrared satellite images in Figure 1.1 cover a nine hour period when TC Dominic may have intensified from an Australian category 3 cyclone to a category 5 cyclone if the Dvorak T numbers are used to determine the current ntensity.

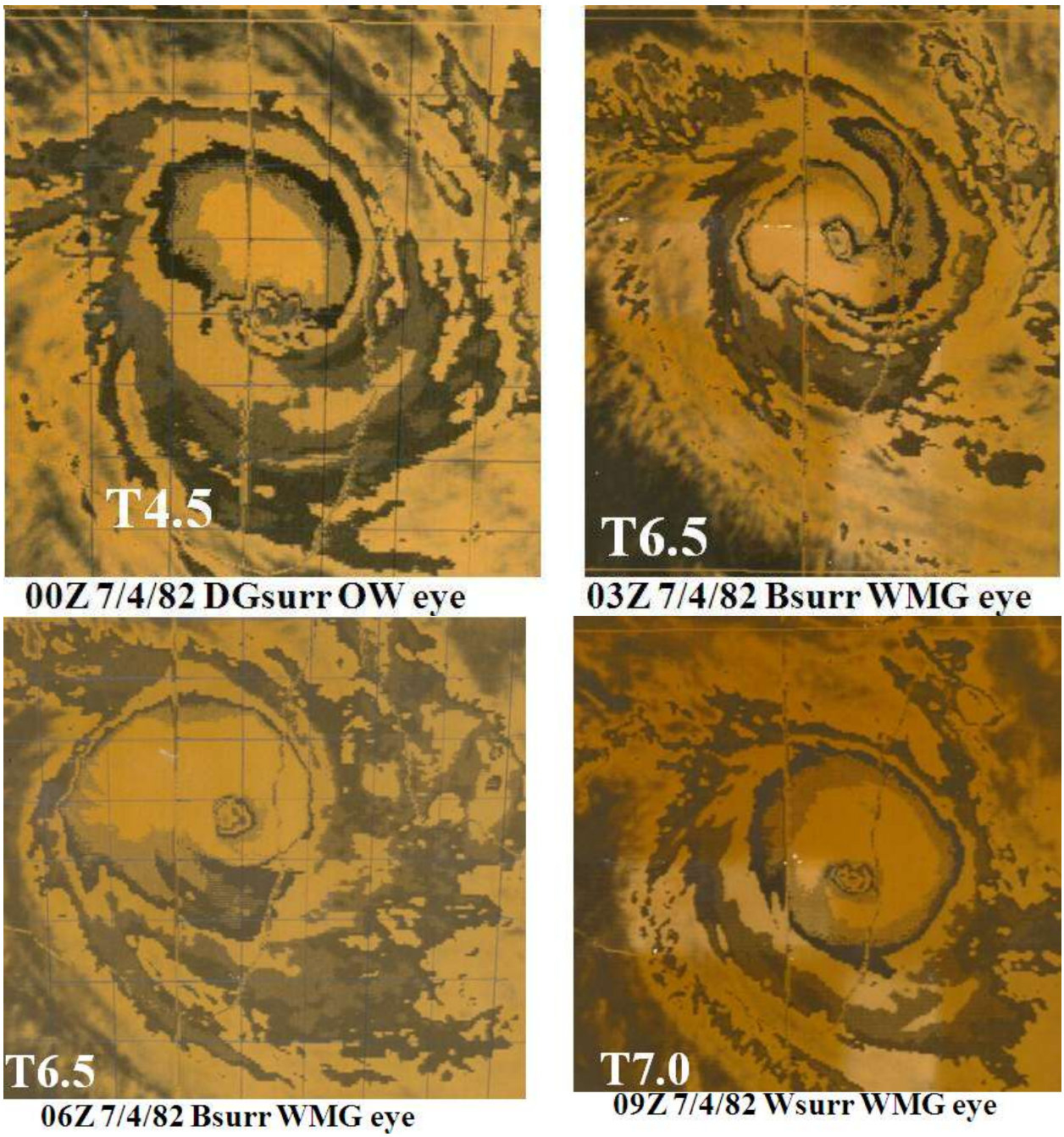

Figure 1.1 In this enhancement used in Australia at the time it differed slightly to the usual grey scale in that black was the same (-64^{0}C to -69^{0}C) the next coldest shade above (medium grey) was the same as the Dvorak white i.e. (-70^{0}C to -75^{0}C) and the white was equivalent to the Dvorak coldest medium gray i.e. (-76^{0}C to -80^{0}C)

Impact

Dominic crossed the coast near Cape Keerweer. Just prior to landfall satellite imagery showed a clear eye around 40 km in diameter surrounded by cloud tops colder than -70^{0}C (7.0 on the Dvorak T scale). There was damage to buildings and power lines at Edward River Mission. At Aurukun damage was assessed at $(1982)200,000. Tides were 1 m above normal at Weipa and 1.5 m above normal at Karumba. A detailed report of the damage in the remote Cape Keerweer area was provided by the log of The Round Australia Kayak expedition. Tree damage commenced at Wallaby Island (mouth of Archer R.) And extended south of Edward River Mission. The most extensive damage was from Love River To Holyrod River. There, all seashore Casuarinas were killed presumably due to salt water in root system. North of Cape Keerweer tree damage suggested onshore winds. One mile north of Cape Keerweer was an area devoid of all vegetation (no grass or trees) - the area appeared like a ploughed field for one mile inland.

Modified best track for *Dominic* with changes in red:

198115	Dominic_1982	04/04/1982 2100	-11.40	139.70	1002	289	25knots
198115	Dominic_1982	05/04/1982 0000	-11.50	139.60	1000	303	27knots
198115	Dominic_1982	05/04/1982 0300	-11.60	139.50	998	317	30kniots
198115	Dominic_1982	05/04/1982 0600	-11.50	139.30	994	334	35knots
198115	Dominic_1982	05/04/1982 0900	-11.30	139.20	990	339	42knots
198115	Dominic_1982	05/04/1982 1200	-11.20	139.30	990	326	42knots
198115	Dominic_1982	05/04/1982 1500	-11.40	139.30	988	331	45knots
198115	Dominic_1982	05/04/1982 1800	-11.50	139.40	986	324	45knots
198115	Dominic_1982	05/04/1982 2100	-11.70	139.40	984	331	50knots
198115	Dominic_1982	06/04/1982 0000	-11.80	139.40	982	335	52knots
198115	Dominic_1982	06/04/1982 0300	-12.10	139.40	980	350	52knots
198115	Dominic_1982	06/04/1982 0600	-12.30	139.50	977	352	56knots
198115	Dominic_1982	06/04/1982 0900	-12.60	139.60	974	362	60knots
198115	Dominic_1982	06/04/1982 1200	-12.90	139.80	972	367	64knots
198115	Dominic_1982	06/04/1982 1500	-13.00	140.00	968	360	65knots
198115	Dominic_1982	06/04/1982 1800	-13.10	140.10	965	361	66knots
198115	Dominic_1982	06/04/1982 2100	-13.30	140.20	962	372	70knots
198115	Dominic_1982	07/04/1982 0000	-13.80	140.30	960	412	75knots
198115	Dominic_1982	07/04/1982 0300	-14.10	140.40	948	436	95knots
198115	Dominic_1982	07/04/1982 0600	-14.20	140.80	930	428	105knots
198115	Dominic_1982	07/04/1982 0900	-14.30	141.10	920	428	115knots
198115	Dominic_1982	07/04/1982 1200	-14.40	141.40	935	431	100 knots
198115	Dominic_1982	07/04/1982 1500	-14.50	141.90	965	434	70knots
198115	Dominic_1982	07/04/1982 1800	-14.60	142.30	980	444	55knots
198115	Dominic_1982	07/04/1982 2100	-14.70	142.60	990	457	40knots
198115	Dominic_1982	08/04/1982 0000	-14.70	143.10	995	465	35knots
198115	Dominic_1982	08/04/1982 0300	-14.70	143.60	997	479	30knots
198115	Dominic_1982	08/04/1982 0600	-14.60	144.20	998	493	28knots

2. TC *Ivor*

David Ambrose (07 38471847) was on board the vessel *Mustique,* which encountered sustained winds of 114.5 knots (maximum reading on the anemometer). They spent the period steaming between Flinders and Stanley Islands in Princess Charlotte Bay. David Curnock , a dentist in Cairns was one of the crew and he recalled the ship's barometer falling to 928hPa The windward side of trees were stripped of bark.

Figure 2.1 location where the vessel Mustique steamed while the eye of severe TC Ivor passed over it.

At 0731 UTC 19 March 1990 (Figure 2.2) there was a large blow up of intense convection near the *Mustique.* Two hours later there was and eye evident on enhanced infrared imagery (Figure 2.3) with warmest eye temperature in the range -54^{0}C to -61^{0}C surrounded by band -70^{0}C to -75^{0}C which yields T6.0 or Australian Category 4 intensity. This would agree with observations from the *Mustique*.

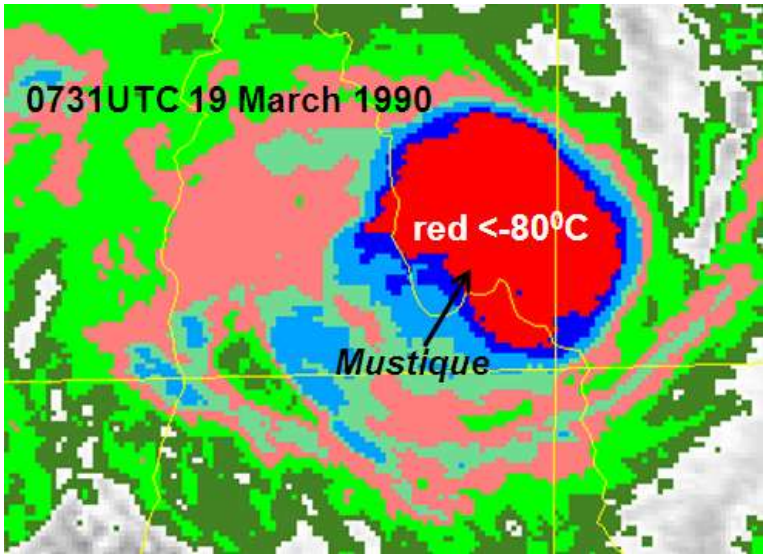

Figure 2.2 Enhanced coloured infrared satellite imagery at 0731 UTC 19 March 1990 (as in Figure 1). The location of the Mustique in marked.

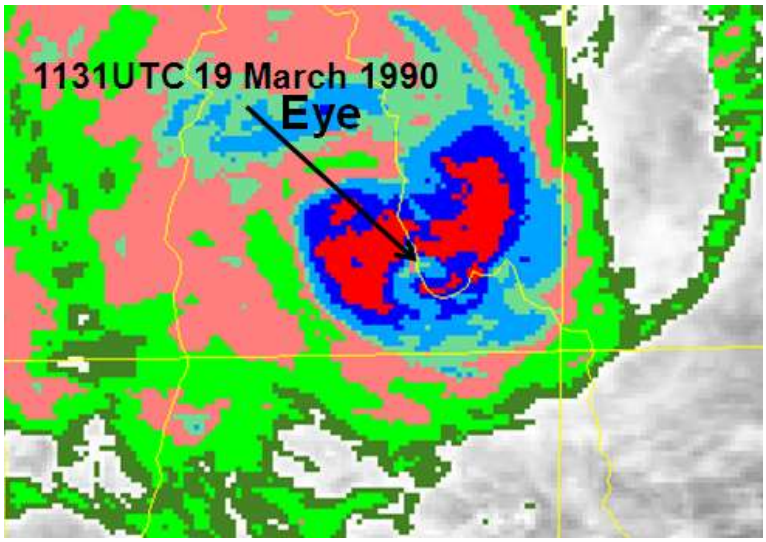

Figure 2.3 As in Figure 2.2 except for 1131 UTC 19 March 1990.

Modified best track for *Ivor* with changes in red:

http://www.bom.gov.au/tmp/aus1989198910.html

Ivor_1990	16/03/1990 0000	-15.80	160.80	995	2094	21.4knots
Ivor_1990	16/03/1990 0600	-16.80	158.80	995	1920	27.2knots
Ivor_1990	16/03/1990 1200	-17.00	156.80	992	1728	35knots
Ivor_1990	16/03/1990 1800	-16.60	155.20	992	1553	36.9knots
Ivor_1990	17/03/1990 0000	-16.10	153.80	990	1394	40.8knots
Ivor_1990	17/03/1990 0600	-15.30	152.10	990	1192	42.8knots
Ivor_1990	17/03/1990 1200	-14.40	150.70	984	1014	48.6knots
Ivor_1990	17/03/1990 1800	-14.20	150.10	980	945	54.4knots
Ivor_1990	18/03/1990 0000	-14.10	148.90	976	824	60.3knots
Ivor_1990	18/03/1990 0600	-14.00	147.90	971	724	62.2knots
Ivor_1990	18/03/1990 1200	-13.60	147.50	969	664	64.1knots
Ivor_1990	18/03/1990 1800	-13.50	146.90	966	603	70knots
Ivor_1990	19/03/1990 0000	-14.00	146.00	965	558	70knots
New intensity	**19/03/1990 0000**	**-14.00**	**146.00**	**960**	**558**	**75knots**
Ivor_1990	19/03/1990 0600	-14.10	145.00	970	492	64.1knots
New intensity	**19/03/1990 0600**	**-14.10**	**145.0**	**950**	**492**	**85knots**
Ivor_1990	19/03/1990 1200	-14.10	144.20	980	444	54.4knots
New intensity	**19/03/1990 1200**	**-14.10**	**144.20**	**930**	**444**	**100knots**
Ivor_1990	19/03/1990 1800	-14.00	143.40	983	399	50.5knots
New intensity	**19/03/1990 1800**	**-14.00**	**143.40**	**970**	**399**	**65knots**
Ivor_1990	20/03/1990 0000	-13.80	142.80	986	361	48.6knots
Ivor_1990	20/03/1990 0600	-13.90	142.40	988	367	46.7knots
Ivor_1990	20/03/1990 1200	-14.00	141.80	988	380	46.7knots
Ivor_1990	20/03/1990 1800	-14.00	141.50	986	386	48.6knots
Ivor_1990	21/03/1990 0000	-14.20	141.50	984	407	50.5knots
Ivor_1990	21/03/1990 0600	-14.80	141.50	988	473	46.7knots
Ivor_1990	21/03/1990 1200	-15.10	141.50	992	505	40.8knots
Ivor_1990	21/03/1990 1800	-15.20	141.90	994	512	35knots
Ivor_1990	22/03/1990 0000	-15.30	142.70	1001	524	29.2knots
Ivor_1990	22/03/1990 0600	-15.50	143.60	998	564	33knots
Ivor_1990	22/03/1990 1200	-15.70	144.30	999	609	29.2knots
Ivor_1990	22/03/1990 1800	-16.20	145.10	999	695	29.2knots
Ivor_1990	23/03/1990 0000	-16.90	145.90	1001	804	25.3knots
Ivor_1990	23/03/1990 0600	-17.10	145.40	999	798	27.2knots
Ivor_1990	23/03/1990 1200	-17.00	146.20	1001	830	21.4knots
Ivor_1990	23/03/1990 1800	-17.30	146.90	999	898	21.4knots
Ivor_1990	24/03/1990 0000	-18.30	146.90	1000	991	21.4knots

3.TC *Agnes*

The postion of Tropical Cylone *Agnes* at 1800UTC 16 April 1985 (Figure 3.1) showed that it was located 496km from Thuesday Island. Therefore it should be included in the climatology. It is also important as it was so intense and close to the latitude of the Torres Strait Islands. The enhanced infrared imagery (Figure 3.2) indicated that the Dvorak T number reached 6.5 2hile reamining near T 6.0 for some time. This is not reflected in the best track data and we have made some amendments (see below).

Figure 3.1 closest postion of Agnes with respect to Thursdayisland.

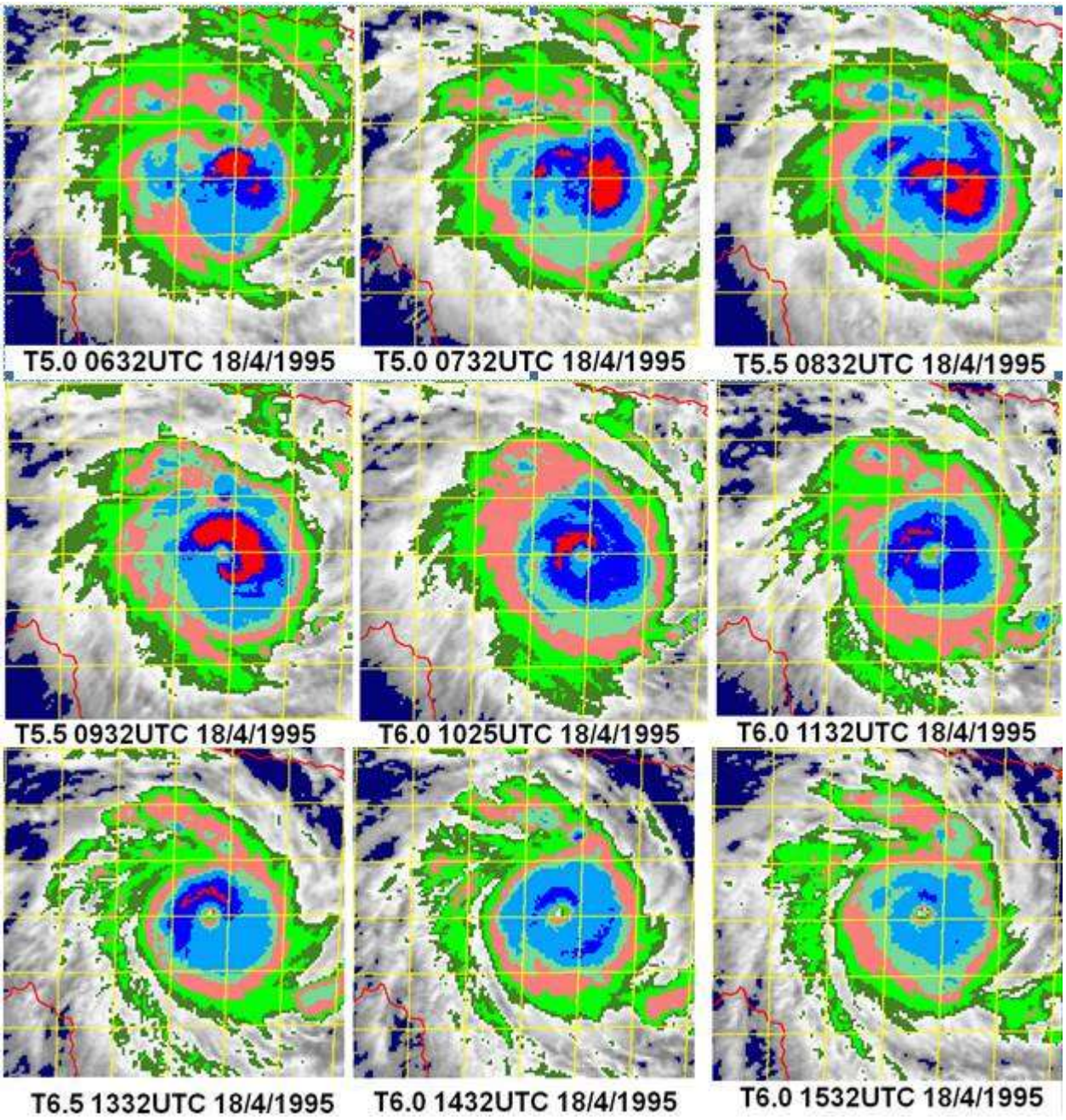
T5.0 0632UTC 18/4/1995
T5.0 0732UTC 18/4/1995
T5.5 0832UTC 18/4/1995
T5.5 0932UTC 18/4/1995
T6.0 1025UTC 18/4/1995
T6.0 1132UTC 18/4/1995
T6.5 1332UTC 18/4/1995
T6.0 1432UTC 18/4/1995
T6.0 1532UTC 18/4/1995

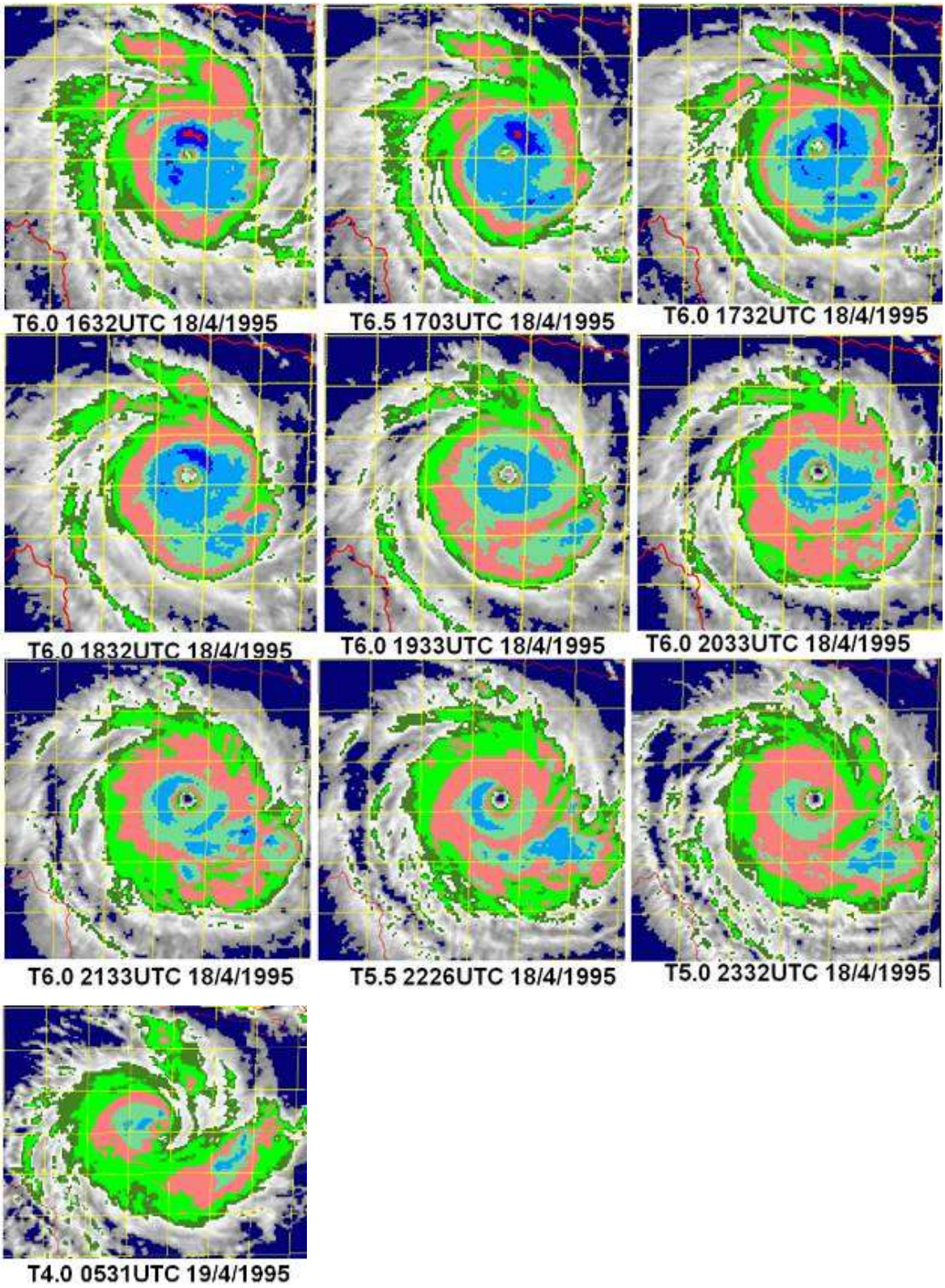

Figure 3.2 Enhanced coloured infrared satellite imagery from 0632 UTC 18 April 1995 to 0531UTC 19 April 1995.

Amended best track of TC *Agnes* with changes in red:

16 April 1995 1800UTC 11.3S 146.7E 995hPa 35knots
17 April 1995 0000UTC 11.8S 147.4E 990hPa 41knots
17 April 1995 0600UTC 12.1S 147.6E 985hPa 51knots
17 April 1995 1200UTC 12.3S 147.8E 975hPa 60knots
17 April 1995 1800UTC 12.5S 147.9E 975hPa 60knots
18 April 1995 0000UTC 12.8S 148.1E 970hPa 64knots
18 April 1995 0600UTC 13.0S 146.7E 960hPa 80knots
18 April 1995 1200UTC 13.1S 147.8E 945hPa 89knots
18 April 1995 1200UTC 13.1S 147.8E 945hPa 100knots T6.0 CI 6.0
18 April 1995 1800UTC 13.0S 147.7E 995hPa 89knots
18 April 1995 1800UTC 13.0S 147.7E 945hPa 100knots T6.0 CI 6.0
19 April 1995 0000UTC 12.8S 147.6E 945hPa 89knots
19 April 1995 0000UTC 12.8S 147.6E 945hPa 100knots T5.0 CI 6.0
19 April 1995 0600UTC 12.9S 147.6E 945hPa 89knots
19 April 1995 0600UTC 12.9S 147.6E 955hPa 90knots T4.0 CI 5.0
19 April 1995 1200UTC 13.1S 147.6E ~~**955**~~ **965hPa** 80knots
19 April 1995 1800UTC 13.1S 147.6E ~~**955**~~ **965hPa** 80nots
20 April 1995 0000UTC 13.1S 147.6E 970hPa 70knots
20 April 1995 0600UTC 13.1S 147.6E 970hPa 70knots
20 April 1995 1200UTC 13.1S 147.6E 970hPa 70knots
20 April 1995 1800UTC 12.6S 147.7E 975hPa 60knots
21 April 1995 0000UTC 12.1S 147.8E 980hPa 54knots
21 April 1995 0600UTC 11.8S 147.9E 985hPa 50knots
21 April 1995 1200UTC 11.6S 148.1E 985hPa 50knots
21 April 1995 1800UTC 11.1S 148.1E 985hPa 50knots
22 April 1995 0000UTC 10.8S 147.8E 985hPa 50knots
22 April 1995 0600UTC 10.5S 147.5E 990hPa 41knots
22 April 1995 1200UTC 10.1S 147.1E 995hPa 35knots

4. TC *Nina*

The Dvorak coloured (Figure 4.1) enhancements leading up to landfall indicate that the T number reached T5.0. The best track data has been amended below to accommodate intensities associated with T5.0.

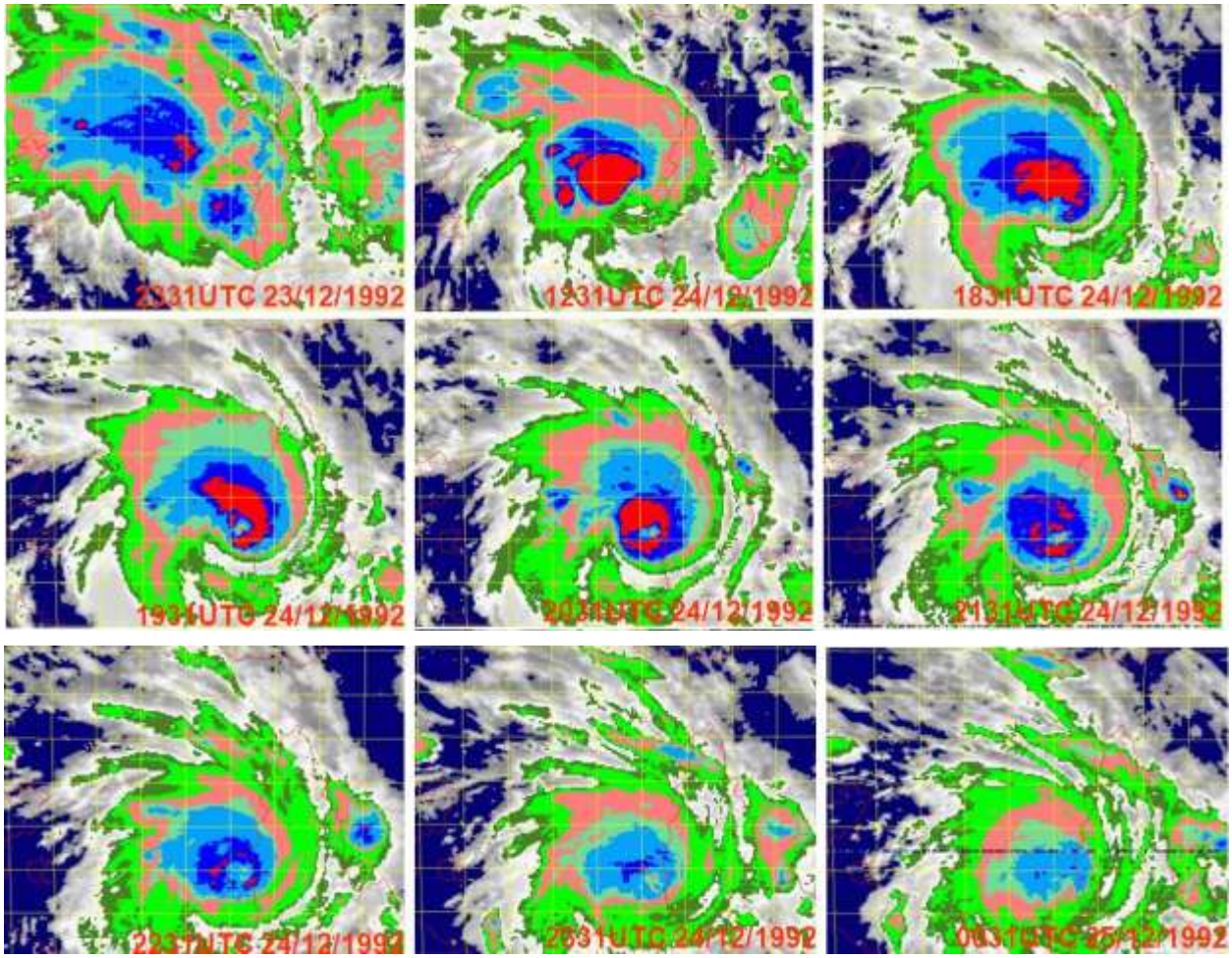

Figure 4.1 Enhanced infrared satellite image for TC Nina.

Best track changes for TC *Nina* in red.

Nina_1992 23/12/1992 0000 -13.00 140.00 996 31knots
Nina_1992 23/12/1992 0600 -12.50 139.50 996 31knots
Nina_1992 23/12/1992 1200 -12.00 139.50 995 35knots
Nina_1992 23/12/1992 1800 -12.10 140.10 995 35knots
Nina_1992 24/12/1992 0000 -12.30 140.30 990 41knots
Nina_1992 24/12/1992 0600 -12.60 140.30 985 50knots
Nina_1992 24/12/1992 1200 -12.80 140.80 975 60knots
Nina_1992 24/12/1992 1800 -13.30 141.10 970 ~~60knots~~/65knots
Nina_1992 25/12/1992 0000 -14.10 141.30 ~~965~~(970) ~~60knots~~/75knots T5.0
Nina_1992 25/12/1992 0600 -14.30 141.60 970 ~~60knots~~/65knots
Nina_1992 25/12/1992 1200 -14.30 141.80 975 ~~55knots/~~60knots
Nina_1992 25/12/1992 1800 -14.30 142.00 980 ~~50knots~~/55knots
Nina_1992 26/12/1992 0000 -14.30 142.30 985 ~~45knots/~~50knots
Nina_1992 26/12/1992 0600 -14.50 142.60 985 ~~45knots~~/50knots
Nina_1992 26/12/1992 1200 -14.30 143.10 990 45knots
Nina_1992 26/12/1992 1800 -14.0 143.10 990 45knots
Nina_1992 27/12/1992 0000 -13.30 143.30 990 45knots
Nina_1992 27/12/1992 0600 -13.50 144.10 990 45knots
Nina_1992 27/12/1992 1200 -13.50 144.10 995 ~~31knots~~35knots
Nina_1992 27/12/1992 1800 -13.10 144.50 995 ~~31knots~~35knots
Nina_1992 28/12/1992 0000 -13.00 145.50 ~~995~~(990) 41knots
Nina_1992 28/12/1992 0600 -13.00 145.50 990 41knots
Nina_1992 28/12/1992 1200 -13.60 146.80 990 41knots
Nina_1992 28/12/1992 1800 -13.60 147.10 990 41knots
Nina_1992 29/12/1992 0000 -14.30 148.80 990 41knots
Nina_1992 29/12/1992 0600 -14.60 150.00 985 50knots
Nina_1992 29/12/1992 1200 -15.10 150.80 975 60knots
Nina_1992 29/12/1992 1800 -15.10 151.30 975 60knots
Nina_1992 30/12/1992 0000 -14.80 152.00 970 64knots
Nina_1992 30/12/1992 0600 -14.60 152.50 ~~965~~(970) 70knots
Nina_1992 30/12/1992 1200 -14.50 153.30 ~~965~~(970) 70knots
Nina_1992 30/12/1992 1800 -14.00 153.50 970 64knots
Nina_1992 31/12/1992 0000 -13.30 154.60 970 64knots
Nina_1992 31/12/1992 0600 -13.10 155.10 965 ~~64knots~~70knots
Nina_1992 31/12/1992 1200 -12.80 155.80 965 70knots
Nina_1992 31/12/1992 1800 -12.60 156.80 960 ~~70knots~~75knots
Nina_1992 01/01/1993 0000 -11.80 158.10 960 75knots
Nina_1992 01/01/1993 0600 -11.60 159.30 960 75knots
Nina_1992 01/01/1993 1200 -11.60 160.50 960 75knots

5.TC *Dora* 2-9 February 1964

Dora made landfall on the eastern Gulf coast and devastated the Edward and Mitchell River missions on the 3rd. Trees over a wide area of western Cape York Peninsula were blown down or completely defoliated in winds of around 100 mph (87 knots).

The eye passed directly over Rutland Plains which experienced a 3 hour calm and gave the eye diameter as 12 nm. The winds at Edward River Mission reached hurricane force easterlies at noon on the 3rd. These winds backed to the northwesterly and maintained hurricane force before decreasing after midnight.

Mitchell River. At Mitchell River easterly winds reached hurricane force at 3.30 pm on the 3rd, thereafter veering to the southeast and increasing in force. A near calm period was observed there between 8.30 pm and 10.30 pm after which the wind veered southwest, then west, slackening in speed at 3.30 am on the 4th.

Rutland Plains. Rutland Plains experienced destructive easterly winds from 3pm to 10.30 pm on the 3rd with the strongest winds between 8pm and 10 pm. A complete calm then occurred until 1.30 am on the 4th after which westerly winds of slightly less speed persisted until 6.30 am. Damage was reported as far north as Aurukun Mission, extending to Miranda Downs and Karumba in the south. A strip almost 480 km in length. Maximum damage was a 130 km strip from near Edward River to the Nassua River. The Edward River Mission reported little damage 8km east of the mission- the strip was therefore very narrow in the north and widened to about 48 km in the south . In this maximum damage zone one quarter of the trees were blown down and those left standing were defoliated with major limb damage. At Wallaby Island at the mouth of the Mitchell River extensive and dense belts of Mangrove 10 metres high were completely destroyed and flattened like grass. The two mission stations and Rutland Plains all suffered severe damage. For the two mission stations the damage was estimated at 300,000 pounds(1964).

Rainfall. *Dora* was accompanied by torrential rainfall over a long period. Example of large 24 hour totals were Yirrkala 248mm on the 1st, Edward River 197mm 4th, Croydon 368mm 5th, Mary Kathleen 228mm 7th, Disraeli 320mm 8th and Iffley 247 mm 9th. The Norman, Flinders, Leichhardt and Gregory experienced record floods with river levels in many instances breaking records. The total discharge was estimated at nearly double the average annual discharge of the Murray/Darling systems. The Norman River was 8 inches higher than the 1951 record at Normanton.

Storm Surge. A large storm surge came ashore with the cyclone – the Superintendent reported the sea came right over the beach ridge, a rise of approximately 18 feet. The beach was left strewn with many dead marine creatures like porpoises and sea snakes.

Lowest pressure at landfall in the best track data 974hPa at 0000UTC 3 January 1964 which implies a high category 2. Considering the severe structural wind damage and the severe storm surge we will make it comparable with *Flora* below 955hPa at landfall with mean winds to 85knots.

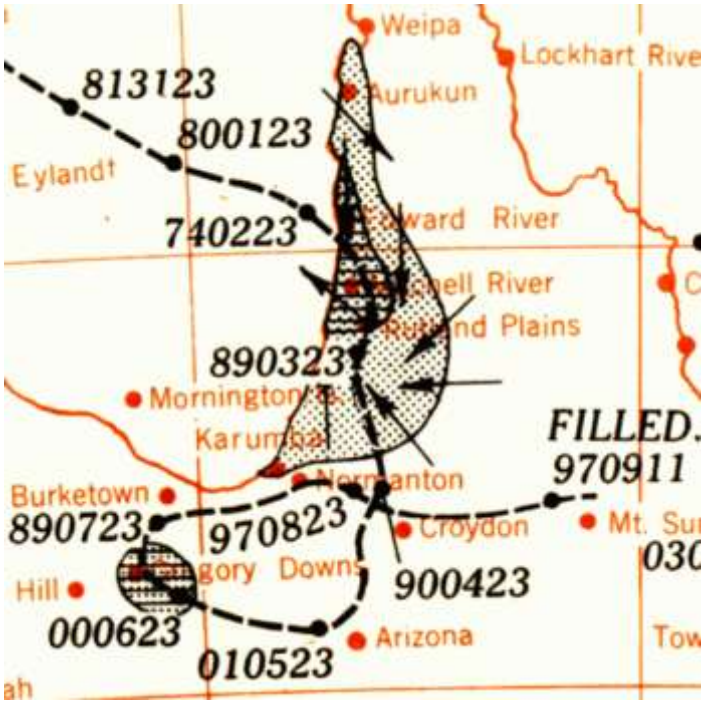

Figure 5.1 Hatching Areas of wind damage Horizontal hatching Areas of maximum wind damage (20% of timber down) Arrows show reported direction of tree fall

Best track for *Dora* with changes in red:

196305	Dora_1964	27/01/1964	2300	-9.20	131.00	1006	20knots
196305	Dora_1964	28/01/1964	0500	-9.50	131.60	1006	20knots
196305	Dora_1964	28/01/1964	1100	-9.70	132.20	1005	20knots
196305	Dora_1964	28/01/1964	1700	-9.90	132.70	1006	20knots
196305	Dora_1964	28/01/1964	2300	-10.00	133.20	1006	20knots
196305	Dora_1964	29/01/1964	0500	-10.30	133.90	1005	20knots
196305	Dora_1964	29/01/1964	1100	-10.60	134.50	1003	24knots
196305	Dora_1964	29/01/1964	1700	-10.80	135.10	1001	28knots
196305	Dora_1964	29/01/1964	2300	-11.00	135.70	999	30knots
196305	Dora_1964	30/01/1964	0500	-11.20	136.30	998	30knots
196305	Dora_1964	30/01/1964	1100	-11.40	136.90	997	30knots
196305	Dora_1964	30/01/1964	1700	-11.60	137.20	991	40knots
196305	Dora_1964	30/01/1964	2300	-11.70	137.50	985	50knots
196305	Dora_1964	31/01/1964	0500	-12.10	137.70	983	55knots
196305	Dora_1964	31/01/1964	1100	-12.50	137.90	981	55knots
196305	Dora_1964	31/01/1964	1700	-12.80	138.20	981	55knots
196305	Dora_1964	31/01/1964	2300	-13.10	138.50	981	55knots
196305	Dora_1964	01/02/1964	0500	-13.40	138.90	981	55knots
196305	Dora_1964	01/02/1964	1100	-13.70	139.20	980	55knots
196305	Dora_1964	01/02/1964	1700	-13.90	139.50	980	55knots
196305	Dora_1964	01/02/1964	2300	-14.00	139.70	~~980~~ 975	60knots
196305	Dora_1964	02/02/1964	0500	-14.20	140.20	~~979~~ 970	65knots
196305	Dora_1964	02/02/1964	1100	-14.30	140.60	~~977~~ 965	70knots

196305	Dora_1964	02/02/1964	1700	-14.50	141.00	~~976~~ 960	75knots
196305	Dora_1964	02/02/1964	2300	-14.70	141.40	~~974~~ 955	85knots
196305	Dora_1964	03/02/1964	0500	-15.20	141.80	~~974~~ 955	85knots
196305	Dora_1964	03/02/1964	1100	-15.60	141.70	~~975~~ 970	65knots
196305	Dora_1964	03/02/1964	1700	-16.00	141.70	~~982~~ 980	55knots
196305	Dora_1964	03/02/1964	2300	-16.30	141.60	989	45knots
196305	Dora_1964	04/02/1964	0500	-16.70	141.60	991	40knots
196305	Dora_1964	04/02/1964	1100	-17.10	141.60	993	35knots
196305	Dora_1964	04/02/1964	1700	-17.60	141.70	996	30knots
196305	Dora_1964	04/02/1964	2300	-18.00	141.70	998	30knots
196305	Dora_1964	05/02/1964	0500	-18.40	141.70	999	30knots
196305	Dora_1964	05/02/1964	1100	-18.80	141.70	999	30knots
196305	Dora_1964	05/02/1964	1700	-19.20	141.50	1000	30knots
196305	Dora_1964	05/02/1964	2300	-19.50	141.20	1001	25knots
196305	Dora_1964	06/02/1964	0500	-19.40	140.70	1001	25knots
196305	Dora_1964	06/02/1964	1100	-19.30	140.20	1000	30knots
196305	Dora_1964	06/02/1964	1700	-19.10	140.00	1000	30knots
196305	Dora_1964	06/02/1964	2300	-18.90	139.80	1000	30knots
196305	Dora_1964	07/02/1964	0500	-18.60	139.60	996	30knots
196305	Dora_1964	07/02/1964	1100	-18.30	139.40	991	40knots
196305	Dora_1964	07/02/1964	1700	-18.20	139.60	991	40knots
196305	Dora_1964	07/02/1964	2300	-18.00	139.70	991	40knots

6. TC *Flora* December 1964

Flora crossed the southern Gulf passing to the north of Mornington Island and making landfall near Inkerman Station at 9pm. The station (7 km inland) felt the full effects and the native's quarters, the butcher shop and a 2 room house were demolished. The northeast side of the homestead was lifted, 2-way radio aerials disappeared and rain penetrated all buildings. Large trees were snapped off or blown down .

Storm surge. A surge of sea water accompanied the winds and the sea came up the creek with a terrific rush. The bridge weighing approximately 2 tons was lifted and carried upstream about 800 metres and dumped approximately 90 metres up a ridge. The bridge was located 10 miles from the mouth of the creek.

Dunbar Station. Further north and 95km inland, Dunbar Station was subjected to damaging winds between 6.30 pm and 7.25pm. Mango trees were blown over in a strip 200 metres wide, houses were flattened, while roofing iron was deposited 800 metres away and twisted beyond use.

Vanrook Station. Vanrook Station (80 km inland) estimated hurricane ESE winds followed by a lull between 2.30 am and 3.30 am and then storm force SW winds. Buildings were unroofed and structures badly damaged and trees uprooted.

Miranda. At Miranda wireless aerials were blown down, roofing iron lifted, trees stripped of branches and many birds were found dead. There was heavy flooding and around Burketown about 100 stations were isolated.

Landfall data in the data base is 16.5S 141.4E 992hPa 10.58S 142.2E which implies at category 1 TC at landfall. Whereas the impact above includes severe structural wind damage and an incredible storm surge. This would suggest a strong category 3 cyclone at least. We estimate a central pressure at landfall of 955hPa and mean winds to 85knots.

Best track for *Flora* with changes in red:

1964 302330UTC November 10.7S 134.5E 1002hPa 25knots
1964 010230UTC December 10.8S 134.1E 1002hPa 25knots
1964 010530UTC December 11.0S 134.0E 1002hPa 25knots
1964 010830UTC December 11.1S 133.8E 1002hPa 25knots
1964 011130UTC December 11.2S 133.6E 1001hPa 30knots
1964 011430UTC December 11.3S 133.1E 1000hPa 30knots
1964 011730UTC December 11.3S 133.1E 1000hPa 30knots
1964 012030UTC December 11.4S 132.9E 1000hPa 30knots
1964 012330UTC December 11.5S 132.7E 1000hPa 30knots
1964 020230UTC December 11.6S 132.5E 1000hPa 30knots
1964 020530UTC December 11.8S 132.2E 998hPa 35knots
1964 020830UTC December 12.0S 132.1E 997hPa 35knots
1964 021130UTC December 12.1S 132.0E 995hPa 35knots
1964 021300UTC December 12.2S 131.8E 995hPa 35knots
1964 021430UTC December 12.4S 131.8E 996hPa 35knots
1964 021730UTC December 12.5S 131.6E 997hPa 35knots
1964 022030UTC December 12.8S 131.6E 996hPa 35knots
1964 022330UTC December 13.1S 131.6E 996hPa 35knots
1964 030230UTC December 13.2S 131.8E 996hPa 35knots
1964 030530UTC December 13.5S 132.3E 998hPa 30knots
1964 031130UTC December 13.7S 132.7E 998hPa 30knots
1964 031730UTC December 13.8S 133.2E 998hPa 30knots
1964 032030UTC December 13.8S 133.8E 998hPa 30knots
1964 032330UTC December 13.8S 134.3E 998hPa 30knots
1964 040230UTC December 14.0S 134.8E 998hPa 30knots
1964 040530UTC December 14.3S 135.0E 998hPa 30knots
1964 040830UTC December 14.6S 135.6E 996hpa 35knots
1964 041430UTC December 15.2S 136.7E ~~994hPa~~ 970hPa 70knots
1964 042300UTC December 15.9S 138.6E ~~993hPa~~ 962hPa 78knots
1964 051000UTC December 16.5S 141.2E ~~992hPa~~ 958hPa 80knots
1964 051100UTC December 16.5S 141.4E ~~992hPa~~ 955hPa 85knots
1964 051400UTC December 16.7S 141.8E ~~994hPa~~ 970hPa 65knots
1964 051600UTC December 17.0S 141.9E ~~995hPa~~ 975hPa 60knots
1964 051700UTC December 17.2S 142.3E ~~995hPa~~ 985hPa 50knots
1964 052000UTC December 17.6S 142.7E 995hPa 35knots
1964 052300UTC December 17.7S 143.5E 996hPa 30knots
1964 060200UTC December 17.5S 143.8E 996hPa 30knots
1964 060800UTC December 17.5S 145.0E 996hPa 30knots
1964 061200UTC December 17.8S 146.1E 996hPa 35knots
1964 062300UTC December 18.5S 147.9E 996hPa 35knots
1964 071100UTC December 19.0S 149.2E 998hPa 35knots
1964 072300UTC December 19.2S 150.1E 1000hPa 35knots

7.TC *Fiona* February 1971

Satellite analyses.

Below is the satellite analyses from Bureau of Meteorology 1973.

From ITOS 1 the first indication of an eye appeared on the imagery at 1744UTC 17 February 1971 with an irregular eye evident in a circular bright cloud feature just over one degree in diameter. This suggests about T4.0 from visual imagery Dvorak analyses today. We will a lot the central pressure around then as 975hPa maximum 10 minute winds as 60knots.

ESSA 8 imagery at 2324UTC 17 February 1971 showed a ragged eye with a large 2 to 3 degree sized overcast which would imply still around T4.0 or 975hPa mean winds to 60knots.

ITOS 1 0556UTC 18 February 1971 there was no eye evident in the imagery.

Subsequent imagery was also indefinite with no eye so it may have been a T 3.5 to T4.0 over this period.

ESSA 8 0008UTC 19 February 1971 an eye was visible again. It was a faint but well shaped eye embedded in 4 to 5 degree dense overcast. Possibly T5.5 from Dvorak visible imagery analysis and 945hPa mean wind to 90knots.

ITOS 1 imagery at 0652UTC 19 February 1971, about 2 hours before landfall, the cyclone had a very clear well shaped eye with a small bright convective ring surrounding it and a bright overcast cloud canopy surrounding this three latitude degrees in diameter. This indicated a very severe TC and from Dvorak analysis using the visual imagery with the clear eye embedded more than 1 degree into the dense overcast gives an eye pattern E7 and given the clear well shaped eye would result in a T 7 without adding more for banding features. Given the damage it caused and in particular the large storm surge it generated this cyclone was probably a category 5 storm or at least a high category 4 at landfall. We have called it 925hPa mean wind 110 knots.

Impact of *Fiona.* *Fiona* crossed the east coast of the Gulf of Carpentaria at the Nassua River mouth while rapidly intensifying. From the extensive defoliation and damage to the few buildings there , it was most likely accompanied by hurricane force winds .An outstation of Inkerman Station is located at the Nassua River mouth and a brief calm was noted at 0930 UTC preceded by east southeasterly winds and followed by west northwesterly. The destructive winds lasted about 2 hours and flattened timber and demolished buildings. About 50 % of the trees were left standing and these were damaged, some stripped of bark. The wharf was destroyed and 4 four 55,000 litre fuel tanks lifted and scattered up to a mile away. Forty four gallon drums were scattered widely like confetti.

Storm surge. The caretaker of the outstation observed a tidal wave was seen to come up from the mouth of the Nassua River and split at Cattle Creek. The wave came over the flats and washed away 3m high walls. It was 4.6 m high and travelled inland for approximately 2 km.

Edward River Mission At Edward River Mission the sea washed out a road on one of the sand ridges 2.7 m above sea level.

Aurukin. At Aurukun a tidal surge of 0.9 m was observed in the river about 5 miles from the Gulf.

Best track for *Fiona* with amendments in red:

197016	Fiona_1971	16/02/1971 2300	-16.00	140.80	1004	25knots
197016	Fiona_1971	17/02/1971 0500	-16.00	140.20	~~1001~~995	30knots
197016	Fiona_1971	17/02/1971 1100	-16.00	139.50	~~997~~985	50knots
197016	Fiona_1971	17/02/1971 1700	-15.80	138.80	~~992~~975	60knots
197016	Fiona_1971	17/02/1971 2300	-15.60	138.10	~~986~~975	60knots
197016	Fiona_1971	18/02/1971 0500	-15.00	137.50	~~984~~975	60knots
197016	Fiona_1971	18/02/1971 1100	-14.00	137.50	~~980~~975	60knots
197016	Fiona_1971	18/02/1971 1700	-13.50	138.50	970	65knots
197016	Fiona_1971	18/02/1971 2300	-14.00	139.70	~~969~~945	90knots
197016	Fiona_1971	19/02/1971 0500	-15.10	140.70	~~963~~925	110knots
197016	Fiona_1971	19/02/1971 1100	-16.10	141.60	~~965~~940	95knots
197016	Fiona_1971	19/02/1971 1700	-17.10	142.30	980	55knots
197016	Fiona_1971	19/02/1971 2300	-18.30	143.10	990	40knots
197016	Fiona_1971	20/02/1971 0500	-19.30	144.70	993	35knots
197016	Fiona_1971	20/02/1971 1100	-20.30	146.30	995	35knots
197016	Fiona_1971	20/02/1971 1700	-21.20	147.70	996	35knots
197016	Fiona_1971	20/02/1971 2300	-22.10	149.00	996	35knots
197016	Fiona_1971	21/02/1971 0500	-22.90	150.10	995	35knots
197016	Fiona_1971	21/02/1971 1100	-23.30	151.10	996	35knots

Bureau of Meteorology 1973. Tropical Cyclones in the Northern Australian Region, Meteorological Summary 95 pages.

8. TC Ted December 1976.

TC *Ted* passed just to the west of Gununa on Mornington Island at 0215UTC 19 December 1976. It then crossed the Australian mainland coast (see Figure 8.1) before moving over the small town of Burketown which experienced the calm conditions inside the eye between 0915UTC and 1050UTC 19 December. A barograph was located at Burketown and a central pressure of 950 hPa was recorded in the eye.

Damage in the path of *Ted* was almost total. On Mornington Island 700 inhabitants were rendered homeless with 95% of its buildings damaged and Burketown was similarly affected. A large storm surge accompanied the cyclone and it extended 20 km inland near Burketown where logs were piled 2-3 m high and a small wharf was destroyed. Tides at Karumba were 2 metres above normal and badly damaged the wharf and prawn processing installations. Magowra Station (SW of Normanton) reported that the sea came 30 km inland. Extensive flooding and wind damage occurred in stations inland from Burketown. The hurricane force winds extended a long way inland, for example Cowan Downs (see Figure 1) near the Burke and Wills Roadhouse had out buildings unroofed, windows blown out of the main building, telephone posts bent to ground level and trees 4 feet in diameter snapped. Livestock losses over the Gulf Country and adjacent areas caused by drowning and low temperatures combined with wet and windy conditions were estimated to be 250,000.

From Figure 8.2 from 2324UTC 17 December 1976 satellite imagery showed an eye had formed which by 1136UTC 18 December was a compact circular eye well embedded in the dense white (cold) cloud tops. With the lack of enhanced infrared satellite imagery in those days the circular nature of the eye along with the degree the eye was embedded in cold cloud tops is a strong indication of intensity. The embedded distance was at least 100km and from current Dvorak visual imagery techniques such an embedded distance equates to an E6. The T number can be less than this if the eye is ragged or irregular and can be more if circular bands exist outside the central core of the cyclone. Therefore we consider a T6 or more is appropriate at 1136UTC 18 December. A T6 gives a central pressure of around 930hPa -925hPa with 10min winds 95-100knots.

By 2349Z 18 December as *Ted* was near Mornington Island the eye has become ragged indicating weakening of the system. By 1000UTC 19 December we know that the central pressure was 950hPa so it is reasonable to assume that at 1136UTC 18 December that the central pressure was 930hPa or less.

Size of *Ted*

From Figure 8.3 we can see that the size of the circulation of TC Ted was relatively large.

Figure 8.1 Track of *Ted* and location mentioned in text.

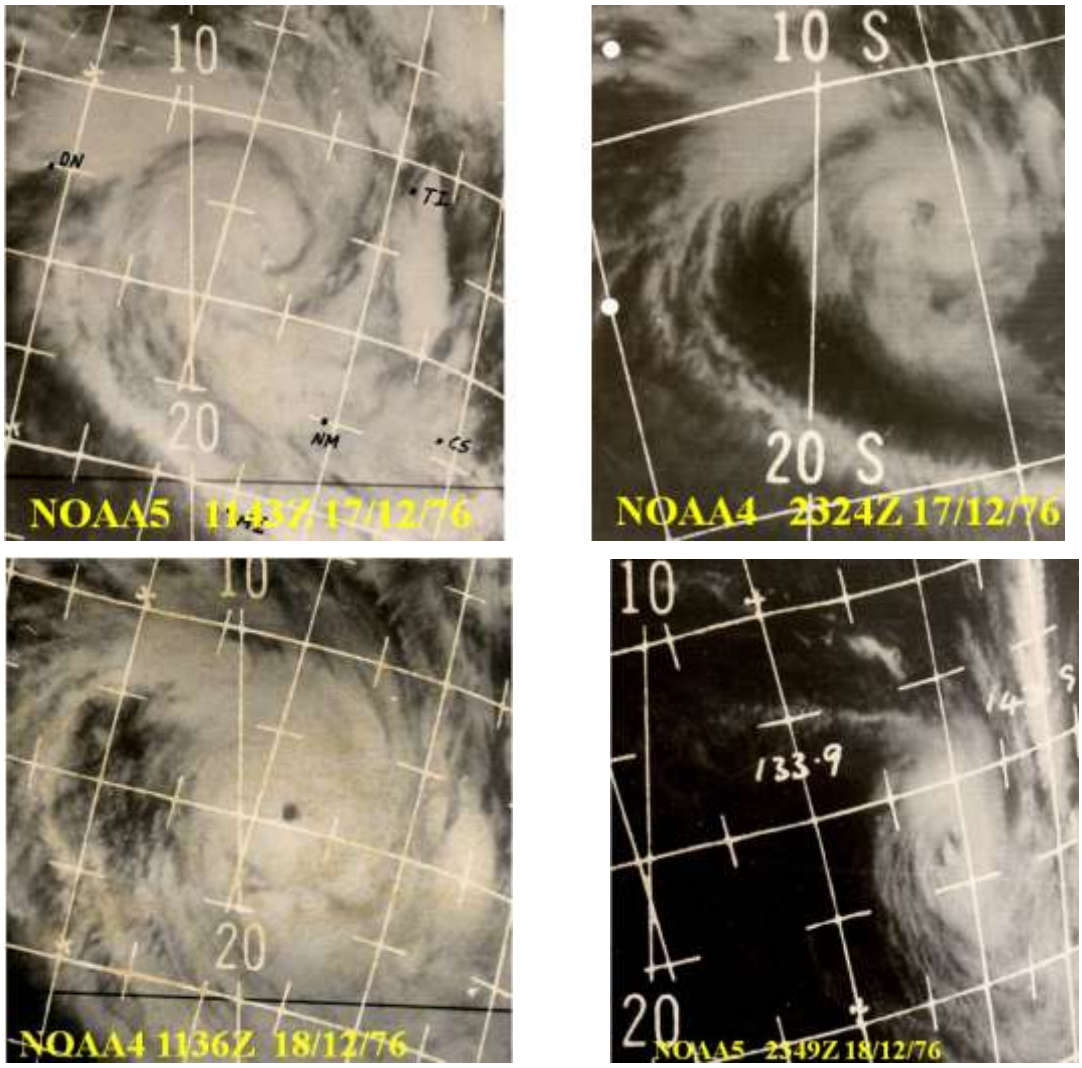

Figure 8.2 Satellite imagery of TC *Ted* at 1143UTC 17 December 1976 (top left), 2324UTC 17 December 1976 (top right), 1136 UTC 18 December 1976 (lower left) and 2349UTC 18 December 1976 (lower right).

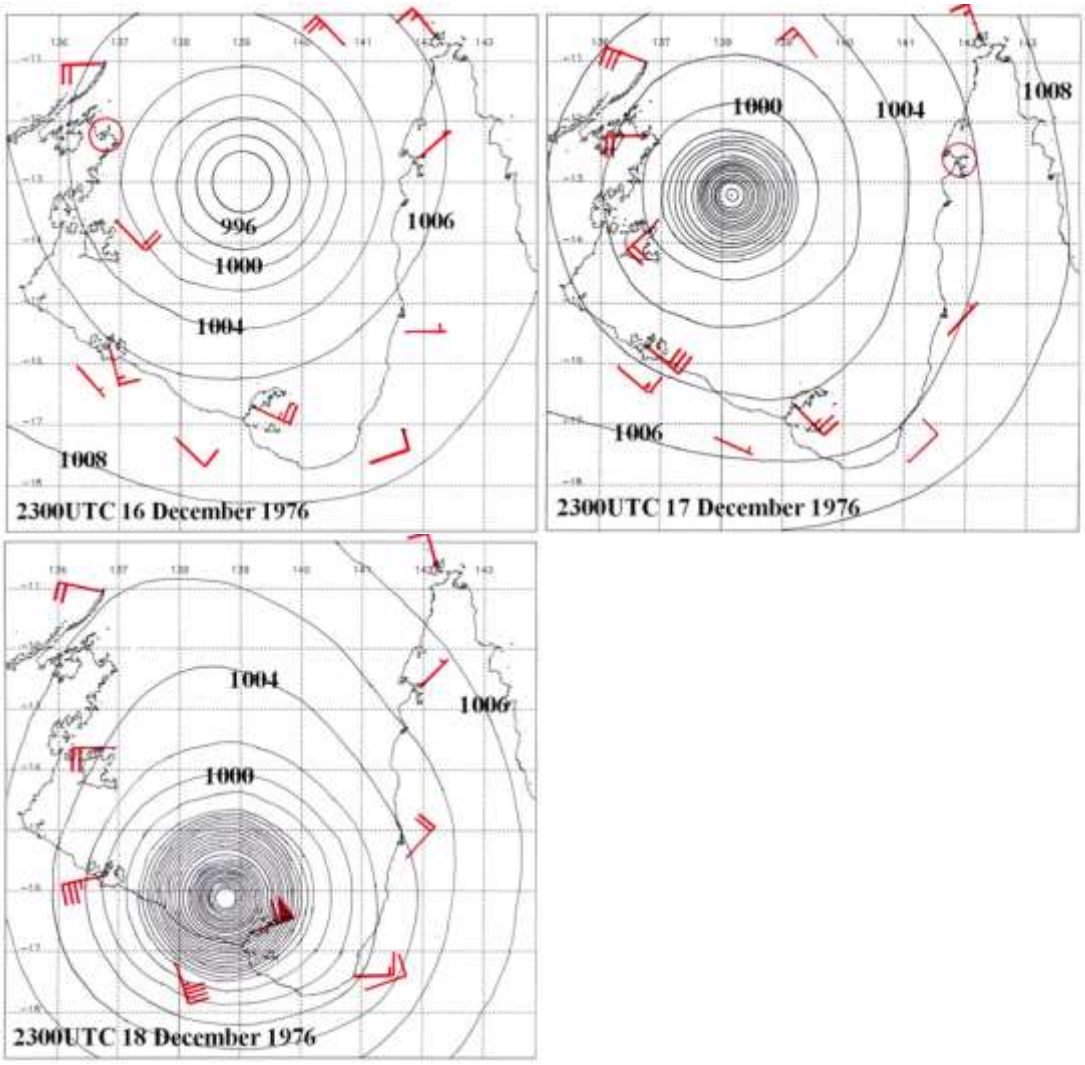

Figure 8.3 Mean sea level analyses for TC *Ted*.

9.TC *Felicity* 1989.

Figure 9.1 shows the rapid development of *Felicity* with a Dvorak analysis of T5.5 (lower right frame) at landfall. The surrounding cloud tops are the pink colour (-54^{0}C to -63^{0}C) with the dark green (-31^{0}C to -41^{0}C) which yields and eye number 5.0. For the eye correction the surrounding cloud is the blue (-70^{0}C to -75^{0}C) which adds 0.5 resulting in a T number of 5.5.

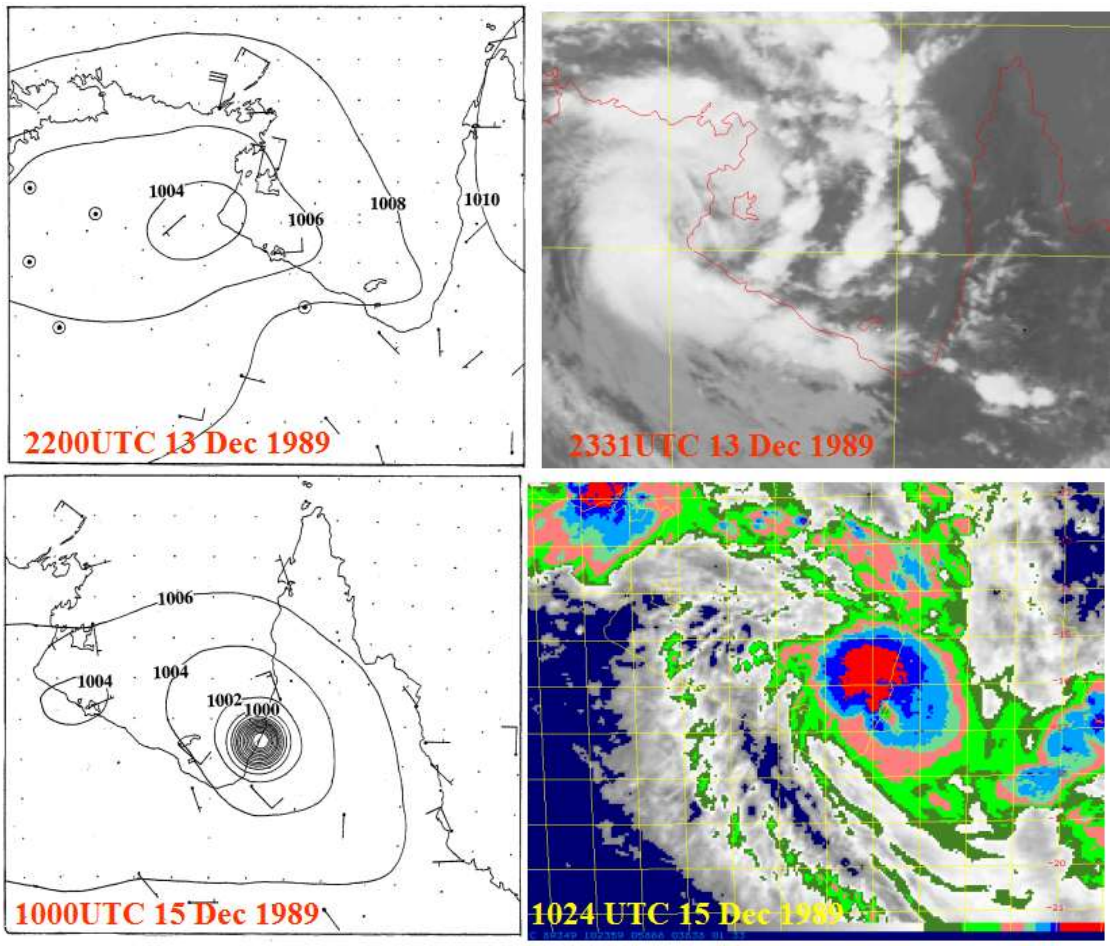

Figure 9.1 MSL charts and satellite imagery showing the rapid intensification of Felicity to a near category 4 storm.

The impact was severe. A Barramundi fisherman, Gordon Bell, has his house 12 feet above the high tide level and the sea came up to within 4 feet of the house which is an 8 ft(2.5m) surge. The house remained in offshore winds so that the surge would have been greater to the north. The strongest winds were from the SE and 80% of the trees were blown down and all trees were stripped of leaves. The wind was of sufficient strength to blow over a heavy stove which took 4 men to lift. Mr Bell was in Townsville during the landfall of TC *Althea* and his impression was that *Felicity* was more intense.

Best track for *Felicity* with changes in red:

1989 122300UTC December 11.6S 134.0E 1001hPa 15knots
1989 130600UTC December 12.1S 134.0E 997hPa 20knots
1989 131200UTC December 12.9S 134.2E 1000hPa 20knots
1989 131800UTC December 13.7S 134.9E 1001hPa 20knots
1989 140000UTC December 14.4S 135.4E 1000hPa 20knots
1989 140600UTC December 14.6S 136.1E 995hPa ~~15knots~~35knots
1989 141200UTC December 15.1S 137.0E 995hPa ~~15knots~~35knots
1989 141800UTC December 15.5S 138.0E ~~995hPa~~ 990hPa~~20knots~~ 40knots
1989 150000UTC December 15.8S 139.2E 985hPa ~~20knots~~ 50knots
1989 150600UTC December 16.2S 140.5E 975hPa ~~40knots~~ 60knots
1989 151100UTC December 16.6S 141.4E 950hPa 85knots
1989 151200UTC December 16.7S 141.5E ~~985hPa~~ 965hPa ~~25knots~~ 75knots
1989 151800UTC December 17.3S 142.5E 1000hPa 40knots
1989 160000UTC December 17.5S 144.0E 1000hPa 40knots
1989 160600UTC December 17.3S 145.8E 999hPa ~~25knots~~ 40knots

10. 1-2 December 1952

A small TC (estimated 50miles wide) struck Thursday Island from the west just before midnight (1st Dec) damaging most buildings with roofing iron flying through the town. Power lines were blown down and four hotels were partly unroofed and two had verandas blown away. The pearling lugger *Naianga* was smashed and sunk and three other luggers were blown ashore. Several other vessels were damaged by the pounding they received. No official BoM track is available.

Possible track for the Dec 1952 event:

1800UTC 30 November 1952 10.0S 138.0E 998hPa 30knots
0000UTC 1 December 1952 10.2S 139.0E 995hPa 35knots
0600UTC 1 December 1952 10.5S 140.0E 990hPa 45knots
1200UTC 1 December 1952 10.7S 141.0E 982hPa 55knots
1800UTC 1 December 1952 11.0S 142.0E 982hPa 55knots
0000UTC 2 December 1952 11.3S 143.0E 988hPa 45knots
0600UTC 2 December 1952 11.5S 144.0E 990hPa 40knots
1200UTC 2 December 1952 11.7S 145.0E 1000hPa 30knots

Appendix H

Compendium of Meteorological Analyses and Tropical Cyclone Impacts

J.J. Callaghan

H.1 The Meteorology Associated with Torres Strait Storm Surges

Following a spate of inundation events through Torres Strain Islands over the last 4 years we have examined the synoptic systems producing these storm surge events and how their frequency compares with the known impacts over longer term.

The east coast of Queensland has experienced a reduction in impacts from TCs from around 1977 to 2003 with an increase in impacts over recent years. This has been attributed to a change in the occurrences of El Nino and La Nina episodes.

Changes in Australia's annual rainfall are associated with year-to-year fluctuations in sea surface temperatures in the tropical Pacific Ocean. Variations in ocean temperatures are often associated with The El Niño/Southern Oscillation (ENSO), the most important coupled ocean-atmosphere phenomenon causing global climate variability on inter-annual time scales. A useful measure of ENSO activity is the Southern Oscillation Index (SOI) which is defined here as ten times the normalised difference in monthly pressure anomaly between Tahiti and Darwin. The negative phase of the SOI corresponds with El Niño, when tropical waters around Australia often have relatively cool temperatures and waters over the equatorial Eastern Pacific are anomalously warm. El Niño is often associated with drought in Australia (eg Nicholls 1992, Allan 1991).

The positive phase of the SOI corresponds with La Niña, when tropical waters around Australia have relatively warm temperatures while waters over the equatorial Eastern Pacific are anomalously cool. La Niña is associated with increased rainfall in Australia.

Wang (1995) described long term changes since 1950 in the tropical Pacific Ocean SST pattern which have affected the manner in which El Niño events evolve. Considering recent decades, the SST long term pattern changed around 1977 in the Pacific, resulting in warming along the equator and eastern Pacific and cooling in the southwest Pacific. Figure 1 illustrates how the SOI altered from a tendency to remain positive in the 27 years prior to January 1977 and negative in the following 27 years.

Research (Power et al 1999) has highlighted the potential importance of a long term cycle of rising and falling sea surface temperatures in the Pacific Ocean, called the Inter-decadal Pacific Oscillation (IPO), for Australian climate. While El Niño and La Niña are generally year-to-year events, the IPO has been shown to last decades - 10, 20 or even 30 years. When the IPO either warms or cools the central Pacific, it alters the impact of El Niño and La Niña. The IPO appears to affect the occurrences of El Niño and La Niña events. For example between 1949 and 1998, the four strongest La Niña (El Niño) episodes occurred before (after) 1977 corresponding with negative (positive) IPO indices.

The relationship between the number of TCs in the Australian region and the Southern Oscillation Index (SOI) is well-known (eg. Nicholls, 1979, 1984, 1985, 1992; Solow and Nicholls, 1990; Basher and Zheng, 1995). This relationship can be used to predict cyclone activity. Low values of the SOI, typically associated with an El Niño, during the Southern Hemisphere spring usually indicate that the ensuing cyclone season will have fewer than normal cyclones. During such years cyclone activity usually increases in the central South Pacific (Basher and Zheng, 1995).

In Figure 2, generated from http://www.bom.gov.au/cgi-bin/silo/cyclones.cgi TCs passing within 200 km of 10^0S 143^0E in the 27 seasons before and after 1977 is

shown and the period after 1977 is characterised by a reduction in tropical cyclones passing through Torres Strait. So it appears that the IPO had some affect on the Torres Strait region.

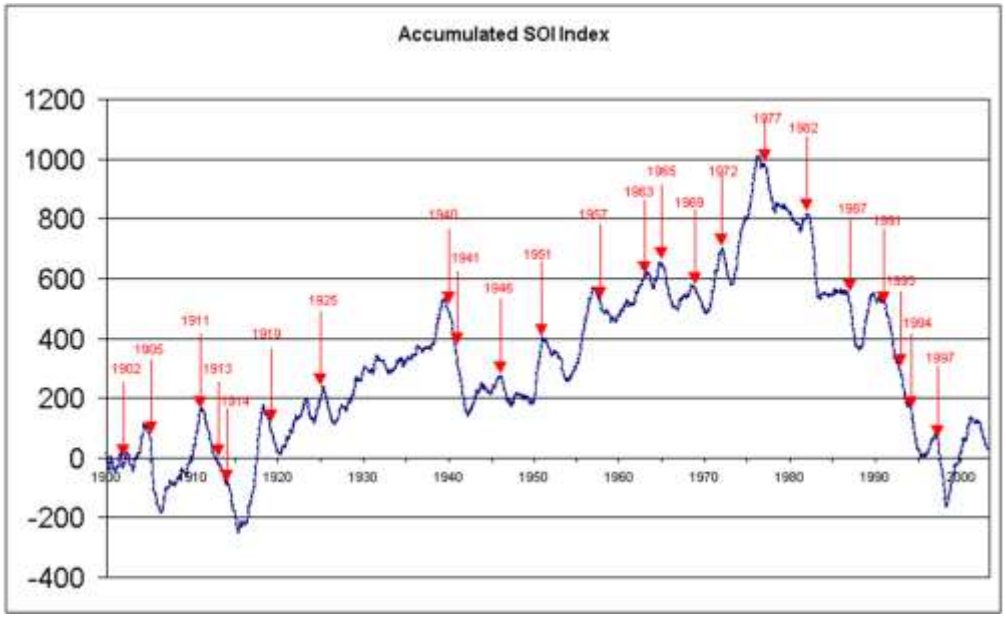

Figure 1 This graph is generated by adding the monthly value of the SOI so that consecutive positive monthly values will cause the graph to rise and similarly negative values will cause the graph to fall.

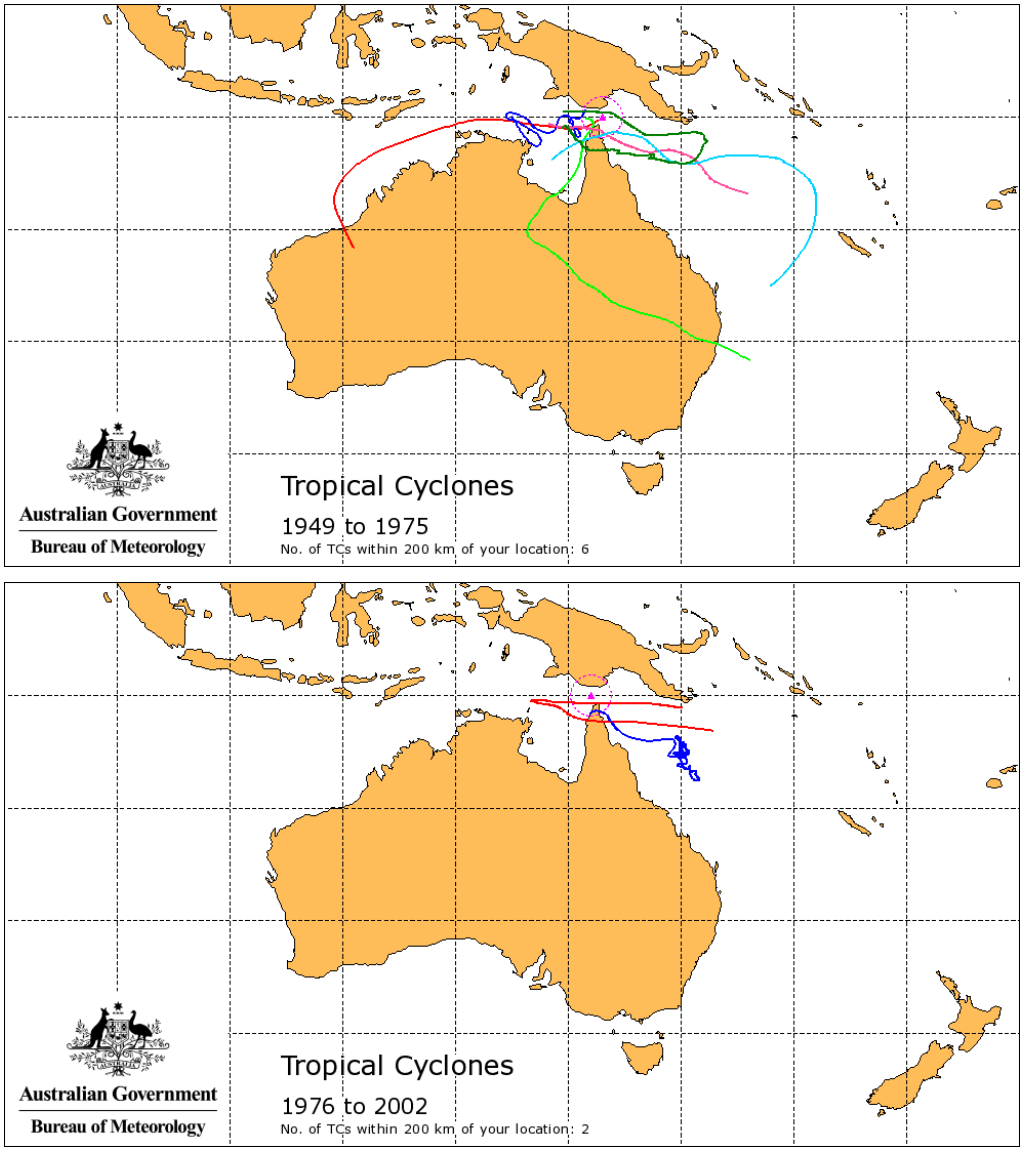

Figure 2 Tropical cyclones within 200km of 10degrees south and 143degrees east for the 27 seasons 1949/1950 to 1975/1976 (top) and for the 27 seasons 1976/1977 to 2002/2003 (bottom).

H.2 Recent events

2005/2006.

Full details of these events are in Appendix H-1 and these include

1. TC *Ingrid* March 2005 (most impact in PNG). Very intense westward moving cyclone just south of Torres Strait.

2. Winter gales July 2005 impact both Torres Strait and PNG).

3. Port Moresby Cyclone April 2005. This was a rapidly developing eastward moving cyclone just north of Torres Strait. Extremely rapid development as it moved off the land into the Gulf of Papua.

4. Intense monsoon low January 2006 overland Northern Australia with large impact storm surge Torres Strait.

5. TC *Kate* February 2006. Impact on Torres Strait Islands as the cyclone developed.

2007/2009

Detailed in Appendix H-2 are three large cyclonic circulations in the southern part of the Gulf of Carpentaria which all brought large waves and elevated sea levels into the Torres Strait region due to the extensive areas of strong to gale force winds across the Arafura Sea. Two were associated with damaging storm surges in Torres Strait while the third involving TC Nelson in 2007 was not as bad due to lower astronomical tides at the time.

Monsoon winds

These recent events indicate that since 2005 the monsoon westerlies may have become more active again at least in January and below in Figure 3 we compare the strength of the westerlies in January since 2005 with those in the 27 seasons before and after 1977. The active period pre 1977 had similar strength in the low level westerlies to the recent period while the post 1977 period has weaker average westerlies which are consistent with a quiet quarter of a century since the mid seventies.

The following figures have been obtained from http://www.cdc.noaa.gov/cgi-bin/data/composites/printpage.pl/hour/index.html

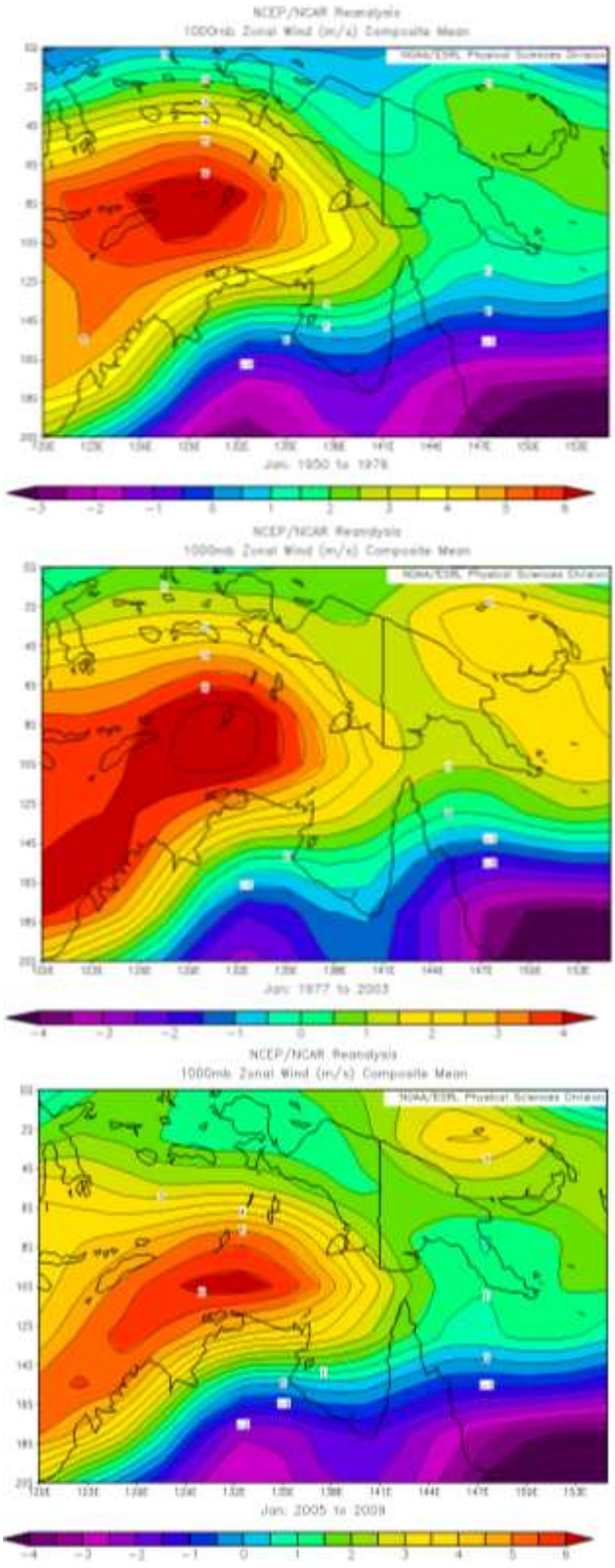

1000hPa zonal winds (westerlies are positive and easterlies are negative for January 1950-1976 (top), 1977-2003 (centre) and 2005-2009 (bottom)

H-3 Known Impacts prior to 2005

Here we detail known impacts in the Torres Strait region back to 1923 and there does appear to be less impact since the mid nineteen seventies.

Major Cyclones Torres Strait

23-25 March 1923. This was the so called *Douglas Mawson* cyclone as it sunk that vessel with the loss of 20 lives in the Gulf of Carpentaria where it also generated a 7 metre storm surge at Groote Island. The track below shows its passage through the Torres Strait Islands it may have been much more intense than indicated.

The eastern islands of Torres Strait (usually cyclone free) were badly damaged. Darnley, Coconut, Mabuiag and Murray Islands suffered much damage - houses unroofed, trees down, gardens damaged, luggers dismasted and Darnley settlement was virtually destroyed and banks of living coral 4 to 5 feet high were dashed up by the waves .

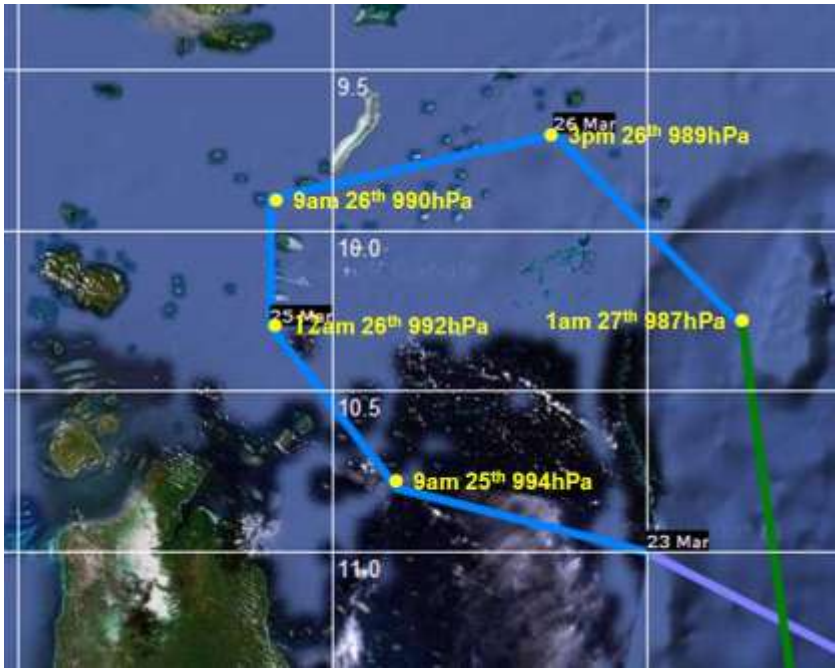

Track of *Douglas Mawson* cyclone in March 1923

6 January 1948 This cyclone moved eastwards towards Thursday Island causing structural damage there. Possible devastating storm surge Saibai Island.

From http://www.cmar.csiro.au/e-print/open/greendl_2006a.pdf

Prior to these recent inundation incidents, the islands' last major floods in living memory occurred at the end of 1947 and in early 1948 when a TC combined with high tides to create a storm tide that inundated Boigu and Saibai. At least two elderly Islanders on Boigu still remember this incident. One informant described her childhood memory of how she had to wade through chest high water to get to the church which was built on the highest ground on the island. Most of the community

waited at the church for several hours until the flood waters had subsided. In response to this event, some of the community decided to move off the island and onto mainland Australia. Many of the inhabitants of Bamaga community on the tip of Cape York are descendents of these relocated Islanders.

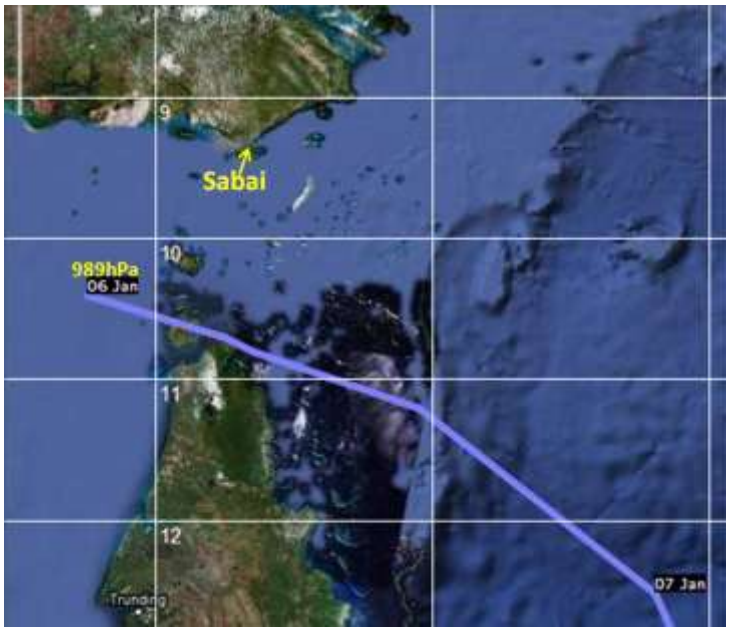

Track of 6-7 January 1948 TC

20 January 1952 A TC made landfall near Weipa and then turned and passed over Normanton. Thursday Island had wind gusts to 70 knots on 19th and 20th.

Track of 18-19 January 1952 TC

1-2 December 1952. A small TC (50miles wide) struck Thursday Island from the west just before midnight (1st) damaging most buildings with roofing iron flying through the town. Power lines were blown down and four hotels were partly unroofed and two had verandas blown away. The pearling lugger *Naianga* was smashed and sunk and three other luggers were blown ashore. Several other vessels were damaged by the pounding they received. No official track is available.

25-26 December 1959 A TC crossed the Gulf from Gove to Edward River Mission. At 9am 26th Thursday Island recorded wind gusts to 69 knots and 63 knots at 3pm. At Thursday Island fences were flattened, trees uprooted and 3 luggers crashed into a jetty. A number of pearl culture oyster beds were destroyed along the NE Gulf coast when large waves sank oyster pontoons. The *MV Windarra* in the Gulf reported injuries to the crew from large waves. Considerable flooding occurred in the Gulf Country when the cyclone crossed the Peninsula and water entered some homesteads.

Track of December 1959 TC.

TC *Dawn* February 1970

Between 0800UTC and 2000UTC 11 February 1970 Booby Island Lighthouse recorded sustained SW/40kts and Thursday Island W/38kts.

Between 0200Z and 0500Z 11th a ship southeast of Cape York recorded NW/44kts and -Thursday Island W/40kts with gusts to 54kts

The ship *Jeparit* 95km W of Thursday Island reported sustained W/45kts.

Several houses were unroofed at Port Moresby and on 12 February the ship *Laurabada* enroute Port Moresby to Daru was damaged by the seas and returned to Port Moresby.

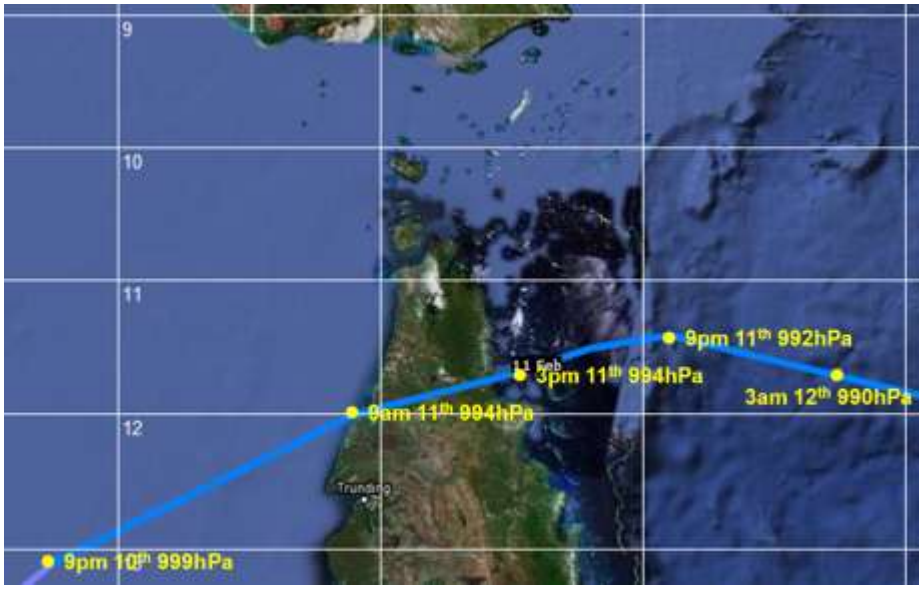

Track of TC *Dawn* February 1970.

TC *Faith* April 1972

Torrential rain at Thursday Island as the disturbance developed with 453mmin recorded in the 24h to 9am 9 April 1972.

At 10am 11th the Ship *John Bourke* reported NW/30kts 48km N of centre with rough seas and a heavy swell- During the day the *John Bourke* reported storm force NW winds averaging 50kts- The same ship at 7am 12th at a bearing 050/65km from centre reported a moderate W swell and at 1pm 12th on a bearing 360/28km reported Heavy increasing W swell.

At 7pm 12th there was a relatively dense network of ships indicating gales 120900Z 80 to 160km from centre. Gusts to 45kts at Aurukun 9pm 13th snapped off trees 23cm diameter.

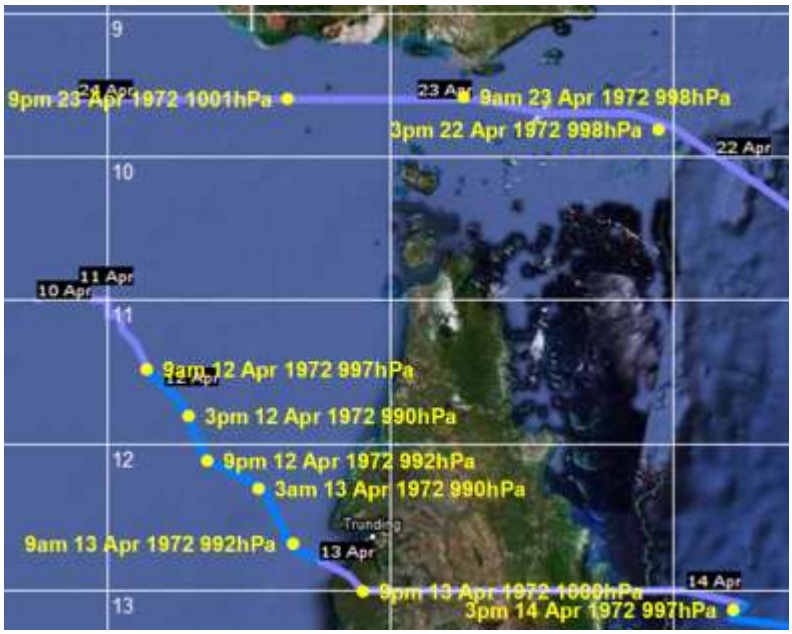

Track of TC *Faith* April 1972

Moderate effect Torres Strait

11-12 January 1955 TC near Stationary Gulf Coast just to the north of Weipa. Heavy rain and gales. Thursday Island recorded a gust of 56 knots on the 11th and a gust of 48 knots on 12th .

2-8 March 1961

A ship 7pm on the 2nd reported NW/33kts whole 30nm NW of Thursday Island. At 3am 3rd gales and gusts to 49kts at Thursday Island. At 9am 3rd Thursday Island mean winds were 31kts and 900hPa (1km elevation) were wind 44kts.

25-26 March 1963 NW gales at Thursday Island.

26-30 March 1963 NW gales Thursday Island max gust 58kts 270820Z

TC *Audrey* 7-14 January 1964 Thursday Island brief NW gales 7th with gust 53kts-however on the 8th mean winds of 30kts throughout the day with a peak gust of 57kts at 082300Z 60kt gust 090025Z then mean winds decreased although 55kt gust at 091435Z and an isolated gust 58kts at 101115Z

TC *Flora* 30 Nov 8 Dec 1964

050200Z Weipa gusts 40knots; 900hPa wind at Thursday Island 042300Z 310/37kts and 050500Z 300/45kts

Disturbance 12-21 Jan 1965 Gales 310/34kts 131700Z Thursday Island

TC *Dixie* 25-28 Jan 1968

Ship 30nm W of Weipa 262300Z NNW/30kts and heavy NW swell and at 270500Z WNW 35kts and heavy NW swell continued to report heavy NW swell until 271100Z as it steamed north.

TC *Bronwyn* 6-15 Jan 1972

Booby Island Lighthouse 061200Z to 070000Z NW 30kts gusts 45kts Thursday Island 25kts.

7 Mar 1977 TC *Otto*

Otto crossed the coast between Aurukun and Weipa. The only damage reported was tree damage at Weipa. Messmate trees (shallow rooted) with girths to 6 ft were blown down

TC *Greta* 19 January 1979

Greta crossed the coast 20 km south of Weipa. Weipa recorded a maximum wind gust of 42 knots and a 30 min calm in the eye where a central pressure of 986 hPa was recorded. Little damage was experienced.

TC *Stan* 16-15 April 1979

A 0.5 storm surge was reported at Weipa.

TC *Dominic* 7 Apr 1982

Very intense cyclone crossed near Cape Keerweer. Tides were 1 m above normal at Weipa

TC *Rebecca* 22 February 1985,

Rebecca crossed the coast just to the north of Weipa. Tree damage at Weipa with trees with girths to 60 cm blown down.

TC *Mark* 10 January 1992

Mark crossed the coast near Weipa, which suffered widespread minor damage with falling trees largely responsible for house damage and power line damage. Wave action caused $3.5 (1994 million) damage to the Kaolin loading facility at the Port. The maximum wind gust at Weipa Met Office was 63 knots from the NW. A maximum gust of 75 knots was recorded from an anemometer located at Lorim Point.

TC *Nina* 25 December 1992

Nina crossed the coast near Cape Keerweer. Aurukun reported 4 houses structurally damaged, **widespread tree damage** and the VHF aerial lost from the Council roof. Archer River reported severe flooding with 4 people isolated at the Roadhouse. **Severe tree damage**, heavy rain and one house was unroofed at Pormpuraaw.

TC *Ethel* 9 Mar 1996

Ethel crossed the coast north of Weipa. The strongest wind gust of 56 knots at Weipa Meteorological Office was recorded at 1030 UTC 9 March 1996 when an outer rainband passed through the station. This was at the time the peak storm surge of 1.18 metres was recorded at Weipa. The water level exceeded the highest astronomical tide at Weipa by .26 metres. Around this time a waverider buoy located 8 km west southwest of Weipa recorded a significant wave height of 3.76m and a peak wave height 6.69 m. The peak height reading is the largest wave observed at the Weipa. Larger wave effects were observed north of Weipa.

TC *Craig* 7-12 March 2003

Craig tracked from near Gove to Kowanyama. Weipa, which was well to the north of the cyclone's centre, recorded a storm surge of 1.1 metres, significant wave heights of 3 metres, and peak wave heights of 5 metres.

H-34 References

Allan, R.J. ,1991: In: Teleconnections linking worldwide climate anomalies. Glantz, M, et al (Eds), Cambridge Uni. Press, Cambridge, UK, 73-120 pp.

Nicholls, N., 1984: The Southern Oscillation, sea-surface temperature, and interannual fluctuations in Australian tropical cyclone activity. *J. Climatol*., 4, 661-670.

Nicholls,N.,1985: Towards the prediction of major Australian Droughts. *J. Climatol* 5, 553-560

Nicholls, N., 1985: Predictability of interannual variations of Australian seasonal tropical cyclone activity. *Mon. Weath. Rev*., 113, 1144-1149.

Nicholls,N.,1992: Historical El Niño/Southern Osscillation variability in the Australian region. In Nicholls, N., 1992: Recent performance of a method for forecasting Australian seasonal tropical cyclone activity. *Aust. Meteor. Mag*., 40, 105-110.

Power, S., Casey, T., Folland, C., Colman, A., Mehta, V. 1999. Inter-decadal modulation of the impact of ENSO on Australia, *Climate Dynamics* 15, 319-324.

Appendix H-1 Events during 2005 and 2006.

TC *Ingrid*

As Ingrid approached the Queensland Coast is generated southerly swells which were directed towards PNG and five lives were lost in the Coral Sea on the eighth near Kerema on the Papua New Guinea coat as a boat was capsized by the large swells.

Storm surges on the 9th caused considerable damage to villages southeast of Port Moresby.

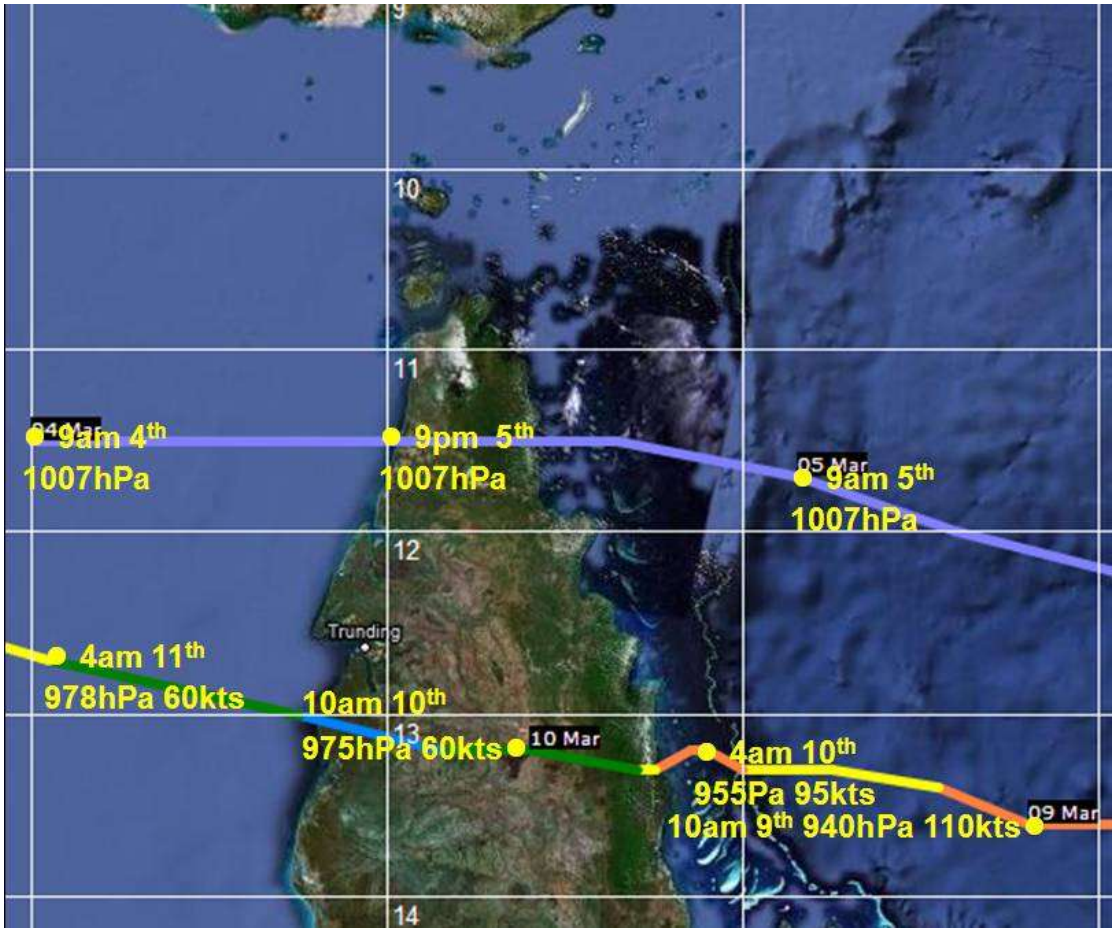

Track of TC *Ingrid* March 2005

Port Moresby Cyclone

This system rapidly developed as it moved off the New Guinea mainland into the Gulf of Papua. There were reports of sustained winds of 50 knots from an oil rig at 3.30am 15 April 2005. The Port Moresby gradient wind (elevation 1km) at 0000Z 15 April 2005 49 knots.

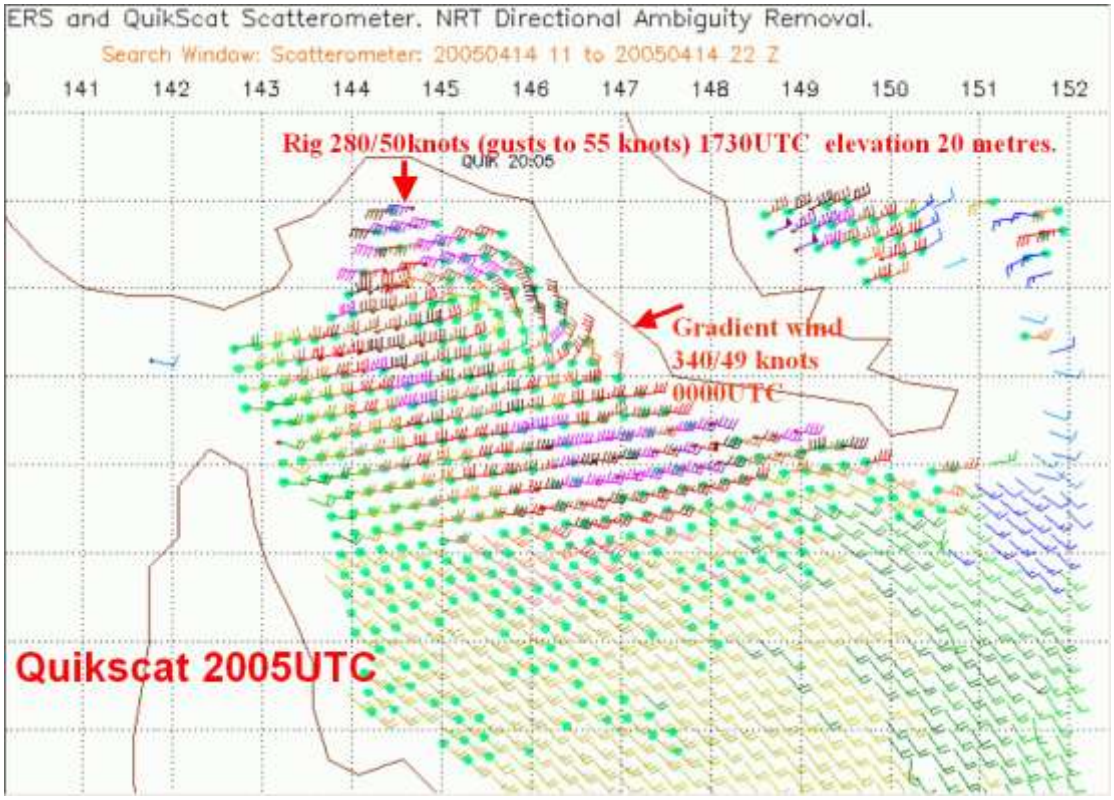

Quikscat winds at 6.05am 15 April 2005 show gale to storm force winds circling the developing cyclone.

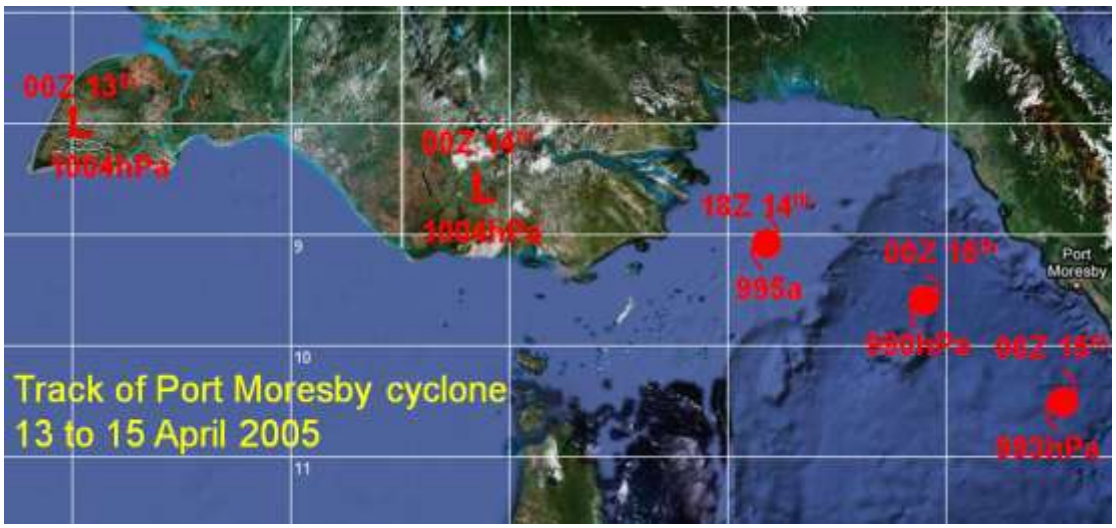

The track of the Port Moresby cyclone.

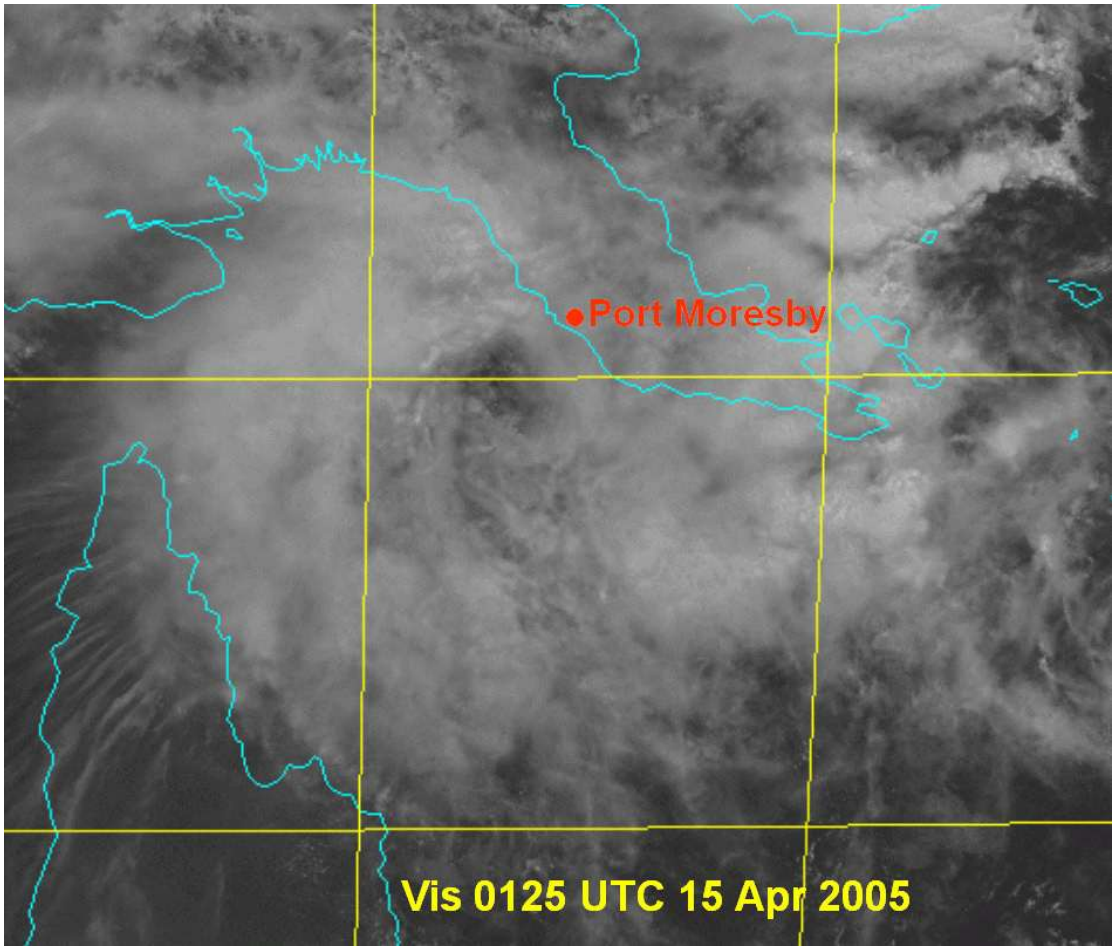

Eye type feature from the visible satellite imagery at its closest approach to Port Moresby

July 2005- A large Storm surge in Torres Strait and PNG.

Impact Torres Strait

Yorke Island had a large storm surge and Warraber Island lost about 20 metres. There was inundation on Mer, a high tide flooded several houses. Several houses had about 60cm of sand dumped at their front door. In one of the flooded houses, the water partially submerged a child's bed. Fortunately the family managed to rescue the child and flee higher ground until the flood waters subsided

Impact PNG

More than 200 homes, mostly in Western Province and at least one village on the Gulf and Central Province border, have been destroyed by surging high tides. Gulf Governor Chris Haiveta said at least 200 homes had been destroyed on Daru island over the past two weeks. "In my own province, I was at home during the weekend and I inspected at least five villages where considerable damage has been done," Mr Haiveta said. "I've also got reports coming in; I received one from a village called Laulava in the eastern part of the province on the border of Central (Province) where

seven houses have also been destroyed." He called on Inter-Government Relations Minister Sir Peter Barter to send National Disaster and Emergency Services officers to investigate the effects of the high tides on people's lives. Sir Peter said the problem of rising tides was not restricted to the southern part of Papua New Guinea and included Madang, New Ireland and Milne Bay provinces.He said "unprecedented levels of water" had swept into food gardens on Carteret Island, Mortlocks and Tasman islands in Bougainville and some of the Trobriand Islands. 10 fisherman were missing near Daru.

Meteorological situation causing the storm surge.

Mean Sea Level Charts

These charts below show the intense pressure gradient across North Queensland and Torres Strait. This was the period of strongest winds in the affected areas, which reached gale force over large areas of open sea.

Scatterometer winds

The winds derived from the Quikscat satellite data below from 8am EST 21 July 2005 until 8pm 21 July 2005 indicate gale force winds in the red areas for winds at 10 metres elevation over the ocean.

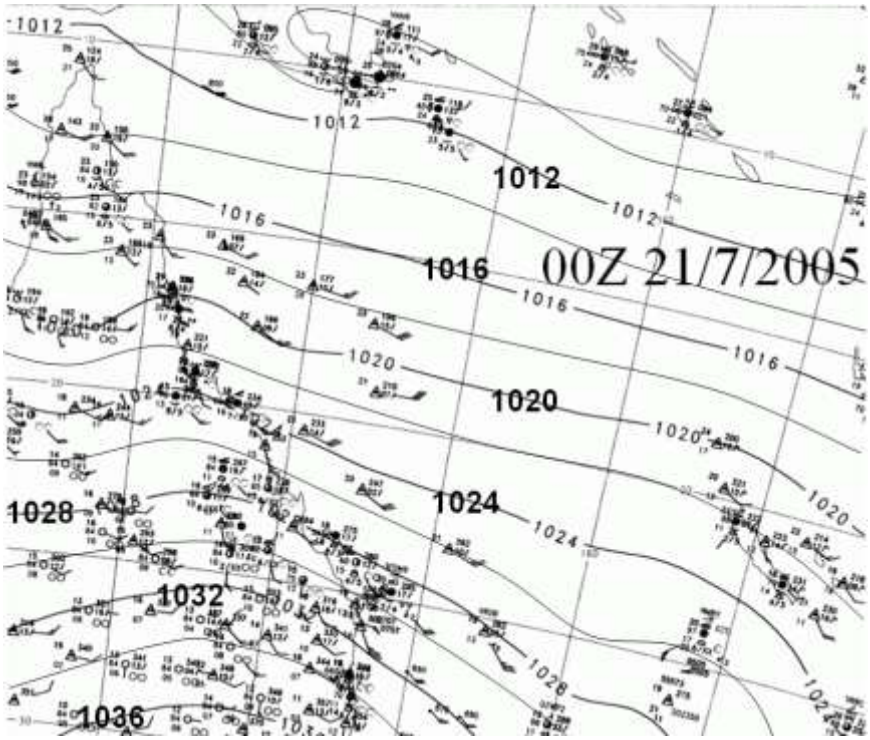

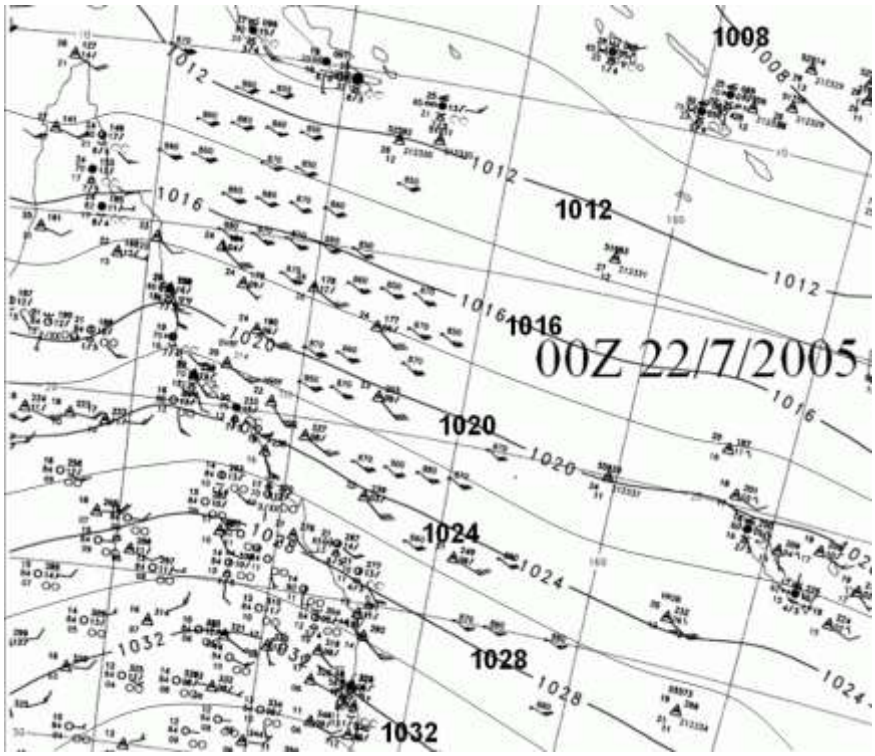

MSL synoptic charts showing the intense pressure gradient across North Queensland and Torres strait at 9am 21 July 2005 (top) and 9am 22 July 2005 (bottom).

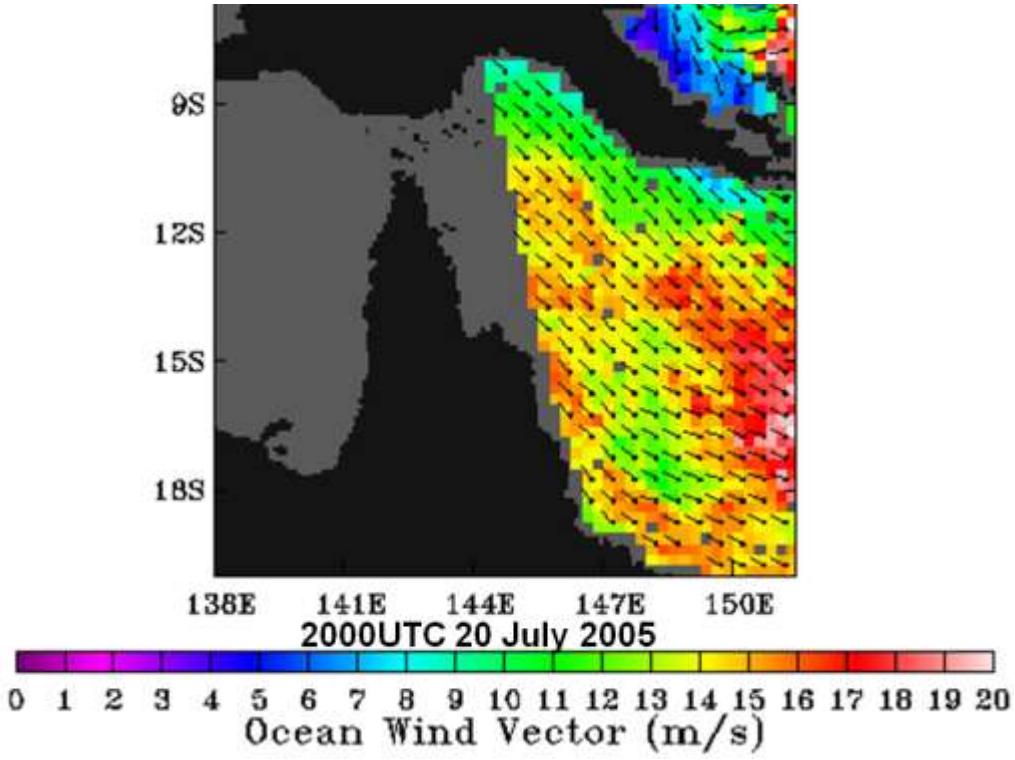

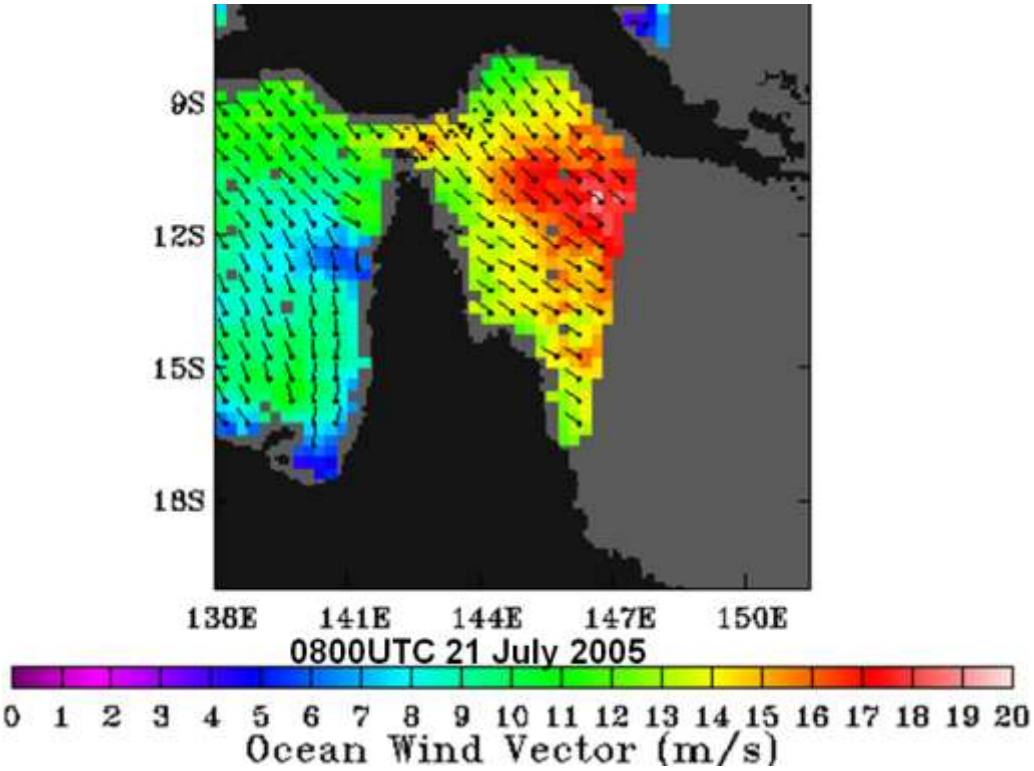

Winds derived from the Quikscat satellite from 8am EST 21 July 2005 until 8pm 21 July 2005. The red areas indicate winds at 10 metres elevation over the ocean averaging more than 33 knots (gale force).

Intense Monsoon Low developing over the Northern Territory January 2006

These systems have been called agukabams from the aboriginal word roots “agu”, meaning land and “kabam” meaning storm (see reference *A Hypothesis for the Redevelopment of Warm-Core Cyclones over Northern Australia* by Kerry Emanuel, Jeff Callaghan and Peter Otto, Monthly Weather Review 136, 3863-3872.)

This was a high impact event in Torres Strait see:

http://www.epa.qld.gov.au/publications/p01864aa.pdf/2006_King_Tides_in_Torres_Strait.pdf

Tides Data

The Weipa and Booby Island tide gauges below show the prolonged period of levels exceeding highest astronomical tides (HAT) at Weipa and Booby Island.

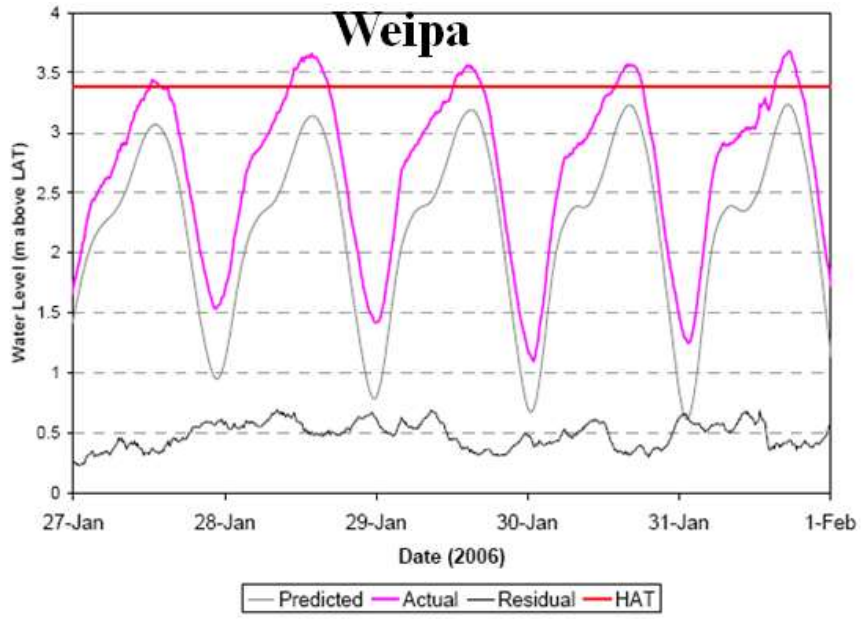

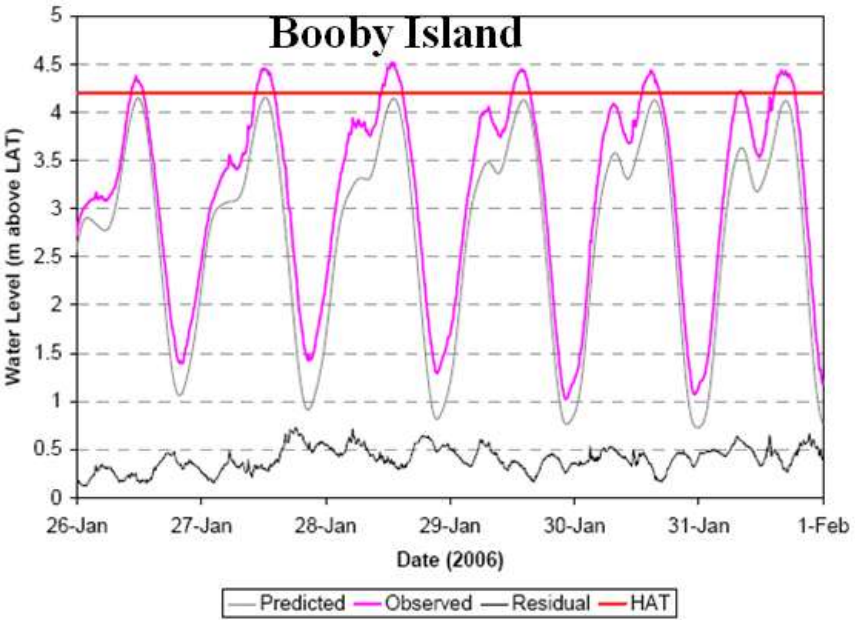

Waves

There were large waves in areas exposed to the west. Wave measurements at Weipa showed that the significant wave heights increased up to 2.45m.

Mean sea level (MSL) synoptic pattern

The MSL charts from 27-31 January 2006 show an intense low pressure develop over the Northern Territory with a strong pressure gradient to its north.

There are no quikscat images available during this period however near surface winds (925hPa level) from the US reanalysis site http://www.nomad3.ncep.noaa.gov/ncep_data/ indicate very strong WNW winds across an extensive zone of the Arafura Sea (see below).

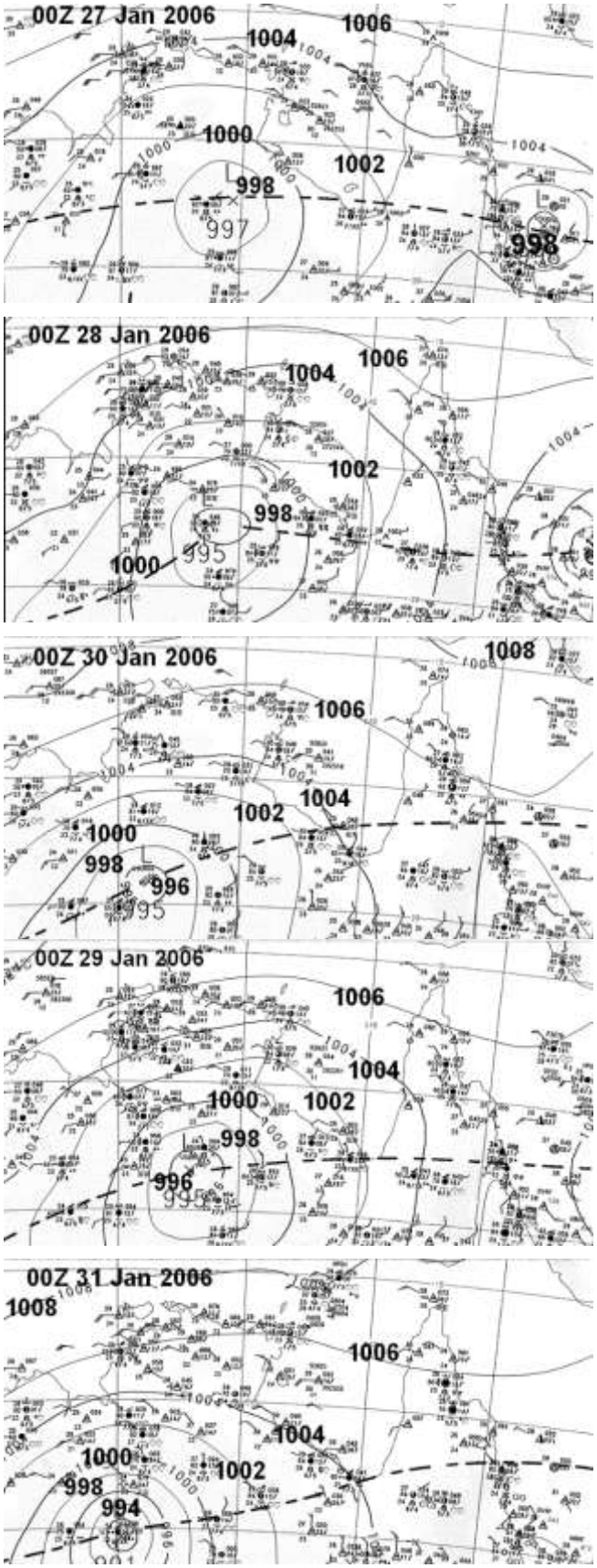

Sequence of MSL charts 27 January 2006 to 31 january 2006.

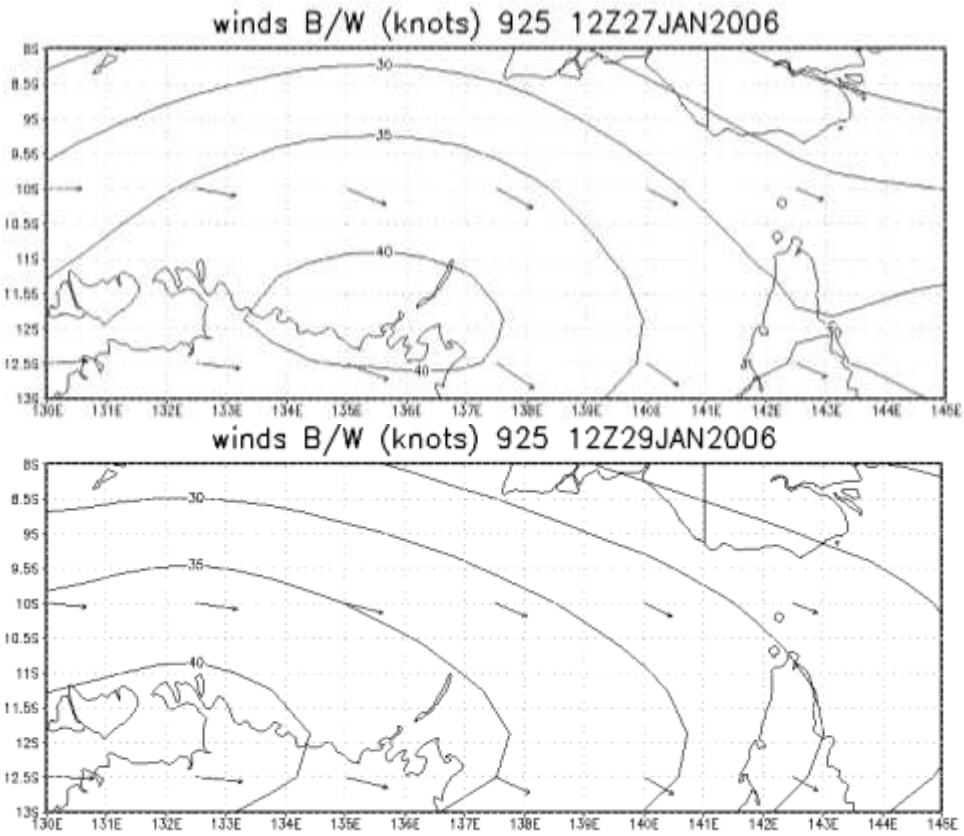

Near surface winds from http://www.nomad3.ncep.noaa.gov/ncep_data/

22-24 Feb2006 TC Kate. *Kate* had an impact on Torres Strait Islands where it washed away a jetty and added to the erosion damage caused by the gales last July and *Ingrid* and the Port Moresby cyclone last summer.

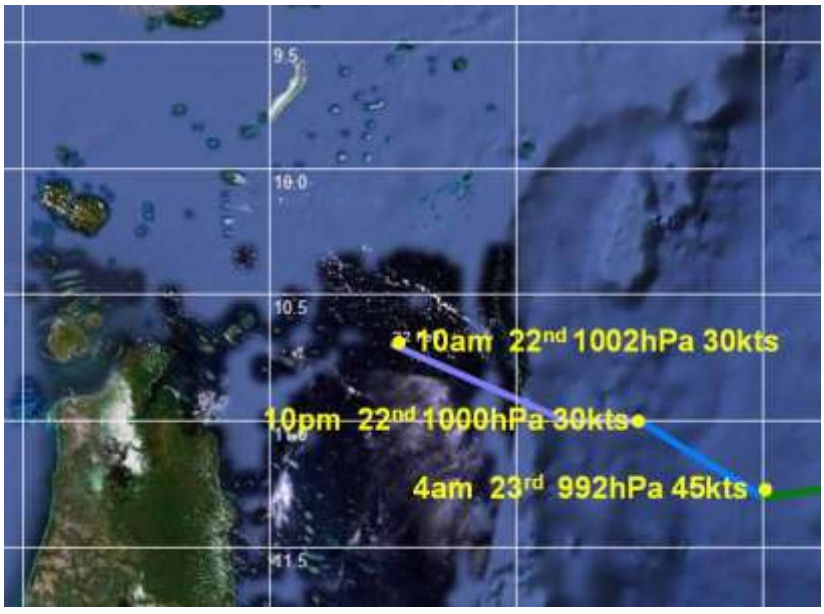

Track of TC *Kate* February 2006.

Appendix H-2 Events occurring from 2007 to 2009.

TC Nelson February 2007

This was another large system which brought large waves and storm surges into the area where Weipa wave rider buoy again measured significant wave heights over 3 metres (not shown) and the tide gauge recorded levels of over a metre above predicted levels (see below). However the astronomical tides were lower so that water levels just exceeded highest astronomical tide levels (HAT).

The mean sea level charts below show the large size of the circulation extending strong to gale force winds into the northern Gulf of Carpentaria. The near surface winds (925hPa level) from the US reanalysis site http://www.nomad3.ncep.noaa.gov/ncep_data/ indicate very strong WNW to NW winds across an extensive zone of the Arafura Sea and reaching 50knots in Torres Strait (see below).

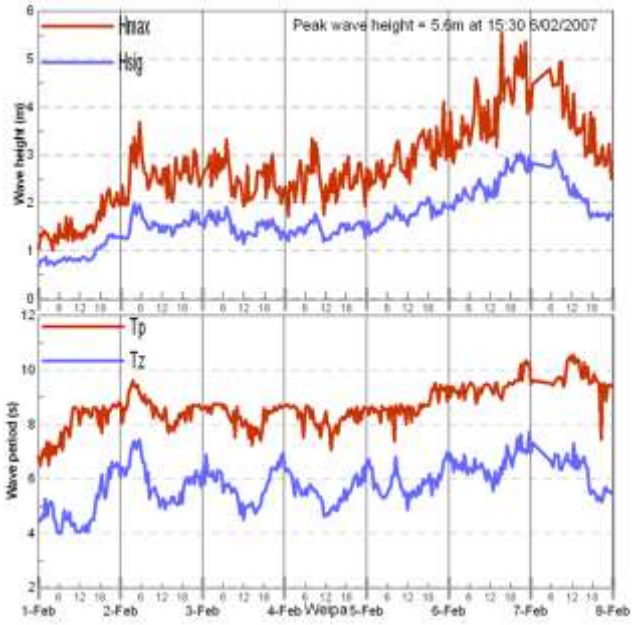

Weipa wave rider buoy data

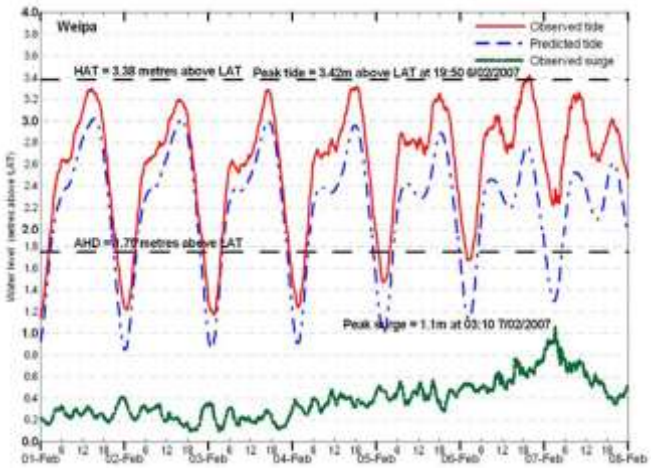

Weipa tide gauge data.

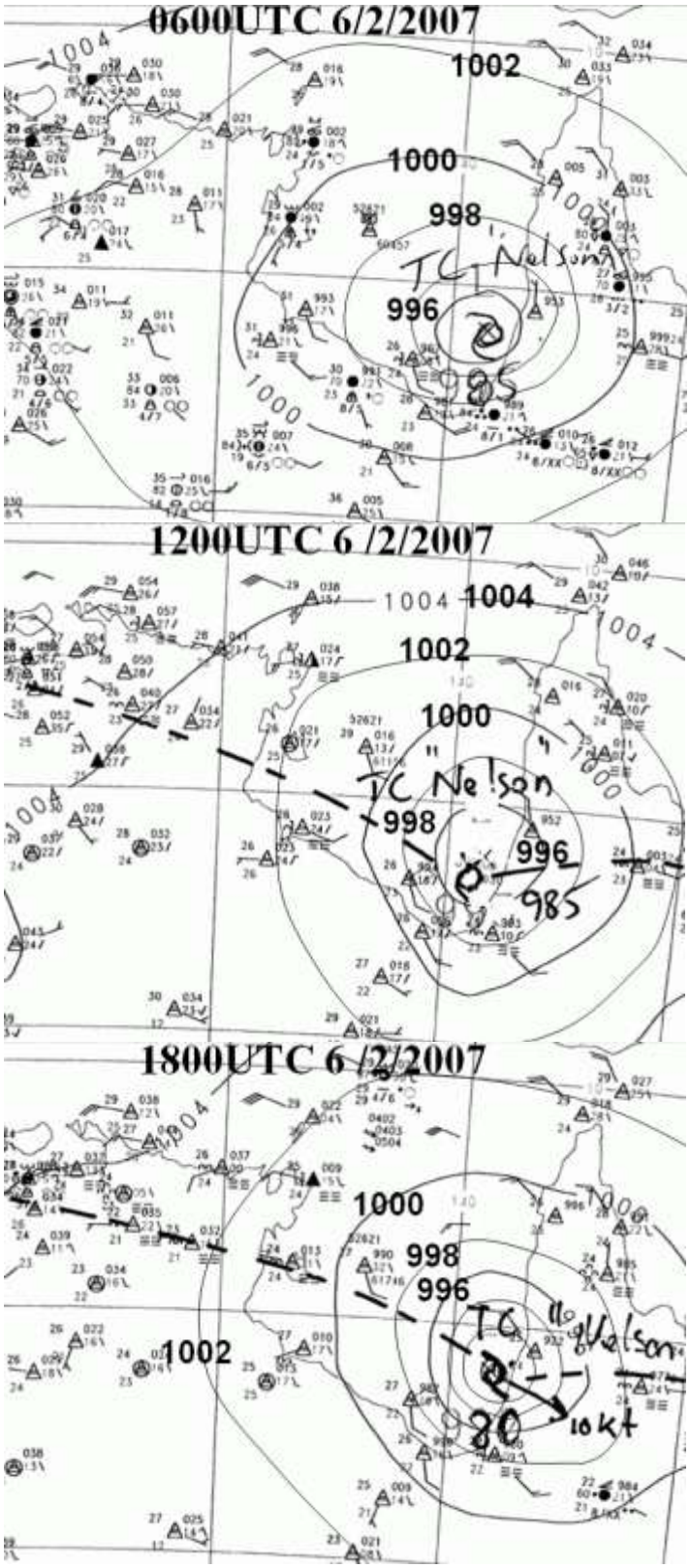

Sequence of MSL charts for 4pm 6 February 2007 to 4am 7February 2007.

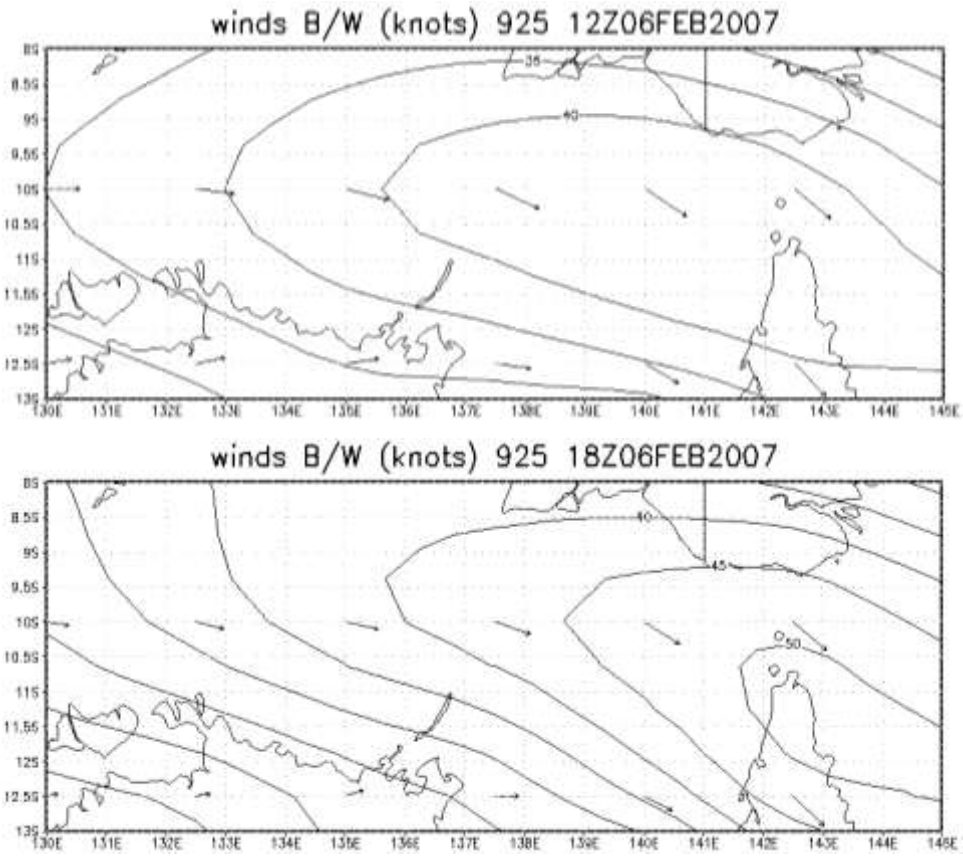

Near surface winds from http://www.nomad3.ncep.noaa.gov/ncep_data/

Ex TC Helen January 2008

This system brought also large waves and storm surges into the area where Weipa wave rider buoy again measured significant wave heights over 3 metres (not shown) and the tide gauge recorded levels of over a metre above predicted levels (see below).

The MSL charts and Quikscat satellite wind observations (below) both indicate the large size of the circulation extending strong to gale force winds into the northern Gulf.

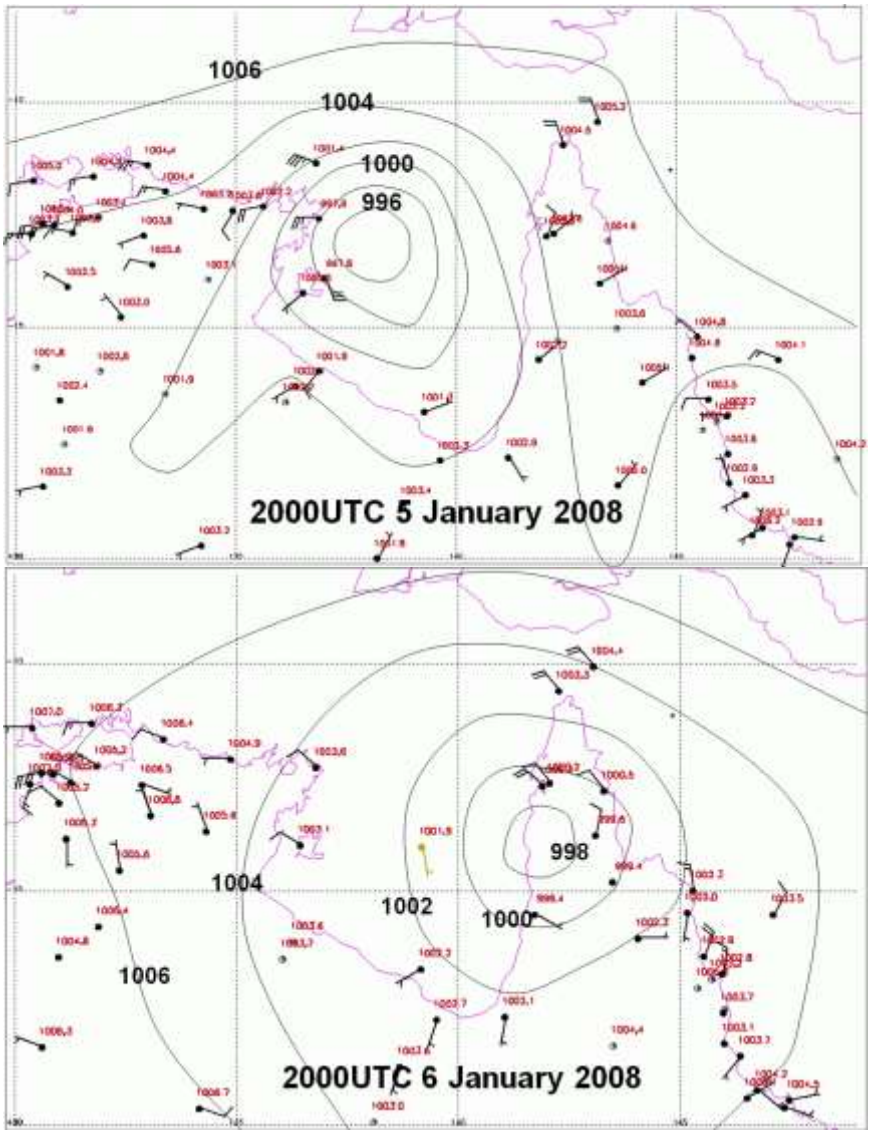

Manual pressure analyses of mean sea level pressure distribution at 6am EST 6 January 2009 (top) and 6am 7 January 2008 (lower frame) with observations of wind speed and direction with mean sea level pressure for verification.

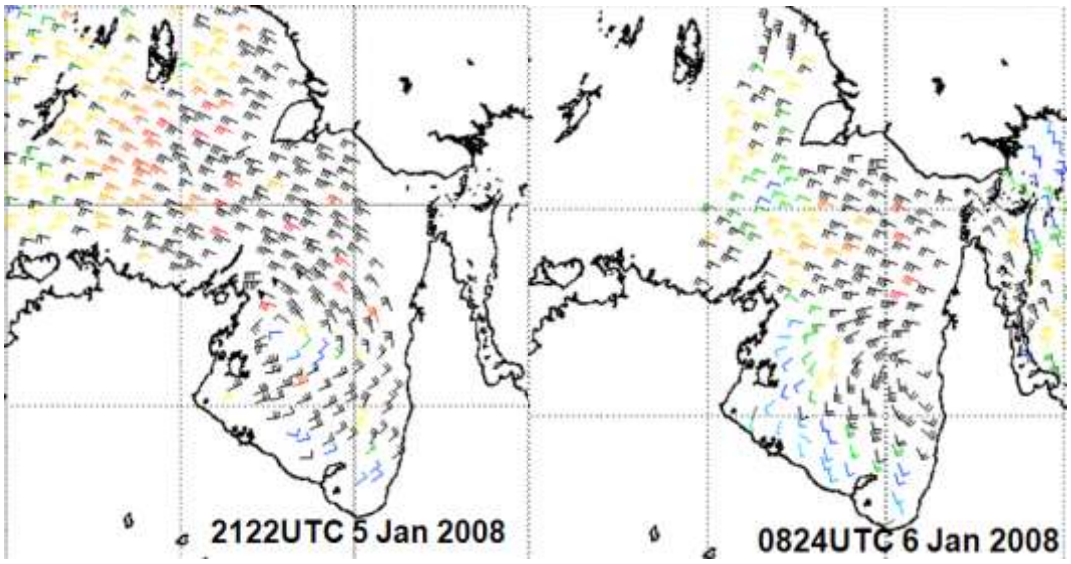

Surface wind observations derived from the quikscat satellite at 7.22am 6 January 2008 (left) and 6.24pm 6 January 2008(right).

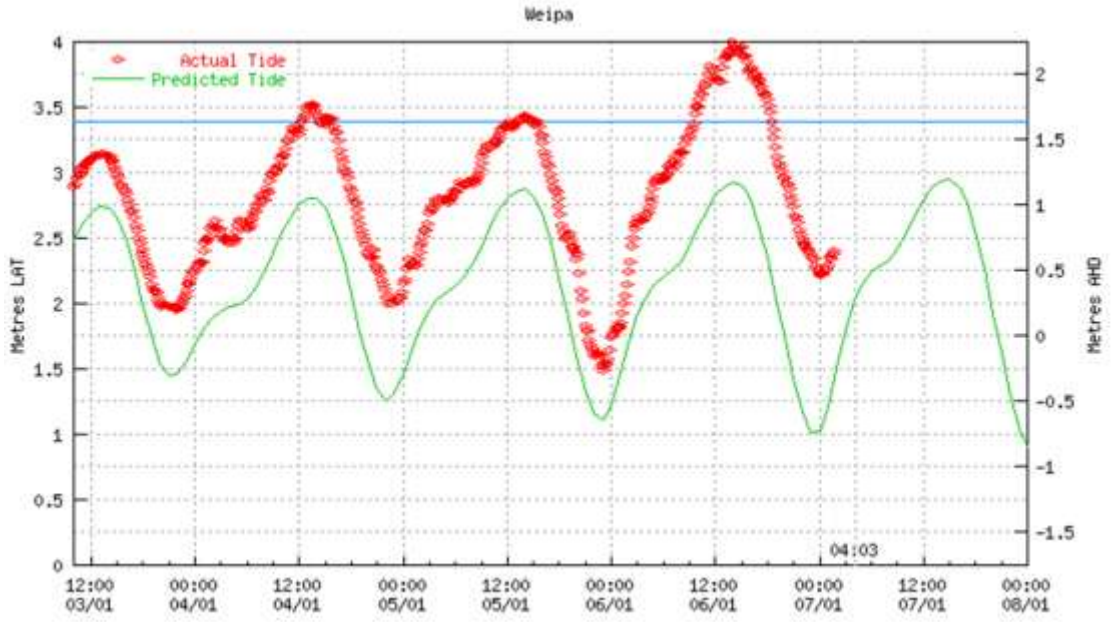

Weipa tide gauge data with the time in EST showing the actual tide levels exceeding predicted levels by over a metre.

TC Charlotte January 2009

This system brought large waves and storm surges into the area where Weipa wave rider buoy measured significant wave heights over 3 metres and the tide gauge recorded levels of over a metre above predicted levels (see below) Peak wave heights just exceeded 6 metres while the peak energy wave period exceeded 10 seconds which indicate high energy wave conditions.

Below are the mean sea level charts together with quikscat satellite wind observations which indicate the large size of the circulation.

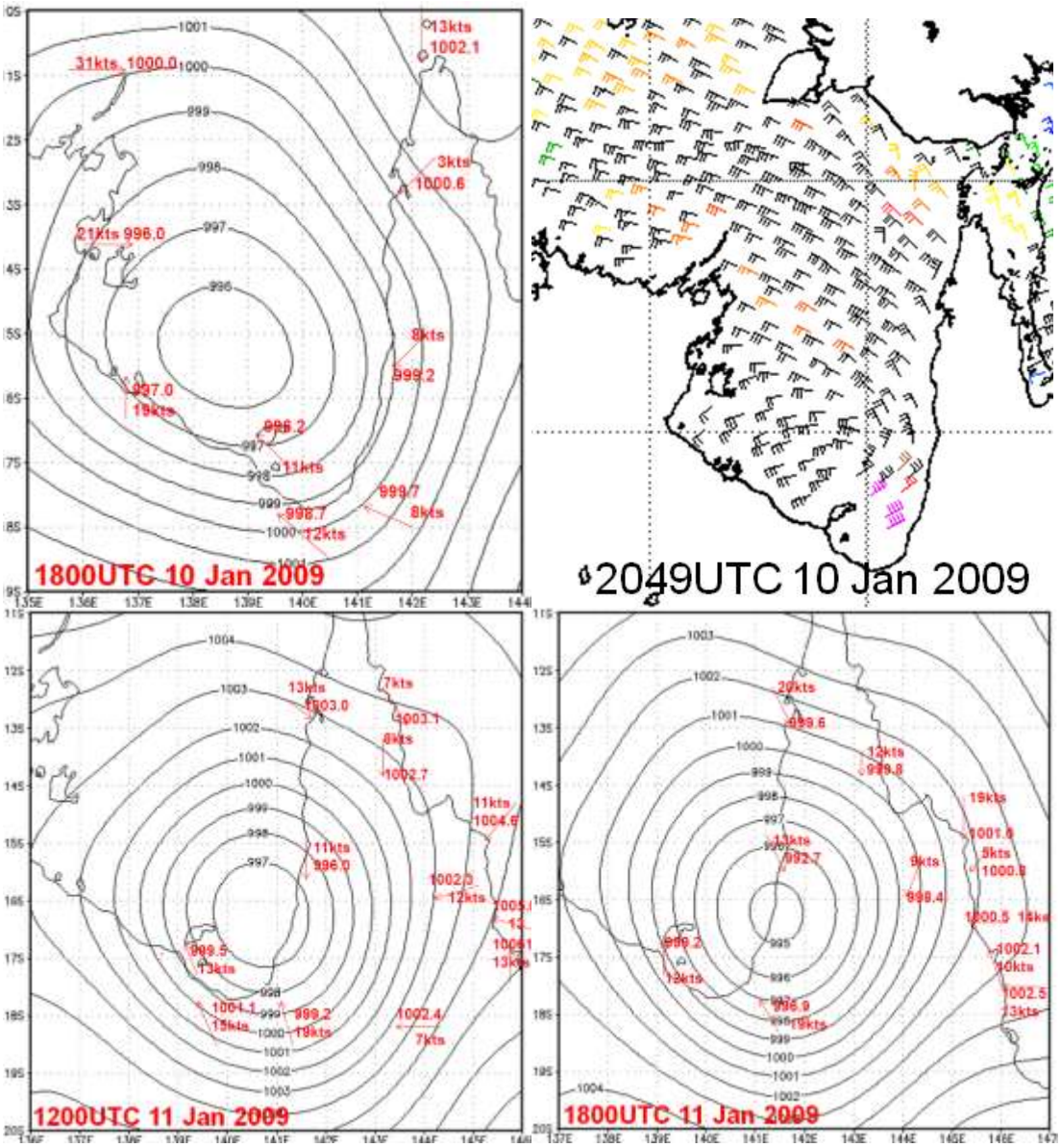

US high resolution computer analyses of mean sea level pressure distribution at 6am EST 11 January 2009 (top left), 10pm 11 January 2009 (lower left) and 4am 12 January 2009 (lower right) with observations of wind speed and direction with mean sea level pressure for verification. The top right are surface wind observations derived from the quikscat satellite at 6.49am 11 January 2009.

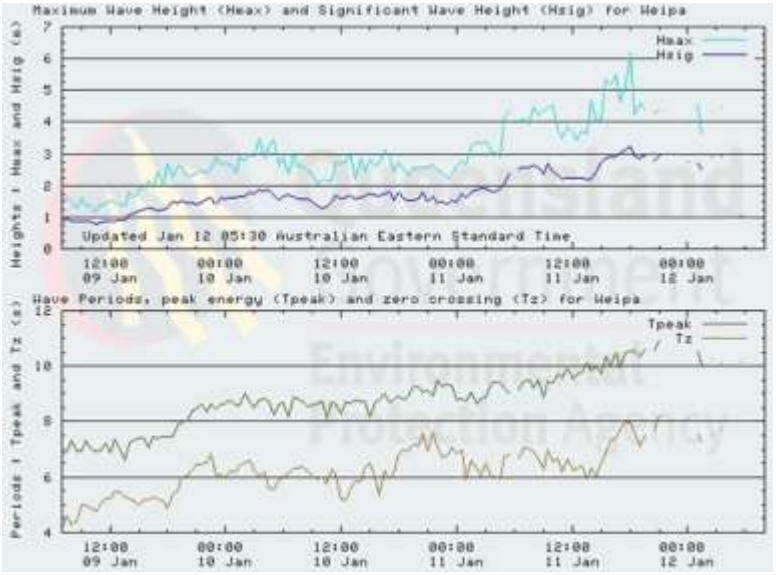

Weipa wave rider buoy data with the time in EST showing the significant wave heights peaking over 3 metres around 11pm 11 January 2009 and the peak heights exceeded 6 metres around the same time.

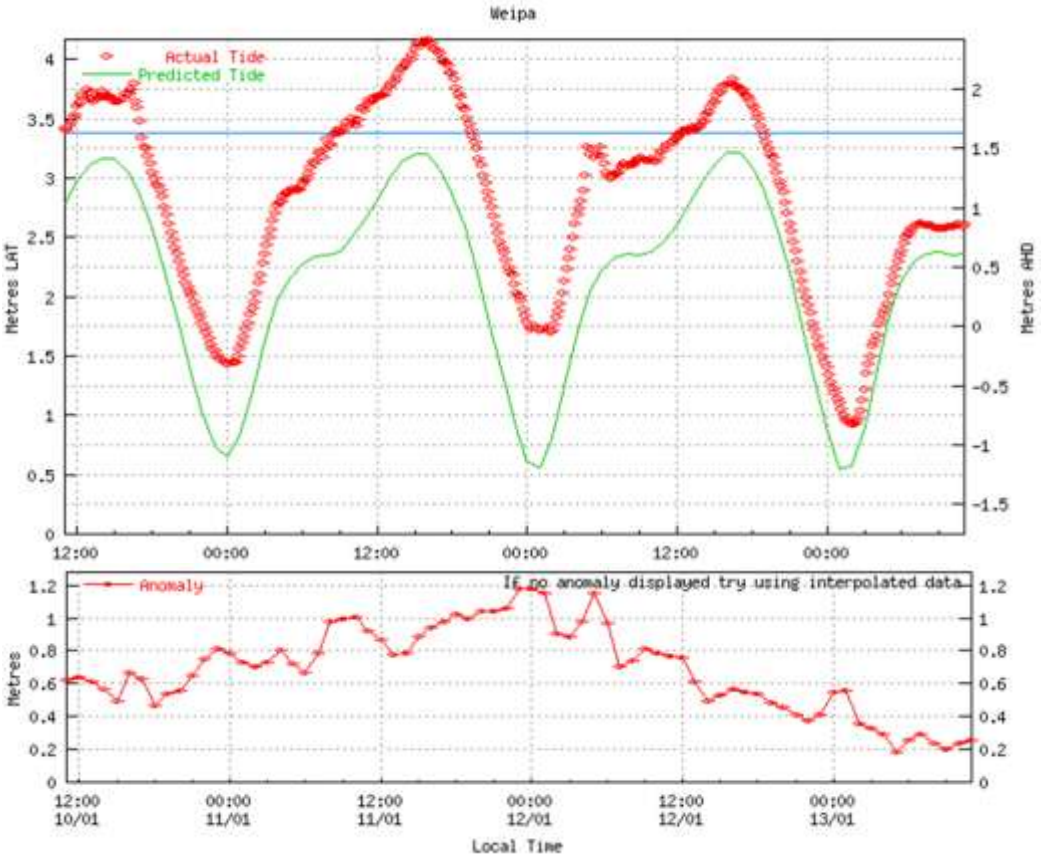

Weipa tide gauge data with the time in EST showing the actual tide levels exceeding predicted levels by over a metre. The lower graph is actual tide minus predicted tide.

Appendix I

Modelled Tropical Cyclone Storm Surge Scenarios

Example Category 4 Storm:

p_c = 940 hPa

R = 20 km

B = 1.8

V_{fm} = 4 ms^{-1}

I-1 West to East over Badu Island

I-2 South West to North East over Dauan Island

I-3 North West to South East west of Prince of Wales Island

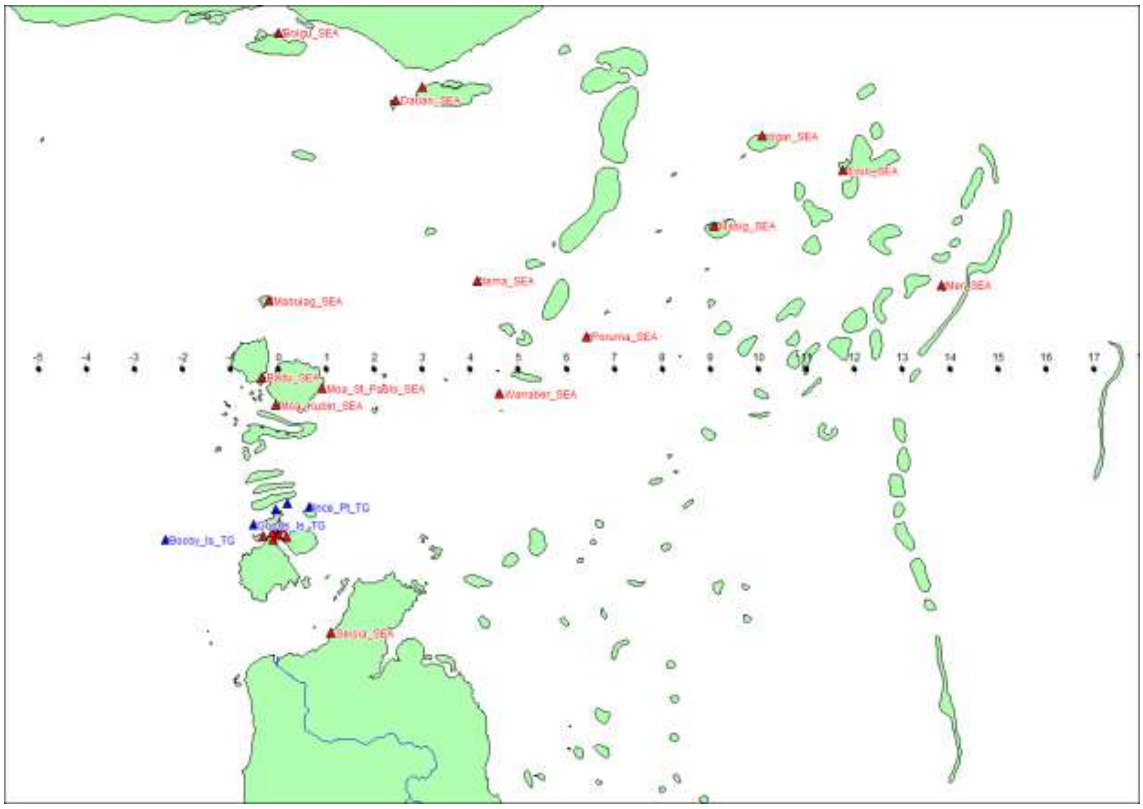

Figure I-1a Example W-E Category 4 TC (track and times)

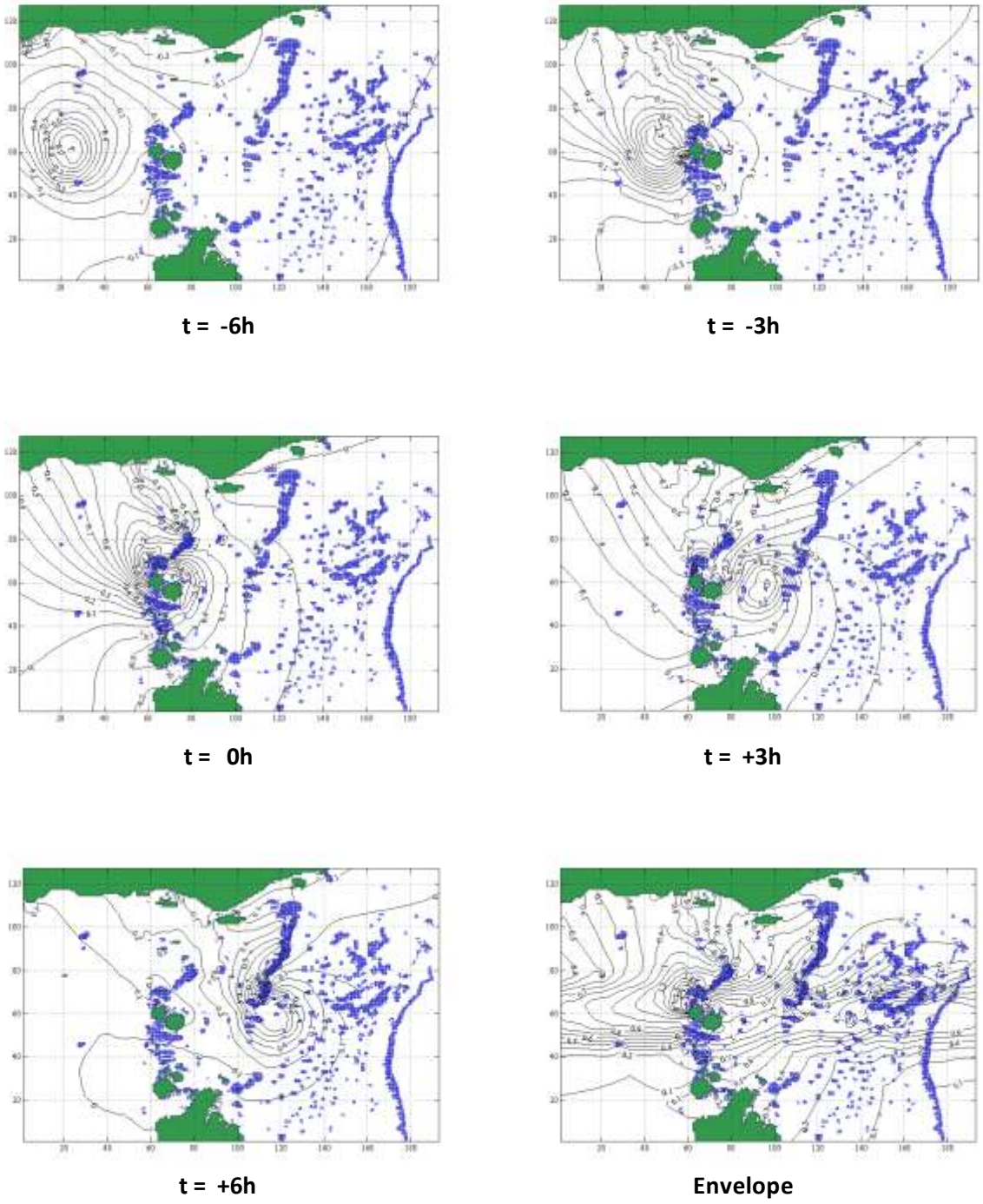

Figure I–1b Example W-E Category 4 TC (surge)

Surge magnitude relative to MSL (0.10m contour interval)

Time in hours shown relative to passing line perpendicular to track through Thursday Island. Envelope is the surface of maximum surge magnitude (0.10m contour interval).

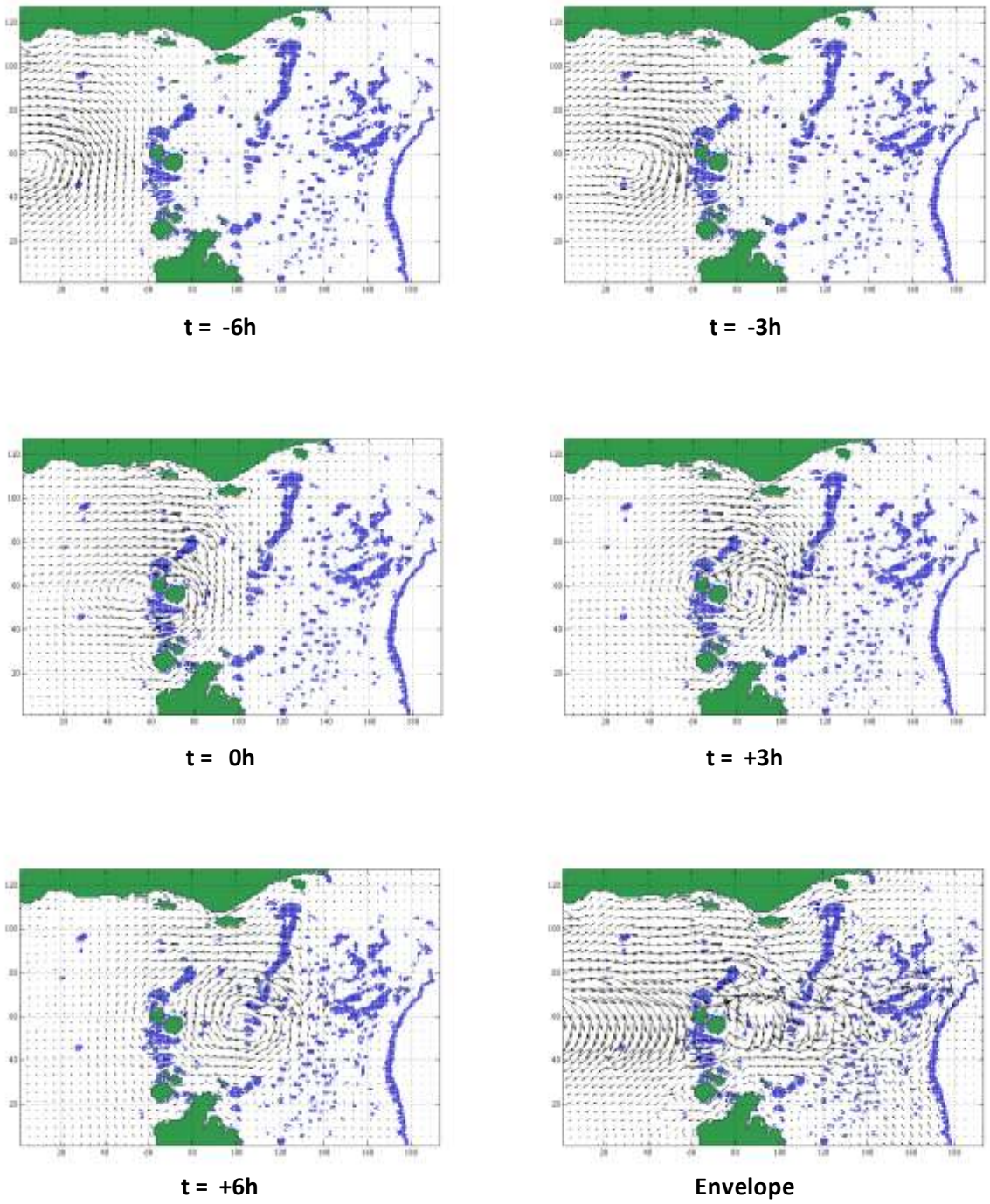

Figure I–1c Example W-E Category 4 TC (currents)

Vector currents(scaled)

Time in hours shown relative to passing line perpendicular to track through Thursday Island. Envelope is the maximum vector current.

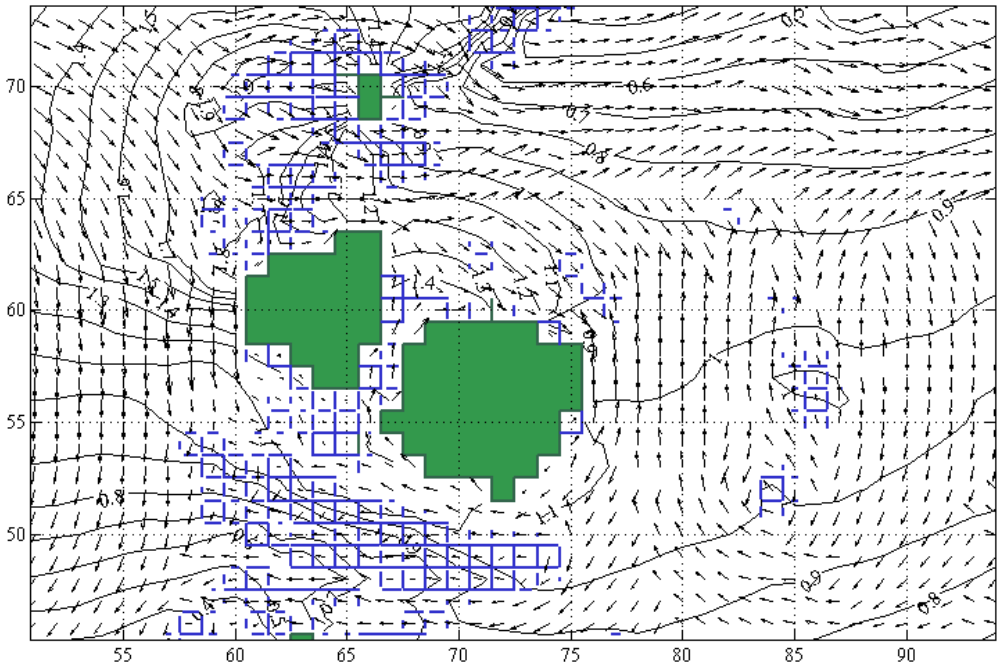

Figure I–1d Example W-E Category 4 TC (detail envelope surge and currents in vicinity Badu)

Badu Island and Moa Island detail showing influence of sub-scale reefs on current and water level envelope patterns.

Table I-1 Summary of W-E peak surge levels.

Community	Surge	Community	Surge
	m		m
Badu_SEA	1.36	Moa_Kubin_SEA	1.18
Boigu_SEA	0.65	Moa_St_Pauls_SEA	1.18
Dauan_SEA	0.37	Muralag_SEA	0.56
Erub_SEA	0.17	Ngurupai_SEA	0.53
Gealug_SEA	0.14	Poruma_SEA	0.70
Hammond_SEA	0.48	Saibai_SEA	0.3
Iama_SEA	0.66	Seisia_SEA	0.13
Mabuiag_SEA	0.97	Ugar_SEA	0.17
Masig_SEA	0.33	Waiben_S_SEA	0.34
Mer_SEA	0.38	Warraber_SEA	0.87

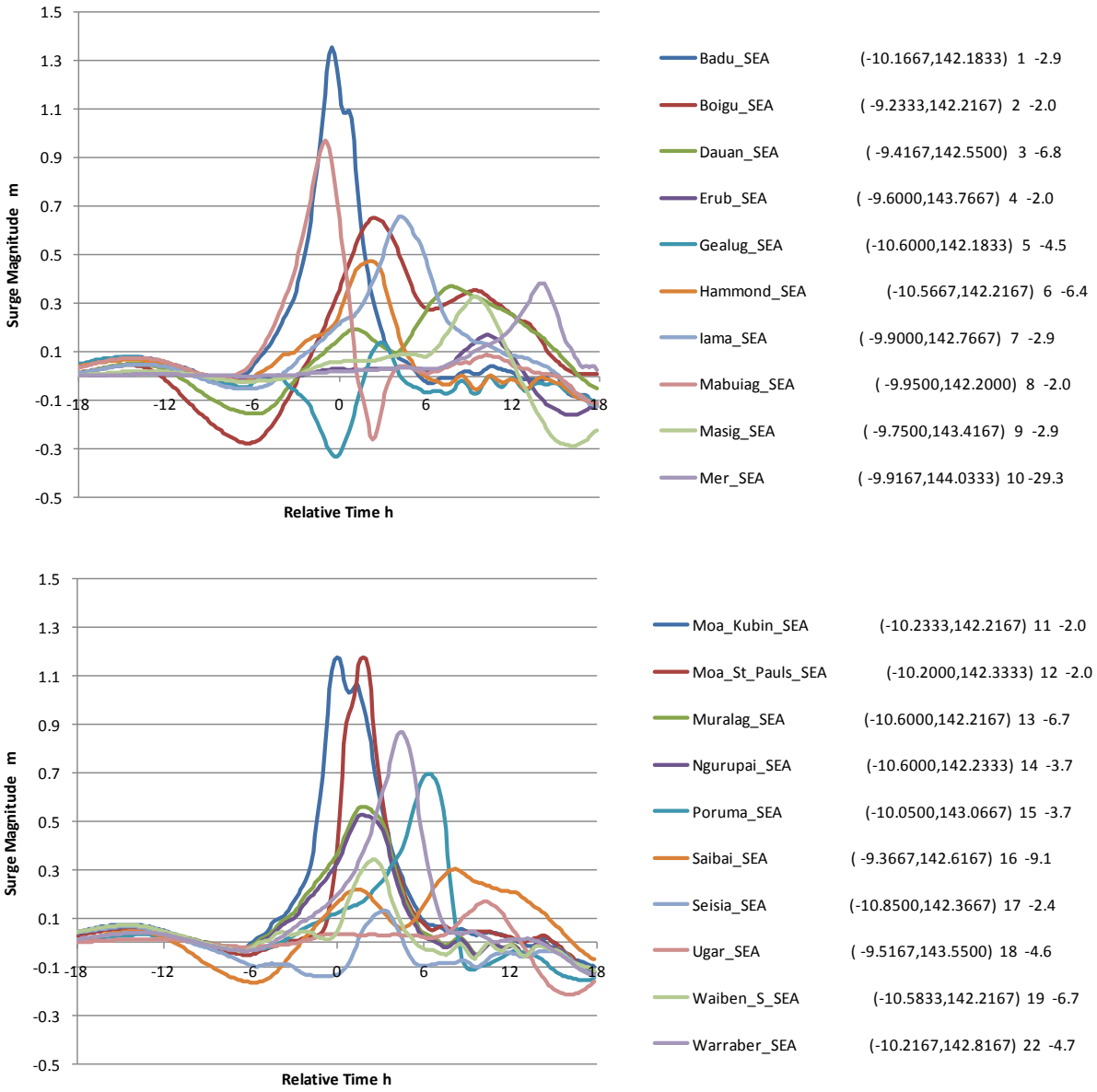

Figure I-1e Example W-E Category 4 TC (time history surge each TSRA community).

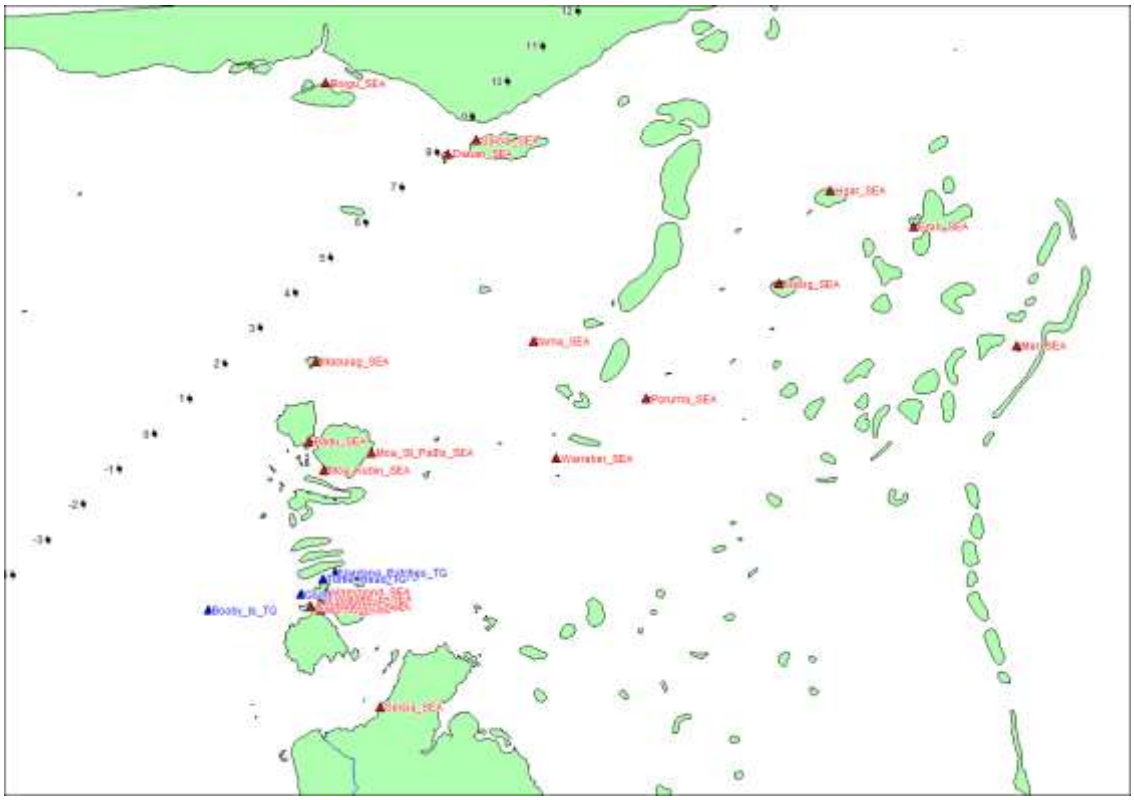

Figure I-2a Example SW-NE Category 4 TC (track and times)

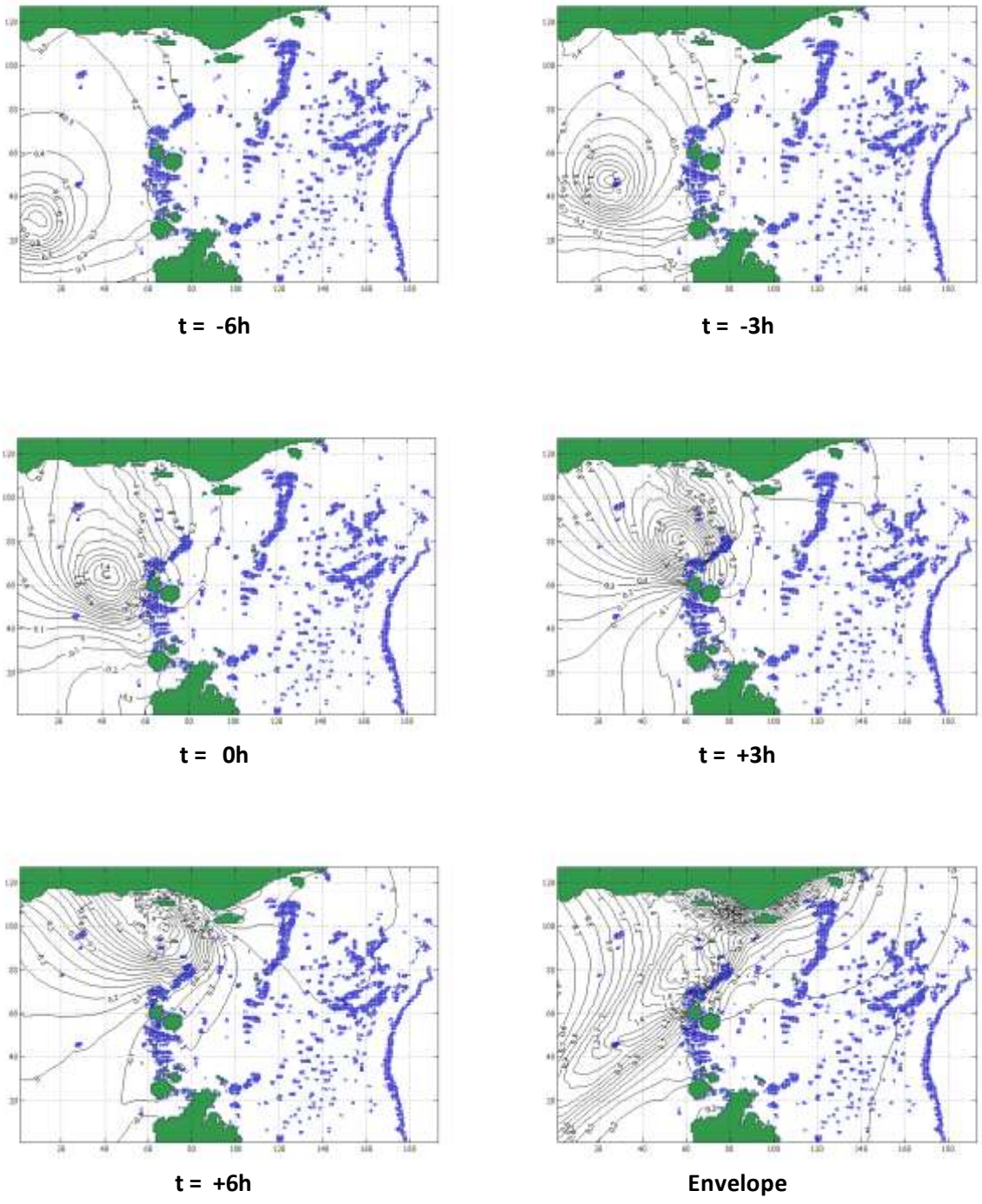

Figure I-2b Example SW-NE Category 4 TC (surge)

Surge magnitude relative to MSL (0.10m contour interval)

Time in hours shown relative to passing line perpendicular to track through Thursday Island. Envelope is the surface of maximum surge magnitude (0.10m contour interval).

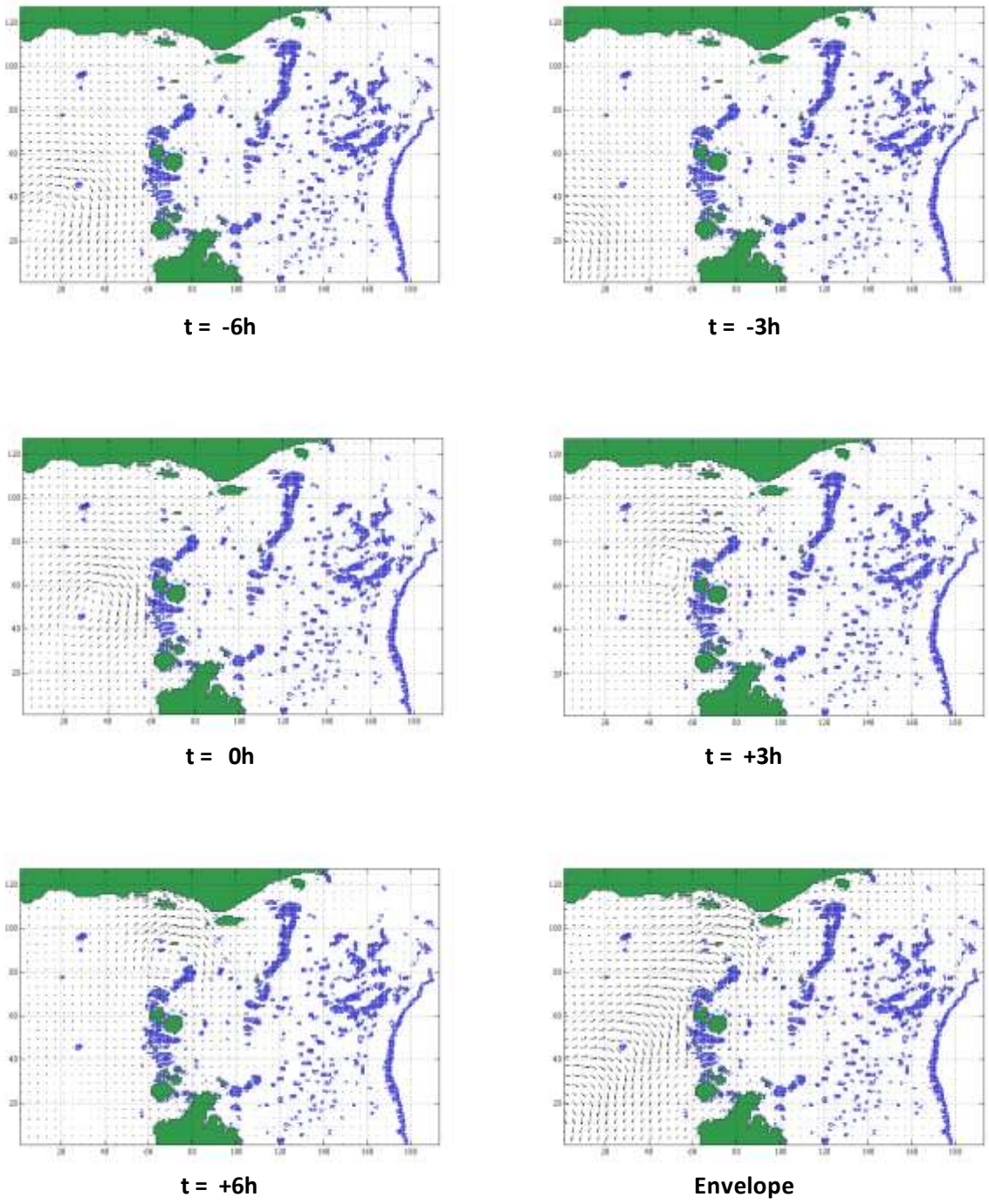

Figure I-2c Example SW-NE Category 4 TC (currents)

Vector currents(scaled)

Time in hours shown relative to passing line perpendicular to track through Thursday Island.Envelope is the maximum vector current.

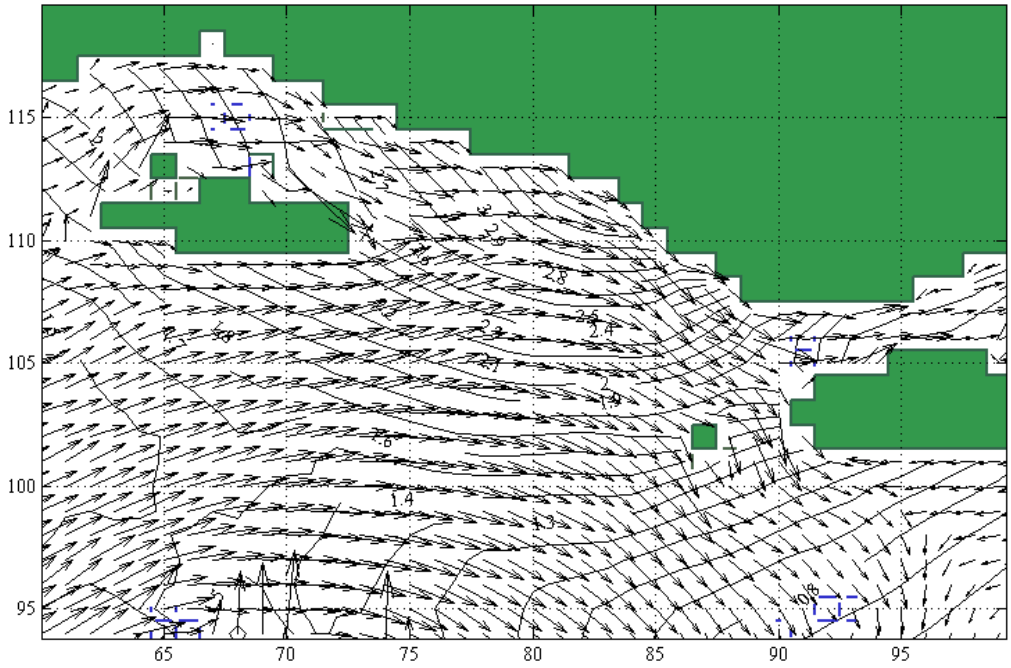

Figure I-2d Example SW-NE Category 4 TC (detail envelope surge and currents in vicinity Boigu and Saibai)

Boigu Island, Dauan and Saibai Island detail showing peak of about 3.5m along coast.

Table I-2 Summary of SW-NE peak surge levels.

Community	Surge	Community	Surge
	m		m
Badu_SEA	0.48	Moa_Kubin_SEA	0.24
Boigu_SEA	2.34	Moa_St_Pauls_SEA	0.15
Dauan_SEA	1.51	Muralag_SEA	0.21
Erub_SEA	0.17	Ngurupai_SEA	0.21
Gealug_SEA	0.27	Poruma_SEA	0.19
Hammond_SEA	0.19	Saibai_SEA	1.64
Iama_SEA	0.22	Seisia_SEA	0.20
Mabuiag_SEA	1.34	Ugar_SEA	0.24
Masig_SEA	0.23	Waiben_S_SEA	0.20
Mer_SEA	0.06	Warraber_SEA	0.18

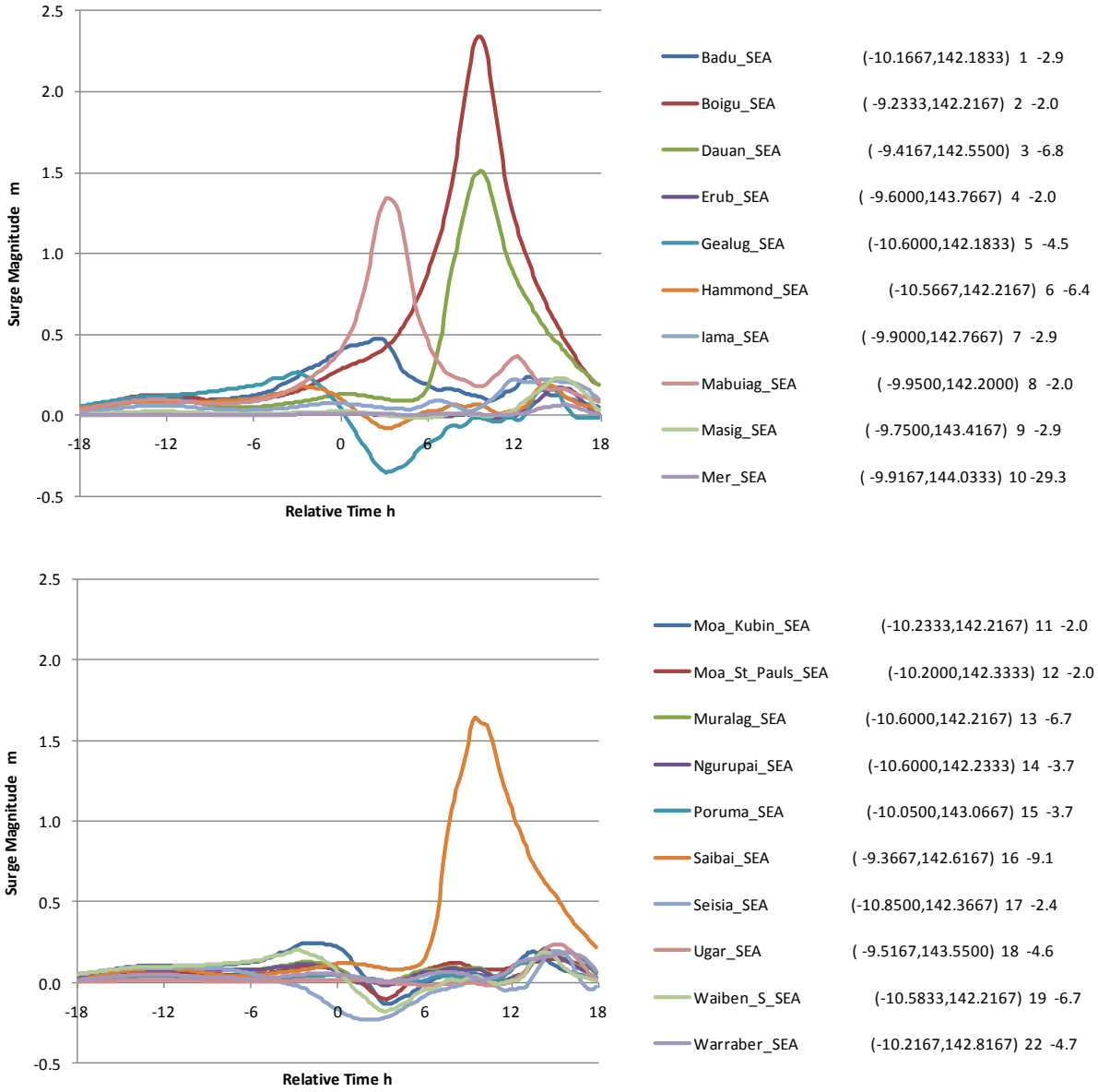

Figure I-2e Example SW-NE Category 4 TC (time history surge each TSRA community)

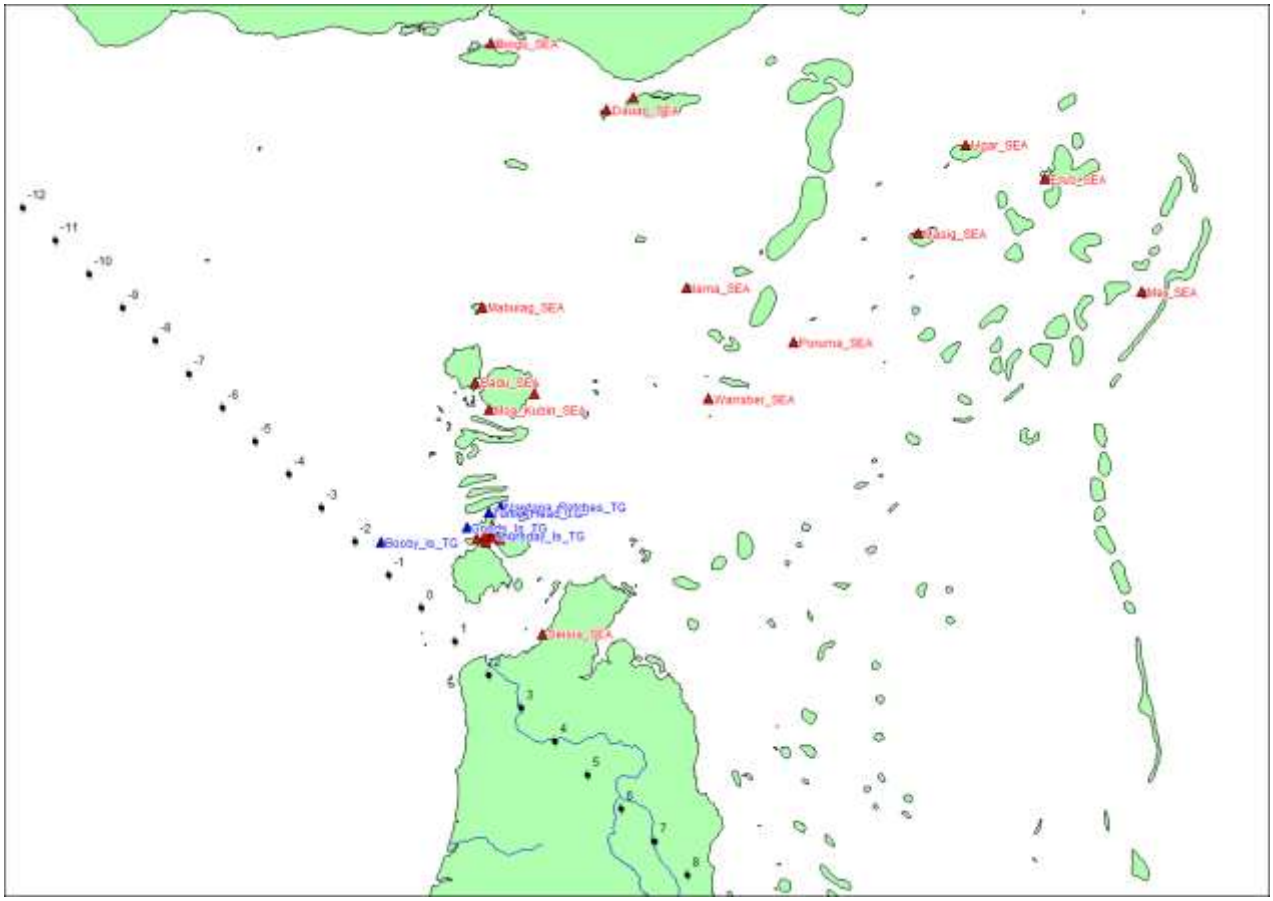

Figure I-3a Example NW-SE Category 4 TC (track and times)

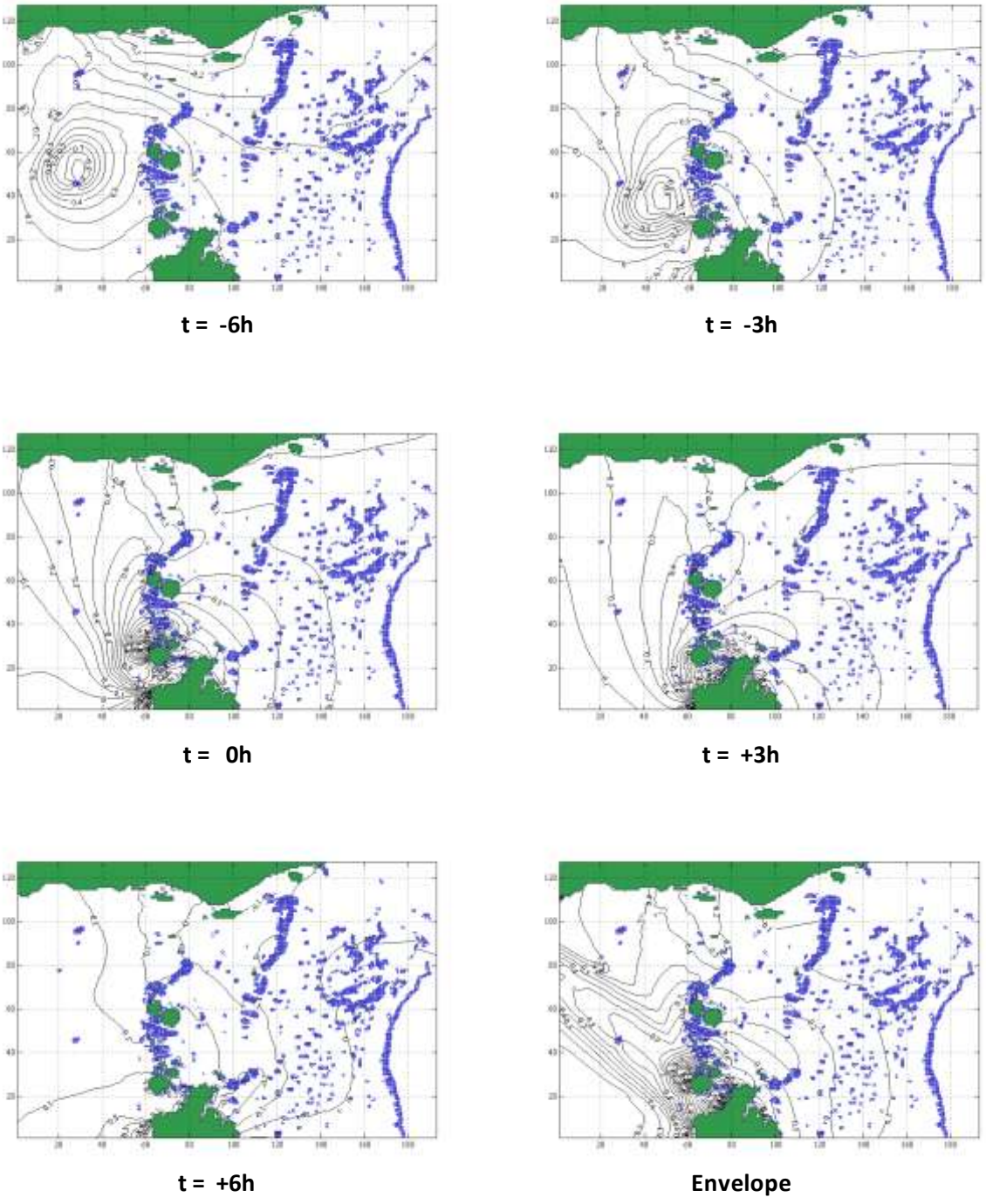

Figure I-3b Example NW-SE Category 4 TC (surge)

Surge magnitude relative to MSL (0.10m contour interval)

Time in hours shown relative to passing line perpendicular to track through Thursday Island. Envelope is the surface of maximum surge magnitude (0.10m contour interval).

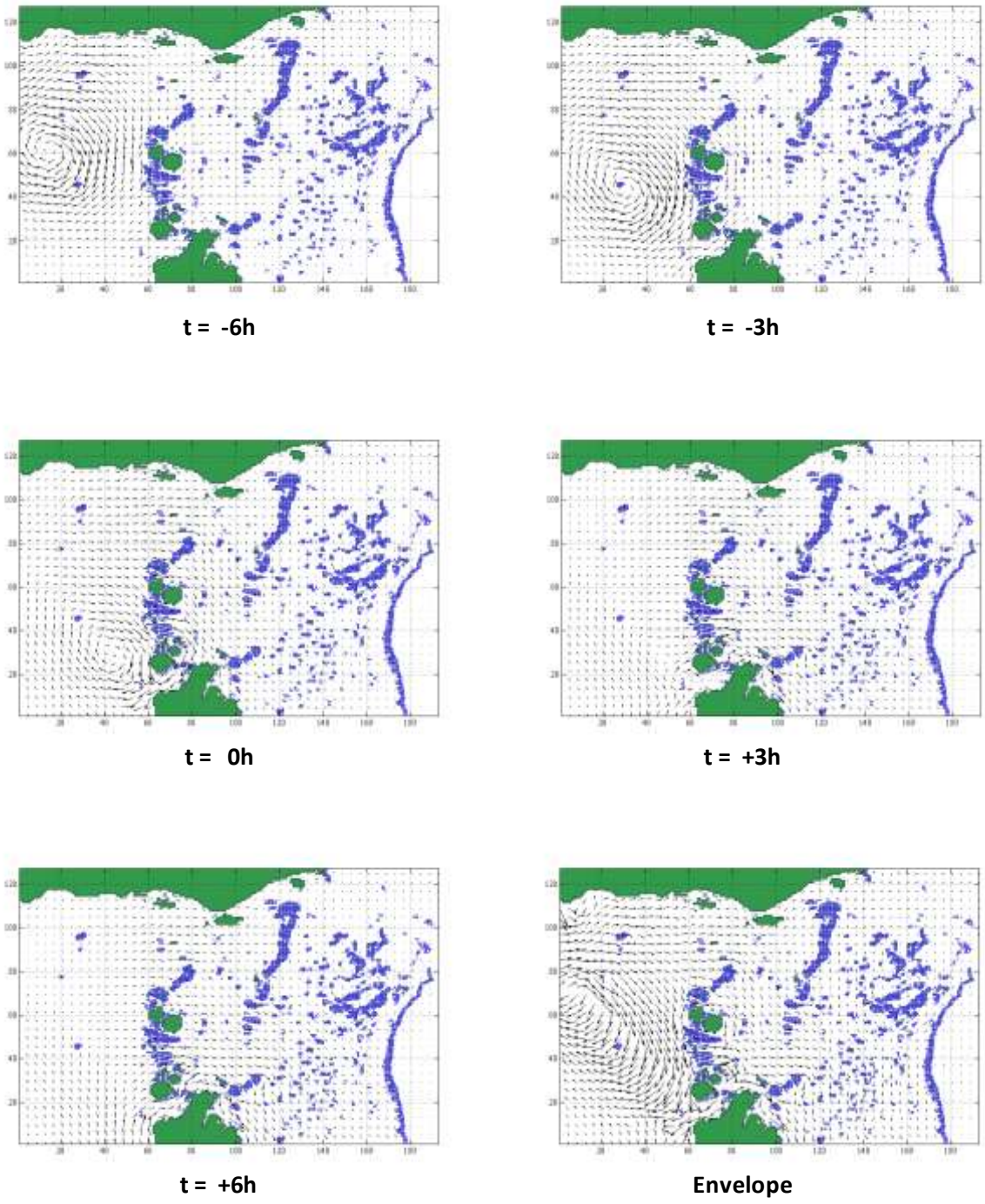

Figure I-3c Example NW-SE Category 4 TC (currents)

Vector currents(scaled to be 0.25 m/s per grid size, every 4th vector shown)

Time in hours shown relative to passing line perpendicular to track through Thursday Island. Envelope is the maximum vector current.

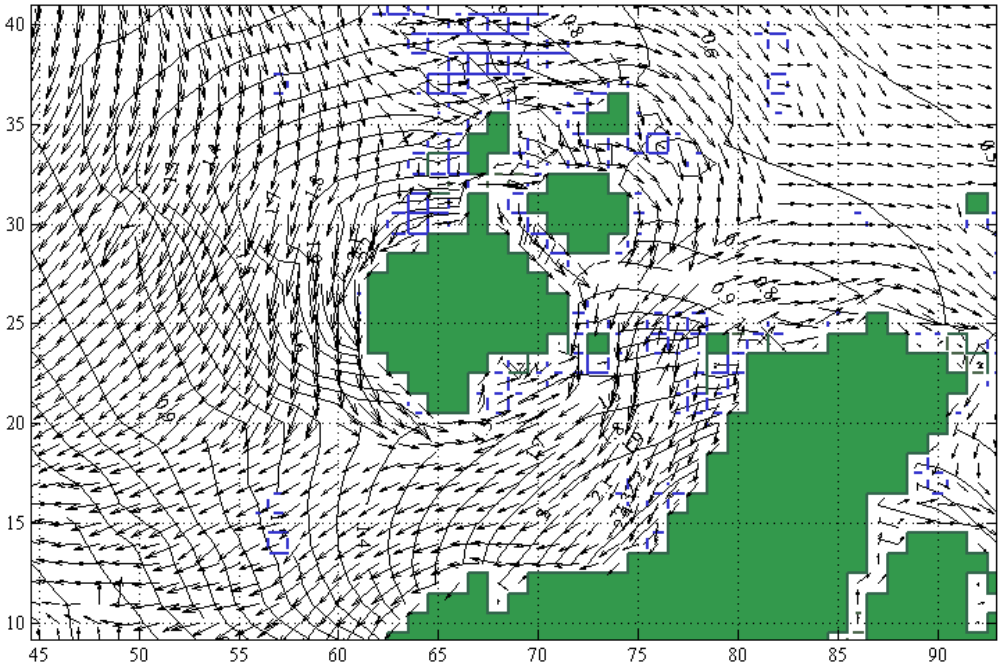

Figure I-3d Example NW-SE Category 4 TC (detail envelope surge and currents in vicinity of Cape York and Seisa)

Table I-3 Summary of NW-SE Category 4 peak surge levels.

Community	Surge	Community	Surge
	m		m
Badu_SEA	0.53	Moa_Kubin_SEA	0.64
Boigu_SEA	0.25	Moa_St_Pauls_SEA	0.26
Dauan_SEA	0.12	Muralag_SEA	1.66
Erub_SEA	0.04	Ngurupai_SEA	1.66
Gealug_SEA	2.27	Poruma_SEA	0.14
Hammond_Sea	1.24	Saibai_SEA	0.12
Iama_SEA	0.16	Seisia_SEA	2.74
Mabuiag_SEA	0.30	Ugar_SEA	0.04
Masig_SEA	0.07	Waiben_S_SEA	1.60
Mer_SEA	0.02	Warraber_SEA	0.25

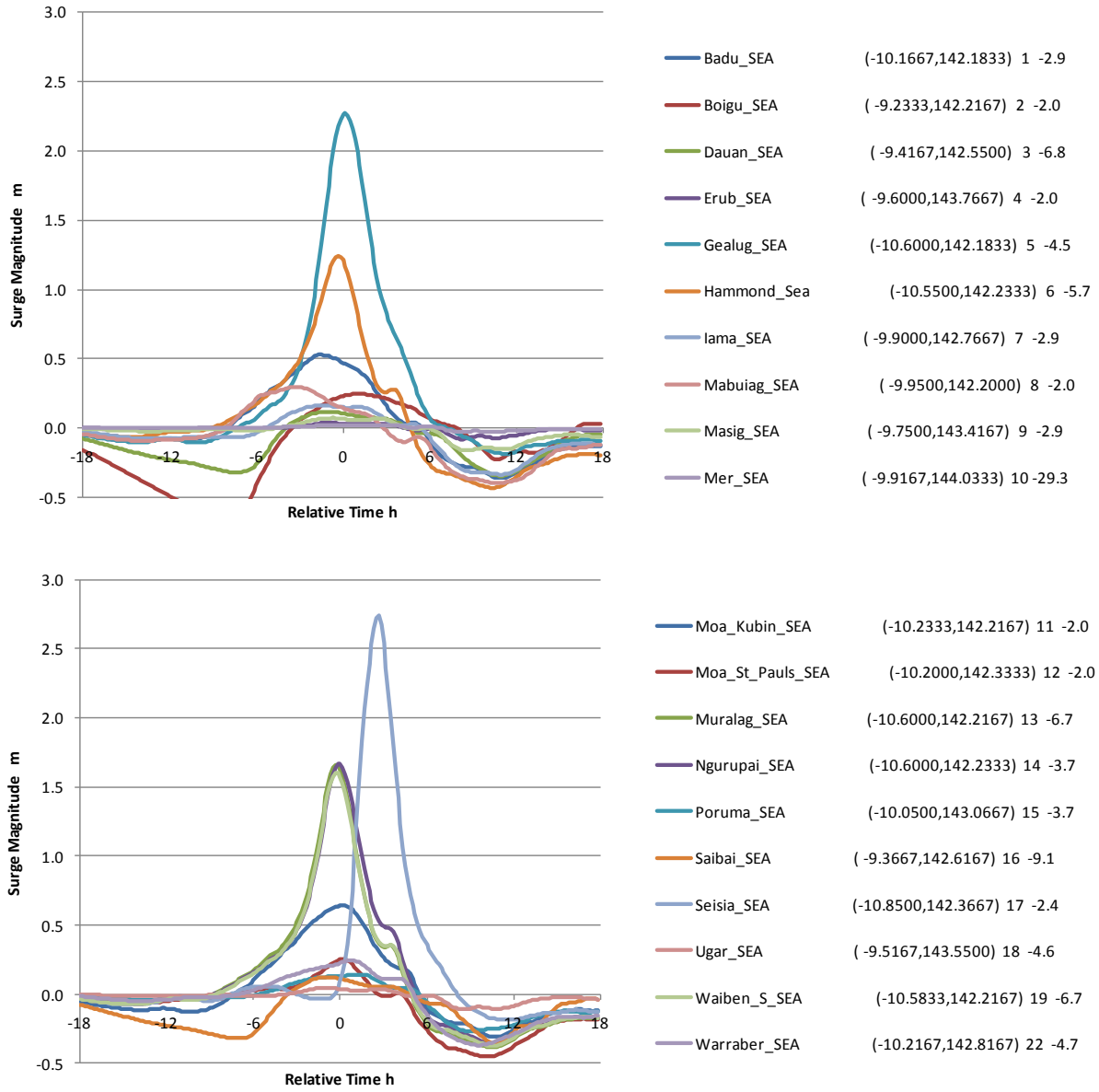

Figure I-3e Example NW-SE Category 4 TC (time history surge each TSRA community)

Appendix J

Tropical Cyclone Storm Surge Model Resolution Sensitivity Testing

Two C domain 371 m sub-grids were tested to determine if the B domain 1853 m resolution would still be satisfactory in the Thursday Island and northernmost island situations where it was thought some loss of resolution might adversely affect the results.

A NW-SE Category 4 TC (refer previous Appendix) was chosen to test the Thursday Island situation and a SW-NW TC for the northernmost sites.

Table I-1 summarises the peak modelled surge levels for the Thursday Island case, showing the results for co-located B and C locations and the true C location. Figures I-2 and I-3 illustrate the issue that required some minor correction of depths, reefs and barriers near Thursday Island to obtain these results. No corrections were needed to adequately reproduce tides.

Table I-2 summarises the peak modelled surge levels for the northernmost islands case, again showing the results for co-located B and C locations and the true C location. No changes to the B domain were required to achieve these results.

These extreme TC events are used as examples of the worst case scenarios likely to affect any of these locations.

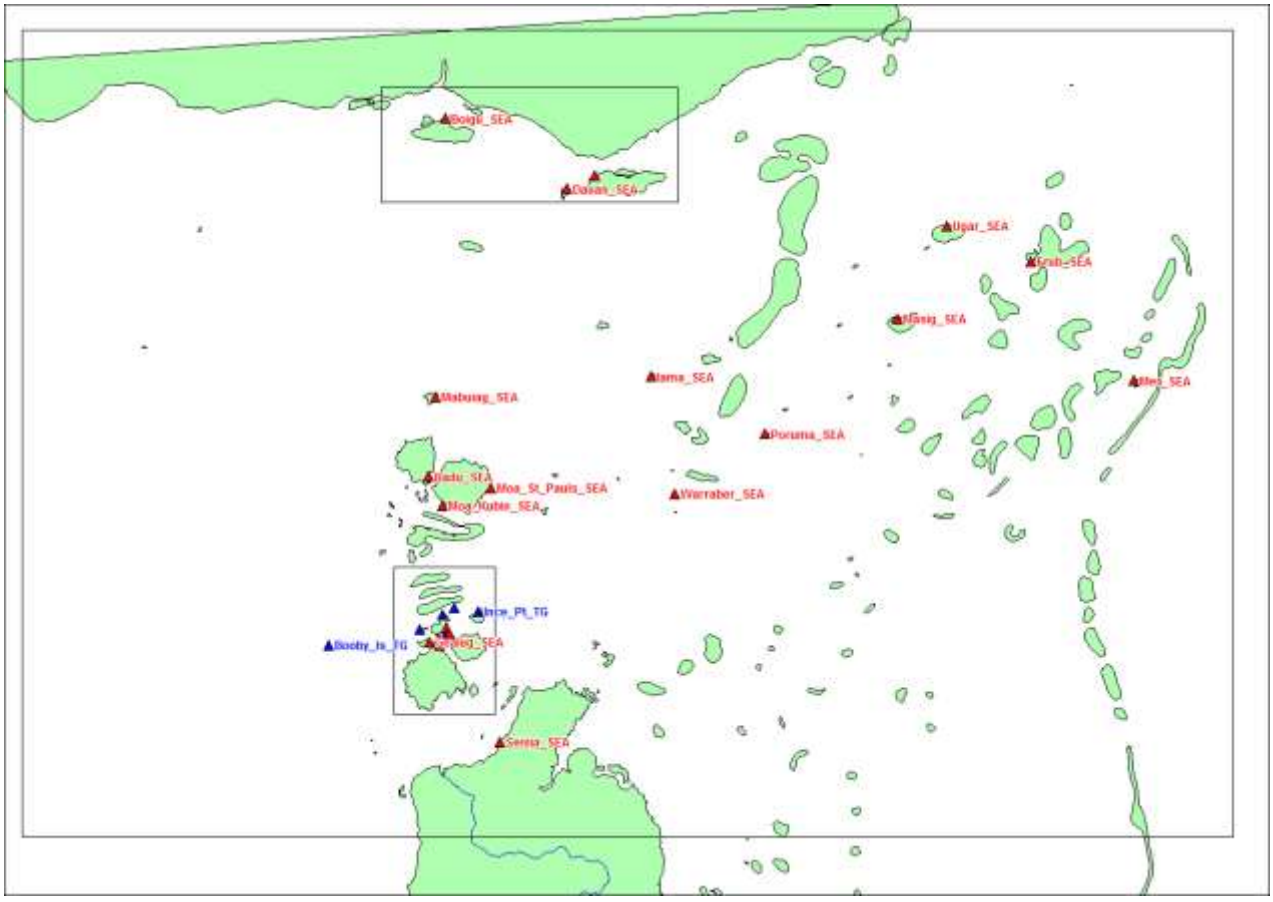

Figure J-1 Location of 371 m resolution C grids used for model resolution sensitivity testing using NW-SE track (vicinity Thursday Island) and SW-NE track (vicinity Boigu and Saibai Islands).

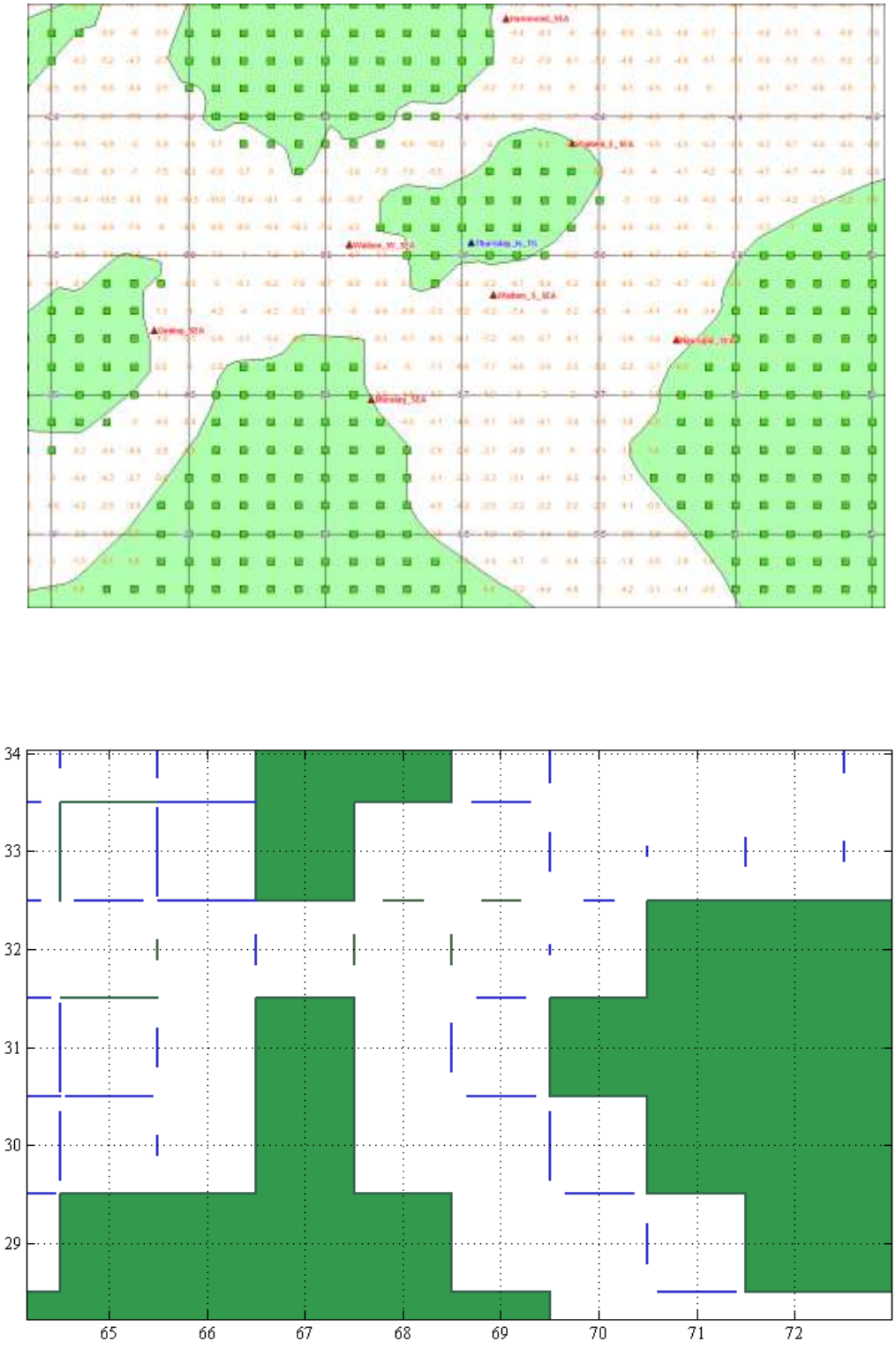

Figure J-2 Similar areas of the MMUSURGE C grid (above) showing depths and the B grid (below) in the vicinity of Thursday Island.

The C grid has no sub-scale flow features, while the B grid has a combination of reef and barrier boundary conditions to make up for the fact that Thursday Island is too small to resolve on the 1 nmile grid (shown as background grid in top figure).

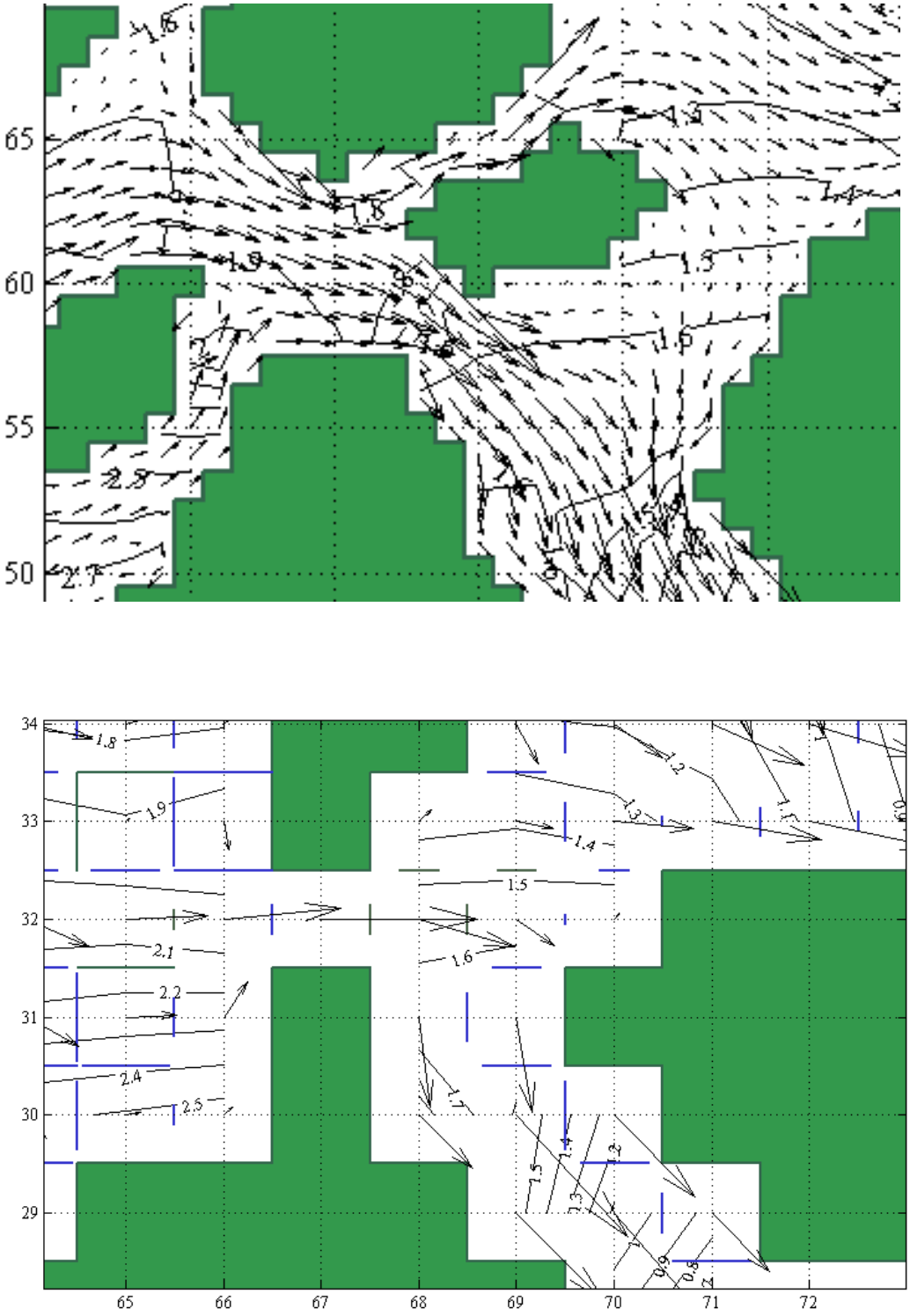

Figure J-3 Surge contours and flow vectors for the SE example at time 0hr in the C grid (above) and the B grid (below) in the vicinity of Thursday Island.

Surge magnitude relative to MSL (0.10m contour interval)

Current vectors are scaled to be 1 m/s relative to the grid size in each case.

Table J-1 Summary of NW-SE Category 4 peak surge level (m) sensitivity.

		C Grid Location Matched to B			C Grid Location True		
	B	C	B->C	%	C	B->C	%
Badu_SEA	0.53						
Boigu_SEA	0.25						
Dauan_SEA	0.12						
Gealug_SEA	2.27	2.27	0.00	0.0	1.99	-0.28	-12.3
Hammond_Sea	1.24	1.2	-0.04	-3.2	1.23	-0.01	-0.8
Mabuiag_SEA	0.30						
Moa_Kubin_SEA	0.64						
Moa_St_Pauls_SEA	0.26						
Muralag_SEA	1.66	1.66	0.00	0.0	1.69	0.03	1.8
Ngurupai_SEA	1.66	1.63	-0.03	-1.8	1.68	0.02	1.2
Saibai_SEA	0.12						
Seisia_SEA	2.74						
Waiben_S_SEA	1.60	1.52	-0.08	-5.0	1.54	-0.06	-3.8
Waiben_W_SEA	1.78	1.85	0.07	3.9	1.89	0.11	6.2
Waiben_E_SEA	1.40	1.32	-0.08	-5.7	1.35	-0.05	-3.6

Table J-2 Summary of SW-NE Category 4 peak surge level (m) sensitivity.

		C Grid Location Matched to B Grid			C Grid Location True		
	B	C	B->C	%	C	B->C	%
Badu_SEA	0.48						0.0
Boigu_SEA	2.34	2.34	0.00	0.0	2.34	0.00	0.0
Dauan_SEA	1.51	1.49	-0.02	-1.3	1.55	0.04	2.6
Gealug_SEA	0.25						
Hammond_Sea	0.20						
Mabuiag_SEA	1.34						
Moa_Kubin_SEA	0.24						
Moa_St_Pauls_SEA	0.15						
Muralag_SEA	0.20						
Ngurupai_SEA	0.20						
Saibai_SEA	1.64	1.59	-0.05	-3.0	1.56	-0.08	-4.9
Seisia_SEA	0.20						
Waiben_S_SEA	0.20						
Waiben_W_SEA	0.21						
Waiben_E_SEA	0.20						

Appendix K

Comparison of Steady-State and Unsteady Fetch-Limited Wave Models under Regionally-Modified NCEP Wind Forcing

For the four years 1949 to 1952.

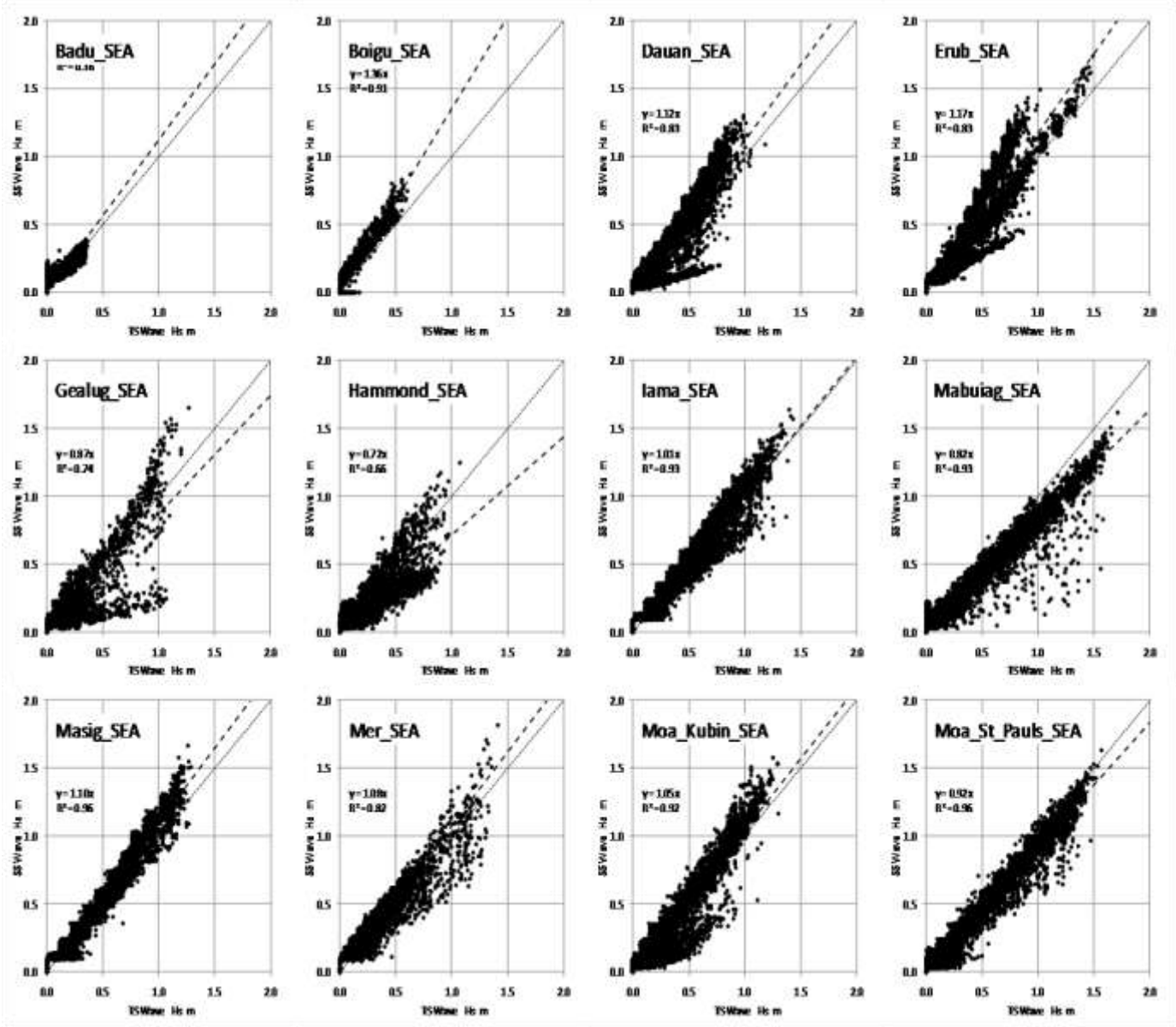
Badu_SEA
Boigu_SEA
y= 1.36x
R²=0.91
Dauan_SEA
y= 1.32x
R²=0.83
Erub_SEA
y= 1.17x
R²=0.83
Gealug_SEA
y= 0.87x
R²=0.74
Hammond_SEA
y= 0.72x
R²=0.66
Iama_SEA
y= 1.03x
R²=0.93
Mabuiag_SEA
y= 0.82x
R²=0.93
Masig_SEA
y= 1.10x
R²=0.96
Mer_SEA
y= 1.08x
R²=0.82
Moa_Kubin_SEA
y= 1.05x
R²=0.92
Moa_St_Pauls_SEA
y= 0.92x
R²=0.96
SS Wave Hs m
TS Wave Hs m
0.0
0.5
1.0
1.5
2.0

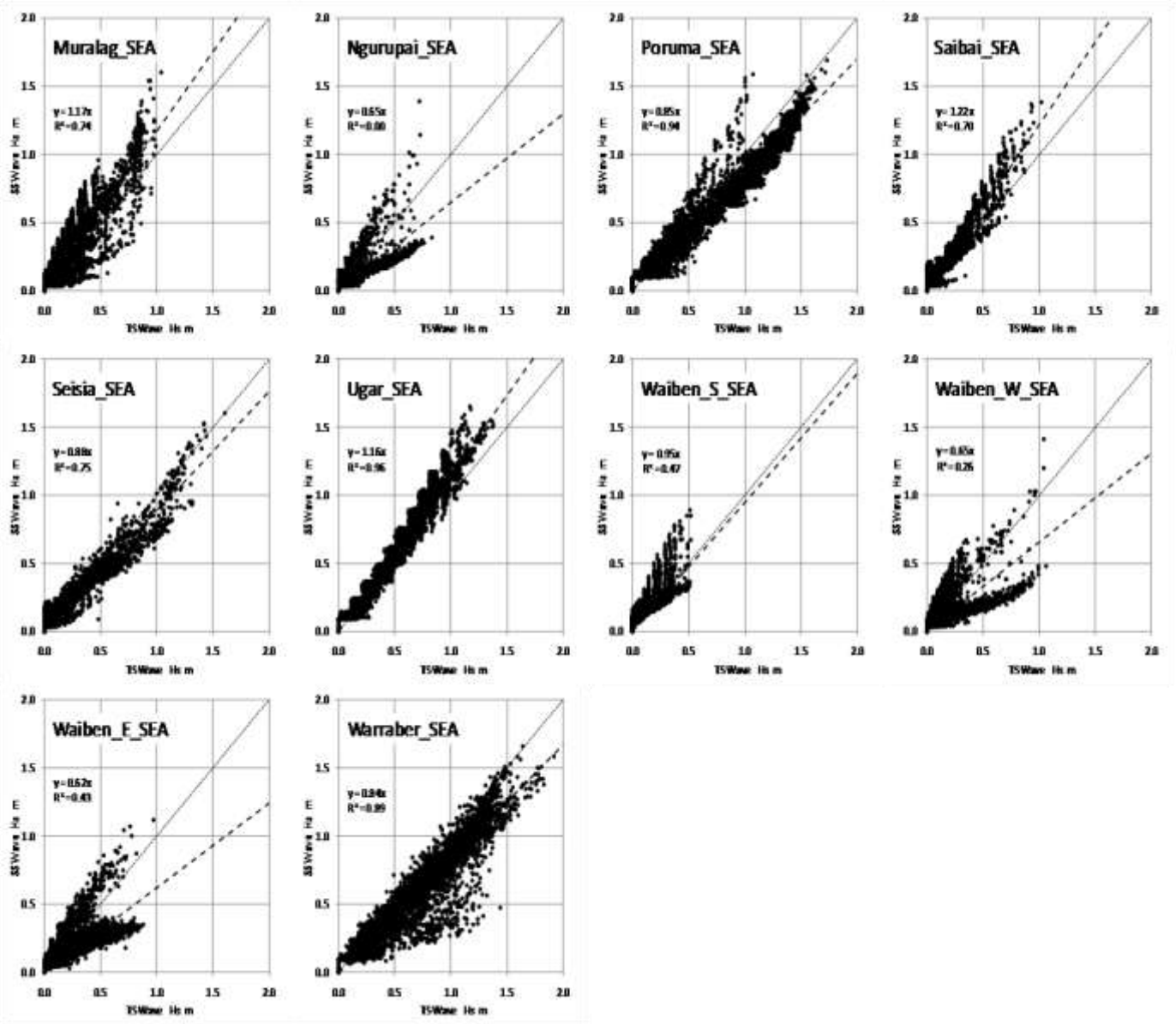
Muralag_SEA
Ngurupai_SEA
Poruma_SEA
Saibai_SEA
Seisia_SEA
Ugar_SEA
Waiben_S_SEA
Waiben_W_SEA
Waiben_E_SEA
Warraber_SEA
TSWave Hs m

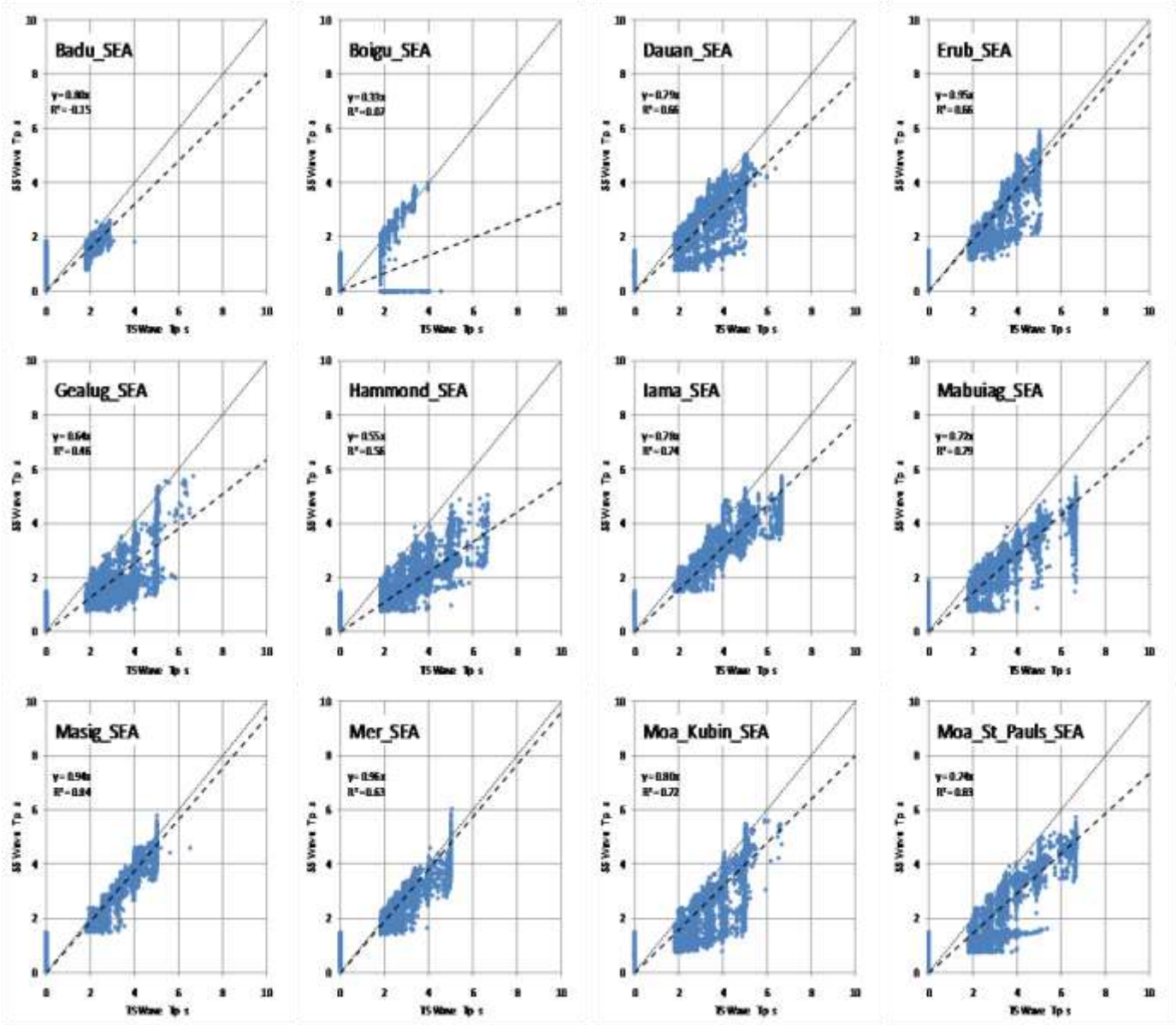
Badu_SEA
Boigu_SEA
Dauan_SEA
Erub_SEA
Gealug_SEA
Hammond_SEA
Iama_SEA
Mabuiag_SEA
Masig_SEA
Mer_SEA
Moa_Kubin_SEA
Moa_St_Pauls_SEA
SS Wave Tp s
TS Wave Tp s

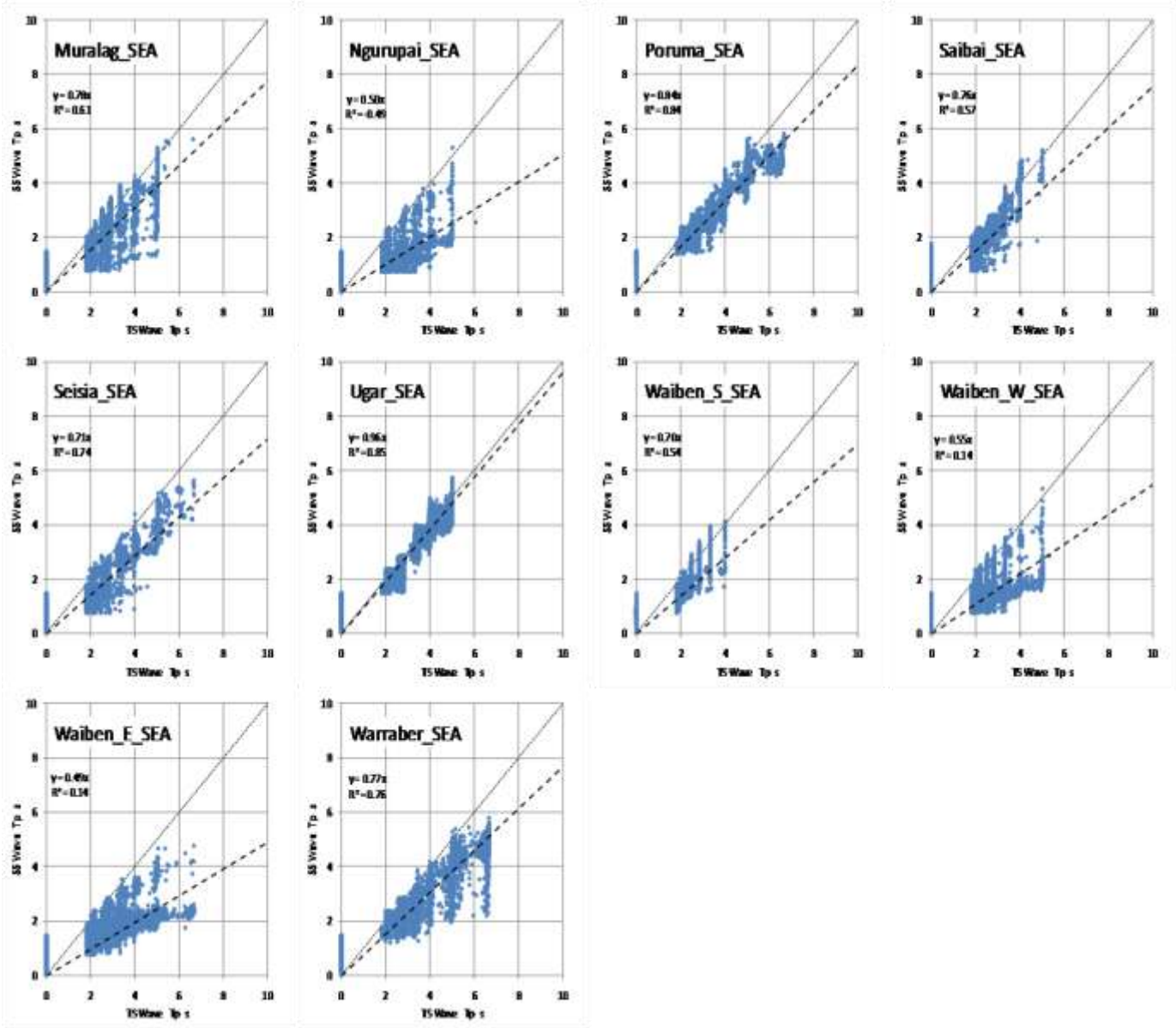
Muralag_SEA
Ngurupai_SEA
Poruma_SEA
Saibai_SEA
Seisia_SEA
Ugar_SEA
Waiben_S_SEA
Waiben_W_SEA
Waiben_E_SEA
Warraber_SEA
TS Wave Tp s

Appendix L

Comparison of Unsteady Fetch-Limited Spectral Wave Model *TS_Wave* and *ADFA1* Spectral Wave Model for Selected Extreme Tropical Cyclone Scenarios

Example Category 4 Storm:

p_c = 940 hPa

R = 20 km

B = 1.8

V_{fm} = 4 ms^{-1}

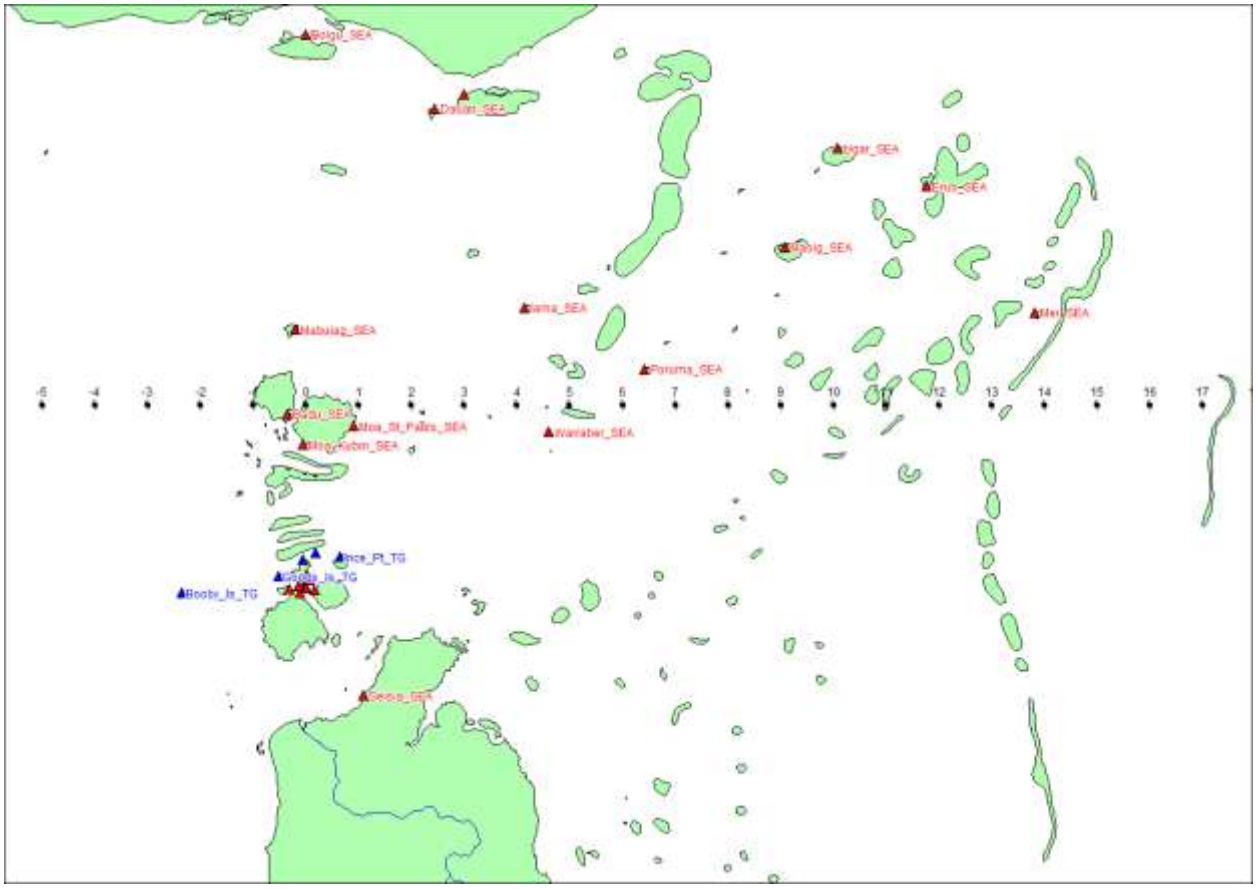

Figure L-1a Example W-E Category 4 TC through Centre (track and times in hours)

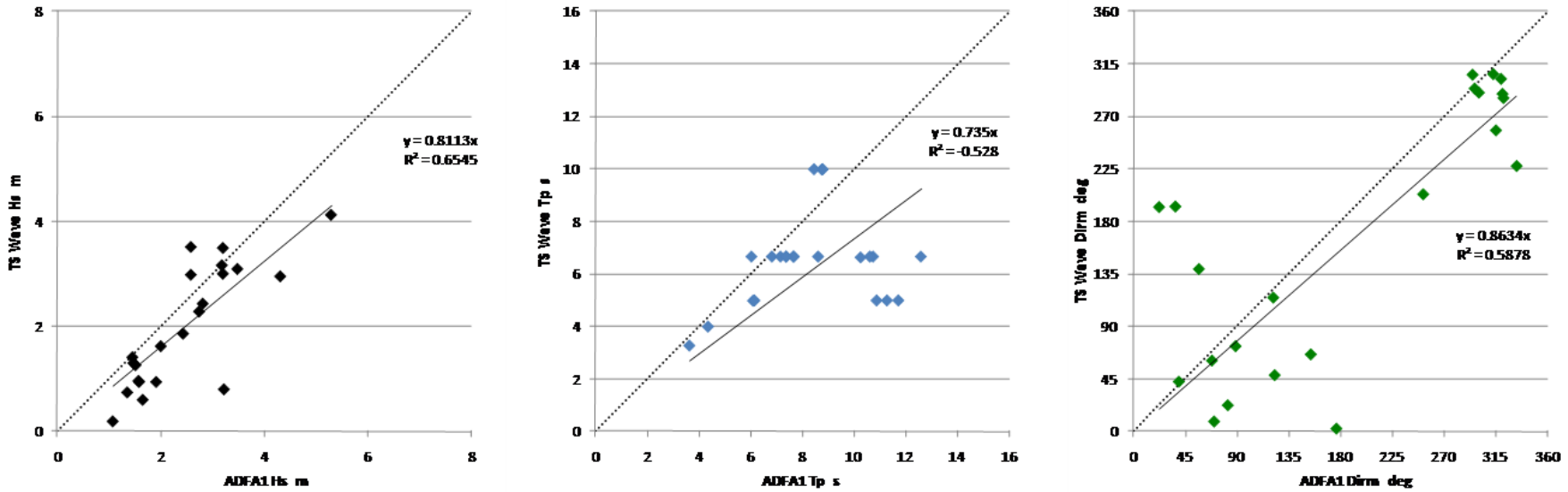

Figure L-1b Example W-E Category 4 TC through Centre (peak site-specific Hs summary and associated Tp and Mean Direction)

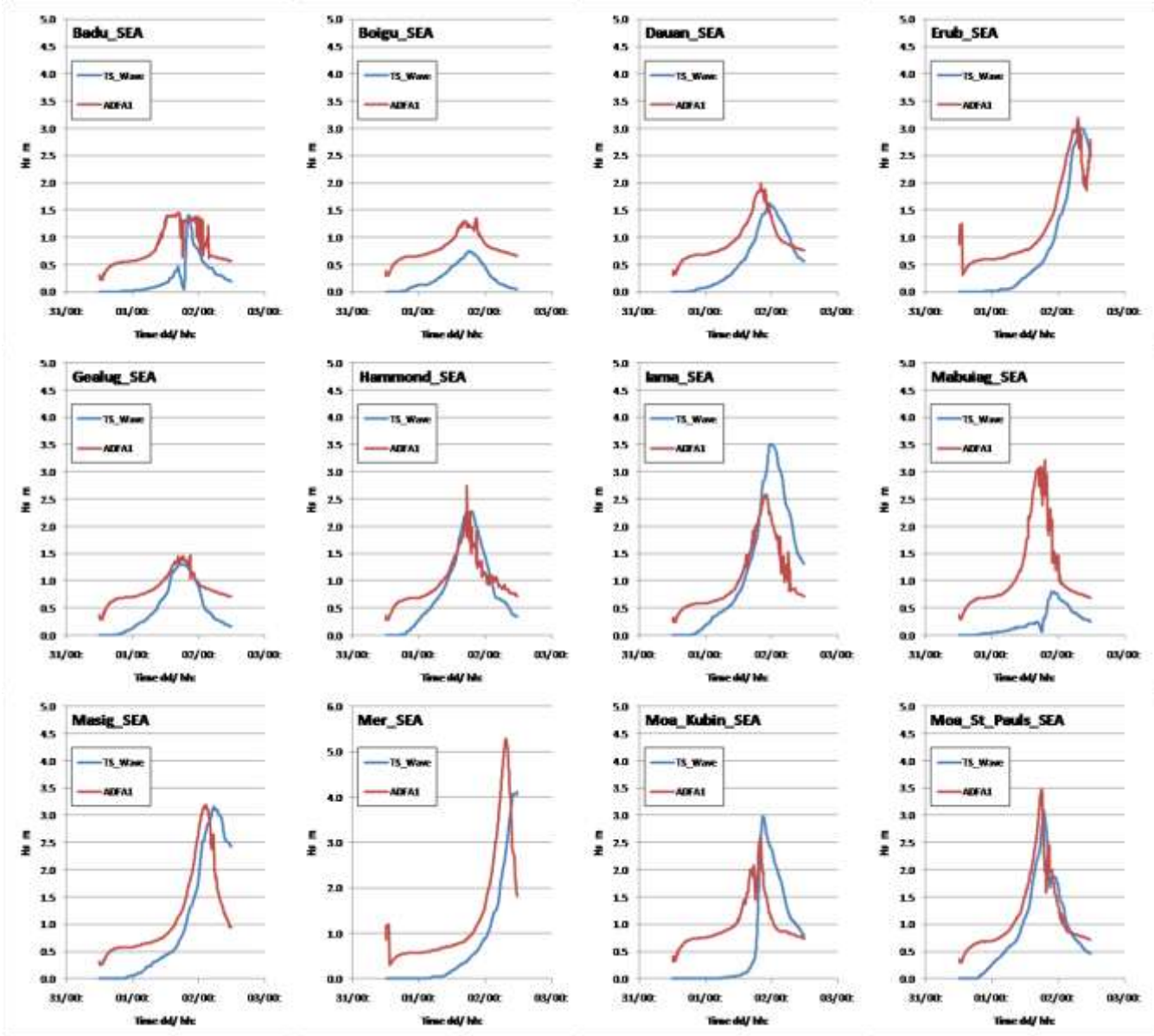

Figure L-1c Example W-E Category 4 TC through Centre (Hs time series comparisons)

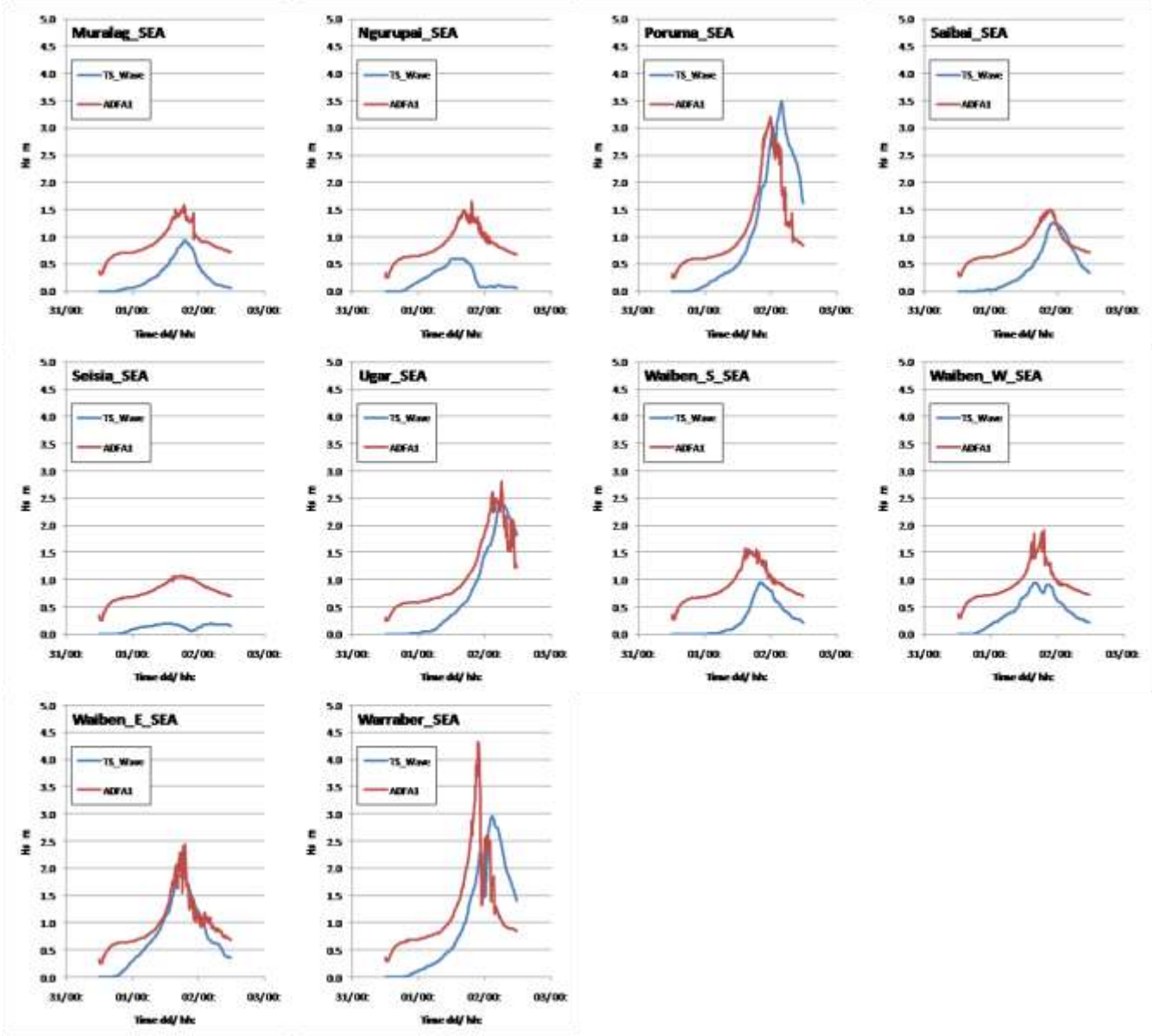

Figure L-1c Example W-E Category 4 TC through Centre (Hs time series comparisons) contd

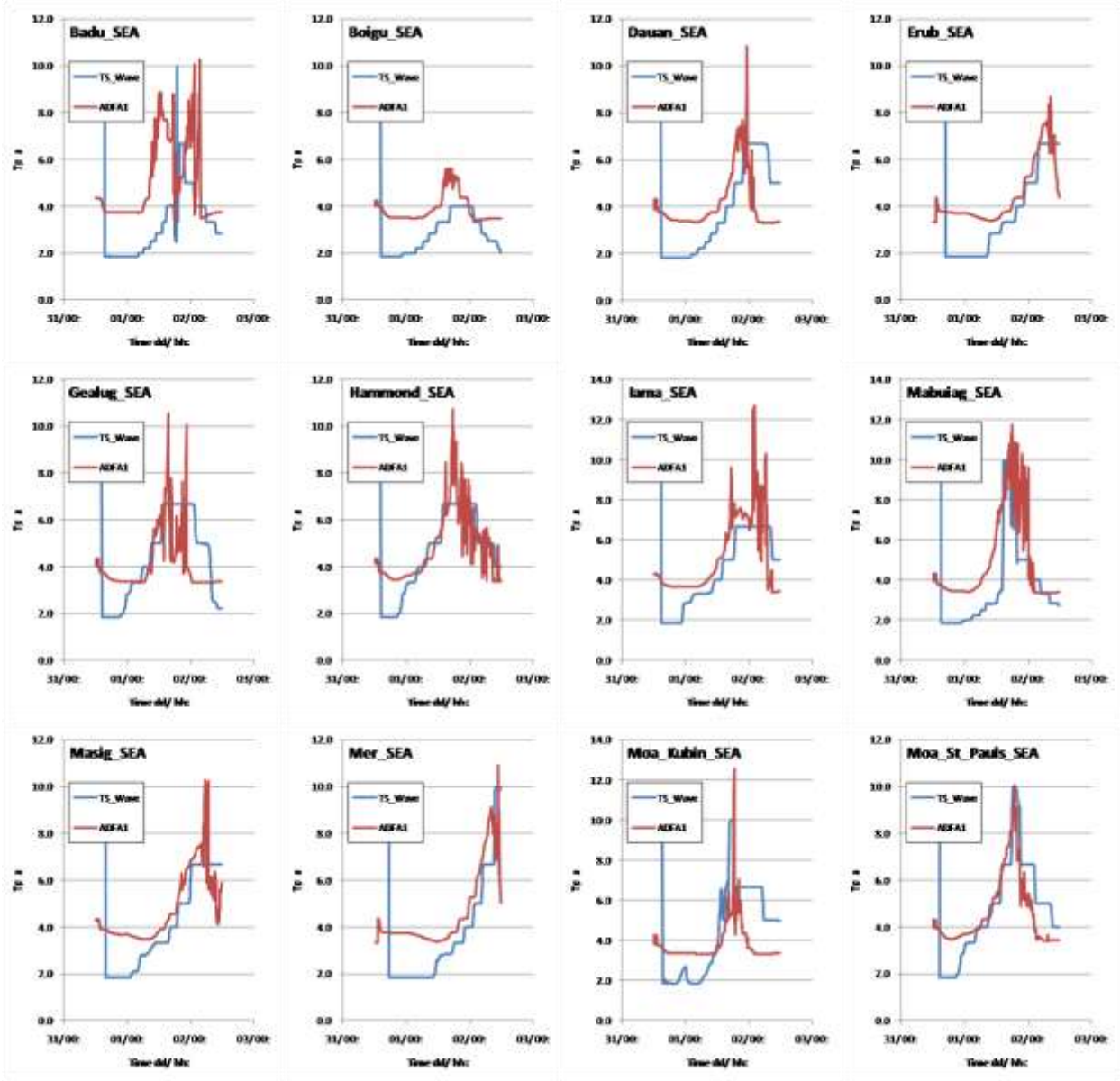

Figure L-1d Example W-E Category 4 TC through Centre (Tp time series comparisons)

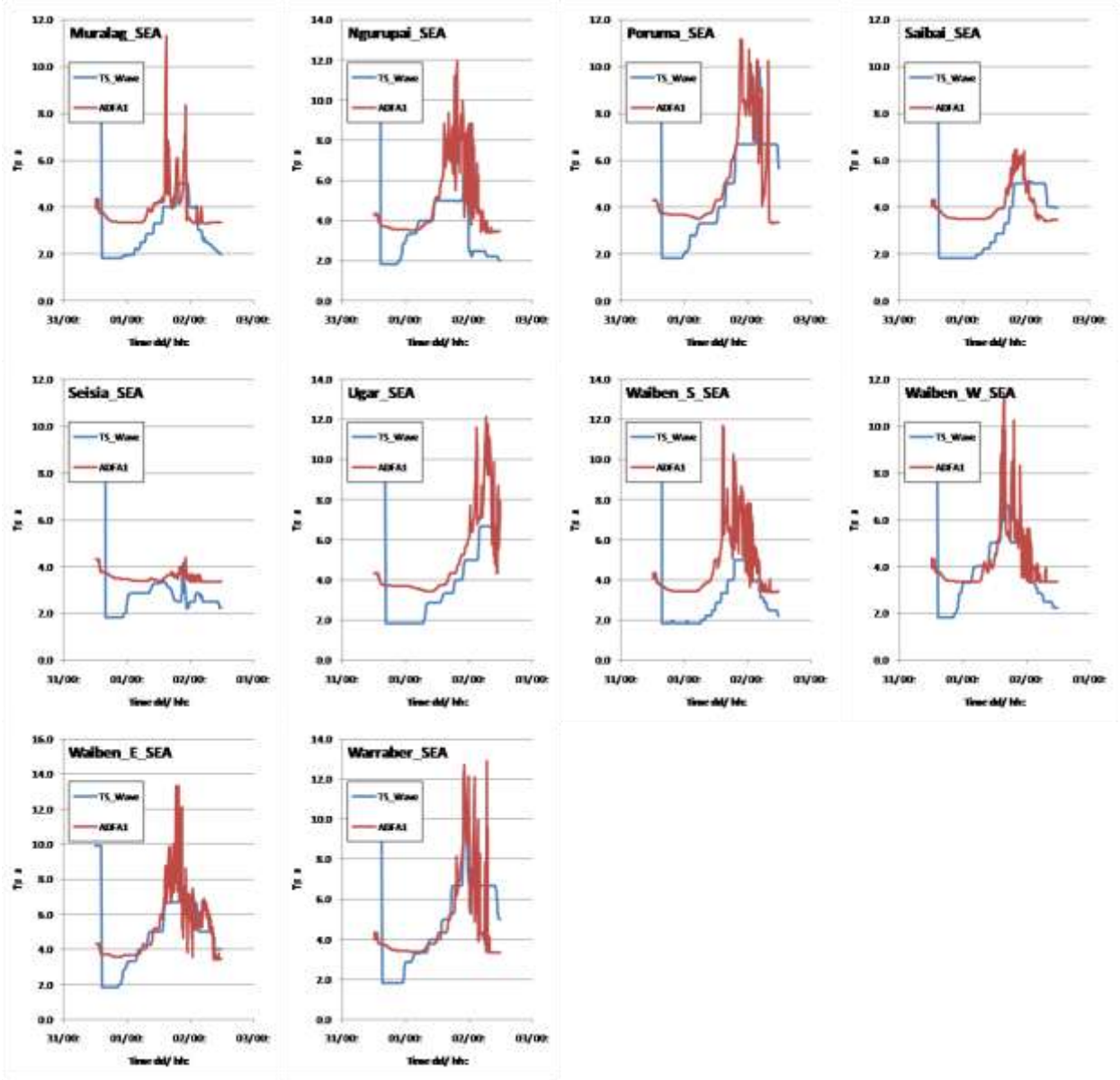

Figure L-1d Example W-E Category 4 TC through Centre (Tp time series comparisons) contd

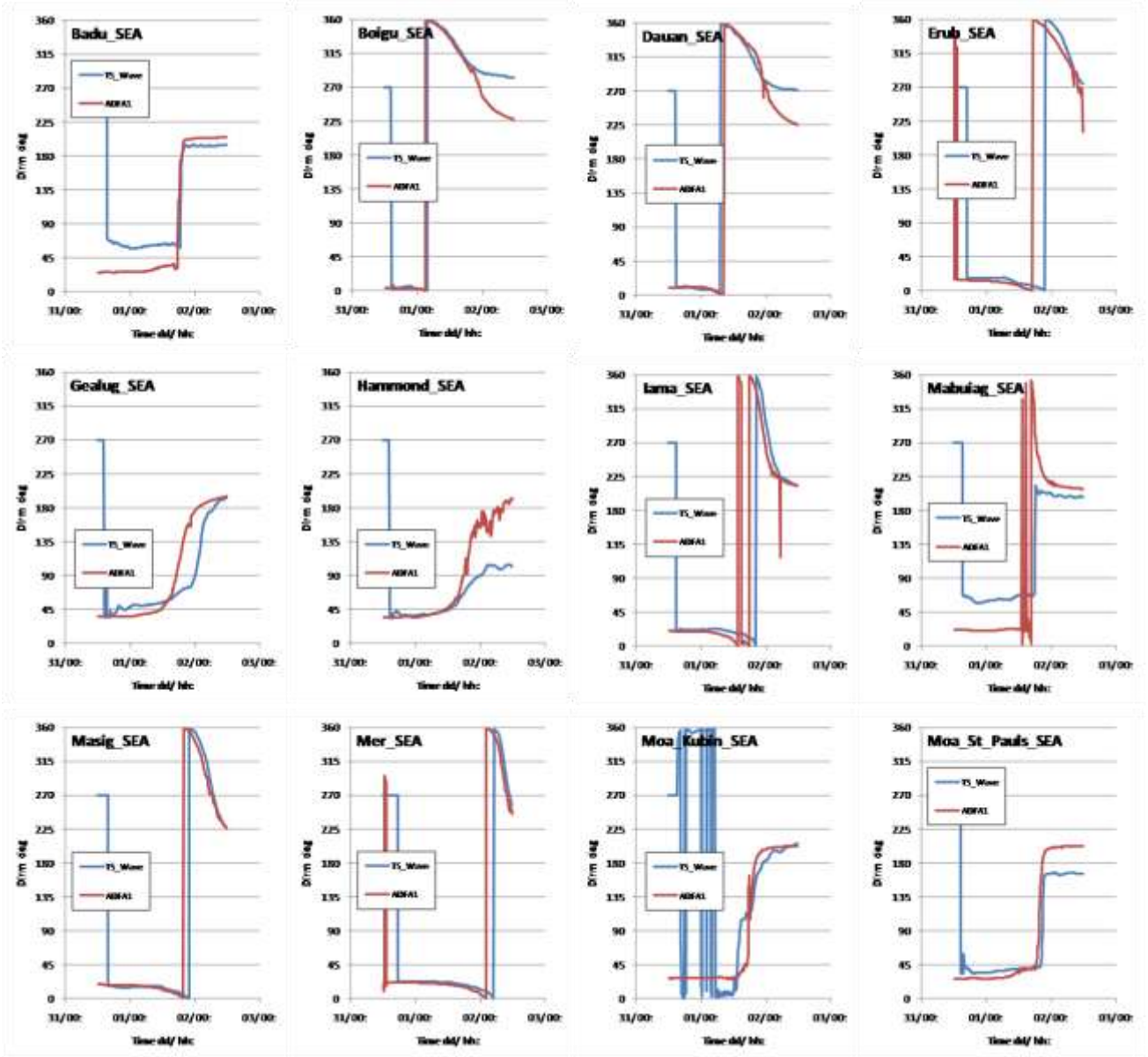

Figure L-1e Example W-E Category 4 TC through Centre (Mean Direction time series comparisons)

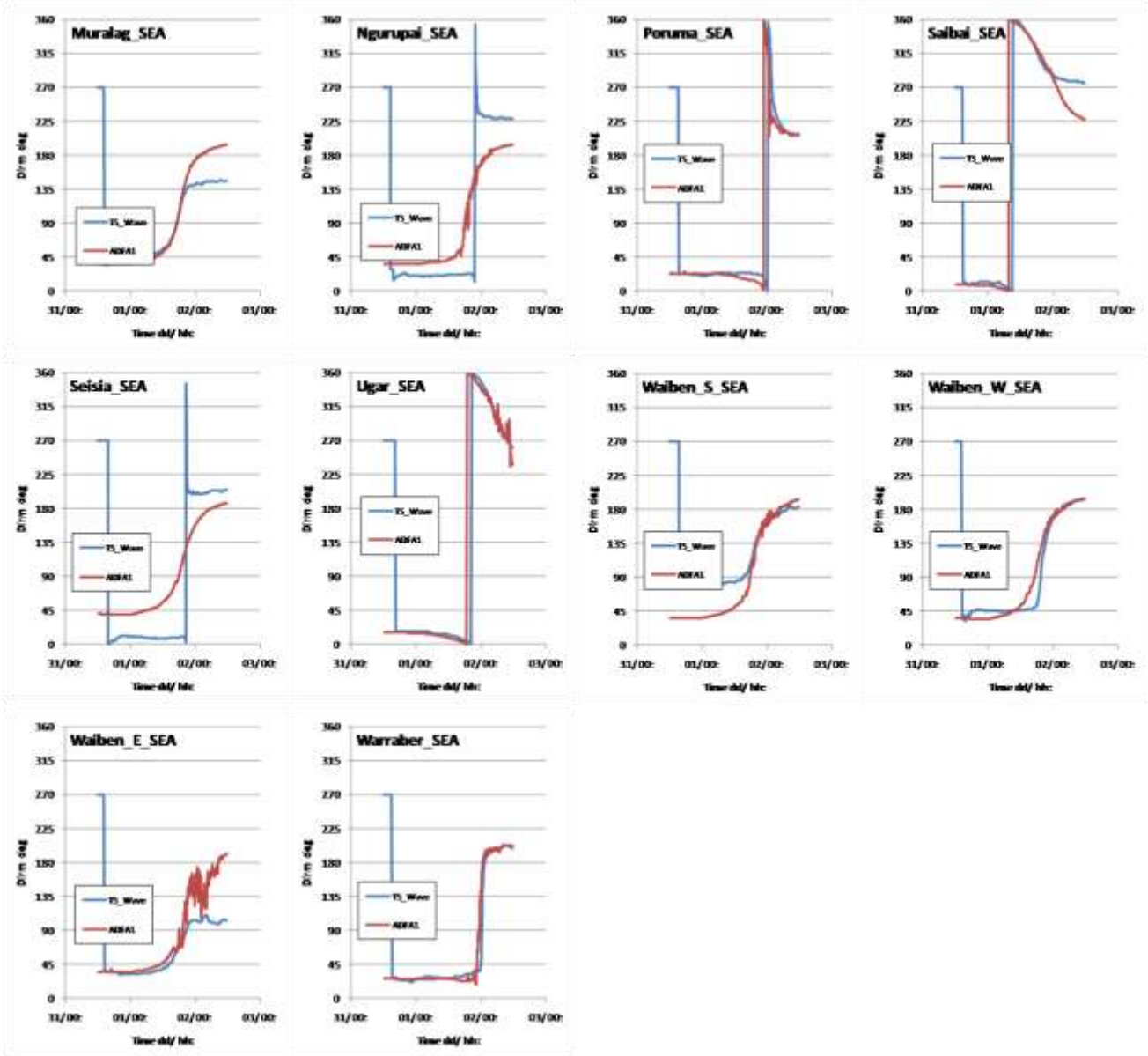

Figure L-1e Example W-E Category 4 TC through Centre (Mean Direction time series comparisons) contd

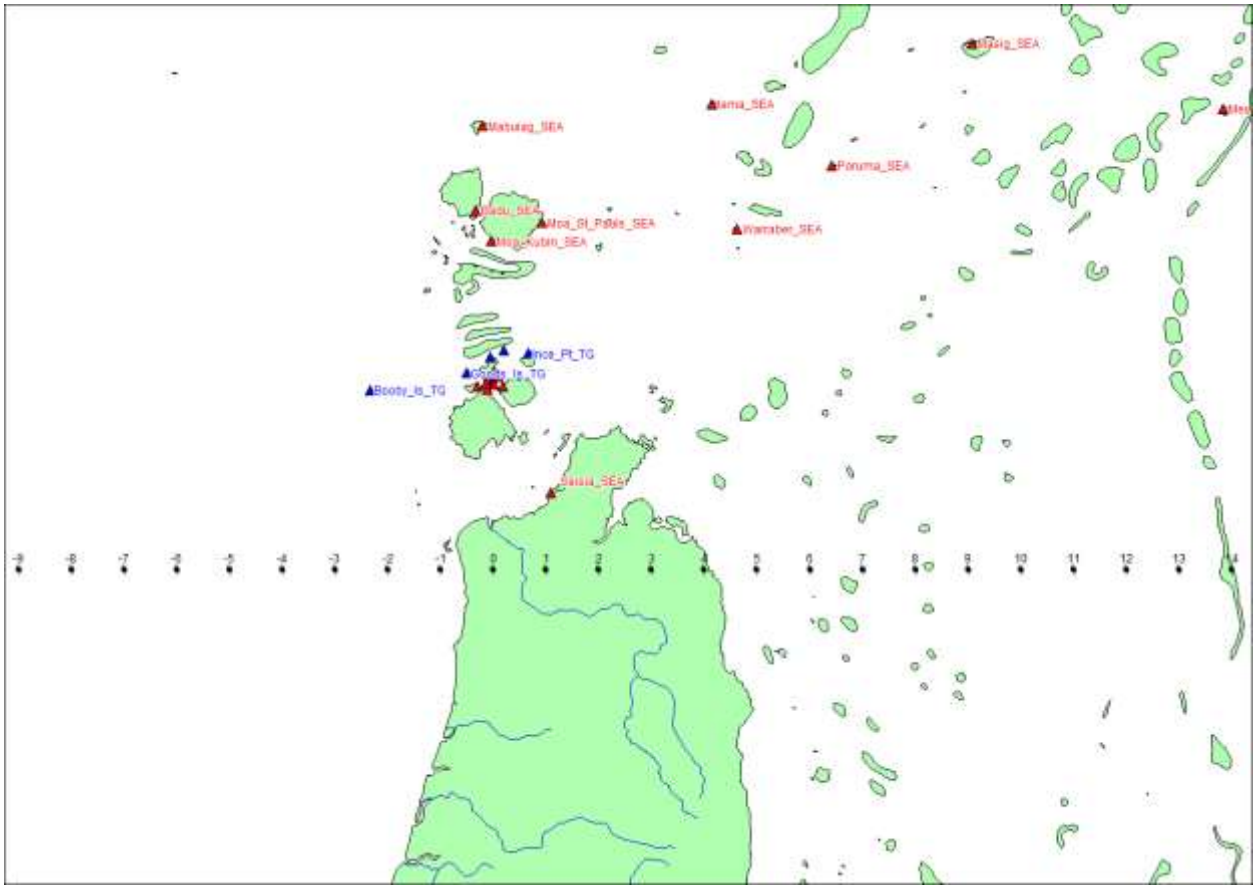

Figure L-2a Example W-E Category 4 TC through Cape York (track and times in hours)

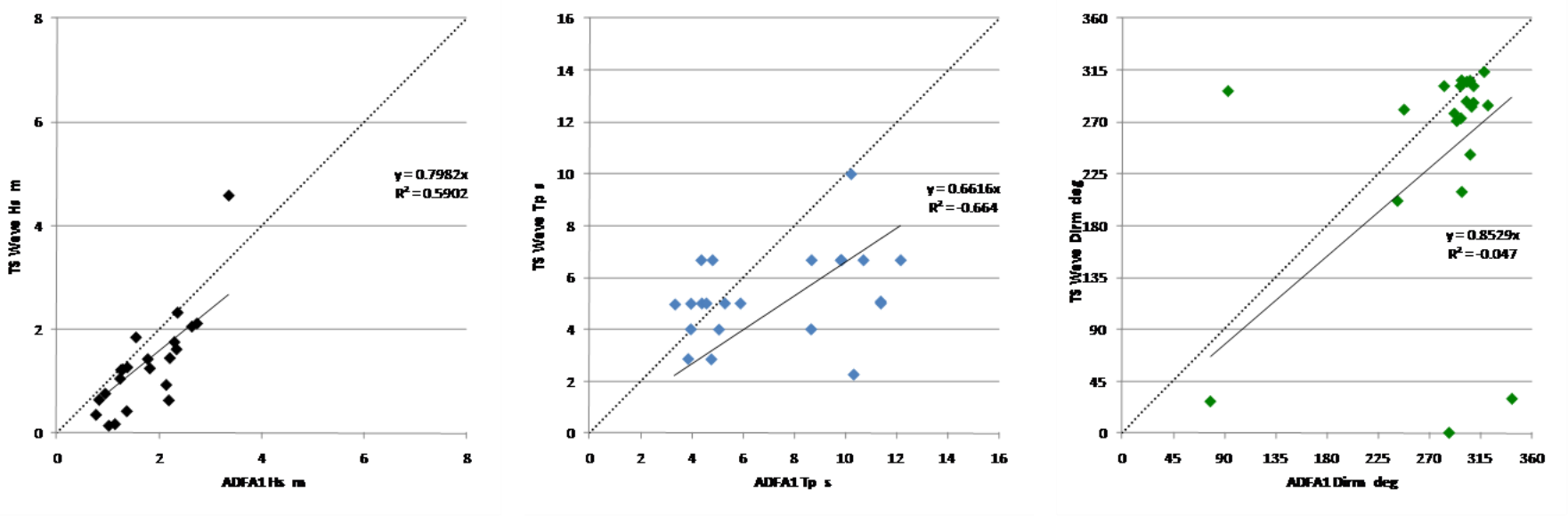

Figure L-2b Example W-E Category 4 TC through Cape York (peak site-specific Hs summary and associated Tp and Mean Direction)

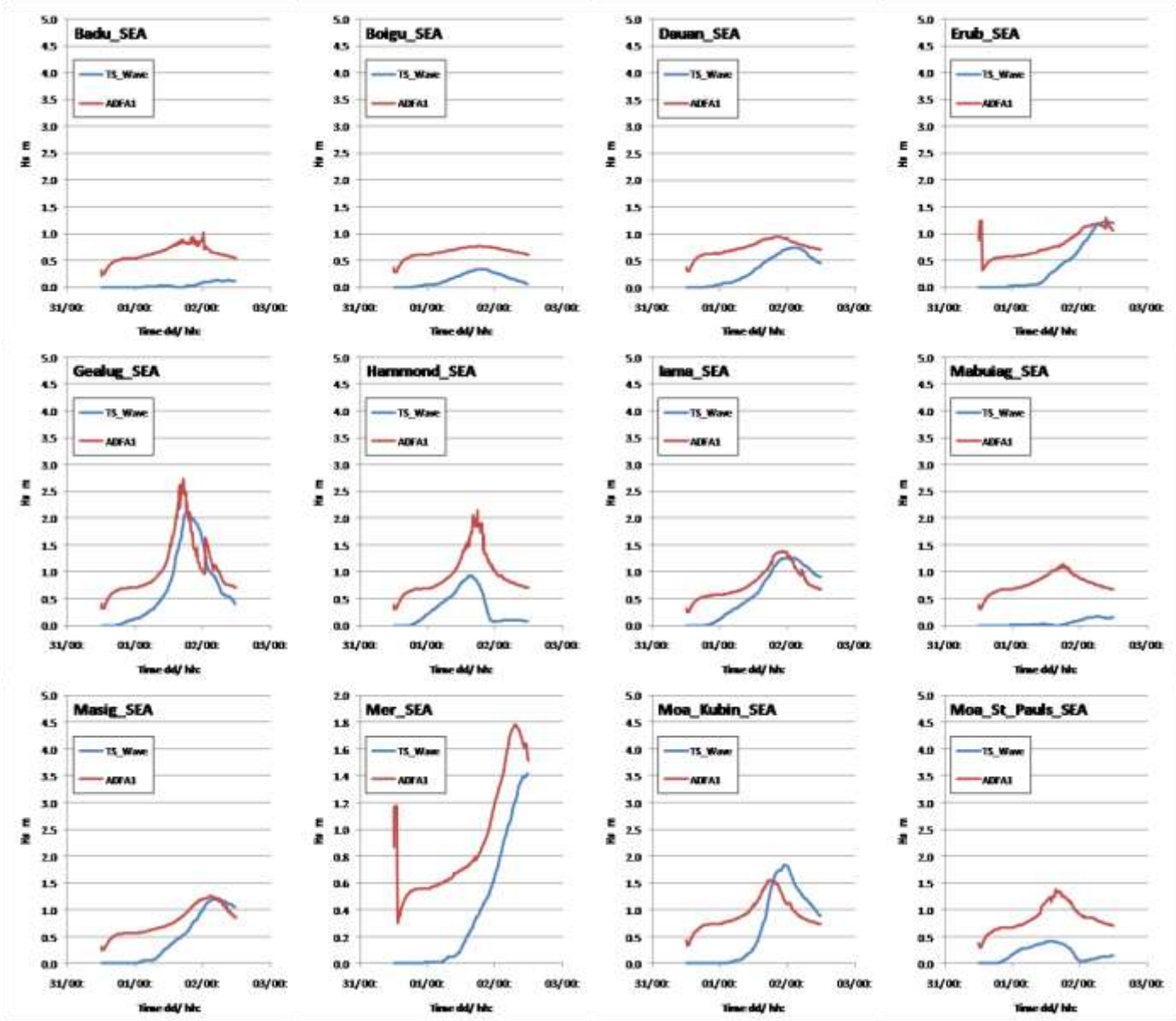

Figure L-2c Example W-E Category 4 TC through Cape York (Hs time series comparisons)

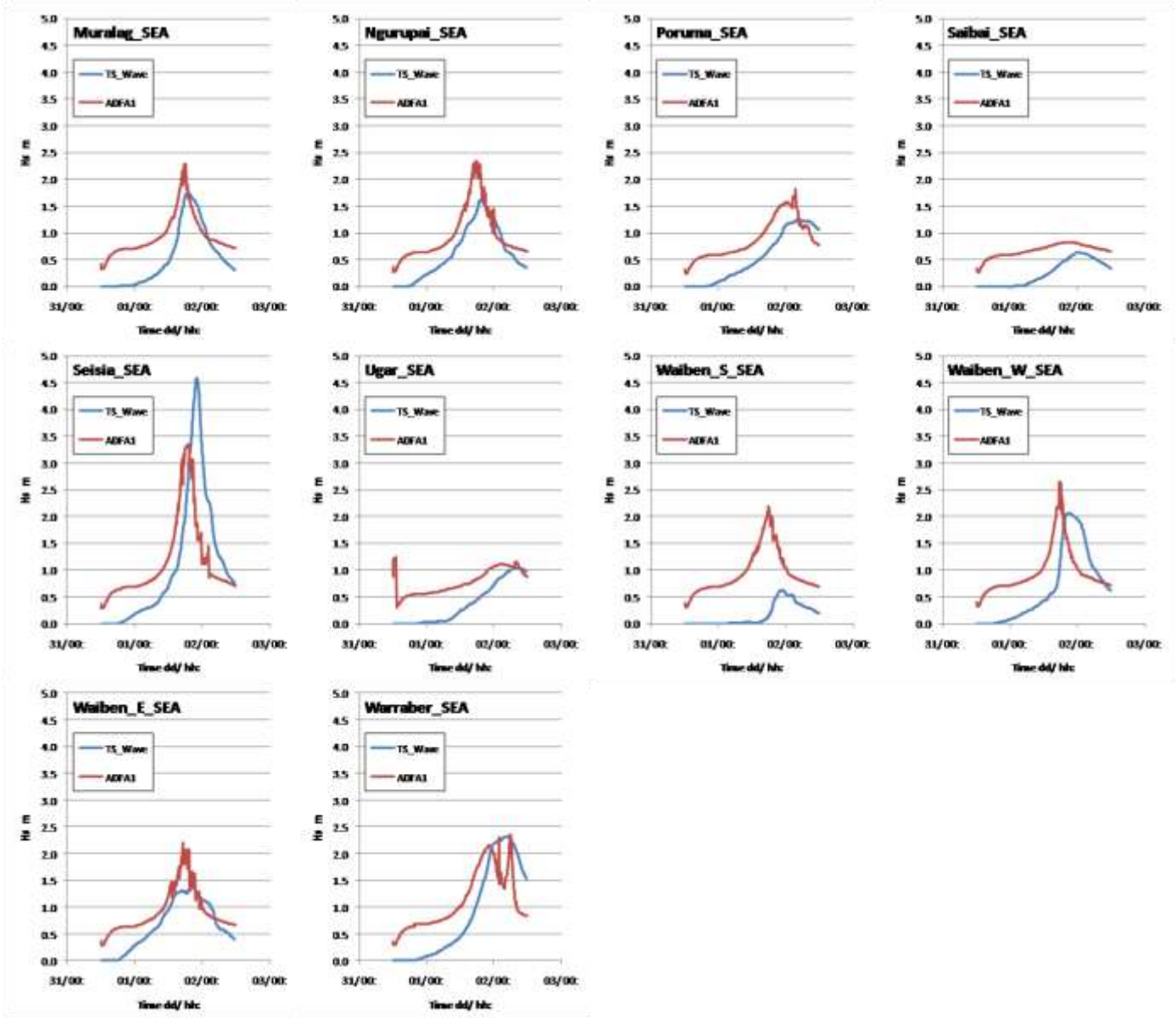

Figure L-2c Example W-E Category 4 TC through Cape York (Hs time series comparisons) contd

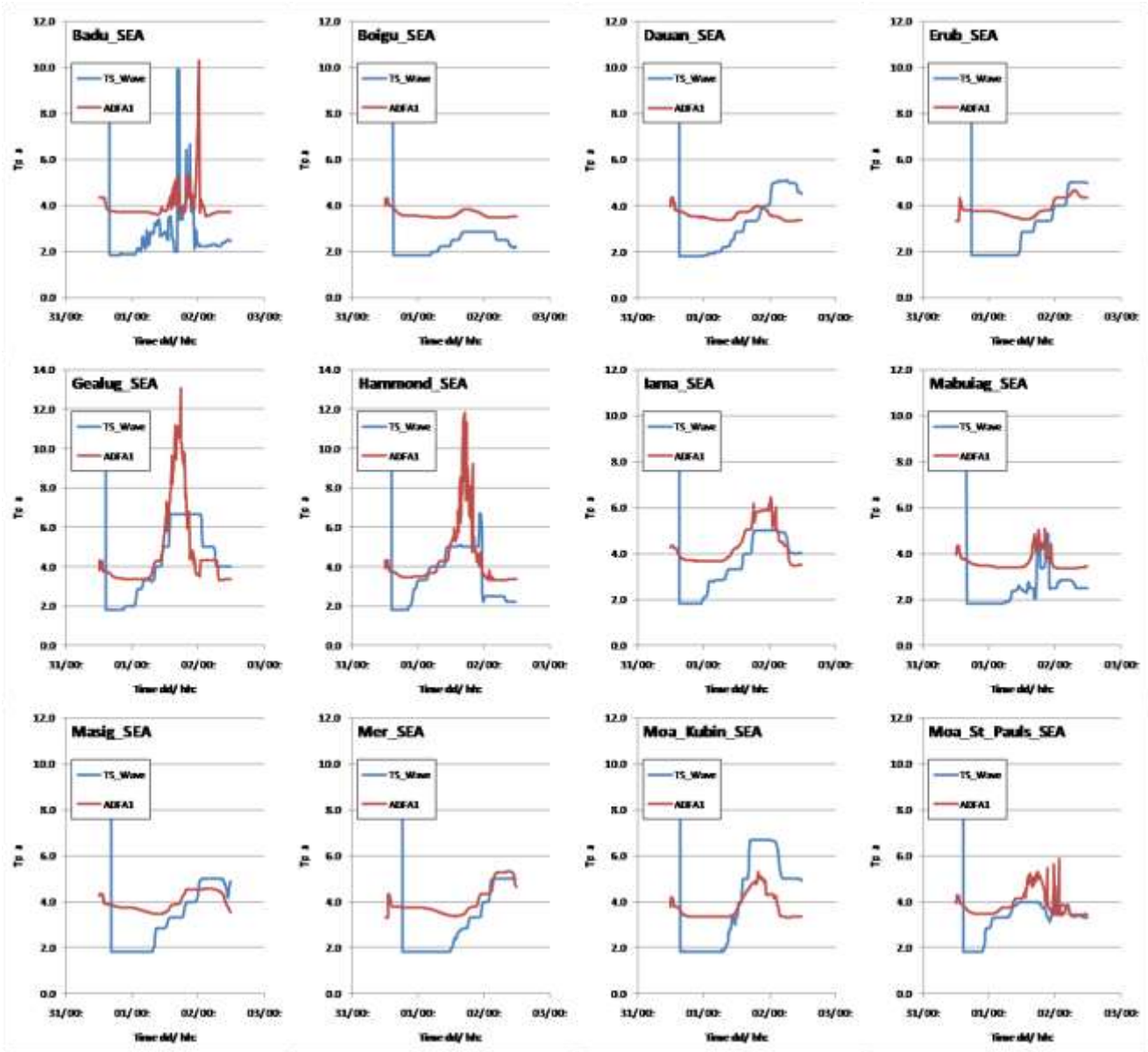

Figure L-2d Example W-E Category 4 TC through Cape York (Tp time series comparisons)

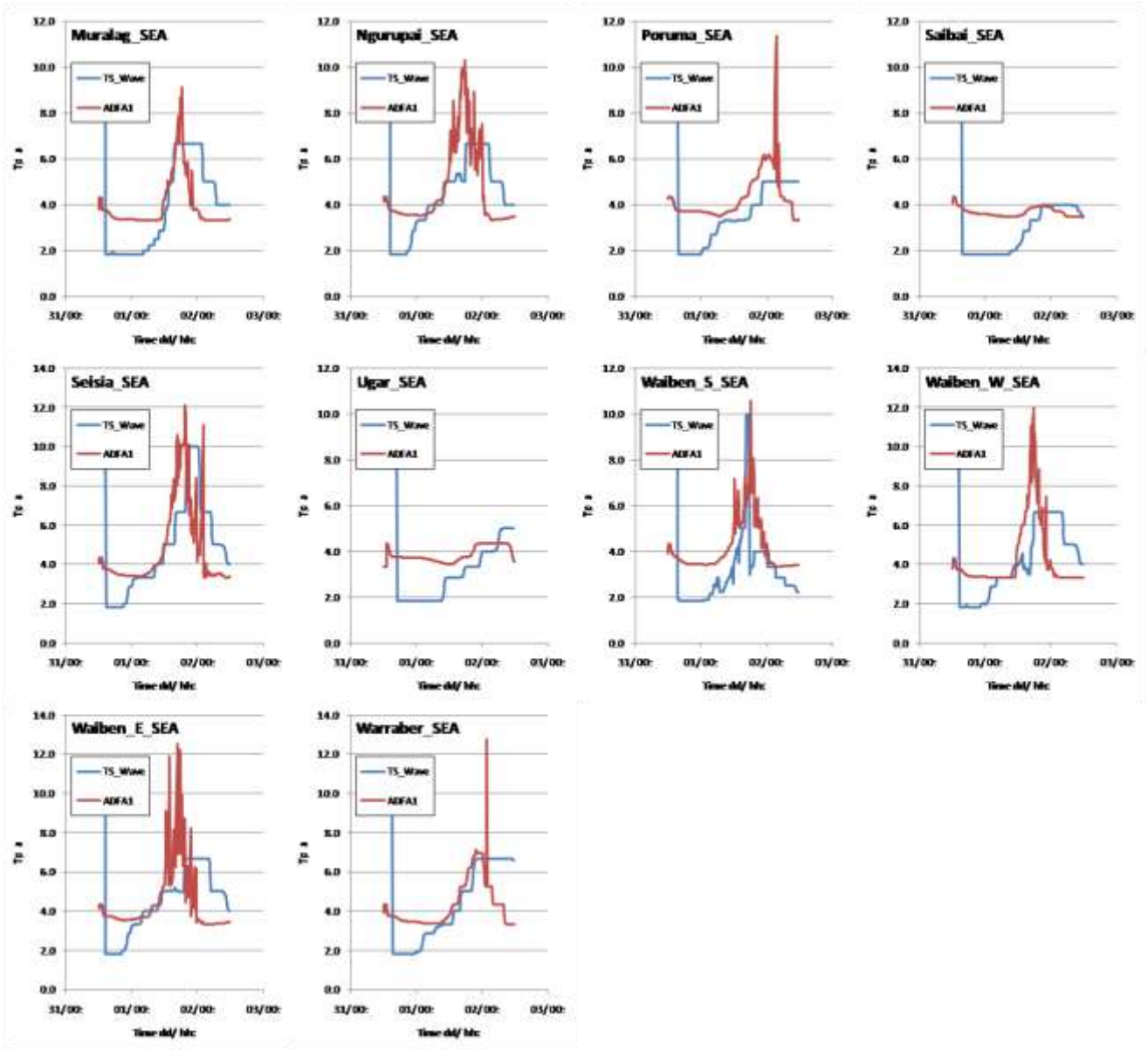

Figure L-2d Example W-E Category 4 TC through Cape York (Tp time series comparisons) contd

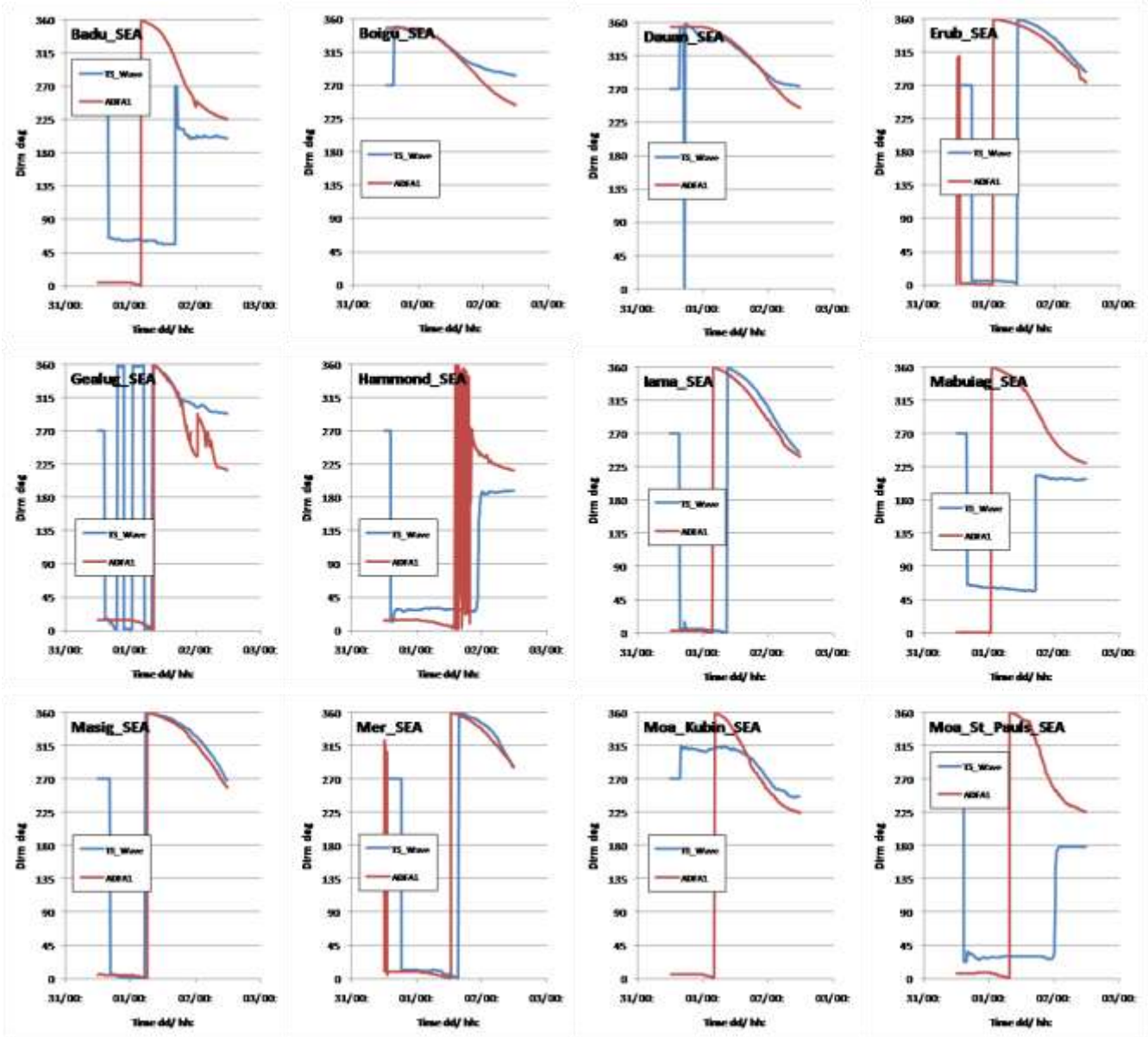

Figure L-2e Example W-E Category 4 TC through Cape York (Mean Direction time series comparisons)

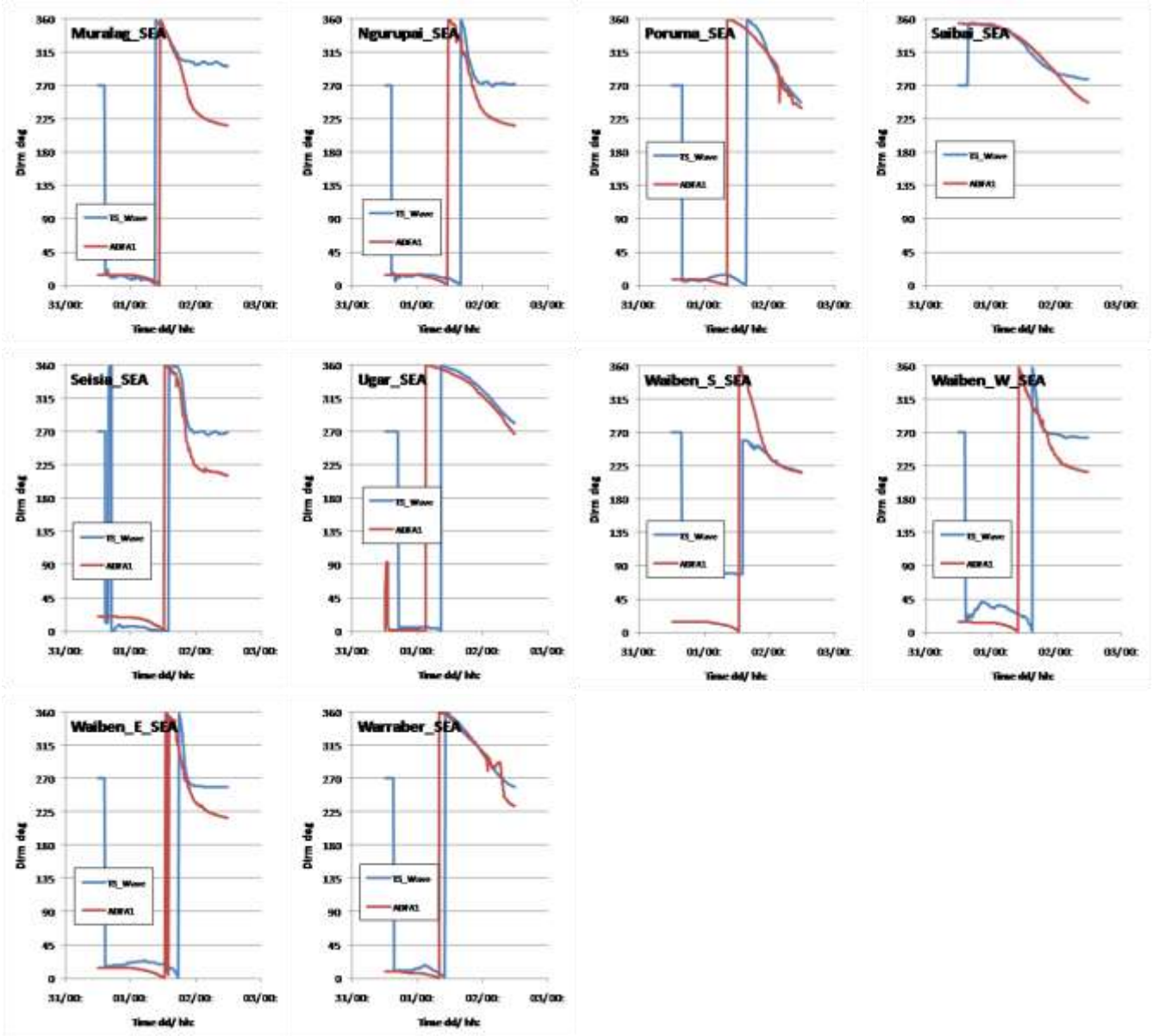

Figure L-2e Example W-E Category 4 TC through Cape York (Mean Direction time series comparisons) contd

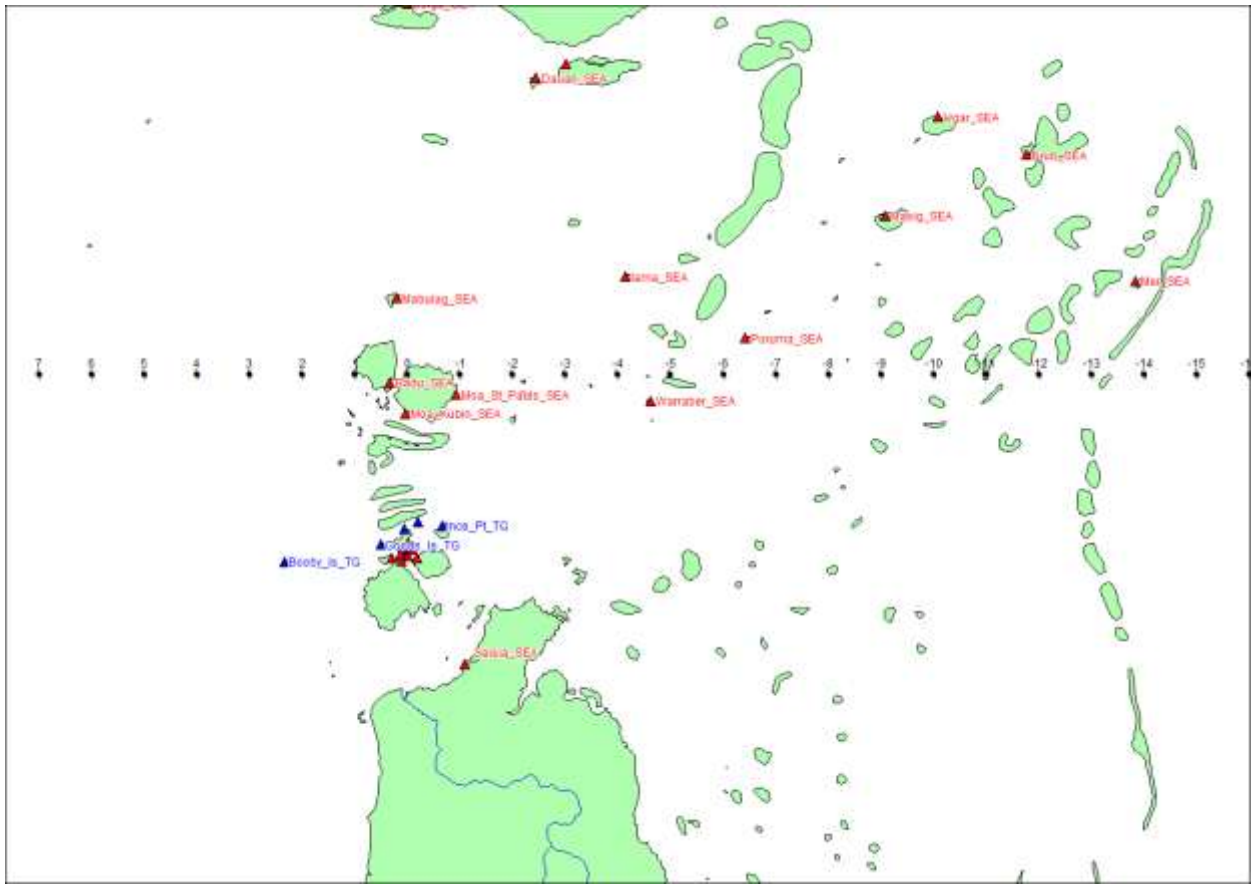

Figure L-3a Example E-W Category 4 TC through Centre (track and times in hours)

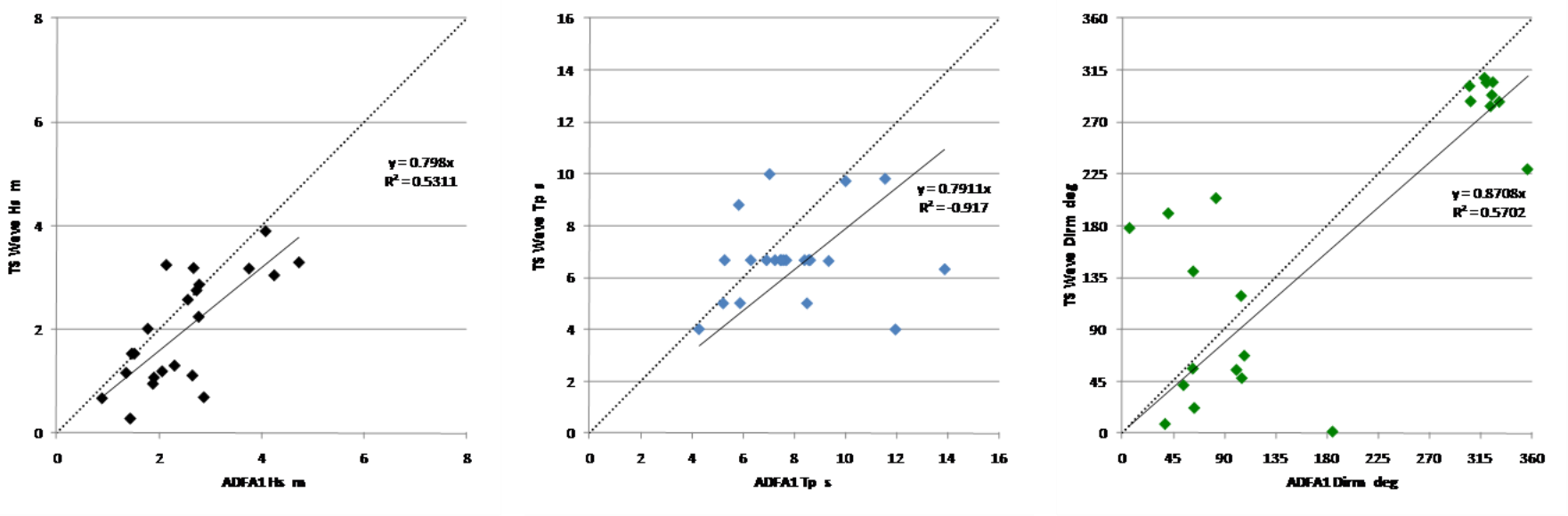

Figure L-3b Example E-W Category 4 TC through Centre (peak site-specific Hs summary and associated Tp and Mean Direction)

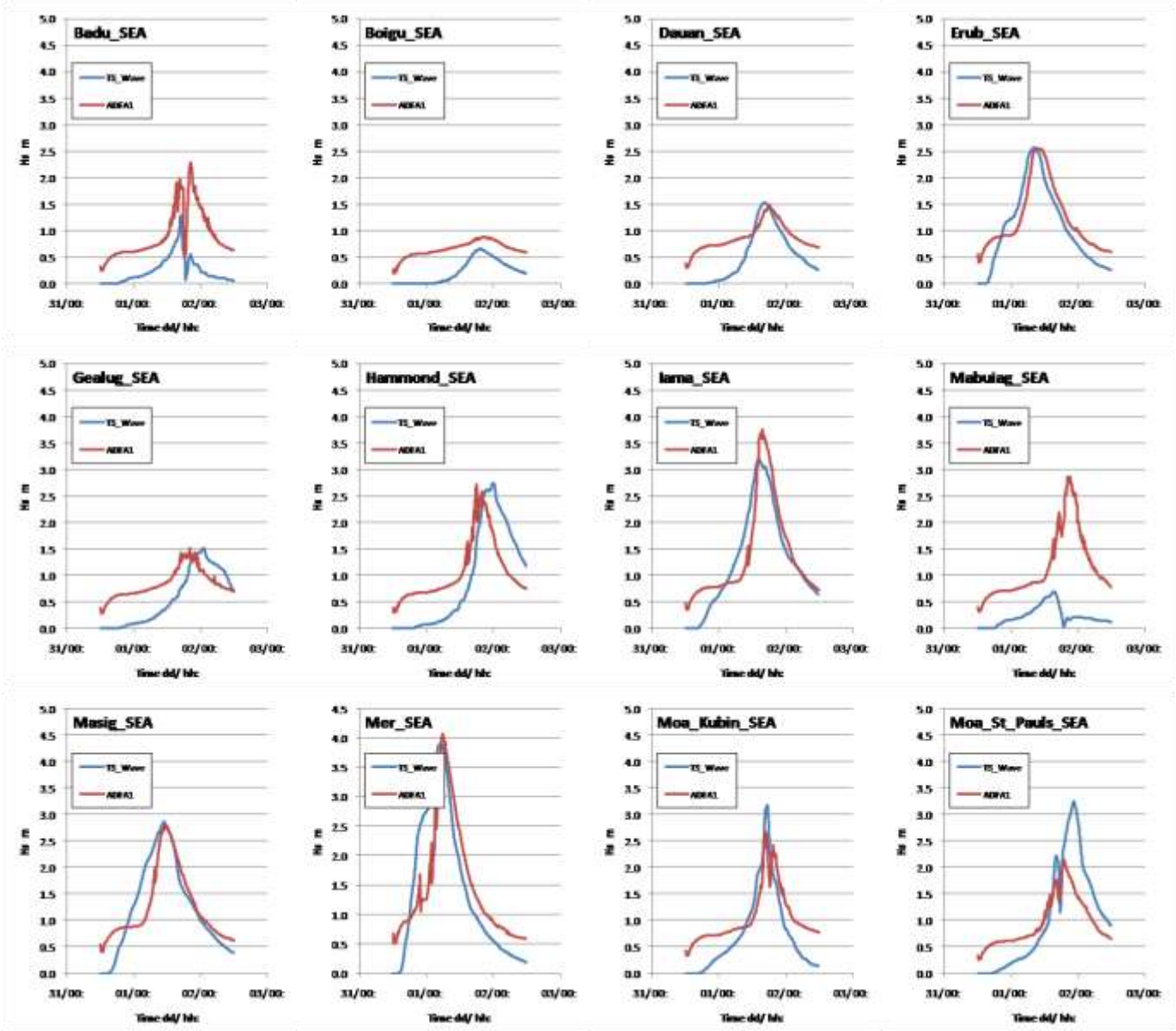

Figure L-3c Example E-W Category 4 TC through Centre (Hs time series comparisons)

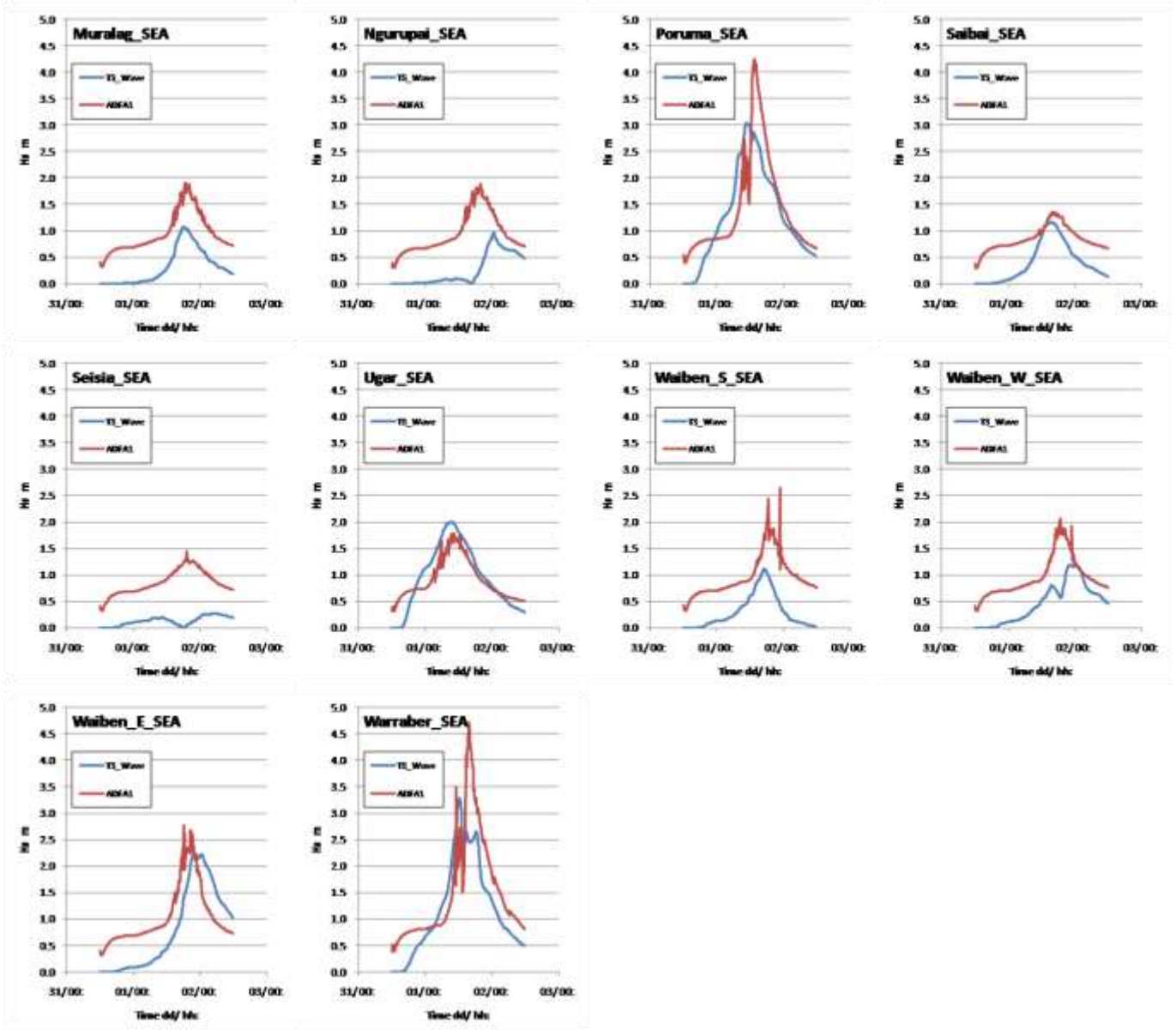

Figure L-3c Example E-W Category 4 TC through Centre (Hs time series comparisons) contd

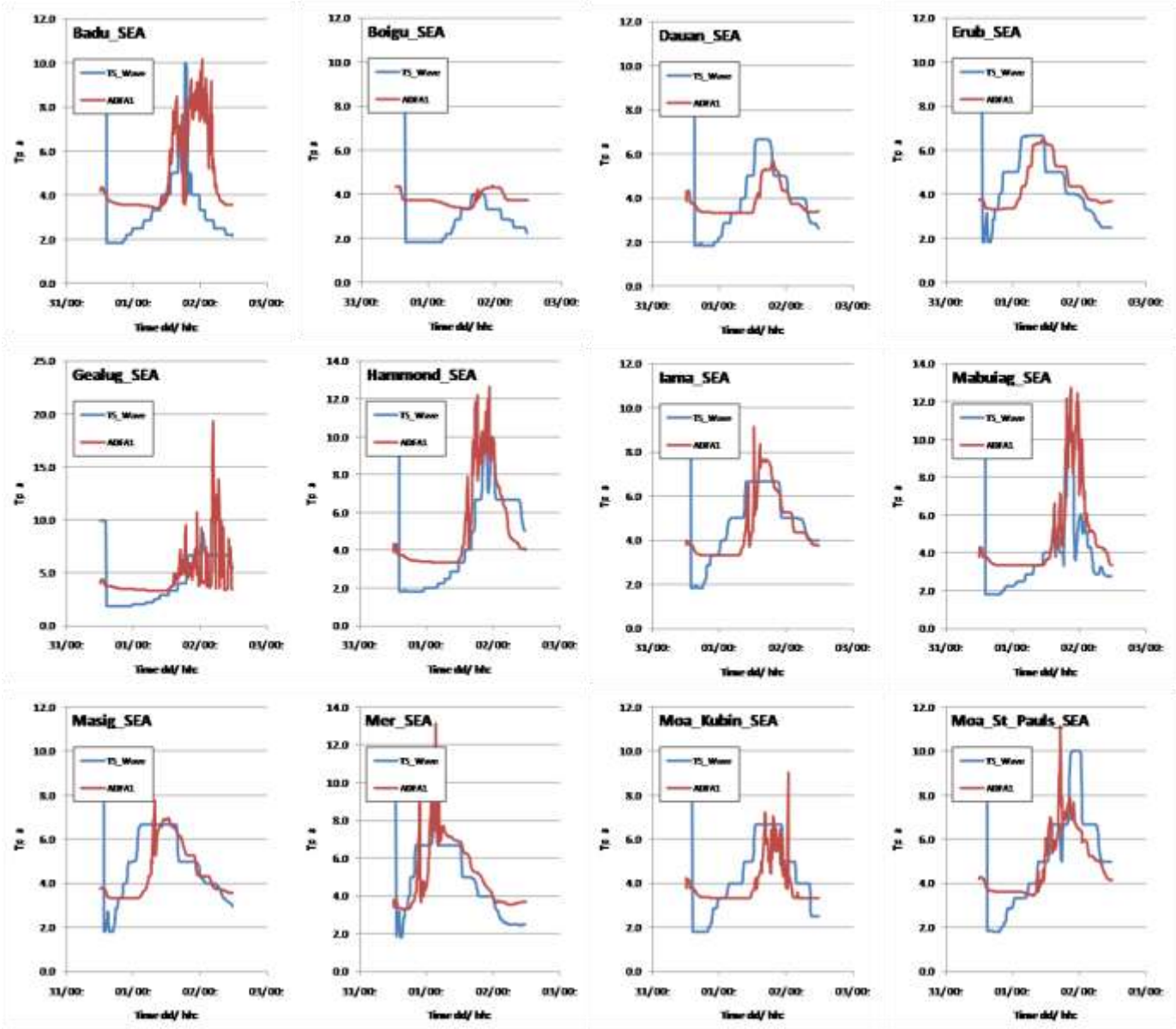

Figure L-3d Example E-W Category 4 TC through Centre (Tp time series comparisons)

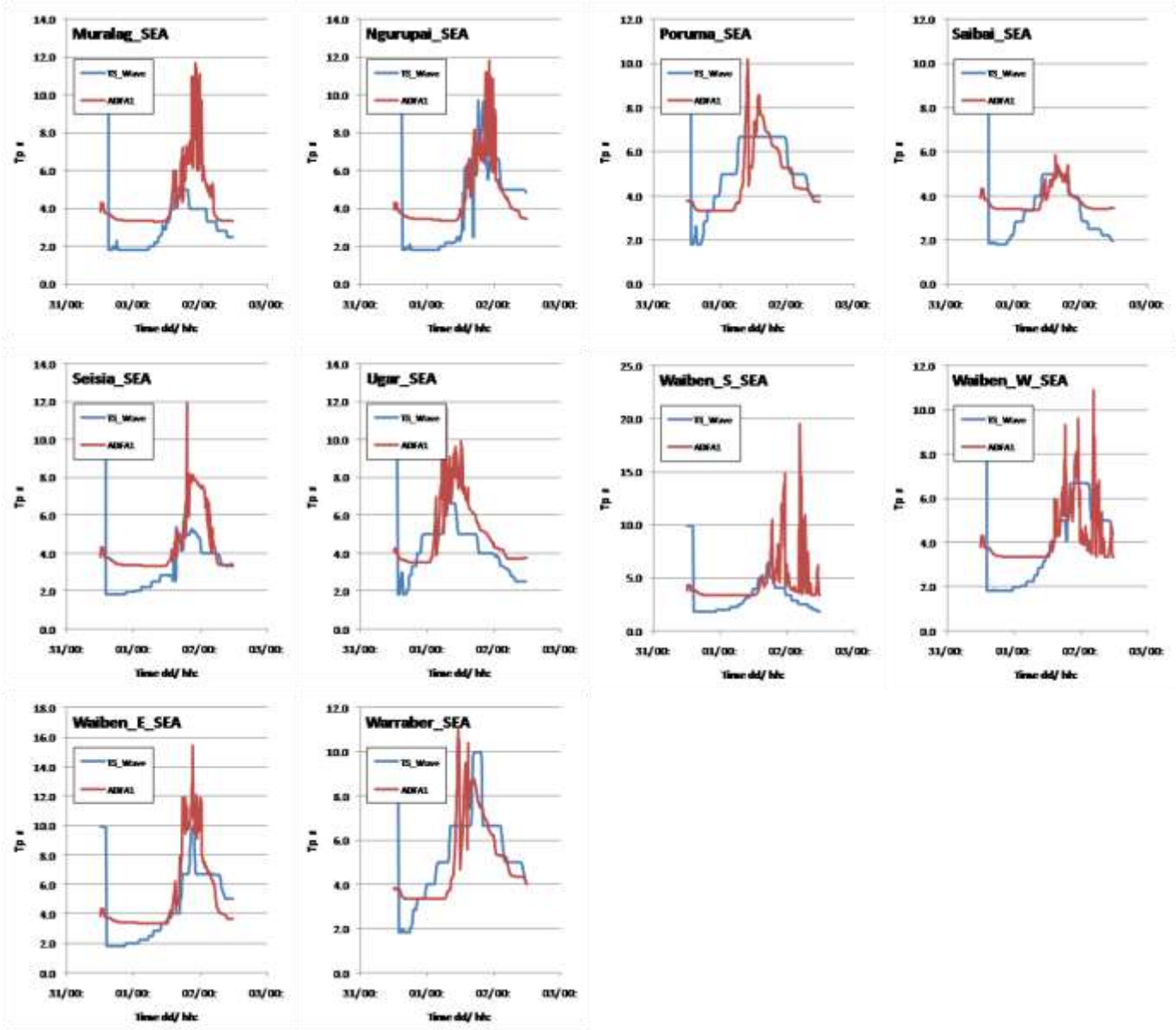

Figure L-3d Example E-W Category 4 TC through Centre (Tp time series comparisons) contd

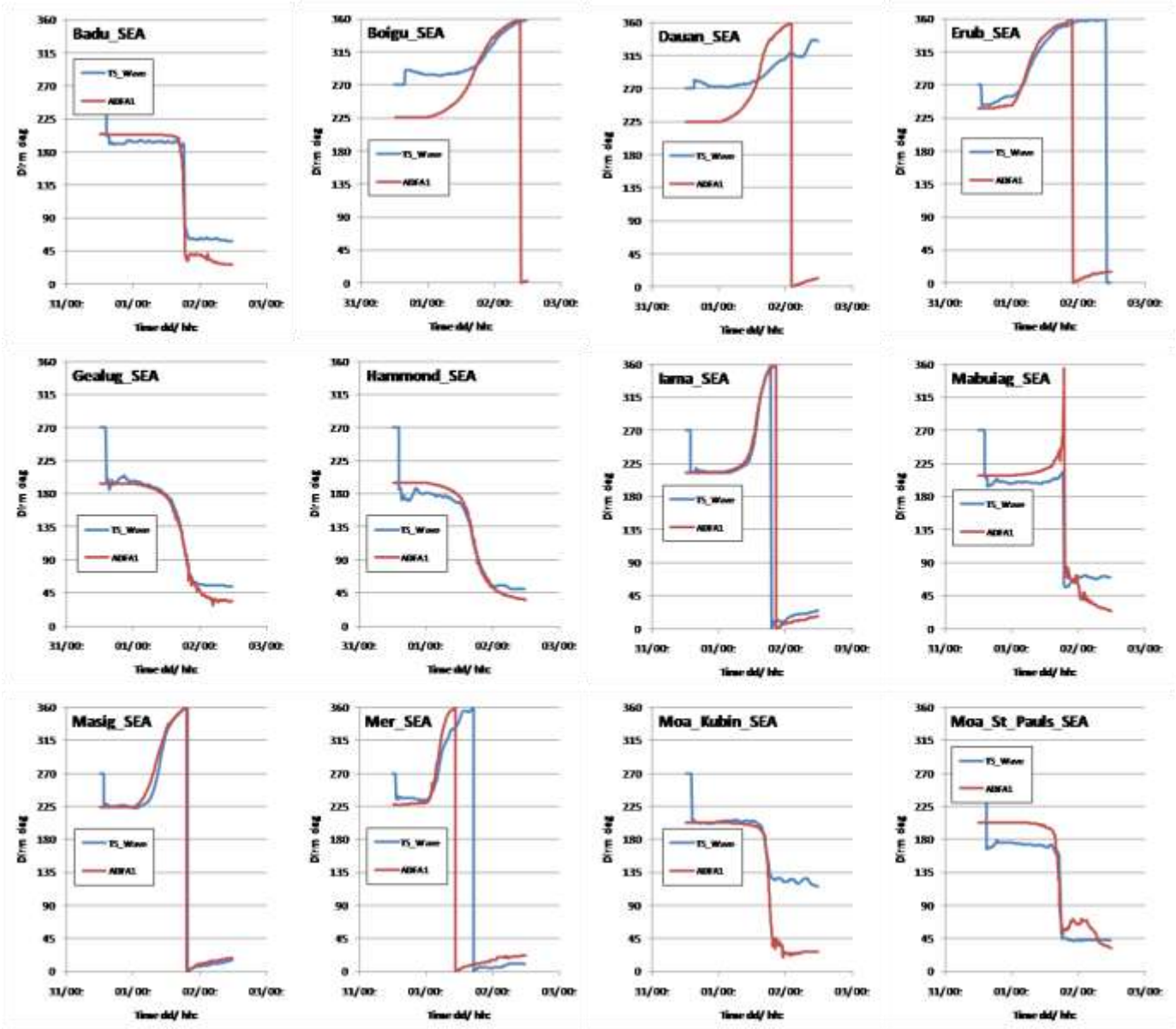

Figure L-3e Example E-W Category 4 TC through Centre (Mean Direction time series comparisons)

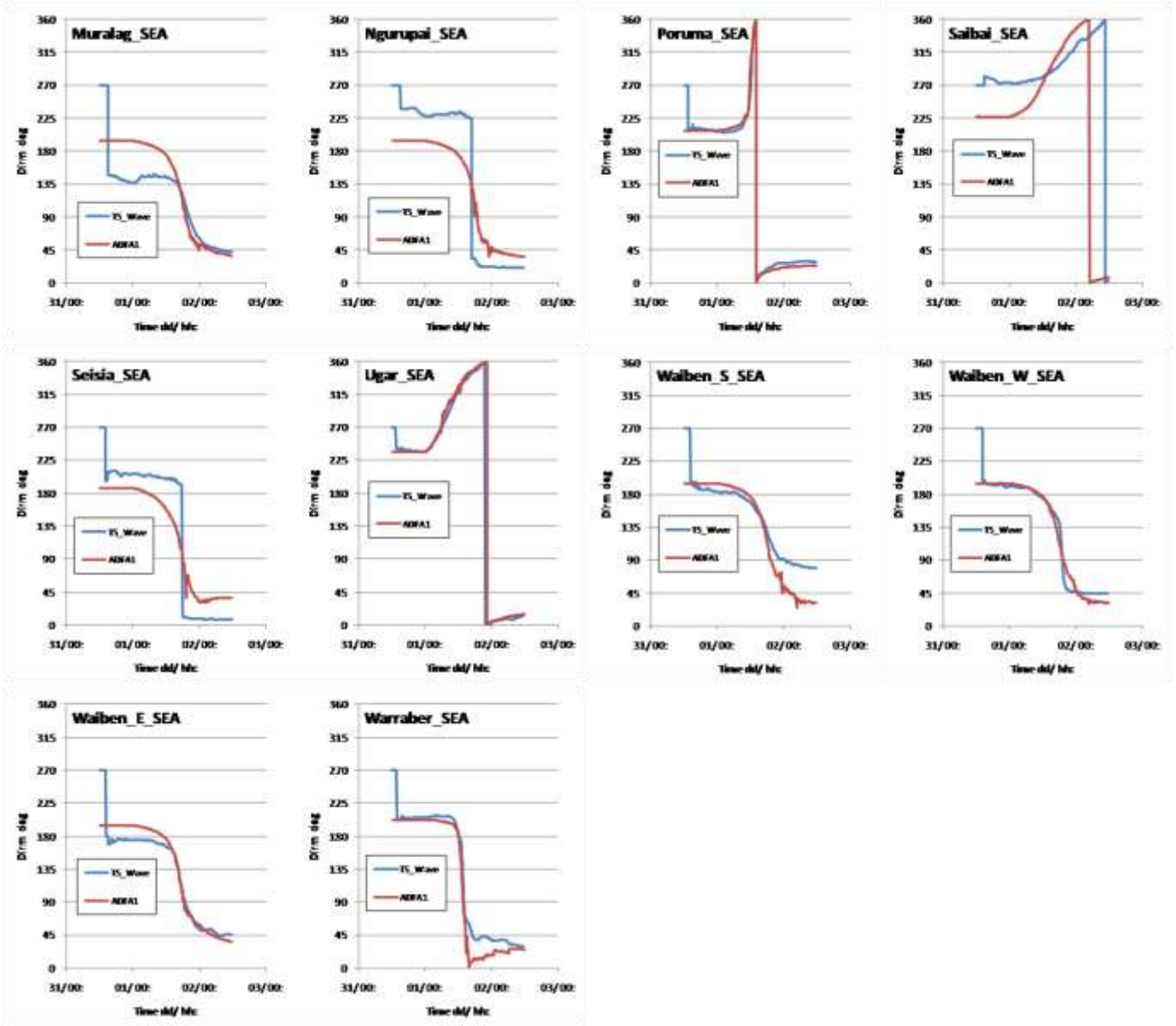

Figure L-3e Example E-W Category 4 TC through Centre (Mean Direction time series comparisons) contd

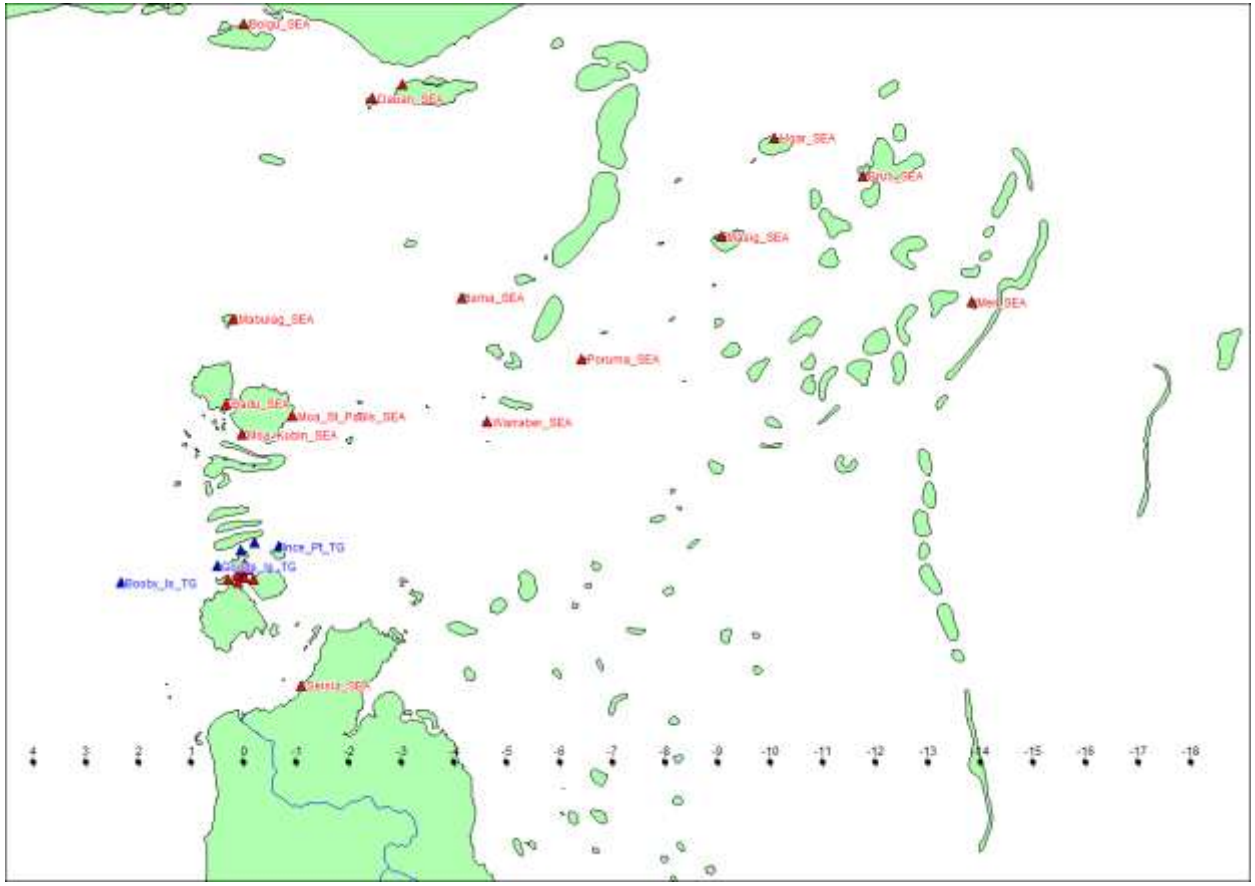

Figure L-4a Example E-W Category 4 TC through Cape York (track and times in hours)

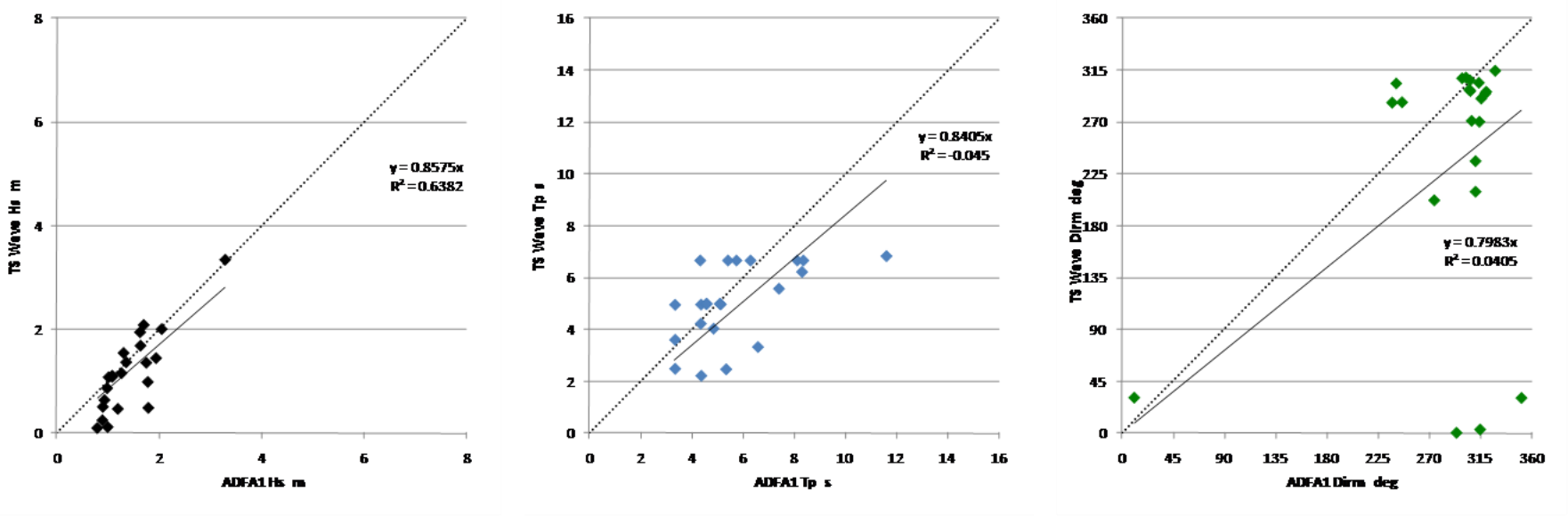

Figure L-4b Example E-W Category 4 TC through Cape York (peak site-specific Hs summary and associated Tp and Mean Direction)

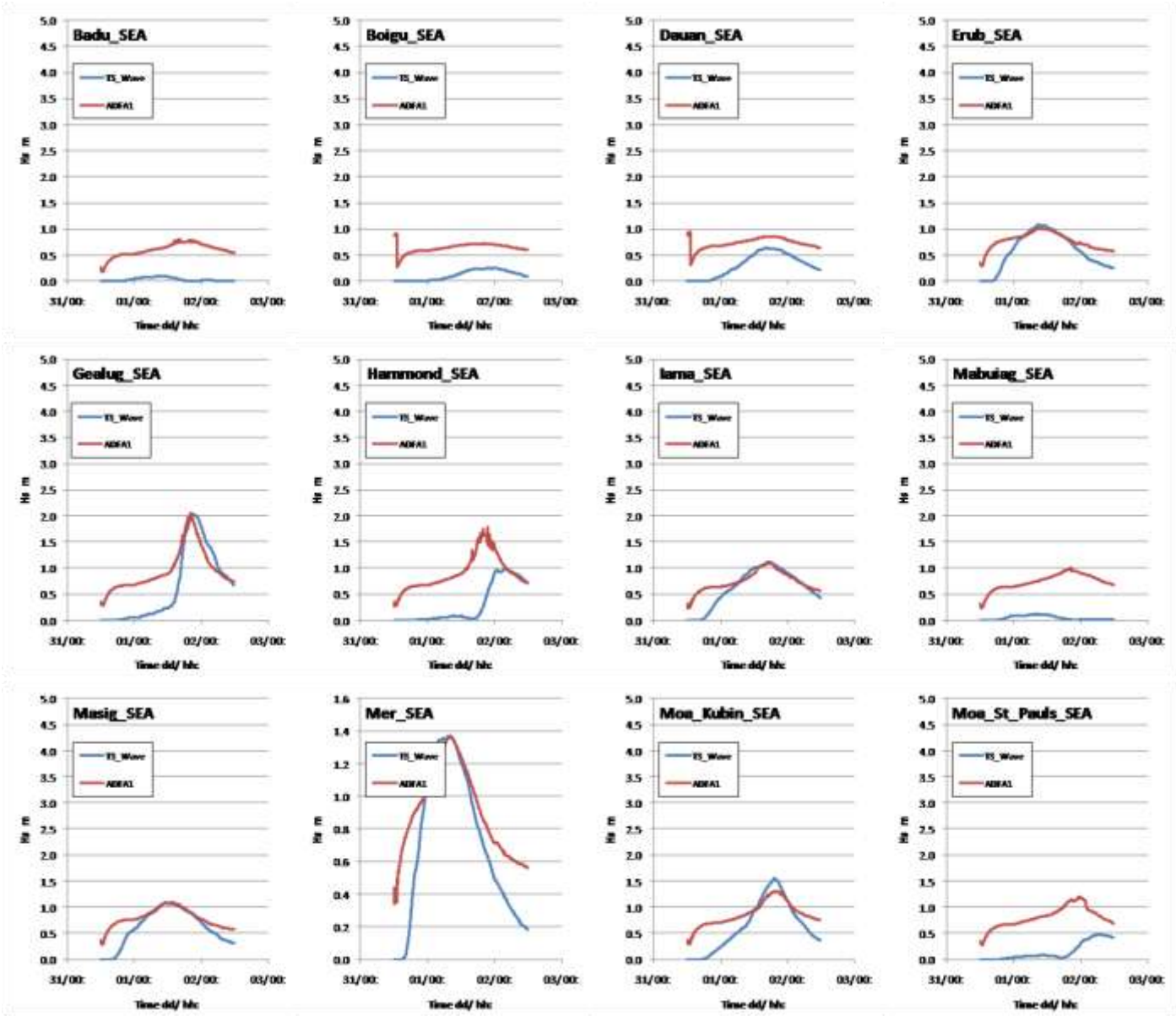

Figure L-4c Example E-W Category 4 TC through Cape York (Hs time series comparisons)

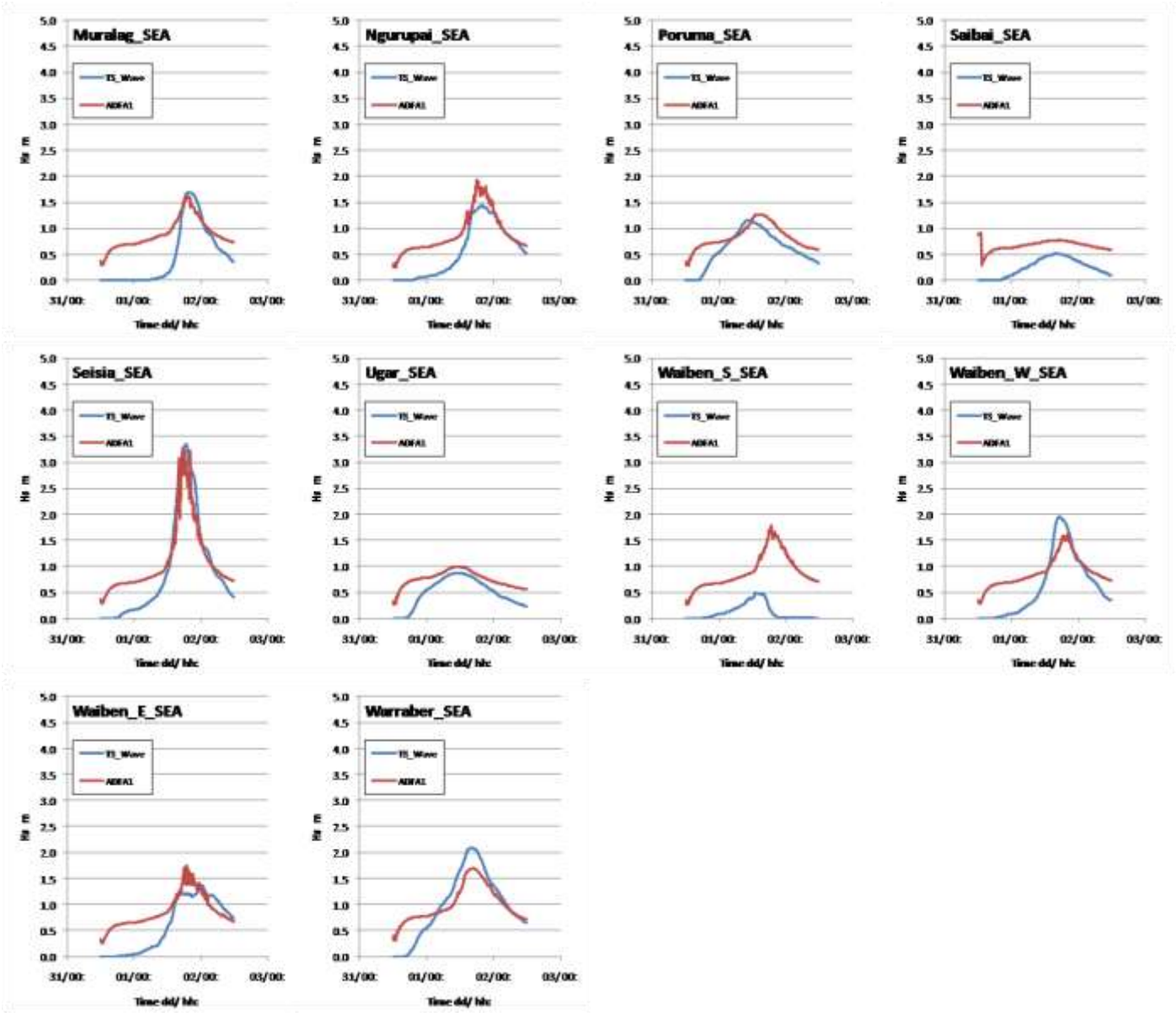

Figure L-4c Example E-W Category 4 TC through Cape York (Hs time series comparisons) contd

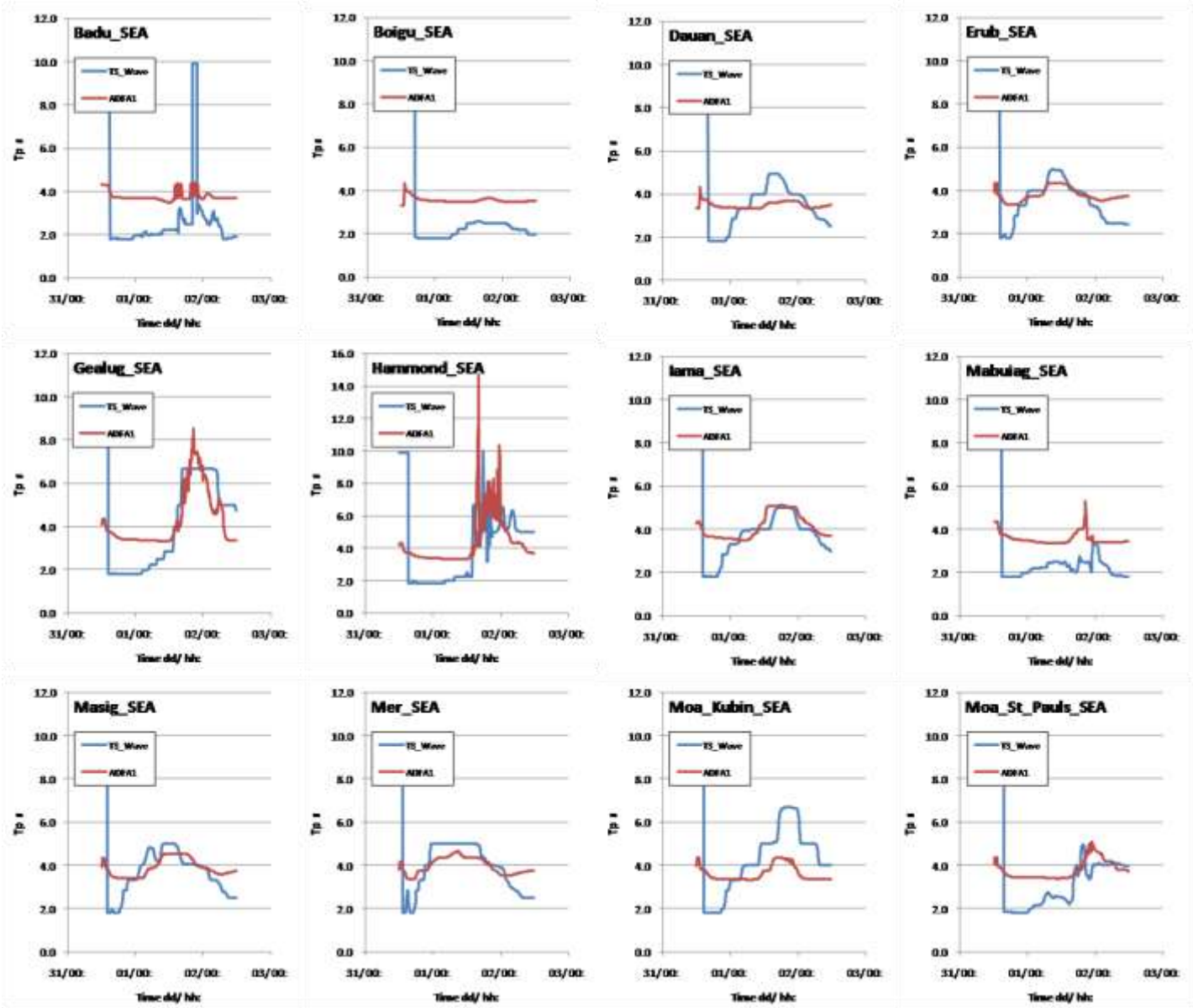

Figure L-4d Example E-W Category 4 TC through Cape York (Tp time series comparisons)

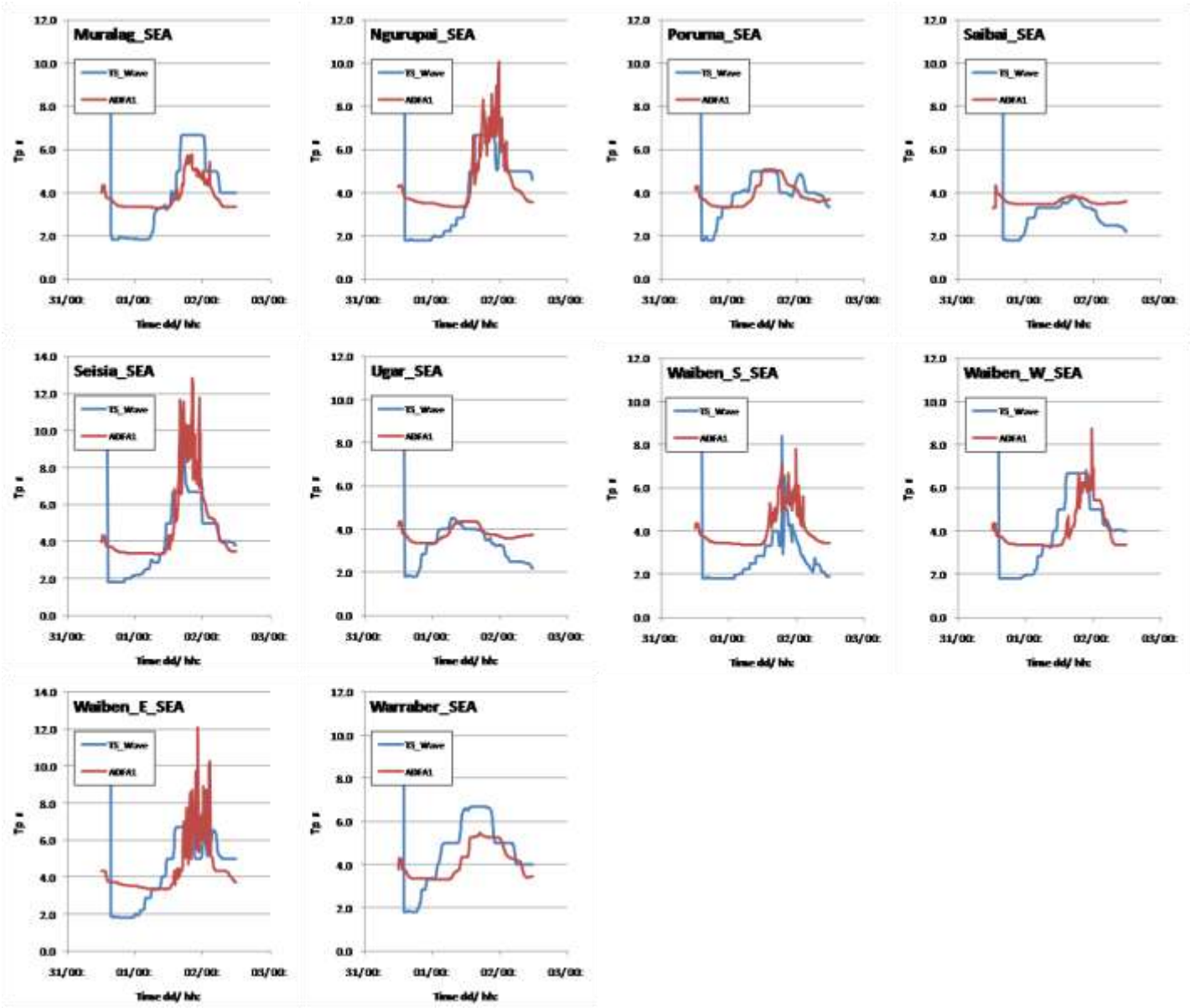

Figure L-4d Example E-W Category 4 TC through Cape York (Tp time series comparisons) contd

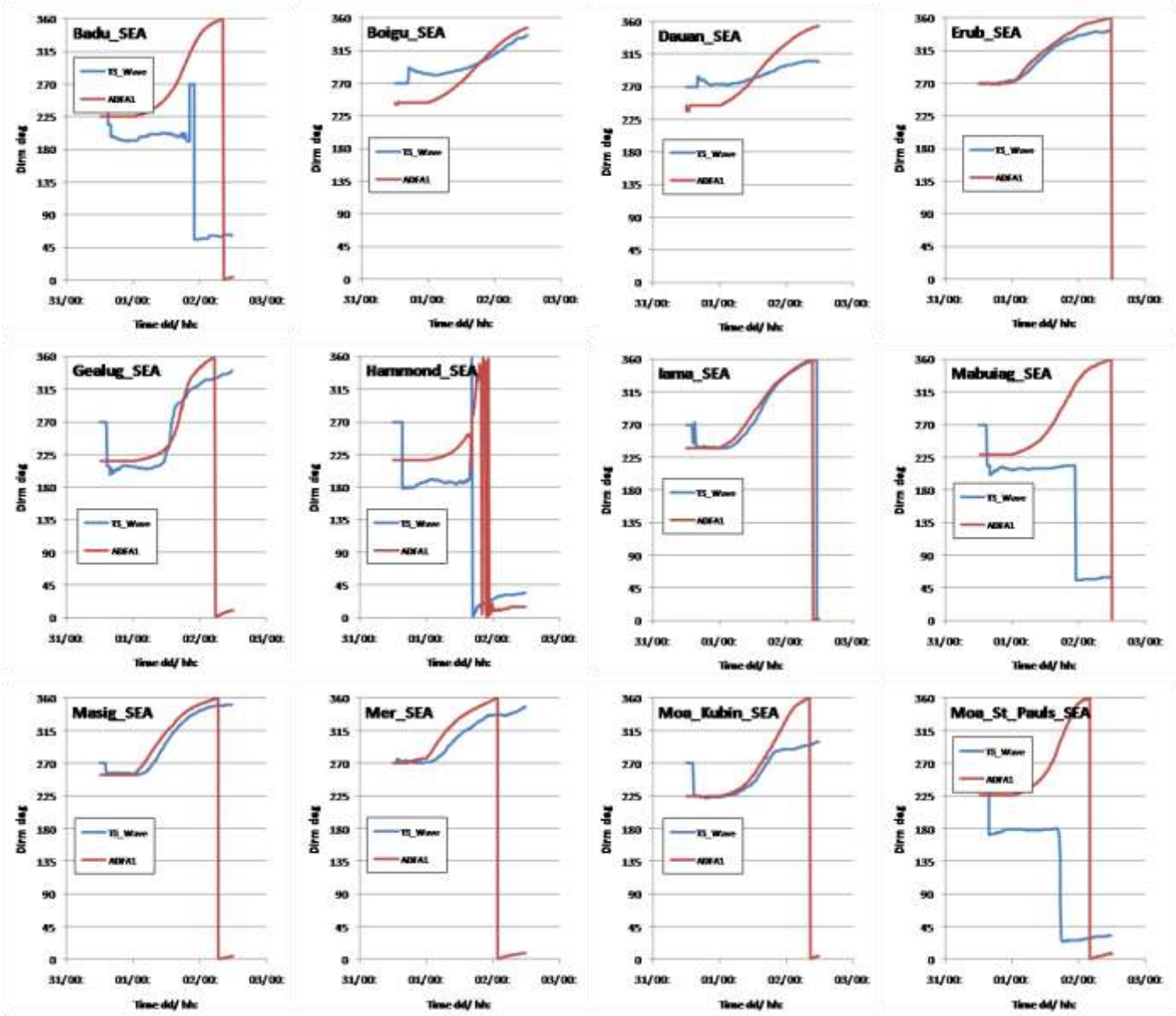

Figure L-4e Example E-W Category 4 TC through Cape York (Mean Direction time series comparisons)

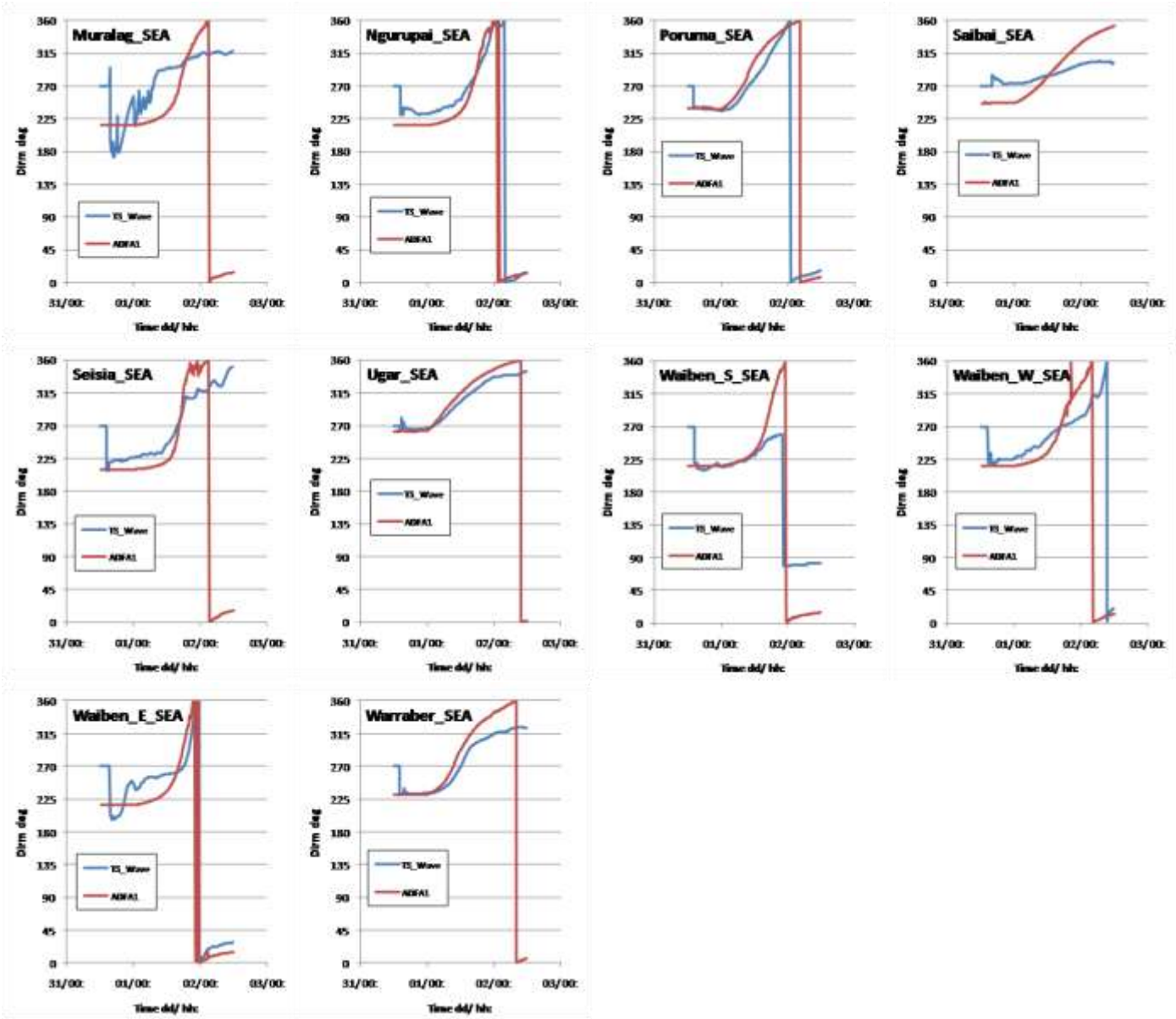

Figure L-4e Example E-W Category 4 TC through Cape York (Mean Direction time series comparisons) contd

Appendix M

Comments on the seasonal components of the MSQ (2009) report "Torres Strait Tidal Survey, Datum Analysis"

L.B. Mason

26/03/2010
Australian Maritime College
University of Tasmania

The seasonal signal in water level, are mainly a consequence of seasonal changes in wind patterns and atmospheric pressure although other processes such as fresh water inflow/rain also contribute. This signal is often treated as a tide and are associated with the S_a and S_{sa}, the yearly and half-yearly, tidal constituents. Because the S_a and S_{sa} represent the effect of weather patterns the NTC used a frequency for S_a the is tied to the tropical year rather than the astronomical frequency which has a slowly varying phase relative to the yearly climate.

In the MSQ (2009) report the S_a constituent is used for two purposes (a) to estimate the tidal HAT and LAT and, (b) to adjust the measured MWL obtained by GU in the short (35d) measurement program to MSL. For these purposes MSQ has for (a) used published estimate of S_a and for (b) used a constant 0.07m correction for all the GU stations (Zier et al. 2009). This comment considers whether an improved outcome could be obtained by using present modelled results obtained for the 60 y simulation of the water level in the Torres Strait.

M.1 Estimation of HAT and LAT

Accurate estimates of the weather induced S_a can only be obtained from multi-year analyses of measured water levels. The available multi-year records are mostly located at stations around the Prince of Wales shipping channel and are used for the safe navigation of the channel (see first four stations in Table M-1). A multi-year record also exists for Thursday Island. Yam Island also has a tidal record is greater than one year but this is made up of shorter records over a two year period (*Personal Comm*. Zarina Jayaswal). Other estimates of S_a in the Torres Strait have been inferenced from short records or are suspect because they are likely to originate from instruments measuring water pressure with no correction for atmospheric pressure (e.g. Twin Island and Albany Island).

The modelled estimates for the amplitude and phase of S_a are shown here in Figures M-1 and M-2. These results indicate a large change in amplitude and phase across the strait. The amplitude varies from approximately 0.28 m to 0.07 m from the western to eastern side of the strait. This sharp amplitude change and the phase change can be attributed to the wind patterns that cause the S_a signal in combination of the shallow frictional water of the Torres Strait. In winter the trade winds tend to setup water on the eastern side while causing a drawdown on the western side. The opposite is true during the monsoons. The high tidally induced friction across the strait suppresses the cross-strait flow and sharpens the gradients in amplitude and phase.

Comparisons with available data (Table M-1) indicate that the model does a reasonable job of reproducing the S_a amplitude and phase. In the Gulf of Carpentaria, the Booby Island the modelled results are a very good match to the data. On the eastern side of the strait the modelled results deteriorate slightly with the phase being delayed by about 10° as indicated by the Yam Island and Ince Point data in Table M-1. A slightly smaller phase lag also exists for Port Moresby and Cairns which suggests that this discrepancy originates from the model boundaries.

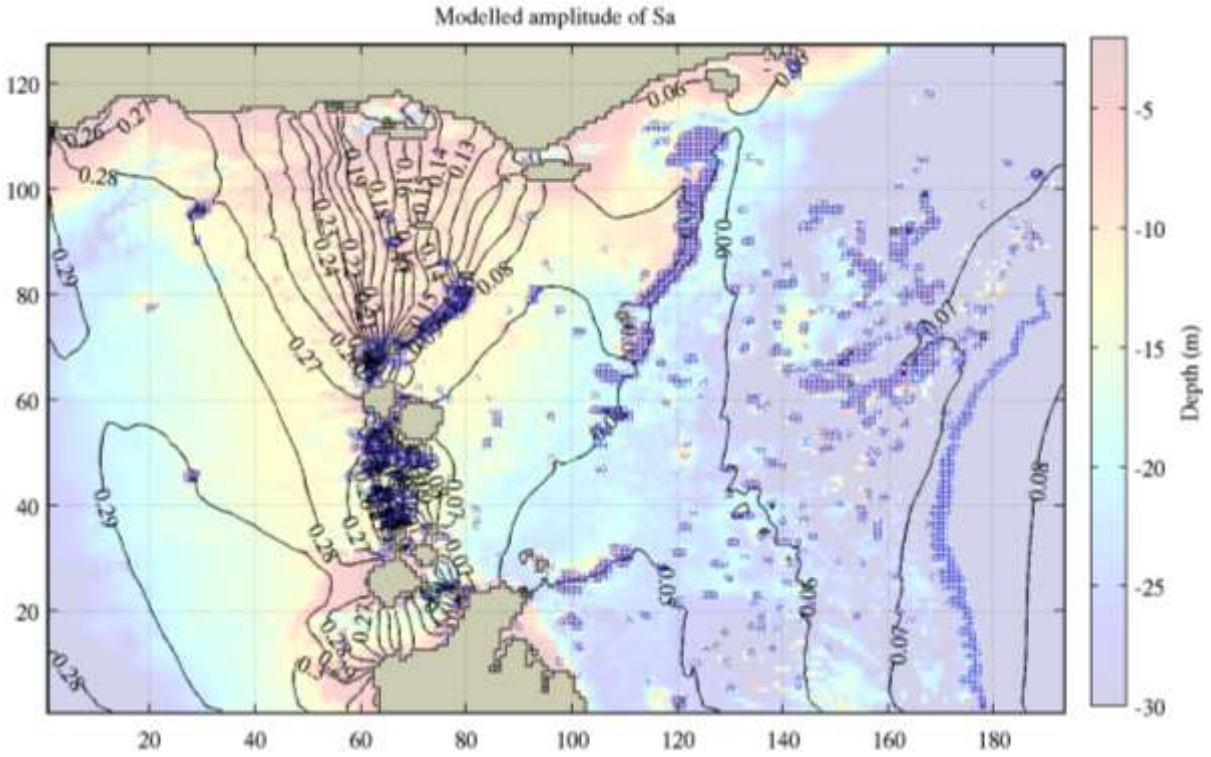

Figure M-1 Amplitude of the modelled S_a.

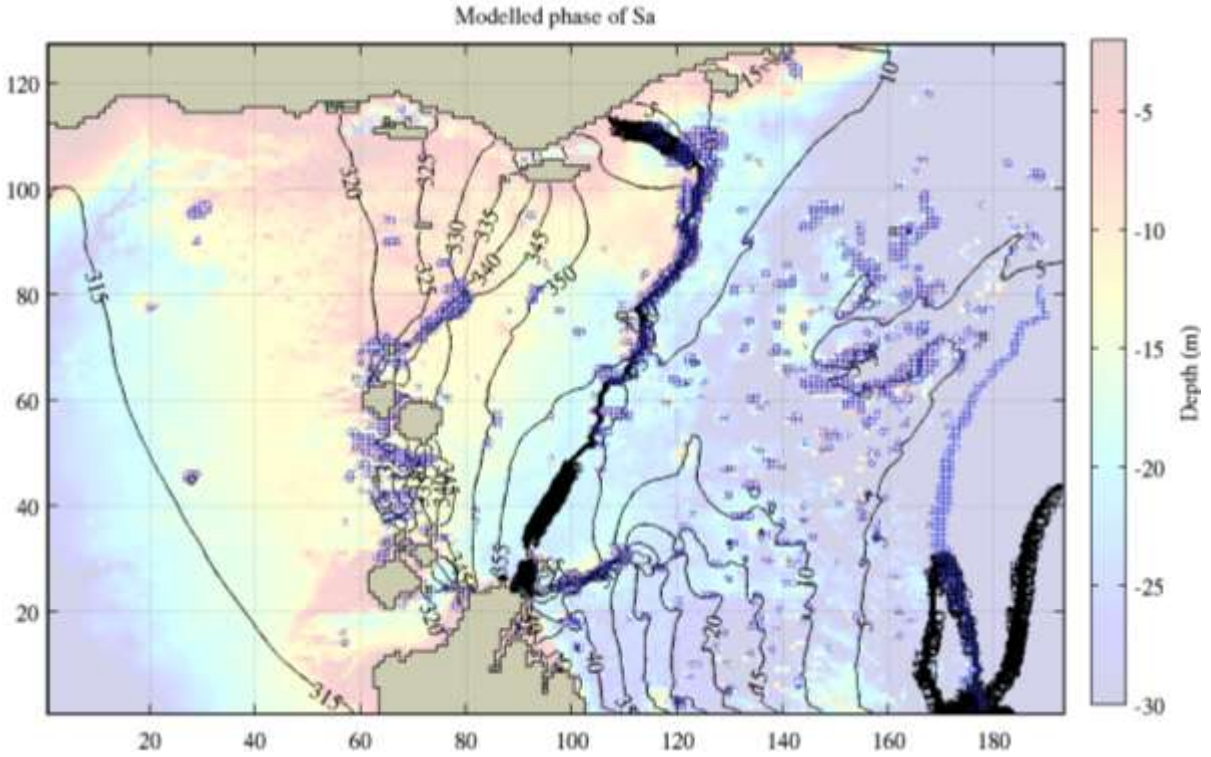

Figure M-2 Phase of the modelled S_a.

Table M-1 - Measured and modelled estimates of the weather induced S_a

Station Name	Measured S_a Amplitude/Phase	Modelled S_a (AMC) Amplitude/Phase	Modelled S_a (OCCAM) Amplitude/Phase
Booby Island	0.295/314.5 (AMC)	0.289/315.8	
Goods Island	0.256/310.4 (AMC)	0.262/317.4	
Turtle Head	0.164/316.1 (AMC)	0.189/320.6	
Ince Point	0.092/327.7 (AMC)	0.085/337.5	0.159/313.7
Thursday Island	0.114/322.9 (AMC)	0.130/326.3	
Boigu Island	0.261/308.7 (ANTT)	0.171/322.5	
Yam Island	0.077/339.9 (ANTT)	0.069/352.5	
Port Moresby	0.045/358.1 (ANTT)	0.077/4.7	0.068/348.2
Cairns	0.091/359.3 (ANTT)	0.110/4.8	
Coral Sea (144.5^{O},-10.5^{O})		0.084/359.5	0.050/344.6

Also shown in Table M-1 are some values of S_a derived from output of OCCAM, a UK derived global ocean model (http://gcmd.nasa.gov/records/GCMD_OCCAM.html) and is used to obtain a different perspective of the variation of S_a on the eastern side of the Torres Strait. For OCCAM the modelled phases lead the measured values near Ince Point and Port Moresby by about 10°. It also produces smaller amplitudes then the current modelling in the deeper water of the Coral Sea. Again this suggests some error in the boundaries of the current modelling.

Recommendations on the use of the modelled S_a for estimating HAT and LAT

The current modelling shows reasonable skill at reproducing the amplitude and phase variation across the Torres Strait and with a small modification to the phases the current work should provide a better estimate of S_a than used in the MSQ report. For stations east of Yam Island (e.g. Coconut Island to Murray Island) and Saibai Island the modelled phase should be reduced by 10° to obtain the best of HAT and LAT.

As noted in the MSQ report, there is a large difference in amplitude between the modelled and published values at Boigu Island. However, because published value is inferred from other stations and the model show some skill, suggest that the modelled value is more accurate and should be used.

M.2 MWL to MSL adjustment for GU stations

Like the estimation of S_a obtaining a good value for MSL requires multi-year water level records. This is particularly so on the western side of the Torres Strait where the seasonal variations in level are large. MSQ have used a constant 0.07m value to adjust the measured MWL to MSL for all sites in the GU measurement program. This value was obtained by calculating seasonal MWL variation from MSL at Thursday Island for the 35d period of the GU program.

To assess validity of using a constant MWL to MSL adjustment for all sites the equivalent modelled variations are computed and shown in Table M-2 (column labelled “Modelled GU Mean - Modelled MSL”). That is the computed MSL is subtracted from the computed MWL for the 35d of the GU project, where the total simulation time was 60 years. In this form the MSQ adjustment would be -0.07m. As can be seen from these results varies significantly meaning that the use of a

constant adjustment could possibly be in error by -0.18m (last column), assuming the model is accurate.

The accuracy of the modelled adjustments can be investigated by comparing them to those calculated from stations with multi-year records. Table M-3 presents modelled and measured adjustments computed for the MSQ stations spaning the Prince of Wales channel. These data show that there is indeed a significant discrepancy, ranging from 0.05 to 0.11m, between the modelled and measured estimates. The source of this difference is not obvious but probably originates from the weakest component of the modelling, the very long period variations in water level which are introduced into the system as boundary water levels computed by a simple linear model correlated to the SOI. These models only explain 77% and 48% of the long term variance on the western and eastern sides of the Torres Strait, respectively. Another but less likely source of error are the wind and pressure fields. This would require a significant bias in the wind over the 35d period of the GU program.

Table M-2 - Modelled seasonal corrections for GU sites. Modelled GU Mean's are mean water levels during the period (35d) when the GU data was collected.

Station Name	Station Longitude	Station Latitude	Modelled GU Mean - Modelled MSL	Variation from the 0.07m seasonal correction made by MSQ
Badu	142.1681	-10.17011667	-0.062152	-0.007848
Mabuiag	142.2012833	-9.95123333	0.047873	-0.117873
Hammond	142.2193611	-10.56138889	0.019141	-0.089141
Thursday	142.2215664	-10.58612194	-0.03713	-0.03287
Saibai	142.6136111	-9.38	0.056393	-0.126393
Yam	142.7662472	-9.89967111	0.093972	-0.163972
Warraber	142.8225031	-10.20459861	0.10132	-0.17132
Coconut	143.0639753	-10.04928139	0.10971	-0.17971
Yorke	143.4016156	-9.74890527	0.10606	-0.17606
Boigu	142.219	-9.23	-0.03102	-0.03898
Stephen	143.546905	-9.50482694	0.10588	-0.17588
Darnley	143.7600831	-9.59744778	0.10259	-0.17259
Murray	144.0397222	-9.915	0.097671	-0.167671

Table M-3 - Measured seasonal corrections calculated from the multi-year tidal stations. Measured GU Mean's are mean water levels during the period (35d) when the GU data was collected

Station Name	Station Longitude	Station Latitude	Modelled GU Mean - Modelled MSL	Measured GU Mean - Measured MSL (approx 10y)	Difference between the measured and modelled offsets
Booby Island	141.91667	-10.6	-0.1368	-0.2032	-0.0664
Goods Island	142.16667	-10.56667	-0.1109	-0.1606	-0.0497
Turtle Head	142.21666	-10.51667	-0.0376	-0.13	-0.0924
Ince Point	142.31667	-10.5	0.0669	-0.0426	-0.1095

Recommendations on the use of the modelled MWL to MSL adjustment

In this case it is clear that there is no obvious superior option. The constant adjustment use by MSQ is clearly in error given the model results however the model has its own issues underestimating the correction by 0.08m on average at the MSQ Prince of Wales stations. If one is convinced that this error is mainly due to the inaccurate estimation of the very long period water levels then a simple offset to the

model results would produce a better outcome than the constant adjustment used by MSQ.

Table M-4 presents MWL to MSL adjustments assuming a simple 0.08m (0.0795m) long period error in the modelled water. When this assumption is made the difference between the modelled adjustment and the constant 0.07m MSQ adjustment vary from -0.1 to 0.1 m, as see in the last column of Table M-4.

Table M-4 - Adjusted modelled seasonal corrections for GU sites.

Station Name	Station Longitude	Station Latitude	Modelled GU Mean WL - Modelled MSL, Adjusted by -0.0795m	Variation from the 0.07m seasonal correction made by MSQ
Badu	142.1681	-10.17011667	-0.141652	0.071652
Mabuiag	142.2012833	-9.95123333	-0.031627	-0.038373
Hammond	142.2193611	-10.56138889	-0.060359	-0.009641
Thursday	142.2215664	-10.58612194	-0.11663	0.04663
Saibai	142.6136111	-9.38	-0.023107	-0.046893
Yam	142.7662472	-9.89967111	0.014472	-0.084472
Warraber	142.8225031	-10.20459861	0.02182	-0.09182
Coconut	143.0639753	-10.04928139	0.03021	-0.10021
Yorke	143.4016156	-9.74890527	0.02656	-0.09656
Boigu	142.219	-9.23	-0.11052	0.04052
Stephen	143.546905	-9.50482694	0.02638	-0.09638
Darnley	143.7600831	-9.59744778	0.02309	-0.09309
Murray	144.0397222	-9.915	0.018171	-0.088171

M.3 Conclusion

Use of the modelled results should improve both the estimation of both S_a and the seasonal correction for the GU program. However modelling cannot take the place of measured data when trying to set datums. It is therefore recommended that a comprehensive program be set up to collect multi-year water level records that have accurate datum control. The instruments should preferably measure the water level directly. Although pressure gauges are cheaper to purchase and run it is more difficult to determine a datum. They also require an atmospheric pressure correction and an accurate estimate of the water density which is determined by the water temperature and salinity.

Appendix N

Summary of Selected Site-Specific Simulation Model Parameters

Site ID	Site Name	Lat	Lon	Nominal Depth	Dune Crest	Beach Slope	STIF %low	STIF %high	STIF LAT	STIF HAT	Tide Tamp	Wave Hs_f	Wave Tp_f	Reef?	Zreef	Zedge	Reef Top	Rim Width	Rim Slope	Kp	Kp'
		deg_GDA94	deg_GDA94	m_MSL	m_MSL	tan()	-	-	m_MSL	m_MSL	-	-	-	0_or_1	m	m	m	m	tan()	-	-
1	"Badu"	-10.16157	142.17463	3.0	6.5	0.12	5.0	-5.0	-2.0	2.0	1.0	2.23	1.60	1	-1.0	-1.5	400	480	0.02	0.50	0.50
2	"Boigu"	-9.22943	142.21921	3.0	2.5	0.40	10.0	-10.0	-2.0	2.0	1.0	1.98	1.20	0	0.0	0.0	0	0	0.00	0.00	0.00
3	"Dauan"	-9.41237	142.54124	3.5	6.5	0.12	5.0	-5.0	-2.0	2.0	1.0	1.20	0.81	1	-1.0	-1.5	90	100	0.02	0.50	0.50
4	"Erub"	-9.60218	143.76704	12.5	3.5	0.11	0.0	0.0	-2.0	2.0	1.0	1.01	0.95	1	-1.0	-1.5	400	500	0.02	0.50	0.50
5	"Gealug"	-10.59227	142.17916	3.0	5.0	0.12	5.0	-5.0	-2.0	2.0	1.0	1.10	1.04	0	0.0	0.0	0	0	0.00	0.00	0.00
6	"Hammond"	-10.55496	142.22207	5.5	5.5	0.10	10.0	-5.0	-2.0	2.0	1.0	1.42	1.50	1	-1.0	-1.5	200	250	0.02	0.50	0.50
7	"Iama"	-9.90120	142.76511	3.0	3.0	0.10	3.0	-3.0	-2.0	2.0	1.0	0.97	1.10	1	-1.0	-1.5	200	250	0.02	0.50	0.50
8	"Mabuiag"	-9.95447	142.19322	3.0	5.0	0.14	5.0	-5.0	-2.0	2.0	1.0	1.30	1.89	1	-1.0	-1.5	700	850	0.02	0.50	0.50
9	"Masig"	-9.75179	143.41413	3.0	2.5	0.12	5.0	-5.0	-2.0	2.0	1.0	1.00	0.98	1	-1.0	-1.5	350	450	0.02	0.50	0.50
10	"Mer"	-9.91242	144.03923	14.0	5.5	0.12	0.0	0.0	-2.0	2.0	1.0	1.13	0.99	1	-1.0	-1.5	50	150	0.02	0.50	0.50
11	"Moa_Kubin"	-10.23713	142.21352	8.5	10.0	0.12	10.0	-10.0	-2.0	2.0	1.0	0.85	0.81	1	-1.0	-1.5	550	660	0.02	0.50	0.50
12	"Moa_St_Pauls"	-10.19152	142.33972	3.0	5.0	0.12	10.0	-10.0	-2.0	2.0	1.0	1.29	0.95	1	-1.0	-1.5	510	550	0.02	0.50	0.50
13	"Muralag"	-10.60055	142.20561	3.0	5.0	0.12	10.0	-10.0	-2.0	2.0	1.0	1.36	1.11	0	0.0	0.0	0	0	0.00	0.00	0.00
14	"Ngurupai"	-10.59344	142.24283	3.0	5.0	0.06	10.0	-10.0	-2.0	2.0	1.0	1.74	1.42	0	0.0	0.0	0	0	0.00	0.00	0.00
15	"Poruma"	-10.05164	143.06392	6.0	4.0	0.12	3.0	-3.0	-2.0	2.0	1.0	1.18	1.18	1	-1.0	-1.5	100	150	0.02	0.50	0.50
16	"Saibai"	-9.37754	142.61555	3.0	2.0	1.00	10.0	-10.0	-2.0	2.0	1.0	1.33	1.03	0	0.0	0.0	0	0	0.00	0.00	0.00
17	"Seisia"	-10.85327	142.36299	5.0	4.0	0.05	20.0	-20.0	-2.0	2.0	1.0	1.45	1.42	0	0.0	0.0	0	0	0.00	0.00	0.00
18	"Ugar"	-9.50906	143.54676	3.0	8.5	0.14	5.0	-5.0	-2.0	2.0	1.0	1.08	1.05	1	-1.0	-1.5	500	750	0.02	0.50	0.50
19	"Waiben_S"	-10.58808	142.22051	3.0	5.0	0.07	10.0	-5.0	-2.0	2.0	1.0	2.52	2.16	0	0.0	0.0	0	0	0.00	0.00	0.00
20	"Waiben_W"	-10.58205	142.20294	4.0	5.0	0.14	10.0	-5.0	-2.0	2.0	1.0	1.31	1.22	1	-1.0	-1.5	400	420	0.02	0.50	0.50
21	"Waiben_E"	-10.56990	142.23007	3.0	5.0	0.14	10.0	-10.0	-2.0	2.0	1.0	1.33	1.42	0	0.0	0.0	0	0	0.00	0.00	0.00
22	"Warraber"	-10.20657	142.82713	3.0	3.5	0.13	5.0	-5.0	-2.0	2.0	1.0	1.11	0.93	1	-1.0	-1.5	550	600	0.02	0.50	0.50

Legend:

STIF Surge-tide interaction factors

Tamp Tide amplification factors (not used here as variation derived from broadscale modelling)

Hs_f Significant wave height calibration factor derived from inter-model comparisons

Tp_f Peak spectral wave period calibration factor derived from inter-model comparisons

ID	Name	Other Name	Location	Exposure	Type	Comment
1	"Badu"		mid-eastern	S?	granitic	
2	"Boigu"		north-western	NW	mud island	Ceebee wall
3	"Dauan"		north-eastern	NE	granitic	
4	"Erub"	Darnley_Island	southern side	S	volcanic	
5	"Gealug"	Friday_Island	eastern-end	E?	granitic	
6	"Hammond"		eastern side	E	granitic	
7	"Iama"	Yam_Island	western end	SW	granitic	
8	"Mabuiag"		eastern side	E	granitic	
9	"Masig"	Yorke_Island	eastern end	E	coral cay	taken on northern side
10	"Mer"	Murray_Island	north-western	N	volcanic	
11	"Moa_Kubin"		southern side	W	granitic	
12	"Moa_St_Pauls"		eastern side	E	granitic	
13	"Muralag"	Prince_of_Wales_Island	north-eastern	E	granitic	
14	"Ngurupai"	Horn_Island	north-western	W	granitic	
15	"Poruma"	Coconut_Island	western end	N	coral cay	taken on northern side
16	"Saibai"		north-western	W	mud island	near vert low seawall
17	"Seisia"	Bamaga/Cape_York	western end	W	granitic	
18	"Ugar"	Stephen_Island	eastern end	N	volcanic	
19	"Waiben_S"	Thursday_Island	southern side	S	granitic	very minor reef ignored
20	"Waiben_W"	Thursday_Island	western end	W	granitic	
21	"Waiben_E"	Thursday_Island	eastern end	E	granitic	very minor reef ignored
22	"Warraber"	Sue_Island	eastern end	SE	coral cay	taken on northern side

Appendix O

Summary Simulation Model Results for Present Climate 2010

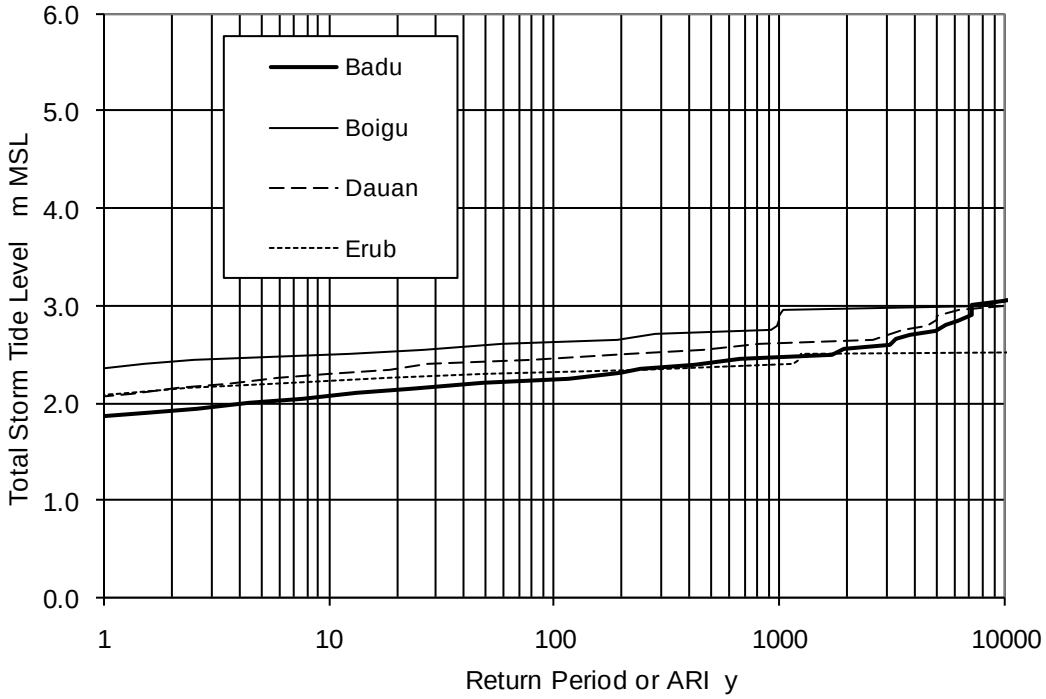
6.0
5.0
4.0
3.0
2.0
1.0
0.0
Total Storm Tide Level m MSL
Badu
Boigu
Dauan
Erub
1
10
100
1000
10000
Return Period or ARI y

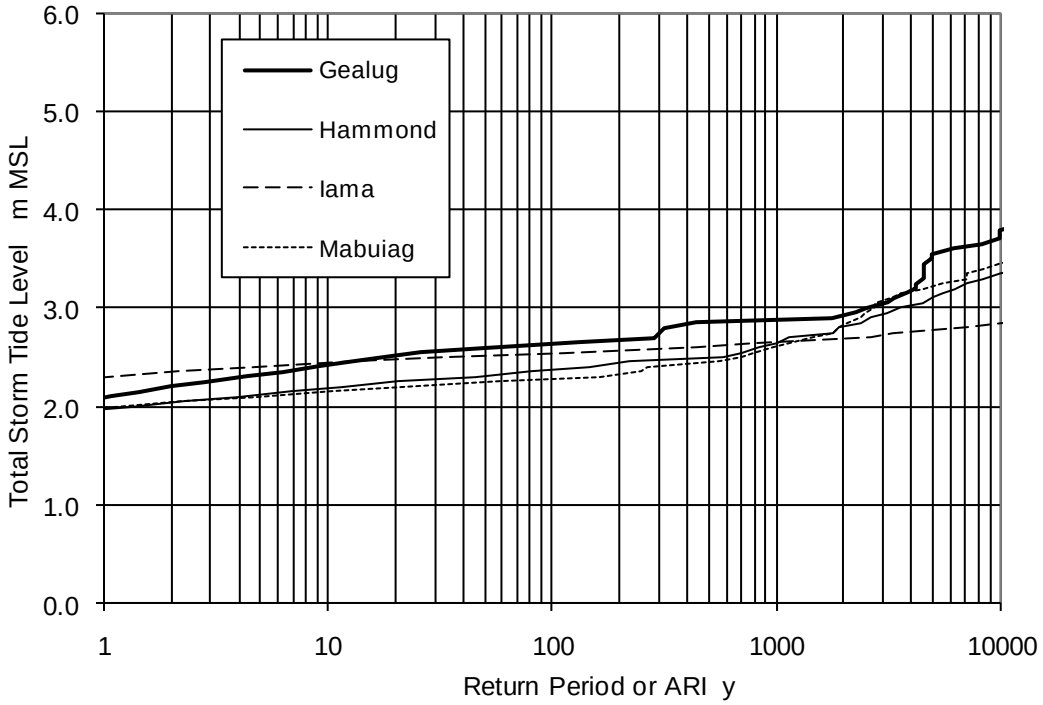
6.0
5.0
4.0
3.0
2.0
1.0
0.0
Total Storm Tide Level m MSL
Gealug
Hammond
Iama
Mabuiag
1
10
100
1000
10000
Return Period or ARI y

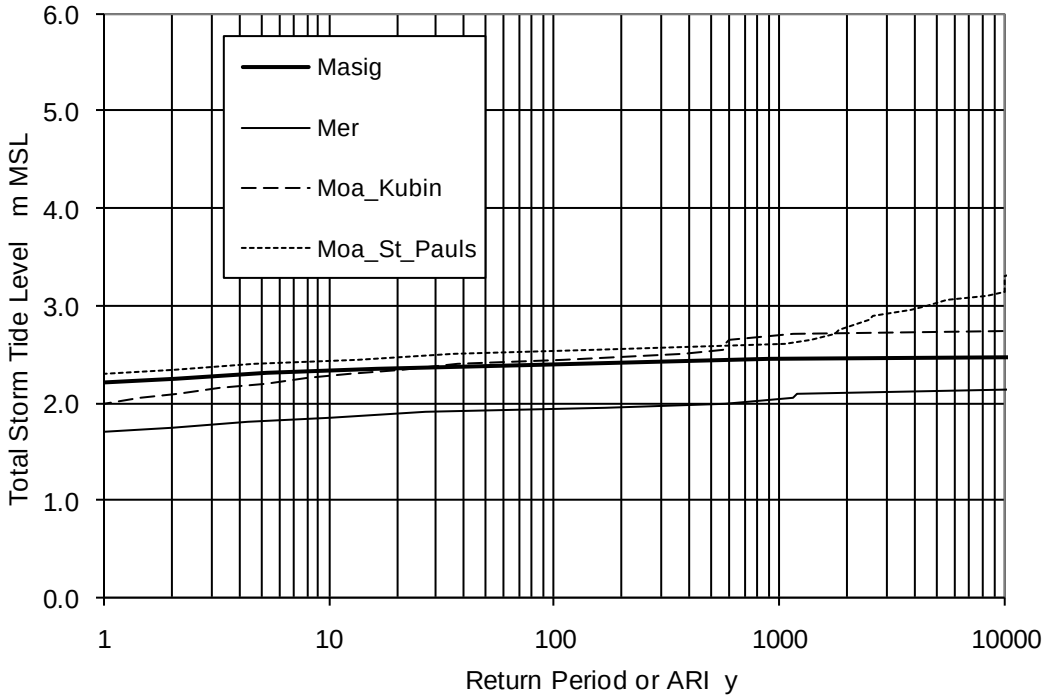
6.0
5.0
4.0
3.0
2.0
1.0
0.0
Total Storm Tide Level m MSL
Masig
Mer
Moa_Kubin
Moa_St_Pauls
1
10
100
1000
10000
Return Period or ARI y

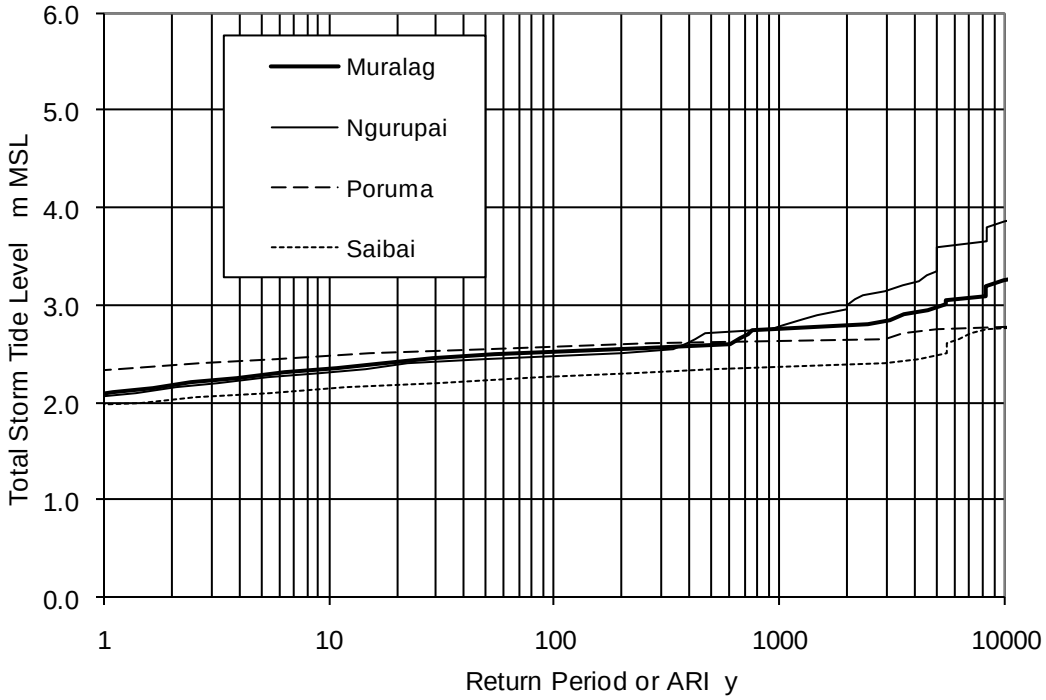
6.0
5.0
4.0
3.0
2.0
1.0
0.0
Total Storm Tide Level m MSL
Muralag
Ngurupai
Poruma
Saibai
1
10
100
1000
10000
Return Period or ARI y

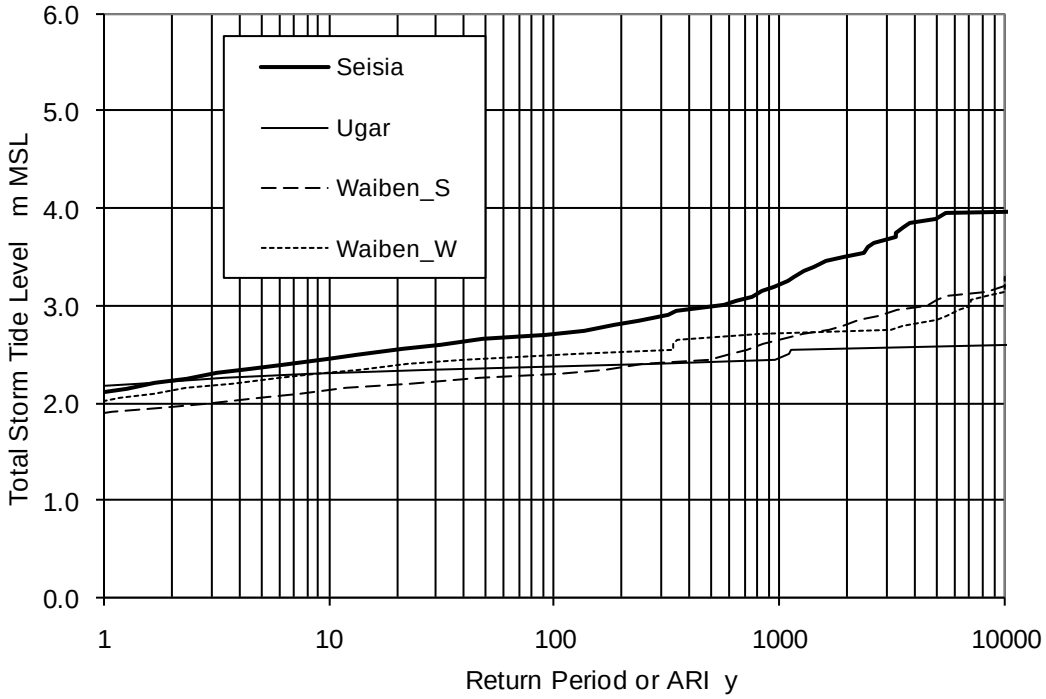
Seisia
Ugar
Waiben_S
Waiben_W
Total Storm Tide Level m MSL
Return Period or ARI y
6.0
5.0
4.0
3.0
2.0
1.0
0.0
1
10
100
1000
10000

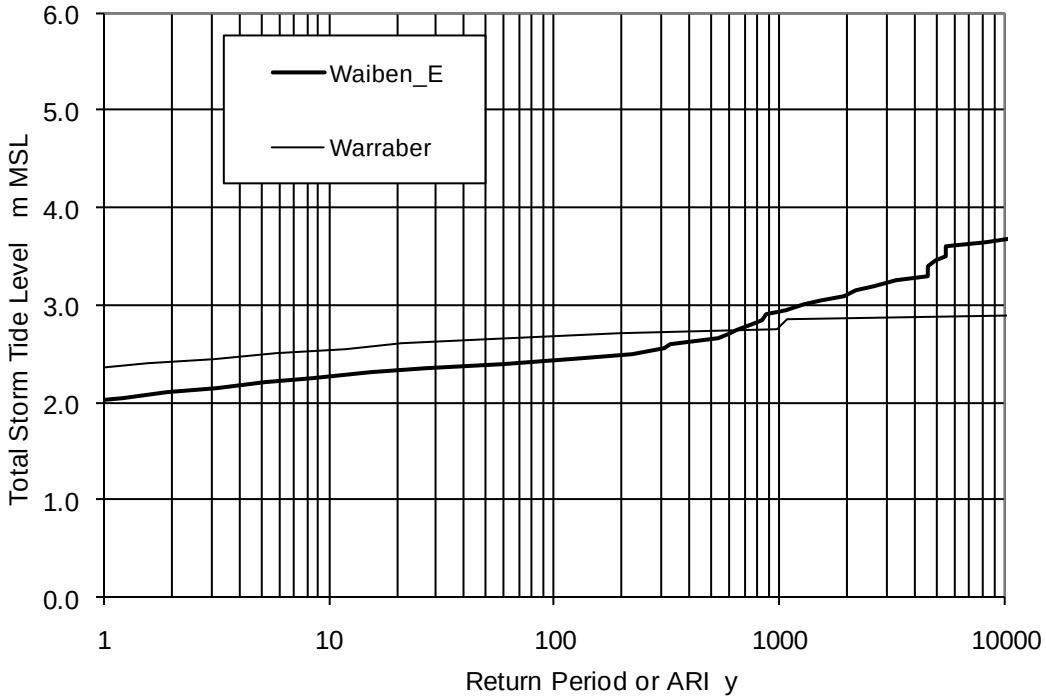
Waiben_E
Warraber
Total Storm Tide Level m MSL
Return Period or ARI y
6.0
5.0
4.0
3.0
2.0
1.0
0.0
1
10
100
1000
10000

Appendix P

Detailed Site-Specific Simulation Model Results for Present Climate 2010

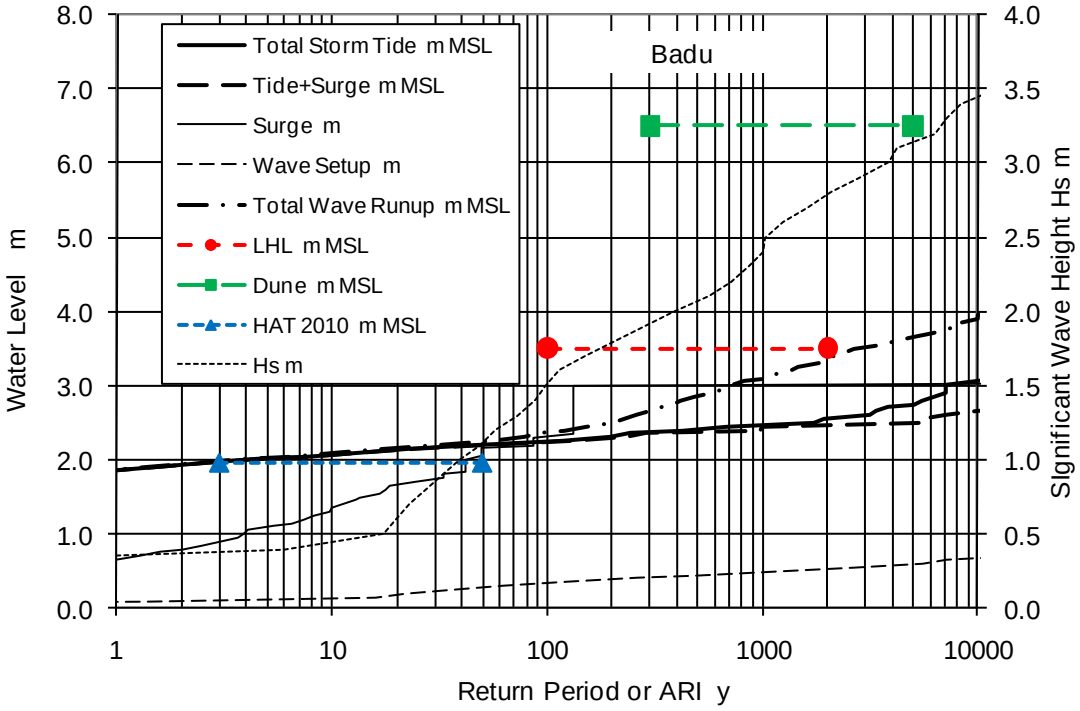
Badu
Total Storm Tide m MSL
Tide+Surge m MSL
Surge m
Wave Setup m
Total Wave Runup m MSL
LHL m MSL
Dune m MSL
HAT 2010 m MSL
Hs m
Water Level m
Significant Wave Height Hs m
Return Period or ARI y
8.0
7.0
6.0
5.0
4.0
3.0
2.0
1.0
0.0
4.0
3.5
3.0
2.5
2.0
1.5
1.0
0.5
0.0
1
10
100
1000
10000

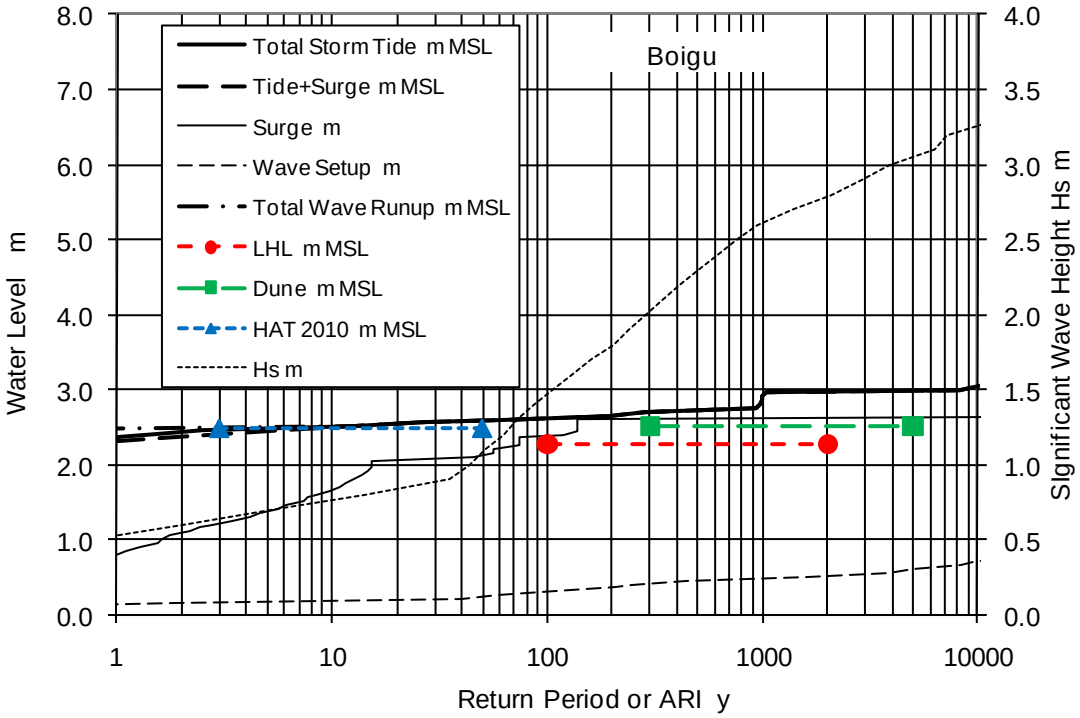
Boigu
Total Storm Tide m MSL
Tide+Surge m MSL
Surge m
Wave Setup m
Total Wave Runup m MSL
LHL m MSL
Dune m MSL
HAT 2010 m MSL
Hs m
Water Level m
Significant Wave Height Hs m
Return Period or ARI y
8.0
7.0
6.0
5.0
4.0
3.0
2.0
1.0
0.0
4.0
3.5
3.0
2.5
2.0
1.5
1.0
0.5
0.0
1
10
100
1000
10000

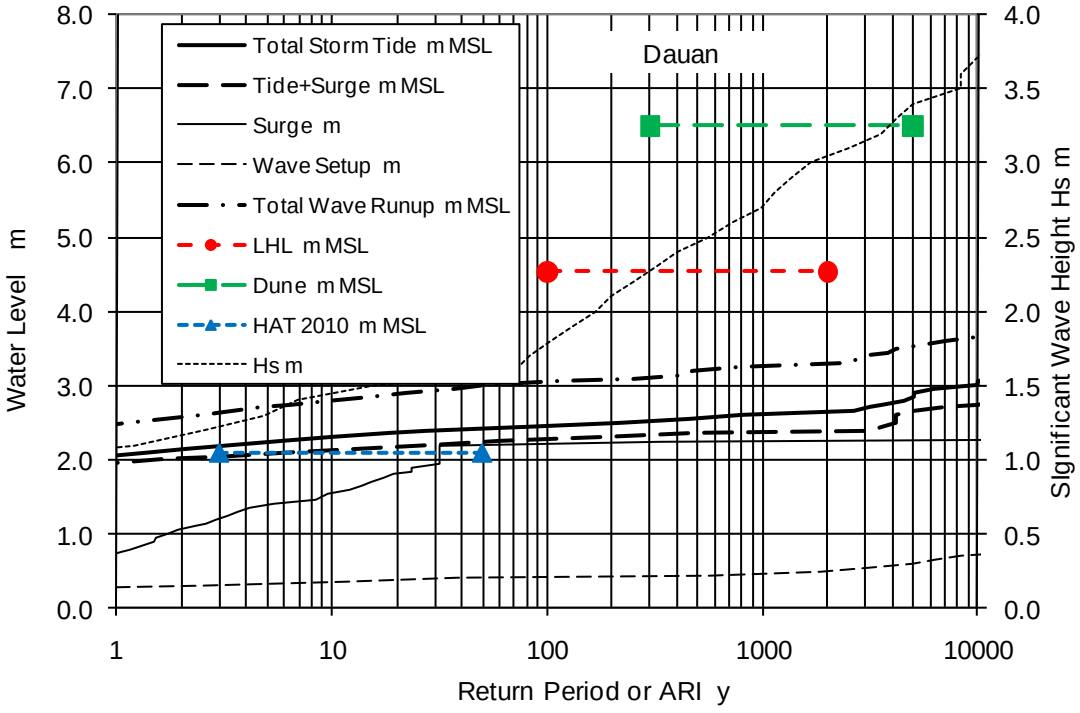
Dauan
Total Storm Tide m MSL
Tide+Surge m MSL
Surge m
Wave Setup m
Total Wave Runup m MSL
LHL m MSL
Dune m MSL
HAT 2010 m MSL
Hs m
Water Level m
Significant Wave Height Hs m
Return Period or ARI y
8.0
7.0
6.0
5.0
4.0
3.0
2.0
1.0
0.0
4.0
3.5
3.0
2.5
2.0
1.5
1.0
0.5
0.0
1
10
100
1000
10000

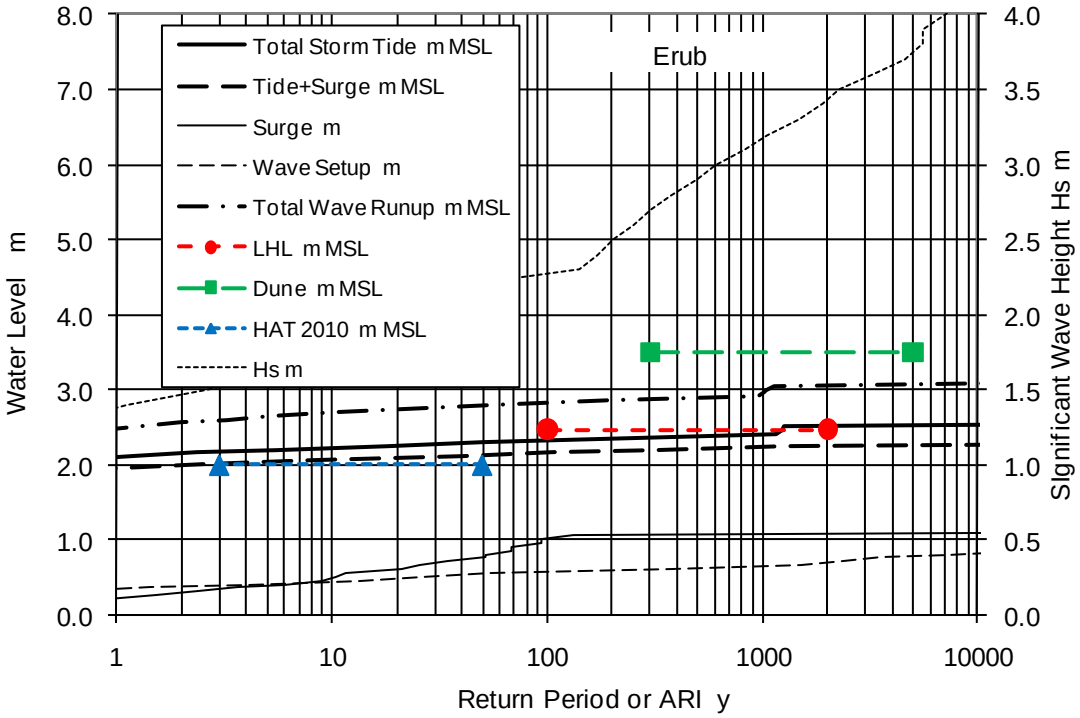
Erub
Total Storm Tide m MSL
Tide+Surge m MSL
Surge m
Wave Setup m
Total Wave Runup m MSL
LHL m MSL
Dune m MSL
HAT 2010 m MSL
Hs m
Water Level m
Significant Wave Height Hs m
Return Period or ARI y
8.0
7.0
6.0
5.0
4.0
3.0
2.0
1.0
0.0
4.0
3.5
3.0
2.5
2.0
1.5
1.0
0.5
0.0
1
10
100
1000
10000

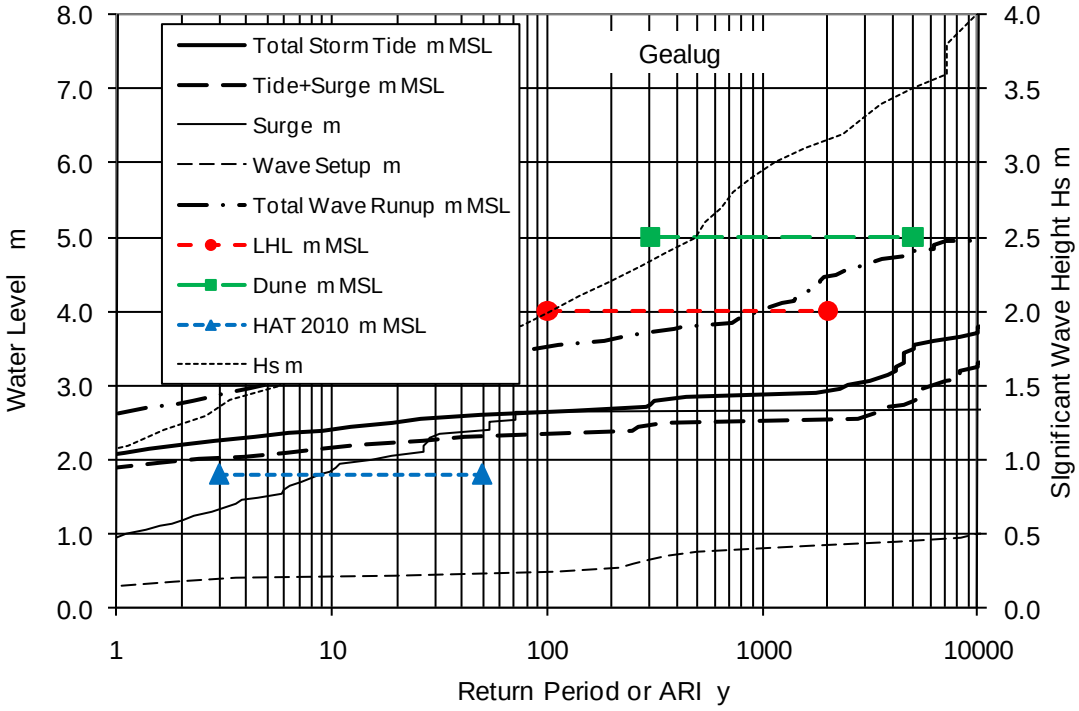
Gealug
Total Storm Tide m MSL
Tide+Surge m MSL
Surge m
Wave Setup m
Total Wave Runup m MSL
LHL m MSL
Dune m MSL
HAT 2010 m MSL
Hs m
Water Level m
Significant Wave Height Hs m
Return Period or ARI y
8.0
7.0
6.0
5.0
4.0
3.0
2.0
1.0
0.0
4.0
3.5
3.0
2.5
2.0
1.5
1.0
0.5
0.0
1
10
100
1000
10000

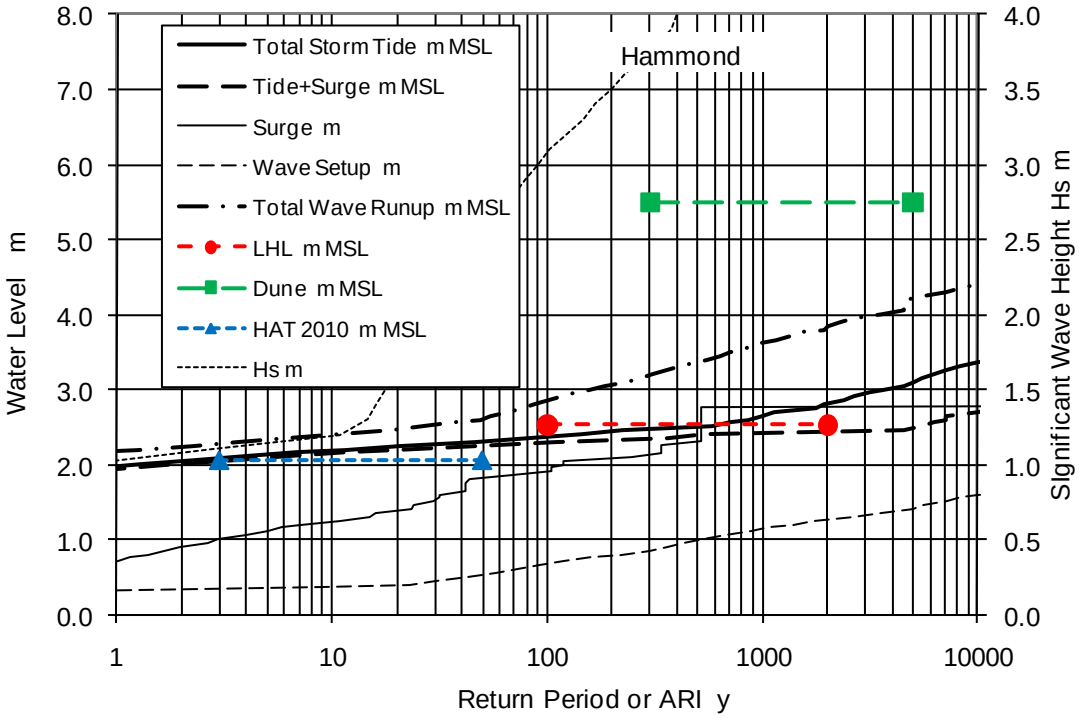
Hammond
Total Storm Tide m MSL
Tide+Surge m MSL
Surge m
Wave Setup m
Total Wave Runup m MSL
LHL m MSL
Dune m MSL
HAT 2010 m MSL
Hs m
Water Level m
Significant Wave Height Hs m
Return Period or ARI y
8.0
7.0
6.0
5.0
4.0
3.0
2.0
1.0
0.0
4.0
3.5
3.0
2.5
2.0
1.5
1.0
0.5
0.0
1
10
100
1000
10000

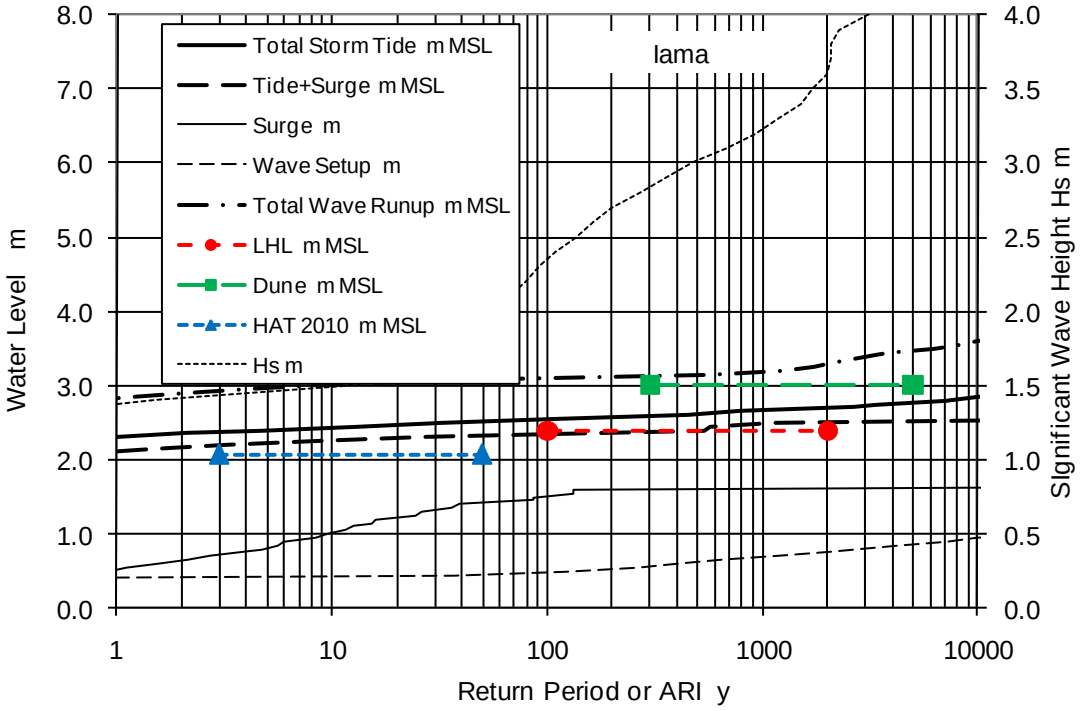
Iama
Total Storm Tide m MSL
Tide+Surge m MSL
Surge m
Wave Setup m
Total Wave Runup m MSL
LHL m MSL
Dune m MSL
HAT 2010 m MSL
Hs m
Water Level m
Significant Wave Height Hs m
Return Period or ARI y
8.0
7.0
6.0
5.0
4.0
3.0
2.0
1.0
0.0
4.0
3.5
3.0
2.5
2.0
1.5
1.0
0.5
0.0
1
10
100
1000
10000

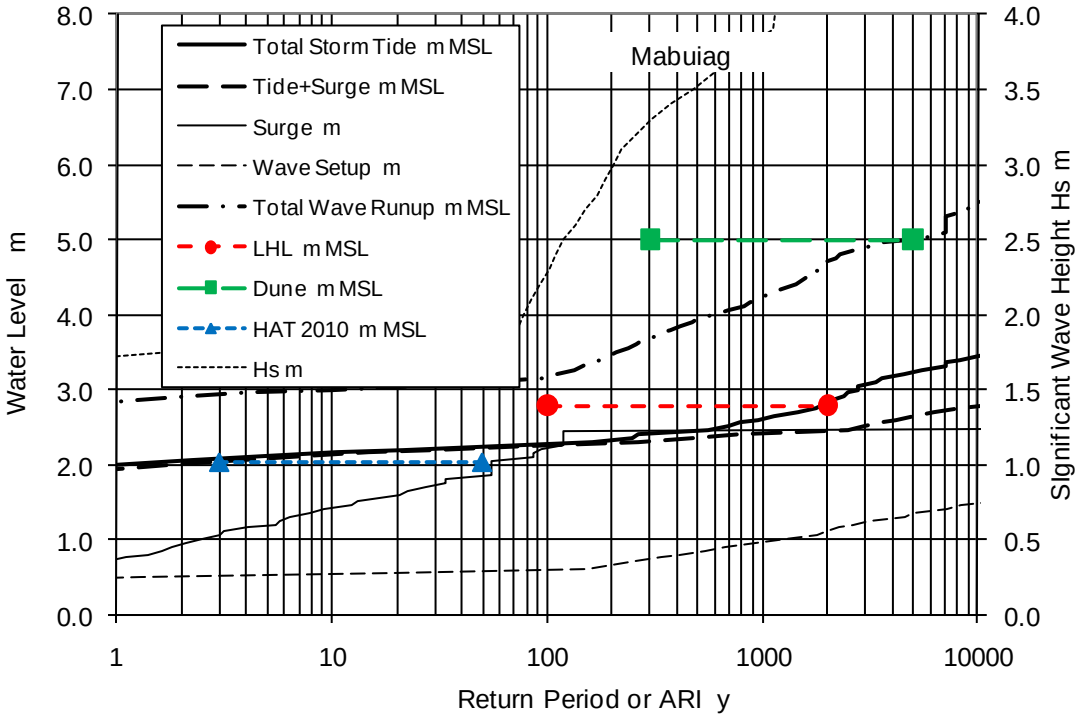
Mabuiag
Total Storm Tide m MSL
Tide+Surge m MSL
Surge m
Wave Setup m
Total Wave Runup m MSL
LHL m MSL
Dune m MSL
HAT 2010 m MSL
Hs m
Water Level m
Significant Wave Height Hs m
Return Period or ARI y
8.0
7.0
6.0
5.0
4.0
3.0
2.0
1.0
0.0
4.0
3.5
3.0
2.5
2.0
1.5
1.0
0.5
0.0
1
10
100
1000
10000

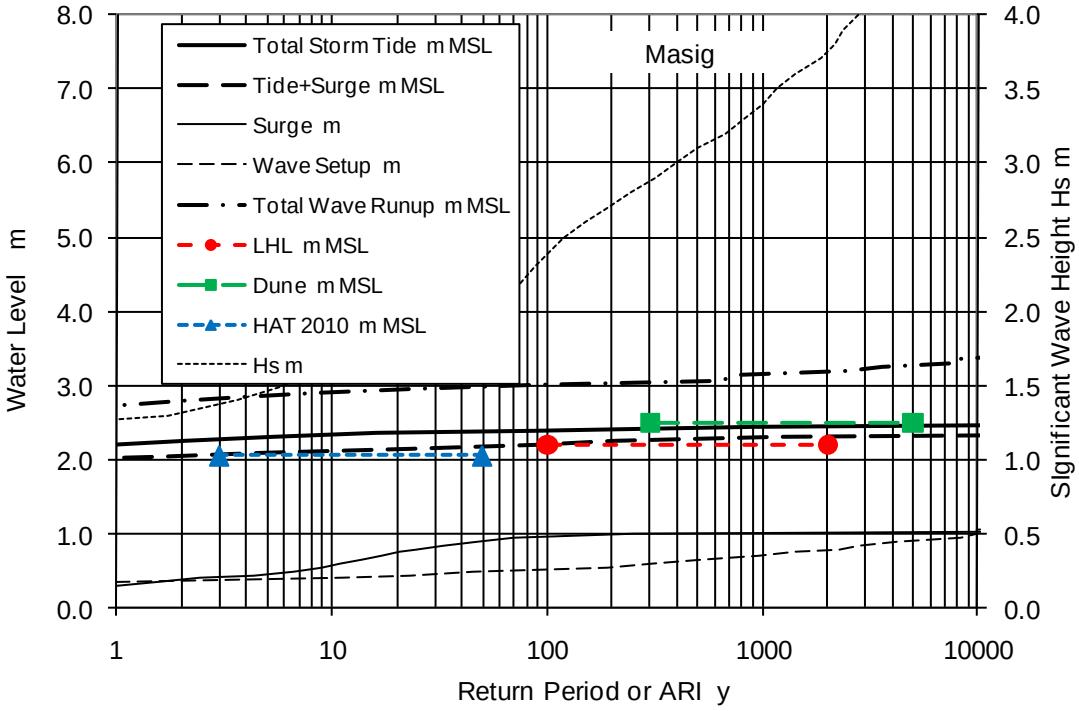
Masig
Total Storm Tide m MSL
Tide+Surge m MSL
Surge m
Wave Setup m
Total Wave Runup m MSL
LHL m MSL
Dune m MSL
HAT 2010 m MSL
Hs m
Water Level m
Significant Wave Height Hs m
Return Period or ARI y
8.0
7.0
6.0
5.0
4.0
3.0
2.0
1.0
0.0
4.0
3.5
3.0
2.5
2.0
1.5
1.0
0.5
0.0
1
10
100
1000
10000

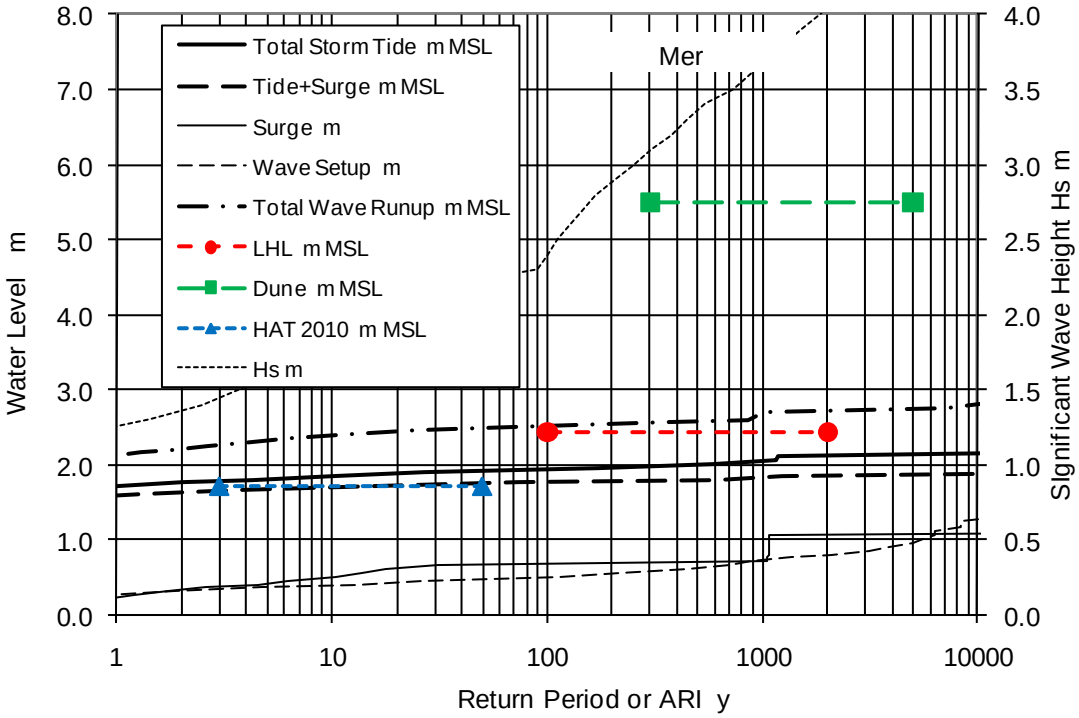
Mer
Total Storm Tide m MSL
Tide+Surge m MSL
Surge m
Wave Setup m
Total Wave Runup m MSL
LHL m MSL
Dune m MSL
HAT 2010 m MSL
Hs m
Water Level m
Significant Wave Height Hs m
Return Period or ARI y
8.0
7.0
6.0
5.0
4.0
3.0
2.0
1.0
0.0
4.0
3.5
3.0
2.5
2.0
1.5
1.0
0.5
0.0
1
10
100
1000
10000

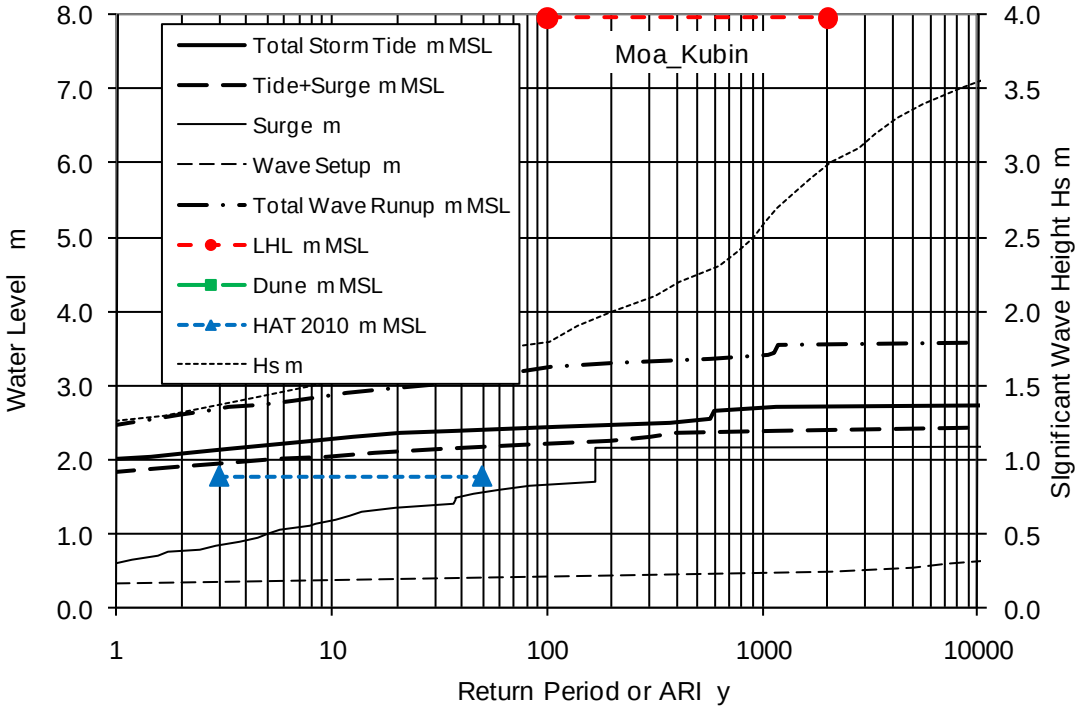
Moa_Kubin
Total Storm Tide m MSL
Tide+Surge m MSL
Surge m
Wave Setup m
Total Wave Runup m MSL
LHL m MSL
Dune m MSL
HAT 2010 m MSL
Hs m
Water Level m
Significant Wave Height Hs m
Return Period or ARI y
8.0
7.0
6.0
5.0
4.0
3.0
2.0
1.0
0.0
4.0
3.5
3.0
2.5
2.0
1.5
1.0
0.5
0.0
1
10
100
1000
10000

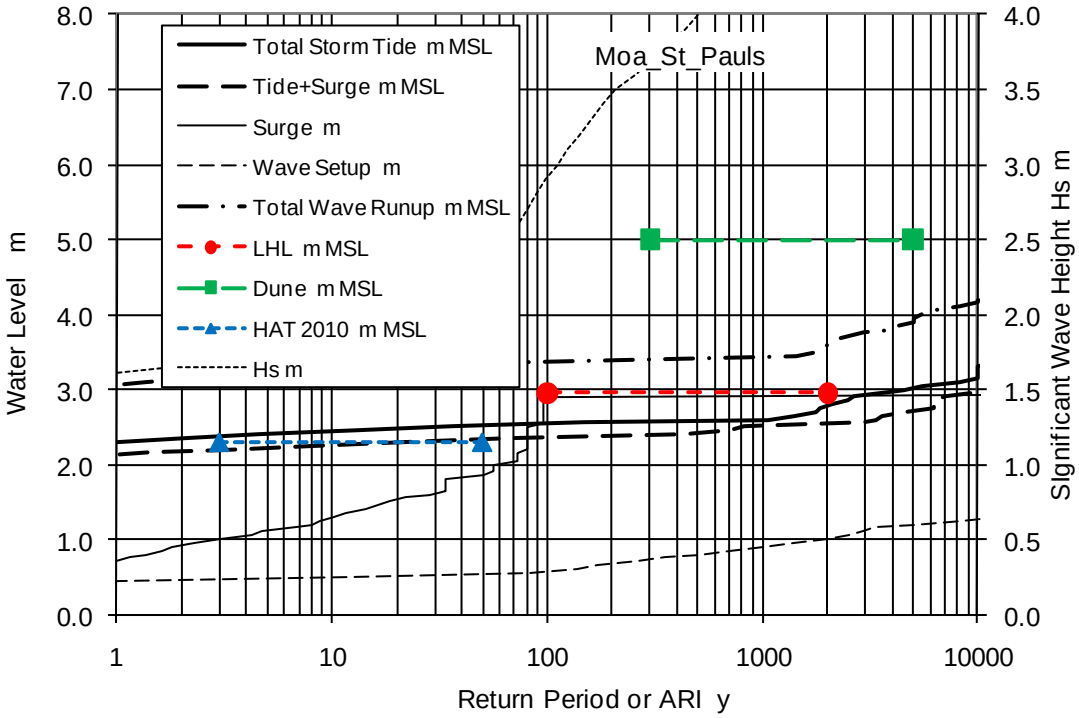
Moa_St_Pauls
Total Storm Tide m MSL
Tide+Surge m MSL
Surge m
Wave Setup m
Total Wave Runup m MSL
LHL m MSL
Dune m MSL
HAT 2010 m MSL
Hs m
Water Level m
Significant Wave Height Hs m
Return Period or ARI y
8.0
7.0
6.0
5.0
4.0
3.0
2.0
1.0
0.0
4.0
3.5
3.0
2.5
2.0
1.5
1.0
0.5
0.0
1
10
100
1000
10000

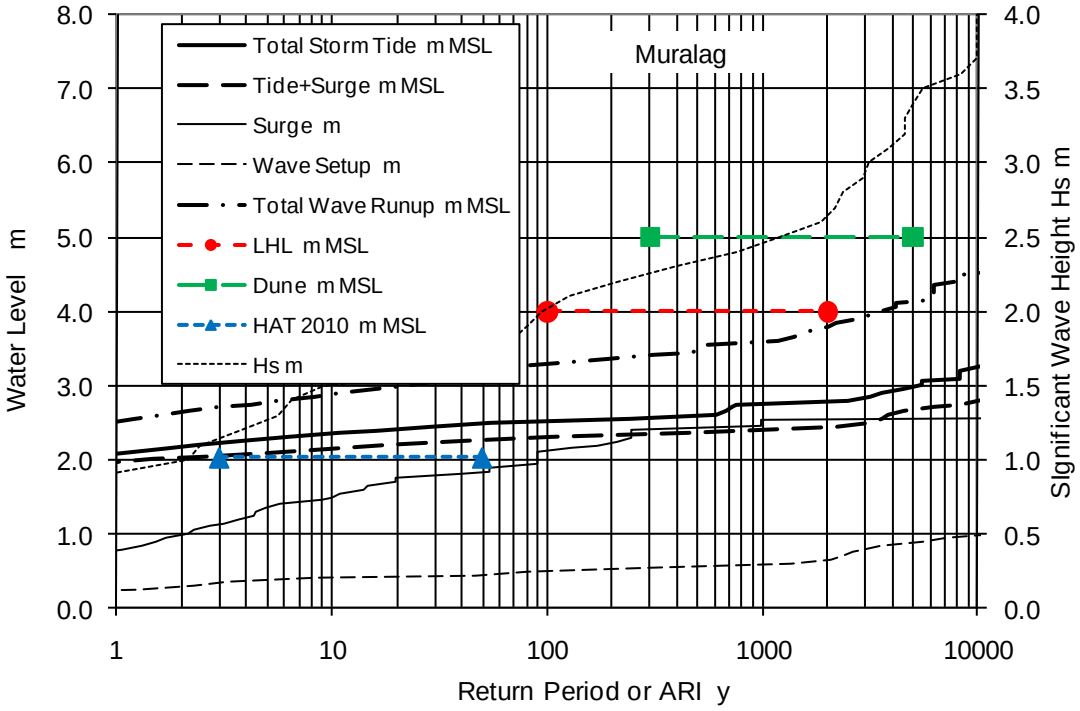
Muralag
Total Storm Tide m MSL
Tide+Surge m MSL
Surge m
Wave Setup m
Total Wave Runup m MSL
LHL m MSL
Dune m MSL
HAT 2010 m MSL
Hs m
Water Level m
Significant Wave Height Hs m
Return Period or ARI y
8.0
7.0
6.0
5.0
4.0
3.0
2.0
1.0
0.0
4.0
3.5
3.0
2.5
2.0
1.5
1.0
0.5
0.0
1
10
100
1000
10000

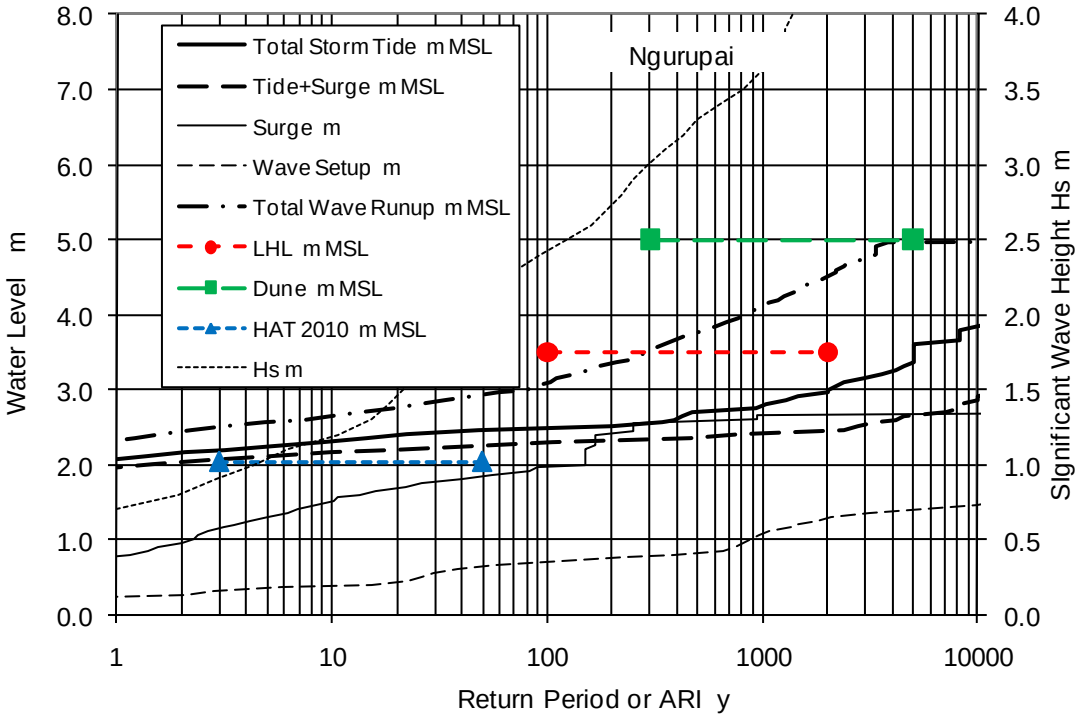
Ngurupai
Total Storm Tide m MSL
Tide+Surge m MSL
Surge m
Wave Setup m
Total Wave Runup m MSL
LHL m MSL
Dune m MSL
HAT 2010 m MSL
Hs m
Water Level m
Significant Wave Height Hs m
Return Period or ARI y
8.0
7.0
6.0
5.0
4.0
3.0
2.0
1.0
0.0
4.0
3.5
3.0
2.5
2.0
1.5
1.0
0.5
0.0
1
10
100
1000
10000

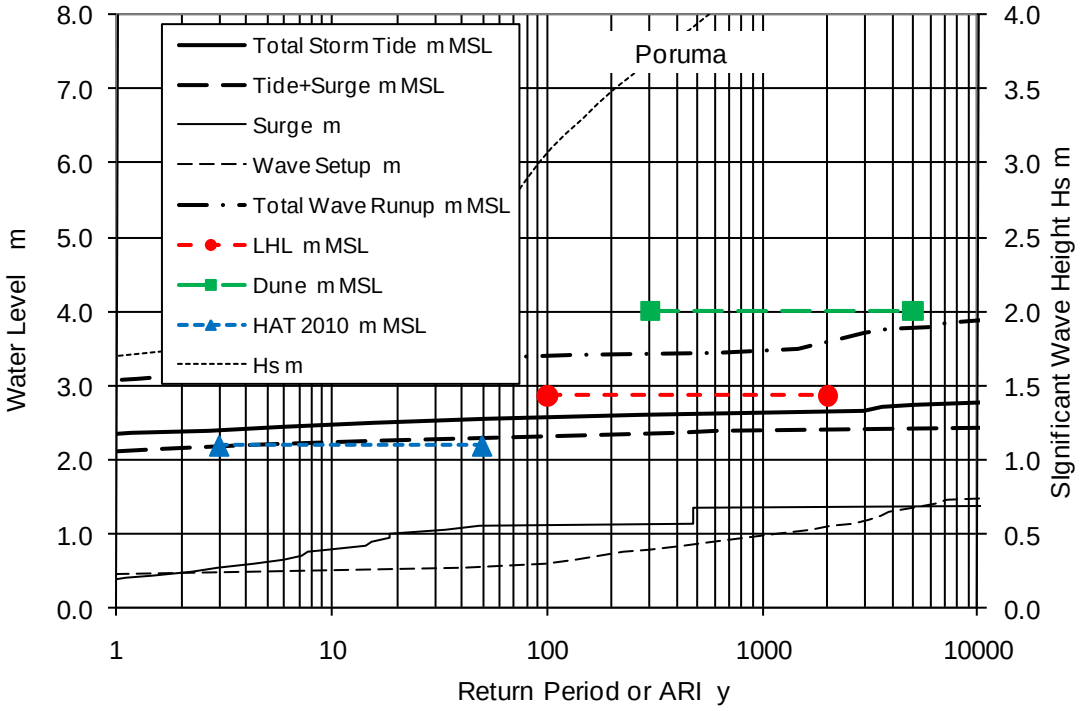
Poruma
Total Storm Tide m MSL
Tide+Surge m MSL
Surge m
Wave Setup m
Total Wave Runup m MSL
LHL m MSL
Dune m MSL
HAT 2010 m MSL
Hs m
Water Level m
Significant Wave Height Hs m
Return Period or ARI y
8.0
7.0
6.0
5.0
4.0
3.0
2.0
1.0
0.0
4.0
3.5
3.0
2.5
2.0
1.5
1.0
0.5
0.0
1
10
100
1000
10000

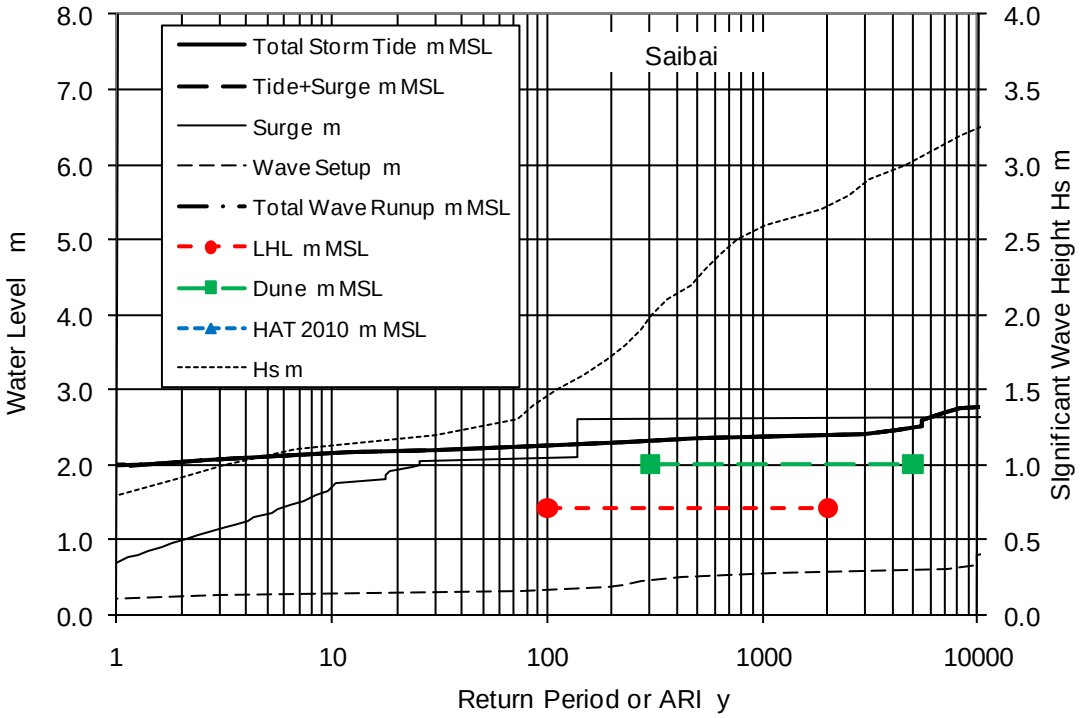
Saibai
Total Storm Tide m MSL
Tide+Surge m MSL
Surge m
Wave Setup m
Total Wave Runup m MSL
LHL m MSL
Dune m MSL
HAT 2010 m MSL
Hs m
Water Level m
Significant Wave Height Hs m
Return Period or ARI y
8.0
7.0
6.0
5.0
4.0
3.0
2.0
1.0
0.0
4.0
3.5
3.0
2.5
2.0
1.5
1.0
0.5
0.0
1
10
100
1000
10000

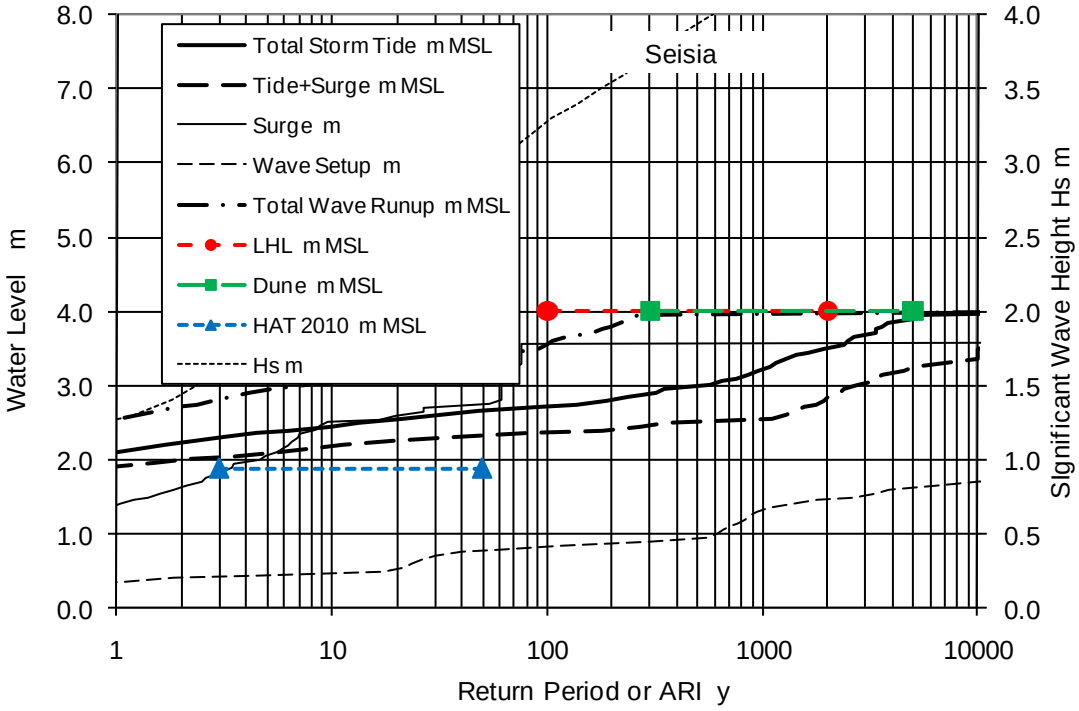
Seisia
Total Storm Tide m MSL
Tide+Surge m MSL
Surge m
Wave Setup m
Total Wave Runup m MSL
LHL m MSL
Dune m MSL
HAT 2010 m MSL
Hs m
Water Level m
Significant Wave Height Hs m
Return Period or ARI y
8.0
7.0
6.0
5.0
4.0
3.0
2.0
1.0
0.0
4.0
3.5
3.0
2.5
2.0
1.5
1.0
0.5
0.0
1
10
100
1000
10000

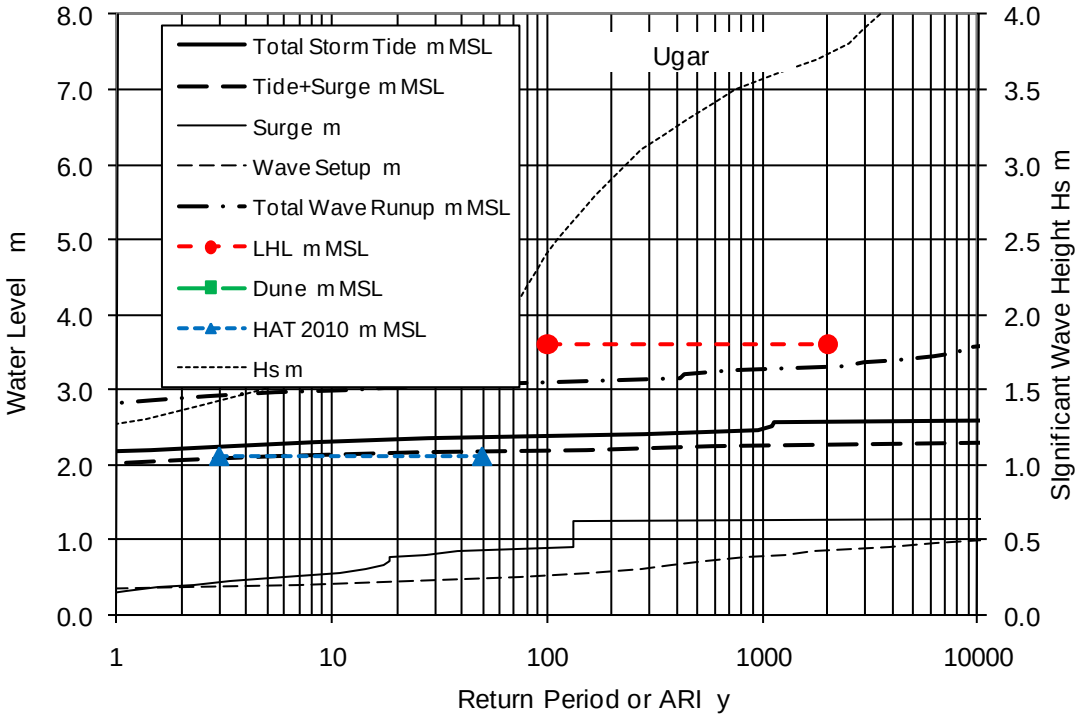
Ugar
Total Storm Tide m MSL
Tide+Surge m MSL
Surge m
Wave Setup m
Total Wave Runup m MSL
LHL m MSL
Dune m MSL
HAT 2010 m MSL
Hs m
Water Level m
Significant Wave Height Hs m
Return Period or ARI y
8.0
7.0
6.0
5.0
4.0
3.0
2.0
1.0
0.0
4.0
3.5
3.0
2.5
2.0
1.5
1.0
0.5
0.0
1
10
100
1000
10000

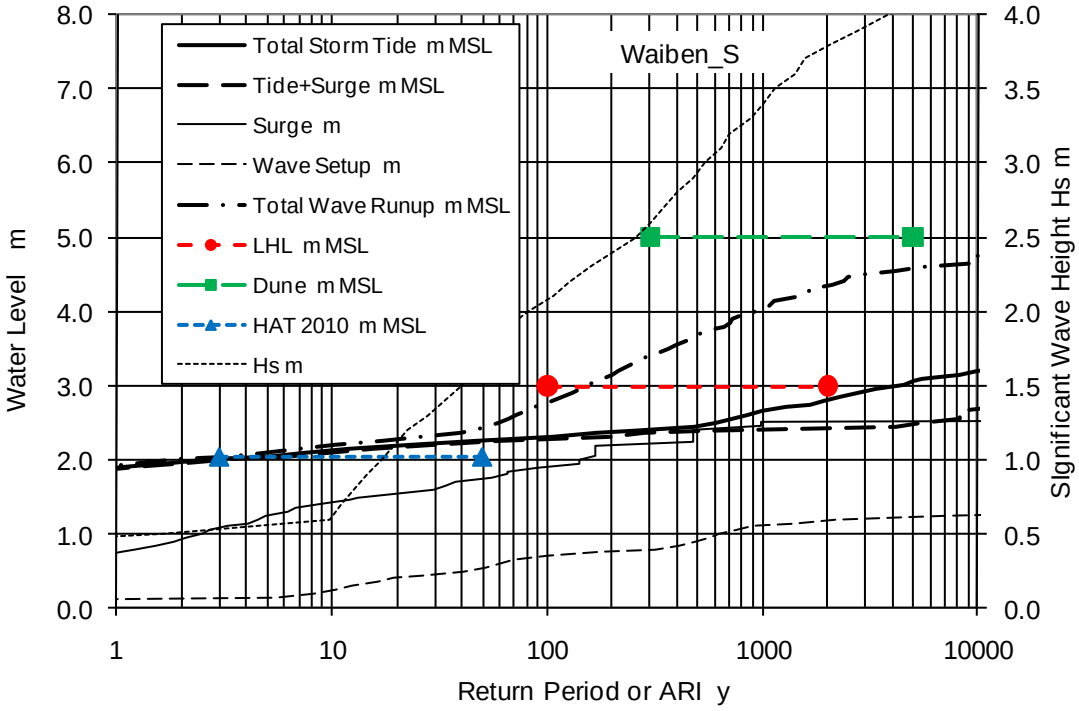
Waiben_S
Total Storm Tide m MSL
Tide+Surge m MSL
Surge m
Wave Setup m
Total Wave Runup m MSL
LHL m MSL
Dune m MSL
HAT 2010 m MSL
Hs m
Water Level m
Significant Wave Height Hs m
Return Period or ARI y
8.0
7.0
6.0
5.0
4.0
3.0
2.0
1.0
0.0
4.0
3.5
3.0
2.5
2.0
1.5
1.0
0.5
0.0
1
10
100
1000
10000

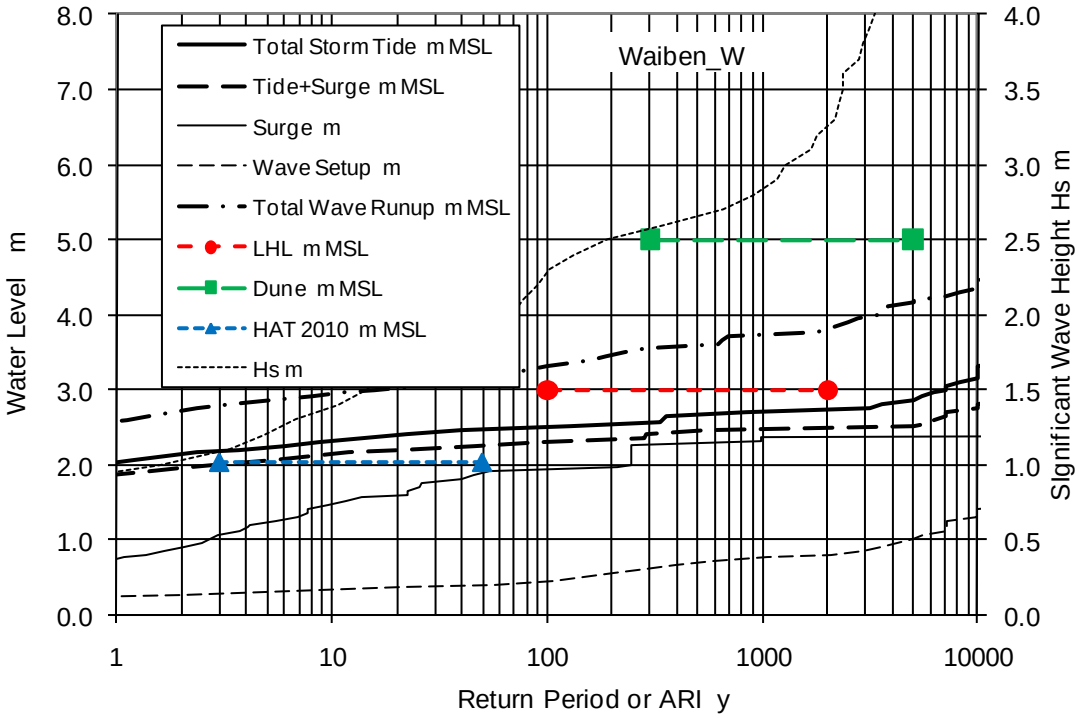
Waiben_W
Total Storm Tide m MSL
Tide+Surge m MSL
Surge m
Wave Setup m
Total Wave Runup m MSL
LHL m MSL
Dune m MSL
HAT 2010 m MSL
Hs m
Water Level m
Significant Wave Height Hs m
Return Period or ARI y
8.0
7.0
6.0
5.0
4.0
3.0
2.0
1.0
0.0
4.0
3.5
3.0
2.5
2.0
1.5
1.0
0.5
0.0
1
10
100
1000
10000

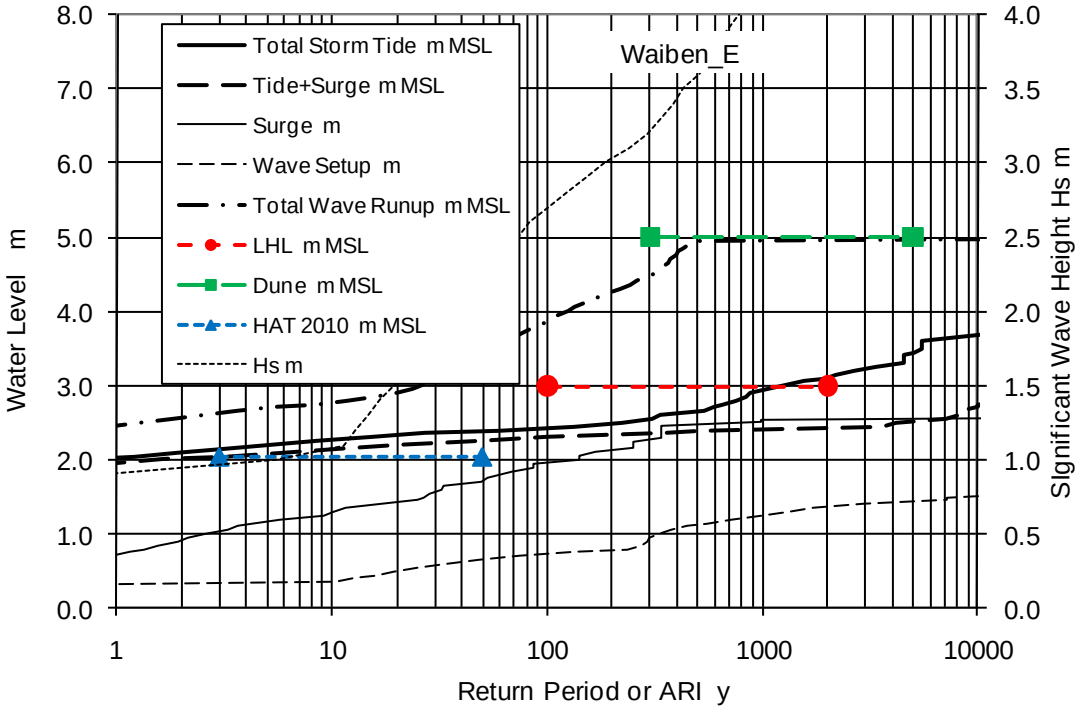
Waiben_E
Total Storm Tide m MSL
Tide+Surge m MSL
Surge m
Wave Setup m
Total Wave Runup m MSL
LHL m MSL
Dune m MSL
HAT 2010 m MSL
Hs m
Water Level m
Significant Wave Height Hs m
Return Period or ARI y
8.0
7.0
6.0
5.0
4.0
3.0
2.0
1.0
0.0
4.0
3.5
3.0
2.5
2.0
1.5
1.0
0.5
0.0
1
10
100
1000
10000

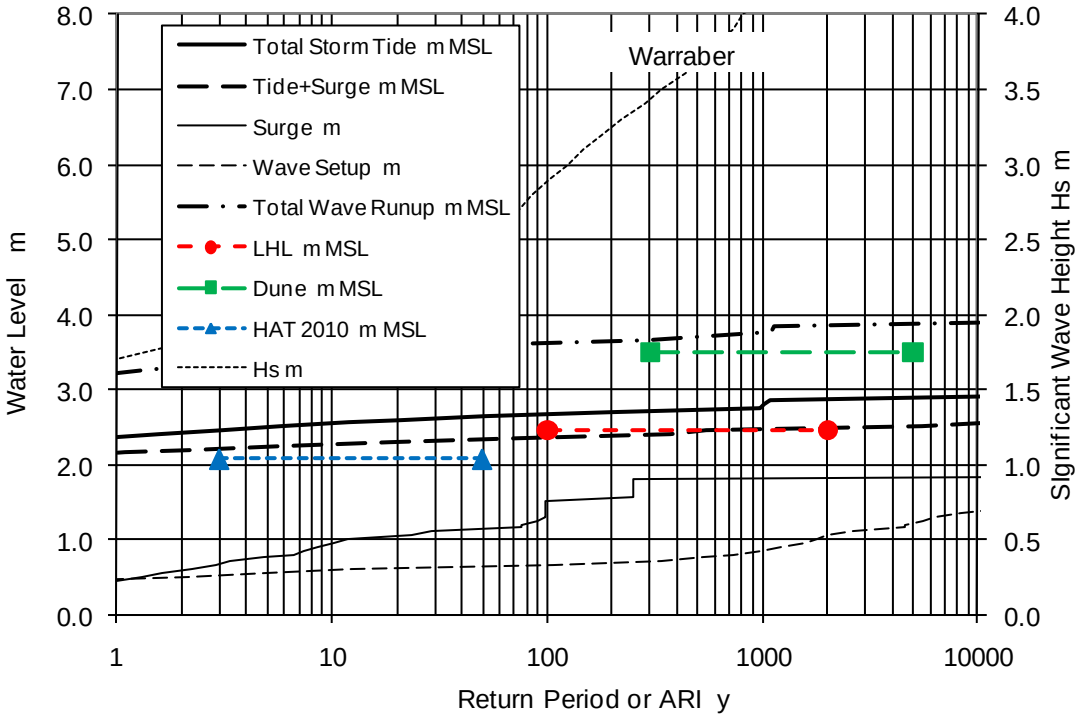
Warraber
Total Storm Tide m MSL
Tide+Surge m MSL
Surge m
Wave Setup m
Total Wave Runup m MSL
LHL m MSL
Dune m MSL
HAT 2010 m MSL
Hs m
Water Level m
Significant Wave Height Hs m
Return Period or ARI y
8.0
7.0
6.0
5.0
4.0
3.0
2.0
1.0
0.0
4.0
3.5
3.0
2.5
2.0
1.5
1.0
0.5
0.0
1
10
100
1000
10000

Appendix Q

Site-Specific Simulation Model Comparisons of Total Storm Tide in Present 2010 Climate with Projected Future Climates 2050 and 2100

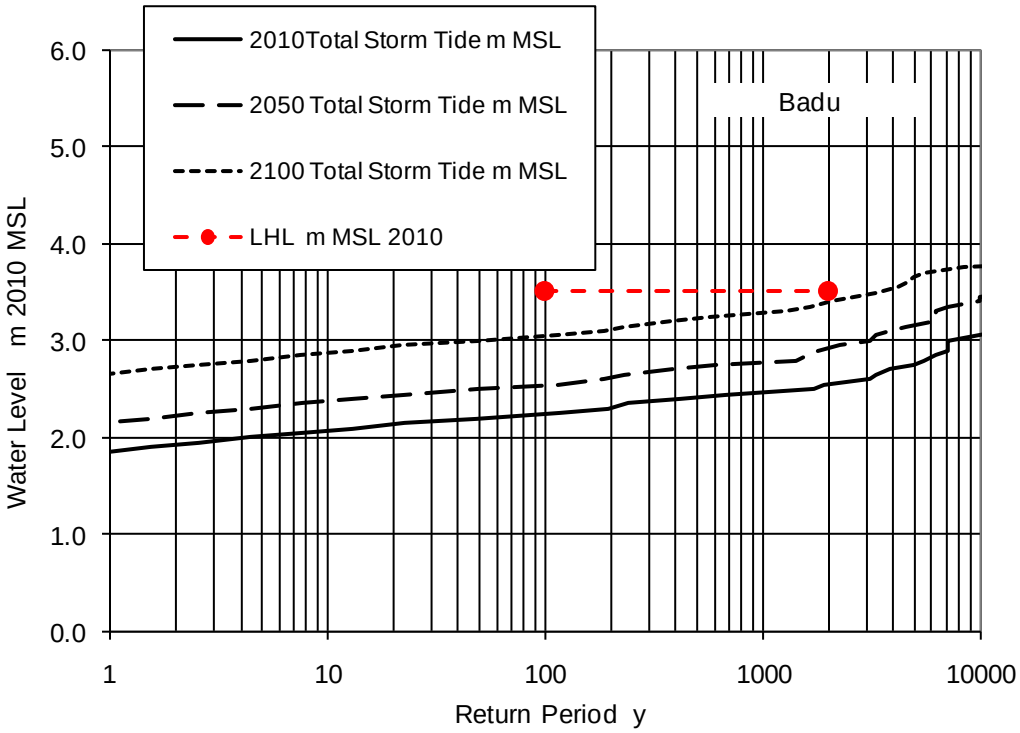
2010Total Storm Tide m MSL
2050 Total Storm Tide m MSL
2100 Total Storm Tide m MSL
LHL m MSL 2010
Badu
Water Level m 2010 MSL
6.0
5.0
4.0
3.0
2.0
1.0
0.0
1
10
100
1000
10000
Return Period y

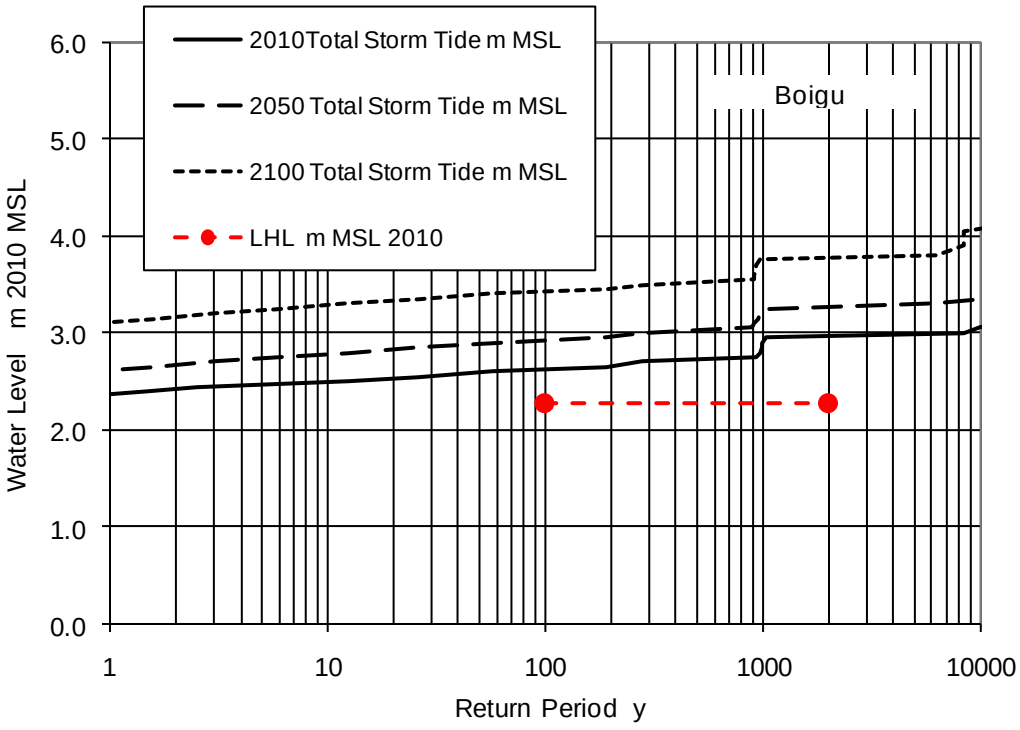
2010Total Storm Tide m MSL
2050 Total Storm Tide m MSL
2100 Total Storm Tide m MSL
LHL m MSL 2010
Boigu
Water Level m 2010 MSL
6.0
5.0
4.0
3.0
2.0
1.0
0.0
1
10
100
1000
10000
Return Period y

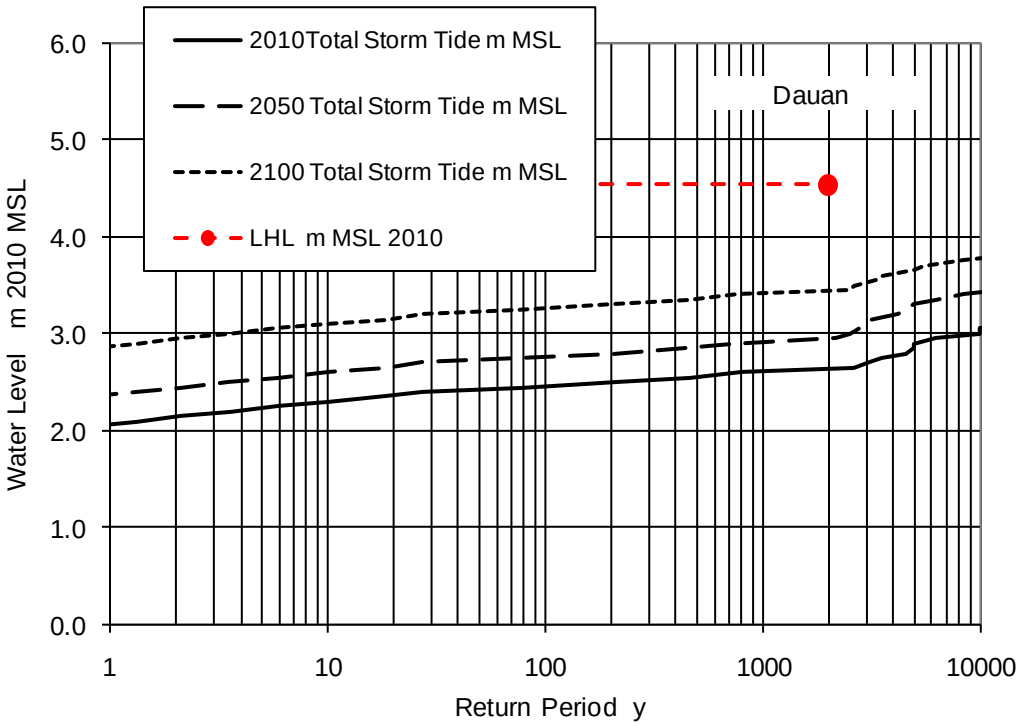
2010Total Storm Tide m MSL
2050 Total Storm Tide m MSL
2100 Total Storm Tide m MSL
LHL m MSL 2010
Dauan
Water Level m 2010 MSL
6.0
5.0
4.0
3.0
2.0
1.0
0.0
1
10
100
1000
10000
Return Period y

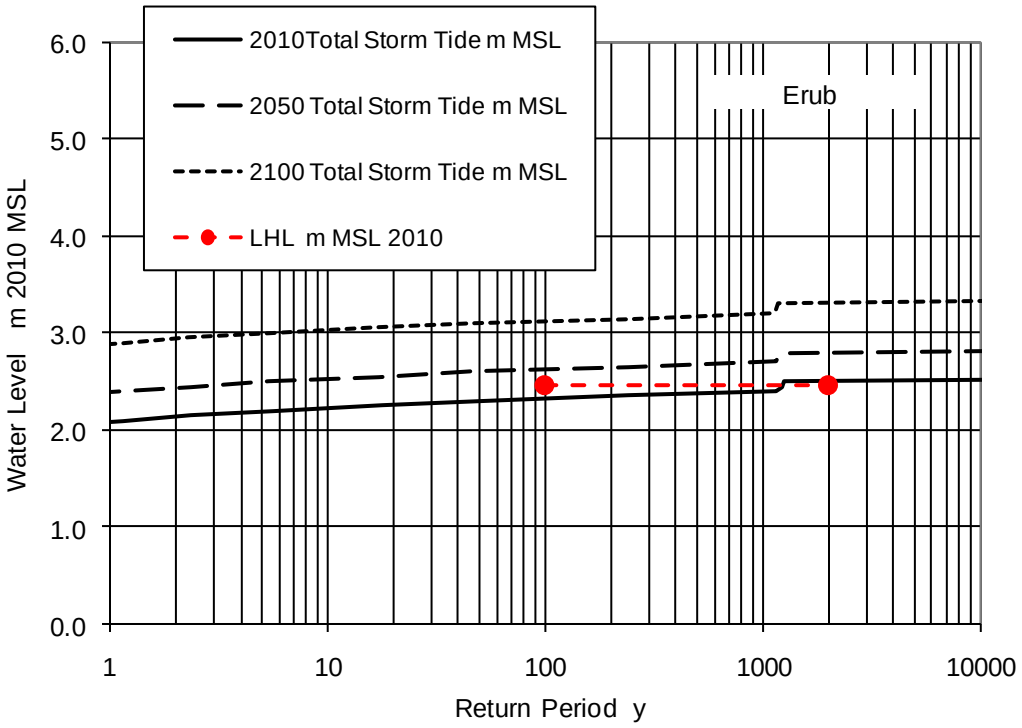
2010Total Storm Tide m MSL
2050 Total Storm Tide m MSL
2100 Total Storm Tide m MSL
LHL m MSL 2010
Erub
Water Level m 2010 MSL
6.0
5.0
4.0
3.0
2.0
1.0
0.0
1
10
100
1000
10000
Return Period y

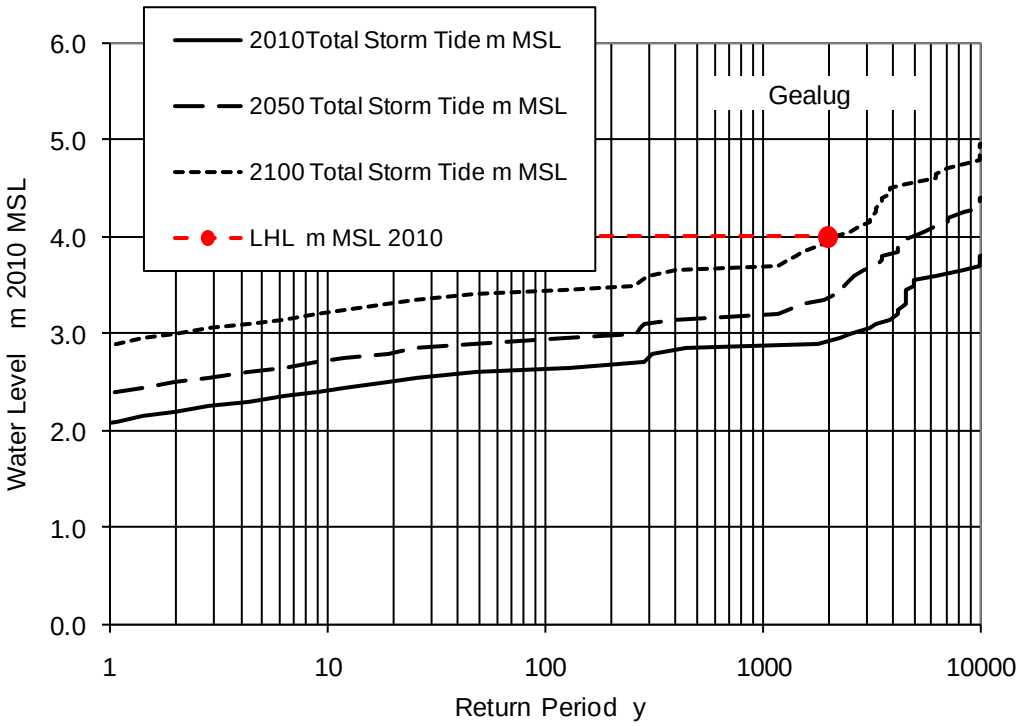
2010Total Storm Tide m MSL
2050 Total Storm Tide m MSL
2100 Total Storm Tide m MSL
LHL m MSL 2010
Gealug
Water Level m 2010 MSL
6.0
5.0
4.0
3.0
2.0
1.0
0.0
1
10
100
1000
10000
Return Period y

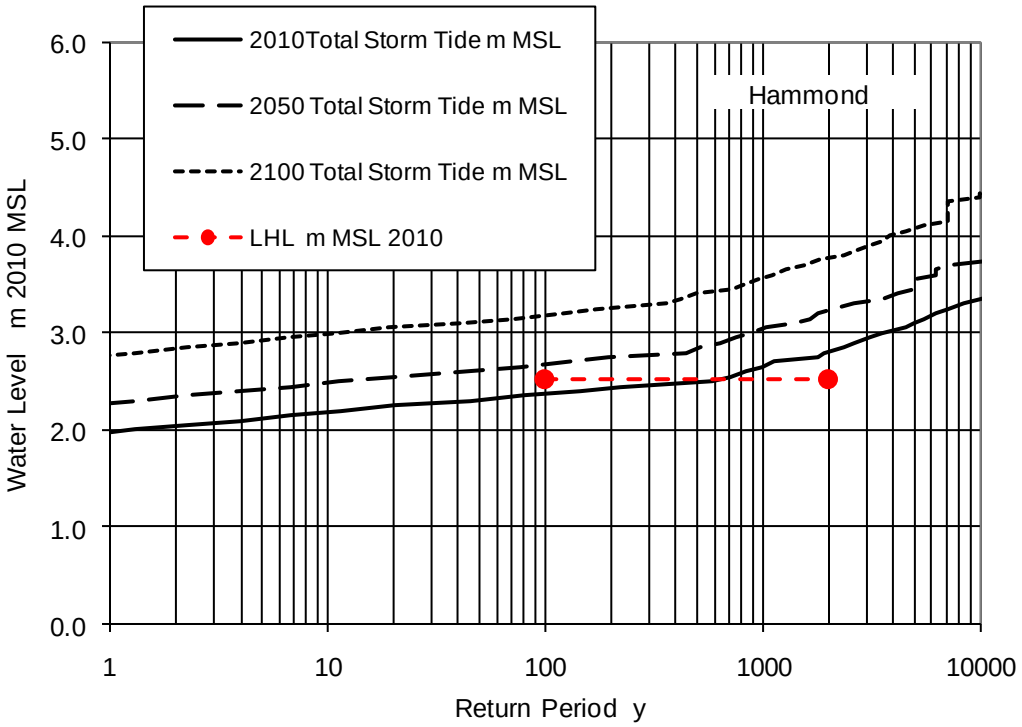
2010Total Storm Tide m MSL
2050 Total Storm Tide m MSL
2100 Total Storm Tide m MSL
LHL m MSL 2010
Hammond
Water Level m 2010 MSL
6.0
5.0
4.0
3.0
2.0
1.0
0.0
1
10
100
1000
10000
Return Period y

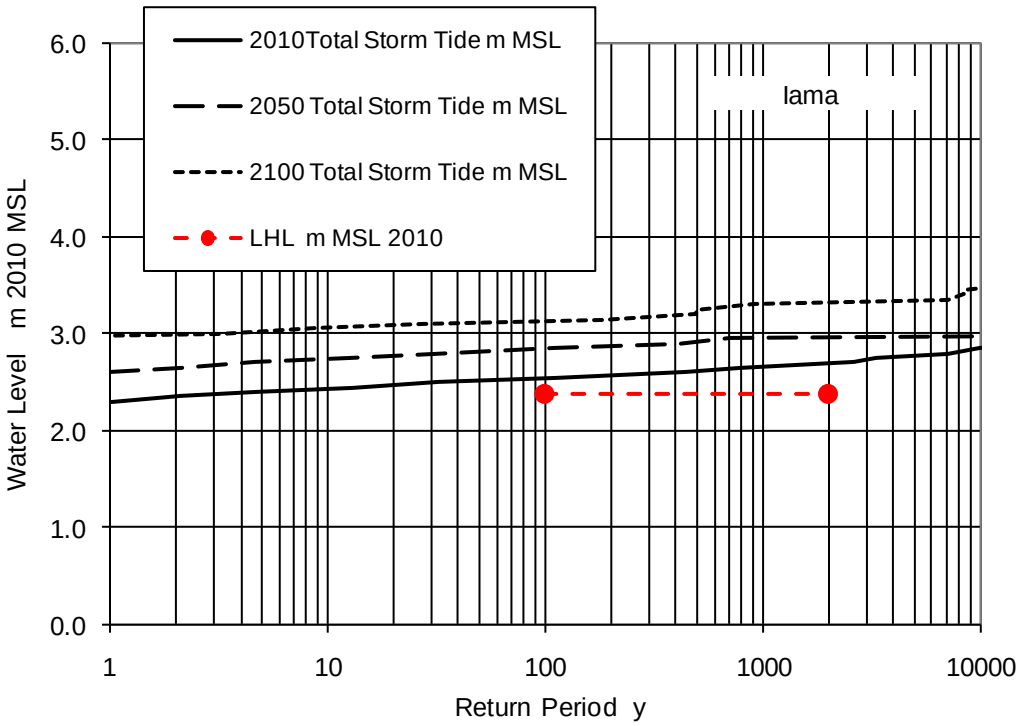
2010Total Storm Tide m MSL
2050 Total Storm Tide m MSL
2100 Total Storm Tide m MSL
LHL m MSL 2010
Iama
Water Level m 2010 MSL
6.0
5.0
4.0
3.0
2.0
1.0
0.0
1
10
100
1000
10000
Return Period y

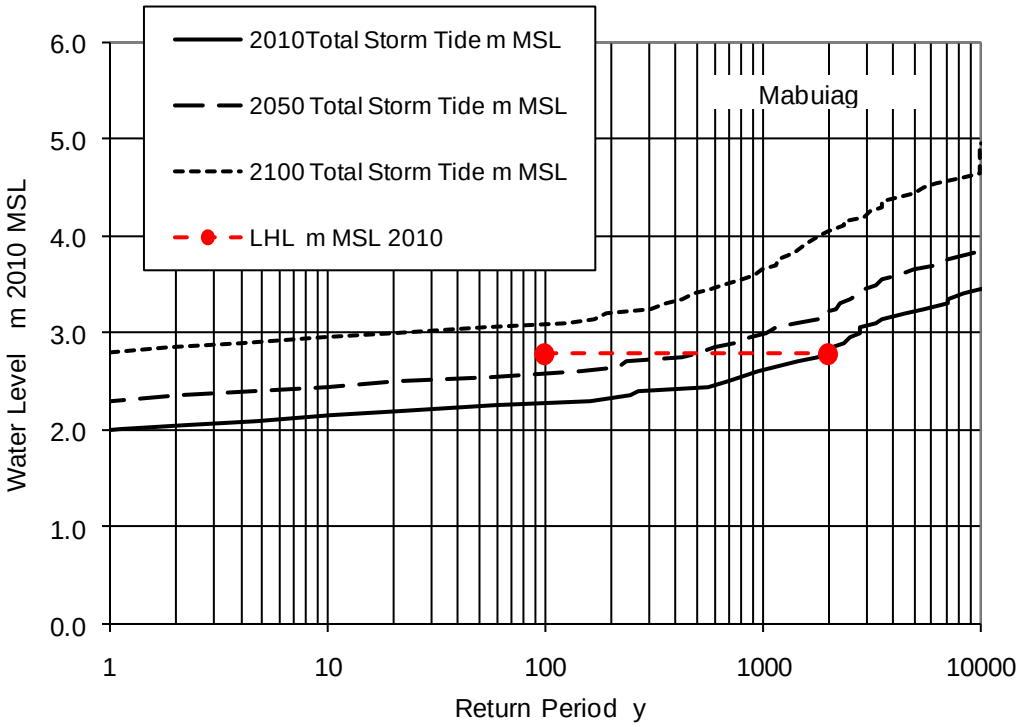
2010Total Storm Tide m MSL
2050 Total Storm Tide m MSL
2100 Total Storm Tide m MSL
LHL m MSL 2010
Mabuiag
Water Level m 2010 MSL
6.0
5.0
4.0
3.0
2.0
1.0
0.0
1
10
100
1000
10000
Return Period y

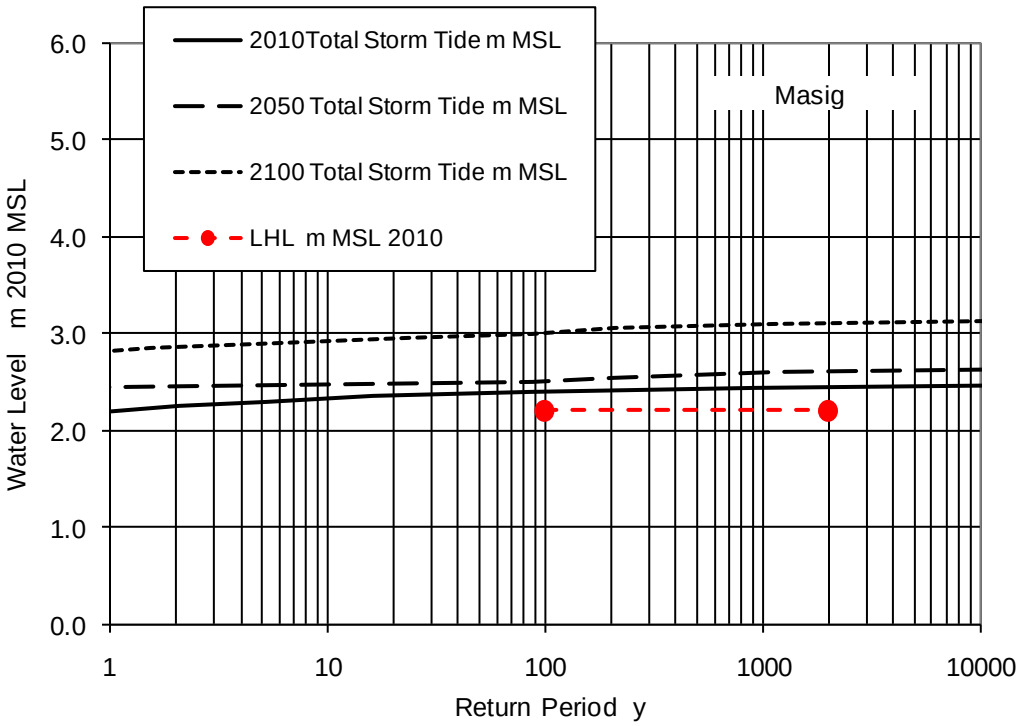
2010Total Storm Tide m MSL
2050 Total Storm Tide m MSL
2100 Total Storm Tide m MSL
LHL m MSL 2010
Masig
Water Level m 2010 MSL
6.0
5.0
4.0
3.0
2.0
1.0
0.0
1
10
100
1000
10000
Return Period y

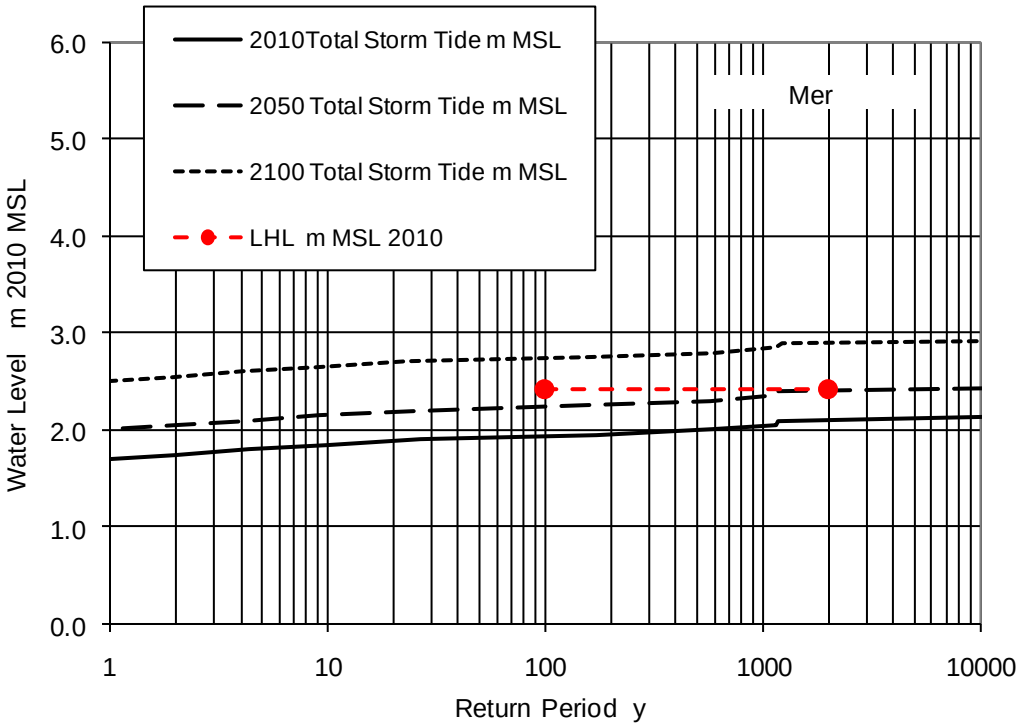
2010Total Storm Tide m MSL
2050 Total Storm Tide m MSL
2100 Total Storm Tide m MSL
LHL m MSL 2010
Mer
Water Level m 2010 MSL
6.0
5.0
4.0
3.0
2.0
1.0
0.0
1
10
100
1000
10000
Return Period y

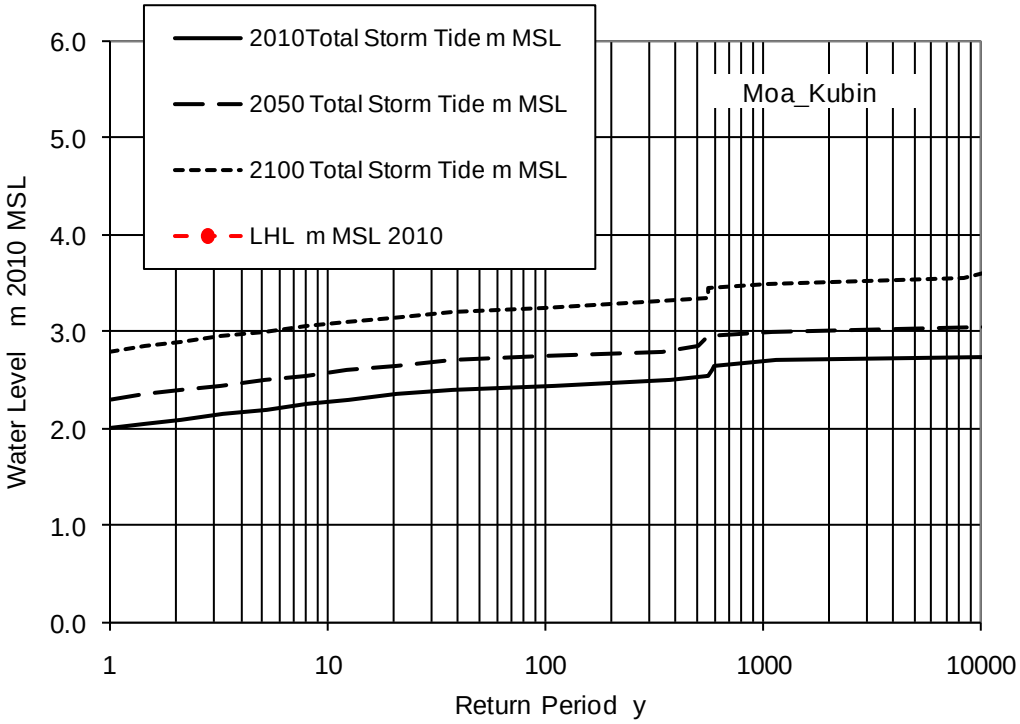
2010Total Storm Tide m MSL
2050 Total Storm Tide m MSL
2100 Total Storm Tide m MSL
LHL m MSL 2010
Moa_Kubin
Water Level m 2010 MSL
6.0
5.0
4.0
3.0
2.0
1.0
0.0
1
10
100
1000
10000
Return Period y

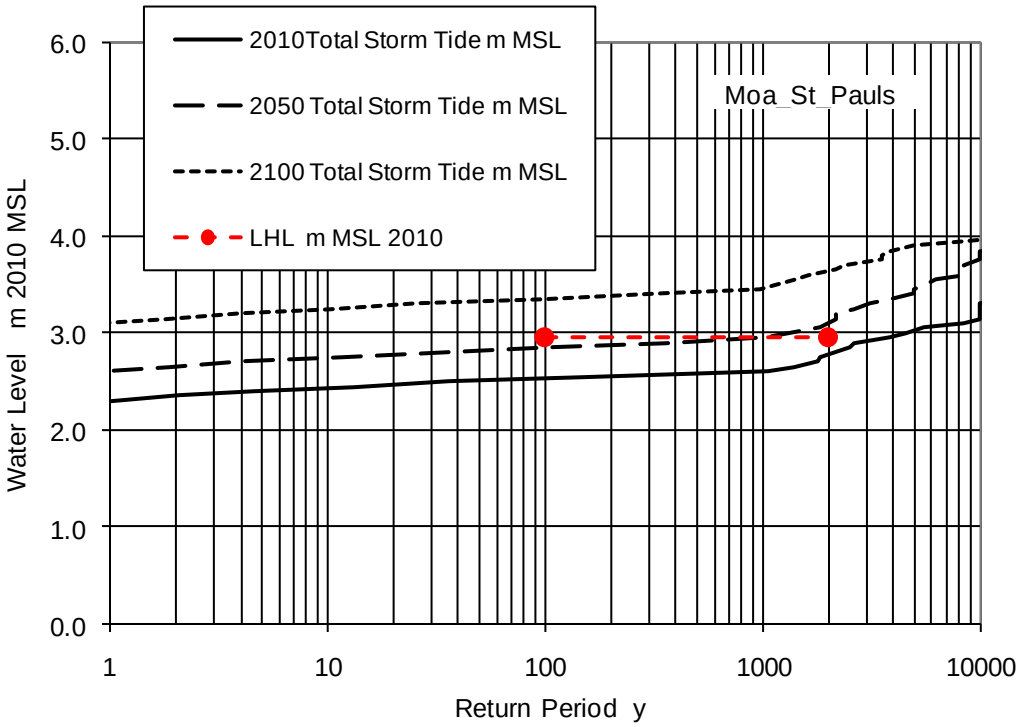
2010Total Storm Tide m MSL
2050 Total Storm Tide m MSL
2100 Total Storm Tide m MSL
LHL m MSL 2010
Moa_St_Pauls
Water Level m 2010 MSL
6.0
5.0
4.0
3.0
2.0
1.0
0.0
1
10
100
1000
10000
Return Period y

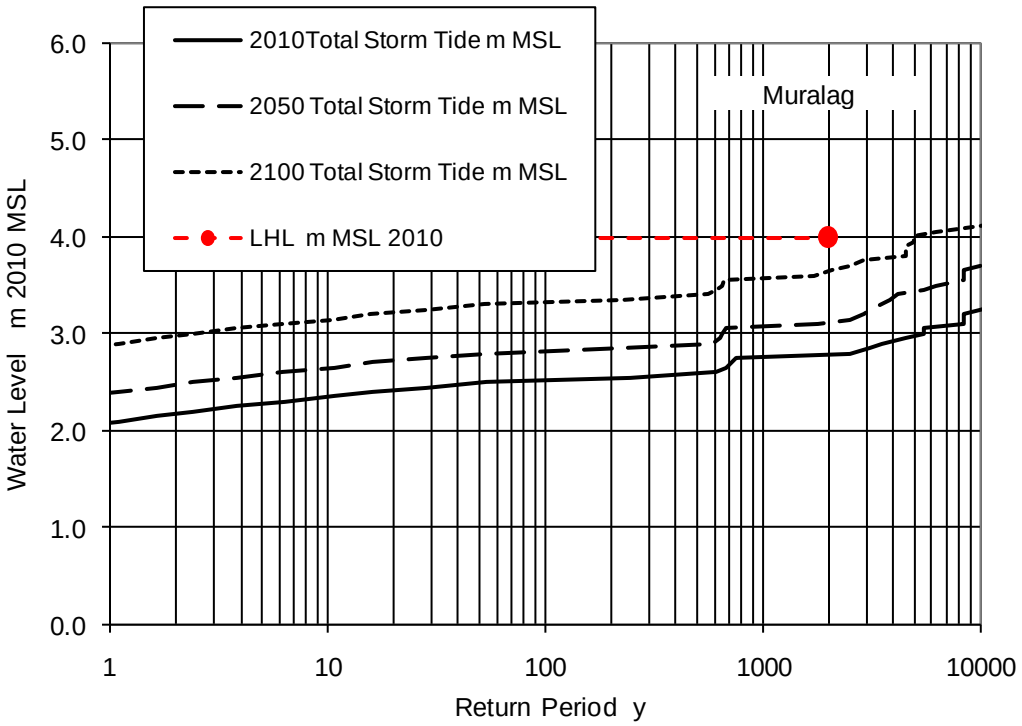
2010Total Storm Tide m MSL
2050 Total Storm Tide m MSL
2100 Total Storm Tide m MSL
LHL m MSL 2010
Muralag
Water Level m 2010 MSL
6.0
5.0
4.0
3.0
2.0
1.0
0.0
1
10
100
1000
10000
Return Period y

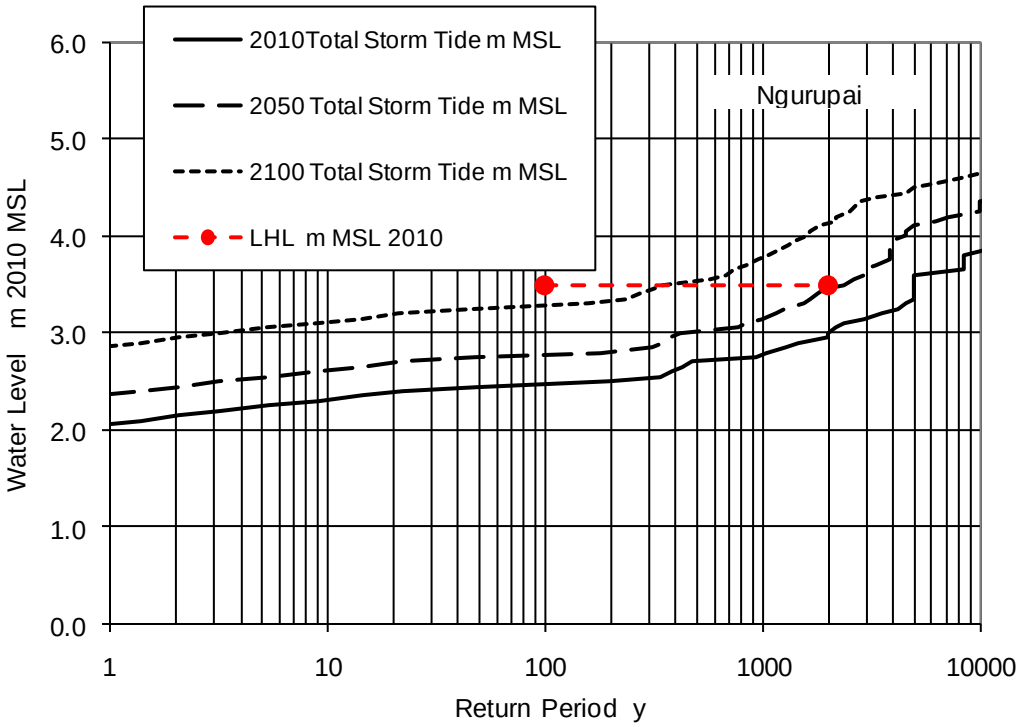
2010Total Storm Tide m MSL
2050 Total Storm Tide m MSL
2100 Total Storm Tide m MSL
LHL m MSL 2010
Ngurupai
Water Level m 2010 MSL
6.0
5.0
4.0
3.0
2.0
1.0
0.0
1
10
100
1000
10000
Return Period y

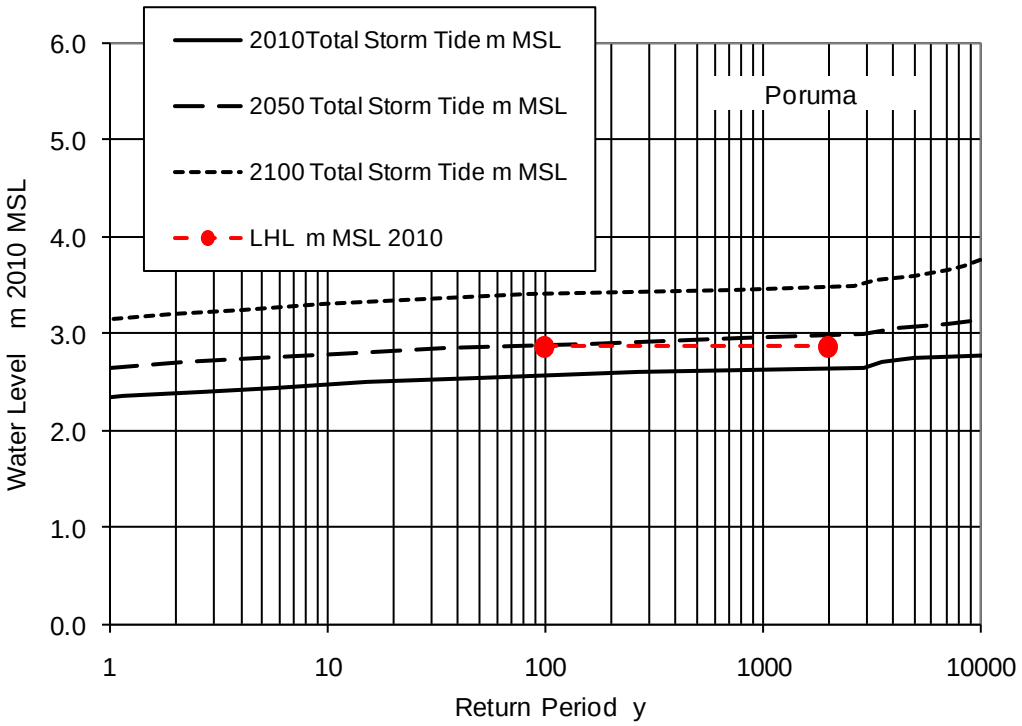
2010Total Storm Tide m MSL
2050 Total Storm Tide m MSL
2100 Total Storm Tide m MSL
LHL m MSL 2010
Poruma
Water Level m 2010 MSL
6.0
5.0
4.0
3.0
2.0
1.0
0.0
1
10
100
1000
10000
Return Period y

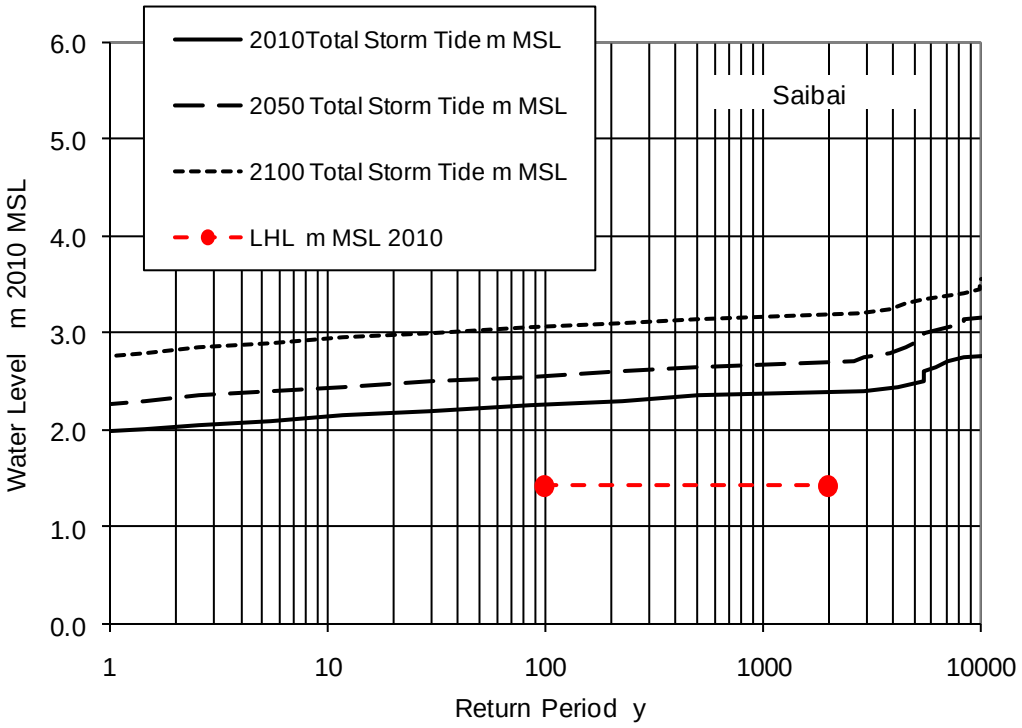
2010Total Storm Tide m MSL
2050 Total Storm Tide m MSL
2100 Total Storm Tide m MSL
LHL m MSL 2010
Saibai
Water Level m 2010 MSL
6.0
5.0
4.0
3.0
2.0
1.0
0.0
1
10
100
1000
10000
Return Period y

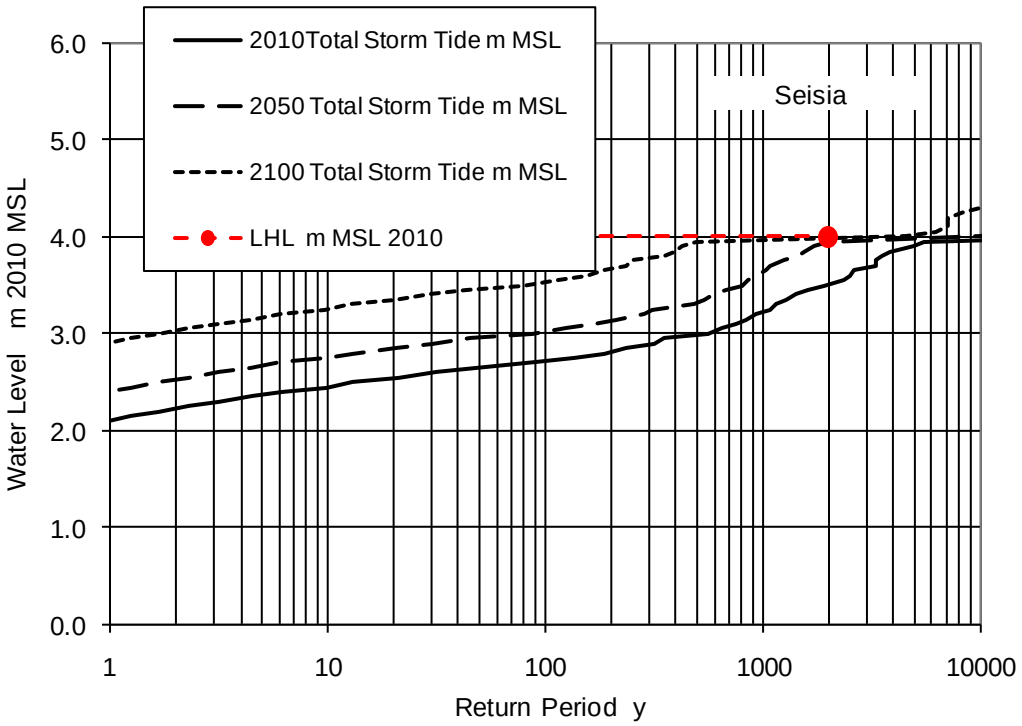
2010Total Storm Tide m MSL
2050 Total Storm Tide m MSL
2100 Total Storm Tide m MSL
LHL m MSL 2010
Seisia
Water Level m 2010 MSL
6.0
5.0
4.0
3.0
2.0
1.0
0.0
1
10
100
1000
10000
Return Period y

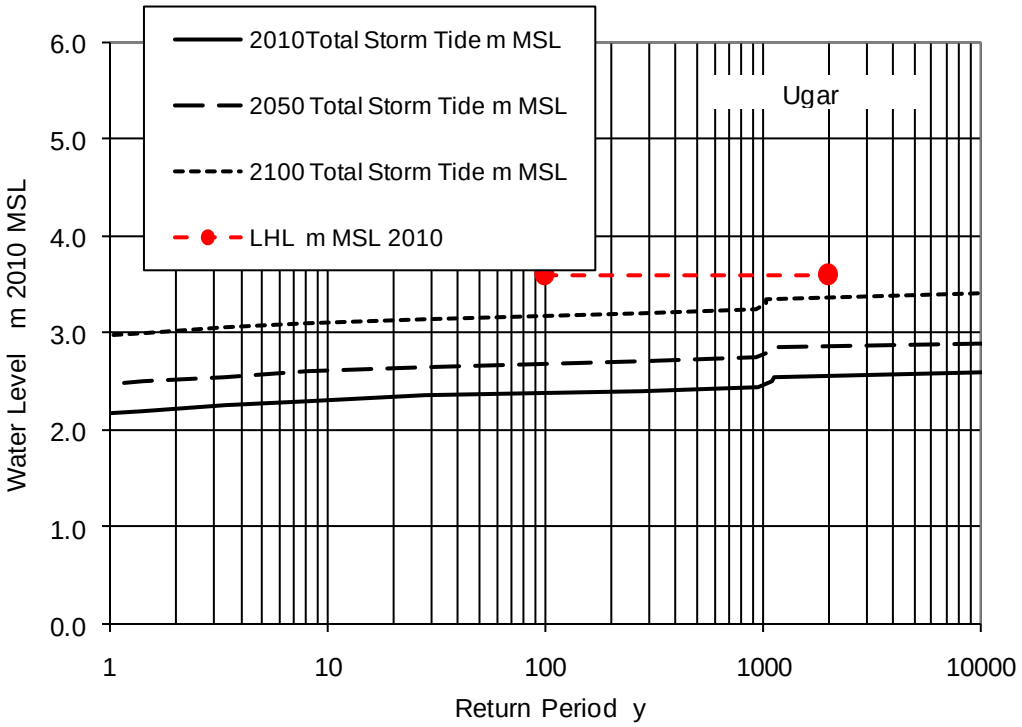
2010Total Storm Tide m MSL
2050 Total Storm Tide m MSL
2100 Total Storm Tide m MSL
LHL m MSL 2010
Ugar
Water Level m 2010 MSL
6.0
5.0
4.0
3.0
2.0
1.0
0.0
1
10
100
1000
10000
Return Period y

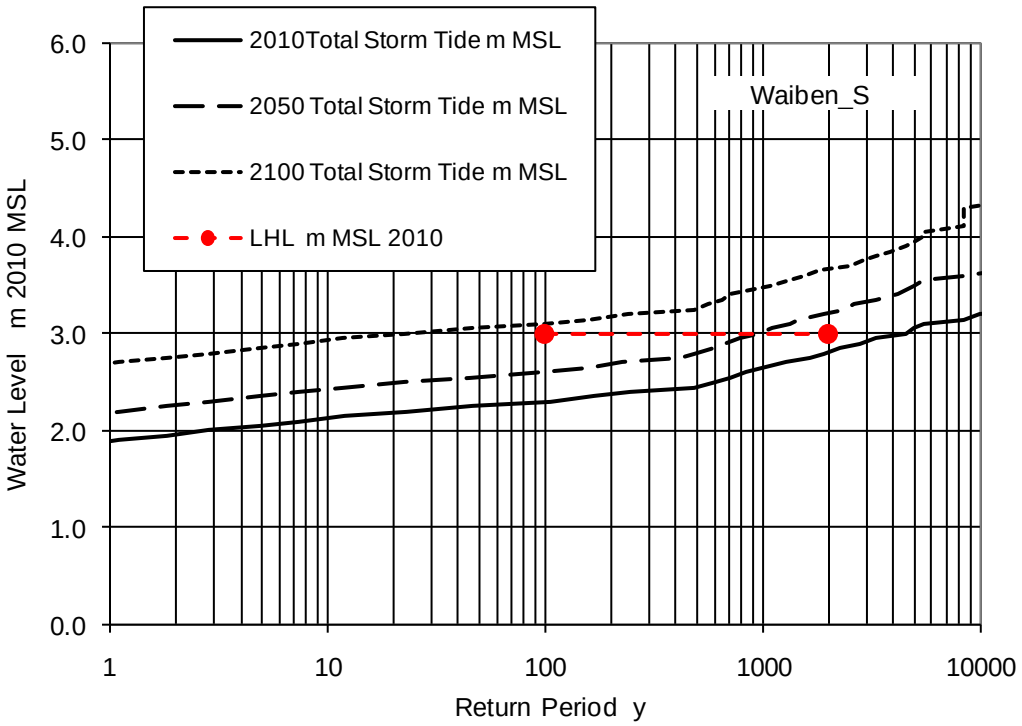
2010Total Storm Tide m MSL
2050 Total Storm Tide m MSL
2100 Total Storm Tide m MSL
LHL m MSL 2010
Waiben_S
Water Level m 2010 MSL
Return Period y
6.0
5.0
4.0
3.0
2.0
1.0
0.0
1
10
100
1000
10000

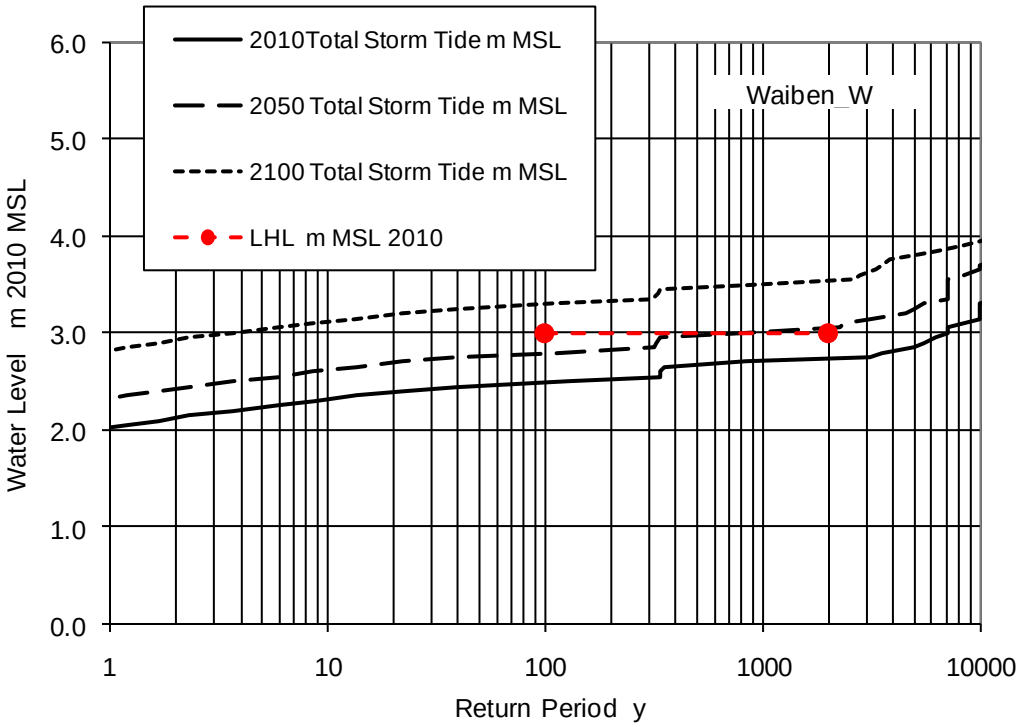
2010Total Storm Tide m MSL
2050 Total Storm Tide m MSL
2100 Total Storm Tide m MSL
LHL m MSL 2010
Waiben_W
Water Level m 2010 MSL
Return Period y
6.0
5.0
4.0
3.0
2.0
1.0
0.0
1
10
100
1000
10000

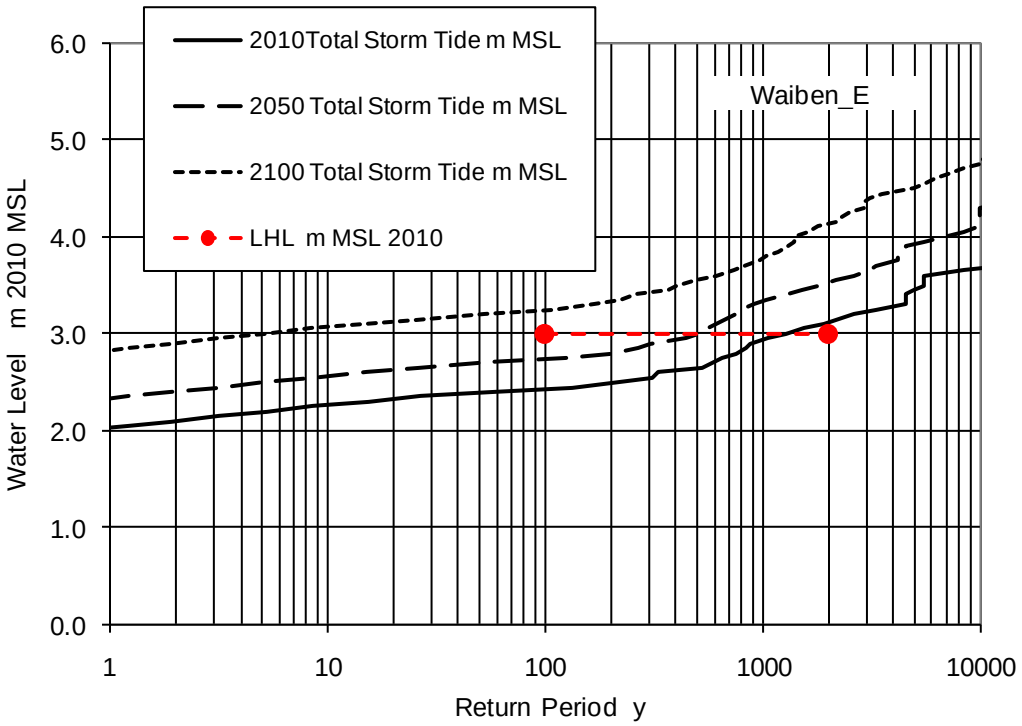
2010Total Storm Tide m MSL
2050 Total Storm Tide m MSL
2100 Total Storm Tide m MSL
LHL m MSL 2010
Waiben_E
Water Level m 2010 MSL
Return Period y
6.0
5.0
4.0
3.0
2.0
1.0
0.0
1
10
100
1000
10000

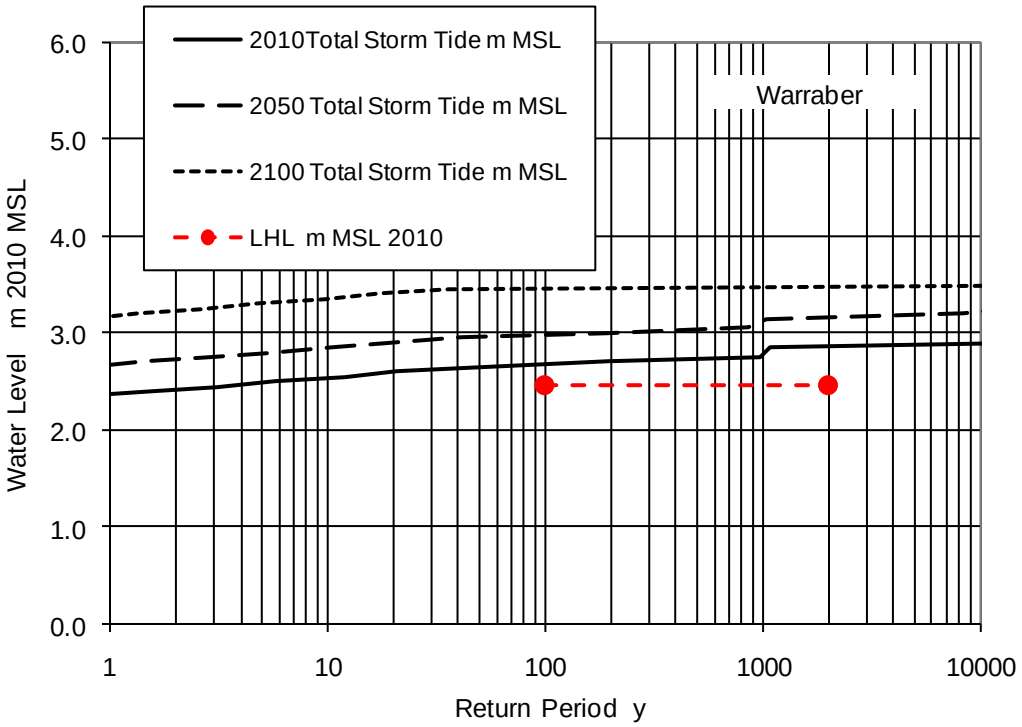
2010Total Storm Tide m MSL
2050 Total Storm Tide m MSL
2100 Total Storm Tide m MSL
LHL m MSL 2010
Warraber
Water Level m 2010 MSL
Return Period y
6.0
5.0
4.0
3.0
2.0
1.0
0.0
1
10
100
1000
10000

Appendix R

Site-Specific Simulation Model Differences between Projected Future Climate 2050 and 2100 Total Storm Tide Levels and Present 2010 Climate

2050	Estimated Return Period of Total Storm Tide Level (shown as difference from 2010)							
	5	10	25	50	100	500	1000	10000
Site	m MSL	m MSL	m MSL	m MSL	m MSL	m MSL	m MSL	m MSL
Badu	0.30	0.30	0.30	0.30	0.30	0.30	0.30	0.30
Boigu	0.25	0.24	0.27	0.29	0.30	0.30	0.30	0.30
Dauan	0.30	0.30	0.30	0.30	0.30	0.30	0.30	0.30
Erub	0.30	0.30	0.30	0.30	0.30	0.30	0.30	0.30
Gealug	0.30	0.30	0.30	0.30	0.31	0.30	0.30	0.31
Hammond	0.30	0.30	0.30	0.31	0.30	0.30	0.31	0.35
Iama	0.30	0.31	0.30	0.30	0.30	0.30	0.30	0.30
Mabuiag	0.31	0.31	0.30	0.30	0.30	0.30	0.30	0.36
Masig	0.25	0.20	0.15	0.14	0.10	0.11	0.10	0.13
Mer	0.30	0.30	0.30	0.30	0.31	0.30	0.30	0.30
Moa_Kubin	0.30	0.30	0.31	0.30	0.30	0.30	0.31	0.32
Moa_St_Pauls	0.30	0.30	0.31	0.31	0.31	0.30	0.32	0.34
Muralag	0.30	0.30	0.30	0.30	0.30	0.30	0.30	0.31
Ngurupai	0.30	0.31	0.30	0.30	0.30	0.30	0.30	0.31
Poruma	0.32	0.31	0.31	0.32	0.32	0.31	0.32	0.33
Saibai	0.28	0.30	0.30	0.30	0.30	0.30	0.30	0.30
Seisia	0.30	0.31	0.31	0.30	0.30	0.31	0.31	0.34
Ugar	0.30	0.30	0.30	0.30	0.30	0.30	0.30	0.30
Waiben_S	0.30	0.30	0.30	0.30	0.31	0.30	0.30	0.34
Waiben_W	0.30	0.31	0.30	0.30	0.30	0.30	0.31	0.30
Waiben_E	0.30	0.30	0.31	0.30	0.30	0.30	0.30	0.35
Warraber	0.31	0.31	0.31	0.32	0.31	0.30	0.30	0.30
Average =	0.30	0.30	0.29	0.30	0.29	0.29	0.29	0.31
Less static rise =	0.00	0.00	-0.01	0.00	-0.01	-0.01	-0.01	0.01

2100	Estimated Return Period of Total Storm Tide Level (shown as difference from 2010)							
	5	10	25	50	100	500	1000	10000
Site	m MSL	m MSL	m MSL	m MSL	m MSL	m MSL	m MSL	m MSL
Badu	0.80	0.80	0.80	0.80	0.80	0.80	0.80	0.81
Boigu	0.75	0.74	0.77	0.79	0.80	0.80	0.80	0.80
Dauan	0.80	0.80	0.80	0.80	0.80	0.80	0.80	0.80
Erub	0.80	0.80	0.80	0.80	0.80	0.80	0.80	0.80
Gealug	0.80	0.80	0.80	0.80	0.81	0.80	0.80	0.81
Hammond	0.80	0.80	0.80	0.81	0.80	0.81	0.82	0.91
Iama	0.66	0.64	0.62	0.62	0.61	0.60	0.58	0.64
Mabuiag	0.82	0.81	0.81	0.80	0.80	0.81	0.81	0.97
Masig	0.62	0.61	0.60	0.59	0.59	0.60	0.60	0.64
Mer	0.80	0.80	0.80	0.80	0.81	0.80	0.80	0.80
Moa_Kubin	0.80	0.80	0.81	0.80	0.80	0.80	0.81	0.81
Moa_St_Pauls	0.80	0.80	0.81	0.82	0.82	0.81	0.82	0.84
Muralag	0.80	0.80	0.80	0.80	0.80	0.80	0.80	0.81
Ngurupai	0.80	0.81	0.80	0.80	0.80	0.80	0.80	0.83
Poruma	0.82	0.82	0.82	0.83	0.84	0.82	0.84	0.83
Saibai	0.78	0.80	0.80	0.80	0.80	0.80	0.80	0.80
Seisia	0.80	0.81	0.81	0.80	0.80	0.81	0.82	0.97
Ugar	0.80	0.80	0.80	0.80	0.80	0.80	0.80	0.80
Waiben_S	0.80	0.80	0.80	0.80	0.80	0.80	0.80	0.80
Waiben_W	0.80	0.81	0.80	0.80	0.80	0.80	0.81	0.80
Waiben_E	0.80	0.80	0.81	0.80	0.81	0.80	0.81	0.91
Warraber	0.81	0.82	0.81	0.82	0.81	0.80	0.78	0.73
Average =	0.78	0.79	0.79	0.79	0.79	0.78	0.79	0.81
Less static rise =	-0.12	-0.12	-0.12	-0.11	-0.11	-0.12	-0.11	-0.09

Appendix S

A Note on the Interpretation of Statistical Return Periods

S.1 General

This study has presented its analyses of risk in terms of the so-called *Return Period* (or *Average Recurrence Interval ARI*). The return period is the "average" number of years between successive events of the same or greater magnitude. For example, if the 100-year return period storm tide level is 3.0 m AHD then on average, a 3.0 m AHD level storm tide *or greater* will occur due to a single event once every 100 years, but sometimes it may occur more or less frequently than 100 years. It is important to note that in any "N"-year period, the "N"-year return period event has a 64% chance of being equalled or exceeded. This means that the example 3.0 m storm tide has a better-than-even chance of being exceeded by the end of any 100-year period. If the 100-year event were to occur, then there is still a finite possibility that it could occur again soon, even in the same year, or that the 1000 year event could occur, for example, next year. Clearly if such multiple events continue unchecked then the basis for the estimate of, say, the 100 year event might then need to be questioned, but statistically this type of behaviour can be expected.

A more consistent way of considering the above (NCCOE 2004) is to include the concepts of "design life" and "encounter probability" which, when linked with the return period, provide better insight into the problem and can better assist management risk decision making. These various elements are linked by the following formula (Borgman 1963):

$$T = - N / ln [1 - p]$$

Where p	=	encounter probability	$0 \leq 1$
N	=	the design life	(years)
T	=	the return period	(years)

This equation describes the complete continuum of risk when considering the prospect of at least one event of interest occurring. More complex equations describe other possibilities such as the risk of only two events in a given period or only one event occurring.

Figure S.1 illustrates the above equation graphically. It presents the variation in probability of at least one event occurring (the encounter probability) versus the period of time considered (the design life). The intersection of any of these chosen variables leads to a particular return period and a selection of common return periods is indicated. For example, this shows that the 200-year return period has a 40% chance of being equalled or exceeded in any 100-year period.

The level of risk acceptable in any situation is necessarily a corporate or business decision. Table S.1, based on Figure S.1, is provided to assist in this decision making process by showing a selection of risk options. Using Table S.1, combinations of design life and a comfortable risk of occurrence over that design life can be used to yield the appropriate return period to consider. For example, accepting a 5% chance of occurrence in a design life of 50 years means that the 1000-year return period event should be considered. A similar level of risk is represented by a 1% chance in 10 years. By comparison, the 100 year return period is equivalent to about a 10% chance in 10 years. AS1170.2 (Standards Australia 2002), for example, dictates a 10% chance in 50 years criteria or the 500-year return period as the minimum risk level for wind speed loadings on engineered structures.

S.2 References

NCCOE (2004) Guidelines for responding to the effects of climate change in coastal and ocean engineering – 2004 update. The National Committee on Coastal and Ocean Engineering, ENGINEERS AUSTRALIA, Canberra, EA Books, 75pp.

Borgman L. (1963) Risk Criteria. Journal of the Waterway, Port, Coastal and Ocean Division, ASCE, Vol 89, No. WW3, Aug, 1 - 35.

Standards Australia (2002) AS/NZS 1170.2 – 2002. Structural design actions - Part 2: wind actions. 88pp, as amended.

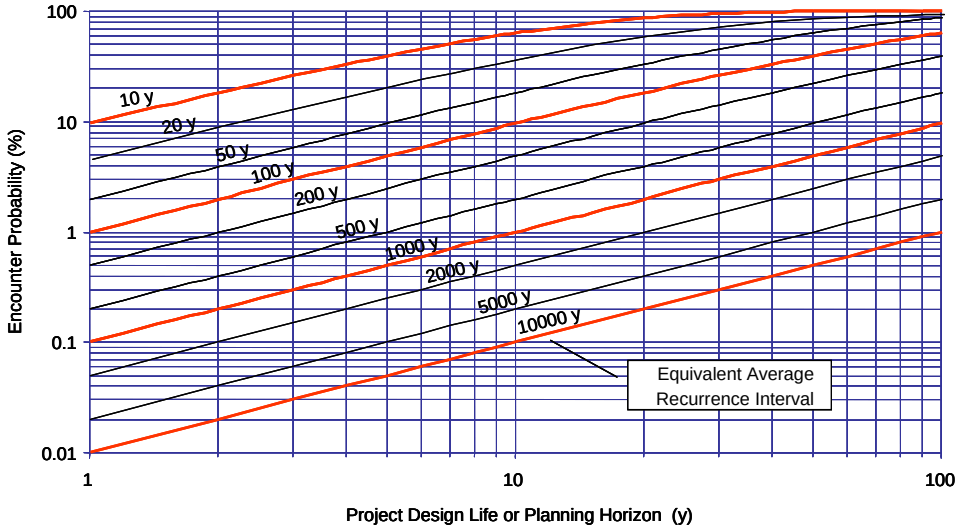

Figure S.1 Relationship between Return Period and Encounter probability

Table S.1 Risk selection based on encounter probability concepts.

Considered Design Life or Planning Horizon	Chosen Level of Risk of at Least One Event Occurring					
	% Chance					
y	**1**	**2**	**5**	**10**	**20**	**30**
	Equivalent Return Period (y)					
10	995	495	195	95	45	29
20	1990	990	390	190	90	57
30	2985	1485	585	285	135	85
40	3980	1980	780	380	180	113
50	4975	2475	975	475	225	141